Assessing Climate-related Fire Danger across the Central Grassland Biome of South Africa

by

Abraham Stephanus (Stephan) Steyn

(2003141922)

Submitted in partial fulfilment of the requirements

for the degree

Philosophiae Doctor in Agrometeorology

in the

Department of Soil, Crop and Climate Sciences

Faculty of Natural and Agricultural Sciences

University of the Free State

Supervisor: Prof C.J. Stigter (*emortuus*)

Co-supervisor: Prof A.C. Franke

Bloemfontein

2020

DECLARATION

“I, Abraham Stephanus Steyn, declare that the research thesis that I herewith submit for the Philosophiae Doctor Degree in Agrometeorology at the University of the Free State is my independent work, and that I have not previously submitted it for a qualification at another institution of higher education.”

I furthermore cede copyright of the thesis in favor of the University of the Free State.

A.S. Steyn

Date: January 2020

Place: Bloemfontein, South Africa.

ABSTRACT

The grasslands of the South African interior plateau are subject to seasonal wildfires that occasionally inflict serious damage to livestock production systems and infrastructure. Recent and future projected changes in the climate imply long-term changes in the fire regime, which may pose challenges to fire managers and exceed the current suppression capacity. The aim of this study was thus to assess historical and future fire danger across the central grassland biome of South Africa.

Both actual observed fires (i.e. total burned area obtained through satellite remote sensing) and climatological fire danger (i.e. fire danger indices calculated from reanalysis climate data) were considered over the historical period (1981 – 2010). Self-organizing map (SOM) analysis was also used to identify the 850 hPa synoptic weather patterns related to increased climatological fire danger over the historical period, while projections from six ensemble members were used in evaluating climate-related fire danger under the A2 scenario over three future periods (i.e. 2011 – 2040, 2041 – 2070 and 2071 – 2100).

Results showed that enhanced rainfall during the antecedent mid-summer season lead to increased burning due to higher fuel loads. There was a large inter-annual variability in the total burned area, ranging from 478 000 to 1.6 million ha per annum, with a significant decreasing trend of about 34 000 ha per annum over the historical period. This was in contrast to the significant increase in climatological fire danger, particularly during the last decade. Climatological fire danger was shown to be considerably higher in the south-western part of the central grassland, where extreme days occurred on 5 – 9 days during the fire season. SOM analysis revealed that very dangerous fire conditions were mostly associated with the warm, dry and windy conditions typically experienced to the east of a well-developed frontal trough over the subcontinent.

Projections from various ensemble members did not support a continued increase in climate-related fire danger over the current climate epoch and had broadly inconsistent spatial patterns of change in very dangerous occurrences. The bulk of

the ensemble members projected relatively small changes in fire danger over the southern Highveld, while the largest increases occurred in the north-west. An increase of between 5 – 15 very dangerous days was predicted for the near-future climate epoch, and 5 – 45 days for the distant future epoch (double these values for FFDI under MIROC3.2). The pattern and magnitude of change generally corresponded to different degrees of warming. The shift towards higher fire danger seemed to be more prominent from mid-century onwards. The projections from two ensemble members, CSIRO Mk3.5 and GFDL-CM2.1, differed considerably from the others. They predicted a decrease of between 5 – 15 very dangerous days over the central and southern parts of the study area for the current and near-future climate epochs, and decreases of less than 5 days for the distant future epoch. Discrepancies among future climate scenarios and unrepresented processes (e.g. vegetation dynamics), contribute to uncertainty about the accuracy of these predictions. Nonetheless, the results of this study underscore the potentially large impacts of climate change on the central grassland biome.

Keywords: *burned area, climate change, fire danger index, future projections, SOM analysis*

TABLE OF CONTENTS

ACKNOWLEDGEMENTS

I would like to acknowledge the following people and institutions for their kind assistance:

- Inkaba yeAfrica (now Iphakade) for funding;
- Copernicus Climate Change Service Climate Data Store for providing the ERA5 reanalysis near-surface data;
- KNMI Climate Explorer for providing the ERA5 reanalysis daily total precipitation data;
- ARC – ISCW for providing historical station climate data;
- SAWS for providing historical station climate data;
- Lufuno Vhengani of the CSIR – Meraka Institute for supplying the MODIS district level monthly burned area data;
- Francois Engelbrecht for providing the CCAM data and initial program code for ingesting it;
- Christien Engelbrecht for her expert guidance and assistance with the SOM analysis;
- Fanie Riekert for assisting me with access to, and software installations on, the UFS High Performance Computing cluster;
- The various contributors to Stackoverflow for their sporadic assistance with problematic program code;
- My supervisors, Kees Stigter and Linus Franke, for their guidance and encouragement;
- Jaqui Stigter for her warm hospitality when I visited them in the Netherlands;
- My family and friends for their support and encouragement;
- Pippa, Rolo, Keke and Johan for being there; and
- The Greater Power for instilling an interest in the atmospheric sciences in me.

LIST OF ABBREVIATIONS

AFIS	Advanced Fire Information System
Ann	Annual
AOH	South Atlantic Ocean High Pressure Cell
ARC-ISCW	Agricultural Research Council – Institute for Soil, Climate and Water
AR5	Fifth Assessment Report of the IPCC
AU	Animal Unit
BI	Burning Index
BUI	Buildup Index
CAB	Congo Air Boundary
CCAM	Conformal-Cubic Atmospheric Model
CDF	Cumulative Distribution Function
CDS	Climate Data Store
CDSR	Canadian Daily Severity Rating
CFFDRS	Canadian Forest Fire Danger Rating System
CFWI	Canadian Fire Weather Index
CMIP5	Phase five of the Coupled Model Intercomparison Project
CO_2	Carbon dioxide
CSIR	Council for Scientific and Industrial Research (South Africa)
CSIRO	Commonwealth Scientific and Industrial Research Organisation (Australia)
C3S	Copernicus Climate Change Service
DAFF	Department of Agriculture, Forestry and Fisheries
DC	Drought Code
DMC	Duff Moisture Code
DSR	Daily Severity Rating
ECHAM	A GCM developed at the Max Planck Institute for Meteorology
ECMWF	European Centre for Medium-Range Weather Forecasts
EM	Ensemble Member
EQMC	Equilibrium Moisture Content
EWS	Early Warning System

FAO	Food and Agriculture Organization of the United Nations
FDI	Fire Danger Index
FDRS	Fire Danger Rating System
FFDI	Forest Fire Danger Index (McArthur)
FFMC	Fine Fuel Moisture Code
FMC	Fuel Moisture Content
FPA	Fire Protection Association
FS	Fire Season
FWI	Fire Weather Index (Canadian)
GCM	Global Climate Model
GFDI	Grassland Fire Danger Index (McArthur)
GFDL	Geophysical Fluid Dynamics Laboratory
GHG	Greenhouse Gas
GMT	Greenwich Mean Time
GrADS	Grid Analysis and Display System
GRIB	GRIdded Information in Binary form
IFSTA	International Fire Service Training Association
IPCC	Intergovernmental Panel on Climate Change
IOH	South Indian Ocean High Pressure Cell
ISI	Initial Spread Index
ITCZ	Inter-Tropical Convergence Zone
KNMI	Koninklijk Nederlands Meteorologisch Instituut
LFDI	Lowveld Fire Danger Index
LST	Local Standard Time
LULC	Land Use Land Cover
MCA	Medieval Climate Anomaly
MIROC	Model for Interdisciplinary Research on Climate
MODIS	Moderate Resolution Imaging Spectroradiometer
MSR	Monthly Severity Rating
NCEP	National Centers for Environmental Prediction
NetCDF	Network Common Data Form
PDF	Probability Density Function
RCF	Rainfall Correction Factor
RCP	Representative Concentration Pathway

RH	Relative Humidity at a height of 2 m
SAWS	South African Weather Service
SOM	Self-Organizing Map
SRES	Special Report on Emission Scenarios
SSR	Seasonal Severity Rating
T	Air temperature at a height of 2 m
UCT-CSAG	University of Cape Town – Climate System Analysis Group
UFS	University of the Free State
UKMO	United Kingdom Met Office
UKZN	University of KwaZulu-Natal
UM	Unified Model
US NFDRS	United States National Fire Danger Rating System
VCAA	Victorian Curriculum and Assessment Authority
WAMIS	Wide Area Monitoring Information System
WF	Wind Factor
WS_{10}	Wind Speed at a height of 10 m
WUI	Wildland-Urban Interface
z_{850}	850 hPa geopotential heights

Fire is a good servant but a bad master

- English proverb –

CHAPTER 1

INTRODUCTION

1.1 BACKGROUND

The presence of an oxygen-rich atmosphere and large continental regions covered in vegetation that is subjected to seasonally dry climates and numerous (natural and anthropogenic) ignition sources, makes for an ineluctably flammable planet. Fire is regarded as a natural environmental factor and has occurred throughout Earth's history. The presence of charcoal in geological records indicates that wildfires commenced soon after the appearance of terrestrial plants about 420 million years ago (Bowman *et al*., 2009). Many aspects of the global environment, including ecosystem distribution, biodiversity, the carbon cycle, atmospheric chemistry and climate are influenced by fire (Bowman *et al*., 2009; Power *et al*., 2010; Aldersley *et al*., 2011). It plays an essential ecological role in plant communities as it is a primary driving force of terrestrial ecosystem dynamics (Weber & Flannigan, 1997; cited by de Groot *et al*., 2013) and can also be used as a management tool in grassland production.

Wildland fires are regarded as "one of the most devastating and terrifying forces of nature" (Bytnerowicz *et al*., 2009). Annually, wildland fires burn an estimated 330 – 608 million hectares of vegetation worldwide (Mouillot & Field, 2005; Giglio *et al*., 2013; Liu *et al*., 2014), while an increase in fire activity has been reported in many regions (de Groot *et al*., 2006; Higuera, 2015). An estimated 86% of global fire occurs in grasslands and savannas (Figure 1.1), mainly in Africa and Australia, but also in South Asia and South America, while approximately 11% occurs in the world's forests (Mouillot & Field, 2005; Global EWS, 2015). Many of these fires had grave negative impacts on human safety, health, regional economies, global climate change, and ecosystems in non-fire-prone biomes (de Groot *et al*., 2006). Wildland fires are thus increasingly coming under the environmental spotlight in a wide range of world ecosystems (Chuvieco, 2003). Fire suppression expenditures have been increasing globally as a result of attempts to limit the impact of wildland fires (de Groot *et al*., 2006).

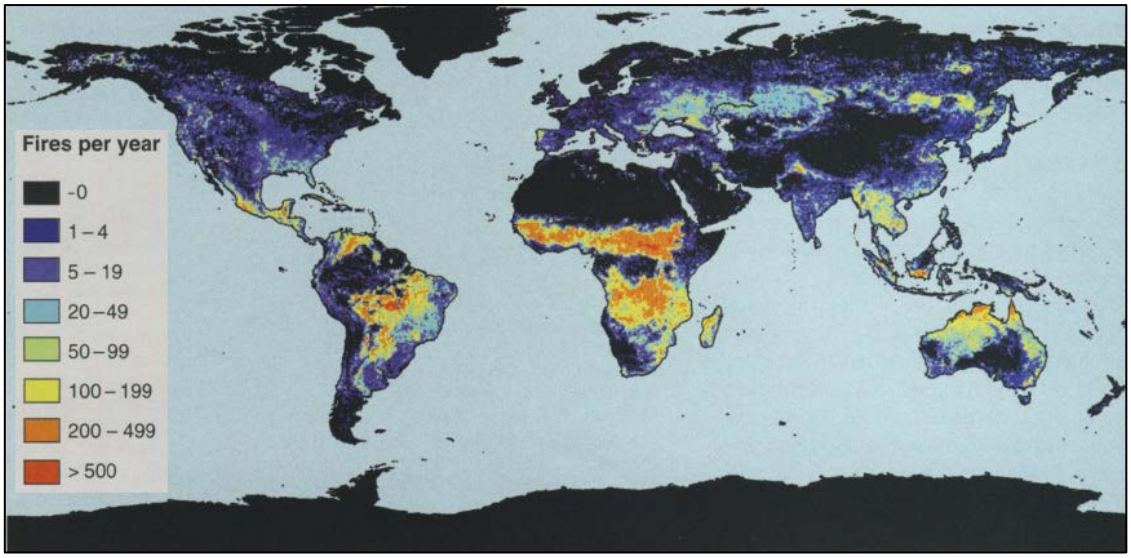

Figure 1.1 **Global fire activity from 2001 to 2006 from MODIS active fire counts (Bowman *et al*., 2009).**

Southern Africa is frequently subjected to wildland fires (Figure 1.2), justifying its earlier designation as "*Terra de Fume*" by Vasco da Gama (Thompson, 1937) who was the first European to sail around the southern tip of Africa in 1497 to discover an ocean route to the East. David Livingstone, in his travels through southern Africa (1849 – 1856), also mentioned the practice of veld burning and even compared the vapour rising from Victoria falls to the smoke rising from a veld fire (Livingstone, 1905).

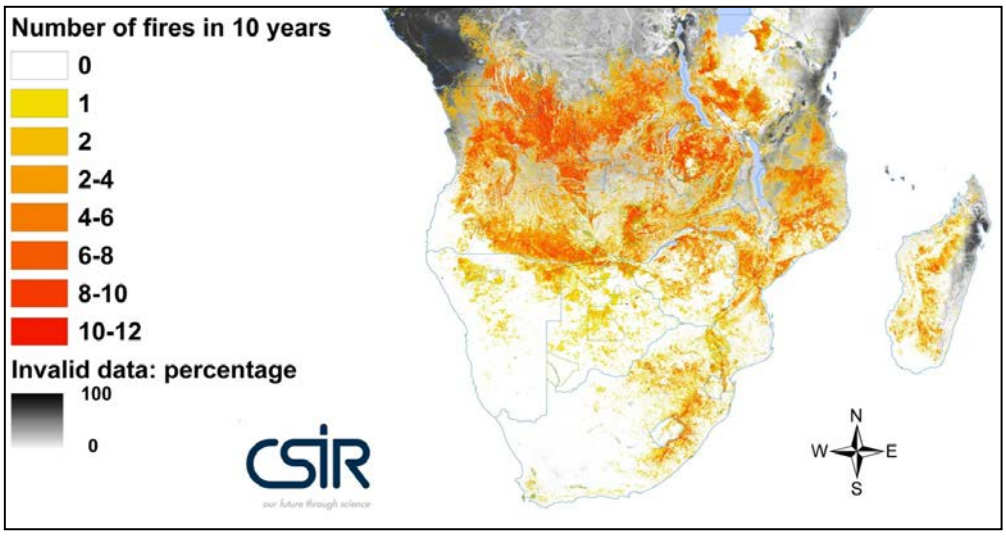

Figure 1.2 **Fire frequency map of southern Africa for the period May 2000 – April 2010 (WAMIS, 2014).**

The primary fuel type in southern Africa is grassland and savannah (de Groot *et al*., 2010). Dead grass and other fine fuels are the first to become flammable in dry

conditions and have the ability to easily sustain high intensity fires under high wind speeds (de Groot *et al*., 2010). The grassland biome is considered to be the most threatened biome in South Africa (Reyers & Tosh, 2003; cited by O'Connor *et al*., 2014), primarily due to urban expansion, mining and agricultural activities.

Weather and climate are the primary factors affecting fire activity (Flannigan *et al*., 2005; Aldersley *et al*.; 2011) and future scenarios of its incidence largely depend on the outcome of climate change (Chuvieco, 2003). Although there will be large spatial and temporal variations in fire activity in response to climate change, a warmer climate in future can potentially lead to more severe fire weather, larger areas burned, more ignitions and a longer fire season (Flannigan *et al*., 2005). Climate change will thus likely result in altered future fire regimes (de Groot *et al*., 2013) as characterised by fire frequency, fire intensity, fire severity (comprising physical and ecological aspects), season of burn, type of fire (crown, surface, ground) and fire size (including shape or pattern) (Weber & Flannigan, 1997 and Gill & Allan, 2008; cited by de Groot *et al*., 2013).

1.2 OBJECTIVES OF THE RESEARCH

PROBLEM STATEMENT

The grasslands of the South African interior plateau are subject to seasonal wildfires that occasionally inflict serious damage to livestock production systems and infrastructure. As indicated in Figure 1.3, observed annual mean surface temperatures over this region exhibited a statistically significant increase of 1.0 – 1.25°C during the period spanning 1901 – 2012 (IPCC, 2013). Multi-model mean projections indicate an annual mean surface temperature increase by the late 21st century for the central interior of South Africa of between 1.0 and 1.5°C under the RCP2.6 scenario, and between 4 and 7°C under the RCP8.5 scenario (Collins *et al*., 2013). This may imply long-term changes in the fire regime, which in turn will impact land cover, thus affecting livestock production, soil erosion, biodiversity and the CO_2 budget. Increased fire weather severity may also pose challenges to fire managers and exceed the current suppression capacity, with a considerable increase in large fires as a result (de Groot *et al*., 2013).

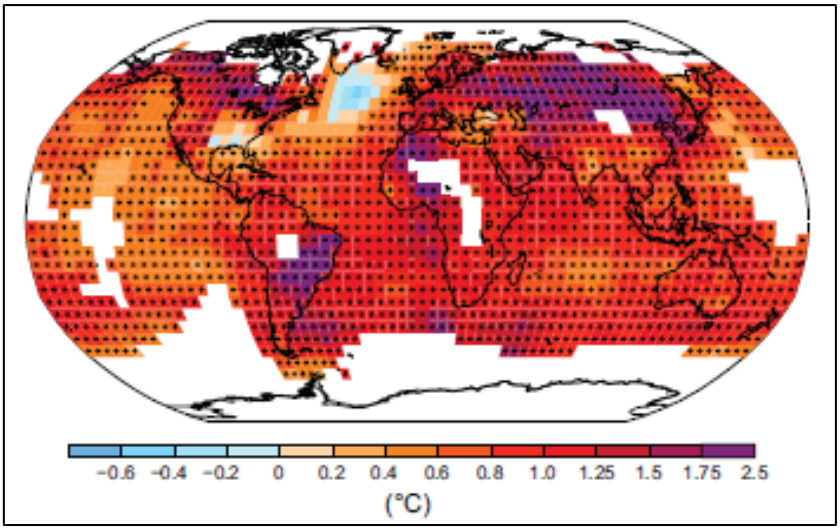

Figure 1.3 **Observed annual mean surface temperature changes from 1901 to 2012. Trends were only calculated for grid boxes with more than 70% complete records and greater than 20% data availability in the first and last 10% of the time period. Grid boxes where the trend is significant at the 10% level are indicated by a + sign (IPCC, 2013).**

RESEARCH QUESTIONS

The following research questions arise with regards to the study area (Section 6.1):

a) Are there noticeable changes in fire regime during the historical observation records? This aspect address spatial changes across the region, as well as the severity of events.
b) What are the specific synoptic weather patterns that result in increased fire danger?
c) Is the fire regime likely to change under future climate scenarios?

OBJECTIVES

The overall objective of this study is to assess historical and future fire danger across the central grassland biome of South Africa. With respect to this study area, the following specific objectives were identified (some definitions of subject specific terms are provided in the glossary at the back of this document):

a) To evaluate the historical fire regime;
b) To identify those synoptic weather patterns that have historically resulted in increased climatological fire danger; and
c) To assess the potential impacts of climate change on climatological fire danger.

CHAPTER 2

FUNDAMENTALS OF WILDLAND FIRE

2.1 PRINCIPLES OF COMBUSTION

The study of fire behaviour necessitates a basic understanding of combustion (Trollope *et al*., 2004). The substances that make up plant biomass (primarily cellulose, hemicellulose and lignin) are quite susceptible to burn (Keane, 2015). In organic fuels flammable gases are generated at around 200°C (The COMET Program, 2010a; Keane, 2015). The combustion of plant material is thus an oxidation process involving a chain reaction during which solar energy originally trapped by photosynthesis is released as heat (Brown & Davis, 1973; cited by Trollope, 1999; Keane, 2015). This is shown in the following general equations:

Photosynthesis:

$$6CO_2 + 5H_2O + \text{solar energy} \rightarrow (C_6H_{10}O_5)n + 6O_2$$

Combustion:

$$(C_6H_{10}O_5)n + 6O_2 + \text{kindling temperature} \rightarrow 6CO_2 + 5H_2O + \text{heat} + \text{secondary compounds}$$

The kindling temperature (also referred to as the ignition temperature) merely plays a catalytic role in initiating and maintaining the combustion process (Trollope, 1999). For wildland fuels the kindling temperature is given as about 315°C by The COMET Program (2009a), 325 – 350°C by Goldammer *et al*. (2009), roughly 300°C by Dupuy and Alexandrian (2010) and 450 – 500°C by Keane (2015).

The principles of fire combustion can be illustrated by means of the fire triangle (Figure 2.1), where each side represents one of the three required components for combustion (Countryman, 1969; cited by Keane, 2015; Goldammer *et al*., 2009; CSIRO, 2013; VCAA, 2016). Ignition of wildland fuels requires a heat source. Natural heat or ignition sources include lightning, volcanic eruptions and sparks from rock falls, while campfires, discarded cigarette buds and welding sparks are examples of anthropogenic sources. Enhanced airflow will increase the intensity of a fire by adding oxygen. Ultimately, some sort of fuel is required for a fire to occur. In wildland fires the fuel is predominantly plant material (e.g. grass, shrubs, trees etc.).

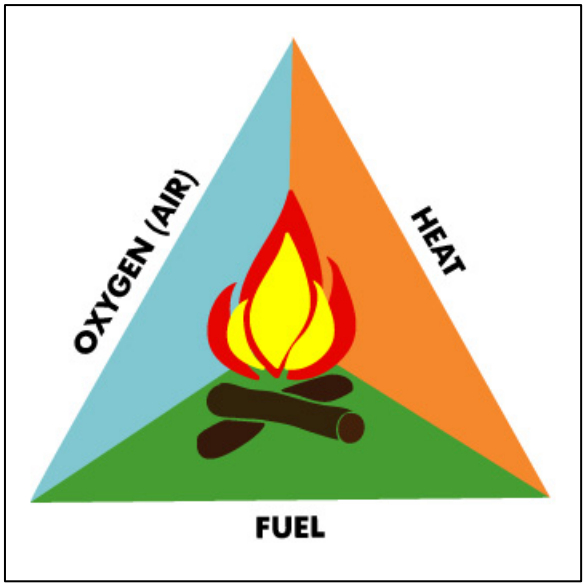

Figure 2.1 The fire triangle (VCAA, 2016).

The fire triangle not only aids in understanding the ignition of a fire, but also hints at possible suppression methods. Removal of any one of the components of the fire triangle will extinguish the fire (IFSTA, 2008; CSIRO, 2013). Fuel can be removed by prescribed burning or clearing a fire line, air (specifically oxygen) can be removed from small fires by covering them with foam or dirt, while heat is usually removed from a fire by applying water (CSIRO, 2013). A recent addition to the fire triangle, referred to as the "fire diamond", aimed to include a fourth component in the form of the chemical chain reaction that sustains the fire and permits it's endurance until at least one of the other components are removed (IFSTA, 2008; Scott *et al*., 2014). Other adaptations attempted to adjust for coarser temporal and spatial scales (Scott *et al*., 2014; Higuera, 2015), impinging on the paradigm of the fire behaviour triangle to be discussed in Chapter 4. In order to address the direct and indirect effects of climate on pyrogeography across a variety of scales, Bradstock (2010) developed a conceptual four-switch model (Figure 2.2). The model shows how four factors (i.e. biomass accumulation, readiness of biomass to burn, capacity for fire to spread and the presence of ignition sources) control fire activity organised on a time axis. The four-switch model is also useful in comprehending how humans can manipulate the limitations imposed by gradients in productivity (Scott *et al*., 2014).

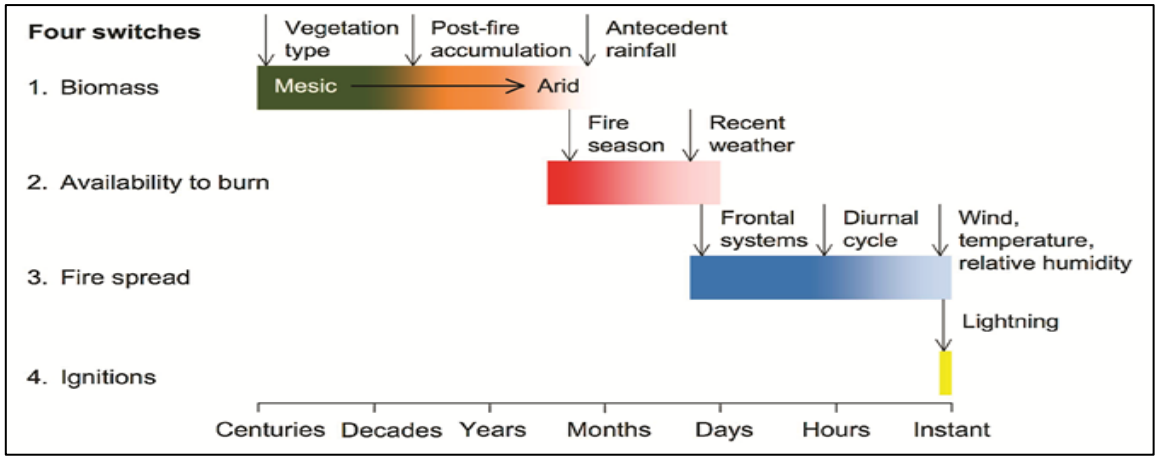

Figure 2.2 **Conceptual model proposed by Bradstock (2010) depicting how four key "switches" control fire activity organised on a time axis (Scott *et al*., 2014).**

When considering the combustion of plant fuels, there are four overlapping phases that occur simultaneously during a fire (Trollope, 1999; Goldammer *et al*., 2009; Scott *et al*., 2014; Keane, 2015):

a) a pre-heating phase (also referred to as the pre-ignition phase) where the temperature of the plant material in front of the blaze is raised by either conduction, convection or radiation to ignition temperature while water and low molecular weight volatiles are evaporated from the fuel;

b) flaming combustion (also referred to as the gaseous phase) where the gasses produced during the pre-heating phase are ignited in the presence of oxygen and biomass is converted into combustible organic vapours, tars, char and ash while giving off energy in the form of heat and light;

c) smouldering combustion takes place after the passage of the active flaming front and involves the surface oxidation of char, while combustible gases are still produced through pyrolysis, but condense to produce a lot of smoke as the temperatures and rate of release are not sufficiently high to support a persistent flame;

d) glowing combustion occurs when most of the volatile gases have been driven off and the residual charcoal is consumed to leave a bit of ash behind.

Smouldering combustion is more likely to occur in fuel types such as rotten logs, duff or organic soils (Sandberg *et al*., 2002) and is less prevalent in fuels with a high surface-to-volume ratio (e.g. grasses, shrubs and twigs). Each stage has a distinct combustion efficiency, thermal energy release and emits a different mixture of

chemical compounds into the atmosphere (Section 2.3) (Sandberg *et al*., 2002; Urbanski *et al*., 2009).

In a wildfire there is a natural progression from one phase to another at a specific point, though they may occur simultaneously and often in close proximity on a landscape (Sandberg *et al*., 2002; Urbanski *et al*., 2009). The maintenance of this chain reaction of combustion involves the transfer of heat, through the processes of radiation, convection and conduction, to the plant material in and ahead of the fire front (Trollope *et al*., 2004; Urbanski *et al*., 2009). This essentially allows a fire to spread, while the rate of spread is governed by the strength of the heat source, the efficiency of the heat transfer processes and the amount of energy required to raise the fuel temperature to the kindling temperature (Dupuy & Alexandrian, 2010). Combustion continues in the wake of the flaming front, with regions of intermittent open flame across the fuel bed (Urbanski *et al*., 2009).

2.2 TYPES OF FIRE

Wildland fires are generally classified into the following three types according to the fuel layer in which they are burning (Trollope, 1999; Keane, 2015):

a) Crown fires that burn in shrub and tree canopies, more or less independently of what is going on at the surface (Figure 2.3a);
b) Surface fires that burn in the surface fuels such as standing grass, litter and small shrubs (Figure 2.3b); and
c) Ground fires that burn in underground layers of organic material (Figure 2.3c).

Surface fires are by far the most common fire type experienced in South Africa, particularly in grassland and savanna areas (Trollope, 1999; Trollope *et al*., 2002). Fires can also be classified according to their spread in relation to the wind direction and their location along the fire perimeter (Trollope *et al*., 2004). As depicted in Figure 2.4, a wildfire spreading from an ignition point will form a roughly elliptical shape, aligned along the direction of the prevailing wind (CSIRO, 2013). The perimeter of the fire can be divided into three main parts (Figure 2.4):

- the head;
- the flank; and
- the back.

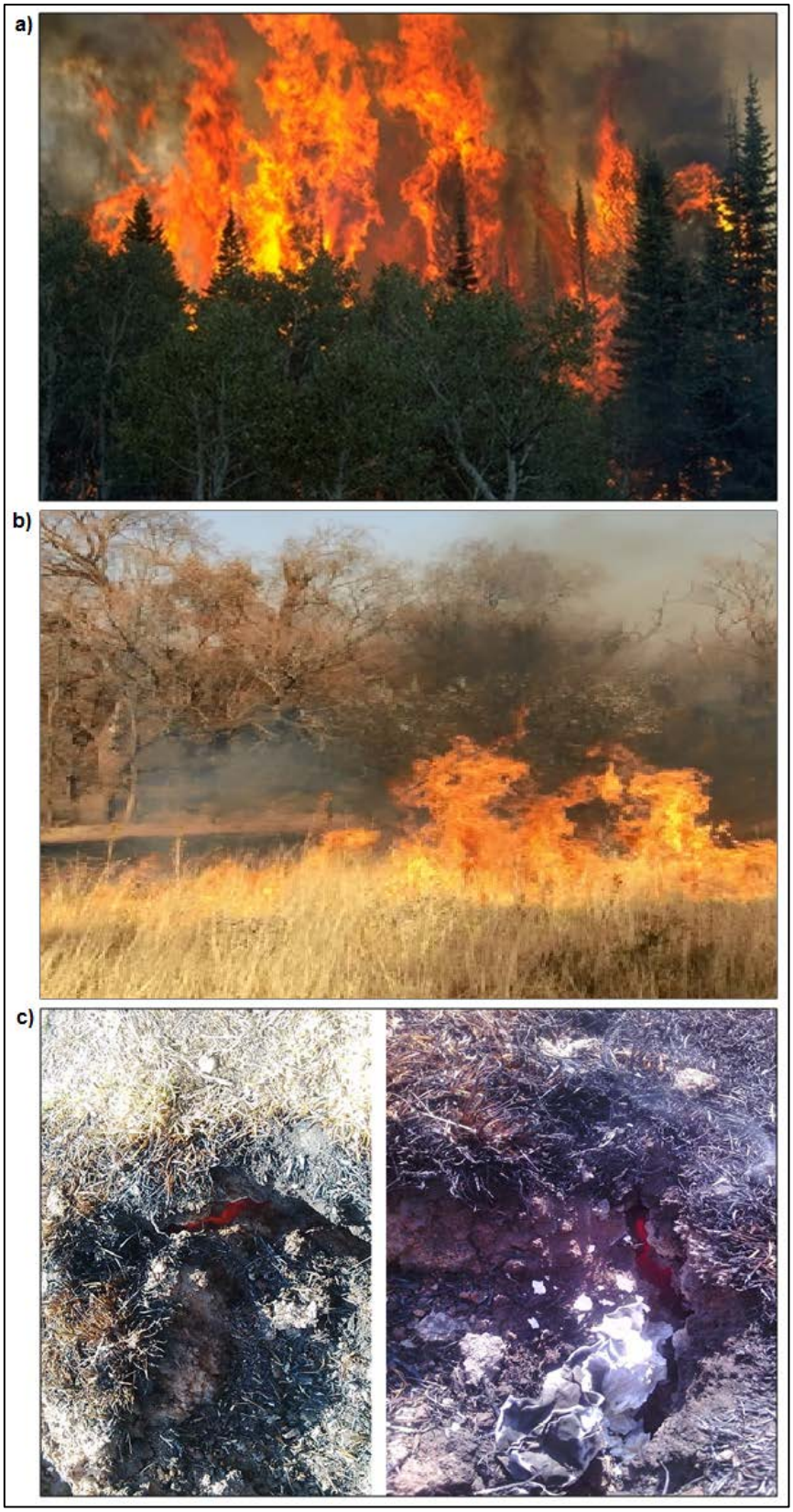

Figure 2.3 **Fire types: (a) crown fire (The COMET Program, 2010b); (b) surface fire near Bloemfontein, South Africa (Author); and (c) ground fire near Groblersdal, South Africa (Ka-Mphezulu, 2016).**

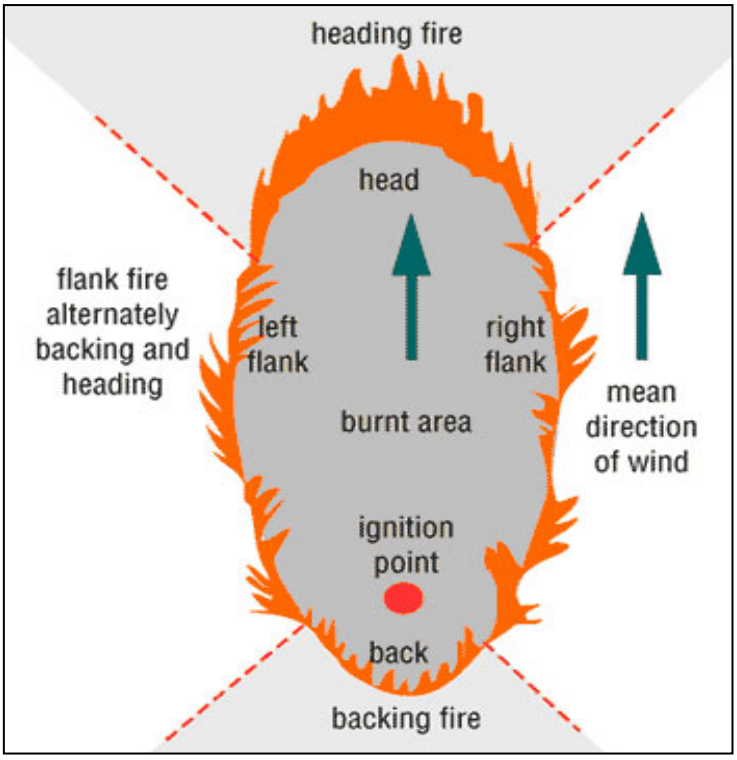

Figure 2.4 The fire perimeter (CSIRO, 2013).

The heading fire (Figure 2.5) is the most rapidly spreading part of the fire perimeter where the flames are driven by wind (or assisted by sloping terrain) towards unburnt fuel (CSIRO, 2013; Trollope *et al*., 2004; The COMET Program, 2009a). Under extreme weather conditions when the fire front advances quite rapidly, combustion can be rather inefficient, resulting in thick black smoke and partially burnt fuel. Often large envelopes of burning gas can be observed as flashes of flame well above the average flame height (CSIRO, 2013).

Figure 2.5 Wind driven flames in a heading fire (The COMET Program, 2009a).

A backing fire (Figure 2.6) propagates against the wind (or down-slope) with the flames leaning over already burnt material (CSIRO, 2013; Trollope *et al*., 2004; The COMET Program, 2009a). Although this part of the fire perimeter burns slowly, combustion is often very efficient and complete, resulting in less smoke than a heading fire (Trollope *et al*., 2004).

Figure 2.6 **Flames spreading against the wind in a backing fire (The COMET Program, 2009a).**

A flank fire is generally aligned parallel to the wind direction with the flames more or less leaning along the flank (CSIRO, 2013). This part of the fire perimeter burns faster and more intense than a back fire, but slower and less intense than a head fire (Trollope *et al*., 2004). Due to changes in wind direction, the flank may turn into a head fire or back fire along any location along the fire perimeter.

In addition to these, spot fires (Figure 2.7) may also occur when burning embers carried by the wind start new fires some distance ahead of the main fire front (Trollope *et al*., 2004; Dupuy & Alexandrian, 2010). This is one of the most treacherous characteristics of large wildfires as fire fighters may become trapped when attempting to attack a head fire from the front. Gustiness can easily trigger spotting by throwing showers of sparks across the fireline (Crosby & Chandler, 2009). Gravity can also be responsible for spotting on steep slopes due to burning or hot material such as pine cones and logs rolling downhill (The COMET Program, 2009a).

Figure 2.7 Spot fires in logging slash (Cathcart, 2006; cited by Cruz & Plucinski, 2007).

The literature also abounds with terms used to describe the rate at which fires spread. Running fires spread rapidly with a well-defined head, while creeping fires burn with a low flame and spread slowly (The COMET Program, 2009a). The rate of spread can be expressed in terms of the forward rate of spread, the increase in the fire perimeter, and the increase in the area of the fire, which is governed by the slope, wind speed and fuel types in the fire environment (The COMET Program, 2009a). Keane (2015) also classified wildland fires according to their effects on vegetation:

- nonlethal surface fires burn in the surface fuel layer with a vegetation mortality of less than 20%;
- lethal surface fires result in a vegetation mortality of at least 20% (the term “stand replacement fire” is also used when most plants and at least 70% of trees are killed); and
- mixed severity fires demonstrate a spatially heterogeneous pattern of both aforementioned types.

2.3 FIRE EMISSIONS

Smoke from the combustion of biomass (Figure 2.8) contains a rich and complex mixture of gases and aerosols that is determined by an array of variables pertaining to fuel characteristics (type, structure, loading, chemistry, moisture content) and burn conditions (smouldering vs. flaming combustion) (Fowler, 2003; Naeher *et al*., 2007;

Urbanski *et al*., 2009). The myriad of emission products include greenhouse gases (water vapour (H_2O), carbon dioxide (CO_2), methane (CH_4), nitrous oxide (N_2O)), photochemically reactive compounds (carbon monoxide (CO), non-methane volatile organic carbon (NMVOC), nitrogen oxides (NO_x)), sulphur dioxide (SO_2), ammonia (NH_3) as well as fine and coarse particulate matter (PM) (Bell & Adams, 2009; Johnston *et al*., 2012). Of these, H_2O and CO_2 are the most prominent products of biomass combustion (Sandberg *et al*., 2002). Table 2.1 lists the most abundant gases (excluding H_2O) emitted by savanna fuels in Africa. A more comprehensive list can be found in Andreae and Merlet (2001) or Urbanski *et al*. (2009) who compiled emission factor data for different generalized vegetation cover types.

Figure 2.8 Smoke rising from a surface fire near Modimolle, South Africa (Author).

As already mentioned, the actual chemical composition and the plume dynamics of smoke are significantly influenced by the phase of combustion (Section 2.1). Volatile organic compounds (VOCs) are evaporated from fuels during the early and later combustion process as lignin and cellulose are decomposed through pyrolysis (Bell & Adams, 2009). Flaming combustion is a highly exothermic process that produces more highly oxidized compounds (e.g. CO_2, NO_x, molecular N_2 and SO_2), aerosols with a substantial but highly variable portion of elemental carbon and subsequent convective

lofting (Bell & Adams, 2009; Urbanski *et al*., 2009). Lower temperatures and higher fuel moisture contents will give rise to smouldering combustion (Bell & Adams, 2009; Scott *et al*., 2014). During smouldering combustion the reduced rate of pyrolysis results in lower heat production and products of char oxidation (e.g. CO, CH_4, NH_3, C2-C3 hydrocarbons, methanol, formic and acetic acids and formaldehyde), while the smoke frequently lingers close to the ground (Urbanski *et al*., 2009). Heading fires (Section 2.2) have also been shown to produce two to three times more emissions than backing fires (Trollope *et al*., 2004; Bell & Adams, 2009). The smoke plume rising from a wildfire most likely contains a mixture of emissions produced by flaming and smouldering combustion due to entrainment.

Table 2.1 The top trace gas emissions (excluding H_2O) in African savanna fuels and their emission ratios relative to CO_2 (Christian *et al*., 2003)

Compound	Emission Ratio (mmol/mol CO_2)	Emission Factor (g kg^{-1})
Carbon dioxide (CO_2)	1000	1689
Carbon monoxide (CO)	66.4	71.4
Hydrogen (H_2)	12.6	0.97
Methane (CH_4)	3.53	2.17
Nitrogen oxides (NO_x and NO)	3.04	3.50
Nitrogen (N_2)	2.87	3.08
Ethylene (C_2H_4)	1.14	1.23
Acetic acid (CH_3COOH)	1.06	2.44
Formaldehyde (HCHO)	0.97	1.12
Methanol (CH_3OH)	0.96	1.18
Sulphur dioxide (SO_2)	0.85	2.09
Hydrogen cyanide (HCN)	0.57	0.59
Ammonia (NH_3)	0.46	0.30
Acetaldehyde (CH_3CHO)	0.45	0.76
Formic acid (HCOOH)	0.39	0.69
Acetylene (C_2H_2)	0.29	0.29
Phenol (C_6H_5OH)	0.23	0.83
Acetol (C_3H_6O2)	0.22	0.62
Glycolaldehyde ($C_2H_4O_2$)	0.21	0.48
Propylene (C_3H_6)	0.20	0.32
Ethane (C_2H_6)	0.19	0.22
Methylvinylether (C_3H_6O)	0.11	0.24
Furan (C_4H_4O)	0.085	0.21
Acetone (C_3H_6O)	0.085	0.19
Acetonitrile (CH_3CN)	0.082	0.13
Benzene (C_6H_6)	0.069	0.21
Toluene ($C_6H_5CH_3$)	0.052	0.18
Chloromethane (CH_3Cl)	0.037	0.072
Propane (C_3H_8)	0.035	0.059
1, 3 Butadiene (C_4H_6)	0.035	0.073
1-butene (C_4H_8)	0.03	0.064
Propenenitrile (C_3H_3N)	0.03	0.061
Propanenitrile (C_3H_5N)	0.02	0.042

In addition to the aforementioned primary pollutants emitted by wildfires, secondary pollutants (e.g. ozone (O_3), secondary organic aerosols (SOA) and peroxyacetyl nitrate (PAN)) are also formed when gaseous precursors such as NMVOC and NO_x undergo photochemical processing (Urbanski *et al*., 2009; Ward *et al*., 2012; Wigder

et al., 2013). Photochemical production within smoke plumes can carry on for days and increase O_3 concentrations in locations distant to a fire (Ward *et al*., 2012). A study by Kang *et al*. (2014) revealed an increased O_3 concentration of over 10 ppbv in both urban and rural areas that fell within smoke plumes some 600 km downwind from large wildfires in Canada. These peaks coincided with that of CO, NO_x and PM2.5, while the latter also managed to affect indoor air quality (Kang *et al*., 2014). PM, consisting mostly of organic material from the incomplete combustion, distillation and recondensation of tarry substances, is both a primary and secondary pollutant (Andreae, 1997; Wigder *et al*., 2013).

2.4 FACTORS PERTINENT TO FIRE EFFECTS

The impact that a fire will have on the natural environment is primarily determined by the amount, rate and the vertical level at which the heat energy is released during biomass combustion (Trollope *et al*., 2002). The spatial extent and timing of the impact may further compound the overall influence of a fire, albeit on biotic components (e.g. plants, animals etc.) or abiotic ones (e.g. soil, air quality etc.). While this section briefly focuses on some of the factors pertinent to fire effects (mainly on vegetation), a more elaborate discussion of the imposed impacts on flora, fauna, soil, air quality and health, climate and the economy is provided in Chapter 3. How the heat is released and the factors influencing it involve the study of fire behaviour, which will be considered in Chapter 4.

2.4.1 Available Heat Energy

During a fire, the fuel load largely determines the variation of the total amount of heat energy released (Luke & McArthur, 1978; cited by Trollope, 1999). Trollope (1999) showed there is little difference between the combustion heat of different surface fuel types. The combustion heat is defined as the "total amount of heat energy contained per unit mass of fuel" (Trollope *et al*., 2002). In the U.S.A. and Australia average combustion heat values are estimated at around 20 000 kJ kg^{-1}, which doesn't differ much from the measured 18 000 ± 150 kJ kg^{-1} for grass fuels in the savanna areas of the Eastern Cape (Table 2.2). Surface fuels in the form of grass constitute the bulk of the fuel load in African savannas and grasslands (Trollope *et al*., 2002).

Table 2.2 Combustion heat of different grass species commonly burnt in surface fires in the thornveld areas of the Eastern Cape (after Trollope, 1999)

Grass species	Type of material	Combustion heat of dry material (kJ kg^{-1})
Cymbopogon plurinodis	Vegetative leafy	17 650 ± 50
	Mature leaf/culm	18 150 ± 50
Digitaria eriantha	Vegetative leafy	16 700 ± 150
	Mature leaf/culm	17 550 ± 100
Panicum maximum	Vegetative leafy	17 950 ± 150
	Mature leaf/culm	17 700 ± 50
Sporobolus fimbriatus	Vegetative leafy	17 550 ± 150
	Mature leaf/culm	17 200 ± 50
Themeda triandra	Vegetative leafy	17 150 ± 50
	Mature leaf/culm	17 750 ± 50
All species	**Composite grass sample**	**18 000 ± 150**

Some of the energy contained in a fuel is used to evaporate moisture, while another portion remains in partially combusted material (Trollope, 1999; Trollope *et al*., 2002), implying that not all the energy contained in a fuel is released. The actual amount of heat released during a fire is referred to as the heat yield and is closely related to the fuel's moisture content (FMC) (Trollope, 1999). The amount of heat released is the product of the fuel load (kg m^{-2}) and the heat yield of the fuel (kJ kg^{-1}) and is expressed in kJ m^{-2}. According to Baker (1983; cited by Ubysz & Valette, 2010) the heat yield of grass and forest fuels increases with the richness of the tissues in lignin (25 600 kJ kg^{-1}) and decreases with cellulose content (18 600 to 23 200 kJ kg^{-1}). Furthermore, Trollope (1999) found that more heat was released from backing fires than from heading fires (Table 2.3). The South African values quoted in Table 2.3 correspond well with the average heat yield for Australian (16 000 kJ kg^{-1}), US (18 640 kJ kg^{-1}) and European (18 500 kJ kg^{-1}) grass and forest fuels (Luke & McArthur, 1978; cited by Trollope, 1999; Ubysz & Valette, 2010). The fire intensity and the resultant maximum temperature are strongly influenced by the fuel load (Tunstal *et al*., 1976; cited by Trollope, 1999).

Table 2.3 Heat yield of fully cured, dormant winter grass fuels in the thornveld areas of the Eastern Cape (after Trollope, 1999)

Type of fire	Heat yield (kJ kg^{-1})	Fuel moisture (%)
Heading fire	16 890	32
Backing fire	17 780	36

2.4.2 Rate of Heat Energy Release

The amount of heat energy released per unit time per unit length of the fire front is defined as the fire intensity and can be calculated using the following fire intensity index (Byram, 1959; cited by Trollope, 1999; Trollope *et al*., 2002):

$$I = Hwr$$

where: I = fire intensity (kJ s^{-1} m^{-1})

H = heat yield (kJ kg^{-1})

w = mass of available fuel (kg m^{-2})

r = rate of spread of fire front (m s^{-1})

Fire intensity can vary greatly within the confines of a single burn, depending among others on fuel properties (Section 4.1), weather conditions (Section 4.2), topography (Section 4.3), and characteristics of any previous disturbances (Flannigan *et al*., 2000). When fully cured the grasslands of southern Africa are notorious for the fast rate at which the fire front spreads. However, these grassland fires exhibited somewhat lower fire intensities than forest fires where the forest floor was littered by leaves or needles (Trollope *et al*., 2004). Trollope *et al*. (2002) developed the following multiple regression fire intensity model based on 200 surface heading fires in grassland and savanna areas of South Africa:

$$I = 2729 + 0.8684x_1 - 530x_2^{0.5} - 0.907x_3^2 - 596x_4^{-1}$$

where: x_1 = fuel load (kg ha^{-1})

x_2 = fuel moisture (%)

x_3 = relative humidity (%)

x_4 = wind speed (m s^{-1})

The locally developed fire intensity prediction equation yielded a coefficient of determination (R^2) of 0.56 against independent data and mean fire intensities of about 2 560 kJ s^{-1} m^{-1} (ranging from 136 to 12 912 kJ s^{-1} m^{-1}) (Trollope *et al*., 2002). Backing fires were found to be less variable than heading fires in terms of fire intensity, while the latter were roughly seven times more intense. Field observations also indicated a strong relationship between fire intensity and the height of lethal scorching (topkill) of trees and shrubs (Trollope *et al*., 2002).

Flame length (not necessarily the same as the vertical flame height) is sometimes used as a proxy for fireline intensity (The COMET Program, 2009a). The vertical development of a fire and its associated smoke column is determined by the fire intensity (The COMET Program, 2009a). Low intensity fires have a limited influence on the immediate environment as they are characterised by weak indrafts and poorly developed smoke or convective columns over the fire. In contrast, high intensity fires have the ability to significantly modify the immediate environment as they possess much stronger indrafts which aid well-developed smoke or convective columns to build to tremendous altitudes (The COMET Program, 2009a). Such fires are often marked by torching, fire whirls and well-developed smoke plumes (Section 4.4).

2.4.3 Vertical Distribution of Heat Energy

During burning trials conducted by Trollope *et al*. (2002), temperatures were measured at three heights (i.e. at ground level, at grass canopy level and 1 m above the grass canopy) during heading and backing fires in South Africa and Kenya. Although the maximum temperatures of both heading and backing fires were observed to be higher at canopy level than at ground level, noteworthy differences regarding the vertical temperature profile were revealed between these two types. Most significantly, the majority of heading fires were comparatively hotter above the canopy of the grass sward, while back fires were generally hotter at ground level (Trollope *et al*., 2002).

The perpendicular flame height is thought to be a reliable indicator of the vertical distribution of heat energy released during a fire and should correlate well with temperatures recorded at different heights above the ground (Trollope, 1999; Trollope *et al*., 2002). Flame height has been shown to influence the topkill of stems and branches on trees, with taller flames being able to introduce lethal scorching at higher levels (Section 3.1).

CHAPTER 3

IMPACTS OF WILDLAND FIRE

Fires are global occurrences that interact with the biosphere, atmosphere and cryosphere to influence land and ice surface energy budgets, biogeochemical and hydrological cycles and subsequently the climate (Ward *et al*., 2012). The effects of fire may vary across a range of temporal and spatial scales (Binkley *et al*., 1993; Ward *et al*., 2012). Wildland fires have both immediate and long-term impacts on social and ecological systems (Higuera, 2015), while such effects can be spatially heterogeneous due to the variability of the various factors that influence fire behaviour (Morgan *et al*., 2014). A complex web of fire effects thus arises as local topography, microclimate and ambient weather conditions, fuel characteristics and previous disturbance histories interact (Morgan *et al*., 2014). Frequent, low-intensity fires have considerably different impacts than occasional, high-intensity fires (Hantson *et al*., 2014). Fires that burn for days on end exhibit variation in severity due to variations in fuel load, weather conditions and local topography. Large fires tend to shape homogeneous landscapes, whereas spatial patchiness may result in a mixture of ecosystems with divergent compositions and structures (Binkley *et al*., 1993; Bowman *et al*., 2009). It is important to consider both the detrimental and beneficial effects of fire in order to develop a more comprehensive view of its role in nature and society and to better inform fire management policies and practices.

3.1 FIRE EFFECTS ON FLORA

Fire impacts plants principally through the destruction or heat damage to regenerative tissue such as the vascular cambium and buds, post-fire necrosis of phloem and reduced hydraulic conductivity of xylem in the stem (Michaletz *et al*., 2012; Scott *et al*., 2014). The location of the buds (i.e. above-, at or below-ground) is particularly important in a plant's ability to survive a fire, while the type of fire determines the vertical distribution of heat release (Section 2.4.3). Trees and shrubs have bud tissues above-ground (phanerophytes), while grasses' growth points are more protected at ground level (hemicryptophytes) (Scott *et al*., 2014).

Since heading fires release the bulk of their heat above-ground, away from the growing points of grasses, trees and shrubs sustain more damage from such fires due to crown scorch and cambium injury (Figure 3.1) whereas grasses can recover faster (Trollope *et al*., 2002; Scott *et al*., 2014). Slower moving surface backing fires, on the other hand, tend to have the opposite effect as they result in more heat being released at ground level (Section 2.4.3) where a critical threshold temperature of 95°C is maintained several seconds longer (Trollope *et al*., 2002; Trollope, 2007). Backing fires causes more damage to shoot apices of grasses, thus impeding their regrowth (Trollope, 2007). Figure 3.1 shows that in savanna and woodlands, trees become less susceptible to fire damage as they grow taller (particularly when heights surpass 2 m).

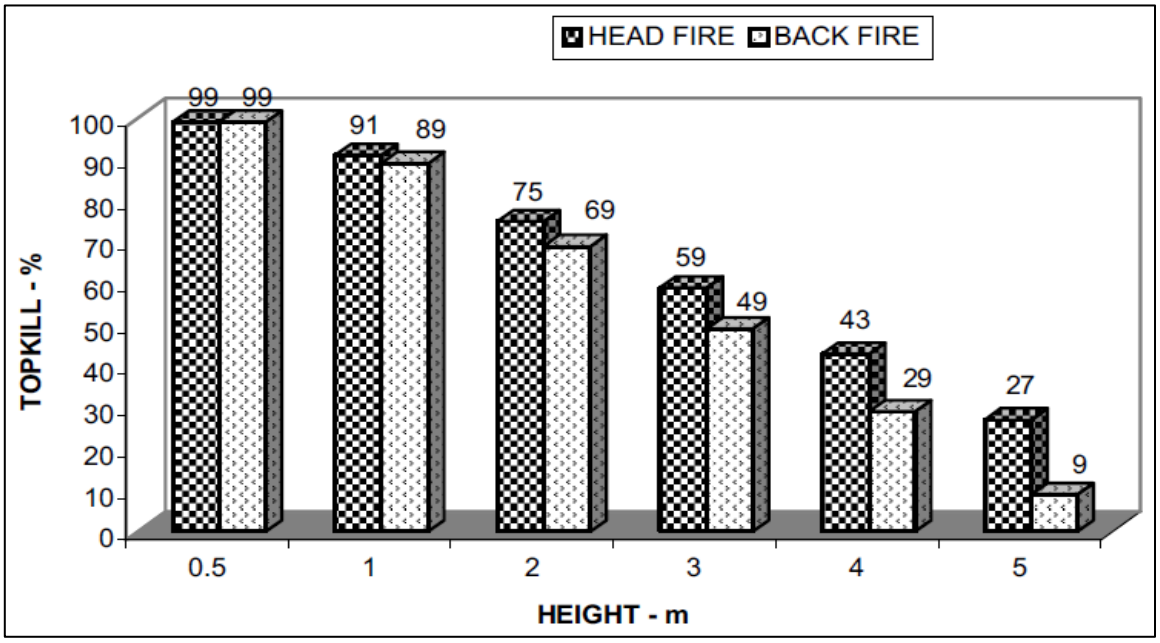

Figure 3.1 **Portion of topkill under trees and shrubs of all species attributed to heading and backing fires within the Lewa Wildlife Conservancy and Hopcraft Ranch, Kenya (Trollope *et al*., 2002).**

Hydraulic failure is even more fatal than heat damage to cambial tissue (Michaletz *et al*., 2012; Scott *et al*., 2014). Heating of sap within the stem causes surface tension in the xylem conduits to become too low, resulting in water column breakage (cavitation) and the formation of gas bubbles (embolisms) (Borghetti *et al*., 1993). Heating also causes thermal softening and deformation of the xylem conduit walls at temperatures above about 60°C (Figure 3.2) (Michaletz *et al*., 2012). This leads to the disruption of water supply to above-ground parts and to the dispersal of photosynthates (Michaletz *et al*., 2012; Scott *et al*., 2014). The ensuing post-fire canopy die-off is similar to severe

drought and acts much faster in killing a tree than cambium injury (ring-barking). Studies suggest that it is fire damage to the stem rather than to the canopy crown (topkill) that kills trees (Balfour & Midgley, 2006; Lawes *et al*., 2011; Michaletz *et al*., 2012). This view is supported by Joubert *et al*. (2012) who concluded that the survival rate of saplings and mature shrubs in arid savanna fires were positively correlated to stem diameter. Bark thickness, which generally increases with stem diameter, is also a key component determining tree mortality due to fire in boreal forest (de Groot *et al*., 2003; Shuman *et al*., 2017).

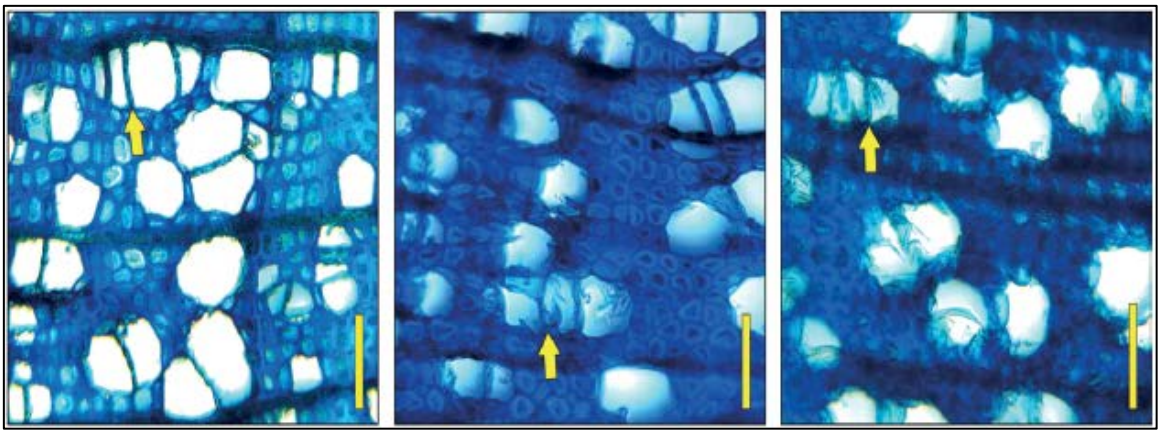

Figure 3.2 **Magnified cross-sections of xylem conduit structure in *Populus balsamifera* branches, with arrows drawing attention to typically observed features, in control (left), 65°C treatment (centre) and 95°C treatment (right). Cross-sections are oriented with the cambium to the left and the mature xylem to the right. The photographs are merely comparisons between similar geometries from different branches and not before-and-after photos of the same branch. Scale bars = 50 µm (Michaletz *et al*., 2012).**

Fire has several direct and indirect impacts on vegetation patterns within a web of ecological interactions (Scott *et al*., 2014). Natural fires function as an extrinsic disturbance factor in the environment that can interrupt or change plant community development, regenerate growth and help determine community structure and composition, and maintains biological and biogeochemical processes (Goldammer & Crutzen, 1993). By burning established plants, space is created for new seedlings under conditions generally characterised by more light, higher temperatures, higher water availability and higher nutrient levels (Bond & van Wilgen, 1996). Fire is therefore an essential element in the vegetation dynamics of some biomes, shaping the landscape mosaic (Geldenhuys, 1994; Flannigan *et al*., 2000; de Groot *et al*., 2003; Curt *et al*., 2011; Schaffhauser *et al*., 2011; Wood *et al*., 2011; Murphy & Bowman, 2012; Curt *et al*., 2013; Scheiter & Savadogo, 2014; Shuman *et al*., 2017).

Scott *et al*. (2014) argues that fire has caused a decoupling of climatic and vegetation patterns. This can be motivated by observations of closed-canopy forests transitioning to savanna within a short distance in the same ecotope (Murphy & Bowman, 2012), or by the notion that savannas would not exist in a world without fire (addressed later in this section), while grasslands would be confined to very specific climatic or edaphic environments. Closed-cover forests can be viewed as "pyrophobic" on account of them shading out grass fuels and having a cooler and moister microclimate with reduced wind speeds, while more open, lower biomass savannas are "pyrophilic" as frequent burning favours the growth of light-demanding grasses that increase fire risk (Trollope *et al*., 2002; Murphy & Bowman, 2012; Scott *et al*., 2014). Forest trees are also generally more susceptible to whole-tree mortality and topkill than savanna trees (Hoffmann *et al*., 2009; Murphy & Bowman, 2012; Scott *et al*., 2014). Fire and vegetation are thus involved in positive feedback loops (Figure 3.3) that provide stabilizing effects on vegetation patterns. Such stabilizing effects can, however, be overruled by changes in fire regime which constitute key factors when considering the impact of fire on vegetation patterns (Figure 3.4). Under such circumstances the relative importance of bottom-up (resource-dependent) controls are outweighed by top-down (disturbance-dependent) controls (Murphy & Bowman, 2012).

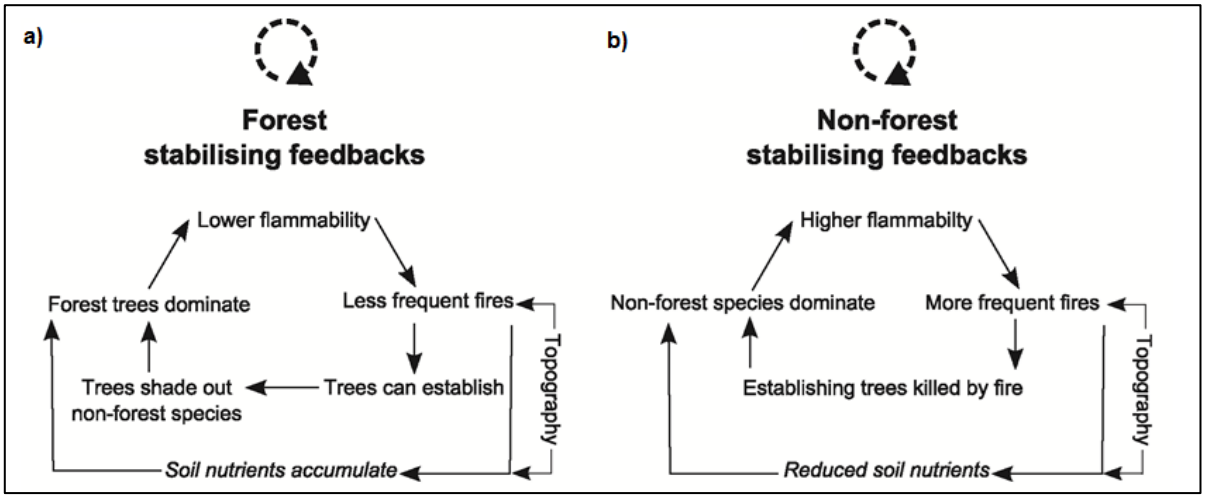

Figure 3.3 **Stabilising feedback loops for the maintenance of (a) forest; and (b) non-forest communities (Scott *et al*., 2014).**

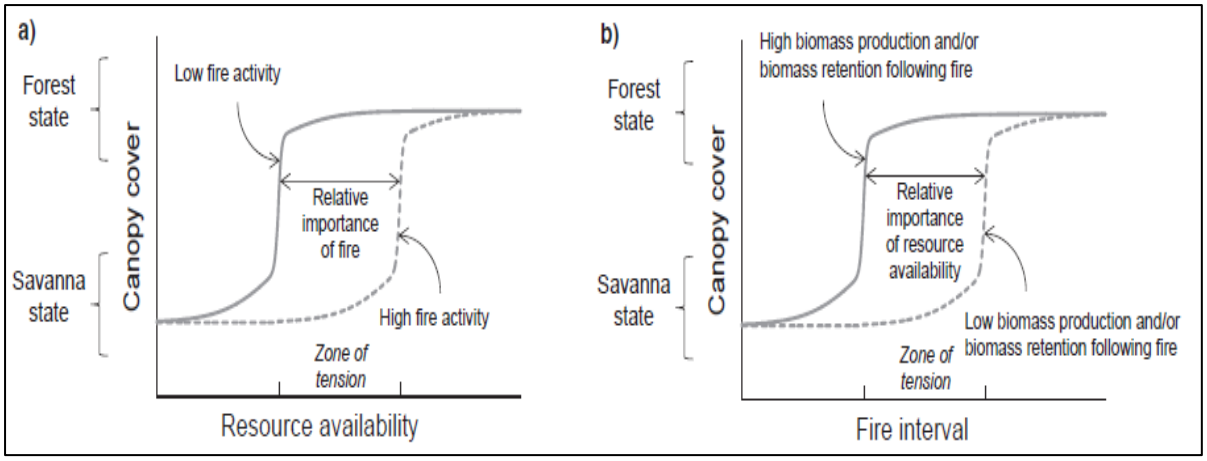

Figure 3.4 **Conceptual model depicting how forest and savanna can switch in response to (a) resource availability; and (b) fire interval. Relatively low fire activity can maintain savannas in low productive environments, while considerably higher fire activity is required in productive environments (Murphy & Bowman, 2012).**

Relatively cool fires (< 600°C) that move rapidly through vegetation tend to leave the plant roots and seed in the soil bank intact (Scott *et al*., 2014). The intensity of the fires (Section 2.4.2) are also important as high intensity fires affect a larger topkill among trees and shrubs, whilst having little bearing on the regrowth of grasses (Trollope *et al*., 2002). The intensity of the fire may also be influenced by time of burn due to seasonal changes in fuel load and moisture content. The timing of the fire also determines the affected plants' seasonal phenological state, their reproductive response and hence the post-fire community structure and composition (Flannigan *et al*., 2000). The size of the burnt area determines landscape patchiness and the distance seed will have to travel for regeneration (Flannigan *et al*., 2000).

The fire return interval (FRI) is of critical importance in stabilizing boundaries between pyrophobic and pyrophilic vegetation types. Rowe (1983; cited by de Groot *et al*., 2003) classified north American boreal plants into different plant functional types by relative FRI, with each group having unique fire survival and post-fire regeneration adaptations. These groups comprised of invaders (e.g. shade-intolerant pioneers with short-lived, wind-disseminated seeds), endurers (e.g. resprouting), evaders (e.g. storing seed in the canopy), resisters (e.g. thick barked) and avoiders (e.g. owing no direct fire survival traits). Longer FRIs generally favour the pyrophobic avoiders, while the more pyrophilic vegetation types (e.g. endurers and evaders) tend to proliferate under shorter FRIs (de Groot *et al*., 2003).

In grasslands a FRI of less than 10 years would kill off any potential tree saplings, while the proportion of woody species (i.e. shrubs and trees) would increase if the FRI is longer (Bond *et al*., 2005; Murphy & Bowman, 2012). In a similar fashion closed-canopy forests could be invaded by more pyrogenic shrubs and grasses under a short FRI as frequent fires defoliate and eventually kill trees (Geldenhuys, 1994; Murphy & Bowman, 2012; Scott *et al*., 2014). Simulations using biophysical models (Bond *et al*., 2003; Bond *et al*., 2005; Scheiter & Savadogo, 2014) seem to confirm field observations (Thompson, 1937; Louppe *et al*., 1995; Bond & van Wilgen, 1996; Bond *et al*., 2003), suggesting that by excluding fire altogether forested areas would increase significantly in size in the savanna and grasslands biomes (Figure 3.5). Observations made by O'Connor *et al*. (2014) in southern Africa suggest that the rate at which woody species increase under fire exclusion is positively correlated to the mean annual rainfall.

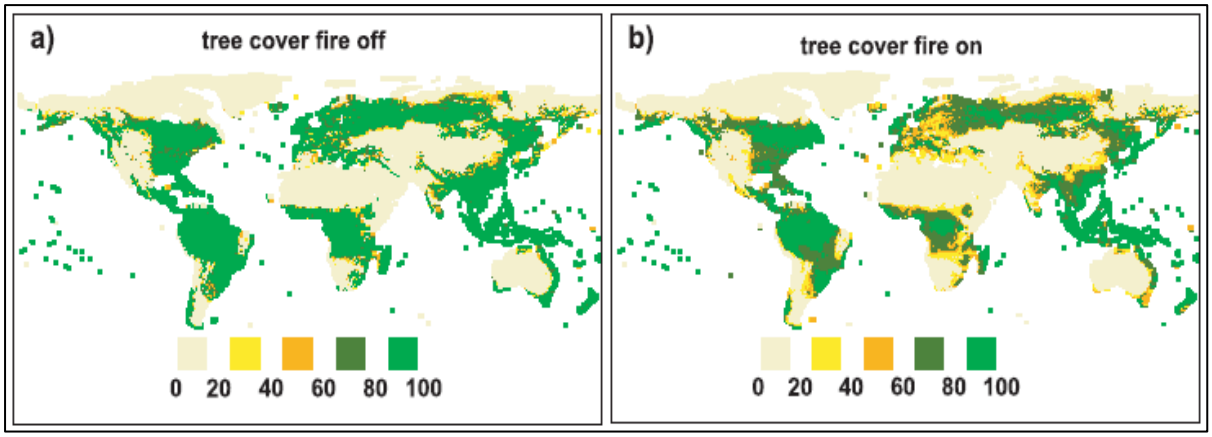

Figure 3.5 **Simulated median tree cover (%) for the 20th century (a) without fire; and (b) with fire. In terms of observed cover 5 – 10% corresponds to scattered trees, 10 – 40% to more closed forms of savanna and other types of woodland, and 40 – 100% to closed forests with no grass understorey (Bond *et al*., 2005).**

The mere observation of distinct survival and reproductive strategies in certain plant species supports the view of fire as a potent biological filter that influences biomass production, vegetation distribution and hence also the risk of fire (Bowman *et al*., 2009). Numerous authors have reported on a variety of fire survival traits at different plant growth stages (e.g. Lotan, 1976; Christensen, 1993; Dixon *et al*., 1995; Bond & van Wilgen, 1996; Gignoux *et al*., 1997; Goubitz *et al*., 2002; Balfour & Midgley, 2006; Choczynska & Johnson, 2009; Moola & Vasseur, 2009; Lamont & Downes, 2011;

Lawes *et al*., 2011; Maurin *et al*., 2014; Scott *et al*., 2014; Causley *et al*., 2016 and Shuman *et al*., 2017).

Fire-stimulated flowering (e.g. *Cyrtanthus purpurea* and *Disa atrorubens*) optimises the fitness benefits of sexual reproduction in an optimal post-fire environment without sacrificing vegetative growth (Christensen, 1993; Bond *et al*., 2004; Lamont & Downes, 2011). Fire-stimulated seed release also aims at exploiting post-fire conditions (Bond & van Wilgen, 1996; Causley *et al*., 2016). Pyriscence occurs as some plants produce serotinous cones or fruit that dehisce in response to heat from a fire (e.g. *Banksia*, *Phaenocoma prolifera*, *Pinus contorta*, *Pinus halepensis* and *Proteaceae*). Some of these cones have a resinous bond that only breaks when exposed to high temperatures, with the ability to store seed for several years until disturbed by wildfire (Lotan, 1976; Bond & van Wilgen, 1996; Goubitz *et al*., 2002; Causley *et al*., 2016). A number of seeds require heat shock (e.g*. Anacardiaceae, Aspalathus*, *Leucospermum* and *Phylica*) or exposure to smoke (e.g. *Actinostrobus acuminatus*, *Emmenanthe pendulifera* and *Themeda triandra*), or a combination of both, in order to germinate (Dixon *et al*., 1995; Goubitz *et al*., 2002; Bond *et al*., 2004; Lamont & Downes, 2011).

Grasses in particular survive fire by continuing leaf growth from intercalary meristems and from new tillers emerging from protected buds in the basal tuft (Choczynska & Johnson, 2009; Scott *et al*., 2014). Other plants have the ability to re-sprout from lignotubers (e.g. *Arctostaphylos*) or by clonal expansion from subterranean rhizomes or roots (e.g. *Andropogon gerardii*, *Gaultheria procumbens*, *Symphoricarpos orbiculatus* and *Vaccinium parvifolium*) (Moola & Vasseur, 2009; Lamont & Downes, 2011; Scott *et al*., 2014). Savanna trees tend to have thicker bark (e.g. *Acacia karroo*, *Buchanania obovate* and *Crossopteryx febrifuga*) that acts as an insulating layer that protects living tissue in the cambium and reduces heat transfer to the stem, as well as the ability to re-sprout from root stocks or stems, making them more tolerant to frequent fires (Gignoux *et al*., 1997; Balfour & Midgley, 2006; Scott *et al*., 2014). Certain trees have epicormic buds embedded in the bark and wood (e.g. *Eucalyptus spp*. and *Pseudotsuga macrocarpa*), allowing them to re-sprout even after the bark was destroyed (Lawes *et al*., 2011; Murphy & Bowman, 2012). A few species that grow too slowly to escape the fire trap (i.e. not tall and thick enough) have developed

extensive underground storage organs and short-lived aerial shoots (e.g. geoxyles such as *Lannea edulis* and *Ziziphus zeyheriana*) (Maurin *et al*., 2014).

Some of these adaptations (e.g. re-sprouting ability) may also enhance a plant's ability to survive frost damage, wind damage or herbivory. These adaptations do enhance species' fitness allowing them to rapidly recover after wildfire occurrences and to release seeds into an optimal post-fire habitat. It can thus be argued that fire and life have shaped each other through "evolutionary adjustment".

3.2 FIRE EFFECTS ON FAUNA

Fire can injure or kill wildlife, domestic animals and people through heat exposure, asphyxiation and inhalation of noxious compounds in smoke (Engstrom, 2010). Survival of animals from these direct effects of fire depends on their location relative to each other (i.e. animal vs. flame), the animals' mobility, as well as the duration of exposure (Engstrom, 2010; Scott *et al*., 2014). Most animals can only tolerate temperatures of up to about 50°C (Schmidt-Nielson, 1997). At higher temperatures cell membrane structures degrade, proteins undergo denaturation, enzyme production falls below the rate at which they unfold, interdependent metabolic reactions are affected and oxygen supply becomes inadequate (Schmidt-Nielson, 1997). The majority of large mammals killed in wildfires, however, succumb to smoke inhalation (Scott *et al*., 2014). Although these effects can be immediate (i.e. pulsed disturbance), impacts on injured individuals such as shortened lifespan or impaired fitness, or on population dynamics of entire species, may only be revealed over a period spanning years to decades following a fire event (i.e. pressed disturbance) (Gresswell, 1999; Engstrom, 2010).

Mortality due to wildfires is generally low because most animals will try to flee or avoid the heat and smoke (de Ronde *et al*., 2004b; Engstrom, 2010). However, flightless arthropods, invertebrates or reptiles undergoing ecdysis, terrestrial vertebrates with poor climbing abilities and low mobility, young animals and camped-in domestic animals are at higher risk (Barlow & Peres, 2004; Engstrom, 2010; Scott *et al*., 2014). A variety of means exist whereby less mobile organisms can avoid fire. These include burrowing or retreating into underground shelters, taking refuge under large rocks or logs, climbing trees or moving into fire resistant sites (e.g. onto bare ground or into

water streams) (de Ronde *et al*., 2004b; Engstrom, 2010). Animals that survived a fire can remain within the burned matrix or emigrate into nearby unburned areas, if available (Barlow & Peres, 2004). Remaining individuals may face increased predation, reduced shelter and severe food shortages. Migrants are typically subjected to density-dependent enhanced competition for food, mates or other resources through territorial aggression from related species and could also be disadvantaged by their poor familiarity with the new area (Barlow & Peres, 2004).

Generally, the indirect impacts on animal populations via the post-fire environment are greater than the direct effects of fire (Scott *et al*., 2014). Lasting negative population responses to fire are believed to be more common in remnant species that occur in small isolated fragments of the landscape (Gresswell, 1999; Engstrom, 2010). Fire can transform habitats within mere minutes, while the extent of alteration to animal habitats is generally proportional to the post-fire changes in vegetation structure (Scott *et al*., 2014). Such changes are typically most dramatic with stand-replacing crown fires in closed-canopy forests (Figure 3.6), while open systems such as savannas and grasslands exhibit small compositional shifts and faster recovery rates (Scott *et al*., 2014).

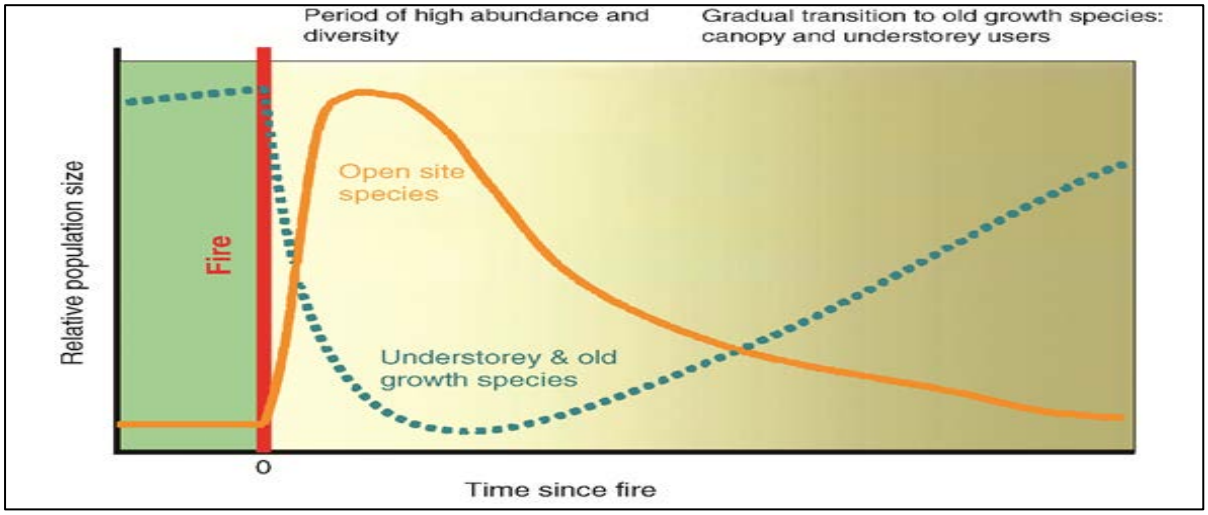

Figure 3.6 **Shifts in the composition of an animal population in response to post-fire changes in vegetation structure. The case presented is that of a stand-replacing crown fire in a closed-canopy forest (Scott *et al*., 2014).**

Barlow and Peres (2004) reported how recurrent fires in the Amazon rainforest led to the decline of most mammals, particularly large arboreal frugivores (e.g. *Pithecia* spp.

and *Chiropotes* spp.) and understorey birds with specialised dietary, foraging or habitat requirements (e.g. *Willisornis* spp.). Caribou have been reported to avoid boreal forests burnt by crown fires for 50 years or more until food sources such as lichens have been re-established (Scott *et al*., 2014). The abundance of duff-dwelling arthropods are expected to decline dramatically in the first year post-fire (Coleman & Rieske, 2006), particularly for species with predisposed traits like remnant habitat dependence; upland habitat preference; low vagility (i.e. ability or tendency to migrate freely); and univoltinism (i.e. one brood of offspring per year). African species such as oribi (*Ourebia ourebi*), sable (*Hippotragus niger*), kudu (*Tragelaphus strepsiceros*) and elephants (*Loxodonta africana*) only return to their former habitat once sufficient regrowth has occurred (de Ronde *et al*., 2004b).

Many animals cope with, or even thrive, in the wake of wildfires. Some animals use the opportunity to catch fleeing or exposed prey. Predators such as bears, lions, raptors and insect-feeding birds (e.g. lilac-brested rollers (*Coracias caudate*) and fork-tailed drongos (*Dicrurus adsimilis*)) have been reported to hunt prey trying to escape the flames (de Ronde *et al*., 2004b; Zielinski, 2014). Woodpeckers (*Picidae* spp.) have been known to fly in and feast on bark beetles in dead and dying trees (Zielinski, 2014), while grey hornbills (*Tockus nasutus*) and bald ibis (*Geronticus calvus*) are also known for feeding on recently burned ground (de Ronde *et al*., 2004b).

In the grasslands and savannas of Africa a few mammals exploit the immediate post-fire conditions, e.g. warthogs (*Phacochoerus aethiopicus*) that feed on exposed roots and tubers and black rhinoceroses (*Diceros biconis*) who favour recently burned twigs (de Ronde *et al*., 2004b). Some herbivores are drawn to post-fire regrowth which usually contain more nutrients than unburned vegetation owing to higher leaf-to-stem ratios, rejuvenation and concentration of nutrients in reduced standing biomass (Van de Vijver, 1999). Such species include zebra (*Equus burchelli*), impala (*Aepyceros melampus*), springbok (*Antidorcas marsupialis*), blesbok (*Damaliscus dorcas phillipsi*), black wildebeest (*Connochaetes gnou*) and white rhinoceros (*Ceratotherium simum*) (de Ronde *et al*., 2004b). The risk of predation may also change in burned open areas due to increased visibility with varying impacts to different taxa (de Ronde *et al*., 2004b).

Some species have evolved to require burned areas as part of their life history – birds such as Kirtland's warblers (*Setophaga kirtlandii*) only nest in young jack pine (*Pinus banksiana*) forests (Zielinski, 2014), while blackwinged plovers (*Vanellus melanopterus*) and bronze-winged coursers (*Rhinoptilus chalcopterus*) choose to breed on recently burned ground as their eggs are dark-coloured and chicks have heavily pigmented down (Figure 3.7) (de Ronde *et al*., 2004b). The red grouse (*Lagopus lagopus scotica*) require patchy habitats with a mix of different post-fire successional stages since it feeds on young re-sprouting shoots but nests in older vegetation (Scott *et al*., 2014). Insects like fire beetles (*Merimna atrata* and *Melanophila* spp.) have specialised infrared receptor organs and actively seek out fires as the dead partially burnt trees create a suitable habitat for its larvae (Engstrom, 2010; Scott *et al*., 2014). Evans (1971; cited by Engstrom, 2010) listed numerous other species of pyrophilous insects.

Figure 3.7 **Bronze-winged courser chicks are camouflaged to resemble tufts of burnt grass (Project Nightjar, 2016).**

Fire regimes impact ecological processes influencing wildlife habitats (Scott *et al*., 2014). Wildfires initiate a succession of changes as plants, microbes, fungi and other living organisms repopulate the affected area. With time the ageing vegetation alters the microclimate (i.e. light, temperature and humidity) along with the availability and quality of food and shelter, so that the composition of the animal population in the area will change in response (Zielinski, 2014).

Fire affects the chemical and physical properties of soil, which sequentially influences the number and type of organisms therein (Section 3.3.3). Fire also affects aquatic organisms (i.e. fish, macroinvertebrates and diatoms) and organisms that have aquatic phases in their life histories (e.g. emergent insects and amphibians). Short term impacts can be attributed to lethal increases in water temperature, potential deadly effects of fire-induced changes in stream pH, and increased concentrations of toxic chemicals (e.g. aluminium, iron, lead and zinc) (Gresswell, 1999). Longer term impacts may result from reduced riparian vegetation, pulse or chronic erosion (Section 3.3.1), channel alterations, the amount and type of floating debris, turbidity and stream sedimentation (Gresswell, 1999; Fowler, 2003; Engstrom, 2010; Scott *et al*., 2014). Engstrom (2010) found that larger water bodies are less likely to be affected than smaller ones and that standing water is less affected than flowing water bodies, while wetlands buffer some of the impacts. The scale and extent of these effects can be related to the fire's size and severity, geomorphology, physical, chemical and biological properties of the watershed as well as timing and intensity of post-fire precipitation events (Gresswell, 1999).

3.3 FIRE EFFECTS ON SOIL

Soil properties can experience short-term, long-term or permanent fire-induced changes (Certini, 2005). As with fire effects on fauna (Section 3.2), the inhomogeneous spatial distribution of fire severity results in an intricate mosaic comprising little affected areas interspersed by seriously impacted ones (Certini, 2005; Mataix-Solera *et al*., 2009). It is therefore next to impossible to generalise soil and geomorphological effects of fire across geographical regions, even those with comparable climates and vegetation (Scott *et al*., 2014).

Surface fires affect the chemical properties (e.g. pH, mineral content), physical properties (e.g. temperature, texture, structure, porosity) and biological properties (e.g. abundance and composition of soil biota) of soil (Table 3.1). The extent of such effects depends critically on the following features (González-Pérez *et al*., 2004; Mataix-Solera *et al*., 2009; Scott *et al*., 2014):

a) Fuel characteristics above and within a soil;
b) The temperatures attained, particularly at the interface and within the soil layer, and the period of time involved; and
c) The inherent properties of the soil itself.

Table 3.1 Soil properties affected by fire (modified from Certini, 2005)

Physical properties	Chemical properties	Biological properties
✶ Temperature regime ✶ Structure stability ✶ Particle size distribution ✶ Bulk density ✶ Mineralogical assemblage ✶ Colour ✶ Water repellency ✶ Water infiltration ✶ Water storage capacity ✶ Erodibility	✶ pH ✶ Quantity and quality of organic matter ✶ Availability of nutrients ✶ Base saturation ✶ Exchangeable capacity ✶ Electrical conductivity	✶ Composition and abundance of soil microbiota ✶ Composition and abundance of soil invertebrates ✶ Rate of biological fixation of nitrogen and conversion to nitrate ✶ Enzyme activity

High fuel loads result in hotter fires, while other fuel characteristics (e.g. size, compaction, distribution, moisture content and vegetation type) will impinge on the rate of spread (Section 4.1). The type, intensity and duration of a fire determine the temperatures attained and the fraction of plant nutrients volatilized (González-Pérez *et al*., 2004; Certini, 2005). For example, a low-temperature, fast moving surface fire might only impact slightly on the underlying soil and plant roots down to a few centimetres, while a hotter fire that lingers over a single site will have a greater influence on the soil (Certini, 2005; Mataix-Solera *et al*., 2009; Scott *et al*., 2014). The impact of fire on soil also depends on the nature of the soil itself. For example, immature granite soils that contain rock fragments and little organic matter behave differently from mature sandy or clay soils or those with a high organic content, while soil water content influences the rate at which heat is transferred downwards (Certini, 2005; Mataix-Solera *et al*., 2009; Scott *et al*., 2014). Table 3.1 attempts to summarise some of the key chemical, biological and physical effects of fire on soil that will be discussed in this section. However, it should be acknowledged that the various properties can interact with and influence each other.

3.3.1 Physical Properties

Combustion and heat transfer creates steep temperature gradients within the soil. According to Úbeda and Outeiro (2009) the physical fire-induced changes in soil become significant only when the temperature reaches 400°C, while different chemical elements are volatilized at different temperatures. During a fire surface temperatures momentarily rise to a typical 200 – 300°C, though instantaneous values can reach 1 150°C in certain vegetation types (Certini, 2005; Mataix-Solera *et al*., 2009). Grass fires, which are of particular interest to this study, can generate temperatures of up to 700°C (Van de Vijver, 1999; Mills & Fey, 2004). The latent heat of vaporisation prevents temperatures in wet soil to exceed 95°C until all the water has evaporated (Certini, 2005; Scott *et al*., 2014). Even relatively low soil water content (20% by volume) is deemed sufficient to impede lethal soil temperatures below the first 2.5 cm (Úbeda & Outeiro, 2009). Soil temperatures at 5 cm rarely exceed 150°C, while no significant heating generally occurs below 20 – 30 cm (Certini, 2005). In the wake of a fire the soil temperatures can remain high for anything from a few minutes to several days, while the profile changes temporarily owing to reduced shading by vegetation cover and the decreased albedo of the surface (Certini, 2005). In a study by Xu *et al*. (2012) the temperature of burned surface soil was 6°C higher than that of control unburned soil two months following fire.

Organic matter (OM) is concentrated at the surface and influences the properties of the underlying mineral soil horizons (Úbeda & Outeiro, 2009). The most obvious alteration soils experience during burning is reductions in OM content through distillation, charring or oxidation (Certini, 2005). Soil OM begins to reduce significantly when temperatures reach about Soil OM begins to reduce significantly when the temperature reaches about 220°C (Mills & Fey, 2004; Xu *et al*., 2012). Thus, fires generally increase soil OM decomposition rates, which in turn influence other soil properties such as aggregate stability and loss of structure, aeration, water infiltration and retention capacity, cation exchange capacity and nutrient cycling (Mills & Fey, 2004; Úbeda & Outeiro, 2009). Although soil OM usually decreases immediately after fire, increases in the surface layers of as much as 30% may occur in the presence of external inputs (e.g. dry leaves and partially burnt plant material originating from the tree canopy layer) (González-Pérez *et al*., 2004). The key impacts of fire on soil OM are (González-Pérez *et al*., 2004; Certini, 2005):

a) overall removal of external oxygen groups that produces materials with relatively lower solubility;
b) decline of the chain length of alkyl compounds (i.e. alcohols, alkanes and fatty acids);
c) aromatisation of lipids and sugars;
d) establishment of heterocyclic N compounds;
e) macromolecular condensation of humic substances; and
f) formation of black carbon (i.e. soot, charcoal or any combustion product that is inert in the biosphere).

The combustion of OM within the mineral soil affects the binding of soil particles and alters the soil structure. OM plays an important role in the A horizon, while the clay mineral is more relevant in the B horizon (Úbeda & Outeiro, 2009). In a process referred to as dihydroxylation, heating to temperatures above 460°C drives off hydroxyl (OH) groups from clays (Úbeda & Outeiro, 2009; Parise & Cannon, 2012), which also result in a loss of soil structure. Mills and Fey (2004) suggested that changes in soil chemistry brought about by frequent burning may influence clay dispersibility and aggregate stability, thereby increasing the tendency of soil to form a surface crust.

Properties such as soil plasticity, elasticity, particle size distribution, soil-aggregate stability, and bulk density can also change during burning (Parise & Cannon, 2012). Structural losses correspond to reduced soil plasticity and elasticity (Parise & Cannon, 2012). Certini (2005) stated that particle-size distribution is not directly affected by fire, although increased erosion can selectively remove finer particles. However, Parise and Cannon (2012) advocated that high temperatures are able to fuse soil particles, creating coarser but less cohesive soil aggregates that are vulnerable to erosion and raveling. Bulk density increases in response to fire due to the collapse of aggregates and the congestion of cavities by ash and disseminated clay minerals (Certini, 2005), with obvious implications for soil porosity and permeability. Snyman (2005) showed that burning in semi-arid grasslands may significantly increase soil compaction and therefore bulk density.

Due to the relatively high temperatures required for dihydroxylation and low clay content in the upper few centimetres (< 5% according to Úbeda and Outeiro (2009)), low to moderate fires do not alter the mineralogical assemblage of soils noticeably (Certini, 2005). When high temperatures occurred for a sufficiently long period of time due to concentrated fuels (e.g. logs or stumps), the upper few centimetres of the soil may exhibit the following changes (Certini, 2005):

- transformation of chlorite, chlorite-vermiculite, vermiculite and hydroxy-interlayered vermiculite to illite;
- reduction of gibbsite concentration;
- conversion of goethite into ultra-fine maghemite; and
- complete decomposition of kaolinite or, under specific conditions, its transformation to a poor crystalline aluminosilicate that is able to act as cementing agent among particles (under extreme conditions clays may even be baked into red brick-like fragments).

Ash (ranging in colour from black to grey to white) may be deposited at the surface, while the colour of the affected layer may change from brown and black to yellow, orange and red (Scott *et al*., 2014). Blackening results from charring, while reddening occurs due to the removal of OM in combination with iron oxide formation (Certini, 2005).

Surface fires can also impact on soil hydrophobicity (i.e. water repellency). Generally, soil water repellence is enhanced through the following mechanisms (Úbeda & Outeiro, 2009; Olorunfemi *et al*., 2014):

- drying of soil OM;
- leaching of organic chemicals from plant litter material which subsequently coat mineral particles;
- formation of hydrophobic by-products of microbial mycelium in the upper soil;
- mixing of hydrophobic OM with mineral soil particles; and
- pyrolysis of organic matter with subsequent precipitation of volatile compounds on soil particles to form a hydrophobic layer.

While high temperatures (> about 300°C) can be instrumental in the removal of organic chemicals originating from certain vegetation types which rendered the surface soil layer hydrophobic, it may also act to alter the depth and enhance the hydrophobicity of existing subsurface water repellent layers (DeBano, 2000; Certini, 2005; Doerr *et al*., 2006; Parise & Cannon, 2012; Scott *et al*., 2014). Severe burns could thus destroy any pre-existing surface soil repellency, rendering the uppermost layer of the soil more permeable, while a more water-repellent layer forms underneath (Figure 3.8). The depth of the subsurface water-repellent layer rarely exceeds 6 – 8 cm and is largely determined by fire severity and soil characteristics such as particle-size distribution and water content (Certini, 2005). The removal of vegetation cover by fire combined with rapid saturation of the newly formed wettable surface layer during heavy downpours may result in its removal by overland flow (Doerr *et al*., 2006). The potentially severe implications for soil fertility and seedbed survival, post-fire ecosystem recovery, river sedimentation and water quality are highlighted in sections to follow.

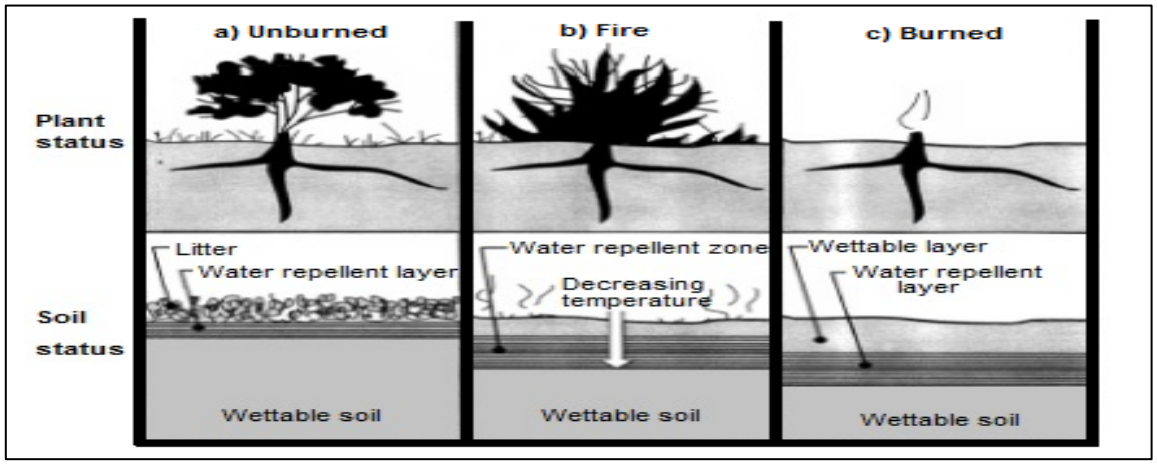

Figure 3.8 **Fire-induced formation of a hydrophobic soil layer. (A) In unburned brush soil water repellency is found in the litter, duff and mineral soil layers immediately beneath the plants; (B) During the fire hydrophobic substances are vaporized, moving downward along the temperature gradient to condensate on cooler mineral soil particles; (C) A post-fire water repellent layer is located below and parallel to the soil surface sandwiched by wettable soil (deBano, 2000).**

A major impact of fire on soil is a reduced saturated hydraulic conductivity (Úbeda & Outeiro, 2009). Water is stored in soil pores by means of capillarity (Úbeda & Outeiro, 2009), while larger pore diameters (such in sandy soils) lead to low water storage capacities per unit volume (the opposite is true for small pore diameters). The loss of OM and structure due to fire has an adverse effect on a soil's ability to retain water.

This is the case because aggregates comprising OM and mineral soil particles create water-holding micropores and enhance the soil structure (Úbeda & Outeiro, 2009). Snyman (2005) showed that burning in semi-arid grasslands decreased the soil water content in the superficial horizons.

Wildfires may accelerate weathering and erosion processes. Post-fire soil losses vary according to soil type and vegetation, fire severity and ensuing weather conditions (Pausas *et al*., 2008). Physical weathering is enhanced by widespread fracturing of rocks and boulders brought about by the heat from severe fires (Scott *et al*., 2014). Fires also reduce the vegetation cover, for up to several seasons after burning (Snyman, 2005; 2006), and destroy the ground surface litter layer and soil OM (Christensen, 1993; Gresswell, 1999; Scott *et al*., 2014). This disposes mineral soils to desiccation and the full impact of falling rain, thus increasing the risk of post-fire erosion (particularly in the case of any significant topography) (Scott *et al*., 2014). A decreased water infiltration rate also results in increased surface runoff, overland flow and erosion (Úbeda & Outeiro, 2009; Parise & Cannon, 2012). Debris flows arise as one of the most destructive consequences of such changes, often leading to widespread damage to human infrastructure (Parise & Cannon, 2012).

Fire-induced soil hydrophobicity is commonly viewed as one of the chief reasons for considerable post-fire increases in hillslope runoff and erosion (Doerr *et al*., 2006). The formation of a surface crust or an enhanced hydrophobic soil layer will prevent the infiltration of water resulting in overland flow (Mills & Fey, 2004; Doerr *et al*., 2006). The strength and position of the enhanced hydrophobic layer plays a key role in post-fire erosion (Figure 3.9). Any discontinuities in the hydrophobic layer may result in the formation of erosional channels wherein sediment can be transported quickly and in large quantities (Scott *et al*., 2014). The erodibility of burned soils increase with an increase in soil heating, with a shorter recovery time to pre-fire erodibility values in less intensely burned areas (Úbeda & Outeiro, 2009). Úbeda and Outeiro (2009) cited the production of four times as much sediment from high-severity burns as compared to low-severity burns on a uniform hill slope. Scott *et al*. (2014) reported post-fire erosion increases of up to 870 times on certain slopes (probably as a result of little erosion before the time).

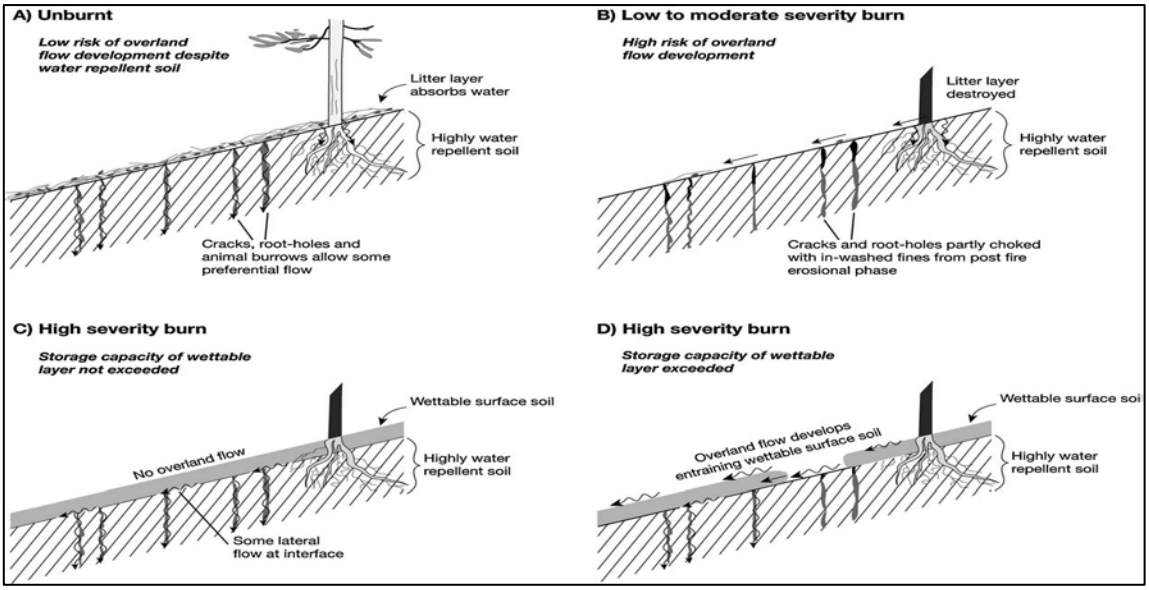

Figure 3.9 **Differences in surface runoff in sloped forested terrain with naturally high water repellent soil for (A) unburnt conditions; (B) following a low-moderate fire; (C) following a high severity fire without exceeding the water storage capacity of the wettable layer; and (D) following a high severity fire and exceeding the water storage capacity of the wettable layer (Doerr *et al*., 2006).**

As previously indicated, wildfires can have far-reaching impacts on the hydrologic response of watersheds. Ash drifting on overland flow and increased soil erosion (e.g. surface erosion, mass wasting and channel erosion) following severe fires can deposit substantial amounts of organic and inorganic material in streams and rivers (Figure 3.10). This sediment may be transported large distances downstream to be deposited onto flood plains or lakebeds, polluting water supplies and silting up reservoirs. In addition, water with a high suspension of sediments will have lower light penetration which can encourage microbial activity and reduce aquatic primary productivity (Fowler, 2003; Scott *et al*., 2014). Sediment input can also alter the water's pH and the availability of nitrates, while water temperatures may increase if vegetation on the embankments was removed. Changes in water temperature can influence species abundance and diversity, egg incubation and offspring survival (Gresswell, 1999). Algal blooms and eutrophication may result from a combination of increased nutrients and warmer conditions (Fowler, 2003; Scott *et al*., 2014). Erosional effects usually peak within 10 years following a fire event (Gresswell, 1999).

Figure 3.10 **Ash and sediment-rich flow from a burned forest after a rain shower in the Stermer Ridge watershed of Arizona, USA (Neary, 2002).**

3.3.2 Chemical Properties

Fire effects on soil chemistry comprise “complex biogeochemical interactions that impact biotic and abiotic cycling of soil components” (Úbeda & Outeiro, 2009). Fire affects the chemical properties of soil by altering the pH, quantity and quality of OM, cycling of nutrients, base saturation, cation exchange capacity and electrical conductivity (Table 3.1).

Soil pH is an important factor affecting the availability of plant nutrients, vegetation type and microbial activity (González-Pérez *et al*., 2004; Certini, 2005; Úbeda & Outeiro, 2009). In most cases wildfires increase soil pH due to the denaturation of organic acids when heated above about 450°C and the deposition of base-rich ash (Menaut *et al*., 1993; Certini, 2005; Úbeda & Outeiro, 2009; Xu *et al*., 2012; Scott *et al*., 2014). Although the topsoil pH could increase by as much as three units

immediately after burning, such fire-induced increases are negligible in soils buffered by carbonates (Certini, 2005). Changes in soil pH, which could last for decades, are determined by post-fire wind and rainfall events and the endurance of ashes at a specific location (Úbeda & Outeiro, 2009).

As stated earlier, the quantity of soil OM decreases immediately following a fire but generally exceeds the pre-fire level in the long run (Certini, 2005). The quality of OM changes considerably, with a relative increase in the fraction that is more recalcitrant to biochemical attack owing to selective burning of fresh residues (leaves, twigs etc.) and newly formed aromatic and highly polymerised (humic-like) compounds (Certini, 2005). The recovery of soil OM is correlated with plant secondary succession and the restoration process of the entire soil ecological system (Xu *et al*., 2012). The residence time of some charred materials, an exclusive product of incomplete combustion, can range from hundreds to thousands of years.

The effect of fire on nutrient dynamics are determined by factors such as fire intensity, vegetation type, composition and structure, the nutrient content of the pre-existing biomass as well as soil properties (Kauffman *et al*., 1994; Scott *et al*., 2014). In what is sometimes referred to as the “fertilizing effect of fire” or the “ashbed effect”, fire can act as a mineralizing agent over the short-term and increase the availability of nutrients for plant growth (Stocks & Trollope, 1993; Snyman, 2003; González-Pérez *et al*., 2004; Úbeda & Outeiro, 2009; Scott *et al*., 2014). Ash (i.e. pure mineral ash and charcoal) enhances nutrient retention through the reduction of leaching (González-Pérez *et al*., 2004; Scott *et al*., 2014) and contains highly soluble oxides of plant nutrients that can be released into the soil (Certini, 2005). Charcoal also acts as a strong sorption agent for germination- and growth- inhibiting phenolic substances (González-Pérez *et al*., 2004; Mataix-Solera *et al*., 2009). The rate at which N is made available depends on levels of microbial activity in the soil, which in turn depends on soil moisture, temperature, pH and the presence and quality of OM (Úbeda & Outeiro, 2009). Over the longer term nutrient losses and redistribution will affect site productivity.

Burning is a rapid physical decomposition process that not only volatizes nutrients, thereby reducing the nutrient content in the soil, but also modifies the remaining organic materials (Úbeda & Outeiro, 2009). The exact temperature at which different

chemical elements are volatilized may vary between organic and inorganic forms of elements. Nitrogen (N) will generally vaporize at > 200°C (Figure 3.11), sulphur (S) at > 300°C, phosphorus (P) and potassium (K) at > 750°C, and calcium (Ca) and magnesium (Mg) at > 1 500°C (Scott *et al*., 2014). By driving changes in vegetation structure in some systems (e.g. reducing tree cover in subtropical savannas), the indirect effect of repeated burning can be just as important for soil nutrients as the direct losses due to volatilization (Coetzee *et al*., 2010; Scott *et al*., 2014).

As already mentioned, higher concentrations of available N are observed immediately following a fire, which is reduced markedly within a few months (Xu *et al*., 2012). Most soil organic N are converted to inorganic form (e.g. ammonium (NH_4^+) and nitrate (NO_3^-)) by moderate to high intensity fires (Certini, 2005). Certini (2005) cited several studies that reported higher post-fire NH_4^+ and NO_3^- levels for the first one to two years in forest soils, while stressing that plant recolonization play an important role in the conservation of soil N in burnt areas.

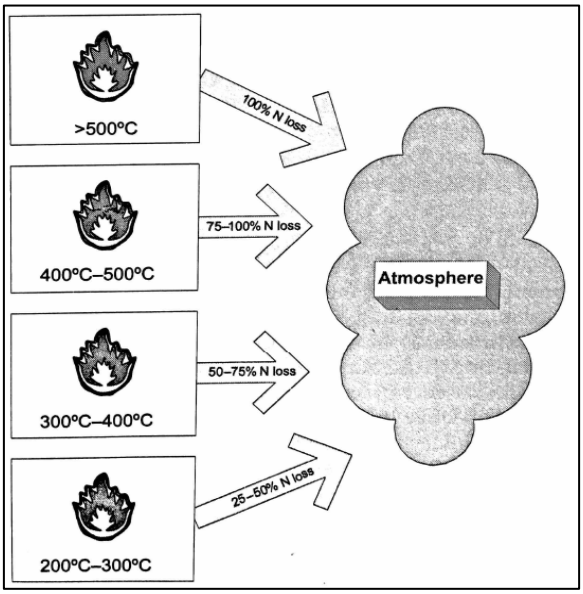

Figure 3.11 Fire-related nitrogen losses at various temperatures (Úbeda & Outeiro, 2009).

Although losses of soil P through volatilisation or leaching are small in natural systems, burning does result in an increase in labile P, while decreases of total organic P and less labile organic P are observed beneath the ashbed (Úbeda & Outeiro, 2009). Fires lead to the conversion of P to orthophosphate which is available to biota (Certini, 2005; Xu *et al*., 2012). The orthophosphate will bind to Al, Fe and Mn-oxides in acidic soils,

while it binds to Ca-minerals or precipitates as discrete Ca-phosphate in neutral or alkaline soils (Certini, 2005). The fact that fire can alter soil pH is important for P availability, since P forms insoluble compounds at either low or high pH levels (Úbeda & Outeiro, 2009). Depending on the original pH level, any fire-induced changes in soil pH toward alkalinity will have a negative influence on the P bioavailability (Xu *et al*., 2012). In a slightly acid soil (as is usually the case in Africa), an increase in pH improves soil available P levels.

Changes to soil nutrient cycles other than N and P due to fire are generally minor and short-lived (Certini, 2005). Exchangeable Mg, K and Na levels may increase for a brief period following the combustion of soil OM, while thermal shock to the soil microbial community (e.g. microorganisms such as mycorrhizal fungi that release Fe) can affect nutrient availability indirectly (Certini, 2005). González-Pérez *et al*. (2004) claimed that a higher pH is also associated with an increase in exchangeable cations. After fires, monovalent cations such as K and Na are present largely as chlorides and carbonates that are readily mobilised, while divalent ions such as Ca and Mg which are also present as oxides and carbonates are less mobile (Úbeda & Outeiro, 2009). The latter group is more likely to be retained on the cation exchange sites, elevating surface levels for extended periods, while Mg, K and Na are relatively soluble and can be leached deeper into the soil (Úbeda & Outeiro, 2009). The transformation of minerals at high temperatures also increase available K content (Xu *et al*., 2012). In addition, nutrients can be leached out of the soil or removed off-site in particulate form by convection of fly ash in smoke columns during a fire, by surface wind transport or water erosion (Certini, 2005).

Kauffman *et al*. (1994) showed that when compared to evergreen forests, subtropical grassland fires exhibited a proportionally greater loss of above-ground N, K, P, Ca, S and C, probably due to higher fire front intensities and subsequent volatilization in the finer fuel type. Most of the other nutrients are replaced by atmospheric inputs within about a year (Scott *et al*., 2014). A study by Snyman (2003) revealed that burning of semi-arid grasslands significantly reduced organic C and total N content in the top soil layer.

The amount and composition of inorganic cations govern base saturation in soils (Úbeda & Outeiro, 2009). The base saturation generally increases due to the predominant release of bases from combusting OM (Certini, 2005).

Cation exchange capacity (CEC) is used as an indicator of soil fertility, nutrient retention capacity and the ability to shield groundwater from cation contamination (Úbeda & Outeiro, 2009). Due to the loss of soil OM, cations (that are stronger related to soil OM than to clay mineralogy) should follow a similar decreasing trend (Menaut *et al*., 1993). Fires thus normally reduce the soil CEC (Certini, 2005), although it may increase in cases where organic rich substrates that originated from fire are deposited (Úbeda & Outeiro, 2009). Mills and Fey (2004) reported an increase in the exchangeable sodium percentage (ESP) in the top centimetre of soil in burned plots, which they attributed to "preferential removal of Ca, Mg and K from the soil profile by plants and the loss of these nutrients when ash is washed off-site by surface runoff".

Soil electrical conductivity (EC), which provides a measure of the total dissolved solids, generally increases after fire, although it strongly depends on the land use history of the area (Úbeda & Outeiro, 2009). Certini (2005) indicated that such increases in EC may only be temporary. Mills and Fey (2004), on the other hand, reported a lower EC in burnt compared to unburnt plots in the southern Kruger National Park, probably due to the export of ash in overland flow.

3.3.3 Biological Properties

Living organisms in the soil include macro-, meso- and microfauna as well as microflora. Temperatures of about 40 – 121°C are easily reached within the first few centimetres of soil during a wildfire and are considered as the threshold for biological disruption (Mataix-Solera *et al*., 2009). The thermal shock and fumigation by organic pollutants emanating from the combustion process causes an immediate and drastic reduction in soil biota, particularly in microbial biomass and activity (González-Pérez *et al*., 2004; Certini, 2005; Mataix-Solera *et al*., 2009; Xu *et al*., 2012). Both beneficial (e.g. mycorrhiza) and detrimental biota (e.g. root pathogens) may be destroyed by severe fires (Scott *et al*., 2014), while in extreme cases the topsoil can experience complete sterilisation (Certini, 2005; Mataix-Solera *et al*., 2009). Changes to soil chemistry and physical properties also influence soil biota, which in turn may influence

soil development, nutrient availability and uptake as well as plant growth (Certini, 2005; Engstrom, 2010; Scott *et al*., 2014). In addition, the activity of certain soil enzymes increases with increasing temperatures up to about 60 – 70°C (Mataix-Solera *et al*., 2009). However, at higher temperatures enzyme activity is reduced due to thermal denaturation, while complete inactivation occurs at about 180°C (Certini, 2005; Mataix-Solera *et al*., 2009).

Following a fire, the short-term increase of soluble carbon and nutrients in the soil, combined with higher pH levels, may facilitate an increased presence of microbes, particularly N-fixing bacteria (González-Pérez *et al*., 2004; Mataix-Solera *et al*., 2009). The added presence of charcoal stimulates the activity of ectomycorrhyzae and increases soil microbial respiration in locations dominated by phenol-rich vegetation such as ericaceous shrubs (González-Pérez *et al*., 2004). With time, however, the organic compounds become increasingly recalcitrant to microbial attack, resulting in a general decrease in microbial activity (González-Pérez *et al*., 2004; Certini, 2005; Mataix-Solera *et al*., 2009).

Burning may alter the composition of the soil microbial community due to the following factors (Mataix-Solera *et al*., 2009):

- differences in temperature sensitivity;
- differential survival strategies;
- differential colonization mechanisms;
- differential tolerance to soil and microclimate changes (e.g. OM, pH, moisture and temperature);
- alterations in biomass and composition of above-ground vegetation; and
- the devastation and establishment of ecological niches.

For example, fungi are generally less tolerant to high temperatures than bacteria and actinomycetes so that burning is less detrimental to the latter (Certini, 2005; Mataix-Solera *et al*., 2009). Xu *et al*. (2012) found that the microbial diversity declined significantly immediately (i.e. one day) after a wildfire but recovered to unburned levels one year later.

In comparison to microorganisms, the direct effects of fire on soil-dwelling invertebrates are not as striking. This can be attributed to the higher mobility of invertebrates, affording them a better chance to escape the heat by burrowing deeper into the soil (Certini, 2005; Mataix-Solera *et al*., 2009). However, the indirect effects of fire (e.g. changes in above-ground vegetation, reduction in the litter mass and soil OM, and altered microclimate) generally result in a sharp decrease in both the total mass and types of invertebrates (Certini, 2005; Mataix-Solera *et al*., 2009). According to Mataix-Solera *et al*. (2009) inconsistent results were reported by individual studies focusing on the effects of repeated burns on micro-arthropod populations.

3.4 FIRE EFFECTS ON AIR QUALITY AND HEALTH

Air pollution may be defined as “the presence in the outdoor atmosphere of one or more contaminants or combinations thereof in such quantities and of such duration as may be, or may tend to be injurious to human, plant or animal life, or property, or which unreasonably interfere with the comfortable enjoyment of life, or property, or the conduct of business” (Mishra, 2014). Emissions from wildfires result in higher levels of pollutants in the atmosphere that are harmful to human health and ecosystems and reduce visibility, leading to hazardous or overall taxing conditions (Urbanski *et al*., 2009). The problem becomes a transboundary issue when plumes transgress international boundaries (Johnston *et al*., 2012). Under certain weather conditions smoke plumes and haze layers resulting from wildfires can persist for extended periods of time, while their chemical and optical properties are also determined by prevailing conditions (Miranda *et al*., 2009). Generally, the extent of air pollution encountered at a site is determined by (Oke, 1987):

a) the nature of relevant emissions; and
b) the state of the atmosphere.

The first factor relates to the rate, type (i.e. physical and chemical nature) and source of emission (which includes the location, area, effective height and duration). The second factor relates to its dispersal (as governed by the stability profile, wind and turbulence), transformation (determined by radiation, temperature, humidity and presence of other atmospheric substances) and removal (by precipitation scavenging, gravitational settling or surface adsorption and impaction) in/from the atmosphere. The

composition of smoke from biomass fires were discussed in Section 2.3, while certain aspects of smoke dispersal are dealt with in Section 4.2.3.

3.4.1 Health Impacts

Wildfires have major impacts on human health which stem from burns, smoke inhalation and post-fire psychological trauma (Pitman *et al*., 2007). Although wildfire emissions are natural, they are not benevolent. There is a substantial and growing body of epidemiological and toxicological evidence suggesting that both acute and chronic exposures to smoke from wildfires are linked to adverse health impacts in humans. Extensive reviews of such studies are provided by Fowler (2003), Naeher *et al*. (2007), Kochi *et al*. (2010), Dennekamp and Abramson (2011) and Liu *et al*. (2015). Exposure to smoke pollutants occurs through inhalation (the most common pathway), ingestion and dermal absorption (Fowler, 2003). Epidemiological studies have also indicated that the potential for health impacts depends on factors such as individual age, the pre-existence of respiratory and cardiovascular diseases or infections, smoke chemical composition and particle size (Schwela, 2001; Liu *et al*., 2015). The most vulnerable groups appear to be young children (< 4 years of age), the elderly (> 65 years of age) and those with underlying chronic diseases (Naeher *et al*., 2007; Liu *et al*., 2015).

Human exposure to smoke from vegetation fires causes a range of medically important biophysical effects, ranging from temporary and relatively benign eye, nose and throat irritation to more permanent and progressive respiratory and cardiovascular diseases and even premature death (Malilay, 1999; Fowler, 2003; Ayres *et al*., 2006; Naeher *et al*., 2007; Kochi *et al*., 2010; Moeltner *et al*., 2013; Liu *et al*., 2015). Sluggish reflexes, reduced manual skills and work capacity, disorientation, fatigue and impaired mental ability are some of the symptoms of carboxyhemoglobin, a condition brought about by inhaling excessive amounts of CO (Fowler, 2003). Most of the studied large wildfire smoke events (e.g. California, U.S.A., 1987, 1999 and 2003; Southeast Asia, 1997; Florida, U.S.A., 1998; Northern Territory, Australia, 2000, 2004 and 2005; Lithuania, 2002; British Columbia, Canada, 2003; Mato Grasso, Brazil, 2004/05; northern Portugal, 2005; central Russia, 2010) have seen a dramatic increase in medication use, the number of emergency room visits and/or hospital admissions for asthma, acute bronchitis, angina, chronic obstructive pulmonary disease (COPD), pneumonia

and myocardial infarction (Mercer *et al*., 2000; Schwela, 2001; Fowler, 2003; Naeher *et al*., 2007; Kochi *et al*., 2010; Dennekamp & Abramson, 2011; Liu *et al*., 2015). Generally, the proportion of the population affected decreased as the severity of the health effects increased (Figure 3.12).

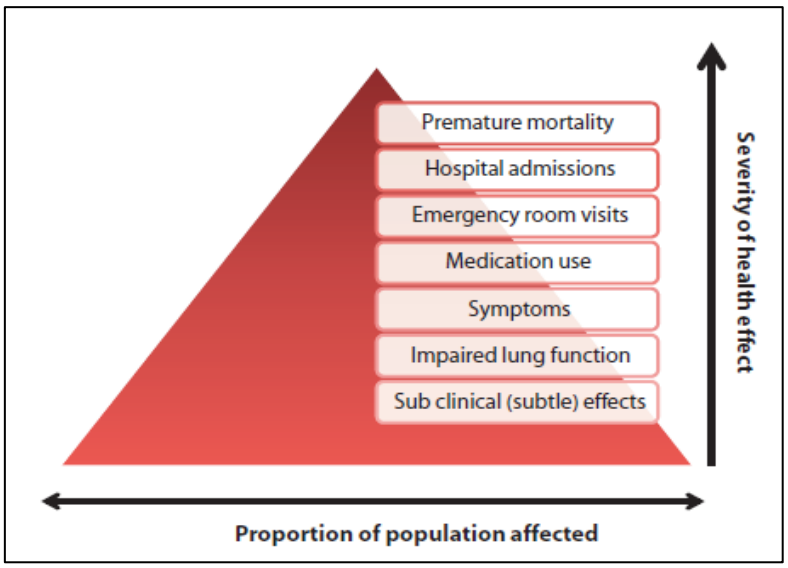

Figure 3.12 The air pollution health effects pyramid (Dennekamp & Abramson, 2011).

The cumulative medical effects of wildfire smoke may only culminate in severe symptoms days to weeks after the initial cardiorespiratory impact (Delfino *et al*., 2009). In addition to the aforementioned short-term health effects, prolonged exposure to biomass smoke may result in reduced life expectancy (Fowler, 2003). Due to changes in immune function or respiratory clearance mechanisms, people that have been exposed to wildfire smoke may become more susceptibility to, or suffer increased severity of, later respiratory infections (Fowler, 2003; Delfino *et al*., 2009). Gaseous compounds ad- or absorbed by particles can also contribute to long-term health effects such cancer (Schwela, 2001; Fowler, 2003). An extreme example of the latter is the remobilization of radioactive materials (e.g. ^{137}Cs) by wildfires in contaminated areas (e.g. Chernobyl) and their subsequent dispersal to previously non-affected regions thousands of kilometres away (Hao *et al*., 2009; Evangeliou *et al*., 2014). Lin *et al*. (2013) also showed how mercury (Hg) emissions from springtime biomass-burning in Southeast Asia were detected downwind between Japan and Taiwan.

Wildfire emissions are thus a substantial health hazard and a significant contributor to global mortality (Johnston *et al*., 2012). Of special concern are the high concentrations

of respirable particulate matter (PM2.5 and PM10), CO, NO_x, SO_2, O_3 and organic compounds such as polycyclic aromatic hydrocarbons (PAHs), benzene, aldehydes and other free radicals (unstable molecular fragments) which are able to move into the lower respiratory tracts (Schwela, 2001; Naeher *et al*., 2007). The most important disease-associated constituent of smoke is probably PM2.5, which mainly consist of organic carbon (OC), black carbon (BC) and smaller contributions from inorganic species with an aerodynamic diameter ≤ 2.5 µm (Naeher *et al*., 2007; Bell & Adams, 2009; Dennekamp & Abramson, 2011; Johnston *et al*., 2012; Ward *et al*., 2012). Australian health guidelines set the maximum limits of exposure to PM2.5 at 25 µg m^{-3} within a 24-hour period and 8 µg m^{-3} over the course of a year (Bell & Adams, 2009).

Johnston *et al*. (2012) used satellite observations and a global chemical transport model to estimate the annual average PM2.5 concentrations from landscape fires for the period 1997 – 2006 (Figure 3.13). With values ranging from 0 to 45 µg m^{-3} annually, it is evident that the highest PM2.5 concentrations occurred over Southeast Asia, sub-Saharan Africa and the Amazon basin in South America. The average annual mortality related to landscape fire smoke exposure (Figure 3.14) was estimated at 110 000 for Southeast Asia, 157 000 for sub-Saharan Africa, 10 000 for South America and 339 000 worldwide. The estimated mortality was shown to be greater during the 1997/98 El Niño year (532 000 worldwide), mainly due to the higher mortality in Southeast Asia (296 000) where this phenomenon is accompanied by drier conditions and increased fire activity (Johnston *et al*., 2012).

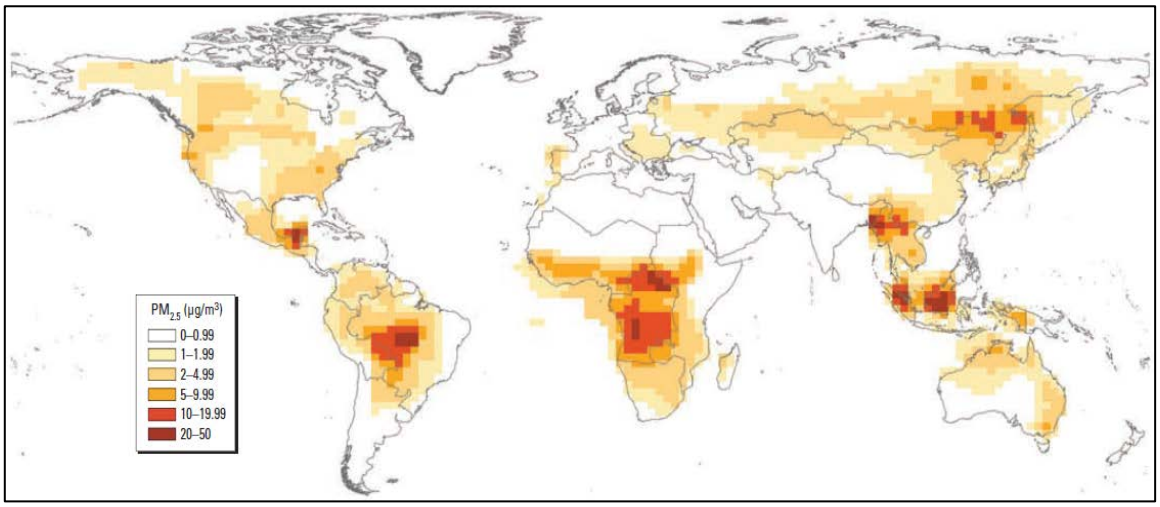

Figure 3.13 **Estimated annual average PM2.5 concentrations from landscape fires for the period 1997 – 2006 (Johnston *et al*., 2012).**

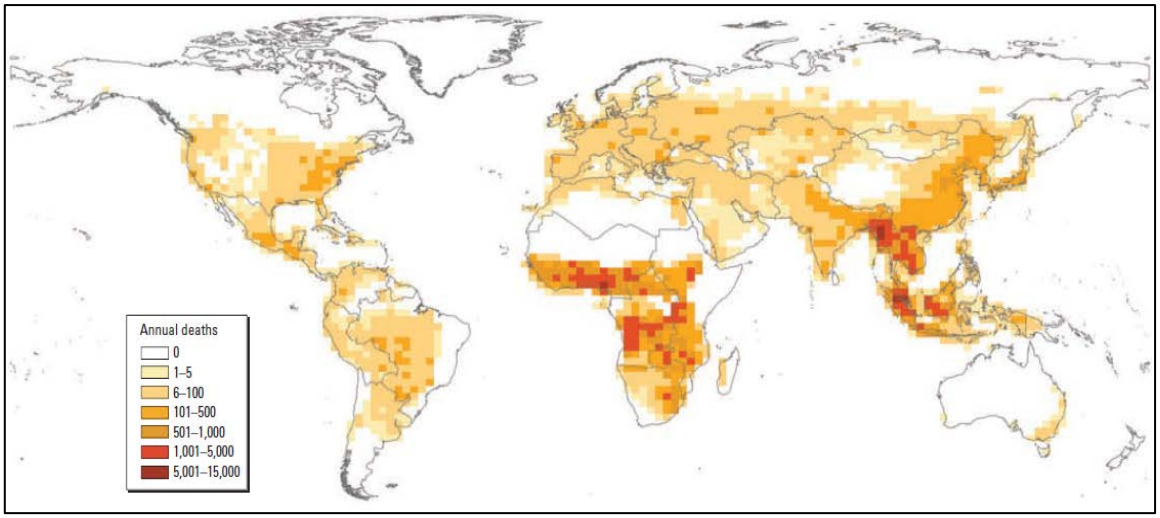

Figure 3.14 Estimated annual average global mortality attributable to exposure to smoke from landscape fires for the period 1997 – 2006 (Johnston *et al*., 2012).

Health impacts and mortality due to wildfire smoke are not limited to humans only (Sections 3.1, 3.2 and 3.3.3). Unfortunately, little information is available on the health effects of wildfire smoke on plants or animals but several studies have focused on the impacts of ambient air pollution. It stands to reason that animal species with higher respiration rates (e.g. small mammals) inhale larger amounts of harmful pollutants (based on the numerous toxicological studies performed on laboratory mice, rats, guinea pigs, rabbits and dogs), while surface O_3 has been shown to induce changes in the soil biotic community (Feng *et al*., 2015; Li *et al*., 2015). Prolonged exposure of animals to SO_2 causes damage to airways (similar to chronic bronchitis in humans), while simultaneous exposure to PM2.5 may aggravate the effect (Bell & Adams, 2009). Formic acid and acrolein are also potent irritants in biomass smoke that can affect lung function (Bell & Adams, 2009).

Wildfire smoke can reach plant and soil surfaces through gaseous uptake or dry and wet deposition. According to Bell and Adams (2009) there is equal opportunity for smoke effects on plants to be beneficial (e.g. promote cell growth) as there is for it to be detrimental (e.g. causing cell injury or death). Uptake of smoke-delivered nutrients (e.g. ammonium and nitrate) should promote plant growth, while the opposite is true for a decreased photosynthetic rate (due to increased shading) and reduced stomatal function (as a response to pollutants like SO_2 and O_3) (Bell & Adams, 2009). The visible and physiological damage of tropospheric O_3 on plants are well documented (Felzer *et al*., 2007; Karnosky *et al*., 2007; Chubarova *et al*., 2009; Feng *et al*., 2015).

Young expanding leaves are probably more sensitive than older leaves, while anatomical and morphological adaptations of fire-prone vegetation may offer them higher protection to harmful pollutants (Bell & Adams, 2009).

3.4.2 Impact on Visibility

Emissions from wildfires can have a considerable impact on tropospheric chemistry and serve as a major source of visible air pollution (Urbanski *et al*., 2009). It is particularly the aerosol particles that render smoke from biomass fires visible to the naked eye, to the extent that it can often be seen from orbiting spacecraft some 400 km above the Earth (Andreae, 1997). Visibility is reduced as the aerosol particles absorb, scatter and reflect visible light, with PM2.5 being most effective scattering agent (Bell & Adams, 2009). Optically thicker smoke is produced during smouldering combustion and the burning of wet fuels (Sections 2.1 and 2.3), while high levels of humidity in the atmosphere will also tend to reduce visibility as more water is available to condensate on PM, increases its ability to scatter light (Fowler, 2003).

Smoke becomes a nuisance when it affects the aesthetics of a vista or hampers outdoor activities (Sandberg *et al*., 2002). Reduced visibility can disrupt road, air and in some cases even maritime traffic, occasionally with fatal consequences. Notorious examples of such disruptions on a regional scale are the large smoke haze events of 1997 and 2015 in Southeast Asia (Mydans, 1997; Rahayu, 2015), 2002 in Florida, U.S.A. (Fowler, 2003) and 2002 and 2010 in western and central Russia (Figure 3.15) (Chubarova *et al*., 2009; Levitov, 2010). Over the interior plateau of southern Africa smoke from wildfires (and to some extent from domestic fires in informal settlements) mostly affect visibility (and hence road and air traffic operations) around dusk and dawn during the winter months (personal experience as a former aviation forecaster). Low visibility brought about by smoke from runaway grassland fires in the Highveld region of South Africa have resulted in road accidents almost every year since 1990 (Trollope *et al*., 2004). Smoke can occasionally combine with fog over the Highveld to form thick smog that may linger over the area, especially when trapped beneath a pronounced surface temperature inversion. Similar conditions, referred to as “super fog”, have been reported in the southern U.S.A. (Sandberg *et al*., 2002; Fowler, 2003). Low visibility in the vicinity of wildfires can likewise hamper firefighting operations (e.g. McGuire, 2015; Seema, 2016).

Figure 3.15 **Smoke from peat fires over the Moscow region (left) as captured by the Moderate Resolution Imaging Spectroradiometer (MODIS) on board the Aqua satellite on 7 August 2010 with red outlines indicating actively burning fires to the east of the city (NASA EOS, 2010). At noon the horizontal visibility was reduced to about 300 m and the vertical visibility to 300 feet at Moscow's Sheremetyevo International Airport (right) (Gutnikov, 2010).**

3.4.3 Soiling of Materials

When soot (i.e. deposited smoke particles) accumulate on the façades of everyday objects (e.g. buildings, statues, motor vehicles, clothing etc.), the light absorbing particles form layers that reduce the amount of light reflected by such surfaces (Pesava *et al*., 1999). This effect, referred to as soiling, is a visual nuisance as it diminishes the aesthetic appeal of such surfaces and could result in physical damage through corrosion (Sandberg *et al*., 2002). Soiling diminishes the light transmission through transparent materials (e.g. windows) and result in power losses from photovoltaic solar panels (Maghami *et al*., 2016). Indoor environments are easily infiltrated by fine smoke particles where it can result in the soiling of fabrics, painted interior walls and works of art (Sandberg *et al*., 2002).

Generally, soiling has been shown to be a function of the PM concentration and time of exposure (Watt *et al*., 2008). While coarser particles like PM10 may initially contribute more to soiling, they are also more easily removed than PM2.5 (Sandberg *et al*., 2002). Studies suggest that a 35% loss in reflectance triggers significant adverse public reaction, warranting the cleaning of such surfaces (Watt *et al*., 2008). Repeated cleaning, washing or repainting of soiled surfaces constitutes an economic burden, can shorten the useful lifetime of the affected material (Sandberg *et al*., 2002) and may lead to the loss of fine detail on historical monuments (Watt *et al*., 2008).

3.5 FIRE EFFECTS ON WEATHER AND CLIMATE

Although weather and climate play a pivotal role in wildfire activity (to be discussed in more detail in Section 4.2), a better understanding of the distribution of fire on Earth has led to a realisation of how fire may be involved in weather modification and climate forcing (Scott *et al*., 2014). As indicated in Section 2.3, wildland fires are large sources of trace gases and aerosols in the atmosphere. These pyrogenic emissions are thought to influence the climate system both directly (through the release of greenhouse gases and aerosols that act as climate forcers) and indirectly (through secondary effects on atmospheric chemistry and cloud microphysical properties) (Bowman *et al*., 2009; Urbanski *et al*., 2009; Johnston *et al*., 2012; Sommers *et al*., 2014).

3.5.1 Impact of Greenhouse Gases

Globally, fires are noteworthy contributors of greenhouse gases (GHG) to the atmosphere (Bowman *et al*., 2009; Miranda *et al*., 2009; Shi *et al*., 2015). It has been estimated that emissions from biomass burning (Section 2.3) account for more than 30% of the global atmospheric NO_x and NMHC, roughly 15% of CH_4, between 40 – 50% of CO (Lindesay, 1997; Mieville *et al*., 2010) and about 20% of CO_2 (Sandberg *et al*., 2002), thus contributing directly to the greenhouse effect.

Recent estimations place the average carbon emissions from biomass fires at about 2.0 Pg C yr^{-1} (Van der Werf *et al*., 2010), which is about a quarter of the amount stemming from fossil fuel combustion and cement production (7.8±0.6 Pg C y^{-1}) (IPCC, 2013). Estimations of emissions from biomass fires vary due to the use of different inventories and the diverse methods used to construct them, examples being the Global Inventory for Chemistry-Climate studies (GICC; Mieville *et al*. (2010)), Global Fire Emissions Database version 3 (GFED3; Van der Werf *et al*. (2010)), Fire Inventory from NCAR version 1.0 (FINN1.0; Wiedinmyer *et al*. (2011)), Global Fire Assimilation System version 1.0 (GFAS1.0; Kaiser *et al*. (2012)) and Global Fire Emissions Database version 4 (GFED4; Giglio *et al*. (2013)). These five global inventories of monthly CO_2 emissions from biomass burning were compared at both global and continental levels by Shi *et al*. (2015) for the period 2002 – 2011 (Figure 3.16). It is not surprising that there is a striking resemblance between the regions with the most frequent fires in Figure 1.1, the highest PM2.5 concentrations in Figure 3.13 and the

highest CO_2 emissions in Figures 3.16 and 3.17, namely Southeast Asia, sub-Saharan Africa and South America south of the equator. Annual CO_2 emissions, as averaged by Shi *et al*. (2015) over the 2002 – 2011 period, range from 6 521.3 to 9 661.5 Tg yr^{-1}.

Emissions for other species (i.e. gases and PM) can either be estimated with the use of emission factors or emission ratios. For each biomass fuel type emission factors (Table 3.2) convey the emission of a target species to the amount of fuel burned (e.g. Andreae & Merlet, 2001; Urbanski *et al*., 2009), while emission ratios relate the emission of the target species to that of a reference species, such as CO_2 (e.g. Mieville *et al*., 2010).

Table 3.2 Emission factors (in gram species per kilogram dry matter burned) of selected pyrogenic species emitted from different biomass fuel types (Andreae & Merlet, 2001)

Species	Grassland and Savanna	Tropical Forest	Extratropical Forest	Agricultural Residues
CO_2	1613 ± 95	1580 ± 90	1569 ± 13	1515 ± 17
CO	65 ± 20	104 ± 20	107 ± 37	92 ± 84
CH_4	2.3 ± 0.9	6.8 ± 2.0	4.7 ± 1.9	2.7
NO_x (as NO)	3.9 ± 2.4	1.6 ± 0.7	3.0 ± 1.4	2.5 ± 1.0
BC	0.48 ± 0.18	0.66 ± 0.31	0.56 ± 0.19	0.69 ± 0.13

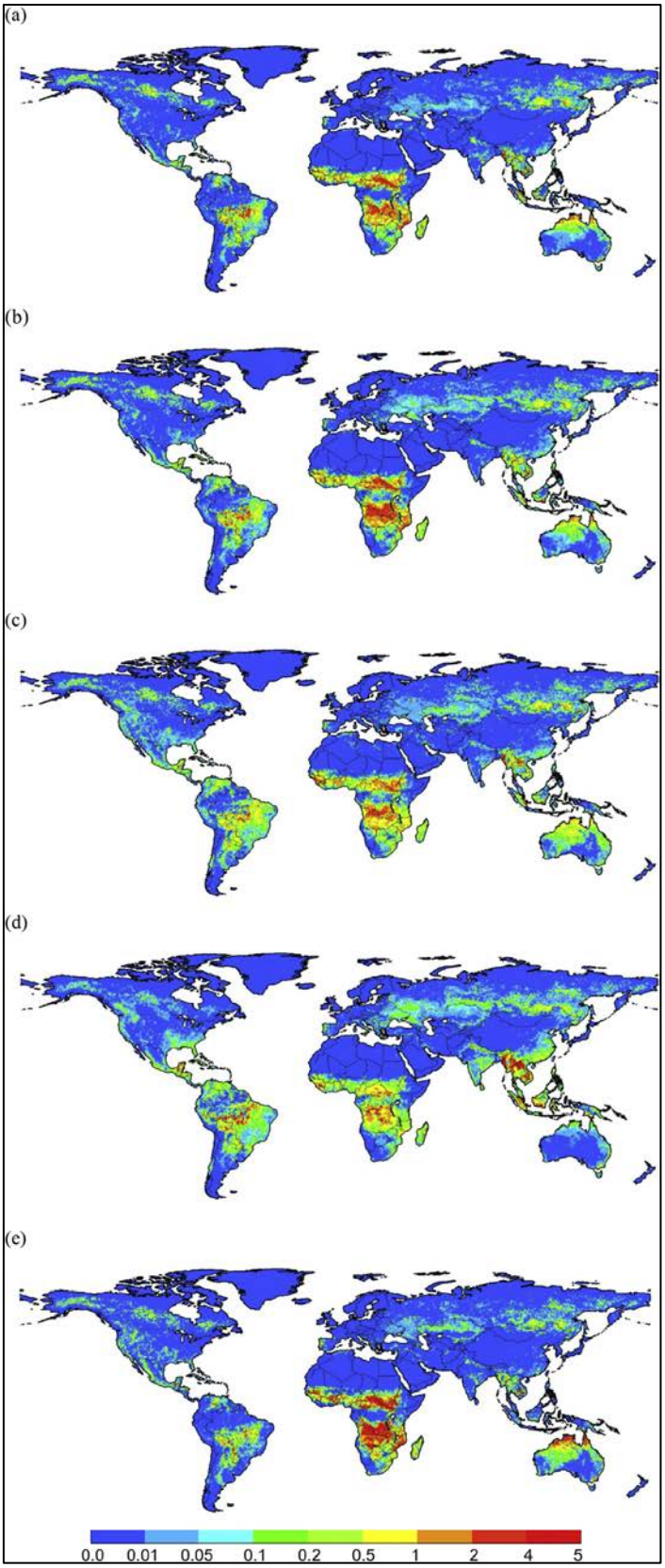

Figure 3.16 **Global distribution of annual CO_2 emissions (in Tg CO_2 yr^{-1}) for the period 2002 – 2011 derived from five distinct inventories: (a) Global Fire Emissions Database version 3 (GFED3); (b) Global Fire Emissions Database version 4 (GFED4); (c) Global Fire Assimilation System version 1.0 (GFAS1.0); (d) Fire Inventory from NCAR version 1.0 (FINN1.0) and (e) Global Inventory for Chemistry-Climate studies (GICC) (Shi *et al.*, 2015).**

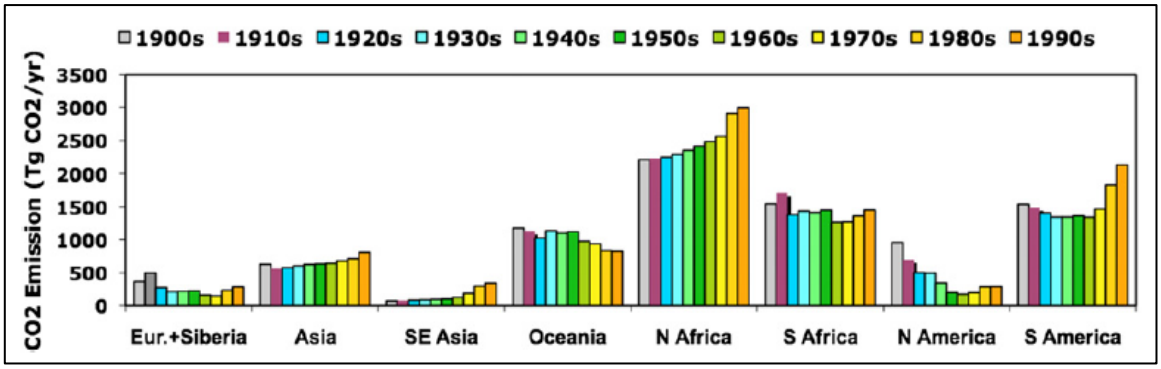

Figure 3.17 The evolution of CO_2 emissions for different world regions from 1900 to 2000 (Mieville *et al*., 2010).

The longer term dataset used by Mieville *et al*. (2010) showed a decrease in global biomass burning emissions between 1900 and 1930, where after it remained relatively stable (at an average of 7 400 Tg CO_2 yr^{-1}) until the 1970s and increased promptly since the 1980s (Figure 3.17). During the 20th century emissions have decreased significantly in North America, Siberia and Australia, while increases was noticed in central and southeast Asia, northern Africa and South America (Figure 3.17). More than half of the global fire emissions originate from Africa (Van der Werf *et al*., 2010; Shi *et al*., 2015).

It is, however, necessary to differentiate between forms of biomass burning that result in a temporary as opposed to a net release of gases such as CO_2 into the atmosphere (Stocks & Trollope, 1993). If regrowth of the same vegetation types takes place after a fire, it is assumed to be neither a source nor a sink for CO_2 (Ward *et al*., 2012). Burning grasslands, for example, release CO_2 into the atmosphere but it is readily absorbed when regrowth takes place (Stocks & Trollope, 1993). Of greater concern is the slash-and-burn agriculture, increased domestic demand for fuelwood and destruction of forests that involve either a net release of CO_2 or a reduced capability of the biosphere to reabsorb CO_2 as readily as in the past (Stocks & Trollope, 1993; Amiro *et al*., 2009). According to Amiro *et al*. (2001) it takes anything from one to three decades for a burned boreal forest to reach the same daytime downward carbon fluxes as a mature unburned one. Shi *et al*. (2015) found that the majority of the global CO_2 emissions came from savanna and grasslands fires (48% or 3366.1 Tg CO_2 yr^{-1}), followed by woodland/forest fires (41% or 2866.7 Tg CO_2 yr^{-1}) and the burning of cultivated areas (11% or 772.3 Tg CO_2 yr^{-1}). Although their estimates may differ, the

relative contributions by these three land cover types are supported by Mieville *et al*. (2010) and Van der Werf *et al*. (2010).

Emissions of GHGs have resulted in significant perturbations in the atmosphere's radiative balance (Mieville *et al*., 2010). The attendant global warming is likely to further increase fire activity (Westerling *et al*., 2006; Higuera, 2015), resulting in a positive feedback with further spikes of GHG emissions. In Section 3.1 the role of fire as a key mechanism in the redistribution of ecosystems was highlighted. This response is especially dynamic when subjected to climate stress, whereas any alterations in the landscape mosaic will subsequently affect the atmosphere-biosphere carbon balance (Goldammer & Crutzen, 1993; Sandberg *et al*., 2002).

3.5.2 Impact of Aerosols

As indicated in Section 2.3, smoke from vegetation fires is a natural source of aerosol particles in the atmosphere. These aerosols perturb regional (and probably global) radiation budgets owing to their surface albedo and light-scattering effects, and their effect on cloud microphysical processes (Andreae & Metlet, 2001; Cotton & Pielke, 2007; Bowman *et al*., 2009; Scott *et al*., 2014). The climatic effect of aerosols is determined by the following features (Andreae, 1997; IPCC, 2013):

- abundance;
- size distribution;
- optical properties;
- solubility; and
- spatial distribution.

Cloud droplets tend to form on aerosol particles that act as cloud condensation nuclei (CCN), with the number of CCN depending on the purity of the air (Anthes *et al*., 1975; Tyson & Preston-Whyte, 2000; Rosenfeld & Woodley, 2001; Rosenfeld *et al*., 2008). Locally, wildfires generate large amounts of heat, capable of producing very strong convergence and uplift of low-level air (Anthes *et al*., 1975; Rosenfeld *et al*., 2007). The rising smoke column offers a greater number of CCN or ice nuclei (IN) that not only facilitate cloud development but also alter their microphysical properties (e.g. drop

size distribution) and consequent precipitation-forming processes (Sandberg *et al*., 2002; Rosenfeld *et al*., 2008).

In terms of the drop size distribution, it is evident that the added CCN in polluted clouds result in a larger number of smaller droplets (Price & Rind, 1994; Rosenfeld & Woodley, 2001; Rosenfeld *et al*., 2007; Scott *et al*., 2014). Smaller droplets take significantly longer to grow into raindrops through collision-coalescence processes in warm clouds or rime onto snowflakes in cold or mixed clouds (Tyson & Preston-Whyte, 2000; Rosenfeld & Woodley, 2001; Rosenfeld *et al*., 2008). The slower conversion of water vapour into raindrops is believed to supress rainfall from shallow, short-lived clouds, while invigorating deep convective clouds with warm bases by delaying the initiation of precipitation and allowing them to enter the ice phase (Bell *et al*., 2008; Rosenfeld *et al*., 2008). The latter implies greater instability for the same amount of rainfall. Rosenfeld *et al*. (2008) concluded that the addition of numerous small CCN in warm-base clouds would lower their precipitation efficiency but enhanced convective overturning (Figure 3.18), while the same action will have the opposite effect on cold-base (above 0°C isotherm) clouds.

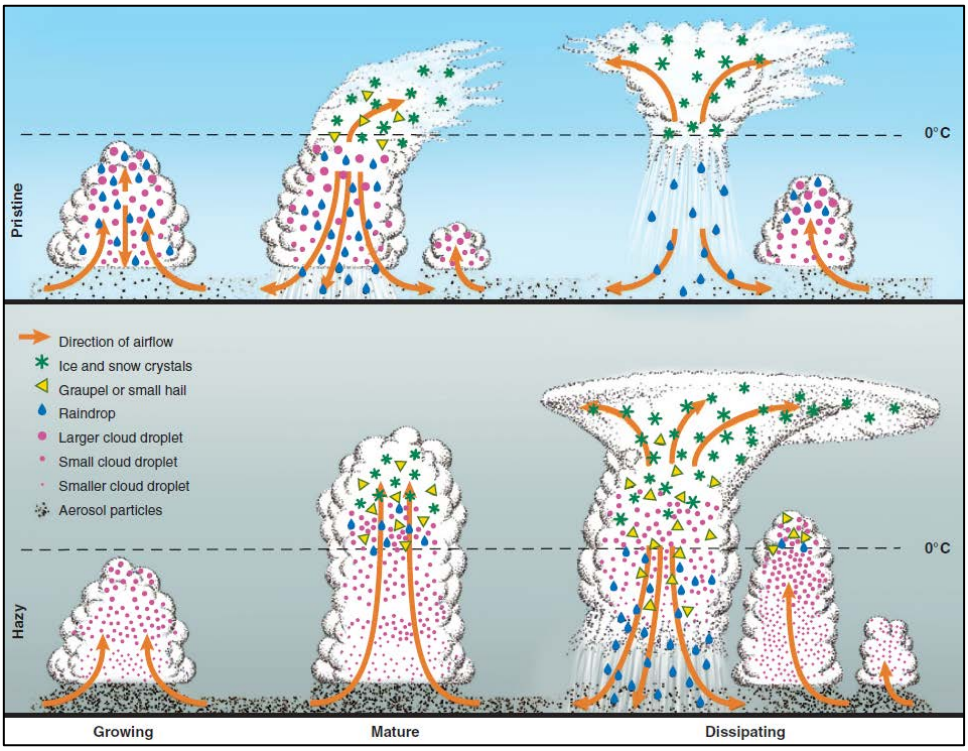

Figure 3.18 **Conceptual model of deep convective clouds developing in the pristine (top) and polluted (bottom) atmosphere. Clouds in pristine air have higher precipitation efficiencies, while those in the polluted atmosphere do not precipitate before they reach supercooled levels (Rosenfeld *et al*., 2008).**

An indirect influence of the aerosols is the slowing down of the growth of precipitation through the ice phase (Rosenfeld & Woodley, 2001). According to Rosenfeld *et al*. (2007) the few large hydrometeors that do form can grow to large hailstones without correspondingly high rain intensity. In fact, the Chisholm (Canada) firestorm of 28 May 2001 was characterised by a violent overshooting updraft, capable of injecting smoke into the lower stratosphere, supressed rainfall and an inordinate amount of positive lightning (Rosenfeld *et al*., 2007). The only precipitation reported during the Canberra, Australia, firestorm (Section 4.4) was soot-blackened hailstones (Fromm *et al*., 2006). On a regional scale, precipitation radar data from the Tropical Rainfall Measuring Mission (TRMM) satellite showed that rainfall was greatly diminished in polluted regions (e.g. the Congo basin), whether the pollution stemmed from industries or massive wildfires (Rosenfeld & Woodley, 2001).

Once airborne, pyrogenic particles may be transported vast distances by winds, traversing the width of entire continents or ocean basins and mixing with other natural and anthropogenic aerosols along the way (Ramanathan & Carmichael, 2008; Bowman *et al*., 2009). The polluted airstream, by virtue of its higher CCN and IN concentration, promotes cloud development with light-reflecting droplets and particles (e.g. sulphates) making the plume hazy and light-absorbing aerosols (e.g. BC) causing it to turn brownish (Ramanathan & Feng, 2008). This gives rise to so-called atmospheric brown clouds (ABCs) with lifetimes of a few weeks or less (Ramanathan & Carmichael, 2008; Ramanathan & Feng, 2008; Ramanathan & Feng, 2009). Within the ABCs, aerosols have two opposing indirect effects that are either microphysical or radiative in nature (Ramanathan & Feng, 2009; Ward *et al*., 2012; Scott *et al*., 2014).

In addition to an increased cloud cover, the higher concentrations of tiny water and ice droplets in ABCs enhance their brightness relative to pristine clouds (Price & Rind, 1994; Rosenfeld & Woodley, 2001; Rosenfeld *et al*., 2007; Ramanathan & Feng, 2009; IPCC, 2013; Scott *et al*., 2014). This is because the net reflected radiation is inversely proportional to the size of the cloud droplets (Rosenfeld & Woodley, 2001). Cloud cover and heights are particularly important over strong absorbing surfaces such as the ocean as ABCs introduce a highly reflective surface in comparison (Ward *et al*., 2012). Generally, the additional solar radiation reflected to space (referred to as the Twomey or cloud albedo effect) exerts a negative radiative forcing that can range from

0.3 to 1.8 W m^{-2} with a central value of 0.7 W m^{-2} (Ramanathan & Feng, 2009). In what is referred to as the Albrecht or cloud lifetime effect, more numerous and smaller droplets within ABCs can also alter their lifetime and hence the overall cloud reflectivity (Cotton & Pielke, 2007; Bond *et al*., 2013). Aerosols such as sulphates, nitrates and some organics also have a direct negative radiative forcing as they reflect solar radiation back to space (Ramanathan & Feng, 2009). According to Rosenfeld and Woodley (2001) the cloud albedo effect masks global warming, which explains why the more polluted northern hemisphere is warming less rapidly than the southern hemisphere.

Black carbon (BC) is "a distinct type of carbonaceous material formed from the incomplete combustion of fossil and biomass based fuels" (IPCC, 2013). BC comprises a substantial fraction of biomass-burning emissions (Table 3.2), augmenting existing atmospheric concentrations from other natural and anthropogenic sources (e.g. volcanic eruptions, fossil and biofuel combustion, etc.) within ABCs. Bond *et al*. (2013) estimated the total global BC emissions in the year 2000 to be around 7 500 Gg BC yr^{-1}(with an uncertainty range of 2 000 to 29 000 Gg yr^{-1}). Globally, BC emissions from open biomass burning (about 2 800 Gg BC yr^{-1}) is second only to energy-related burning (approximately 4 800 Gg BC yr^{-1}) (Bond *et al*., 2013). As was the case with PM2.5 (Figure 3.13) and CO_2 (Figure 3.16), the largest open burning BC emissions occur in Africa, Latin America and Southeast Asia, with Africa constituting the biggest source (Figure 3.19). Grass- and woodland fires contribute about 45% of global open fire emissions of BC (Bond *et al*., 2013) and are the dominant source of such emissions in Africa (Figure 3.19).

In addition to the general aerosol-cloud interactions already mentioned, atmospheric BC has particular climatological significance as it strongly affects the emissivity of ABCs. In fact, BC is the leading absorber of visible and ultraviolet (UV) solar radiation in the atmosphere (Ramanathan & Carmichael, 2008; Ramanathan & Feng, 2008), which results in increased tropospheric heating and tend to intensify greenhouse warming (Bowman *et al*., 2009; Ramanathan & Feng, 2009; Scott *et al*., 2014). According to Ramanathan and Carmichael (2008) the contribution made by BC emissions to current global warming is second only to CO_2. The global annual mean BC direct radiative forcing from all sources is estimated at +0.88 W m^{-2} (ranging from

+0.17 to +1.48 W m^{-2}) but can be significantly higher (~10 W m^{-2}) on a local scale due to its relatively short atmospheric lifetime (Bond *et al*., 2013). A semi-direct effect of atmospheric BC stems from their direct absorption within ABCs that may change the vertical temperature and hence stability profile within the troposphere, while the added heat within the clouds may also aid in their evaporation thereby altering cloud distributions (Ward *et al*., 2012; Bond *et al*., 2013).

The high concentrations of aerosols, especially over continental regions (Figure 3.13), imply that cloud cover and composition are affected by both their microphysical and radiative impacts (Rosenfeld *et al*., 2008). Regionally, the enhanced attenuation of solar radiation by reflection and absorption in ABCs result in a large surface dimming (Ramanathan & Feng, 2009). The dimming reduces surface heating and evapotranspiration, which inhibits convection and slows down the hydrological cycle (Rosenfeld *et al*., 2008; Bowman *et al*., 2009; Ramanathan & Feng, 2009). Since the release of latent heat is closely linked to raincloud formation and precipitation processes, these effects can even induce atmospheric circulation changes (Rosenfeld & Woodley, 2001; Rosenfeld *et al*., 2008). One example is the enhanced mid-week lower-level moisture convergence, uplift and precipitation observed over the south-eastern U.S.A., along with compensatory changes in similar measures over the adjoining ocean (Bell *et al*., 2008). It has also been suggested that the dimming mechanism has contributed to the drying in the Sahel, particularly during the 20th century, as it cooled the North Atlantic Ocean resulting in a southward displacement of the Inter-tropical Convergence Zone (ITCZ) (Rosenfeld *et al*., 2008).

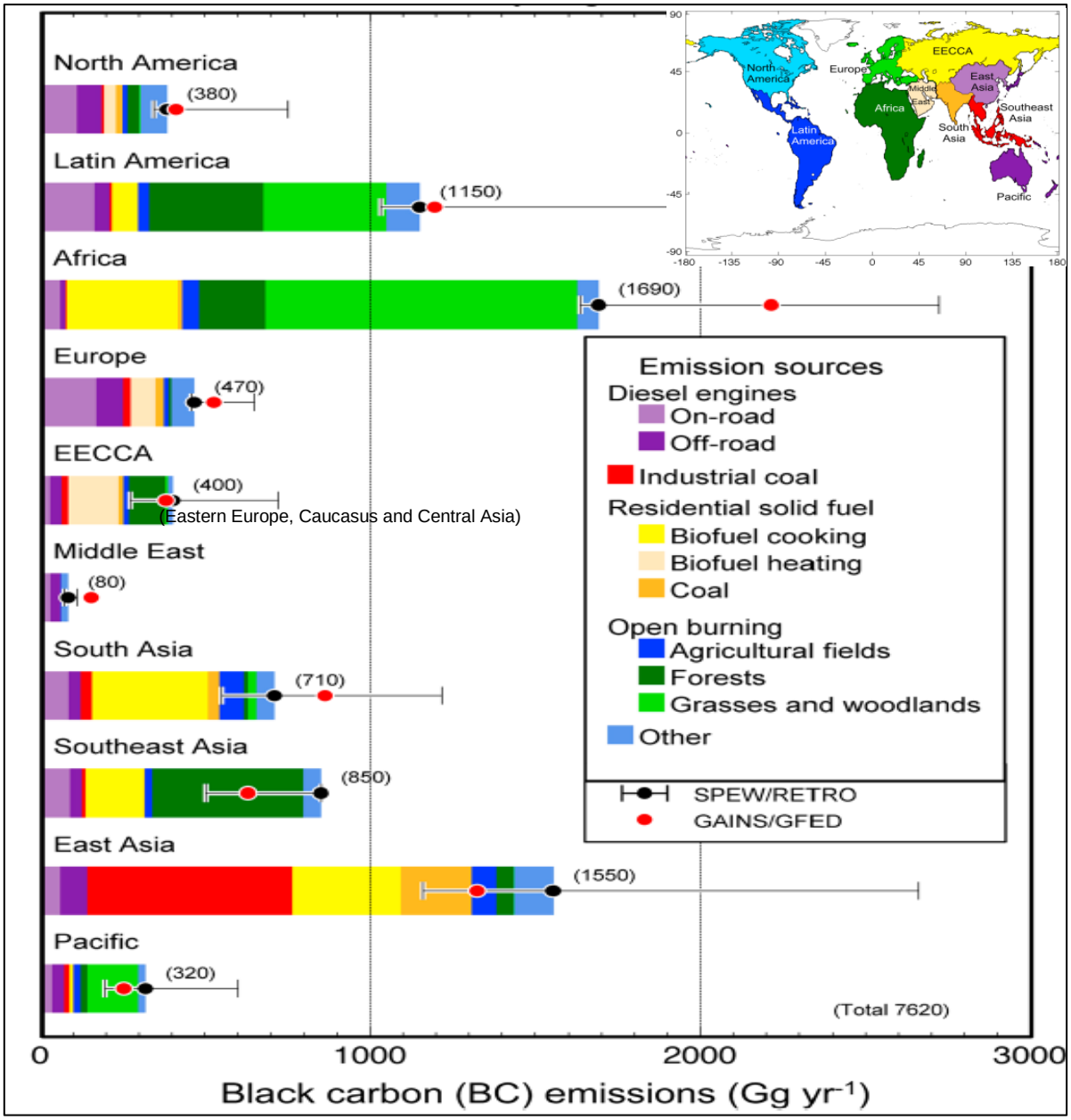

Figure 3.19 **Black carbon emission rates by region and source in the year 2000. Inventories used: SPEW = Speciated Pollutant Emissions Wizard; RETRO = REanalysis of the TROposphere over the last 40 years; GAINS = Greenhouse gas and Air pollution INteractions and Synergies; GFED = Global Fire Emissions Database. SPEW emissions are shown in coloured bars with black horizontal error bars denoting uncertainties. (Bond *et al*., 2013).**

3.5.3 Impact of Surface Albedo Changes

Fires may affect the radiation balance by altering the surface albedo of an area (Bowman *et al*., 2009; Scott *et al*., 2014). Burning can turn a green vegetation cover black, although such surface charring is relatively transitory and usually disappears within a year or two (Ward *et al*., 2012). The annual mean albedo-related radiative forcing due to burn scars over the African continent alone has been estimated at 0.015 W m^{-2} (Figure 3.20a), while monthly local maxima can be as large as 8 W m^{-2} (Myhre *et al*., 2005). The surface albedo-related radiative forcing due to burn scars is generally weaker than the direct radiative forcing from pyrogenic aerosols (Figure 3.20b), since the latter also reduces the amount of incident radiation (Myhre *et al*., 2005). However, over longer time periods repeated burning has been shown to change a dark mesic forest into lighter coloured grassland (Section 3.1). In higher latitudes burning may lead to an overall increase in surface albedo as burn scars are more easily covered by snow (Ward *et al*., 2012; IPCC, 2013), while regrowth in boreal forests tend to be more reflective thus resulting in a negative forcing that peaks during the second decade after fire (Beck *et al*., 2011; Jin *et al*., 2012).

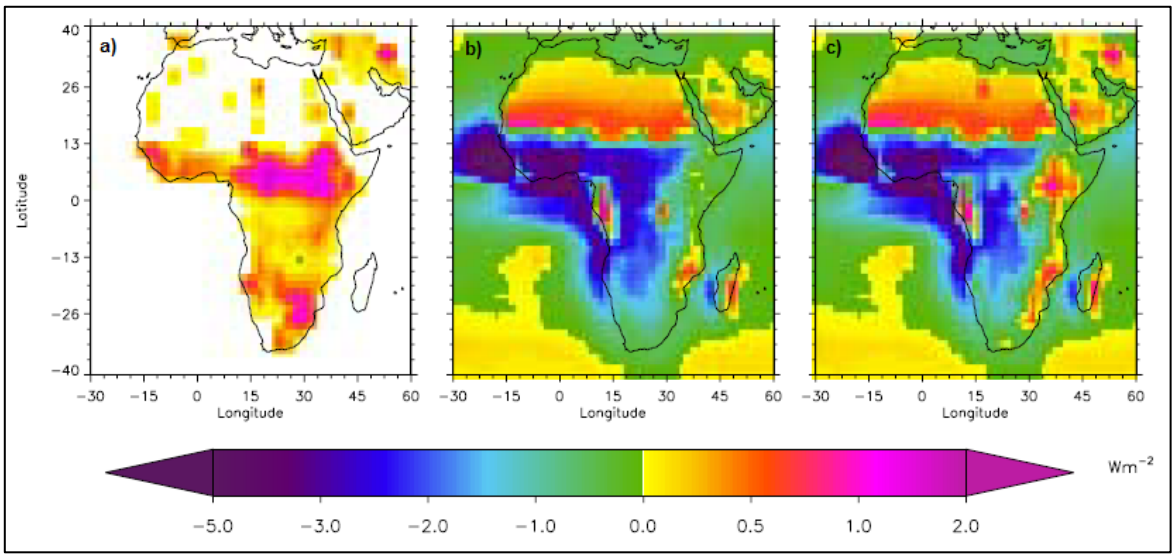

Figure 3.20 **Annual mean radiative forcing due to (a) reduced surface albedo from burn scars; (b) biomass burning aerosols; and (c) combined effect of surface albedo change and biomass aerosols (Myhre *et al*., 2005).**

Contamination of snow by light-absorbing impurities (LAI), typically dominated by BC and mineral dust, or its deposition on glaciers, snowfields or sea ice reduces the reflectivity of such surfaces and cause them to absorb more solar radiation (Hagler *et al*., 2007; Bond *et al*., 2013; Scott *et al*., 2014). Even slight initial reductions in snow

albedo may result in warming which influences snow morphology (grain size), sublimation and melting rates (Hadley & Kirchstetter, 2012; Bond *et al*., 2013; Ming *et al*., 2013). Whereas BC reduces snowpack albedo most noticeably at visible and ultraviolet wavelengths (Figure 3.21b), an increase in snow grain size (a secondary effect of the attendant warming) affects albedo strongly at near-infrared wavelengths (Figure 3.21a). Ming *et al*. (2013) found that BC and increased grain size can reduce the snowpack albedo by 11% and 61%, respectively. Melting and sublimation at the top of the snowpack will cause BC accumulation (Figure 3.22), which further enhances snow albedo reductions (IPCC, 2013).

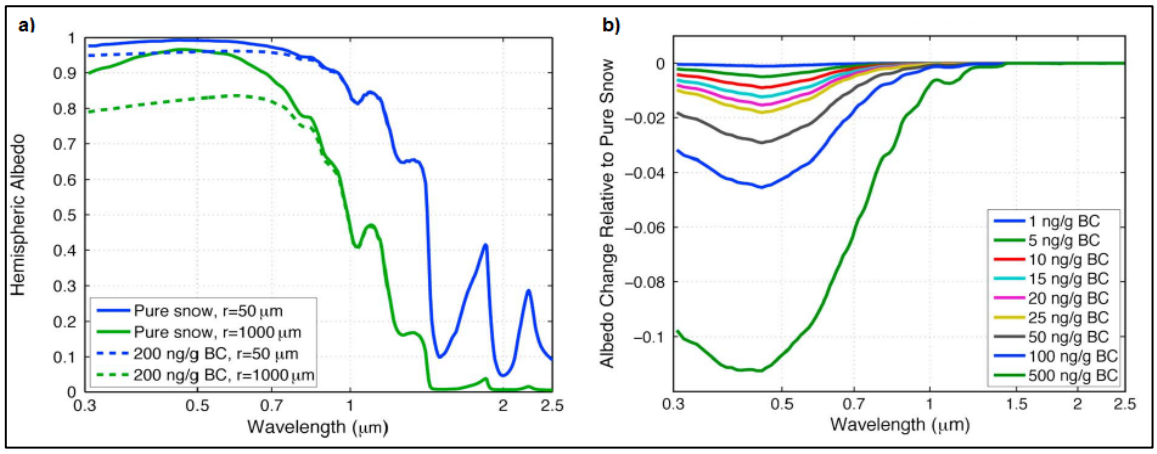

Figure 3.21 **Changes in snow albedo due to black carbon (BC) showing (a) Hemispheric albedo for effective snow grain radii (r) of 50 and 1 000 µm, with and without BC mixing ratios of 200 ng g^{-1} for a semi-infinite snowpack and diffuse incident solar radiation; and (b) Reduction in hemispheric albedo at different BC mixing ratios for a snowpack with effective grain size of 200 µm (Bond *et al*., 2013).**

Figure 3.22 **A canyon carved by meltwater in the Greenland ice sheet. The black material pooled at the bottom of the canyon is referred to as cryoconite – a mixture of windblown mineral dust, small rock particles from volcanic eruptions, black carbon and microbes (Balog, 2010).**

The surface albedo feedback mechanism of “dark snow” has been found to contribute to global warming and speed up the melting of snow and ice surfaces, particularly in middle and high latitudes (Ramanathan & Carmichael, 2008; Hadley & Kirchstetter, 2012; Yasunari *et al*., 2015). In high-altitude regions such as the Himalayas and Tibetan Plateau forcing due to dark snow influences the mass balance of glaciers and the timing of springtime run-off formation due to snowmelt (Bond *et al*., 2013; Lin *et al*., 2013; Jacobi *et al*., 2015). LAI is accredited for about 30% of glacial melt in India (Lang, 2014). Since these glaciers normally supply water through the seasons to several large rivers (e.g. Indus, Ganges, Brahmaputra, Mekong and Yangtze), this would have implications on downstream water resources, hydropower generation and agriculture, possibly affecting a billion people (Bond *et al*., 2013; Jacobi *et al*., 2015). Changes in the cryosphere may further alter the hydrological cycle and disturb the Asian monsoon circulation (Jacobi *et al*., 2015).

3.5.4 Overall Contribution to Climate Change

From the foregoing discussion it is evident that wildfires have significant climatic effects through their impact on vegetation and surface albedo, the emissions of GHGs, aerosols and aerosol precursors and changes to biogeochemical cycles (Figure 3.23). Admittedly, the overall contribution of fires to climate change is difficult to judge due to the various positive and negative radiative forcings described and the mixing of pyrogenic aerosols with those from other natural and anthropogenic sources. The various forcings may even cancel each other out (Bowman *et al*., 2009), while climate feedbacks add even more complexity (Cotton & Pielke, 2007).

According to the fifth assessment report (AR5) of the Intergovernmental Panel for Climate Change (IPCC, 2013), the effective radiative forcing (ERF) due to aerosol-radiation interaction between 1750 and 2011 from all sources is estimated at -0.45 (ranging from -0.95 to +0.05) W m^{-2}, while the ERF due to aerosol-cloud interaction is -0.45 (ranging from -1.2 to 0.0) W m^{-2} (Figure 3.24). The total aerosol ERF (i.e. ERF due to aerosol-radiation and aerosol-cloud interactions from all sources) is estimated to fall between -1.9 and -0.1 W m^{-2} with a best estimate value of -0.9 W m^{-2} (IPCC, 2013). BC on snow and ice (from all sources) constitutes a positive radiative forcing of +0.04 W m^{-2} (ranging from +0.02 to +0.09 W m^{-2}) over the same time period (Figure 3.24) (IPCC, 2013).

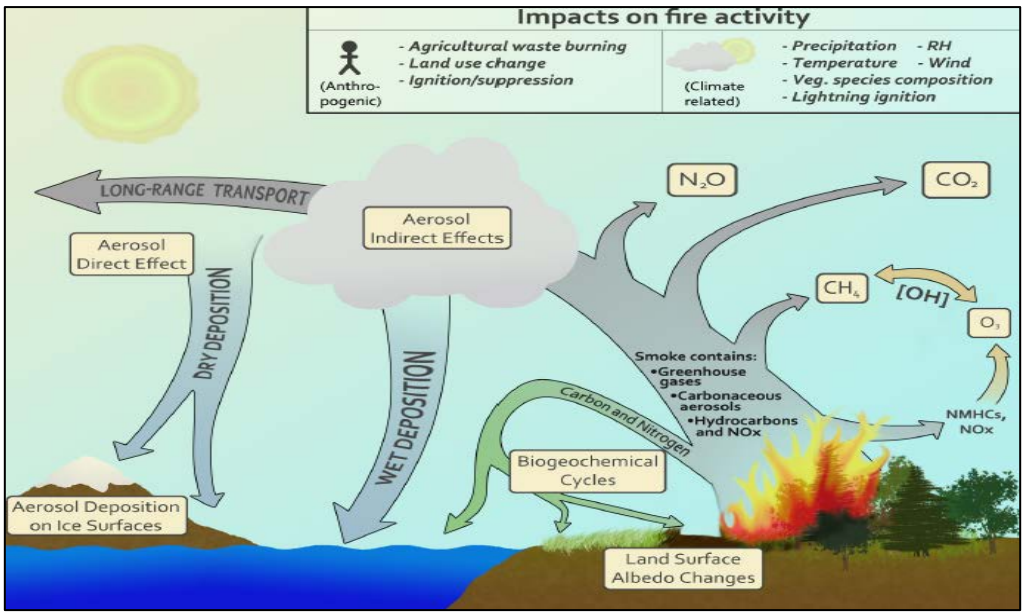

Figure 3.23 The various climate-related impacts of fire (Ward *et al*., 2012).

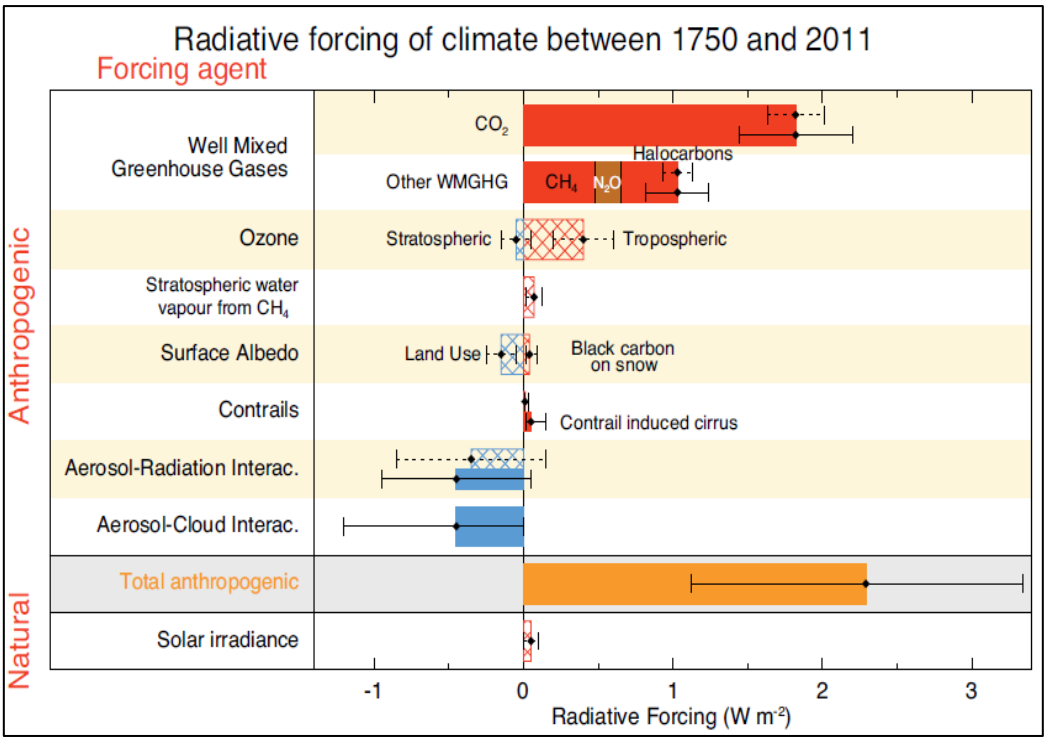

Figure 3.24 All source radiative forcing (hatched bars) and effective radiative forcing (solid bars) for the period 1750 – 2011. Horizontal error bars denote uncertainties (5 to 95% confidence range) (IPCC, 2013).

Ward *et al*. (2012) attempted to consider fire emissions alone when ascribing RFs to the various radiative effects (i.e. removing the RF due to other emission sources). For the current climate Ward *et al*. (2012) computed the RFs summarised in Table 3.3 using fire emissions obtained from the Community Land Model version 3.5 (CLM3).

As indicated, the overall RF due to fire is negative (-0.55 W m^{-2}; Table 3.3), constituting a cooling influence on the global climate. From this estimation the relative strength of the indirect cloud effects are evident. It should be noted that, although the RF of BC deposition on snow and ice surfaces seems negligible, it could culminate in a forcing up to three times greater than CO_2 as snowmelt is accelerated (Ward *et al*., 2012).

Table 3.3 Radiative forcings for various fire impacts (after Ward *et al*., 2012)

Radiative Effect	Radiative Forcing (W m^{-2})
Carbon Dioxide	+0.62
Methane	+0.05
Nitrous Oxide	+0.03
Tropospheric Ozone	+0.03
Direct Effect – All sky	+0.10
Direct Effect – Clear sky*	-0.15
Indirect Cloud Effects	-1.00
Indirect Biogeochemical Effects	-0.08 ± 0.08
Land Albedo Changes	-0.20
Snow/Ice Albedo Changes	0.00
Feedback onto C-cycle	-0.10 ± 0.10
Total	**-0.55**

* not included in the total

Tosca *et al*. (2013) used a global climate model, the Community Atmosphere Model version 5 (CAM5), to evaluate the climate response to pyrogenic aerosol forcing. Two simulations were conducted for the period 1997 – 2009: one with fire aerosol emissions in addition to all other sources (FIRE) and one without the inclusion of fire aerosol emissions (NOFIRE). Inclusion of fire emissions increased the global mean annual aerosol optical depth (AOD) by 10% (Figure 3.25a), which resulted in a 1% (1.3 ± 0.2 W m^{-2}) reduction in the globally averaged all-sky net surface shortwave radiation. The dimming was particularly strong over the major burning regions of sub-Saharan Africa, South America and Southeast Asia (Figure 3.25b), with area-averaged decreases of 8% (-19.1 ± 3.2 W m^{-2}) over southern Africa. In response, global surface temperatures decreased by 0.13 ± 0.01°C (Figure 3.25c), with the anomalies over southern Africa averaging -0.46 ± 0.07°C.

Though global precipitation waned only slightly (1% or $2.9 \times 10^{-2} \pm 0.3 \times 10^{-2}$ mm d^{-1}), a complex spatial pattern of change unfolded with large negative anomalies near the Equator offset by smaller positive ones between 5 and 10° latitude (Figure 3.25d). When considering vertical velocities, it became evident that the knock-on effect of fire aerosols was a reduction in equatorial ascend and a subsequent weakening of the Hadley circulation (indicated by the positive anomalies in the vicinity of the Equator in

Figure 3.25e). A weakening of the Hadley circulation would explain the precipitation decreases indicated over equatorial regions (Figure 3.25d). Although non-aerosol effects were not considered, the results put forward by Tosca *et al*. (2013) demonstrate a plausible link between pyrogenic aerosols and the strength and extent of the Hadley cell, thus affecting global atmospheric circulation.

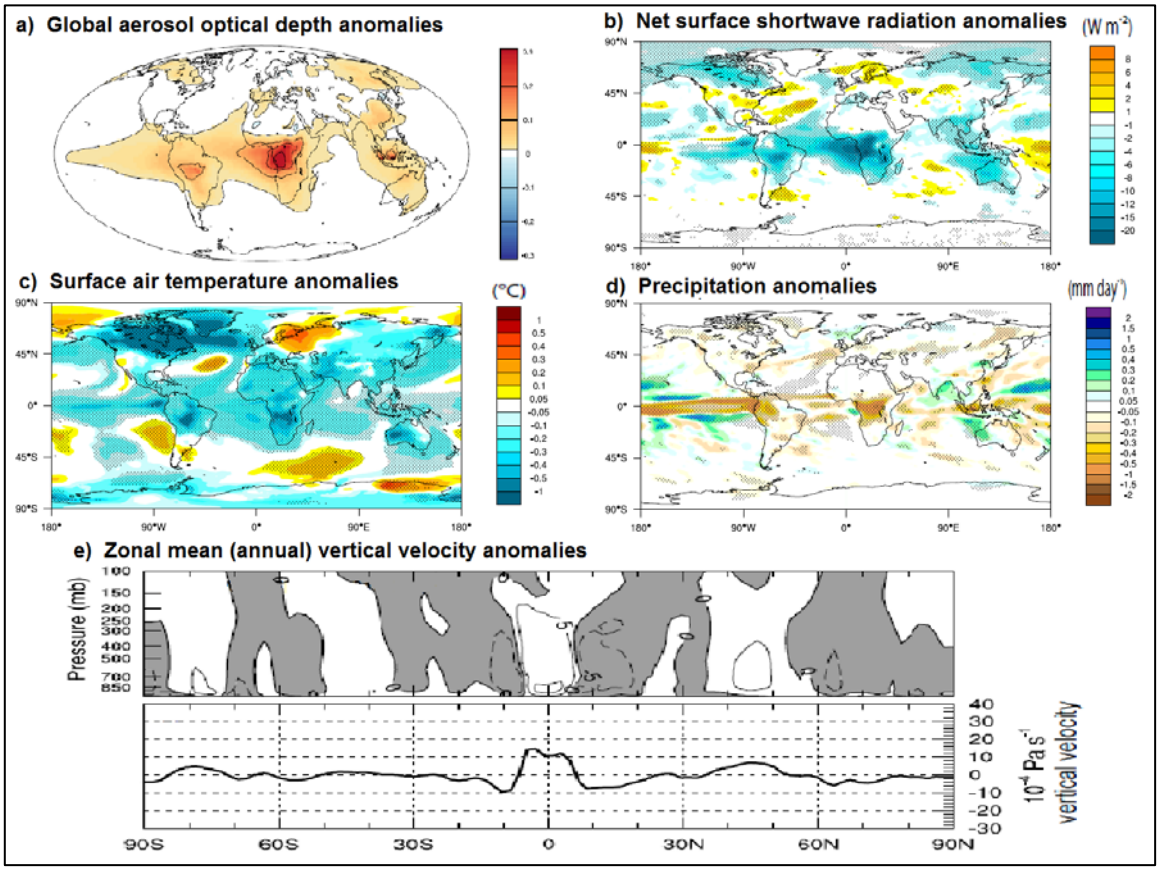

Figure 3.25 **Zonally averaged anomalies (FIRE - NOFIRE) derived from CAM5 simulations: (a) aerosol optical depth (unitless); (b) all-sky net surface shortwave radiation (W m^{-2}); (c) surface temperature (°C); (d) precipitation (mm d^{-1}); and (e) zonal mean (annual) vertical velocities (Pa s^{-1}) with negative values (shaded) indicating increased upward motion and 500 mb anomalies in the insert below (Tosca *et al*., 2013).**

3.6 ECONOMIC EFFECTS OF FIRE

The economics of fire effects are nontrivial (Brown *et al*., 2004). The effect of wildfires on local or regional economies can be both positive and negative (Diaz, 2012). Positive effects stem from economic activity generated by fire suppression and post-fire rebuilding (Diaz, 2012). The influx of firefighting teams into an area has the potential to generate revenue for the community as they patronize local businesses, while additional employment opportunities will also be created if contracting is done

locally (Fowler, 2003; Diaz, 2012). During times of disaster sales of emergency and non-luxury goods (e.g. bottled water, canned food, first aid kits, power generators, fuel etc.) usually skyrocket, occasionally leaving supermarket shelves empty as community members attempt to secure a stockpile in case of a breakdown in normal supply chains. It appears that catastrophic wildfires boost immediate retail at the expense of future purchases (Mercer *et al*., 2000). Although not necessarily based in local communities, fire prevention and suppression can be a lucrative industry (i.e. supply of firefighting gear and equipment) which relies on frequent wild- or controlled fires.

Key aspects that may impact negatively on local or regional economies include (Mercer *et al*., 2000; Brown *et al*., 2004; Rahn, 2009; Diaz, 2012):

- damage to agricultural production (e.g. timber, grazing and cropped lands);
- damage to the natural resource base on which the community relies;
- loss or damage to infrastructure and property (e.g. buildings, roads, bridges, signage, fences, communication facilities, transformers, power lines, water delivery systems etc.);
- loss of businesses, retail and employment;
- cost of fire suppression and protection (e.g. staff, accommodation, meals, equipment, supplies, transportation etc.);
- rescue and evacuation costs;
- watershed and water quality mitigation (e.g. mitigating soil erosion, removing debris from waterways and additional purifying costs);
- cost of post-disaster recovery (e.g. costs of maintenance and damage assessment teams, sensitive species and habitat restoration).
- increased health costs and loss of productivity; and
- forgone recreational and tourism activities and related income.

In addition, governments can cover insurance claims for unemployment or losses to infrastructure if wildfires are declared disasters. Lives lost, damages to ecosystems, cultural and historical resources and climate change related costs, however, are not easily quantified.

Mercer *et al*. (2000) quantified the economic impacts of the catastrophic 1998 wildfires that burned more than 2 000 km^2, mostly in the St. John's River Water Management District (SJRWMD) in north-eastern Florida (U.S.A.). The fire had a huge impact on the local timber industry, destroyed or damaged 337 homes, 33 businesses, several cars and boats, displaced hundreds of people and resulted in tourism-related losses that may have lingered well past the estimation period. The conservatively estimated total cost (which excluded fire-related health costs) of almost $900 million (Table 3.4) rivals that of tropical cyclones (Mercer *et al*., 2000). A similar study was conducted by Rahn (2009) on the series of wildfires that raged in San Diego, California (U.S.A.) in 2003. These fires burned more than 1 500 km^2, killing 16 people and destroying 3 241 homes in the process (Rahn, 2009; Diaz, 2012). The total estimated cost of the San Diego wildfires amounted to about $2.4 billion (Rahn, 2009), while the brunt of the economic impact was borne by the community (Figure 3.26). Stetler *et al*. (2010) also showed that property values in northwest Montana (U.S.A.) were negatively impacted when in proximity to or in view of wildfire burned areas.

Table 3.4 Estimated costs of the 1998 Florida fires (Mercer *et al*., 2000)

Cost Type	Total Estimated Cost	Cost per Acre	Percent Total
Timber (excl. hardwood)	$605 000 000	$1 212	69%
Fire Suppression	$100 000 000	$200	11%
Disaster Relief	$25 000 000	$50	3%
Property Losses (insured only)	$12 000 000	$24	1%
Tourism (excl. Baker and Marion counties)	$138 000 000	$276	16%
TOTAL	**$880 000 000**		

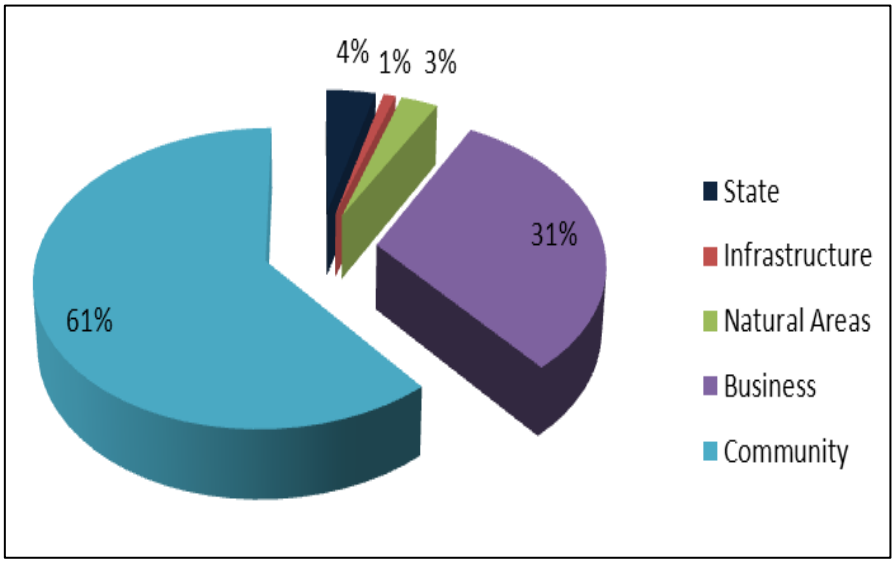

Figure 3.26 Fraction of total economic impact borne by various segments of society in aftermath of the 2003 San Diego wildfires (Rahn, 2009).

HEALTH COSTS

Whereas Mercer *et al*. (2000) neglected to include health costs (i.e. burn injury and exposure to smoke) in their analysis of the 1998 Florida wildfires, Moeltner *et al*. (2013) did manage to show that such costs can be considerable (in the magnitude of several million dollars per fire season) in a relatively small study area in northern Nevada (U.S.A.). Kochi *et al*. (2010) provide a review of the economic cost related to wildfire-smoke induced health effects. The estimated economic total cost, converted to 2007 $US value, of the 1997 haze event in Indonesia alone was $1.19 billion (Kochi *et al*., 2010).

TOURISM

Tourists and recreational facilities are vulnerable to the direct and indirect effects of wildfires (Flannigan *et al*., 2000; GFMC, 2016). Tourism is usually negatively impacted when wildfires threaten places of cultural and natural beauty, national parks, camp grounds and holiday resorts, causing significant downturns in tourism levels both during and after the disaster (Hystad & Keller, 2005; Sanders *et al*., 2008; Diaz, 2012; GFMC, 2016). This is partly due to safety issues (e.g. smoke inhalation, risk of landslides, damaged buildings, trails and bridges etc.) and partly because burned areas tend to be aesthetically unpleasing (Sanders *et al*., 2008). The affected areas are also characterised by a short-term decline in flora and fauna, thereby influencing visitor experience negatively (Sanders *et al*., 2008).

The 1988 wildfires in Yellowstone National Park (U.S.A.) resulted in a 15% decrease in visitation and an estimated loss in tourism economic benefits of about US$ 60 million (Sanders *et al*., 2008). The devastating fires of 2000 and 2001 on the island of Samos (Greece) destroyed mountain forests and several olive groves and vineyards, ruining it's attraction in terms of tourism (TUI, 2016). The 2003 wildfire in northeast Victoria (Australia) caused loss of business of roughly AU$ 20 million within the first month (Sanders *et al*., 2008). The tourism industry of Kelowna in British Columbia (Canada) was severely impacted by the 2003 Okanagan Mountain Park forest fire. During the fire, business revenue declined by 30 – 40%, while losses ranging anywhere from 10 – 90% were still reported several months thereafter (Hystad & Keller, 2005). Small businesses (e.g. restaurants, tour operators and lodges) suffered greater impacts with some forced to close permanently as the fire occurred during the height of the summer

tourist season (Hystad & Keller, 2005). Resorts, restaurants and stores in the popular Big Sur area of California (U.S.A.) also saw substantial reductions in business during the Soberanes Fire of 2016 as many tourists were scared away by the fire and smoke (Murphy, 2016).

3.7 FIRE AS A VELD MANAGEMENT PRACTICE

Even though fires have occurred naturally for millions of years (Bowman *et al*., 2009; Scott *et al*., 2014), aspects such as fire ignition and suppression as well as modification of fire regimes through land use and land cover change have been influenced by humans (Ward *et al*., 2012). Traditionally burning has been used in several parts of the world in a wide range of management objectives (e.g. grazing improvement, burning of agroforestry remains, hunting, etc.) (Lázaro & Montiel, 2010). Fire is used in slash-and-burn agriculture to clear forests for crops and pastures, often in an unsustainable manner (Stocks & Trollope, 1993). Yet controlled burning (also referred to as prescribed burning) as part of the veld management of both wildlife and domestic livestock systems is a well-established practice, particularly in the grasslands and savannas of semi-arid regions of the world (Duffey *et al*., 1974; Trollope *et al*., 2002).

Prescribed burning can be viewed as the application of fire to wildland vegetation under well-defined specific conditions (the prescription) in order to achieve more exact and desirable fire effects (Fernandes, 2010). Judicious prescribed burning therefore depends on the knowledge of both fire behaviour and fire impacts (Trollope, 2007; Fernandes, 2010).

3.7.1 Why Burn?

Burning is a necessary and often unavoidable tool in veld management for the reasons listed below (Thompson, 1937; Duffey *et al*., 1974; Stocks & Trollope, 1993; de Ronde *et al*., 2004a; Trollope, 2007):

- to increase biodiversity;
- to remove unpalatable and innutritious herbaceous grass material that is no longer acceptable to grazing animals;
- to stimulate the growth of nutritious new grass and to prepare seedbeds for natural or artificial seeding of desired forage species;
- to control and prevent invasion by undesirable plants (i.e. bush encroachment);

- to remove a fire hazard; and
- to control parasitic ticks and therefore alleviate the occurrence and spread of tick-borne livestock diseases.

Prescribed burning plays an important role in the removal of moribund and unpalatable grass material that is no longer acceptable to grazers such as cattle and sheep (Trollope, 1989; Stocks & Trollope, 1993; Trollope, 2007; Lohmann *et al*., 2014). The accumulated moribund material of previous seasons is often refused by livestock, while the grazing quality of the veld tends to deteriorate over an extended period of time if it is not removed. This view is supported by early studies which showed that desirable grass species may disappear completely or become stunted in growth and be replaced by vegetation of doubtful value (Thompson, 1937). According to Stocks and Trollope (1993) there is ample evidence to suggest that the botanical composition of the grass sward can be altered considerably by variations in fire regime (e.g. the season and frequency of burning), thereby improving the production potential of rangeland. Although the removal of the accumulated dry material by cutting instead of burning is advocated by some (Thompson, 1937), burning is often the only practical option in uneven terrain and where vegetation cover is relatively sparse. Burning stimulates the growth of nutritious new grass (Thompson, 1937) and prepares seedbeds for natural or artificial seeding of desired forage species (Duffey *et al*., 1974).

Another ecologically acceptable reason for using fire in grasslands and savannas is to prevent invasion by undesirable plants (i.e. bush encroachment) (Thompson, 1937; Trollope, 1989; Stocks & Trollope, 1993; Joubert *et al*., 2012; Lohmann *et al*., 2014). Bush encroachment is defined as a directional increase in the cover of woody species in grasslands and savannas (Smit *et al*., 1999; O'Connor *et al*., 2014), thereby decreasing the overall grazing capacity along with other ecosystem services like water retention and protection from soil erosion (Lohmann *et al*., 2014). Hoffman *et al*. (1999; cited by O'Connor *et al*., 2014) views bush encroachment as one of the biggest rangeland problems across 25% of the magisterial districts of South Africa. Due to the tillering habit of grass plants, burning favours the development of grasses at the expense of woody plants (Stocks & Trollope, 1993). Fire has a marked adverse effect

on the survival, growth, adult recruitment, and seedling regeneration of trees and shrubs (Bond & van Wilgen, 1996; O'Connor *et al*., 2014). Burning therefore constitutes an important ecological agent in maintaining an optimum balance between grass and bush vegetation in savanna ecosystems (Stocks & Trollope, 1993). Lohmann *et al*. (2014) found that the use of fire management to remove moribund material and control bush encroachment significantly increased the long-term average livestock stocking rates in semi-arid savanna rangelands.

Controlled burning can be used to remove a fire hazard. When vegetation is afforded protection and the annual growth not consumed, a serious practical difficulty arises with regards to the permanent prevention of catastrophic wildfires. Such wildfires, fed by higher fuel loads, can cause more devastation than occasional smaller controlled burns. The most devastating wildfire ever recorded in the southern Cape (February 1869) scorched an area of more than 500 km in length and occurred a few years after Brown, in his capacity as Colonial Botanist, secured the prohibition of burning in the then Cape Colony (Thompson, 1937). The term "security burning" is used by de Ronde *et al*. (2004a) to describe the construction of fire breaks (fuel breaks) for the purpose of either reducing the chances of wildfires or prescribed burns of entering areas where property or infrastructure can be damaged, or to restrict fires to a certain area.

Burning is an effective means of killing parasitic ticks and therefore alleviates the occurrence and spreading of tick-borne livestock diseases, although this practice seems poorly justified and a temporary solution when compared to the efficiency of regular dipping (Thompson, 1937). Trollope *et al*. (2003; cited by Trollope, 2007) reported on the successful application of controlled burning to significantly reduce tick populations in the Ngorongoro Crater and Serengeti grasslands of Tanzania.

3.7.2 Where to Burn?

Fire is frequently employed in areas where the annual rainfall exceeds 600 mm as the only practical and economical method of removing moribund material. Conversely, in more arid regions where the annual rainfall is less than 600 mm, the necessity to burn is reduced since the grass remains palatable and retains its nutritive value when mature (Stocks & Trollope, 1993). Before considering the application of fire, the condition of the veld in terms of its botanical composition, ecological status and basal

cover needs to be determined (Trollope, 2007). Trollope (2007) advises that prescribed burning should not be practiced when the grass sward is dominated by Increaser II species (i.e. grass and herbaceous species that increase in response to overgrazing). Under such conditions burning may result in further deterioration (van Oudtshoorn, 2012) and it is better to wait for the grassland to develop to a more productive stage dominated by decreaser species (i.e. grass and herbaceous species that decrease in response to under- and overgrazing). Conversely, Trollope (2007) recommends prescribed burning when the veld is undergrazed and dominated by Increaser I species (i.e. grass and herbaceous species that increase in response to under- or selective grazing). When the grass sward has become overgrown and moribund as a result of excessive self-shading, the standing grass crop is generally found to be greater than 4 000 kg ha^{-1} (Stocks & Trollope, 1993; Trollope, 2007). A Disc Pasture Meter (Bransby & Tainton, 1977) can be used to estimate the standing grass crop (fuel load) with the aid of the following equation (Trollope *et al*., 2004):

$$y = -3019 + 2260\sqrt{x}$$

where: y = mean grass fuel load (kg ha^{-1})

x = mean disc height of 100 readings (cm)

Prescribed burning of rangeland is therefore necessary where the grass fuel load is observed to exceed the 4 000 kg ha^{-1} threshold. Grass fuel loads required for burning to control bush encroachment may differ depending on the encroaching plant species (Trollope, 2007).

When performing prescribed burning for wildlife management, Trollope (2007) recommends that the fraction of burned area should not exceed 33% in arid (annual rainfall < 500 mm) and 50% of the total area in moist (annual rainfall > 700 mm) savanna and grassland ecosystems, respectively. This is to ensure that adequate forage is available for herbivores.

3.7.3 When to Burn?

When burning to remove moribund or to improve rangeland condition, the correct time to burn is determined by the season and the amount of combustible material (Trollope, 2007; van Oudtshoorn, 2012). There is a general consensus amongst rangeland scientists that prescribed burning should always be performed when the grass is

dormant (Thompson, 1937; Duffey *et al*., 1974; Everson *et al*., 1988; Stocks & Trollope, 1993; Trollope, 2007; Lohmann *et al*., 2014). However, early dry-season fires are believed to harm grass meristems, reduce fuel loads and encourage encroachment by undesired woody species (Pricope & Binford, 2012). Van Oudtshoorn (2012) also suggested burning as close as possible to the first seasonal rains so as to avoid exposing the newly stimulated growth to cold and water stress and to curb the removal of soil and nutrient-rich ash by strong winds. Trollope (2007) found that burning in late winter to remove moribund and to improve rangeland condition resulted in a greater recovery of the grass sward during the first post-fire growing season.

In either case, as low intensity fires (< 1 000 kW m^{-1}) are recommended for removing moribund material (Stocks & Trollope, 1993; Trollope, 2007; van Oudtshoorn, 2012) the best time for burning is on days when the fire danger is relatively low (i.e. when the air temperature is < 20°C and relative humidity > 50%). The frequency of burning will depend on the accumulation rate of surplus dry material, which should not exceed 4 000 kg ha^{-1} (Trollope *et al*., 2002). In the higher rainfall regions (annual rainfall exceeding 600 mm) characterised by sourveld (Section 6.2.1), this implies a burn frequency of every two to four years, while this frequency will be much lower in drier regions (Stocks & Trollope, 1993; Trollope, 2007). In fact, burning of sweetveld, typical of more arid regions (Section 6.2.1), is best avoided as the grass remains palatable in winter and will take a long time to recover should follow-up rains fail to occur (van Oudtshoorn, 2012; Snyman, 2005; 2015).

In contrast, when the aim is to remove unwanted woody species, burning should take place on days when the fire danger is relatively high (i.e. when the air temperature is > 25°C and relative humidity < 30%) and grass fuel loads exceed 4 000 kg ha^{-1} (Trollope *et al*., 2002). For safety reasons, prescribed burning is best avoided when wind speeds exceed 20 km h^{-1} (Trollope, 1999; 2007). Lohmann *et al*. (2014) found that the application of prescribed fires in the second season after germination was just as effective in reducing tree seedlings as when applied in the first season. This makes it possible for rangeland managers to burn only 50% of the land invaded by shrub or tree saplings (leaving the remainder to be burned the following year), thereby securing continued grazing (Lohmann *et al*., 2014).

The burning of rangeland to stimulate out-of-season green grazing (i.e. burning in summer or autumn) is totally unacceptable as it reduces the vigour and basal cover of the grass sward and results in increased rainwater run-off and soil erosion (Stocks & Trollope, 1993; Trollope, 2007). Thompson (1937), Everson *et al*. (1988) and Van de Vijver (1999) agree that such burning during the growing season caused a significant reduction in the abundance of *Themeda triandra* (Figure 3.27) and therefore did not enhance grazing.

Figure 3.27 ***Themeda triandra*, commonly known as red grass, is an important grazing grass in the open grassland regions of southern and East Africa (van Oudtshoorn, 2012).**

The botanical composition of grasslands is highly affected by the frequency of burning. Trollope (2007) found that frequent burning favoured species such as *Themeda triandra* that is sensitive to low light conditions under overgrown conditions, while species with a lower grazing value such as narrow-leaved turpentine grass (*Cymbopogon pospischilii*) and hairy trident grass (*Tristachya leucothrix*) do not share this fate and could survive extended periods of non-defoliation. These results were obtained for the arid savanna of the Eastern Cape, the moist grassland of KwaZulu-Natal and grasslands of the central highlands of Kenya. The influence of burn frequency on woody species is not so straightforward, suggesting that factors such as fire type and intensity is of greater importance (Trollope, 2007; O'Connor *et al*., 2014). As highlighted in Section 3.1, withholding fire for several years will result in an increase

in density and size of tree and shrub species (Thompson, 1937; Trollope, 2007; O'Connor *et al*., 2014). This suggests that the frequency of suitable fires (i.e. intensity and type) is vital for ensuring its efficiency in controlling bush encroachment.

If the prescribed burning is performed for wildlife management purposes, it is useful to apply a series of patch burns at regular intervals throughout the duration of the dry dormant season (Trollope, 2007). This will ensure different types of fires in response to weather changes during the burning period and hence a range of fire effects intended to increase habitat diversity (Section 3.2). A diverse mosaic of fire ages and fire histories will accommodate the needs of multiple animal species (Troloppe *et al*., 2002; de Ronde *et al*., 2004b; Scott *et al*., 2014), giving rise to the phrase "pyrodiversity begets biodiversity" in land management circles. The hazard of overgrazing is also reduced when grazers can successively track from one burned area to the next when regrowth takes place. Nimmo (2014) proposed that the focus should shift to ensuring an optimal mix of fire age classes at the regional scale rather than the local scale. In certain ecosystems it may be worthwhile to consider fire and vertebrate herbivores (wild or domestic) as contending consumers of food/fuel, since manipulation of the one will invariably affect the other (Murphy & Bowman, 2012; Scott *et al*., 2014).

3.7.4 Type of Fire?

The type of fire governs the vertical level at which heat is released with respect to the location of meristematic tissues (Trollope, 2007). Generally, fires burning with the wind as heading fires are preferred in rangeland management because they cause less damage to the grass sward (Trollope, 1999; Trollope, 2007; van Oudtshoorn, 2012). Backing fires, conversely, hamper the regrowth of grass (Section 3.1). As mentioned previously, "cool" or low intensity fires (< 1 000 kW m^{-1}) should be used to remove old accumulated organic material in grassland, while "hot" or high intensity fires (> 2 000 kW m^{-1}) is recommended for controlling bush encroachment (Stocks & Trollope, 1993; Trollope *et al*., 2002; Trollope, 2007; van Oudtshoorn, 2012). As explained in Section 3.1, increasing the fire intensity will have little impact on the recovery of grasses, while a significantly greater topkill of stems and branches of trees and shrubs is achieved due to an increased flame height. Substantial topkill of stems and branches of trees and shrubs up to a height of 3 m can be achieved by applying a hot fire (Trollope,

2007) and on a windy day will cause scorching up to crown-level, with minimal burning at ground level (van Oudtshoorn, 2012).

When performing prescribed burning for wildlife management, it became clear from Section 3.2 that the best practice is to employ either point or perimeter ignitions in order to develop a mosaic of different fire types and therefore warrant greater habitat diversity (Troloppe *et al*., 2002; Trollope, 2007; Scott *et al*., 2014).

3.7.5 Post-fire Management

It is important to apply a rotational resting system wherein a portion of the land is rested for at least one growing season prior to the prescribed burn. When burning to remove moribund and to improve rangeland condition, grazing should be applied as soon as possible after the burn to take advantage of the nutritious regrowth of grass (Trollope, 2007) but not before it has reached a height of at least 100 mm (Van Oudtshoorn, 2012). In this respect grazing by cattle is preferred to grazing by sheep (Kirkman, 2002). Following the initial grazing, the burned area should rest for some weeks after which time livestock should be moved rotationally to avoid overgrazing (Van Oudtshoorn, 2012; Lohmann *et al*., 2014). If camps are not available it is advisable to ensure that large enough sections are burned to avoid overutilization. To combat bush encroachment, van Oudtshoorn (2012) recommends that the burned area be heavily browsed and coppicing material be treated with chemicals.

CHAPTER 4

WILDLAND FIRE BEHAVIOUR

Fire behaviour generally refers to “the release of heat energy during combustion as described by the rate of spread of the fire front, fire intensity, flame characteristics and other related phenomena such as crowning, spotting, fire whirlwinds and fire storms” (Trollope *et al*., 2004) (see definitions provided in the glossary at the back of this document). Fire behaviour also affects safety and suppression decisions. Analysis of fire behaviour requires knowledge of the various factors that influence it. Although fire activity is strongly affected by fuels, weather/climate, ignition agents and human activities (Flannigan *et al*., 2005; Moreira *et al*., 2011), the three principal components of the fire environment that influence fire behaviour (Figure 4.1) reside under the following groupings:

- Fuel characteristics;
- Weather conditions; and
- Topographical features.

Fire behaviour responds to an ever-fluctuating combination of these components. The complexity of this interaction is further highlighted by noting that a fire’s behaviour is influenced by the environment, while the fire itself also affects the environment in which it is burning (The COMET Program, 2009a).

Figure 4.1 The fire behaviour triangle (The COMET Program, 2009a).

The area of the fire behaviour triangle (Figure 4.1) can be related to the severity of fire behaviour. This implies that shrinking any one of the sides of the triangle (e.g. a relatively low fuel load that is moderately cured) necessitates a corresponding increase along one or both of the other sides in order to maintain the same overall potential for fire behaviour (e.g. hot, dry and windy weather).

Research in South Africa has concentrated mainly on the effect of fuel and weather variables on fire intensity in savanna areas due to its close association with other fire behaviour parameters such as rate of spread and the flame height. Worldwide research, however, has focused more on the development of fire danger rating systems based on fuel and weather conditions e.g. the U.S. Fire Danger Rating System (NFDRS) (Rothermal, 1972), the Canadian Fire Weather Index (FWI) (van Wagner, 1987; Lawson & Armitage, 2008), the McArthur Forest Fire Danger Index (FFDI) (McArthur, 1967) and the Lowveld Fire Danger Index (LFDI) (Laing, 1978).

4.1 FUEL CHARACTERISTICS

Fuel characteristics are major controls of fire behaviour (Liu *et al*., 2014; Fischer *et al*., 2015). Fuel refers only to combustible, fire-sustaining material comprising live and/or dead vegetation occurring on a site (The COMET Program, 2008a). Green, high-moisture living plant material is not readily considered as fuel since it does not meet the basic criteria of being combustible (Troloppe *et al*., 2004). However, radiant heat from an approaching fire can dry and ignite nearby live fuel. Fire intensity is influenced by fuel load, fuel particle size and the distribution, compaction and moisture of the fuel. For fire to spread, an adequate quantity and distribution of fuel across the landscape is required as any gaps without sufficient fuel will disrupt the spread of the fire front. Although these fuel characteristics exhibit both temporal and spatial variations, the temporal variations usually occur over a much longer time period than changes in weather (The COMET Program, 2009a). In this respect distinction is made between the physical and chemical properties that remain constant during a fire occurrence, and moisture content that changes continually. Knowledge of how existing fuel characteristics affect fire behaviour is crucial in conducting accurate situational analyses and effectively combatting wildfires.

4.1.1 Fuel Load

This is an important factor affecting fire behaviour as it largely determines the amount of energy available for release during a fire (Section 2.4.1). Under the assumption of a constant heat yield, the intensity of a fire is directly proportional to the amount of fuel available at any given rate of spread of the fire front (Figure 4.2) (Brown & Davis, 1973; cited by Trollope, 1999; Dupuy & Alexandrian, 2010). As indicated in sections to follow, the rate of spread is determined by the wind, terrain slope, fuel moisture content and fuel type.

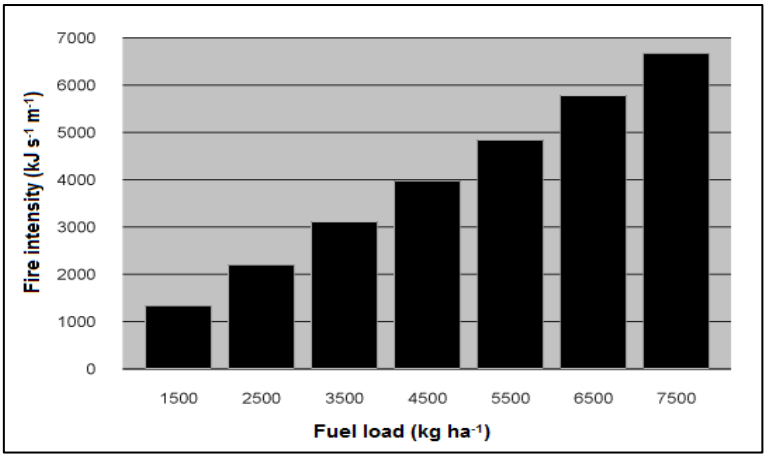

Figure 4.2 Effect of fuel load on fire intensity (Trollope *et al*., 2004).

A critical setup pattern for herbaceous fuels is a wet period (that promotes abundant growth) followed by a dry period (to dry the fuels out) (The COMET Program, 2008a; Fischer *et al*., 2015). The effect can be accumulative and continue over successive years. It has been shown that the fuel load in grasslands is a function of the time since the previous fire (Troloppe *et al*., 2004). On the Highveld sourveld the amount of accumulated fuel following a fire increases from approximately 2 000 kg ha^{-1} after one year, 4 700 kg ha^{-1} after two years, 6 100 kg ha^{-1} after five years, to a maximum of about 7 000 kg ha^{-1} after ten years (Troloppe *et al*., 2004).

4.1.2 Fuel Distribution

Ground, surface and aerial fuels are distinguished. Ground fuels support glowing combustion in the form of ground fires, are difficult to ignite yet extremely persistent and include all combustible material below the loose surface litter such as plant roots, peat and decaying plant material (Trollope *et al*., 2004; Scott *et al*., 2014). Surface

fuels largely comprise of fine fuels such as standing grass, small shrubs, tree seedlings, forbs and loose surface litter and can support intense surface fires (Trollope, 1999). Aerial fuels consist mainly of mosses, lichens, epiphytes and the branches and foliage of trees which are located in the understory and upper canopy layers and thus support crown fires (Trollope, 1999). The term “ladder fuels” are used to refer to a certain arrangement of fuels which enable vertical advancement from surface to crown fires (e.g. tall grass running up to tall shrubs next to trees). According to Trollope *et al*. (2004) the vertical distribution will influence the drying rate of fuel, the fire intensity and to some extent the rate of fire spread. It seems that the height of the fuel alone does not regulate the rate of fire spread, though higher fuels will have higher flames.

The horizontal continuity of a fuel also affects lateral fire spread. Continuous fuels such as cured grassland is easier to traverse, while fire can only move through patchy fuels like Karoo shrubland in the presence of strong winds. The susceptibility of herbaceous fuels (i.e. grassland) to fire events also depends on general land use practices (The COMET Program, 2009b). For example, areas that are heavily grazed tend to have much lower fuel loads and less horizontal continuity, thus impeding fire spread or even ignition (Scott *et al*., 2014).

The rate of spread of surface fires will be higher in open environments such as grassland (where the fuel is more exposed to direct sunlight and stronger wind speeds) than in closed environments as is the case underneath a closed canopy (The COMET Program, 2009b). Continuous aerial fuels such as nearly closed canopies reduce the wind speed beneath them, but can support running crown fires that spread faster than (and independently of) surface fires if ignited (The COMET Program, 2009b). Since surface fires can dry the aerial fuels, a progression of the fire into the canopy layer could result in a reburn. In an open canopy where trees are well separated, individual trees may be consumed entirely (referred to as torching), while the fire rarely spreads faster than at the surface (The COMET Program, 2009b).

4.1.3 Fuel Compaction

Rapid combustion occurs when the fuel is packed loosely enough so that adequate amounts of oxygen can reach the flame zone, but sufficiently dense for efficient heat

to be transferred between burning and unburnt material. Adequate ventilation usually occurs in plant fuels (Luke & McArthur, 1978; cited by Trollope, 1999). Grasslands are considered well-aerated in comparison to compacted litter on a forest floor, and when characterised by a high vertical distribution per unit area will produce an irregular flame pattern with common flare-ups and a fast rate of fire spread (Trollope *et al*., 2004). On the other hand, the compact fuel layer on a forest floor will exhibit a higher fire intensity and a slower rate of fire spread with an even flame distribution and little flare-ups.

Well-aerated fuels also respond quicker to changes in atmospheric humidity. In addition, vertically oriented fuels like grass cure faster than a similar amount of horizontally oriented fuel such as leaf litter and slash (The COMET Program, 2009b).

4.1.4 Fuel Moisture

Fuel moisture is the amount of water in a fuel and is usually expressed as a percentage of the dry weight of the plant material (Teie, 2005; cited by Siwele, 2011; Bianci & Defosse, 2014). All the moisture needs to be heated and converted to water vapour before a fuel will burst into flame (The COMET Program, 2008b; 2010a). In addition, the water vapour released by the burning fuel, may smother the flames by reducing the amount of oxygen in close proximity to the burning plant material thus decreasing the rate of combustion (Brown & Davis, 1973; cited by Trollope, 1999; Trollope *et al*., 2002; Ubysz & Valette, 2010). Fuel moisture thus impinges on the ease of ignition, rate of spread, the fraction of fuel consumed and plant mortality as well as smoke production (Jemison, 1935; Trollope *et al*., 2002; The COMET Program, 2008b; Dupuy & Alexandrian, 2010). The fuel moisture content (FMC) of a particular fuel can be obtained by drying the fuel in an oven for 24 hours at a temperature of 60°C and then calculated using the following formula (Ubysz & Valette, 2010):

$$FMC = \frac{M_i - M_f}{M_f} \times 100$$

where: FMC is the fuel moisture content (as a %);
M_i is the initial mass or wet mass of the fuel (in g or kg); and
M_f is the final mass or its dry mass (in g or kg).

The intensity of the fire also increases as the FMC decreases (Figure 4.3). Various factors influence fuel moisture such as time of day, season, topography (e.g. elevation,

slope, and aspect), fuel type, vegetative state (e.g. living or dead) and exposure (e.g. open or closed canopy) (Jemison, 1935; The COMET Program, 2008b). Most of these factors are discussed in more detail in sections to come.

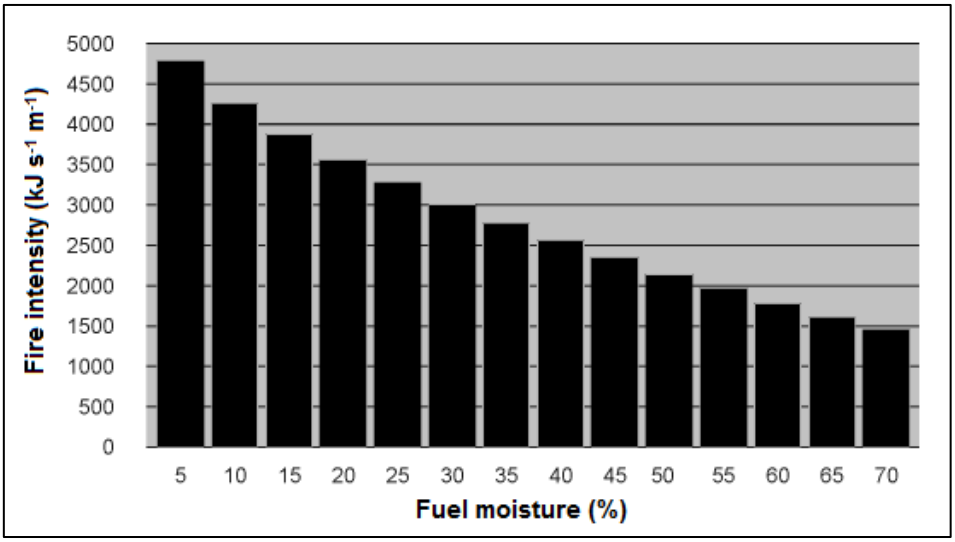

Figure 4.3 Effect of fuel moisture on fire intensity (Trollope *et al*., 2004).

The water content of either live or dead plant material is one of the key factors determining the availability of a fuel to burn (de Groot *el al*., 2005; 2010; The COMET Program, 2010a; Bianci & Defosse, 2014). The strong positive correlation between mean ignition time (MIT) and FMC is visible in Figure 4.4, which is based on *Erica arborea* samples collected during six dry summer periods (2001 to 2006) in the French Mediterranean region (Ubysz & Valette, 2010). Most fuel complexes contain a wide range of moisture contents since a combination of live and dead fuels are usually present (The COMET Program, 2010a). Living plant cells can hold up to three times their weight in water, thus the FMC of live fuels can range from 30 to 300%, depending on species, season and aspect (The COMET Program, 2010a). Live FMC is determined by the balance between the water inputs through the root system and water outputs due to transpiration (Ubysz & Valette, 2010). Live FMC levels change fairly slowly with time, generally over days or weeks, particularly in woody perennials. Live fuels may thus act as a heat sink, requiring a considerably higher ignition temperature to preheat the fuel in order to reach combustion (Tanskanen, 2007; The COMET Program, 2008a). In contrast, the FMC in dead plant material is not regulated by physiological mechanisms, usually falls between 3 and 40% (The COMET

Program, 2009b) and can vary rapidly over time and space as it is strongly influenced by changes in weather and topography (Sections 4.2 and 4.3).

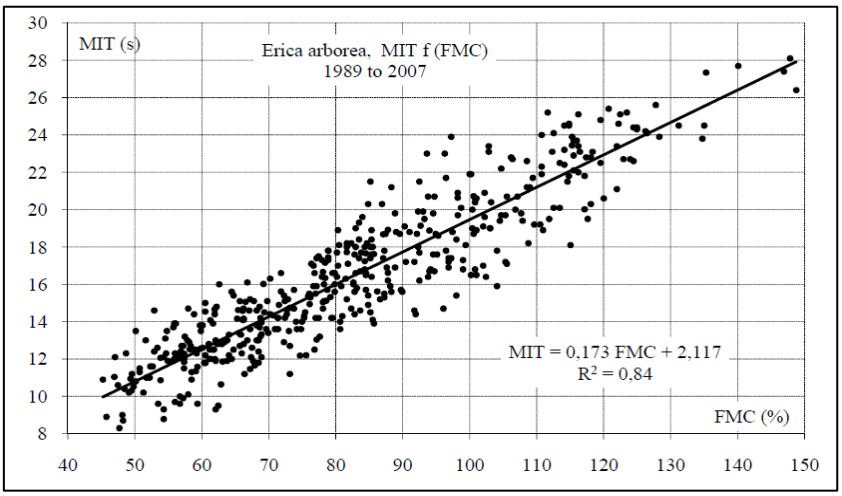

Figure 4.4 **Mean Ignition Time (MIT) versus Fuel Moisture Content (FMC) of *Erica arborea* (Ubysz & Valette, 2010).**

Curing refers to the proportion of dead plant material in a fuel complex (see definitions provided in the glossary at the back of this document). In the case of grassland, ignition will usually begin when green grass is at between 50 and 60% curing (Figure 4.5), and will occur with little difficulty when the grass is about 70% cured (de Ronde *et al*., 2004a). The moisture content of cured plant material is mainly affected by absorption and desorption in response to changes in the relative humidity of the adjacent atmosphere, precipitation and the soil (Trollope *et al*., 2004). For example, combustion will not occur easily in a cool, well-watered field of shrubs, but the same stand may erupt into flame after a long, hot drought period (The COMET Program, 2009b).

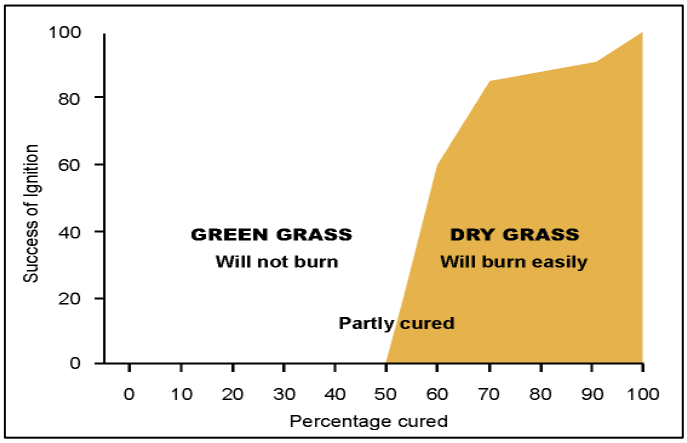

Figure 4.5 **Relationship between success of ignition and percentage curing of grass (de Ronde *et al*., 2004a).**

Equilibrium Moisture Content (EMC) is achieved “when there is no net gain or loss of moisture between fuels and the surrounding air” (The COMET Program, 2010a), implying that the vapour pressure of the air must equal the vapour pressure of the fuel moisture. Laing (1978) defined EMC as “the moisture content a dead fuel would have if it were allowed to gain or lose moisture for a sufficiently long period at a constant temperature and humidity”. EMC fluctuates in response to changes in air temperature and relative humidity, and the lower the EMC value, the drier the fuel (Laing, 1978). Over the summer rainfall region of southern Africa, the EMC typically decreases during the winter months and increases in response to higher relative humidity values with the approach of the rainy season. Although the winter months are naturally associated with lower air temperature values, the following equation illustrates that the lower relative humidity has a dominating effect on the EMC values (Laing, 1978):

$$EMC = 2.22749 + 0.160107RH - 0.014784T$$

where: *EMC* = Equilibrium Moisture Content (%)

RH = relative humidity (%)

T = air temperature (°C)

Various fuel types require different periods of time to approach the EMC, while fuel moisture changes commence quickly and begin to slow as values approach the EMC. Time lag categories allow the classification of fuels according to its response to changes in atmospheric moisture (The COMET Program, 2009b). The time lag is defined as the time required for a fuel particle to lose approximately 63% of the difference between its initial moisture content and the EMC (The COMET Program, 2010a). Fine fuels can experience substantial moisture changes in relatively short time periods and can reach their ECM within an hour. Heavier fuels respond much more slowly and are classified as 10-, 100- or 1000-hour fuels based on their size (The COMET Program, 2009b). More detail on these time lag categories are provided in Section 4.1.5. While 1-hour fuels are considered to be the primary carriers of fire, the moisture content of 10-hour fuels are also thought to influence fire behaviour. The moisture content of 100-hour and 1000-hour fuels provides information on drought conditions and the general severity of a fire season (The COMET Program, 2010a). Fire spread models suggest that a 1% change in the moisture content of 1-hour fuels can lead to a 10% change in the rate of fire spread (The COMET Program, 2010a).

Krawchuk & Moritz (2011) showed that in subtropical/tropical biomes with medium to high annual long-term net primary productivity where fuel resources are always available for burning during the fire season, fuel moisture conditions are a strong limitation on fire activity. In areas where fuel resources are more limiting or variable, such as deserts, xeric shrublands or grasslands/savannas, fuel moisture is a weaker constraint to wildfire.

4.1.5 Fuel Size

Surface-area-to-volume is one of the most important parameters for characterising fuel particles (Ubysz & Valette, 2010). Fuels can either be classed as fine or heavy. Fine fuel burns readily and comprises standing grasses and other herbaceous plants, fallen leaves, bark, twigs and branches with a diameter of less than 6 mm (Trollope, 1999). Fine dead fuels respond quickly to changes in the surrounding moisture conditions owing to their high surface-area-to-volume ratio (The COMET Program, 2010a; Bianchi & Defosse, 2014). Fine fuels thus dry rapidly and ignite easily. While almost complete combustion occurs in fine fuels (Ubysz & Valette, 2010), combustion is often incomplete in heavy fuels such as thick branches, logs and snags that dominate in forests. Heavy fuels dry slowly and require more heat to ignite due to its lower surface-area-to-volume ratio (Trollope *et al*., 2004; The COMET Program, 2009b). Thus, a large amount of fine fuels encourages fire occurrence and spread, whereas heavier fuels will enhance fire duration and intensity (Fischer *et al*., 2015).

As mentioned in the foregoing discussion on fuel moisture, fuels can be classed into the following size categories according to their time lags (Mathewson *et al*., 2008; The COMET Program, 2010a):

a) 1-hour fuels: 0 – 6 mm (¼ inch) in diameter;
b) 10-hour fuels: 6 – 25 mm (¼ – 1 inch) in diameter;
c) 100-hour fuels: 25 – 76 mm (1 – 3 inches) in diameter;
d) 1000-hour fuels: 76 – 203 mm (3 – 8 inches) in diameter; and
e) 10 000-hour fuels: larger than 203 mm (8 inches) in diameter.

1000- and 10 000-hour fuels are unlikely to reach EMC because environmental conditions will not stay constant for such extended periods. Figure 4.6 shows the fuel moisture responses for three different dead fuel size categories. It is evident that the

moisture content of the longer time lag fuels increases more slowly during a precipitation event (the influence of precipitation amount is not shown).

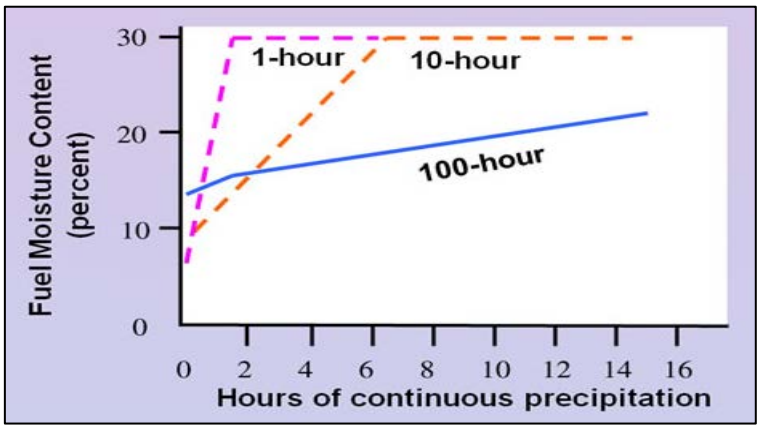

Figure 4.6 **Fuel moisture responses of three different fuel size categories to a wetting event (The COMET Program, 2010a).**

The size and shape of firebrands are also important in predicting the severity of spotting. Small firebrands such as bark flakes can travel several kilometres but burn out quickly, while larger ones like round logs can only travel short distances downhill though they keep burning longer.

4.1.6 Vegetation Type and State

Fuel type determines the amount of heat energy released during the flaming and glowing combustion phases. Light fuel types such as grasses release the bulk of their heat energy during the process of flaming combustion, whereas heavy fuels like tree trunks do so during glowing combustion (Trollope, 1999). The dead fine FMC threshold above which ignition seldom occurs and fire cannot be sustained (i.e. moisture of extinction), varies widely depending on the species and fuel type (de Groot *et al*., 2005; Bianci & Defosse, 2014).

Plant species differ in terms of their calorific values and mineral contents (Scott *et al*., 2014). Certain vegetation types such as grasses and forbs are generally non-volatile fuels that ignite readily when dry and are consumed quickly. In contrast, many woody fuels are volatile on account of them being high in fats, resins and volatile oils (de Ronde *et al*., 2004a; The COMET Program, 2009b; Scott *et al*., 2014). The latter makes for fast-burning, high intensity fires that often produces firebrands capable of

igniting fuels a distance ahead of the fire front. Examples of volatile woody fuels are *Erica arborea*, *Eucalyptus spp.*, *Euclea crispa, Pinus halepensis*, *Rhus lancea* and *Vitex rehmannii* (de Ronde *et al*., 2004a; The COMET Program, 2010b; Ubysz & Valette, 2010). This implies that biomass alone could be a poor indicator of flammability. As an example the Mediterranean-type climate region of the south-western Cape can be considered, where dense thickets occur in the same landscape as fynbos with similar total above-ground biomass. The fynbos, with many fire-adapted species, is much more prone to burning owing to differences in leaf size, leaf texture, shrub architecture and retention of dead branches (Scott *et al*., 2014).

After the occurrence of a fire, certain fuel types display a rapid fuel build-up, while others will go for a long time with fuel loads insufficient to support a new fire (Curt *et al.*, 2013). The properties of leaf litter (i.e. size and compaction) between pyrophilic and pyrophobic plant species (Section 3.1) usually differ to the extent that the latter are less flammable and tend to reduce fire spread (Scott *et al*., 2014). The potential for firebrand production also depends on vegetation type since spotting will only take place when the plant material can be transported effectively and at least still be glowing by the time it reaches the new area. Inherent differences in flammability thus lead to dissimilar fire regimes in vegetation otherwise exposed to the same climate and terrain features.

Vegetation type and state also affect weather variables such as air temperature and relative humidity (e.g. forested areas are likely to be cooler and more humid during the day than adjacent open grasslands) (The COMET Program, 2008b; Murphy & Bowman, 2012). Large wildfires, however, are not very sensitive to fuel type (Castellnou *et al*., 2010) and also spread into agricultural areas or decorative vegetation.

Pathogen-induced mortality (e.g. root rot, stem rot, sudden oak death, bark beetle etc. in forest stands) and other small-scale disturbance agents (e.g. trees uprooted by strong winds, cutting etc.) result in patchy accumulation of dead fuels (Lundquist, 2007; Valachovic *et al*., 2011; Hansen *et al*., 2015). Such disturbances not only influence fuel loads but also the spatial and vertical continuity of fuels. This will

increase fire intensity, flame length and influence firebrand generation and the rate of spread, thus altering fire effects in fire-prone regions (Valachovic *et al*., 2011).

4.2 WEATHER CONDITIONS

Weather is the most variable component of the fire environment (The COMET Program, 2009a), changing rapidly in time and space in response to air mass changes, diurnal cycles and local influences such as topography. It influences fire behaviour directly during combustion and indirectly by shaping fuel conditions (Tanskanen & Venäläinen, 2008). The main meteorological elements influencing fire behaviour are air temperature, relative humidity, wind speed and direction, precipitation and atmospheric stability. The speed at which fire danger reacts to changes in weather depends in part on the fuel type, condition and loading discussed in the previous section. Inter-annual variability in burned areas is also closely correlated with annual climate indices of drought, temperature or a combination of both (Moreira *et al*., 2011). The meticulous monitoring of weather and understanding how it might influence fire behaviour are essential for making critical fire management decisions (The COMET Program, 2008c).

4.2.1 Air Temperature

There are several factors that may influence the air temperature of a specific location (Lowry, 1972; Robinson & Henderson-Sellers, 1999; Arya, 2001). The intensity of incident solar radiation varies with latitude and time of day or year. Since the air is generally warmed from below, the nature of the underlying surface plays an important role due to such thermal properties as absorptivity, conductivity and specific heat capacity. Large water bodies have a moderating effect on the temperature, while continental locations typically exhibit larger diurnal and seasonal temperature variations. Temperatures near the coast are also influenced by the proximity and temperature of major ocean currents (e.g. cooler conditions along the West Coast of South Africa due to the vicinity of the cold Benguella current). Cloud cover lowers daytime temperatures and increases night-time temperatures. Wind disrupts the effect of radiative cooling during the night by effectively mixing warmer, drier air aloft with cooler air near the surface. Prevailing winds may also advect cold or warm air into an area, while topographical aspects such as elevation (decreasing temperatures with

height) and aspect (north-facing slopes receive more direct solar radiation in the southern hemisphere) will also influence the observed air temperature.

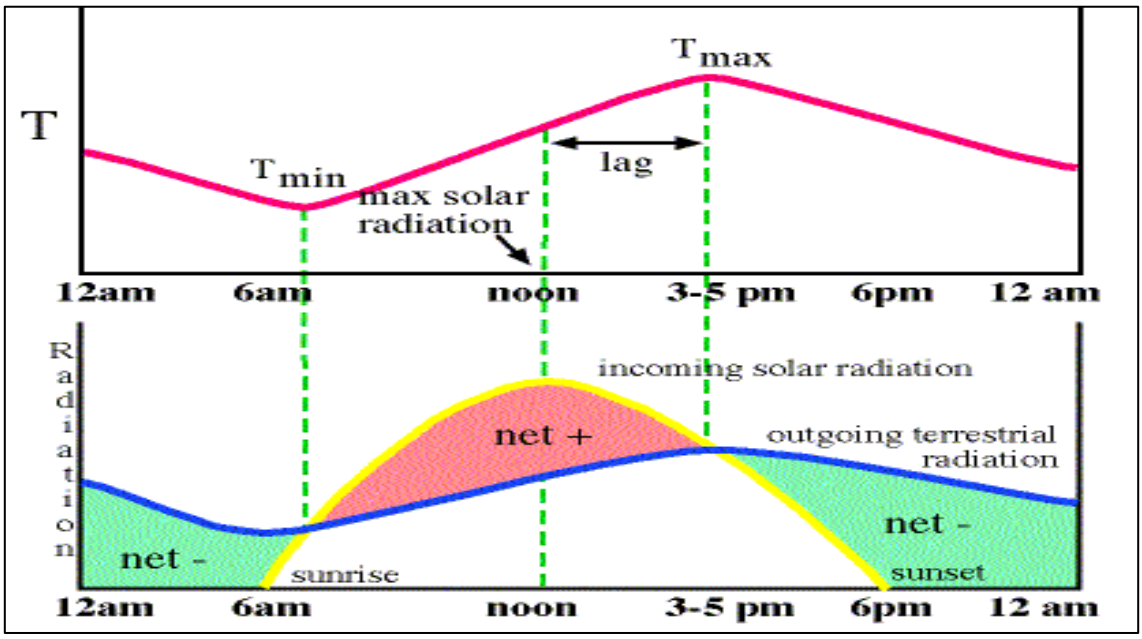

Figure 4.7 **Diurnal variations of incoming solar and outgoing terrestrial radiation (bottom) and air temperature (top) (Atkins, 2014).**

Diurnal and annual variations in air temperature can be explained by considering the budget of incoming solar versus outgoing terrestrial radiation (Figure 4.7 for a day). Normally the daily minimum temperature occurs several minutes after sunrise, while the maximum temperature occurs a few hours after solar noon (Oke, 1987; Tyson & Preston-Whyte, 2000; Atkins, 2014). The annual variation is similar to the diurnal variation with maximum temperature occurring after the summer solstice and minimum temperature occurring after the winter solstice. Instead of being in June and December the minimum and maximum temperatures occur in July and January, respectively in the Southern Hemisphere (Tyson & Preston-Whyte, 2000).

Air temperature directly influences the temperature of the fuel and thus the amount of energy required to reach ignition (Brown & Davis, 1973; cited by Trollope, 1999; Trollope *et al*., 2002). It also has bearing on the relative humidity and evaporative losses from the fuel. Fuel moisture will be higher during the night when air temperatures are normally lower so that it will be easier to bring wildfires under control. Conversely, such fires will become more difficult to suppress during the day, especially in the afternoon when the air temperature normally reaches a maximum and fires

reach their highest intensities (Trollope *et al*., 2004). In the Free State it has been found that 83% of fires start between 9 am and 5 pm (Proctor, 2012; Proctor, 2013, personal communication), presumably due to higher air temperature values and lower relative humidity values during this time of the day. This corresponds well with the findings of Catry *et al*. (2010) who stated that the hourly distribution of wildfire ignitions in Europe peaked between 2 pm and 5 pm. Although fuels require less energy to reach ignition at higher temperatures as indicated above, very low temperature values, specifically associated with severe frost damage, may kill off some vegetation and thereby increase the rate of curing (Laing, 1978; de Ronde *et al*., 2004a).

The relationship between air temperature and fire behaviour is strong enough to be picked-up at longer time scales. A global study conducted by Aldersley *et al*. (2011) for the year 2000 AD showed that burned area (their proxy for wildfire severity) generally increased with higher mean temperatures (Figure 4.8).

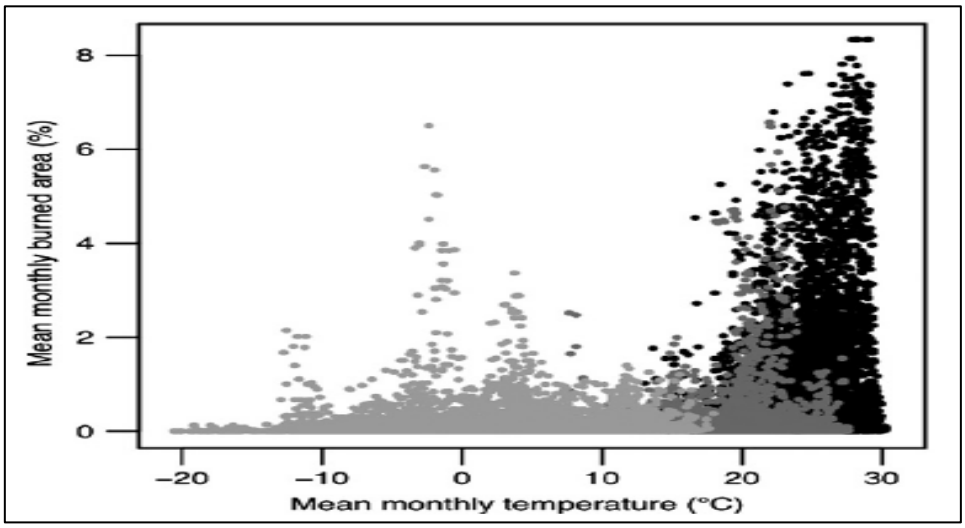

Figure 4.8 **Relationship between mean monthly temperature and burned area. Black dots represent tropical regions (23.5°N to 23.5°S), dark grey subtropical regions (23.5° to 40°N/S) and light grey extratropical regions (beyond 40°N/S) (Aldersley *et al*., 2011).**

4.2.2 Relative Humidity

Relative humidity is defined as the ratio of the amount of water vapour in a parcel of air to the amount that would be present at saturation point, at the same temperature (expressed as a %) (Gedzelman, 1980; Tyson & Preston-Whyte, 2000). Relative humidity can therefore be calculated as the ratio between actual vapour pressure and saturation vapour pressure (Allen *et al*., 1998). Under normal conditions (no airmass

changes or thundershowers) the actual vapour pressure may remain relatively constant during the day, whereas the saturation vapour pressure will vary in response to changes in air temperature (discussed in Section 4.2.1). Consequently, relative humidity exhibits a strong diurnal cycle with a maximum near sunrise and a minimum around early afternoon (Figure 4.9) (Allen *et al*., 1998; Tyson & Preston-Whyte, 2000; Trollope *et al*., 2004). Atmospheric moisture (and hence actual vapour pressure) can increase slowly due to the evaporation of surface water or rather abruptly due to showers or the advection of moist air from a lake or ocean. The dissipation of a low-level inversion is likely to have the opposite effect (The COMET Program, 2008d), while strong vertical mixing from mid- or upper-tropospheric levels can either raise or lower surface humidity (The COMET Program, 2008b).

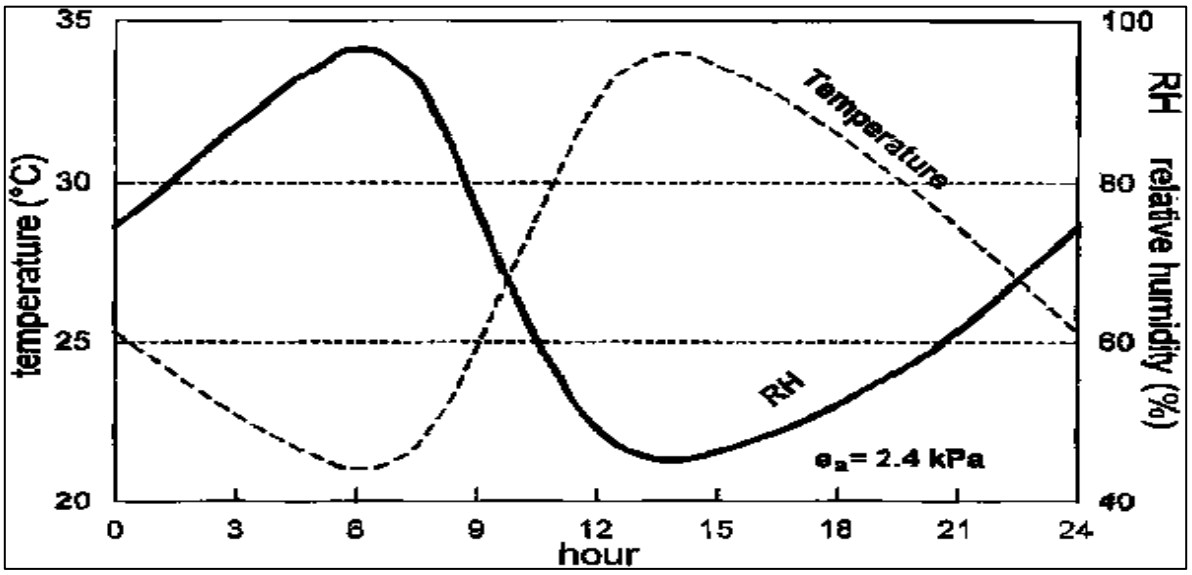

Figure 4.9 **Diurnal variation of relative humidity (solid line) for a constant vapour pressure of 2.4 kPa (Allen *et al*., 1998).**

Vegetation has a moderating effect on local variations in temperature and relative humidity (Scott *et al*., 2014) by intercepting incoming solar radiation by day and outgoing terrestrial radiation by night. Weaker winds within the canopy layer also result in reduced vertical mixing of air. During the day the highest temperature and lowest relative humidity are typically located near the tree tops, while lower temperature and higher relative humidity are found within the canopy layer in tall, dense vegetation (The COMET Program, 2008d). This situation is reversed by night, while the effect is reduced in shorter and sparser vegetation. The local effects of terrain on temperature and relative humidity are dealt with separately in Section 4.3.

The relative humidity of the atmosphere is strongly correlated with the moisture content of fully cured fuels (Wright & Bailey, 1982; cited by Trollope, 1999; Trollope *et al*., 2002). Fine fuels such as cured grasses respond almost immediately to changes in relative humidity, so that the fine dead fuel moisture curve will follow the relative humidity curve with a time lag of approximately one hour (Laing, 1978; van Wagner, 1987; The COMET Program, 2008d; 2010a). As pointed out in Section 4.1.5 large logs will respond significantly slower. In certain circumstances, the fuel moisture content of 1-hour fuels can be estimated by dividing the relative humidity by five (The COMET Program, 2010a), e.g. a relative humidity of 50% translates to a 1-hour fuel moisture content of 10%. This implies that relative humidity influences the combustibility of fine fuels and the subsequent intensity of the fire (Figure 4.10). By virtue of this control of the moisture content of surrounding fuels, relative humidity is the principal weather factor in the initial establishment of fire (Laing, 1978). Wildfires thus become more difficult to suppress during the daytime, especially during very dry conditions when the relative humidity drops below 30% and with fine fuels (Heikkilä *et al*., 1993; cited by Trollope *et al*., 2004).

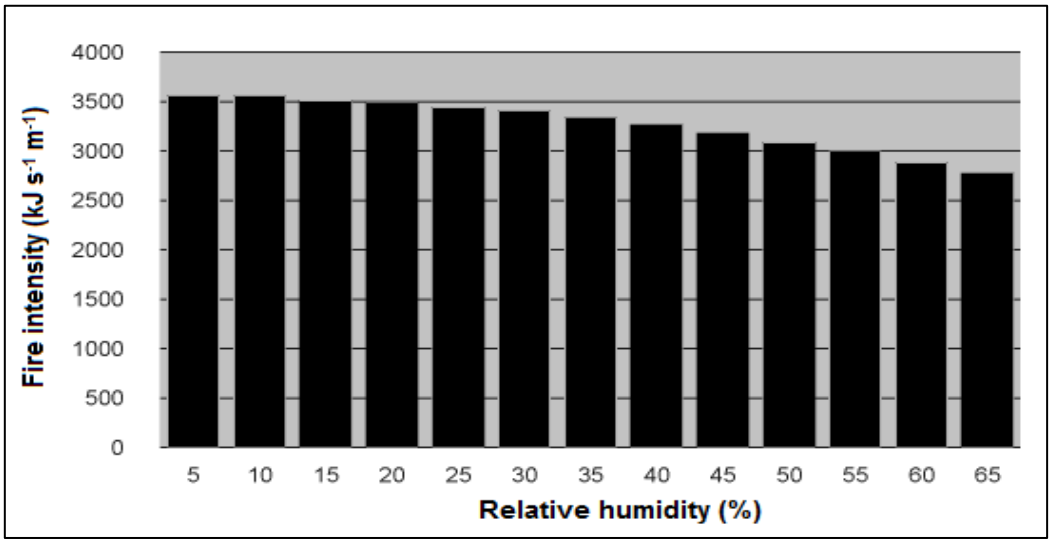

Figure 4.10 Effect of relative humidity on fire intensity in fine fuels (Trollope *et al*., 2004).

4.2.3 Wind

Wind is characterised by its direction, speed, and gustiness. Wind plays an important role in evapotranspiration and the drying of dead fine fuels. During windy conditions fuels tend to approach their EMC faster as evaporation from the fuel is increased and

moist air is removed from the fuel complex (The COMET Program, 2010a). However, the advection of cool, moist air will have the opposite effect.

After the initial establishment of a fire, wind becomes the controlling weather factor in terms of its spread (Laing, 1978; Cheney *et al*., 1993; Sharples *et al*., 2009). Wind speed is often the most important weather factor influencing fire behaviour and fire danger and is also the most variable and difficult to evaluate (Crosby & Chandler, 2009), while wind direction determines the path of a wildfire as well as the resultant smoke transport (The COMET Program, 2009c).

Wind speed determines the rate of oxygen supply to the fire front as well as the angle of the flames (Trollope, 1999; Trollope *et al*., 2002; The COMET Program, 2009c). By driving the flames towards unburned fuel (in head-fires), convecting heat to its surface and by carrying away moist air the wind aids in pre-heating and drying of the fuel ahead of the fire front (Sharples *et al*., 2009). This causes surface head-fires to spread faster (Luke & McArthur, 1978; Cheney, 1981; cited by Trollope, 1999; Dupuy & Alexandrian, 2010) and may facilitate spotting when burning embers are carried forward to new fuels by the wind. Wind speed also governs the residence time of the fire front over a particular location with higher wind speeds resulting in shorter residence times (The COMET Program, 2009c).

The rate of spread of heading fires increases exponentially at wind speeds up to 3.6 m s^{-1}, while backing fires seem unaffected (Beaufait, 1965; Gill, 1980; cited by Trollope *et al*., 2004). Conversely, wind speeds in excess of 14 ms^{-1} may even reduce the rate of spread of heading fires when fuel loads are low (Luke & McArthur, 1978; cited by Trollope, 1999; Trollope *et al*., 2002). Under normal conditions the rate of spread of fires and thus the intensity of fires increase with increasing wind speed (Figure 4.11) (Brown & Davis, 1973; Luke & McArthur, 1978; cited by Trollope *et al*., 2004; Dupuy & Alexandrian, 2010). Stronger wind will also result in greater spotting distances under unstable atmospheric conditions. In terms of its influence on fire intensity, wind therefore plays a significant but non-dominant role.

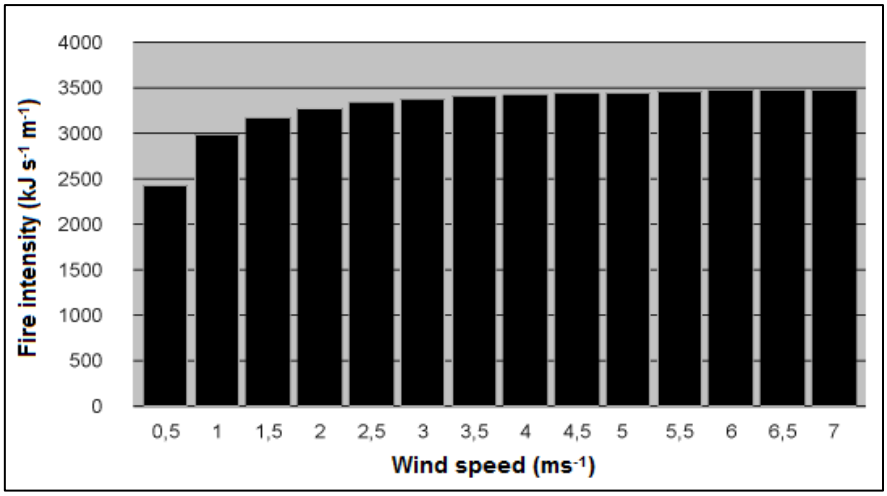

Figure 4.11 Effect of wind speed on fire intensity (Trollope *et al*., 2004).

An increase in wind speed does not necessarily imply increased flame heights due to the flames assuming a more acute angle which may prevent the ignition of aerial fuels (Trollope, 1999; Trollope *et al*., 2002). This offers a partial explanation as to why crown fires do not always occur during high winds. Generally speaking, wind speed attains a maximum during the afternoon when the turbulent mixing layer has reached its maximum depth, but exceptions may occur due to frontal activity or local circulations driven by differential heating of uneven terrain (Tyson & Preston-Whyte, 2000).

Prevailing wind conditions in the landscape during different seasons have a significant impact on the fire regime (Trollope *et al*., 2004; Miller & Schlegel, 2006). An example of this is the hot, dry, gusty downslope winds occurring in different parts of the world (Föhn wind in central Europe, Terral in Spain, Bora in south-eastern Europe, Harmattan in West Africa, Gibli in Libya, Bergwind in South Africa and Namibia, Garnesh in Iran, Oroshi in Japan, Nor'wester in New Zealand, Chinook, Diablo and Santa Ana in North America, Zonda in Argentina and Puelche in Chile). In South Africa Bergwinds can occur any time of the year but are particularly well developed during the winter months and can thus lead to devastating winter fires over large areas of the summer rainfall regions seaward of the main escarpment (i.e. Eastern Cape, KwaZulu-Natal and Lowveld region of Mpumalanga and Limpopo provinces). Over the winter rainfall region of the south-western Cape the impact of these desiccating winds on fire behaviour is more pronounced during the dry summer months. The most devastating wildfire ever recorded in the southern Cape (February 1869) scorched an area of more

than 500 km in length and occurred under Bergwind conditions (Geldenhuys, 1994; Trollope *et al*., 2004). The more recent wildfires that ravaged the Cape Peninsula in March 2015 could also be attributed to Bergwinds which raised the daytime temperature to about 40°C. Bergwinds also fanned the devastating Garden Route fires in June 2017, which killed nine people and completely destroyed a staggering 1 059 houses (Gosling, 2017).

Increasingly gusty winds and warm, unstable atmospheric conditions associated with an approaching cold front often results in extreme fire behaviour over the interior plateau of South Africa. A marked shift in wind direction during a frontal passage could further jeopardise the safety of firefighters as flank fires become head fires. The influence of local winds induced by topographical features on fire behaviour is addressed in Section 4.3.3.

Wind also has a noticeable effect on fire shape since an alteration in wind speed will significantly change the length-to-width ratio of the fire perimeter (Trollope *et al*., 2004). Hargrove *et al*. (2000) determined the probability of a fire spreading to neighbouring cells (depicted as bias factors in Figure 4.12) when subjected to three classes of wind speeds (WS), measured at a height of 6.1 m above the surface. It would appear from this study that an increase in wind speed would result in the head fire spreading quicker downwind, while the spreading rate of the back fire doesn't seem to be affected at all. Wildland fires thus spread in near-elliptical patterns, with the ellipse becoming more elongated as the wind speed increases. However, the actual shape of the fire perimeter is influenced by local factors such as heterogeneous fuels that cause protrusions in the fire perimeter, barriers to the spread of the fire, alterations in slope resulting in variations in spreading rate at the head or flanks, and spotting ahead of or down slope from a fire (The COMET Program, 2009a).

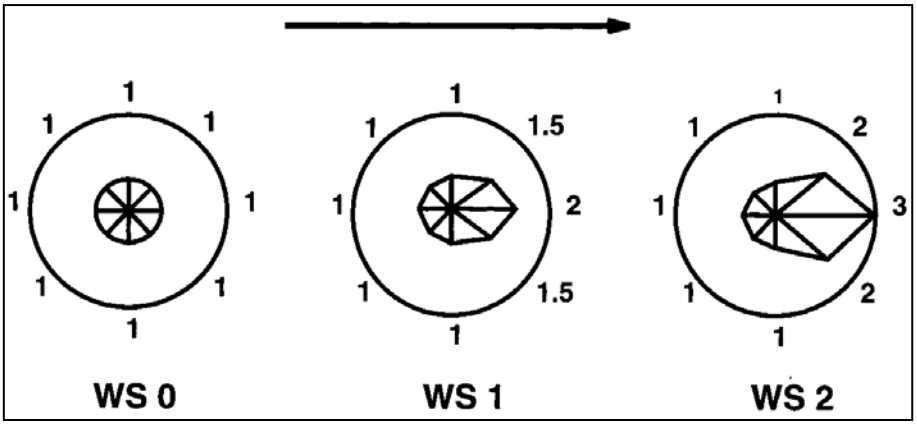

Figure 4.12 **Circular plots of directional bias factors used to simulate wind direction effects under no wind (WS 0, <3.1 km h^{-1}), moderate wind (WS 1, 3.1 – 21.7 km h^{-1}), and strong wind (WS 2, >21.7 km h^{-1}). The arrow indicates the wind direction (Hargrove *et al*., 2000).**

Changes in wind can thus pose serious problems in terms of fire suppression and the safety of firefighters. For example, sudden shifts in wind direction can cause the flank to become the head fire, resulting in a rapid and significant growth in the fire (Flannigan & Wotton, 2001). Fire weather forecasters can use wind direction to infer local wind patterns from large-scale wind flow and topographic features (Lawson & Armitage, 2008).

4.2.4 Cloud

Solar radiation heats the surface whilst decreasing near-surface relative humidity (The COMET Program, 2010a). Cloud cover thus affects fire intensity through its influence on surface air temperature and fine fuel moisture content. When clouds cover less than half of the sky during the day, higher solar radiation levels raise the surface air temperature while speeding up the drying of dead fine fuels. Under such conditions fires generally tend to be more active and flame heights greater (The COMET Program, 2010c). Conversely, fire activity tends to decrease and flame heights lower when daytime clouds cover more than half of the sky. An increase in daytime cloud cover can also alter the stability profile of the lower atmosphere. Extensive cloud cover during the evening, particularly at lower altitudes, will result in higher surface air temperature due to the reradiation of absorbed terrestrial infrared radiation and is associated with higher relative humidity when the vapour increases comparatively more than the saturation vapour pressure.

In addition, different cloud formations can signal potential changes in critical fire weather (The COMET Program, 2009d). Some examples include (The COMET Program, 2009d):

- Cumulonimbus clouds (Figure 4.13a) could spell the sudden onset of lightning, gusty winds, showers of precipitation, drops in air temperature and increases in relative humidity.
- Mountain wave clouds such as altocumulus lenticularis (Figure 4.13b) may herald the onset of strong, gusty downslope winds on the leeside of mountains.
- Altocumulus castellanus clouds (Figure 4.13c) indicate mid-level instability and the possible formation of thunderstorms later in the day.
- Stratus clouds (Figure 4.13d) indicate stable conditions and increased moisture at lower levels and a possibility of drizzle.

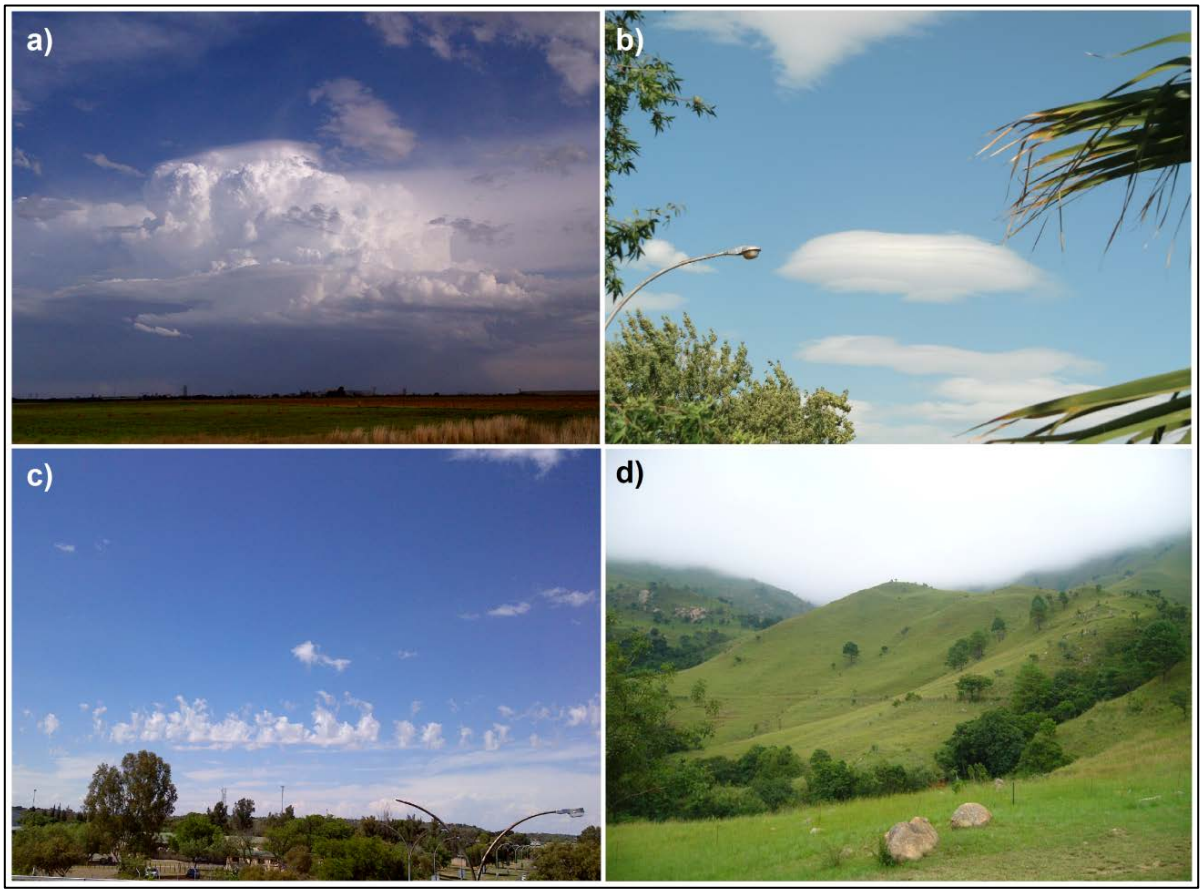

Figure 4.13 **Cloud types pertinent to fire weather: (a) Cumulonimbus; (b) Altocumulus lenticularis; (c) Altocumulus castellanus; and (d) Stratus (Author).**

4.2.5 Precipitation

According to Lawson & Armitage (2008), contact with liquid water can increase the moisture content of live forest fuels to 300% or more, and raise the fibre saturation value for dead woody fuels in a saturated atmosphere to a maximum value of about 30%. It is thus clear that fuel moisture will increase rapidly during precipitation and may even reach the point where combustion can no longer take place. However, the 24-hour accumulated total rainfall must exceed certain threshold amounts before it is considered to have any effect on the FMC (Lawson & Armitage (2008) – fine fuels require smaller amounts than heavy fuel types. Depending on atmospheric conditions influencing the drying rate of the fuels, such conditions will persist for varying time periods after the precipitation event (van Wagner, 1987; Trollope *et al*., 2004).

In the summer rainfall area of South Africa, precipitation is usually in the form of rain showers associated with thunderstorms. These thunderstorms are important for the occurrence and behaviour of fires in three ways: precipitation in the form of thundershowers, thunderstorm-generated winds and fires caused by cloud-to-ground lightning (Trollope *et al*., 2004). Dry thunderstorms are particularly dangerous as they are typically associated with little or no precipitation and well developed gust fronts (The COMET Program, 2009c). Lightning-dominated fire regimes are associated with late-season burning, and larger fires (as opposed to human-dominated fire regimes which are associated with early-season burning, and smaller fires) (Archibald, 2008). The overwhelming majority of wildfires are caused by humans though (de Groot *et al*., 2010).

Fuel loads are positively influenced by precipitation (Crimmins & Comrie, 2004; Aldersley *et al*., 2011). Above-average rainfall seasons may result in a growth spurt of short-lived grasses, thereby producing additional grass fuel loads. However, excessive water can reduce flammability, while sufficiently long dry periods can increase fire susceptibility (Aldersley *et al*., 2011). The dynamic nature of the natural grasslands on the African continent dictates that high summer rainfall can be followed by long dry winter periods, when curing will produce an increased fire hazard (Trollope *et al*., 2004). The lack of rainfall during prolonged droughts not only decreases fuel moisture, but also results in considerable leaf drop and premature curing as a result of water stress in vegetation. Aldersley *et al*. (2011) showed that fuel flammability and

the mean monthly burned area was highest in most global regions when the number of monthly wet days was low, particularly in Africa (Figure 4.14) where there is a strong seasonality in the wet day frequencies.

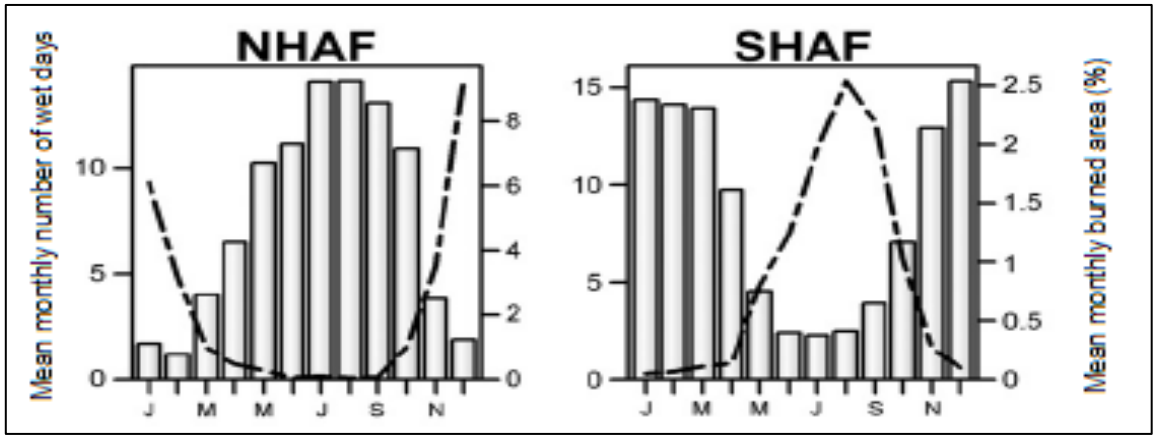

Figure 4.14 **Mean monthly burned area (%) (dashed line) and mean monthly wet day frequency (bars) for Northern Hemisphere Africa (left) and Southern Hemisphere Africa (right) (Aldersley *et al*., 2011).**

4.2.6 Atmospheric Stability

Atmospheric stability (and by proxy the vertical temperature stratification) directly influences the amount of vertical mixing of air between the surface mixing layer and the free atmosphere above (Oke, 1987). When mixing heights are low, smoke will be trapped in the surface layer which will impact negatively on air quality, visibility and fire suppression operations (The COMET Program, 2008e). In contrast, high mixing heights allow deeper vertical mixing within the atmosphere, more effective pollution dispersal and ameliorate air quality and horizontal visibility (The COMET Program, 2008e; Tyson & Preston-Whyte, 2000).

Stable atmospheric conditions tend to suppress wildfires as convection is suppressed and the inflow of fresh air is reduced (The COMET Program, 2008e; 2010c). The persistence of an inversion (i.e. the reversal of the normal lapse rate to lower temperature at higher altitudes) often worsens and extends the effect of wildfire smoke (Allen, 1988). Such layers are very stable and allow little vertical mixing across them, resulting in limited smoke dispersal and poor visibility. Processes which lead to the formation of inversions include (Robinson & Henderson-Sellers, 1999):

- radiative cooling which give rise to surface inversions during clear, calm conditions;

- subsidence that result in compressional warming and the formation of an elevated inversion that gradually builds down towards the surface; and
- warm air advection over a cooler near-surface air mass or surface.

The most persistent inversions are associated with the subsidence that occurs when an almost stationary high-pressure system mantles a region (Allen, 1988). The special case of a radiation inversion within a mountain valley is addresses in Section 4.2.

Unstable atmospheric conditions allow wildfires to grow in intensity and spread faster, while smoke is quickly dispersed up and away from the area. Such conditions give rise to wind turbulence and are most often associated with extreme wildfire behaviour (The COMET Program, 2010c; Dupuy & Alexandrian, 2010) and characterised by large smoke columns (Figure 4.15). Instability also favours the development of thunderstorms, which may cause erratic, gusty winds and lightning that can result in rapid and dangerous changes to fire behaviour.

Figure 4.15 A well-established smoke column and pyro-cumulus cloud (Greene, 2012).

The potential height of the resulting smoke plume is determined by the heat energy of the source and the rise velocity (Sandberg *et al*., 2002). The specific type of plume behaviour to be expected depends intricately on the stability profile of the atmosphere (Bierly & Hewson, 1962; Oke, 1978; Tyson & Preston-Whyte, 2000). Smoke introduced into a strong lapse (unstable) environment will exhibit looping (Figure 4.16a), while coning (Figure 4.16b) will occur when the temperature lapse rate is weak. Smoke introduced below a surface inversion will result in fanning (Figure 4.16c), while lofting (Figure 4.16d) will take place when it is introduced above an inversion layer. An unstable layer capped by a strong inversion may lead to fumigation downstream (Figure 4.16e). Such behaviour patterns can be predicted by evaluating the environmental lapse rate (ELR) relative to the dry adiabatic lapse rate (DALR or Γ) under dry conditions.

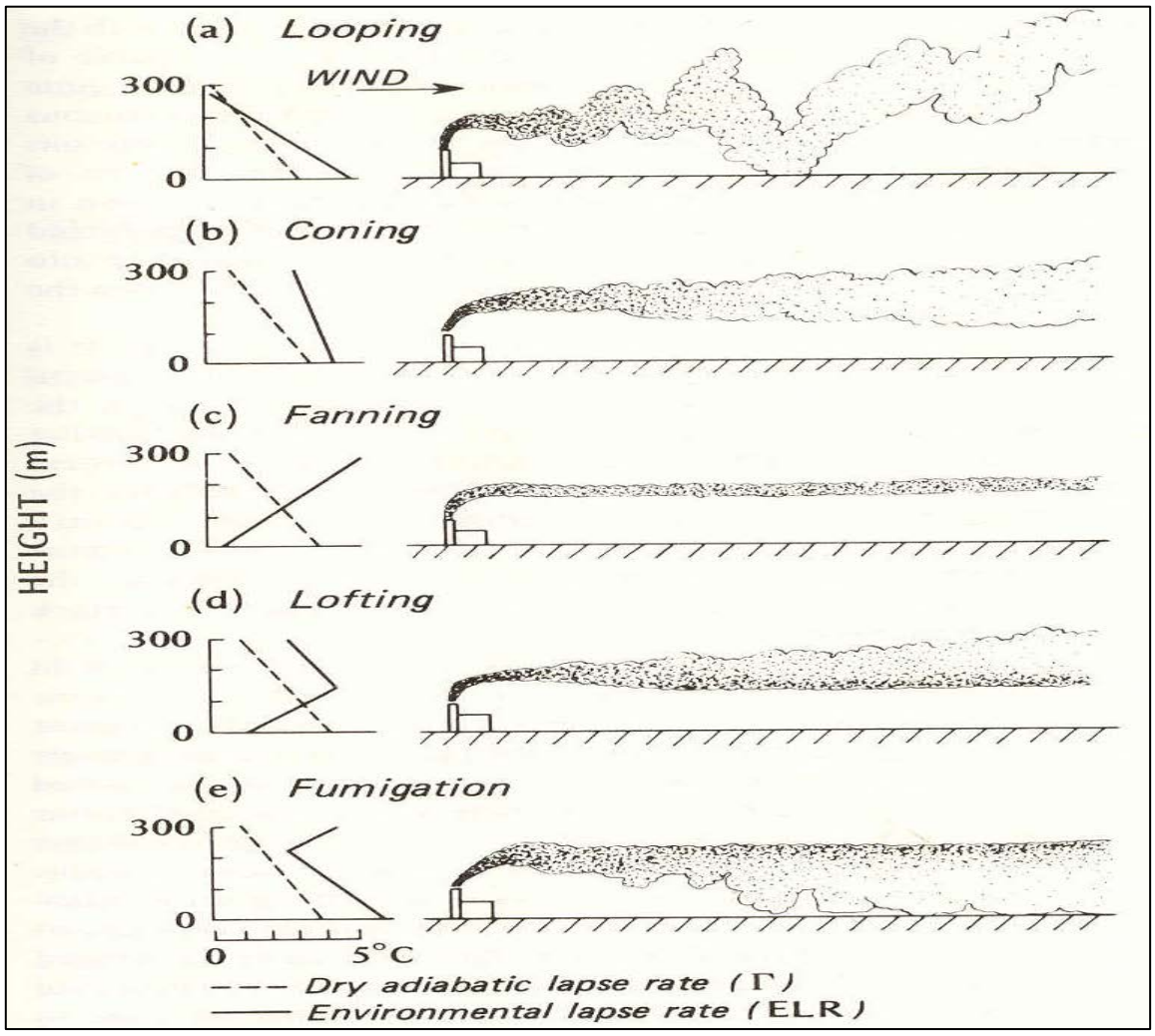

Figure 4.16 **Characteristic smoke plume patterns and their relation to atmospheric stability (Bierly & Hewson, 1962; adapted by Oke, 1978).**

Wind alone can cause short-range spotting, but when combined with strong convective currents firebrands can be carried considerable distances downwind to cause long-range spotting (The COMET Program, 2008e; 2009a). Atmospheric stability will also influence wind speed and direction as unstable air exhibits continuous changes in wind direction and speed. Momentary wind gusts (produced by mechanical and thermal turbulence) are thought to have little effect on the overall rate of spread and fire intensity, but can influence these values over short time periods (Crosby & Chandler, 2009). Certainly, gustiness negatively impacts the ease of fire suppression as it produces variations in flame height and can easily trigger spotting.

Strong lifting motion associated with pronounced wind shear in the vicinity of jet streams, can destabilise the atmospheric column above a wildfire, resulting in the rapid ascent of the smoke column and explosive growth and intensification of the fire (The COMET Program, 2010c; Swetnam, 2014). During such extreme fire weather conditions, the fire front may give rise to a “fire storm” (Trollope *et al*., 2004). More information on extreme fire behaviour is provided in Section 4.4.

4.2.7 Surface Fluxes

Evapotranspiration refers to the total movement of moisture from a surface into the atmosphere (evaporation plus transpiration) and can be seen as the process by which liquid water is converted to water vapour and removed from the evaporative surface (Buckle, 1996). This process takes place continuously, although it reaches a maximum by day. The rate of evapotranspiration is essentially controlled by four factors (Robinson & Henderson-Sellers, 1999):

- Energy availability;
- The humidity gradient away from the surface;
- The wind speed and turbulence immediately above the surface; and
- Water availability.

In addition to some vegetation and environmental factors, evapotranspiration is therefore simultaneously controlled by weather factors such as solar radiation, air temperature, relative humidity and wind (turbulence).

Evapotranspiration will lead to a reduction in the water content of topsoil and vegetation over time. This in turn will influence the rate of curing of the fuel. Furthermore, as soil water content decreases near the surface, more incoming solar radiation will be transformed into heat, rather than being used for affecting a phase change (evaporation of water) (Nielsen & Rasmussen, 2001). Drier soils are thus generally associated with higher daytime temperatures (The COMET Program, 2008b).

In contrast, the effect of condensation (dew) or deposition (hoar frost) on fuel moisture is generally limited to fine fuels (Lawson & Armitage, 2008). Dew forms by water vapour condensing onto a cooled surface when the air close to the surface is chilled to the dew-point temperature, but remains above 0°C (Gałek *et al*., 2015). Hoarfrost forms in a similar fashion, but when the temperature drops below freezing at vapour pressures below 6.11 hPa (Tyson & Preston-Whyte, 2000; Gałek *et al*., 2015). Haines (1979; cited by Lawson & Armitage, 2008) concluded from field experiments in North America that 75% of the fine fuel moisture increase was lost within four hours after sunrise and almost completely lost by noon. It was further noted that dew was more likely in calm, clear conditions in clearings. This relationship between fine FMC and dew formation is used by fire managers to perform prescribed burns in open terrain before sunset (Proctor, 2014, personal communication).

4.3 TOPOGRAPHICAL FEATURES

Fire behaviour becomes increasingly complicated in complex terrain where topography interacts with local wind direction, microclimates and, consequently, vegetation type, fuel loads and fuel moisture content (Moreira *et al*., 2011). Although topography is the most constant component of the fire environment, its features can vary considerably over an area (The COMET Program, 2009a). Topographic features important to wildland fire behaviour include slope, aspect, shape of the terrain, and elevation. Understanding how these topographical features affect fire behaviour can aid in predicting the direction and rate of fire spread, and help in safely and effectively positioning firefighting resources (The COMET Program, 2009e).

4.3.1 Slope

Slope is defined as the degree of inclination or steepness of an area (The COMET Program, 2009e). Slope steepness can influence the value of solar radiation reaching the surface and can have a marked influence on fire behaviour by modifying the extent to which the material ahead of the fire front is pre-heated and dried out (Trollope, 1999; Trollope *et al*., 2004). Though wind direction and speed will modify these properties, in general it is observed that fires burning up-slope attain the characteristics of a heading fire while the flames acquire a very acute angle and become attached to slopes exceeding 15 – 20° (Trollope *et al*., 2002; Trollope *et al*., 2004). On the other hand, fires burning down-slope spread more slowly and acquire the characteristics of a back fire (Trollope, 1999; Trollope *et al*., 2002). Slope reversal (e.g. when a fire crosses over a ridge line or drainage) can thus result in rapid changes in fire type and rate of spread.

In general, the steeper the slope, the taller the flame height (or length) and the faster the fire's rate of spread (The COMET Program, 2009e). The rate of spread of fires has been shown to increase twofold from a moderate (0 – 22°) to a steep (23 – 35°) slope and fourfold to a very steep (36 – 45°) slope (Luke & McArthur, 1978; cited by Trollope, 1999). These rates compare well with those provided in Figure 4.17. Cheney (1981; cited by Trollope *et al*., 2004) provided the following exponential relationship for estimating the spreading rate of surface head fires on slopes gentler than 30° (before the distribution of surface fuel becomes discontinuous):

$$R = R_o e^{0.0693x}$$

where: R = rate of spread (ms^{-1})

R_o = rate of spread on level ground (ms^{-1})

e = exponential function

x = angle of slope (°)

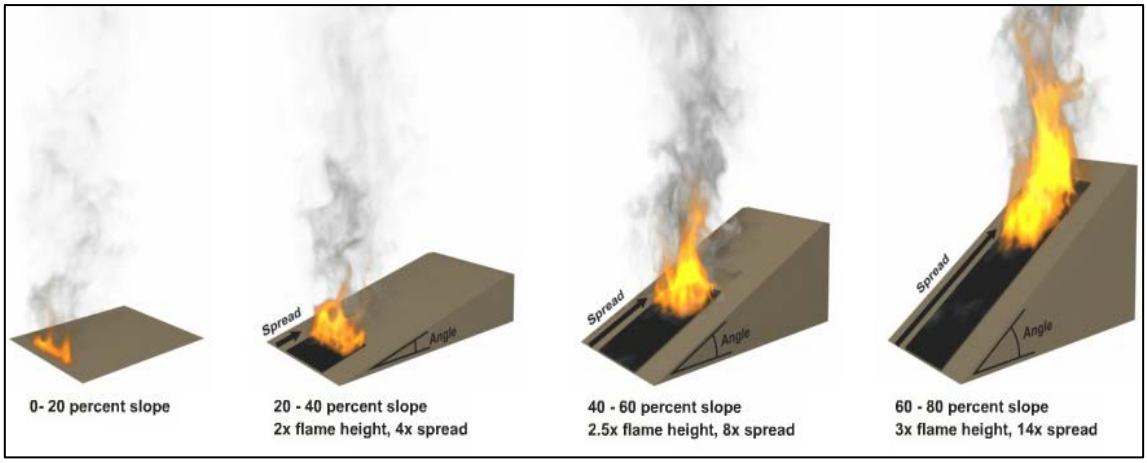

Figure 4.17 Relationship between slope, flame height and rate of fire spread (The COMET Program, 2009e).

The position of a fire on a slope thus affects its size and spread. A fire that starts at the bottom of the slope is likely to become larger than one that starts mid-slope or near the ridge line because the fire has a longer upslope run with more available fuel in its path (The COMET Program, 2009e). Although fires that start mid-slope tend to spread faster uphill, firebrands (pieces of burning debris such as rolling logs or pine cones) can spread fire down-slope (The COMET Program, 2009e).

4.3.2 Aspect

The incident angle of solar radiation on various sloped surfaces changes throughout the day and with the season. Aspect is defined as the compass direction that a slope faces (The COMET Program, 2009e) and can have a marked influence on fuel drying rates and ensuing fire behaviour. In the southern hemisphere, north-facing slopes receive more direct solar radiation and are thus relatively warmer and dryer, while south-facing slopes are more shaded with vegetation retaining moisture for longer periods (Trollope *et al*., 2004). South-facing slopes will thus have a higher propensity for wetter and heavier fuels. East- and west-facing slopes exhibit diurnal variations. East-facing slopes tend to receive more direct solar radiation during the morning hours and less during the afternoon, while the opposite holds true for west-facing slopes (The COMET Program, 2008d; 2009e; 2010a; Adab *et al*., 2013). In some regions mountain ranges constitute climatic dividers with significantly higher rainfall on one side and much drier conditions (rain shadow) on the other. An example of this is the Cape Fold Mountains of the Western and Eastern Cape Provinces in South Africa where northern slopes normally receive less rainfall.

4.3.3 Terrain Shape and Local Circulations

Inhomogeneous terrain most notably gives rise to local wind circulations. Along shorelines the uneven heating/cooling rates of land and water surfaces result in the development of sea/lake breezes during the day, while land breezes form at night (Ahrens, 2003; Jiménez *et al*., 2016). Another example of such a thermal circulation exists in the form of the so-called country breeze that develops due to urban/rural differences and blows towards urban heat islands in the absence of strong synoptic scale winds (Tyson & Preston-Whyte, 2000; Wang & Li, 2016).

In hilly terrain, valleys also produce their own local wind system owing to thermal differences. The local winds of valleys are best developed in anticyclonic weather in summer (Baumbach & Vogt, 1999; Tyson & Preston-Whyte, 2000). Under such conditions, with clear skies and weak large-scale motion, differential warming or cooling of different aspects of the landscape gives rise to horizontal temperature and pressure gradients, which cause wind. The precise nature of these local circulations, termed valley and mountain breezes, depends on the orientation and geometry of the valley. In terms of fire behaviour it should be noted that fire spread can either be enhanced or suppressed by the interaction between the direct effects of topography (e.g. slope, aspect, elevation) and terrain induced flow (The COMET Program, 2008f). Barros *et al*. (2012) found that directional wind channelling by topography were responsible for a large proportion of wildfires being oriented along the main valley.

Commencing early in the morning, heated air, being less dense, rises as a shallow, unstable upslope or anabatic flow (Baumbach & Vogt, 1999; Tyson & Preston-Whyte, 2000; Barry, 2008). To maintain continuity a closed circulation develops across the valley involving air sinking in the valley centre (Figure 4.18 left). The flow taking place up the entire length of the valley is termed the valley breeze. This airflow reaches a peak speed of about 15 to 25 km h^{-1} by midday (Ahrens, 2003; The COMET Program, 2009c). The upslope flow tends to deepen as one progresses up the slope, while the return flow, referred to as an anti-valley breeze, occurs above ridgetop level (Tyson & Preston-Whyte, 2000; The COMET Program, 2007a). The flow reverses by late evening when the valley surfaces cool quickly by the emission of long-wave radiation. The air in contact with these surfaces cools and slides down-slope under the influence of gravity to form a katabatic flow (Figure 4.18 right). This drainage of cold air in a

down-valley flow is known as the mountain breeze which reaches its peak of about 5 to 15 km h^{-1} in the early morning hours, usually just before sunrise (Ahrens, 2003; The COMET Program, 2009c). The downslope flow tends to deepen as one progress down the slope, while the return flow (referred to as an anti-mountain breeze) occurs within the valley (Tyson & Preston-Whyte, 2000; The COMET Program, 2007a). Mountain breezes tend to be shallower and weaker than daytime valley breezes. A general rule-of-thumb estimates the depth of the down-slope flow to be about 5% of the slope's drop in elevation (The COMET Program, 2007a). Nocturnal valley-exit jets tend to develop as the down-valley flow transitions to a shallower layer where a valley opens up onto a plain (Chrust *et al*., 2013). In such cases the strongest winds are observed beyond the valley exit (Zängl, 2004; Chrust *et al*., 2013).

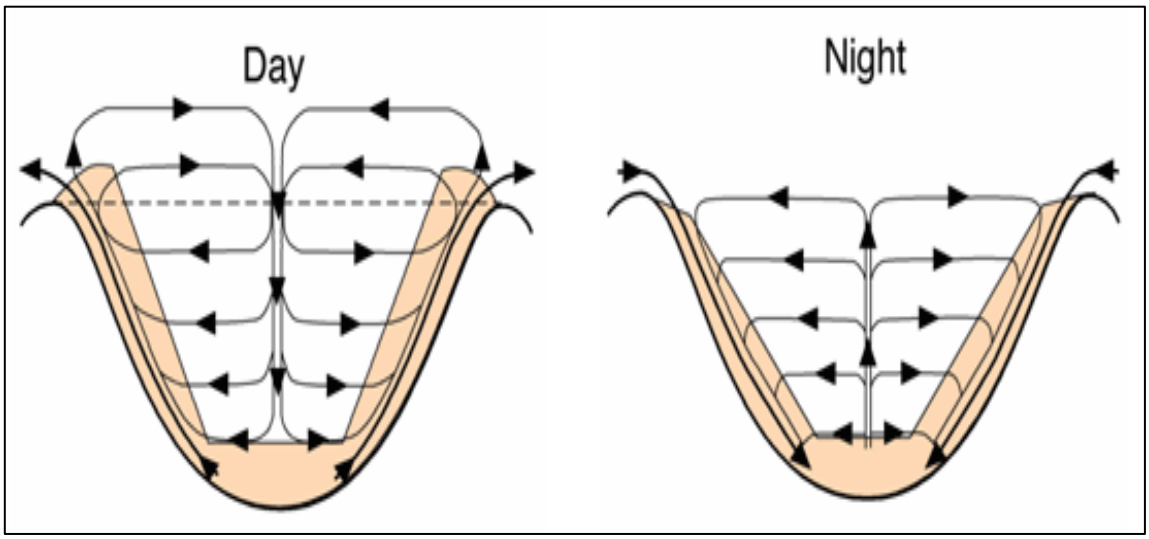

Figure 4.18 **Air circulation in a valley depicting anabatic flow during the day (left) and katabatic flow during the night (right) (The COMET Program, 2007a).**

Transition from katabatic to anabatic flow (or from a mountain to a valley breeze) during the late morning hours can result in dramatic changes in fire behaviour within a matter of minutes, with upslope winds enabling faster spreading rates (The COMET Program, 2009c). As depicted in Figure 4.19 the combined effect of slope winds (i.e. anabatic/katabatic flows) and along-valley flows (i.e. valley/mountain breezes) tend to result in a clockwise rotation (veering) of the wind with time over the valley wall to the right of the drainage, while the rotation is anticlockwise (backing) over the opposite valley wall (The COMET Program, 2007b).

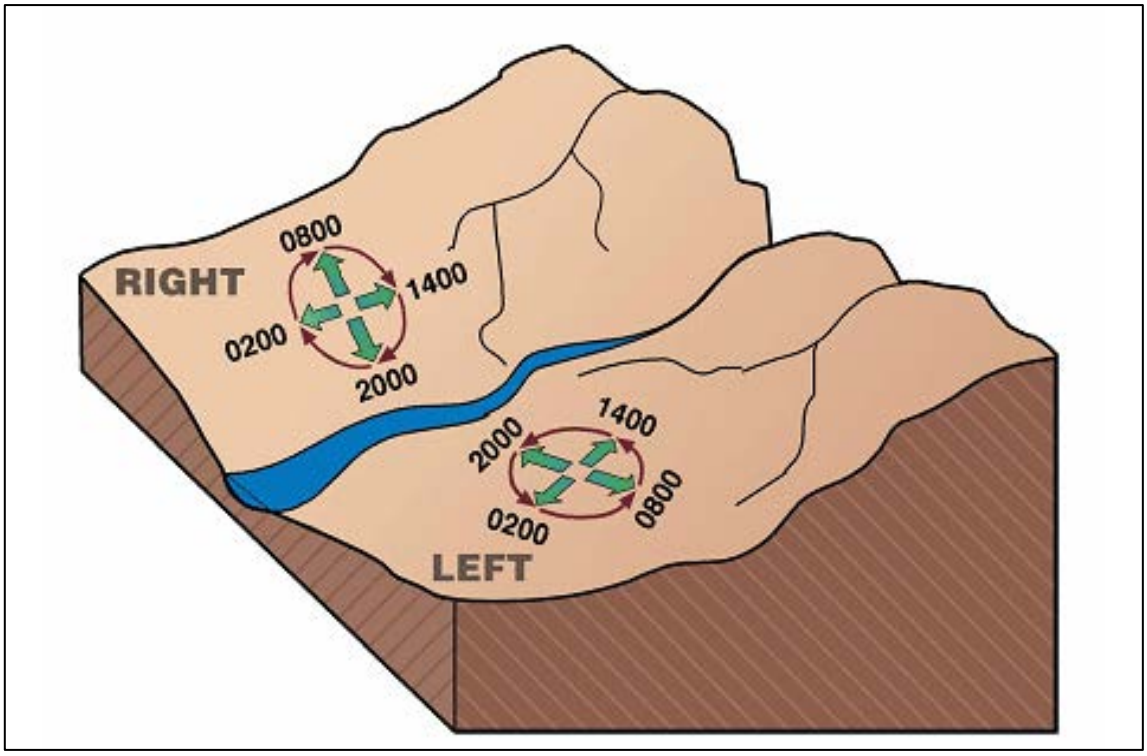

Figure 4.19 Wind direction as a function of local time on opposing slopes within a valley (The COMET Program, 2007b).

The flow pattern may become asymmetric or incomplete during different times of the day (owing to differential heating of opposing slopes) or in valleys possessing intricate geometries (e.g. bends, constrictions, etc.) (Oke, 1987). Warming (cooling) of one slope by the rising (setting) sun while the other slope is cooling (warming) will result in unicellular overturning of air (Figure 4.20). In the case of a bend the wind will bank up and be stronger on the outer slope and be lower and weaker on the inner slope of the bend (Tyson & Preston-Whyte, 2000). Rotors or lee vortices may also develop on the leeside of obstacles to airflow (Robinson & Henderson-Sellers, 1999; Epifanio, 2015) which may cause precarious fire behaviour and smoke downwash.

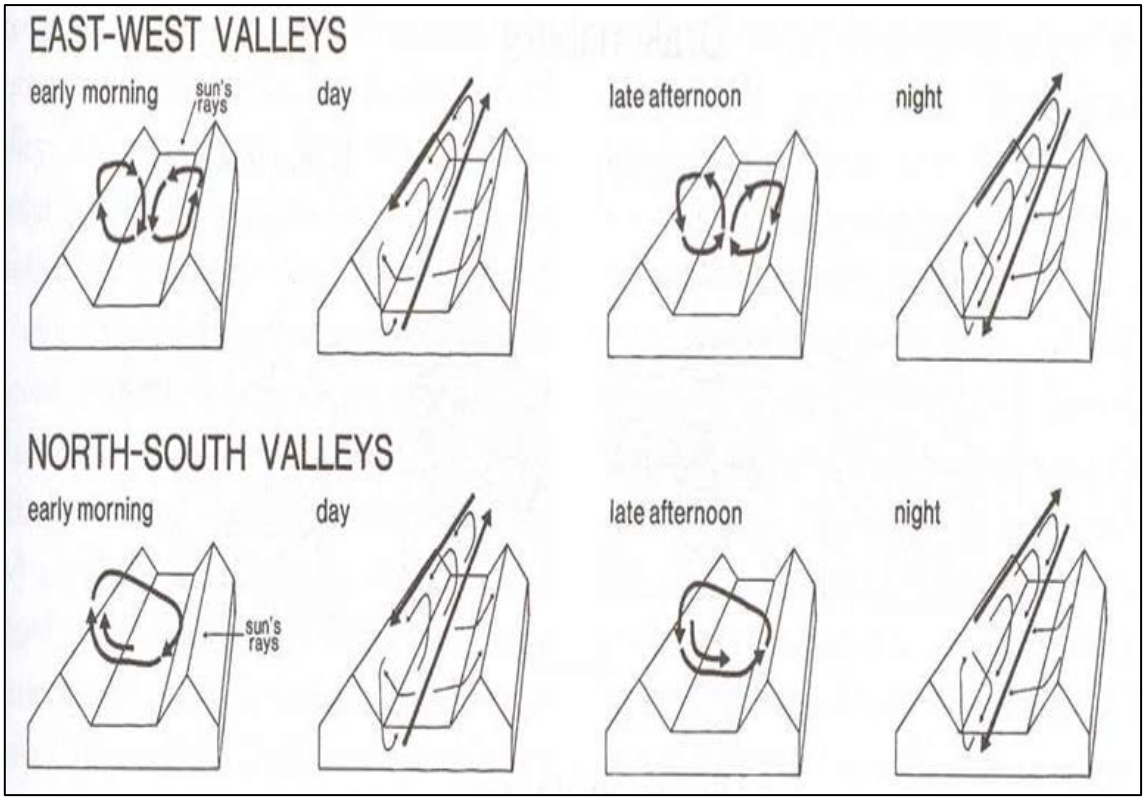

Figure 4.20 **Diurnal variation of local airflow in valleys with an east-west (top) and north-south (bottom) orientation (Tyson & Preston-Whyte, 2000).**

On cold, clear, winter nights, katabatic flow causes cold air to accumulate at the bottom of a valley, forcing warmer air upwards to form a temperature inversion. Any obstructions to katabatic flow will also result in the damming up of cold air, giving rise to frost pockets (Robinson & Henderson-Sellers, 1999). The region along the side of the hill where the air temperature is comparatively higher is known as the thermal belt (Figure 4.21) (Ahrens, 2003). This region of relatively high night-time temperature and low relative humidity is generally associated with greater fire danger than areas above and below (Laing, 1978) and is sometimes associated with continued active burning during the night (The COMET Program, 2010c). The elevation of the thermal belt depends on the locality, season, size and steepness of the valley, and wind conditions (The COMET Program, 2010c). During autumn and winter the thermal belt tends to develop at higher elevations along the slopes, while the same holds true for shallow valleys. During the evening smoke will be trapped beneath the inversion, thereby exasperating the air quality within the valley. However, once the inversion breaks during the mid-morning hours and anabatic flow commences, fire activity can escalate dramatically as wind speed increases and becomes gustier while air temperature rises suddenly.

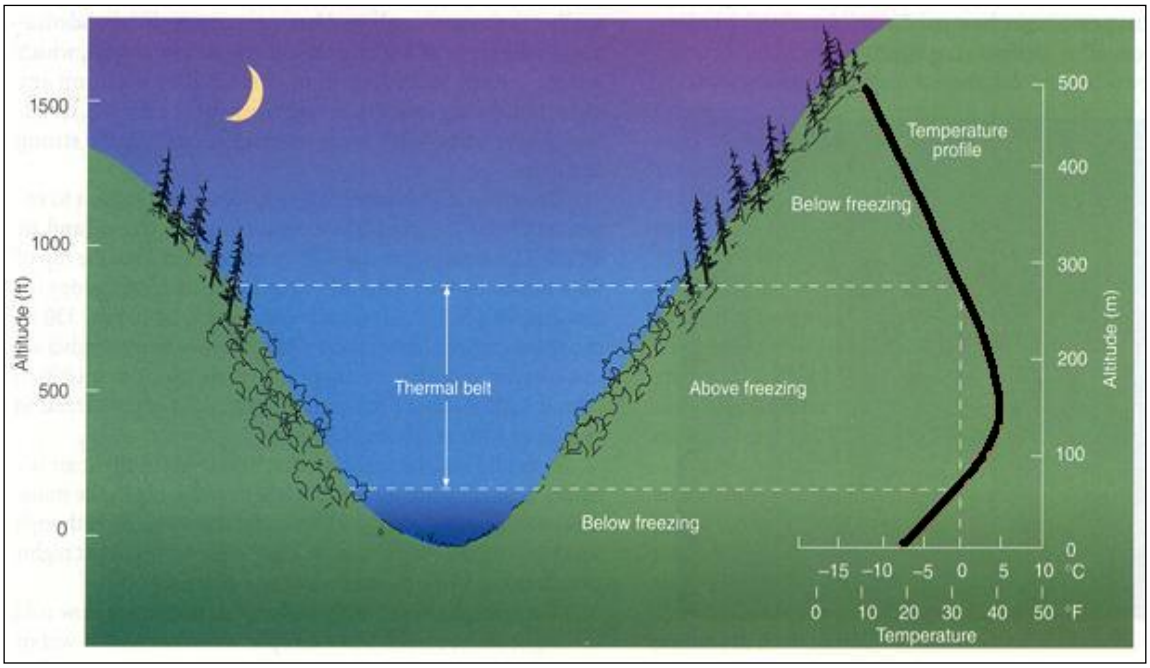

Figure 4.21 **Location of the thermal belt in a valley on a cold, clear winter night (Ahrens, 2003).**

Gap winds develop as airflow accelerates through mountain passages and channels. While earlier conceptual models used the Venturi effect to explain their formation, Sharp and Mass (2002) showed that gap winds develop primarily in response to pressure gradients across the mountain barrier in question. Such winds tend to attain their maximum velocity at the gap exit region (Sharp & Mass, 2002; Marić & Durran, 2009; Chrust *et al*., 2013; Ohashi *et al.*, 2015). Figure 4.22 depicts a gap wind with enhanced diffluence and kinematic divergence at the gap exit region. Since gap winds would fan frequent fires, Geldenhuys (1994) proposed that they could explain the absence of natural forests on the plateaus immediately downstream of the exit regions.

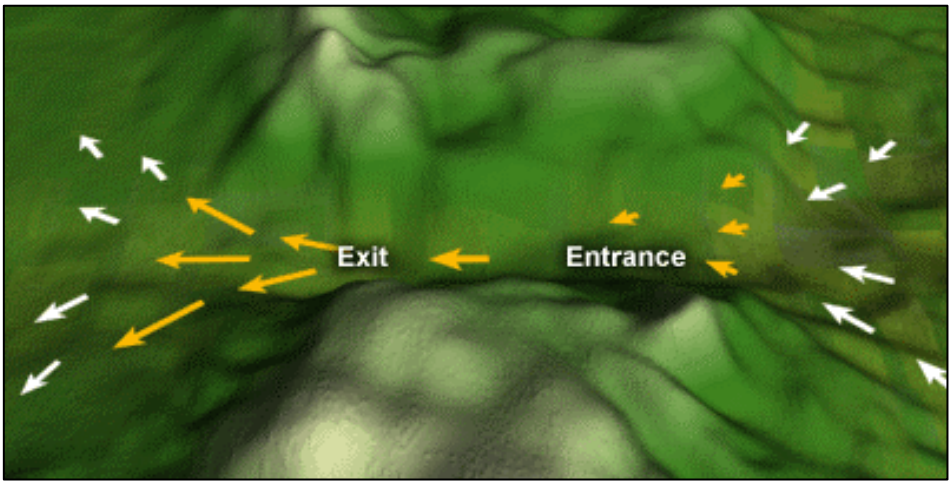

Figure 4.22 **Formation of gap winds at a mountain pass (The COMET Program, 2008g).**

Chutes, saddles and narrow canyons may provide the perfect conditions for a “chimney effect”, increasing fire spread through the funnelling of airflow, rapid transfer of radiant heat and spotting. Wind eddies in the region of intersecting drainages and spur ridges will also cause erratic behaviour, making it difficult to predict the direction of fire spread (The COMET Program, 2009c; 2009e). Rapid burnout in such areas can result in life-threatening conditions for firefighters. On the other hand, certain terrain features deprived of combustible fuels such as streams, lakes and rocky outcrops constitute natural barriers to the direction and rate at which wildfires spread. Variations in topography, in combination with inconsistencies in fuel conditions, can constitute partial barriers by slowing a fire’s rate of spread, but are not very effective in reducing spotting potential (The COMET Program, 2009e).

Mountain waves develop when the regional winds blow within 30° of perpendicular to a long mountain ridge under a stably stratified atmosphere. The exact type of interaction depends on (Barry, 2008): the vertical wind profile; the atmospheric stability structure; and the shape of the obstructing terrain. In this respect, Barry (2008) distinguished between four types of airflow:

- Laminar streaming (Figure 4.23a), characterised by a shallow wave and smooth airflow over the ridge during light winds that remain more-or-less constant with height;
- Standing eddy streaming (Figure 4.23b), depicted by overturning leewards of the barrier during stronger winds that increase moderately with height;
- Wave streaming (Figure 4.23c) when oscillation produced by the mountains set up a train of lee waves (also referred to as transverse waves) with an overturning windwards of the barrier when the winds increase more intensely with height; and
- Rotor streaming (Figure 4.23d), characterised by multiple strong overturning cells leewards of the barrier during strong winds that weaken some distance above the ridgetop.

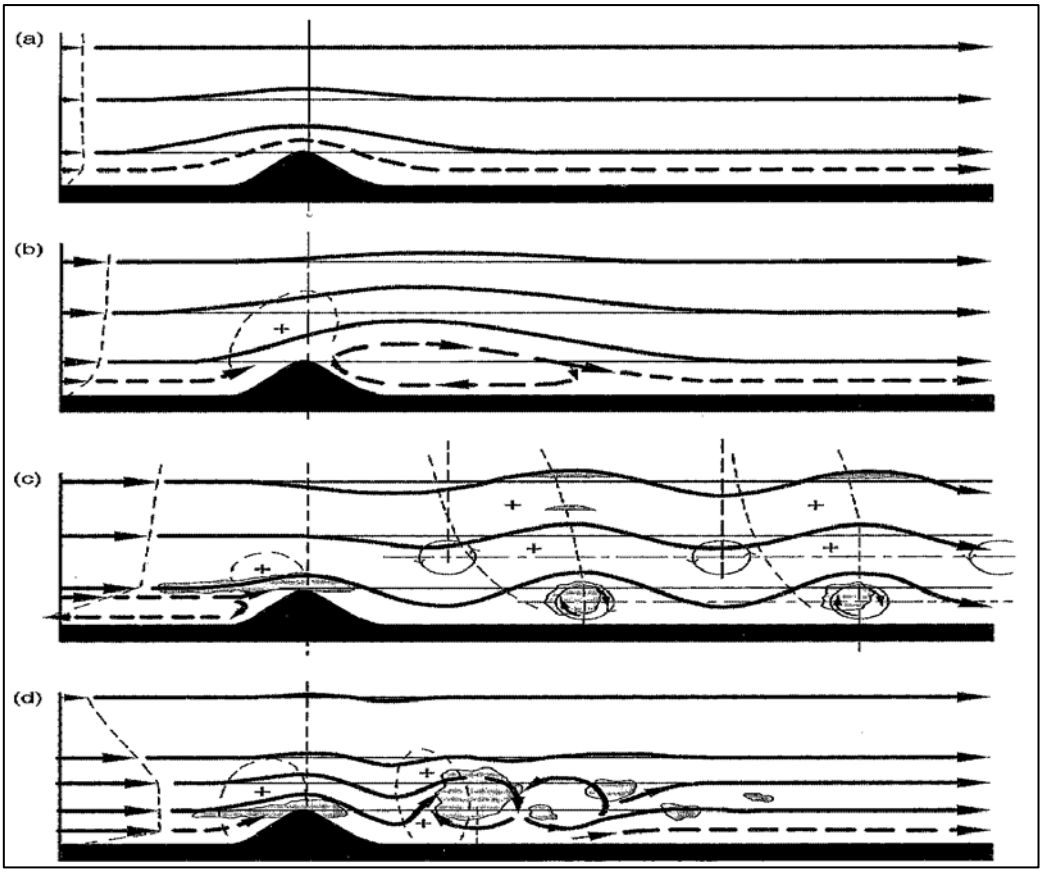

Figure 4.23 Types of airflow over a mountain barrier under stable conditions in relation to vertical wind speed profile (Corby, 1954; cited by Barry, 2008).

Topographic characteristics like slope, aspect, elevation and terrain shape play a key role in explaining the occurrence of fire in the landscape (Geldenhuys, 1994; Wood *et al*., 2011; Scott *et al*., 2014). Geldenhuys (1994) showed that the airflow patterns across topographical barriers explained most of the location pattern of forests in the Tsitsikamma area of South Africa. Here forests persisted in topographic shadow areas of the hot, dry bergwinds which are common during autumn and winter (Figure 4.24). An increase in wind speed across topographic barriers and acuteness of the change in slope between the windward and leeward sides will result in more turbulent airflow (Figure 4.24b) than with gradual slopes (Figure 4.24a). Such turbulence causes the airflow to separate from the ground and to form vertical eddies or rotors with flow in the opposing direction (Figure 4.24b – e). Furthermore, wind tends to also flow around isolated peaks or ridges of limited length. When the leeward slope is significantly steeper than the windward slope, the lee eddy will prevent a fire from burning down the lee slope and forests may persist on such slopes to near the crest (Figure 4.24b and c). These eddies do not develop with gradually changing slopes such as rounded

hills (Figure 4.24a). In broad valleys winds will slow down towards the valley centre, because of the rise of hot air at the fire front. Forests in such topographic situations are confined to valley bottoms (Figure 4.24f). A narrow valley between two ridges provides a refuge for forests due to the formation of a wind shadow (Figure 4.24d and e). Similar topographic fire refugia were reported in southwest Tasmania (Figure 4.25) by Wood *et al*. (2011).

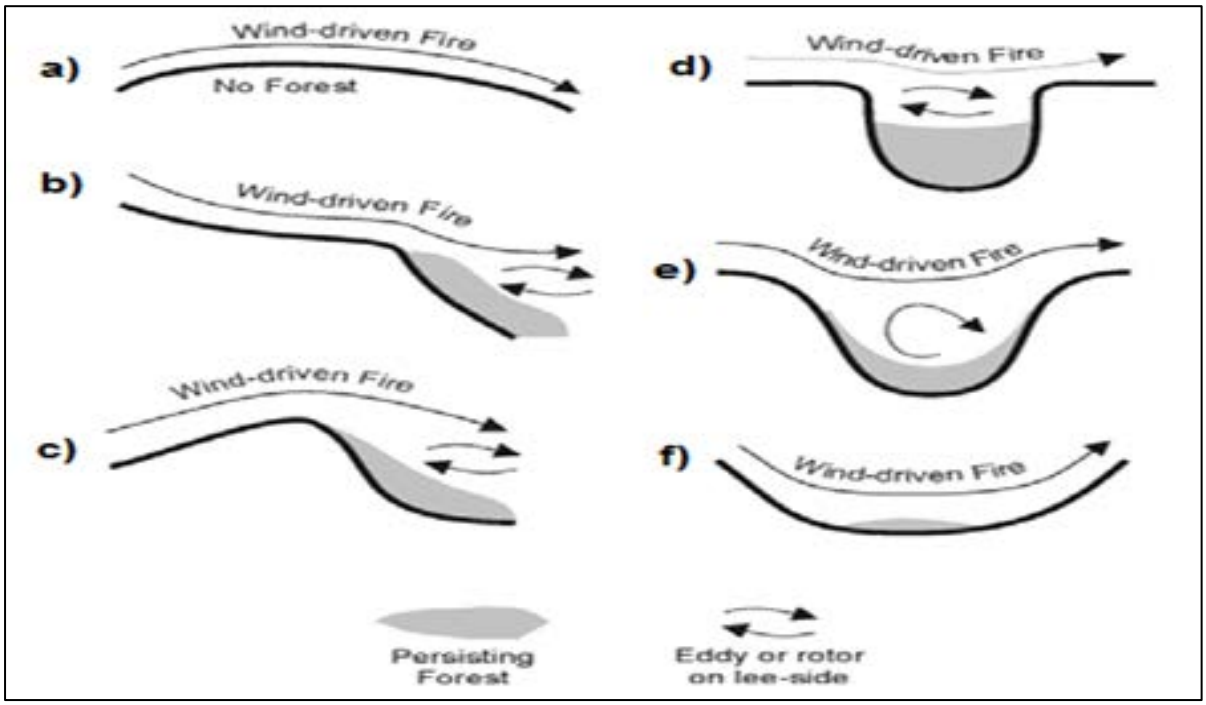

Figure 4.24 **Schematic view of hypothetical airflow across topographic barriers, to show the persistence of forest in wind-shadow areas (adapted from Geldenhuys, 1994).**

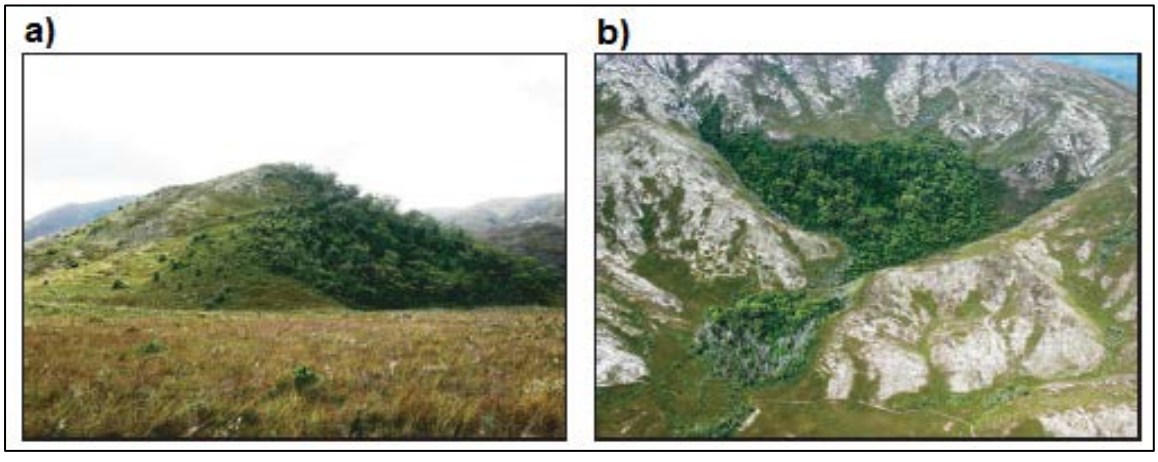

Figure 4.25 **Isolated forests restricted to fire refugia on (a) south-facing slopes; and (b) steep-sided valleys in southwest Tasmania (Wood *et al*., 2011).**

Although not strictly local-scale circulations, some of the larger scale interactions may be attributed to interactions with mountains or high plateaus. Orographically induced ridges and troughs (or in extreme cases lows) frequently develop across escarpments and may alter the wind direction. Piling-up of air and a consequent rise in pressure occurs on the windward side of the barrier, while the opposite takes place on the leeside. Such orographic pressure systems sometimes develop on either side of the Drakensberg Mountains of South Africa (Taljaard, 1995a). Another larger-scale phenomenon relates to cold-air damming and frontal modification (Barry, 2008). Retardation and distortion of fronts with a delay in the advection of cold air to the lee side also results in modifications of the vertical wind profile (Barry, 2008). Taljaard (1995b) described the so-called “left and right hook sequence” of cold front progression over South Africa. In the case of the right-hook sequence the cold front is distorted and delayed by the main escarpment as it tracks eastwards over the subcontinent so that the modified cold air eventually spills over onto the central plateau from the east. Similar frontal distortions have been reported in the vicinity of the Alps (Barry, 2008).

4.3.4 Elevation

Elevation plays a crucial role in fire behaviour as it influences air temperature and humidity as well as fuel moisture and structure (Castro & Chuvieco, 1998; Adab *et al*., 2013). During the day the temperature typically decreases with height, yielding an increase in relative humidity and the moisture content of dead fuels at higher elevations (The COMET Program, 2008d). At night and early in the morning, higher temperature and lower relative humidity values are usually found within the thermal belt (Figure 4.21). Differences in elevation thus contribute to variations in air temperature and relative humidity, which in turn affect the amount of precipitation and curing of vegetation. Soil water content also varies with elevation (The Comet Program, 2008b). These variables influence fuel types and loadings as well as overall fire danger and the duration of the fire season (The COMET Program, 2009e). Higher elevations typically experience cooler and wetter conditions with a propensity for denser and heavier fuels, while the proximity to the ridge line may result in slower rates of fire spread. In contrast, low-lying areas are typically further from the ridge line which may result in faster spreading rates, while mid-slope areas can be viewed as a transition zone (The COMET Program, 2009e).

4.4 EXTREME FIRE BEHAVIOUR

Generally, any fire behaviour that rules out direct fire suppression methods and typically involves one or more of the following characteristics are considered extreme (The COMET Program, 2010b):

- high fire front intensity and rate of spread;
- abundant spotting;
- crowning (Figure 2.3a);
- occurrence of large fire whirls (Figure 4.26); and
- a well-developed convective column (Figure 4.15).

Fires exhibiting these characteristics (also referred to as fire storms) often influence the surrounding environment and create dangerous conditions. They often start out as relatively benign, but suddenly explode when the wind shifts or align with topography (Wilson, 1976). ScienceDaily (2015) defines a fire storm as a conflagration which attains such intensity that it creates and sustains its own wind circulation as the rising hot air draws in more of the surrounding air. The strong updraft creates severe turbulence and erratic winds, while the pronounced wind shear is capable of producing tornado-like features called fire whirls (Figure 4.26).

Figure 4.26 A fire whirl in a grass and shrub surface fire (Author).

As indicated in the introductory paragraph of this chapter, such fire behaviour can be ascribed to an interaction between the various components of the fire environment. Typically, environmental conditions that combine to produce extreme fire behaviour are (The COMET Program, 2010b):

- Abundant fuel (e.g. high fuel loads that are sufficiently dry);
- Extreme weather (e.g. hot and dry with strong, erratic winds and unstable atmospheric conditions); and
- Complex terrain features (e.g. steep slopes, box canyons or chimneys).

Once a fire develops under extreme weather conditions it is next to impossible to limit its spread until the weather moderates (Castellnou *et al*., 2010).

Fires exhibiting extreme fire behaviour can either be topographical, wind-driven or plume-dominated, depending on which of these forcing mechanisms dominate (Castellnou *et al*., 2010; The COMET Program, 2010b). However, most extreme fires are to some extent influenced by a combination of mechanisms. As indicated by the terminology, wind-driven fires occur when the wind dominates the fire spread. Such fires exhibit a tilted low hanging smoke column with spotting (which can be long-range) occurring downwind. Plume-dominated fires develop a tall convective column as the fire begins to modify the wind field in its vicinity. Spread rate and direction thus becomes less predictable while spotting is usually short-ranged but in all directions. A useful diagnostic tool in this respect exists in the form of the Haines Index (Haines, 1988; Potter & Martin, 2001; The COMET Program, 2008e), which acts as an indicator of an atmospheric profile associated with extreme plume-dominated fire behaviour. Wind-driven fires may transition into plume-dominated ones as the convective column grows and starts to modify the prevailing wind field (The COMET Program, 2010b). Outflow winds instigated by the sudden collapse of a convective plume can transport firebrands in all directions and start multiple spot fires (The COMET Program, 2008b).

Fromm *et al*. (2006) provides a discussion of the extreme plume dominated firestorms that devastated Canberra, Australia, in January 2003. An afternoon air temperature of 37°C, relative humidity of 8% and a wind speed of 13 m s^{-1} (with gusts to 22 m s^{-1}) were recorded at the nearby Canberra Airport on the day of peak flaming and fire spread. Combined with very dry vegetation on the back of the 2002/03 El Niño event,

the scene was set for extreme fire behaviour. The ensuing firestorms were characterised by explosive pyro-cumulonimbus development (Figure 4.27), suppressed precipitation, an F2 tornado and black hail, while violent updrafts managed to penetrate the tropopause and inject smoke into the stratosphere. At one stage the combined firefronts occupied 5 000 ha, generating an energy release of 4.3×10^{13} kJ (an equivalent of 22 kT of TNT, more than the 15 kT atomic bomb of Hiroshima). Resultant damage included four human fatalities, 490 human injuries and the destruction of more than 500 houses in Canberra, while almost 70% of the Australian Capital Territory's pastures, forests and nature parks were severely damaged. Rosenfeld *et al*. (2007) also provide a detailed meteorological description of the Chisholm (Canada) firestorm of 28 May 2001.

Figure 4.27 Well-developed pyro-cumulonimbus feeding directly from the heat and smoke of a large wildfire near Canberra, Australia (McRae & Sharples, 2012).

It is perhaps also sensible to list some of the common features of wildfires that proved fatal here. These include (The COMET Program, 2010b):

- small fires or misleadingly quiet zones of large fires;
- light fuels (e.g. grass, herbs and light brush);

- an unforeseen shift in wind direction or increase in wind speed; and
- alignment of topography and wind direction to produce uphill runs.

Another common factor in fireline accidents has been a swift, large increase in the rate of spread (ROS). ROS-ratios (calculated as the ratio of ROS after and before the change) of 60-fold or more have accompanied fire fatalities (The COMET Program, 2010d). Potential factors that may combine to produce large ROS-ratios include changes in wind (~200x), fuel type (~15x) and slope reversal (which can be viewed as an increase in the effective wind speed), and to a limited extend changes in fine dead fuel moisture (~1.5x) (The COMET Program, 2010d). The infamous Black Saturday bushfires which claimed 173 lives in Victoria, Australia, in February 2009 claimed most of these lives when the wind direction shifted suddenly and the fires were driven back at great speed towards towns that had escaped them earlier (Paton-Walsh *et al*., 2012).

CHAPTER 5

FIRE DANGER RATING

Before embarking on a discussion of fire danger rating, it is necessary to distinguish fire danger from fire hazard and fire risk. Fire danger is “the assessment of both the static and dynamic factors of the fire environment which determine the ease of ignition, rate of spread, difficulty of control and impact of a fire” (Wotton, 2009). Fire hazard denotes the potential fire behaviour of a fuel complex, irrespective of its moisture content (Moreira *et al*., 2011), while fire risk represents “the probability of a fire starting due to the potential number of ignition sources in the area” (Wotton, 2009). Fire danger rating involves the regular evaluation and integration of the individual factors (e.g. fuels, weather, topography and risk) that define the elements of fire danger for an area (Schlobohm & Brain, 2002; Wotton, 2009) and is the cornerstone of modern-day fire management programs (Global EWS, 2015; Interagency Standards for Fire and Fire Aviation Operations Group, 2019).

Fire danger rating has developed into a mature science with a history of its implementation to provide early warning of the likelihood of severe wildfires (de Groot *et al*., 2006). In accordance with the National Veld and Forest Fire Act of South Africa (Act 101 of 1998), a fire danger rating system (FDRS) should have the primary purpose of preventing and controlling wildfires. Prevention should transpire through the ability to identify those conditions that result in dangerous fires, and subsequently through the effective deterrence of activities that would lead to the ignition of fires under such conditions (Willis *et al*., 2001).

FDRSs are for the greater part highly adaptable and have demonstrated their early warning ability and usefulness to a wide range of users (de Groot *et al*., 2006; Interagency Standards for Fire and Fire Aviation Operations Group, 2019). These range from remote fire managers (who need to make local fire preparedness and suppression decisions) to national disaster risk centres (who have to issue warnings and deploy personnel) and global fire information centres (who facilitate multinational resource sharing). Stakeholders also include the general public as well as industrial

and other private entities. According to Willis *et al*. (2001) a comprehensive FDRS should consist of the following elements:

a) The capacity to monitor, on a continuous basis, the conditions that affect fire danger;
b) The ability to delimit the regions that are affected by high fire danger conditions;
c) The ability to take relevant factors into account, using appropriate formulae. This requires the use of models which simulate the ease of ignition and potential fire behaviour;
d) The ability to identify high fire danger, and the listing of precautions that should be taken when the fire danger is predicted to be high; and
e) The ability to communicate the fire danger ratings and necessary precautions effectively.

Incorporating all potential factors pertaining to fire danger into a single numerical index is a seemingly impossible task (Sharples *et al*., 2009). However, several FDRSs have been developed to provide numerical indices relating to fire behaviour by integrating selected quantifiable factors contributing to fire danger (Sharples *et al*., 2009). Although some of these FDRSs rely at least partially on a theoretical background, several are based on empirical approaches due to complex interactions between the factors affecting wildland fires (Wastl *et al*., 2012).

A Fire Danger Index (FDI) considers the factors that influence the ease of ignition, rate of spread, difficulty of control and potential impact of fire over a large area (Schlobohm & Brain, 2002; WAMIS, 2014). FDIs are thus used to assess fire behaviour potential, gauge the safety of prescribed burning activities, to improve real-time firefighting preparedness, to aid in the logistic planning of firefighting resources and to inform public awareness of wildfires (Sharples *et al*., 2009; WAMIS, 2014). It should be noted that FDIs are typically implemented as regional measures and do not consider site specific factors related to terrain and fuel characteristics, although they do play an important role in fire behaviour (Sharples *et al*., 2009). This is why it is important to point out that the fire manager's experience and knowledge of a local area must also be taken into consideration when interpreting index values for specific scenarios (Schlobohm & Brain, 2002).

Index values can be derived for current (observed) or future (predicted) conditions. In the latter case they can either be employed to provide guidance for a few days in advance or to compare the severity between days or seasons (Schlobohm & Brain, 2002). Several systems are used around the world. Willis *et al*. (2001) provided a brief overview of the following eight systems currently in use internationally:

a) the Swedish Angstrom Index;
b) the Russian Nesterov Flammability Index;
c) the French Fire Danger Rating System;
d) the Canadian Forest Fire Danger Rating System (CFFDRS);
e) the United States National Fire Danger Rating System (US NFDRS);
f) the Australian (McArthur) Forest Fire Danger Index (FFDI);
g) the Australian (McArthur) Grassland Fire Danger Index (GFDI); and
h) the South African Lowveld Fire Danger Index (LFDI).

Since FDIs are typically non-dimensional and not directly measured variables, there seems to be no clear-cut basis for choosing one over another (Sharples *et al*., 2009). However, the three main FDRSs used internationally are the CFFDRS, the McArthur FDRSs and US NFDRS (Willis *et al*., 2001; Dowdy *et al*., 2009; de Groot *et al*., 2010). These three systems, along with the local LFDI, will be reviewed here, while the results of a few comparison studies are relayed in Section 5.5.

5.1 CANADIAN FOREST FIRE DANGER RATING SYSTEM

The Canadian Forest Fire Danger Rating System (CFFDRS) (van Wagner, 1974; van Wagner, 1987; CWFIS, 2015; Wang *et al*., 2015) has been under continuous development with the original form proposed by Muraro (1968; cited by van Wagner, 1987). It is the national system used for more than 40 years in Canada and conceptually deals with the risk, behaviour and prediction of forest fire occurrence from point-source weather measurements (Lawson & Armitage, 2008). The CFFDRS, or at least its Fire Weather Index (FWI) subsystem, has been tested and/or adapted successfully for use in a number of countries such as Albania, Argentina, Australia, Bosnia and Herzegovina, Bulgaria, China, Croatia, Fiji, France, Greece, Indonesia, Italy, Kosovo, Macedonia, Malaysia, Mexico, Montenegro, New Zealand, Portugal, Romania, Serbia, Slovenia, Spain and U.S.A. (Flannigan *et al*., 2000; Raínha &

Fernandes, 2002; Moriondo *et al*., 2006; Taylor & Alexander, 2006; Vučetić *et al*., 2006; Dowdy *et al*., 2009; Lampin-Maillet *et al*., 2010; Dimitrakopoulos *et al*., 2011; Tian *et al*., 2011; Pereira *et al*. 2013). The European Forest Fire Information System (EFFIS) also uses the FWI system to support fire protection services in the European Union (EU) and neighbouring countries (EFFIS, 2015). The FWI system has also been incorporated into a global early warning system for wildfire danger (de Groot *et al*., 2006). In the latter case the idea was not to replace the many national FDRS already in place, but rather to achieve the following objectives (de Groot *et al*., 2006):

- to allow fire danger predictions over longer time periods by employing advanced numerical weather prediction (NWP) models;
- to provide "a common international metric for implementing international resource sharing agreements during times of fire danger"; and
- to offer early warning capability where national systems are not in place.

The CFFDRS consists of four subsystems (Figure 5.1):

a) the Canadian Forest Fire Weather Index (FWI) system;
b) the Canadian Forest Fire Behaviour Prediction (FBP) system;
c) the Accessory Fuel Moisture (AFM) system; and
d) the Canadian Forest Fire Occurrence Prediction (FOP) system.

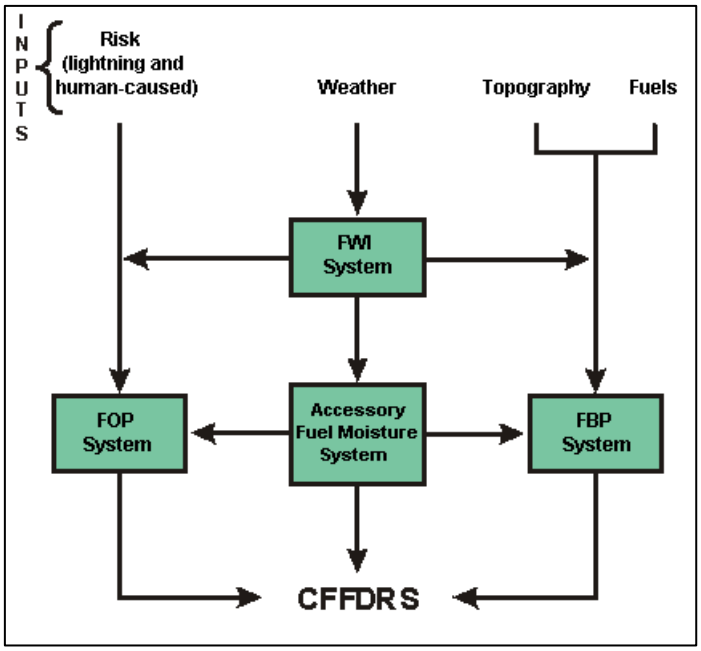

Figure 5.1 **Subsystems of the Canadian Forest Fire Danger Rating System (CFFDRS) (Stocks *et al*., 1989).**

Only subsystems FWI and FBP are used extensively in Canada and internationally (San-Miguel-Ayanz *et al*., 2003; CWFIS, 2015). This discussion will focus primarily on the FWI subsystem, which consist of six components (Figure 5.2) that account for the combined effects of air temperature, relative humidity, wind speed (at 10 m) and 24-hour accumulated precipitation on the forest floor fuel moisture conditions and generalised fire behaviour in a standard jack pine (*Pinus banksiana Lamb.*) stand on level terrain (van Wagner, 1987; San-Miguel-Ayanz *et al*., 2003; Dowdy *et al*., 2009). The intention was that the various indices should be interpreted regionally by experienced fire managers (Wotton, 2009). The system thus employs daily weather observations of these four elements at noon local time, although it actually represents fire danger at its afternoon peak. This discrepancy can be ascribed to the original research on test fires which correlated the fine fuel moisture values in the afternoon to noon weather observations (van Wagner, 1987).

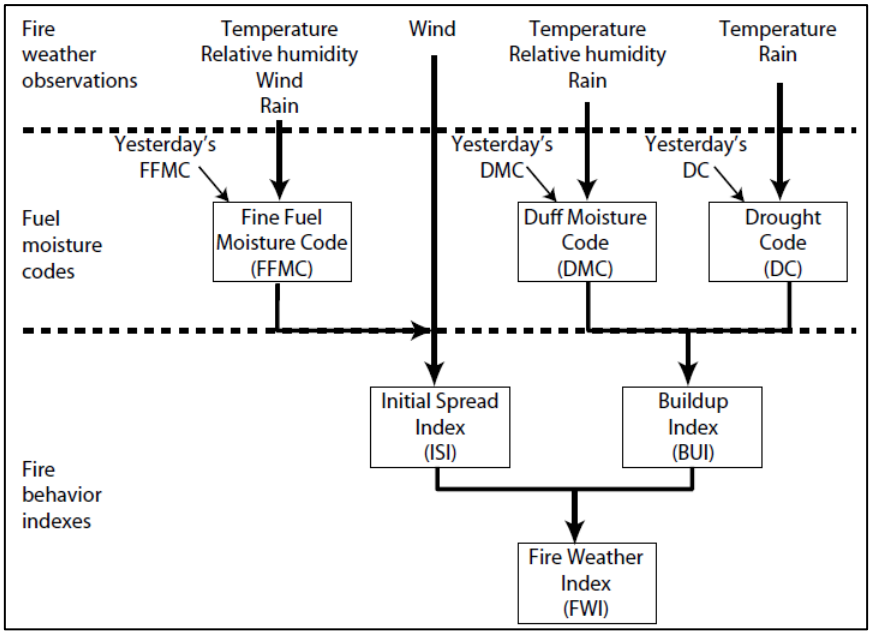

Figure 5.2 **Components of the Canadian Fire Weather Index (FWI) System (Lawson & Armitage, 2008).**

The following three fuel moisture codes are included in the FWI system (Figure 5.2):

- The Fine Fuel Moisture Code (FFMC);
- The Duff Moisture Code (DMC); and
- The Drought Code (DC).

Brief descriptions are provided here, while the actual calculation of these components in various programming languages can be found in Wang *et al*. (2015).

THE FINE FUEL MOISTURE CODE (FFMC)

The moisture in the fine, readily consumed fuels on the surface strongly influences the ignition of fires (Wotton, 2009; Bianchi & Defosse, 2014). The FFMC is a function of the average moisture content of the surface litter (up to 1.2 cm deep) and other cured fine fuels. This code is an indicator of the relative ease of ignition and the flammability of fine fuel with a dry weight of about 0.25 kg m^{-2} (van Wagner, 1987; Wotton, 2009). Higher FFMC values correspond to increased flammability. Such fuels are relatively fast drying, but substantially affected by the previous days' moisture value.

Calculation of the FFMC involves determining the fuel moisture (Figure 5.3) and equilibrium moisture contents, after which a drying/wetting rate (Table 5.1) is applied based on the observed temperature, relative humidity and wind speed (van Wagner, 1987). The temperature and relative humidity in the atmosphere determine a target equilibrium moisture content which the layer attempts to meet by following a simple exponential drying/wetting curve (Wotton, 2009), which is rooted in a physical understanding of how cellulose materials loose or gain moisture in reaction to atmospheric conditions. In the last step the influence of rainfall in increasing FMC is incorporated (only 24-hour accumulated rainfall exceeding 0.5 mm is considered). The FFMC was originally developed as a two digit code (from 00 up to 99) but was later modified to range from 0 (at a maximum FMC of 250%) to 101 (at the minimum FMC of 0%) (van Wagner, 1987; Dowdy *et al*., 2009; Wotton, 2009).

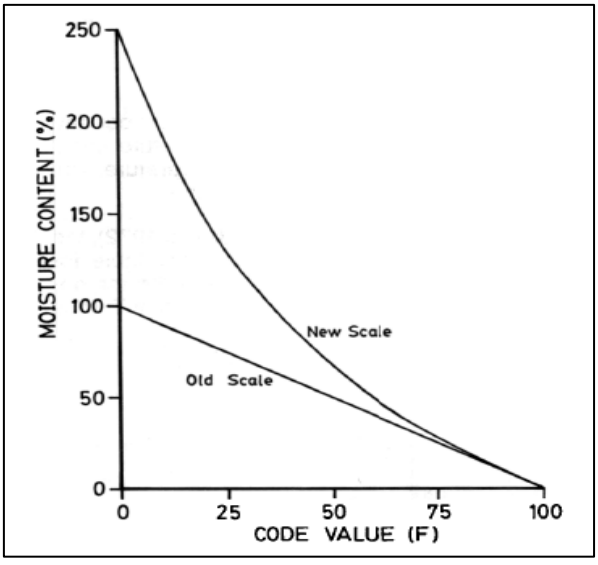

Figure 5.3 **Relationship between fuel moisture content (FMC) and the Fine Fuel Moisture Code (FFMC) (van Wagner, 1987).**

Table 5.1 Recovery of Fine Fuel Moisture Code (FFMC) after rain with three levels of temperature (T), relative humidity (RH), or wind speed (WS), with starting FFMC of 70 (after Lawson & Armitage (2008))

Days since last rainfall	FFMC with variable temperature RH = 45% WS = 18 km h^{-1}			FFMC with variable relative humidity T = 20°C WS = 18 km h^{-1}			FFMC with variable wind speed T = 20°C RH = 45%		
	10°C	20°C	30°C	65%	45%	25%	4 km h^{-1}	18 km h^{-1}	32 km h^{-1}
0	70	70	70	70	70	70	70	70	70
1	80	84	87	79	84	88	82	85	85
2	84	87	89	82	87	91	86	87	87

The FFMC undergoes a sinusoidal diurnal variation, but in the FWI it is only used to describe the afternoon state based on noon observations (Lawson & Armitage, 2008). Although originally designed to track moisture in an idealized pine stand, it should fare reasonably well in other stand types (Wotton, 2009). However, when applied over large geographical areas, the actual FMC might vary from that reflected by the FFMC.

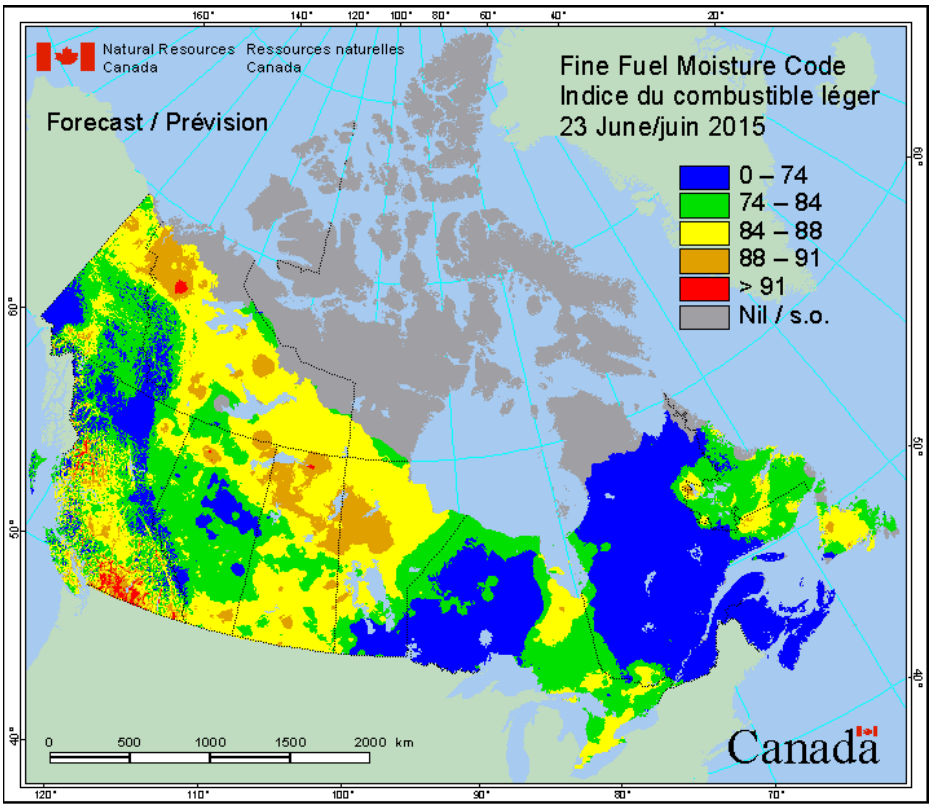

Figure 5.4 Predicted Fine Fuel Moisture Code (FFMC) across Canada on 23 June 2015 (CWFIS, 2015).

The FFMC is often used as an indicator of the receptivity of surface fuels to ignition (de Groot et al., 2005; Wotton, 2009; Global EWS, 2015) and thus is an important element in predicting fire occurrence. Fire managers use their understanding of the

relationships between human-caused fire occurrence and FFMC along with their understanding of potential human activity in the area to make predictions of the number of fires expected to occur each day. An example of its spatial variation is provided in Figure 5.4 which shows the predicted FFMC over Canada on 23 June 2015. Relatively low moisture content values (FFMC > 88) were predicted for parts of the Northwest Territories and Saskatchewan on this day.

THE DUFF MOISTURE CODE (DMC)

The DMC represents the average moisture content of the loosely compacted organic layers of moderate depth (decomposing litter) (CWFIS, 2015). This code provides an indication of fuel consumption in moderate duff layers (approximately 7 cm deep) and medium-sized woody material weighing about 5 kg m^{-2} (van Wagner, 1987; Wotton, 2009). Such fuels are relatively slow-drying. Its calculation involves a rainfall phase and a drying phase. In the rainfall phase the influence of rainfall on FMC is reflected (only 24-hour accumulated rainfall exceeding 1.5 mm is considered), while the drying phase incorporates the combined effects of temperature and relative humidity (van Wagner, 1987; Lawson & Armitage, 2008). Day length is also included since the amount of moisture lost daily from slow-drying fuels is equally dependent on the available time period as on noon weather conditions (van Wagner, 1987). The assumption is made that irrespective of how high the DMC rises, the lowest level of implied forest floor moisture is 20% (Figure 5.5). Although the daily drying factor in the DMC varies linearly with temperature and relative humidity, the relation between relative humidity and implied forest floor moisture content is nonlinear (logarithmic) (Lawson & Armitage, 2008). The DMC is a positive quantity that increases with increasing dryness and has no upper bound (Dowdy *et al*., 2009), although values above 150 are rarely observed (Wotton, 2009).

Whereas FFMC is often as an indicator of receptivity of fuels to human-caused ignitions, the DMC is used by fire managers, along with lightning detection technology, to determine where lightning strikes could potentially ignite the upper organic layer (Wotton, 2009). This is because lightning discharges typically run down tree trunks and ignite the surface or organic material near its base. According to Wotton (2009) this is a real possibility when the DMC exceeds a value of about 20.

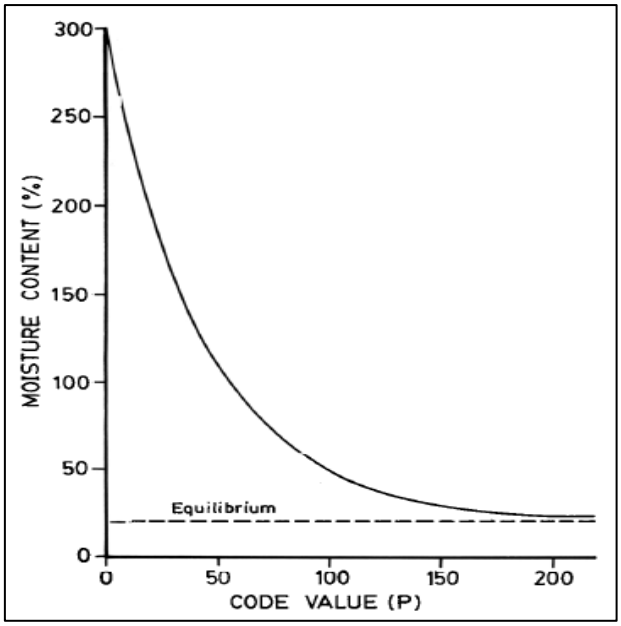

Figure 5.5 **Relationship between fuel moisture content (FMC) and the Duff Moisture Code (DMC) (van Wagner, 1987).**

Figure 5.6 provides an example of the spatial variation in the DMC over Canada on 23 June 2015. Relatively dry conditions (DMC > 60) were predicted for parts of western Canada on this day.

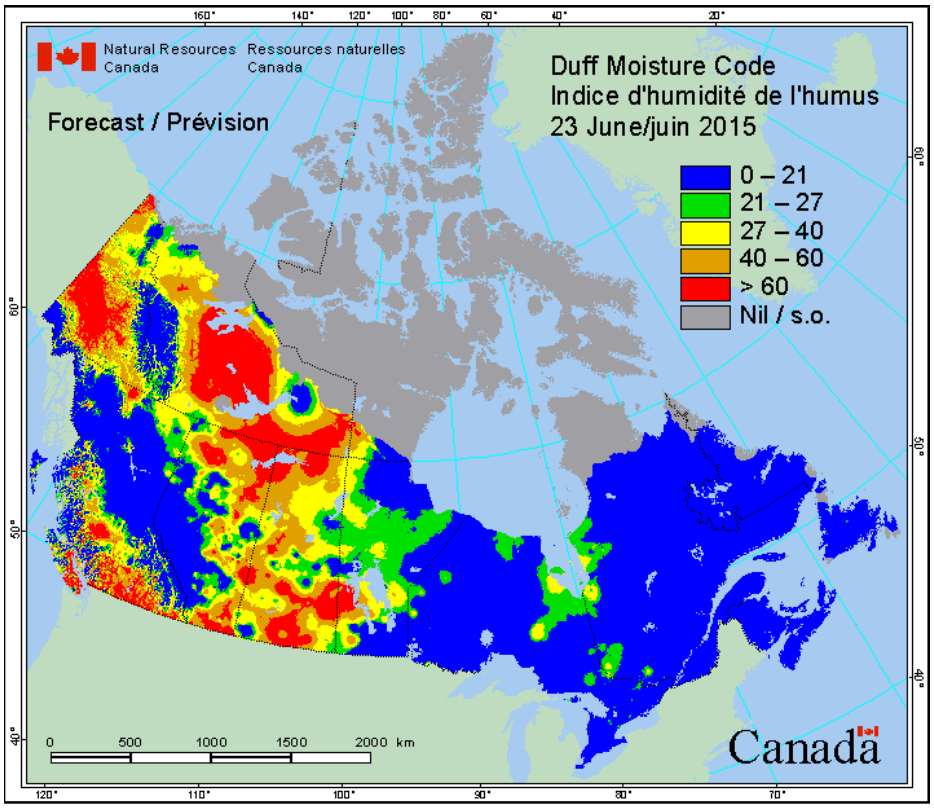

Figure 5.6 **Predicted Duff Moisture Code (DMC) across Canada on 23 June 2015 (CWFIS, 2015).**

THE DROUGHT CODE (DC)

The DC is a numeric rating of the average moisture content of deep, compact organic (humus) layers (CWFIS, 2015). It provides a useful indicator of seasonal drought effects on forest fuels and the amount of smouldering in deep duff layers (up to 18 cm deep) and large logs with a dry weight of about 25 kg m^{-2} (van Wagner, 1987; Wotton, 2009). Such fuels are very slow-drying and in the case of deep duff layers moisture reversals may occur. It is also considered to estimate the availability of water in streams, which may influence the availability of water for fire suppression and containment (Lawson & Armitage, 2008). The code was originally developed to estimate soil water content but was found to be suited to certain heavy fuels (van Wagner, 1987). The DC is thus similar to other drought models such as the Keetch–Byram Drought Index and the Palmer Drought Index (Wotton, 2009). An understanding of the severity of drought provides an indication of the amount of fuel that can be consumed in fires – both on the surface and within the forest floor (Wotton, 2009). Girardin *et al*. (2004) also found a historical correlation between DC and area burned (surface burned per year per climatic region) and forest fire frequency (number of fires per year per climatic region) for Canada.

Its calculation involves a rainfall phase (where the influence of rainfall exceeding 2.8 mm in a 24-hour period on FMC is considered), a drying phase (incorporating the effects of temperature and seasonal day length), and an overwintering phase (whereby a 53-day time lag is applied in order to carry forward the effect of winter precipitation into the new fire season's starting DC value) (Turner & Lawson, 1978; van Wagner, 1987). In contrast to the DMC, a constant equilibrium moisture content of 0% is targeted for this layer (Wotton, 2009). The overwintering phase seems to be of greater importance in high latitude areas and needs careful consideration for application outside Canada (San-Miguel-Ayanz *et al*., 2003; Dowdy *et al*., 2010). The DC is a positive quantity that increases with increasing dryness and has no upper bound (Figure 5.7), although significant differences in fire potential eventually become inconsequential and values exceeding 1 000 are extremely rare (San-Miguel-Ayanz *et al*., 2003; Wotton, 2009).

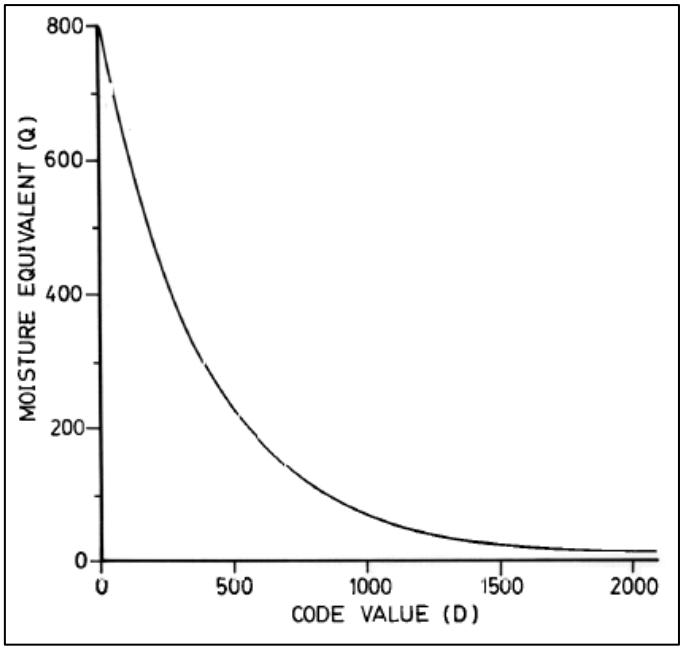

Figure 5.7 **Relationship between moisture equivalent and the Drought Code (DC) (van Wagner, 1987).**

The predicted DC over Canada on 23 June 2015 (Figure 5.8) provides an example of its spatial variation. Relatively dry conditions (DC > 425) were predicted for large parts of western Canada on this day.

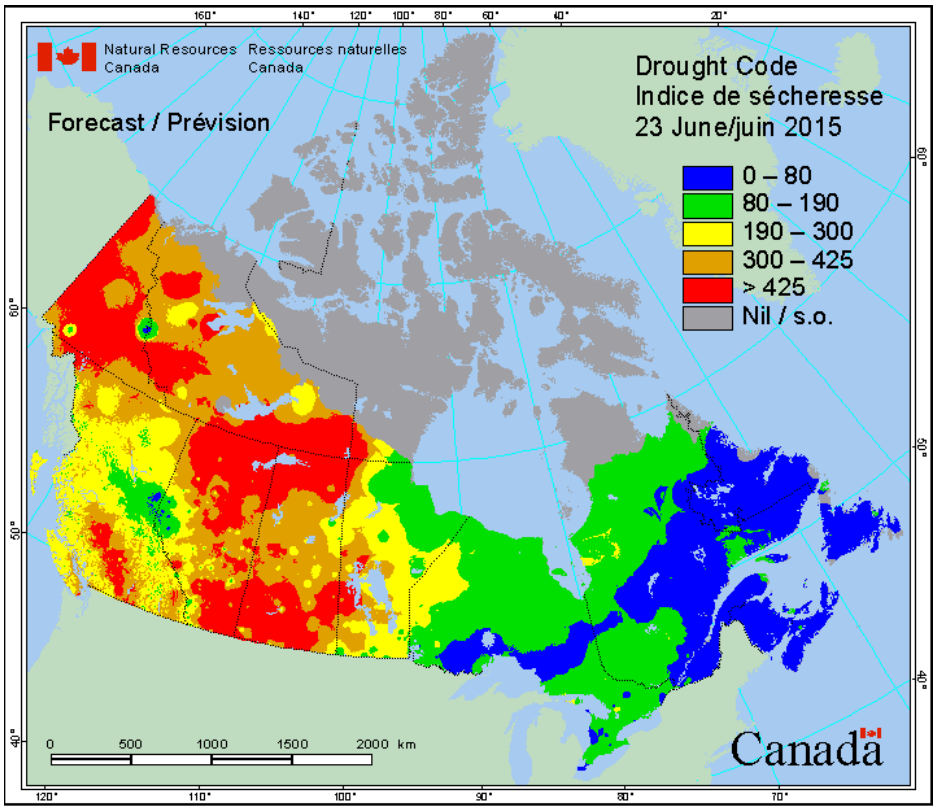

Figure 5.8 **Predicted Drought Code (DC) across Canada on 23 June 2015 (CWFIS, 2015).**

Each of the three fuel moisture codes are calculated on a daily basis using the previous day's value as an input (van Wagner, 1987; Dowdy *et al*., 2010). Stocks *et al*. (1989) likens these moisture codes to a bookkeeping system that adds moisture after rain and subtracts some for each day's drying. It is perhaps also important to note that the three moisture codes need not be in sync with another, as they have different drying/wetting rates and require different rainfall amounts in order to saturate the representative fuel layers. For example, light rain following a long dry spell will result in a low FFMC while the DMC remains high. Each fuel moisture code has direct bearing on various facets of wildfire potential. As an example, Stocks *et al*. (1989) noted that "fires are not likely to spread in surface litter with an FFMC less than about 74, the duff layer does not contribute to frontal fire intensity until the DMC reaches 20, and ground or sub-surface fire activity tends to persist at DC values greater than 400".

The remaining components of the FWI created from the above-mentioned moisture codes, relate to fire behaviour (Figure 5.2) and are described below. As before, formulas pertaining to their actual calculation are provided for different programming languages by Wang *et al*. (2015). The choice to keep these components separate was based on the ideal that each separate index value may convey useful information about the daily fire weather (van Wagner, 1987), capturing fire spread rate, fuel consumption and fireline intensity (Wotton, 2009).

THE INITIAL SPREAD INDEX (ISI)

The ISI represents the potential rate of fire spread by combining the effects of wind speed and the FFMC, without considering the influence of variable quantities of fuel (van Wagner, 1987; Lawson & Armitage, 2008; Wotton, 2009; Dowdy *et al*., 2010). As a general rule of thumb, with FFMC held constant the ISI doubles in value for each wind speed increase of 14 km h^{-1} (Lawson & Armitage, 2008). Similarly, with wind speed held constant, an escalation of five to seven FFMC units is necessary to double the ISI under moderate to severe conditions (Lawson & Armitage, 2008). If the ground is covered by snow or hail at the time of observation, the ISI is kept at zero until it has melted (Lawson & Armitage, 2008). The actual heading fire rate of spread (ROS) can vary from the ISI due to fuel complex differences (Stocks *et al*., 1989; Amiro *et al*., 2001). Figure 5.9 shows how the relationship between ROS and ISI varies across

different fuel complexes. There should be a strong relationship between ISI and area burned (San-Miguel-Ayanz *et al*., 2003).

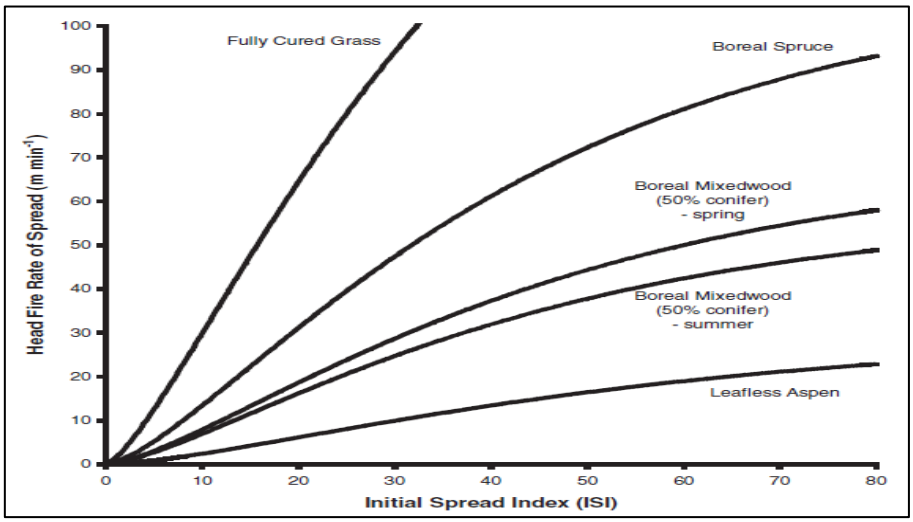

Figure 5.9 **Heading fire rate of spread (ROS) on level terrain as a function of the Initial Spread Index (ISI) for different fuel types (Amiro *et al*., 2001).**

The dependence of the ISI on the FFMC and wind speed is depicted in Figure 5.10. Although the ISI is technically open ended, practical limits apply. Figure 5.11 shows the ISI over Canada on 23 June 2015. Relatively high spreading rates (ISI > 15) were predicted for parts of the Northwest Territories on this day.

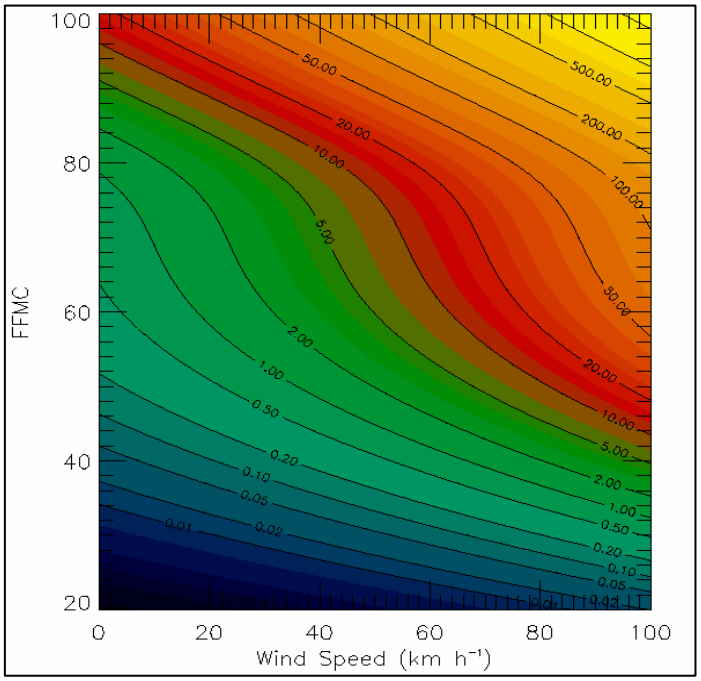

Figure 5.10 **Dependence of the Initial Spread Index (ISI) on the Fine Fuel Moisture Code (FFMC) and the wind speed (Dowdy *et al*., 2009). ISIs are given by the values on the isolines.**

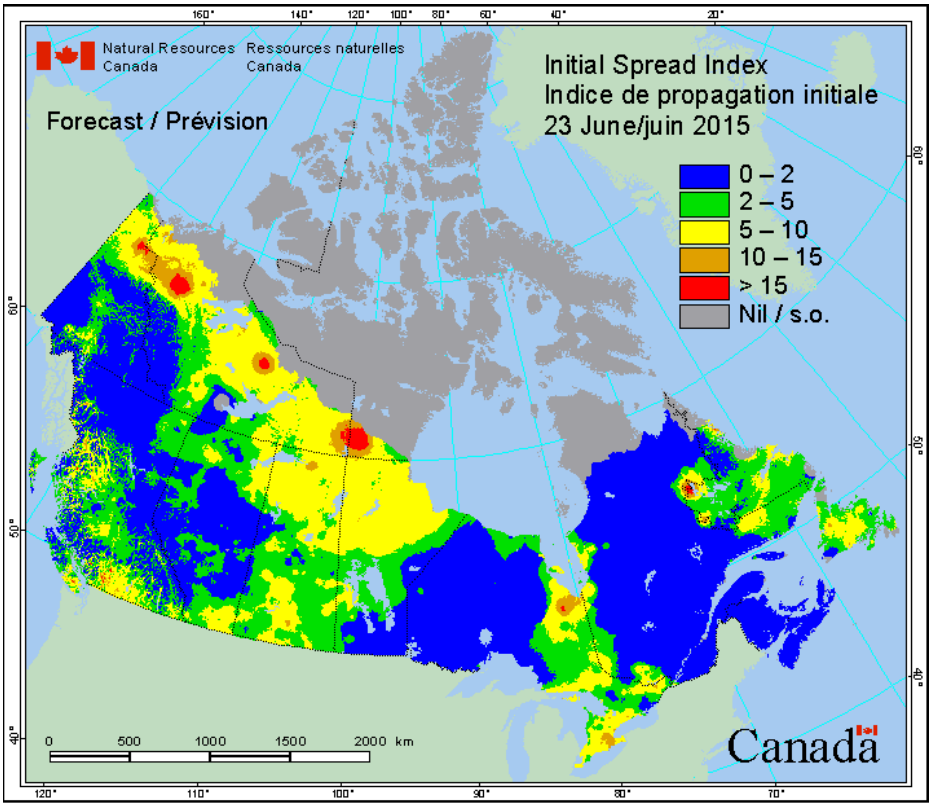

Figure 5.11 **Predicted Initial Spread Index (ISI) across Canada on 23 June 2015 (CWFIS, 2015).**

THE BUILDUP INDEX (BUI)

The BUI is a unitless numeric rating used as a relative indicator of potential fuel available for consumption (consumption of material on and in the forest floor by the passing fire front) (Wotton, 2009; Pereira *et al*., 2013; CFWIS, 2015). The BUI is a weather-index only (Wotton, 2009) and therefore does not take into account actual fuel load on the ground but rather assumes a standard load and fuel arrangement that would be adequate to maintain fire spread. Fire managers often use the BUI as an indicator of the potential tendency of a fire to remain smouldering deep in the ground or in large woody material (Wotton, 2009).

A form of the harmonic mean of the DMC and the DC (the two fuel moisture codes with longer time scales) is used to calculate the BUI (van Wagner, 1987; Lawson & Armitage, 2008; Dowdy *et al*., 2009). Technically the BUI has no upper bounds, but practical limits exist (San-Miguel-Ayanz *et al*., 2003). The dependence of the BUI on the DMC and the DC is depicted in Figure 5.12, while Figure 5.13 shows the predicted BUI values over Canada on 23 June 2015. Note the extremely dry conditions (BUI > 90) predicted for parts of western Canada on this day.

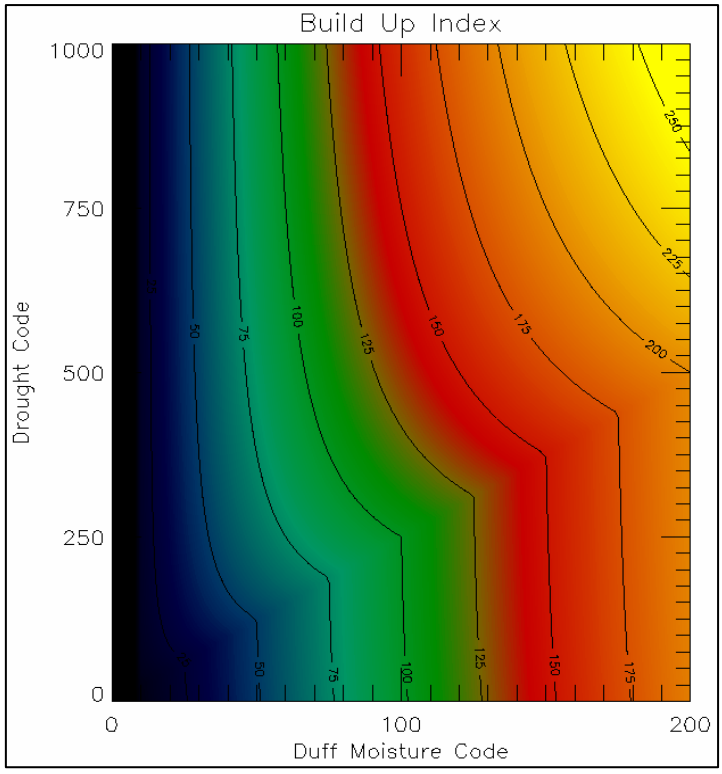

Figure 5.12 **The Buildup Index (BUI) for various values of the Duff Moisture Code (DMC) and the Drought Code (DC) (Dowdy *et al*., 2009). BUIs are given by the values on the isolines.**

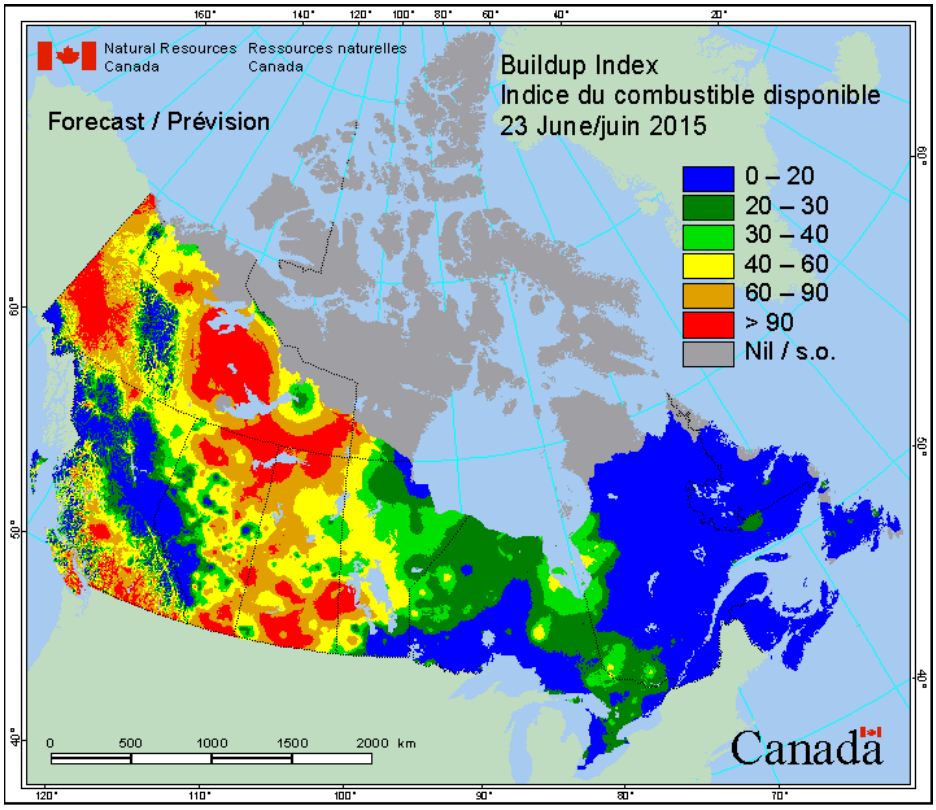

Figure 5.13 **Predicted Buildup Index (BUI) across Canada on 23 June 2015 (CWFIS, 2015).**

THE FIRE WEATHER INDEX (FWI)

The FWI represents the peak intensity of the spreading fire, as the energy output rate per unit length of fire front (van Wagner, 1987; Lawson & Armitage, 2008; Dowdy *et al*., 2009) by combining the ISI and the BUI (Figure 5.14). The FWI is analogous to Byram's fireline intensity (Section 2.4), and therefore also roughly proportional to flame length, another useful measure of fire behaviour (van Wagner, 1987; Wotton, 2009). On a regional scale (Greece and Italy), Hanson and Palutikof (2005; cited by Moriondo *et al*., 2006) established a non-linear relationship between the FWI and forest fire frequency, while Bedia *et al*. (2015) showed that average FWI and annual burned area were significantly correlated over extensive world areas. As a general summary of fire weather and fuel moisture in a region, the FWI – a positive open-ended index – is a useful sole indicator of general fire potential (Wotton, 2009). It is this value that is communicated to the public and used in setting the levels on roadside fire danger signs.

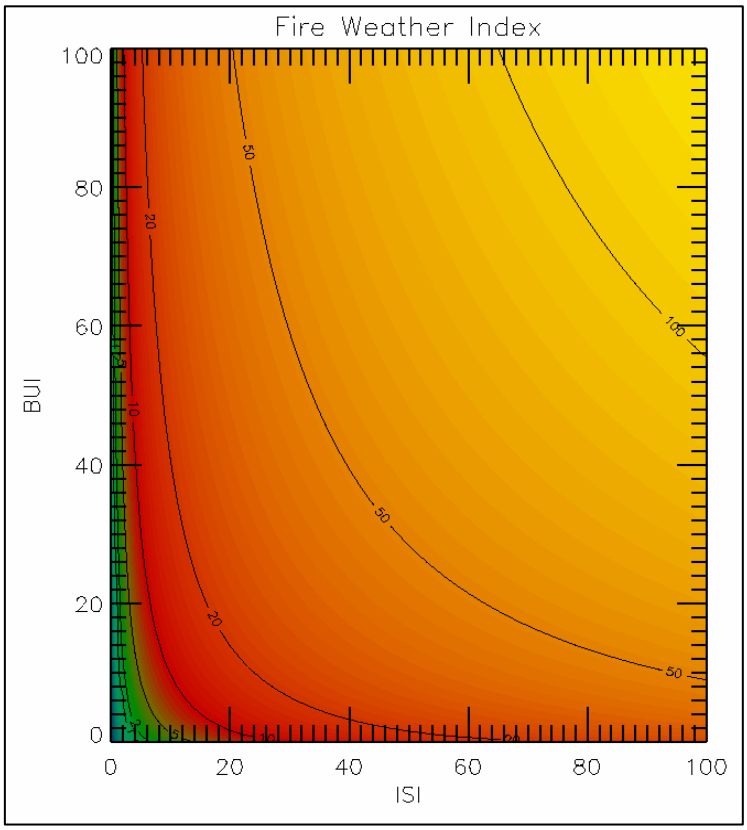

Figure 5.14 **Relationship between the Fire Weather Index (FWI) and its determinant components, the Initial Spread Index (ISI) and the Buildup Index (BUI) (Dowdy *et al*., 2009). FWIS are given by the values on the isolines.**

The FWI system does not portray hourly changes in fire danger conditions, but rather represent conditions during the mid-afternoon peak burning period, assuming a normal diurnal weather pattern (van Wagner, 1987). However, according to Lawson & Armitage (2008) several Canadian fire management agencies have employed an hourly version of the FFMC, together with hourly wind observations, as inputs to the FBP system (Figure 5.1). In the case of rainy days, the effect of the rain is first taken into account before the appropriate drying is applied. The FWI system is dependent on weather only and doesn't consider differences in ignition risk or topography (San-Miguel-Ayanz *et al*., 2003). Variations in fuel type from one season to another or across locations are also not considered (Lawson & Armitage, 2008).

Note the association, but also the differentiation, between high fire weather danger (FWI > 30 in Figure 5.15) predicted over western Canada (the Northwest Territories and Saskatchewan) on 23 June 2015 and the components it is derived from (FFMC > 88 in Figure 5.4; DMC > 60 in Figure 5.6; DC > 425 in Figure 5.8; ISI > 15 in Figure 5.11 and BUI > 90 in Figure 5.13). Numerous wildfires were observed across the region (Figure 5.16) and continued to rage for several days. A smoke plume from these Canadian (and Alaskan) wildfires was later reported to extend all the way through the US Midwest, reaching as far south as Texas and Louisiana (Figure 5.17) (Walker, 2015). Several days later still CNN reported on the evacuation of about 13 000 people in Saskatchewan as hundreds of wildfires continued to burn uncontrollably (Almasy & Gallman, 2015).

Although the FWI system provides a uniform method of rating fire danger and is relatively simple to apply, its outputs can be difficult to interpret without experience since raw output codes and indices have no real physical units (Wotton, 2009). Generally, values from 0 to 8 are considered low, 8 to 17 are considered moderate, 17 to 32 are considered high and values greater than 32 are considered extreme (Lampin-Maillet *et al*., 2010). Anderson and Englefield (2001) found that 95% of observed lightning fire initiations in Saskatchewan occurred at a FWI of 32.4 or higher. However, Mölders (2010) employed FWI threshold values in Alaska of 2, 12 and 27 to designate moderate, high, and extreme fire risk, respectively. Carvalho *et al*. (2011) applied the FWI system to Portugal by using the modified threshold values in Table 5.2. Dimitrakopoulos *et al*. (2011) also derived thresholds for the FWI system which

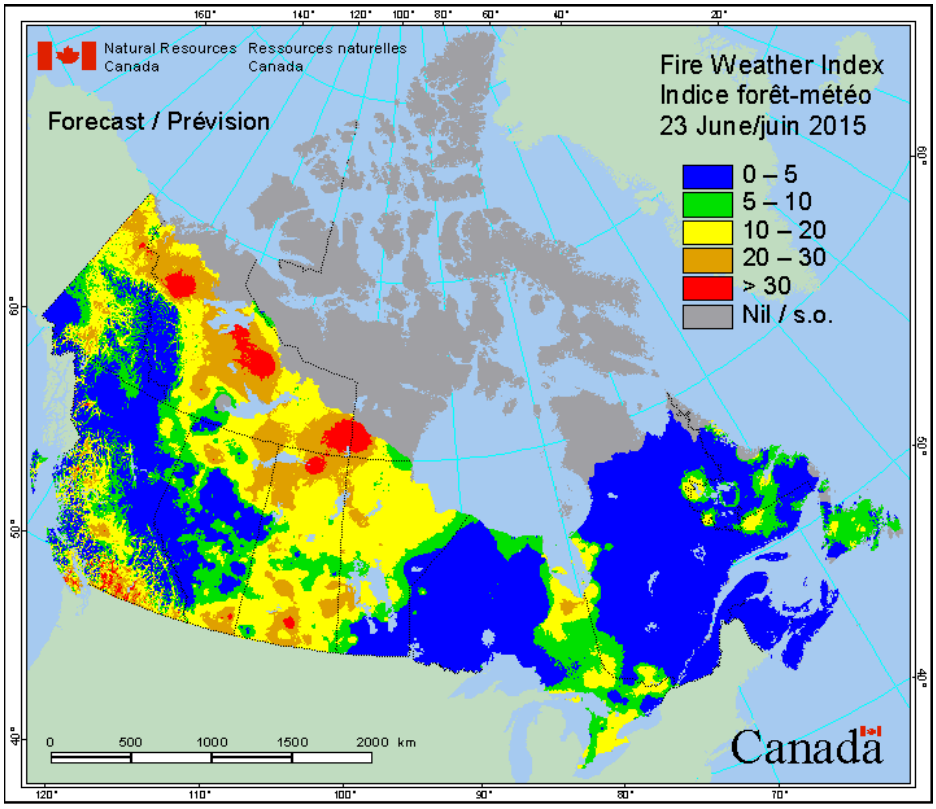

Figure 5.15 **Predicted Fire Weather Index (FWI) across Canada on 23 June 2015 (CWFIS, 2015).**

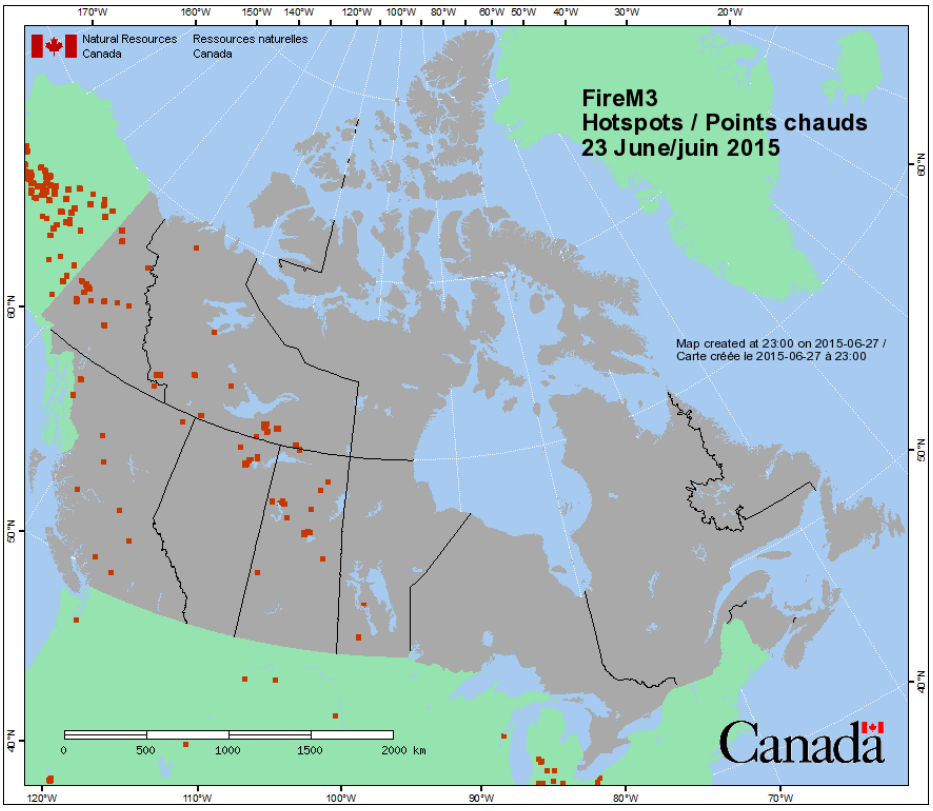

Figure 5.16 **Fire hotspots across North America on 23 June 2015 (CWFIS, 2015).**

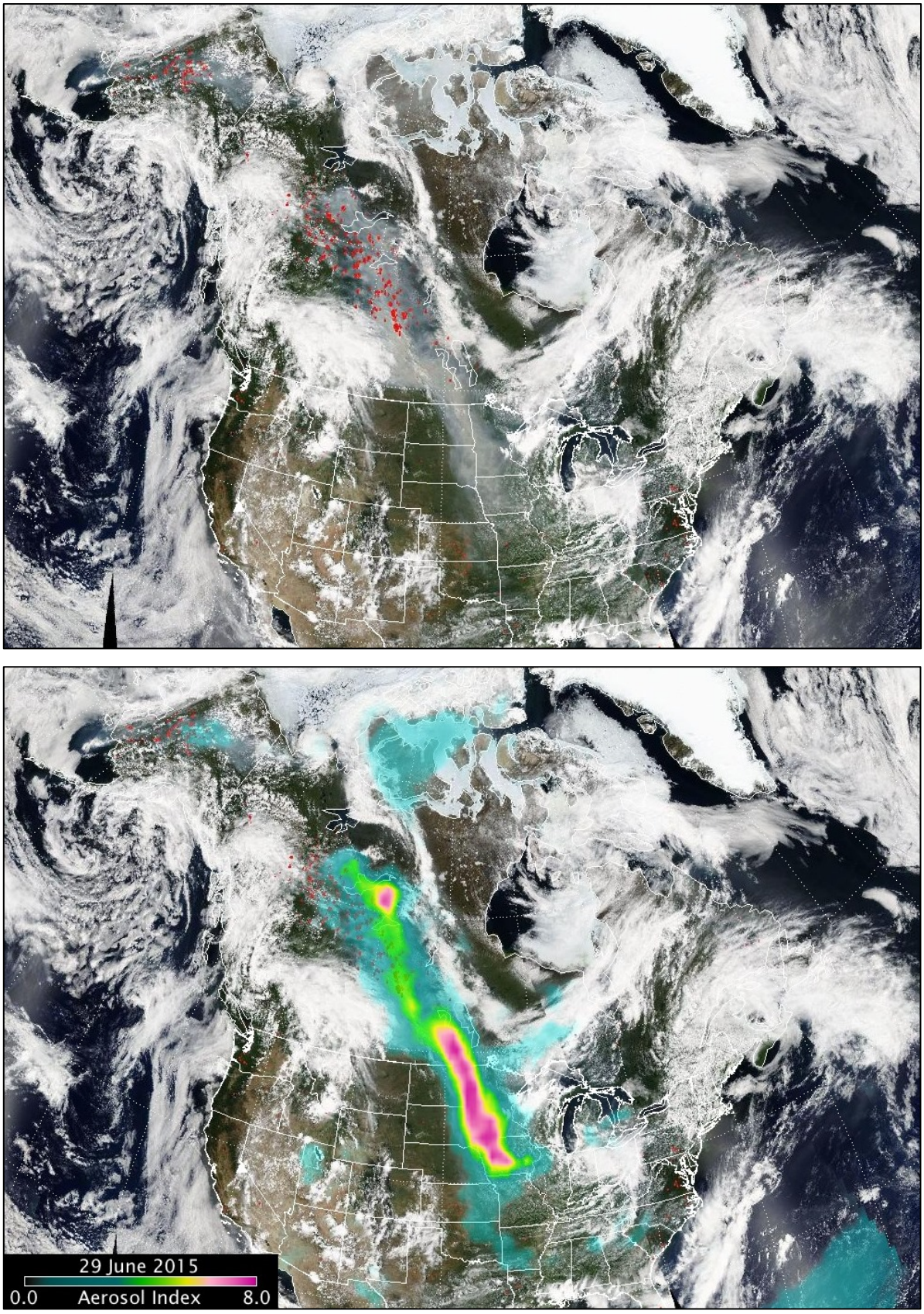

Figure 5.17 **Smoke from wildfires across North America captured by the Aqua MODIS satellite on 29 June 2015. In both cases the colour enhanced image in the visible part of the spectrum is shown over which fire detection (top) and aerosol index (bottom) is superimposed (NASA OMPS, 2015).**

they deemed more appropriate for Mediterranean environments, namely: 0 to 38 for low, 39 to 48 for moderate, 49 to 60 for high, and values greater than 60 for extreme fire danger. It seems likely that such higher thresholds should also apply to conditions in southern Africa.

Table 5.2 Category thresholds of the Fire Weather Index (FWI) System components for use in Portugal (Carvalho *et al*., 2011)

Danger class	FWI system components					
	FFMC	DMC	DC	ISI	BUI	FWI
Low	0 – 18	0 – 19	0 – 78	0 – 1.9	0 – 23	0 – 3
Moderate	82 – 87	20 – 84	78 – 505	2 – 4.9	24 – 115	4 – 17
High	88 – 89	85 – 143	506 – 743	5 – 7.9	116 – 180	18 – 27
Very high	90 – 92	143 – 187	744 – 882	8 – 11.9	181 – 224	28 – 38
Extreme	≥ 93	≥ 188	≥ 883	≥ 12	≥ 225	≥ 39

TEMPORAL OR SEASONAL AVERAGING

The Daily Severity Rating (DSR) provides a relative numeric rating of the difficulty of controlling fires (Pereira *et al*., 2013). It is based on the FWI but more accurately mirrors the amount of work required to suppress a fire (CWFIS, 2015). According to Lawson & Armitage (2008) the FWI itself should be used only as a simple daily value and is not considered suitable for averaging. Any averaging, whether spatially or temporally, should rather be done through the use of the DSR (van Wagner, 1987; Pereira *et al*., 2013). Anderson and Englefield (2001) found that 50% of observed lightning fire initiations in Saskatchewan occurred at a DSR of 3.3 or higher. Figure 5.18 shows the predicted DSR values over Canada on 23 June 2015. Fires that may become difficult to control are indicated in a band stretching across western Canada (the Northwest Territories and Saskatchewan).

The DSR (a non-dimensional variable) and its time-averaged values, the Monthly Severity Rating (MSR) and Seasonal Severity Rating (SSR), are derived from the FWI as follows:

$$DSR = 0.0272 \cdot FWI^{1.77}$$

$MSR = {\sum_{i=1}^{n} DSR_i}/{n}$ where *n* = number of days in month

$SSR = {\sum_{i=1}^{n} DSR_i}/{n}$ where *n* = number of days in season

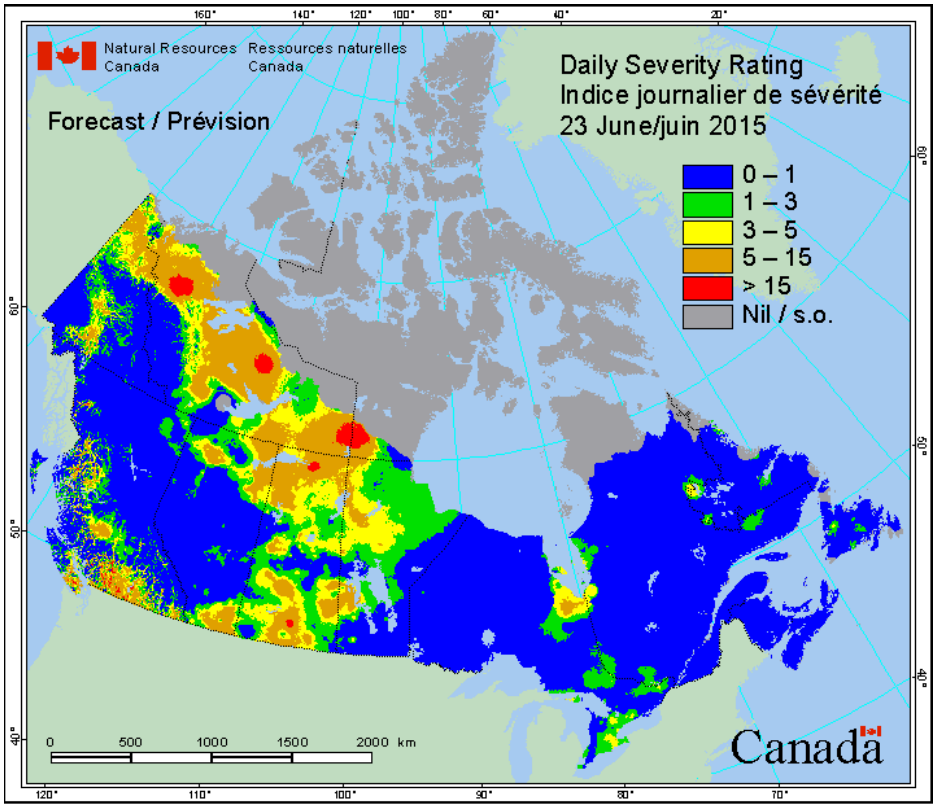

Figure 5.18 **Predicted Daily Severity Rating (DSR) across Canada on 23 June 2015 (CWFIS, 2015).**

The SSR can be used as an objective measure of fire weather from one season to another or of fire climate from one region to another (van Wagner, 1987; Lawson & Armitage, 2008). The classification thresholds provided in Table 5.3 were used by Vučetić *et al*. (2006) in a study conducted for Croatia.

Table 5.3 **Interpretation of Seasonal Severity Rating (SSR) values according to Dimitrov (1998; cited by Vučetić *et al*., 2006)**

SSR	Interpretation
> 7	Very high risk
3 – 7	High risk
1 – 3	Moderate risk
< 1	Low potential risk

IMPLEMENTATION OUTSIDE CANADA

As mentioned earlier, the FWI system has been adapted for use in parts of North, Central and South America, Europe, Asia and Australasia, covering a range of climate regions and vegetation types. The FWI is thus commonly considered useful in defining daily fire risk (Lampin-Maillet *et al*., 2010). Its appeal is mainly ascribed to the fact that the FWI system requires the input of only four weather parameters each day (de Groot

et al., 2006). However, calibration of the classification thresholds is required to suit local climatic conditions (de Groot *et al*., 2006; Dowdy *et al*., 2010).

The six components of the FWI system (Figure 5.2) presented on the global early warning system's website (e.g. Figure 5.19) are currently not calibrated to the local fire regime, i.e. the influences of fuel, ignition sources, climate, fire management/suppression policy, etc. (Global EWS, 2015). Such regional calibration will be an on-going collaborative effort with regional and national agencies. According to Global EWS (2015), frequently applied threshold values that categorise fire weather were used. As such, this "globally-consistent calibration" system allows for the comparison of relative fire danger conditions between countries and biomes, while the short-range forecasts reveal fire danger trends over the next seven days (Global EWS, 2015). As justification it can be argued that the same physical principles govern the water gain/loss of dead fuels, while fire behaviour responds in the same way to variations in fuel conditions, weather and topography worldwide (Taylor & Alexander, 2006; Bianchi & Defosse, 2014).

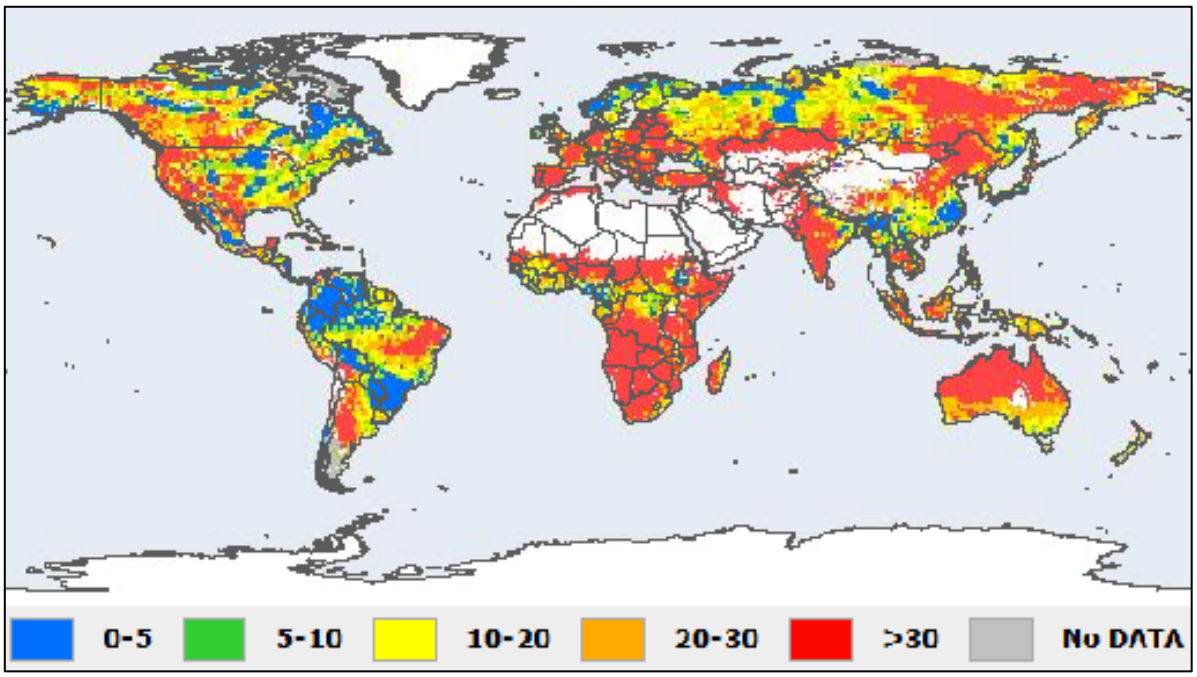

Figure 5.19 Global Fire Weather Index (FWI) predicted for 7 July 2015 (Global EWS, 2015).

However, a site-specific fire danger value holds different meaning in different fire regimes (at least in a fire management context). Because it was developed to represent fire danger and behaviour in a generalised standard fuel type, the FWI system will obviously have different meanings in different fuel types (van Wagner, 1987). Certainly, the very existence of fuel-specific moisture content models such as those developed for fast wetting/drying or slow wetting/drying fuels (Taylor & Alexander, 2006) is a case in point. There is thus additional value in comprehending fire danger in relation to the local fire regime, which includes the influences of fuel, ignition sources, climate, fire management/suppression policy, etc. (Global EWS, 2015). Therefore, regional calibration to adjust the fire danger scales is required. This point is highlighted by the vast areas shaded in red in Figure 5.19.

As a first step, historical weather data can be used to categorize fire danger levels based on frequency of occurrence (Willis *et al*., 2001; de Groot *et al*., 2005; de Groot *et al*., 2006). Further calibration can then focus on the use of remotely sensed hot spot data to calibrate the FFMC as a predictor of fire ignitions (de Groot *et al*., 2006; Global EWS, 2015). Such a trial calibration was performed using one year of MODIS hot spot data for sub-Saharan Africa (Figure 5.20) and corresponding FFMC data (Figure 5.21) for each hot spot location (Global EWS, 2015). However, the only discernible alteration to the FFMC thresholds was a change to the upper boundary of the lowest category from 74 to 76. The procedure was said to provide operational-level information such as potential for fire starts and difficulty of control. Similar calibrations were performed for south-east Asia and Central and South America, yielding very similar FFMC scale calibrations (Global EWS, 2015). Finally, implementing the overwintering scheme is not required for lower latitudes or when daily water balance equations are applied throughout the year (Dowdy *et al*., 2010).

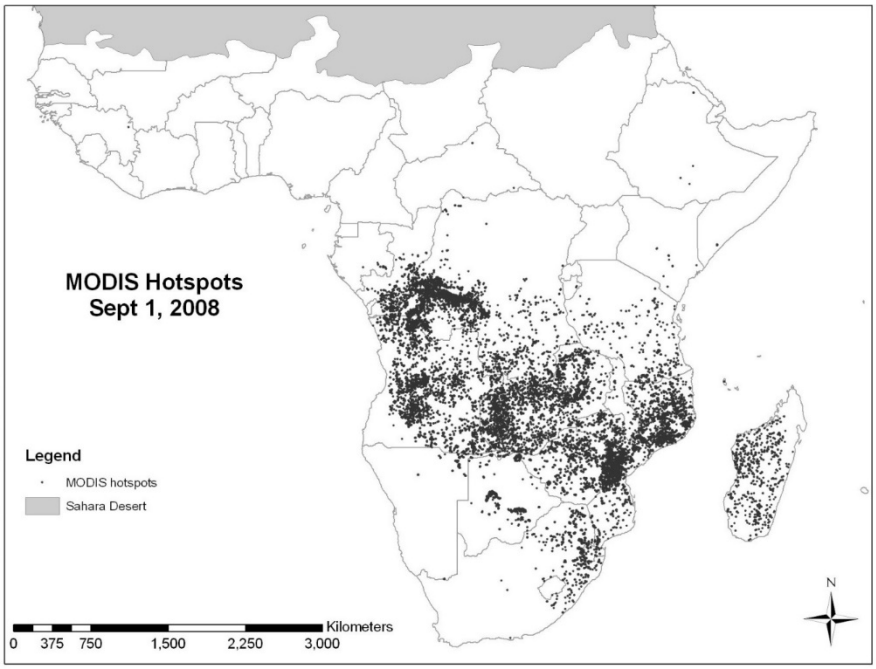

Figure 5.20 **MODIS hot spots for 1 September 2008 over sub-Saharan Africa (Global EWS, 2015).**

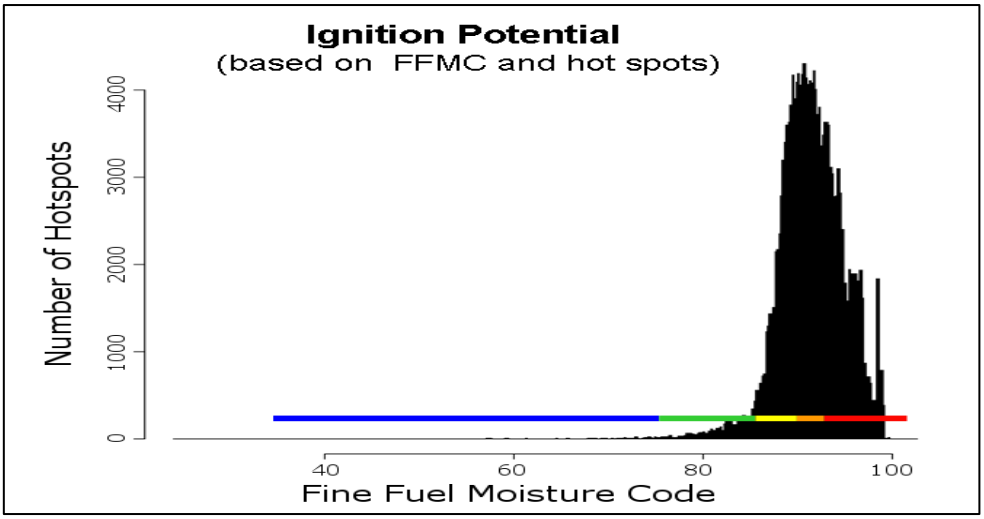

Figure 5.21 **Calibrating the Fine Fuel Moisture Code (FFMC) with satellite-detected hot spots over sub-Saharan Africa to construct a fire start predictor, or "Ignition Potential" indicator (Global EWS, 2015).**

In adapting the FWI system to Indonesia and Malaysia, de Groot *et al*. (2005; 2007) conducted an analysis of historical hot spots (remotely sensed data) along with grass moisture and grass ignition studies (field and laboratory trials). These revealed that fire occurrence and the ability for grass fires to start and spread dramatically increased when the FMC reached a threshold of 35% (Figure 5.22), corresponding to a FFMC of about 82. In south-east Asia, 86% of historical hot spots occurred when the FFMC was ≥ 78. Very high fire intensities were also observed in grasslands when the ISI was

6 or greater. The FFMC scale was subsequently recalibrated by using the average threshold of dead grass ignition (FFMC = 82) as the upper limit of the high category. The extreme category (FFMC > 82) thus represented the range in which fires would ignite and spread with ease. The highest possible FMC at which grass ignition could possibly occur, as defined by the 95% confidence interval limit, corresponded to a FMC of 51% (FFMC = 78). Another interesting result for this part of the world was that historical air quality analysis showed a correspondence between severe haze conditions and a DC exceeding 350.

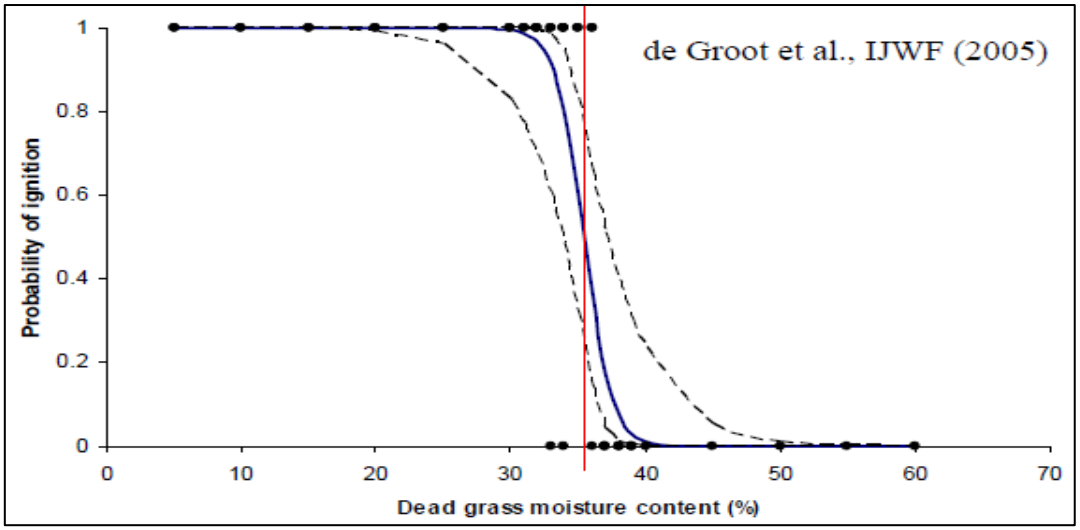

Figure 5.22 **Dataset points and logistic regression model (solid line) showing ignition probability of grass as a function of moisture content (FMC) (de Groot *et al*., 2005).**

In Argentina, Dentoni *et al*., (2007; cited by Bianchi & Defosse, 2014) found a reasonably good relationship between fire occurrence and (uncalibrated) FWI components. However, Bianchi & Defosse (2014) sought to improve the system's overall performance. They conducted lab ignition tests on dead fine surface fuels that were collected at regular intervals over three summer seasons in the forests of north-west Patagonia, Argentina. They also applied a logistic regression model in order to correlate the calculated FFMC with the measured FMC. Results of the ignition tests and of the regressions were subsequently combined to suggest FFMC categories for estimating fire danger in Patagonian forests. The observed FMC varied from 7.3 to 129.6%, while the calculated FFMC varied from 13.4 to 92.6 (Figure 5.24). The ignition threshold occurred at FMC values of 21.5 and 25.0%, depending on tree type (Figure 5.24). It was proposed to divide the FFMC scale into three fire danger categories: Low

(FFMC ≤ 85), High (85 < FFMC ≤ 89) and Extreme (FFMC > 89). According to the regression model (Figure 5.23) the upper limit of FFMC = 85 for the lowest category corresponded to a FMC between 38 and 39%, while the upper limit of FFMC = 89 for the middle category could be associated with a FMC between 6 and 11%. The FFMC calculated over the three seasons indicated that 49.2% of the days can be considered as Low, 34.3% as High and 16.5% as Extreme fire danger.

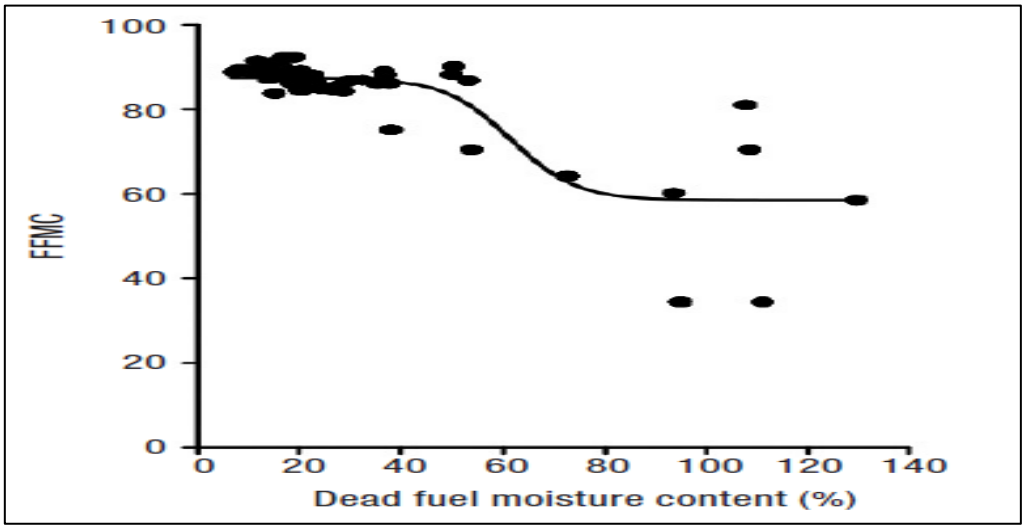

Figure 5.23 **Plots of the four parameter logistic regression model (solid line) relating dead fine surface fuel moisture content (FMC) from native Patagonian forest species and the calculated Fine Fuel Moisture Code (FFMC) (Bianchi & Defosse, 2014).**

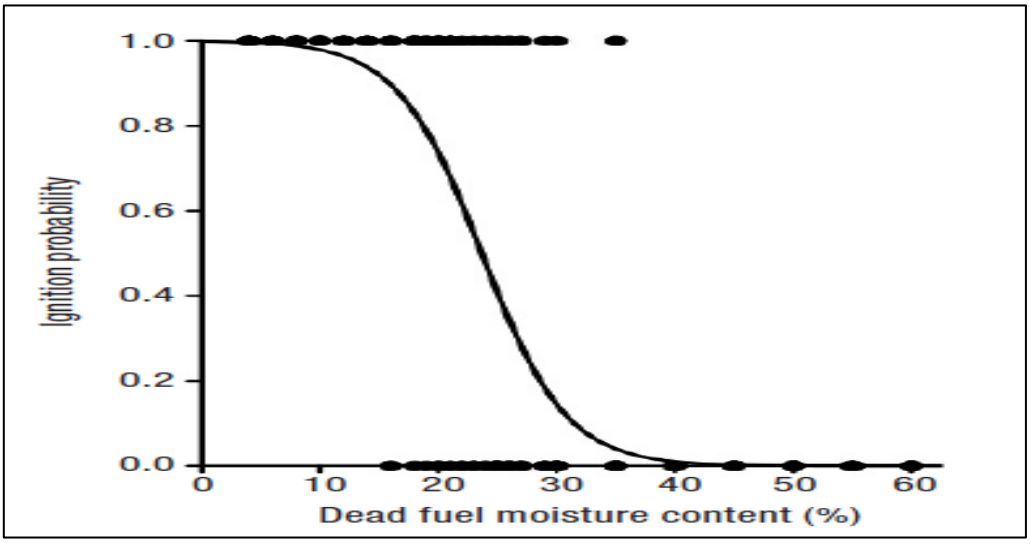

Figure 5.24 **Dataset points and logistic regression model (solid line) showing ignition probability against dead fine surface fuel moisture content (FMC) from native Patagonian forest species (combined results for ñire (*Nothofagus antarctica*) and cypress (*Austrocedrus chilensis*) (Bianchi & Defosse, 2014).**

No specific references could be found on the determination of the dead fine fuel moisture content ignition threshold of the grasses in central South Africa. However, in the "*Wildland Fire Management Handbook for sub-Saharan Africa*" the following relevant statements were made:

a) In Chapter 3 Trollope *et al*. (2004) noted that: "The moisture content of the fuel particles will determine the ease of ignition in dead (cured) grass, e.g. a sustained flame is required for ignition at a moisture content above 15%. Ignition will become progressively easier as the moisture content of dead fuel decreases, and below a moisture content of 6%, very small embers or hot particles are capable of igniting grassy fuels." However, reference is made to Cheney and Sullivan (1997) whose work relates to Australian grasses.
b) In Chapter 12 de Ronde *et al*. (2004a) reported that ignition will usually commence when grass is at between 50 and 60% curing (Figure 4.5), and will occur with little difficulty when the grass is about 70% cured. The relationship between grass curing (GC) and FMC, both as percentages, is provided by the following equation adapted from Trollope *et al*. (2010) for use in grassland and savanna communities in southern Africa:

$$\mathrm{FMC} = 138.46 - 1.28\mathrm{GC}$$

Thus, following the Argentinian example of dividing the FFMC scale into three fire danger categories could yield: Low (GC ≤ 50), High (50 < GC < 70) and Extreme (GC ≥ 70). Applying the above-mentioned result in (b) in order to translate curing into FMC would then give: Low (FMC ≥ 74%), High (49% < FMC < 74%) and Extreme (FMC ≤ 49%).

5.2 UNITED STATES NATIONAL FIRE DANGER RATING SYSTEM

In the U.S.A. research on the relationships between fire danger and weather, fuel moisture and ignition probabilities dates back to 1916 (Hardy & Hardy, 2007). The National Fire Danger Rating System (NFDRS; here referred to as the US NFDRS) was developed in order to obtain consistency among the various organizations and protection agencies operating in the U.S.A., with the initial version released in 1972 (Schlobohm & Brain, 2002). It was a manually operated system comprising numerous lookup tables and alignment charts based on Rothermel's fire behaviour model (Rothermel, 1972; cited by Willis *et al*., 2001; Schlobohm & Brain, 2002). An

automated version was implemented in 1975, with further modifications added in 1978 and 1988 (Schlobohm & Brain, 2002; Hardy & Hardy, 2007). The US NFDRS has been applied across the U.S.A. to a wide range of vegetation (fuel) types and climatic conditions and tested in South Africa, Europe, Asia and Australia (Willis *et al*., 2001).

DESCRIPTION OF THE 1978/88 VERSIONS

A physically based fire behaviour model forms the basis of the system, comprising several mathematical models representing the basic principles of combustion (Schlobohm & Brain, 2002). The system relies heavily on laboratory determined values such as the ignition temperatures of woody material, combustion rates, the moisture of extinction of different types of plant material, the chemical properties of woody debris and heat energy potential (Schlobohm & Brain, 2002). The system thus has the advantage of being mechanistic, but entails relatively complex model parameterisations for new situations (Willis *et al*., 2001). Figure 5.25 provides a schematic outline of the inputs and modules of this system.

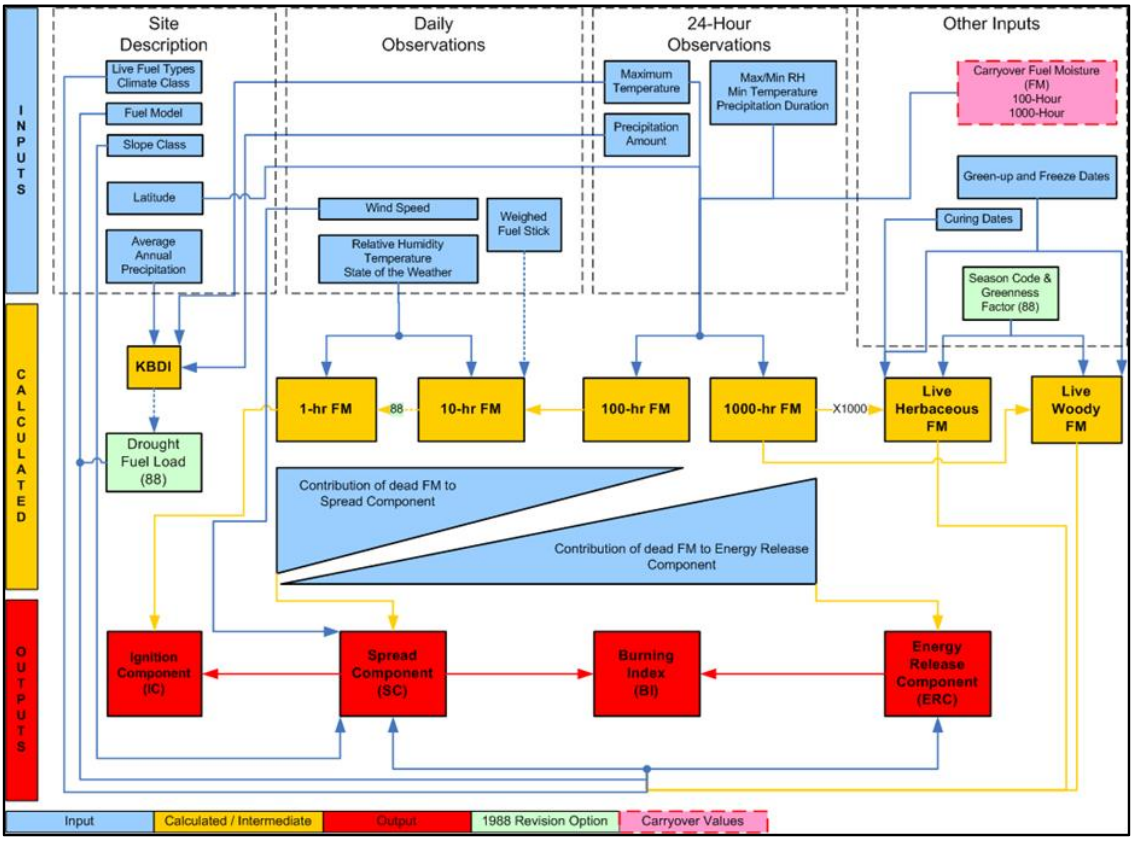

Figure 5.25 Structure of the 1978/88 United States National Fire Danger Rating System (US NFDRS) showing the relationships between observational inputs, intermediate calculations of fuel conditions and output indices. Arrows or blocks labelled as (88) apply only to the 1988 version (Jolly *et al*., 2016).

User specified site descriptors (upper left corner of Figure 5.25) include the most suitable climate class, slope class, fuel model, latitude and the annual average precipitation, which need only be selected once for a particular area (Willis *et al*., 2001; Schlobohm & Brain, 2002; Mölders, 2010). Since all US NFDRS outputs and indices are applied to a so-called Fire Danger Rating Area (FDRA), these site descriptors are either objectively (e.g. climate class and annual precipitation) or subjectively (e.g. slope class and fuel model) chosen to be representative of such a FDRA. FDRA is defined as "a geographical area of generally homogenous fuels, weather and topographic features" so as to create uniform fire danger throughout (Schlobohm & Brain, 2002). The climate class reflects the duration of the growing period when plants are lush and green, with four options representing arid or semi-arid desert or steppe (class 1), semi-humid climate where summertime moisture is deficient (class 2), semi-humid climate where summertime precipitation is adequate to sustain plant growth most of the season (class 3) and wet coastal areas where summertime precipitation and fog are common (class 4) (Schlobohm & Brain, 2002). The slope class should be representative of the whole FDRA with average slopes grouped into five classes labelled 1 through 5 to denote 0 – 25%, 26 – 40%, 41 – 55%, 56 – 75% and > 75%, respectively (Schlobohm & Brain, 2002). The fuel model is a set of descriptors that characterise the dominant vegetation type in an area (Willis *et al*., 2001). A wide range of fuel types (40 in total) are covered and these include live FMC (Jolly *et al*., 2016).

Daily weather inputs to the US NFDRS (upper centre of Figure 5.25) include observed or forecast values of drybulb temperature, relative humidity, dew-point temperature and wind speed, measured at 13:00 LST, while a state of the weather code is used to gauge the contribution of cloud cover and precipitation type to fuel moisture (Schlobohm & Brain, 2002). Minimum and maximum drybulb temperature and relative humidity, as well as total accumulated precipitation, are reported for the preceding 24-hour period. In comparison to the other systems described in this chapter, some of the data required by the US NFDRS (e.g. cloud cover and rainfall duration) are not always readily available (Willis *et al*., 2001).

Other parameters that must be input periodically (upper right corner of Figure 5.25) are the occurrence of a killing frost based on local conditions, starting date of the growing season, an indication whether the local shrub vegetation is deciduous or

evergreen and measured live woody fuel moisture (Schlobohm & Brain, 2002). The latter can be computed solely from weather data but may differ quite substantially from measured values. The season code is meant to represent the various stages of plant development, while the greenness factor is a scaled value from 0 to 20 which corresponds to the observed condition of grasses and shrubs (viz. 0 denoting near dead and 20 representing flush vegetation) (Schlobohm & Brain, 2002).

Outputs from the US NFDRS (central and lower blocks in Figure 5.25) include the 1-, 10-, 100- and 1 000-hour FMC, the Keech-Byram Drought Index (KBDI) as well as four standard fire behaviour indices, namely the spread component (SC), energy release component (ERC), burning index (BI) and ignition component (IC) (Willis *et al*., 2001; Mölders, 2010; Jolly *et al*., 2016). KBDI (Section 5.3) is a stand-alone index used to represent the impacts of seasonal drought on fire potential (Schlobohm & Brain, 2002). Similar to the ISI in the CFFDRS (Section 5.1), the SC estimates the rate at which a heading fire advances and is arguably the most variable of the US NFDRS fire indices as it responds to daily fluctuations in wind speed, fine FMC and live woody FMC (Mölders, 2010). The calculated 1-, 10- and 100-hour dead FMC contribute, in decreasing proportion, to the SC (upper triangle in Figure 5.25). SC is expressed on an open-ended scale in units of feet per minute (Schlobohm & Brain, 2002). The ERC assesses the rate of heat release per unit area (BTU per square foot) during the passage of a fire front and fluctuates least of the US NFDRS indices as it depends on the entire (i.e. living and dead) fuel complex (Schlobohm & Brain, 2002; Hardy & Hardy, 2007; Mölders, 2010). The calculated 1-, 10-, 100- and 1 000-hour dead FMC contribute, in increasing proportion, to the ERC (lower triangle in Figure 5.25). ERC is also expressed on an open-ended scale. The BI is an indicator of fire intensity and indicates the potential effort required to suppress a fire, similar to the FWI in the CFFDRS (Mölders, 2010). Since it is influenced by both SC and ERC, the BI is related to 10 times the potential flame length and is expressed as an open-ended numerical value highly variable as it is sensitive to wind speed (Schlobohm & Brain, 2002; Mölders, 2010). BI is thus highly variable and should be interpreted as representing the near upper limit to be expected over the FDRA.

A cross-reference for BI to potential flame length, fireline intensity and conditions relating to prescribed burning and suppression is provided in Table 5.4. The IC

represents the susceptibility of fine fuels to both human-caused and lightning-caused ignitions that will necessitate suppression activities (Hardy & Hardy, 2007; Mölders, 2010). IC is also highly variable as it depends on FMC and wind speed (Mölders, 2010) and is expressed as a probability ranging from 0 to 100 with the high end indicating that every firebrand will cause a fire requiring suppression (Schlobohm & Brain, 2002). Station data and daily US NFDRS outputs for the contiguous U.S.A. are processed centrally in a Weather Information Management System (WIMS) and accessible via the worldwide web at https://www.wfas.net/.

Table 5.4 Relationship between Burning Index (BI), potential flame length, fireline intensity and conditions pertaining to prescribed burning and suppression (Deeming *et al*., 1977; cited by Schlobohm & Brain, 2002)

Burning Index (BI)	Potential Flame Length (ft)	Fireline Intensity (BTUs/sec/ft)	Narrative Comments
0 – 30	0 – 3	0 – 55	Most prescribed burns are conducted in this range
30 – 40	3 – 4	55 – 110	Generally represent the limit of control for direct attack methods
40 – 60	4 – 6	110 – 280	Machine methods usually necessary or indirect attack should be used
60 – 80	6 – 8	280 – 520	The prospects for direct control by any means are poor above this intensity
80 – 90	8 – 9	520 – 670	The heat load on people within 30 feet of the fire is dangerous
90+	9+	670+	Above this intensity, spotting, fire whirls and crowning should be expected

Some of the application the US NFDRS outputs can be related to (Schlobohm & Brain, 2002):

- Staffing levels (relating fire danger values to fire management actions);
- Pre-plan dispatch actions (provide guidance as to the amount and type of resources required to contain a fire);
- Daily adjective fire danger ratings (standard descriptions for five fire danger levels to be used in public information announcements and fire prevention signs);
- Industrial activity restrictions (regulation of contractors involved in land management undertakings);
- Public use restrictions;
- Regional preparedness levels (assessing the readiness of coordination centres at local, regional and national levels; actions may include pre-positioning existing resources, recalling off-duty personnel or requesting reinforcements from other areas);

- Severity requests (compare seasonal patterns of selected components and/or indices with normal expected and historic worst case values);
- Wildland fire use go/no go decisions (deciding whether or not to suppress a new wildfire or to let it burn under prescribed conditions); and
- Briefings of firefighting personnel (conveying information to fire crews, particularly those unfamiliar with the local area, regarding current and expected conditions).

Staffing Levels (SL) are usually based on an analysis of cumulative frequency of occurrence of either ERC or BI and communicated as numeric class values (ranging from 1 – 5) to which pre-planned management resolutions can be tied (Schlobohm & Brain, 2002). In turn, the daily adjective rating (Table 5.6) is determined by the user selected SL and IC using Table 5.5.

Table 5.5 Determination of adjective fire danger rating according to staffing level and ignition component (Schlobohm & Brain, 2002)

Staffing Levels	Ignition Component (IC)				
	0 – 20	21 – 45	46 – 65	66 – 80	81 – 100
1-, 1, 1+	L	L	L	M	M
2-, 2, 2+	L	M	M	M	H
3-, 3, 3+	M	M	H	H	VH
4-, 4, 4+	M	H	VH	VH	E
5	H	VH	VH	E	E

Table 5.6 Standard adjective description of fire danger levels used in public information releases and fire prevention signing in the United States National Fire Danger Rating System (US NFDRS) (Schlobohm & Brain, 2002)

Fire Danger Rating and Colour Code	Description
Low (L) (Green)	Fuels do not ignite readily from small firebrands although a more intense heat source, such as lightning, may start fires in duff or punky wood. Fires in open cured grasslands may burn freely a few hours after rain, but wood fires spread slowly by creeping or smouldering and burn in irregular fingers. There is little danger of spotting.
Moderate (M) (Blue)	Fires can start from most accidental causes with the exception of lightning fires in some areas; the number of starts is generally low. Fires in open cured grasslands will burn briskly and spread rapidly on windy days. Timber fires spread slowly to moderately fast. The average fire is of moderate intensity, although heavy concentrations of fuel, especially draped fuel, may burn hot. Short-distance spotting may occur, but is not persistent. Fires are not likely to become serious and control is relatively easy.
High (H) (Yellow)	All fine dead fuels ignite readily and fires start easily from most causes. Unattended brush and campfires are likely to escape. Fires spread rapidly and short-distance spotting is common. High-intensity burning may develop on slopes or in concentrations of fine fuels. Fires may become serious and their control difficult unless they are attacked successfully while small.
Very High (VH) (Orange)	Fires start easily from all causes and, immediately after ignition, spread rapidly and increase quickly in intensity. Spot fires are a constant danger. Fires burning in light fuels may quickly develop high intensity characteristics such as long-distance spotting and fire whirlwinds when they burn into heavier fuels.
Extreme (E) (Red)	Fires start quickly, spread furiously and burn intensely. All fires are potentially serious. Development into high intensity burning will usually be faster and occur from smaller fires than in the very high fire danger class. Direct attack is rarely possible and may be dangerous except immediately after ignition. Fires that develop headway in heavy slash or in conifer stands may be unmanageable while the extreme burning condition lasts. Under these conditions the only effective and safe control action is on the flanks until the weather changes or the fuel supply lessens.

DESCRIPTION OF THE 2016 VERSION

The US NFDRS has been criticized in the past for being too complex, while that complexity hardly ever improves the accuracy of predicting of wildfire potential (Willis *et al*., 2001; Steenkamp *et al*., 2013; Jolly *et al*., 2016). Modifications are required to allow the system to reduce human inputs and instead use inputs from remote automated weather stations (RAWS) and gridded datasets from numerical weather prediction (NWP) models (Jolly *et al*., 2016). Figure 5.26 provides a schematic outline of the modified 2016 version of the US NFDRS. According to Jolly *et al*. (2016) these changes will make the system simpler, easier to understand and teach, more reliable and automated. The most noteworthy amendments include (Jolly *et al*., 2016):

a) replacing the state of the weather code with measured solar radiation;
b) substituting the dead fuel moisture model with the Nelson dead fuel moisture model;
c) replacing the live fuel moisture model with the GSI-driven live fuel moisture model; and
d) consolidating the 40 existing fuel models to five fuel response types (viz. grass, grass and shrubs, brush, timber and slash).

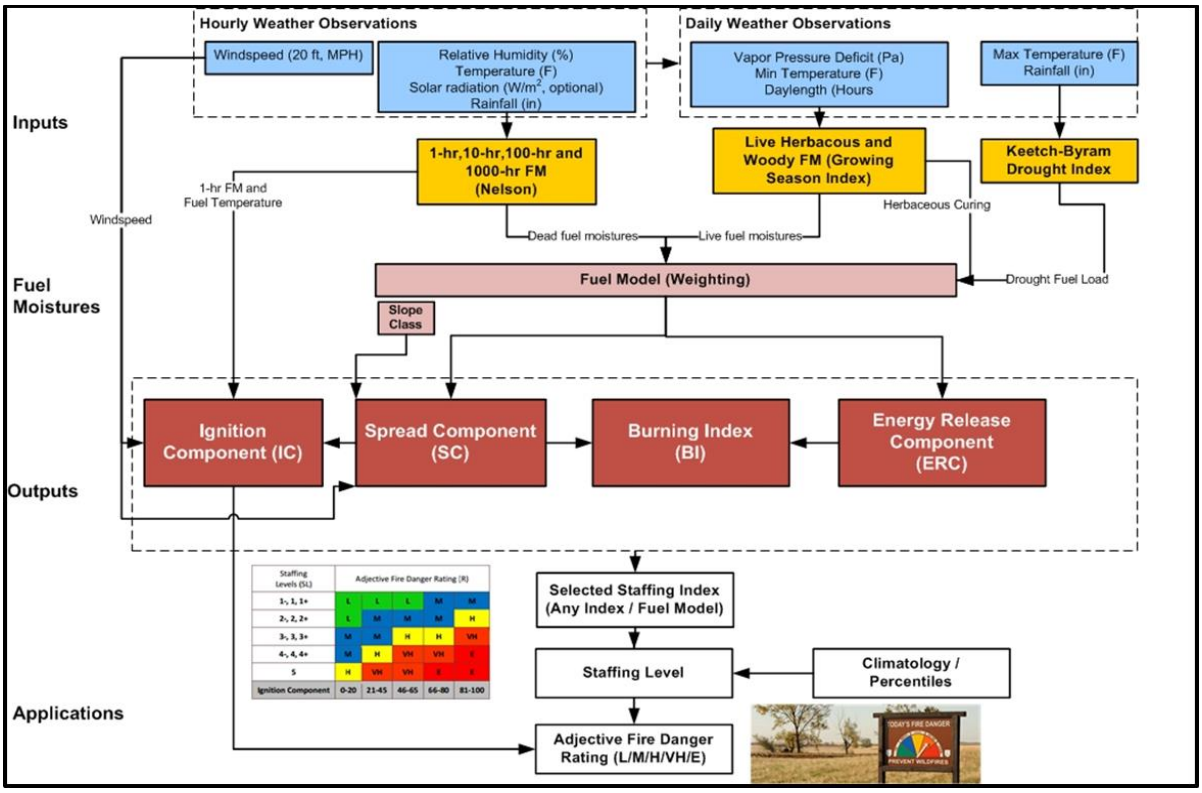

Figure 5.26 Structure of the 2016 United States National Fire Danger Rating System (US NFDRS) (Jolly *et al*., 2016).

5.3 MCARTHUR FIRE DANGER METERS

McArthur's fire danger meters have been used extensively in Australia for issuing fire-danger forecasts and as guides to fire behaviour (Noble *et al*., 1980; Beer, 1990; Williams *et al*., 2009; Dowdy *et al*., 2010). McArthur developed two different meters, the Forest Fire Danger Index (FFDI) and Grassland Fire Danger Index (GFDI), by separating these fuel types and empirically determining the rate of fire spread in representative fuels of each type (Beer, 1990). McArthur's meters were first introduced in 1958 and revised from time to time, with the Mark 4 and 5 versions of the indices in use today (Willis *et al*., 2001; Golding & Betts, 2008).

FOREST FIRE DANGER INDEX

The FFDI is based on an empirical model of fire behaviour fitted to observations from over 800 fires (Noble *et al*., 1980). The Mark 5 version was developed in 1973 and is applicable to open sclerophyll eucalyptus forests, where the fuel is primarily made up of leaf, twig and bark litter as well as a smaller portion of shrubs and grass (Cheney, 1968; cited by Cruz & Plucinski, 2007; Sharples *et al*., 2009). Although fire behaviour varies between open forests, woodlands, shrublands and heathlands, the FFDI can also be applied to these vegetation types as the bulk of the basic fire danger factors are mutual (Willis *et al*., 2001). The FFDI has also been applied or tested in Africa, South America and Southeast Asia (Hoffmann *et al*., 2002; 2003; Forsyth & Van Wilgen, 2008; Golding & Betts, 2008; Steenkamp *et al*., 2013). For vegetation types other than open forest a modification could be applied to the five fire danger classes which rate the difficulty of suppression (Table 5.7). These same thresholds were also used by Forsyth and Van Wilgen (2008) in their analysis of the fire regime in Table Mountain National Park, South Africa. Following the devastating Black Saturday bushfires (Section 4.4; Paton-Walsh *et al*., 2012), the fire danger rating system was reviewed in 2010 to include the new categories proposed by Lucas *et al*. (2007). As evident from the new threshold values in Table 5.8, the most notable modification was the inclusion of a "code red" category to denote catastrophic wildfires in which spreading will proceed so rapidly as to present a critical threat to life and safety (Mackie, 2013; CFA, 2016).

Table 5.7 Original classification thresholds of the McArthur Forest Fire Danger Index (FFDI) (Luke & McArthur, 1986; cited by Dowdy *et al*., 2010)

Fire Danger Rating	FFDI Range
Low	0 – 4
Moderate	5 – 11
High	12 – 24
Very high	25 – 49
Extreme	≥ 50

Table 5.8 Revised classification thresholds of the McArthur Forest Fire Danger Index (FFDI) and Grassland Fire Danger Index (GFDI) (CFA, 2016; Wikipedia, 2016)

Fire Danger Rating	FFDI Range	GFDI
Low - Moderate	0 – 11	0 – 11
High	12 – 24	12 – 24
Very High	25 – 49	25 – 49
Severe	50 – 74	50 – 99
Extreme	75 – 99	100 – 149
Catastrophic (Code Red)	≥ 100	≥ 150

Meteorological inputs required to calculate the FFDI include maximum temperature (°C), wind speed (km h^{-1}) and relative humidity (%), while average annual and 24-hour accumulated rainfall (mm) are also used to determine the drought index and drought factor components (Willis *et al*., 2001; Dowdy *et al*., 2010). The terrain slope, fuel load and fuel moisture content is also needed to calculate other relevant information such as the rate of forward spread of fire, flame height, spotting distance, fire line intensity and heat output (Noble *et al*., 1980; Beer, 1990). In the original version (McArthur, 1966; cited by Noble *et al*., 1980), tables and graphs or circular slide rules were used to read off the fire danger rating but these were later translated to mathematical equations by Noble *et al*. (1980) in order to facilitate modelling applications. Equations for the FFDI Mark 5 are given by (Noble *et al*., 1980; Willis *et al*., 2001; Sharples *et al*., 2009; Williams *et al*., 2009):

$$F = 2e^{-0.45+0.987ln(D)-0.0345RH+0.0338T+0.0234V}$$

$$R = 0.0012FW$$

$$R_m = \frac{1000R}{60}$$

$$R_\theta = Re^{0.069\theta}$$

$$Z = 13R + 0.24W - 2$$

$$S = R(4.17 - 0.033W) - 0.36$$

$$\Psi = 516.7RW$$

$$E = 1860W$$

where: F = fire danger index (unitless);
D = drought factor (unitless);
RH = relative humidity (%);
T = air temperature, either maximum or measured at noon (°C);
V = average wind speed at a height of 10 m (km h^{-1});
W = fuel load (tonnes ha^{-1});
R = forward rate of spread on even or undulating terrain (km h^{-1});
R_m = forward rate of spread on even or undulating terrain (m min^{-1});
R_θ = forward rate of spread on sloped terrain (km h^{-1});
θ = slope of terrain (°);
Z = flame height (m);
S = distance of spotting from fire front (km);
Ψ = fire line intensity (kW m^{-1}); and
E = heat output per unit area (kW m^{-2}).

The drought factor, *D*, is a number ranging from 0 to 10 used to represent fuel state and fine fuel availability (Beer, 1990; Griffiths, 1999; Willis *et al*., 2001; Hoffmann *et al*., 2003). Its determination is based on consideration of long-term rainfall in the form of a drought index (either Mount's Soil Dryness Index, MSDI, or the Keech-Byram Drought Index, KBDI), while a rainfall budgeting procedure for the past 20 days is used to account for the most noteworthy recent wetting event (Griffiths, 1999; Willis *et al*., 2001). Daily rainfall totals of less than 2 mm are assumed to have no significance on fire danger (Griffiths, 1999). Since the drought factor equation proposed by Noble *et al*. (1980) was found not to reproduce McArthur's meter values well, the following improved formula was proposed by Griffiths (1999):

$$y = max \begin{cases} \dfrac{(P-2)}{N^{1.3}}, & N \geq 1 \; and \; P > 2 \\ \dfrac{(P-2)}{0.8^{1.3}}, & N = 0 \; and \; P > 2 \\ 0, & P \leq 2 \end{cases}$$

$$D = \left[10.5\left(1 - e^{\frac{-(I+30)}{40}}\right)\frac{y + 42}{y^2 + 3y + 42}\right]$$

where: y = an index variable calculated for the past 20 days;

P = 24-hour accumulated precipitation (mm);

N = time since last rain event (days);

D = drought factor (unitless and ranging between 0 and 10); and

I = Keetch-Byram drought index (mm).

The KBDI is intended as a direct indicator of accumulated soil water depletion in a virtual soil, between 762 and 889 mm deep, with an assumed field capacity of 203.2 mm (Keetch & Byram, 1968; Garcia-Prats *et al*., 2015). Index values thus range from 0 mm (saturated soil) to a maximum of 203.2 mm in response to wetting (i.e. rainfall) and drying (i.e. evapotranspiration). In accordance with discussions by Keetch and Byram (1968), Alexander (1990), Willis *et al*. (2001), Eastaugh (2012) and Garcia-Prats *et al*. (2015) the procedure for calculating the KBDI on a daily time step is described below.

Calculation of potential evapotranspiration (ET_p) is estimated on a daily basis in the KBDI as a function of the daily maximum temperature and the mean annual rainfall. The actual evapotranspiration (dQ) is subsequently determined on a daily basis as a linear function of soil water depletion (the symbol Q in the original formula has been substituted by the equivalent I_{t-1} here). The next step involves determination of the daily net rainfall (P_n) by subtracting 5.08 mm from the 24-hour accumulated rainfall. In the case of consecutive rainfall days, 5.08 mm is subtracted only once on the day when cumulative rainfall exceeds 5.08 mm. The wet spell is considered ended on the first 24-hour period with no measurable rainfall. Once dQ and P_n is calculated, KBDI for today (I_t) is obtained by adding dQ to yesterday's KBDI value (I_{t-1}) after subtracting the current day's net rainfall (P_n) from it. However, if the result is negative, KBDI is set to zero. Since the KBDI is a cumulative feature, it implies that a drought index record cannot simply automatically start at zero. One option is to initialise the index at a soil moisture content equal to field capacity, thus resetting KBDI to zero (Garcia-Prats *et al*., 2015). According to Schlobohm and Brain (2002) most programs employ a default initiation value of 25.4 mm (100 hundredths of an inch).

$$ET_p = \frac{(0.968e^{0.0875T_{max}+1.5552} - 8.3)}{(1 + 10.88e^{-0.001736P_{ave}})}$$

$$dQ = (203.2 - I_{t-1})ET_p \times 10^{-3}$$

$$dQ = \frac{(203.2 - I_{t-1})(0.968e^{0.0875T_{max}+1.5552} - 8.3)}{10^3(1 + 10.88e^{-0.001736P_{ave}})}$$

$$P_n = \begin{cases} P, & P_{t-1} > 5.08 \\ P - max[(5.08 - P), 0], & 0 < P_{t-1} < 5.08 \\ max[(P - 5.08), 0], & P_{t-1} = 0 \end{cases}$$

$$I_t = (I_{t-1} - P_n) + dQ$$

where: ET_p = potential evapotranspiration (mm);

T_{max} = maximum daily temperature (°C);

P_{ave} = mean annual rainfall (mm);

dQ = actual evapotranspiration or daily addition to soil water deficiency (mm);

I_t = today's Keetch-Byram drought index (mm);

I_{t-1} = yesterday's Keetch-Byram drought index or accumulated soil water deficit (mm);

P = gross 24-hour accumulated rainfall up to this morning (mm);

P_n = net 24-hour rainfall (mm); and

P_{t-1} = yesterday's 24-hour accumulated rainfall (mm), measured yesterday morning.

The KBDI value indicates the amount of net rainfall (in mm) that is required to reduce the index to zero, or bring the top soil layers to saturation (Keech & Byram, 1968; Schlobohm & Brain, 2002). Due to their use of imperial units (viz. rainfall amount measured in hundredths of an inch), Keetch and Byram (1968) expressed drought severity associated with the KBDI as seven categories corresponding to index values ranging from 0 to 800 (Table 5.9). Modified category ranges are also provided in Table 5.9 for assigning drought severity to the metric form employed outside the U.S.A.

Table 5.9 Interpretation of the Keech-Byram Drought Index (KBDI) (adapted from Keech & Byram, 1968)

Index Values (imperial form)	Index Values (metric form)	Drought Stage
0 – 99	0 – 25.3	0
100 – 199	25.4 – 50.7	1
200 – 299	50.8 – 76.1	2
300 – 399	76.2 – 101.5	3
400 – 499	101.6 – 126.9	4
500 – 599	127.0 – 152.3	5
600 – 699	152.4 – 177.7	6
700 – 800	177.8 – 203.2	7

The coefficients in the original version of the actual evapotranspiration (*dQ*) equation were obtained by Keetch and Byram (1968) by setting the reference values for maximum temperature (T_{max}) and mean annual rainfall (P_{ave}) to 26.7°C (80°F) and 1 270 mm (50 in.), respectively. In order to adapt the KBDI to Mediterranean conditions, Ganatsas *et al*. (2011) followed a similar procedure as Keetch and Byram (1968) to derive a modified version (G-KBDI) for a P_{ave} reference value of 762 mm. Ganatsas *et al*. (2011) also set the field capacity of the soil to 200 mm and changed the net rainfall threshold from 5.08 mm to 3 mm. The hydrology-oriented silviculture KBDI (Hydrosil-KDBI; Garcia-Prats *et al*., 2015) attempted to improve on the ET_p expression.

$$dQ = \frac{(200 - I_{t-1})(1.713e^{0.0875T_{max}+1.5552} - 14.59)}{10^3(1 + 10.88e^{-0.001736P_{ave}})}$$

$$dQ = \frac{(203.2 - I_{t-1})(8.057e^{0.0556T_{max}+0.9884} - 3.0116)}{10^3(1 + 10.88e^{-0.001736P_{ave}})}$$

GRASSLAND FIRE DANGER INDEX

The GFDI was developed to account for fire behaviour in slightly grazed temperate perennial grassland on even terrain (Willis *et al*., 2001). It has a similar basis to the FFDI, but instead of the fuel availability module the GFDI includes the degree of grass curing (Noble *et al*., 1980; Willis *et al*., 2001). The FMC is thus governed by the combination of the degree of curing (Section 4.1.4) and the environmental conditions (viz. air temperature and relative humidity) influencing the dead grass moisture content (Willis *et al*., 2001). Rate of fire spread, in turn, is determined by the FFMC and wind speed. The GFDI Mark 5 equations are given by (Noble *et al*., 1980; Sharples *et al*., 2009):

$$M = \frac{(97.7 + 4.06H)}{(T + 6)} - 0.00854H + \frac{3000}{C} - 30$$

$$F = \begin{cases} 3.35We^{(-0.0897M+0.0403V)}, & M < 18.8\% \\ 0.299(30-M)We^{(-1.686+0.0403V)}, & 18.8\% \leq M < 30.0\% \end{cases}$$

$$R = 0.13F$$

where: M = fuel moisture content (%);

H = relative humidity (%);

T = air temperature (°C);

C = degree of curing (%);

F = fire danger index (unitless);

W = fuel load (tonnes ha^{-1}); and

R = forward rate of spread on even or undulating terrain (km h^{-1}).

As pointed out by Sharples *et al*. (2009) the inclusion of *W* in the Mark 5 equations implies that the GFDI cannot be implemented as a regional measure, lest a constant fuel loading over the region is assumed.

5.4 SOUTH AFRICAN NATIONAL FIRE DANGER RATING SYSTEM

The Lowveld Fire Danger Index (LFDI) is an adaptation of a Fire Hazard Index developed in 1968 by staff at Charter Estates in Zimbabwe (then Rhodesia) (Laing, 1978). Although its use as the primary FDRS in South Africa dates back to about 1986 (after Laing's relocation to SAWS, then the South African Weather Bureau), it was only recently adopted as the official South African National Fire Danger Rating System (Notice 1099 of 2013). The LFDI is rooted in operational activities of most local fire management and suppression agencies. The operational activities of the vast majority of local fire management and fire suppression agencies (e.g. the Forest Fire Association, Fire Protection Associations (FPAs), the government's Working on Fire (WoF) programme and South African National Parks (SANParks)) lean heavily on the LFDI (Steenkamp *et al*., 2013). In fact, its initial implementation by the Lowveld and Escarpment FPA followed a preliminary study that indicated a close correlation between plantation areas bunt and the daily LFDI, albeit over a single season (Meikle & Heine, 1987).

BURNING INDEX

The BI is thought to approximate FMC (Laing, 1978). The index is calculated daily using afternoon (14:00 LST) meteorological observations when index values are expected to be at their maximum (Meikle & Heine, 1987) and consequently most dangerous (see Figure 4.9). The first step requires measurements of air temperature (drybulb temperature) and relative humidity in order to calculate a Burning index (BI) with the aid of a simple alignment chart (Figure 5.27). When the alignment chart (Figure 5.27) is used, a straight line is drawn between the dry bulb temperature (°C) on the left hand axis and the relative humidity (%) on the right hand axis, where after the BI is read off at the crossing point with the middle axis. For example, a dry bulb temperature of 15°C and relative humidity of 30% would give a BI of 35.

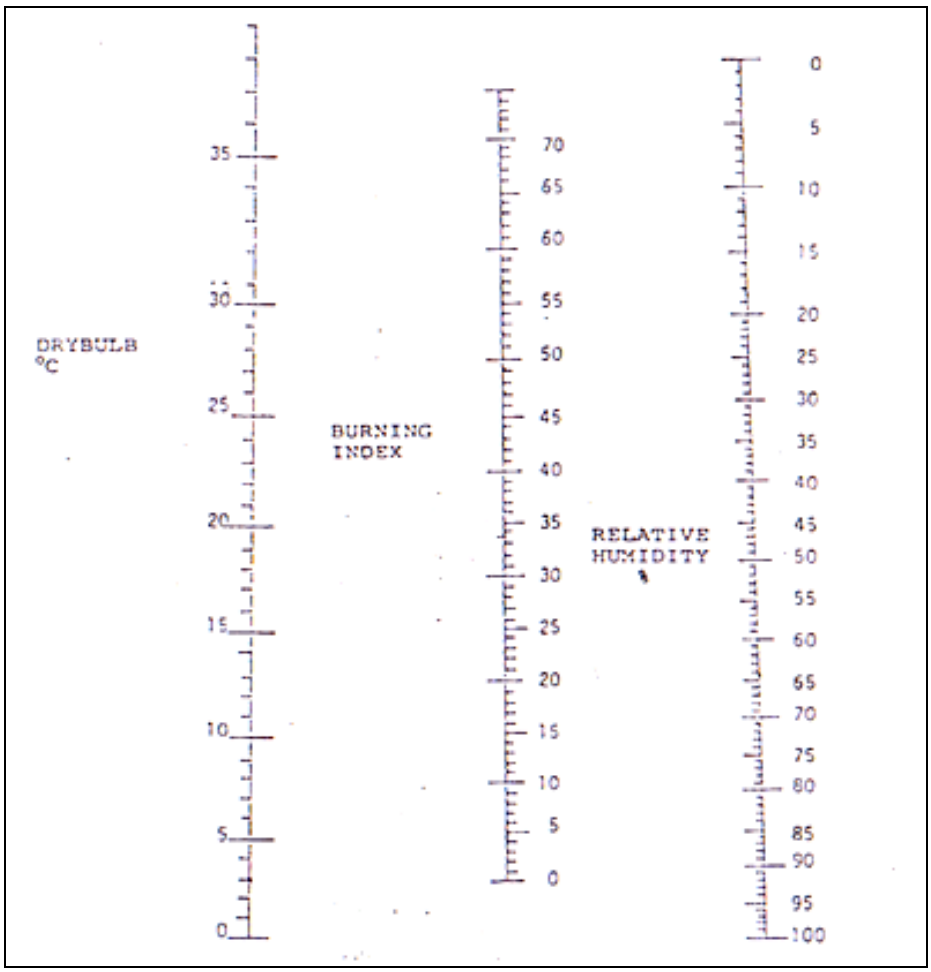

Figure 5.27 **Alignment chart for determining the Burning Index to be used in the calculation of the Lowveld Fire Danger Index (LFDI) (SAWS, 2002).**

The use of the alignment chart in Figure 5.27 to determine the BI is acceptable at a daily station scale, but when a large number of calculations must be made (e.g. for a

large number of stations or daily calculations over a long time period) its usefulness is seriously reduced. For this reason the following empirical equation for calculating the BI was adopted (Notice 1099 of 2013):

$$BI = (T - 35) - \frac{(35 - T)}{30} + 0.37(100 - RH) + 30$$

where: *T* is the (maximum) air temperature (°C)
RH is the (minimum) relative humidity (%)

The aforementioned equation for BI can be written more elegantly as (Lai, 2014, personal communication):

$$BI = 30.834 + 1.033T - 0.37RH$$

WIND FACTOR

The influence of wind speed on fire behaviour was addressed in Section 4.2.3. An adjustment for wind is made by adding a Wind Factor (WF) to the BI in accordance with Table 5.10. It should be noted that this is not the original WF table proposed by Laing (1978), with the most notable change being the addition of categories towards the higher end of the scale. It was interesting to note that Iliopoulos *et al*. (2010) presented an even more detailed WF lookup table, which they used to consider the application of the LFDI during the 2007 and 2008 fire seasons (May – October) across different regions of Greece. Iliopoulos *et al*. (2010) concluded that the LFDI was "applicable and effective". Meikel *et al*. (2012) revealed the likely source to be Forest Fire Association in Nelspruit.

Table 5.10 Determination of the Wind Factor (WF) to be used in the calculation of the Lowveld Fire Danger Index (LFDI) (Notice 1099 of 2013)

Wind speed (km h^{-1})	Wind Factor
≤ 2	0
3 – 8	5
9 – 16	10
17 – 25	15
26 – 32	20
33 – 36	25
37 – 41	30
42 – 45	35
≥ 46	40

RAINFALL CORRECTION FACTOR

The availability of excess moisture (above the plant fibre saturation point) provided by recent rainfall is taken into account by multiplying the sum of the BI and WF with a Rainfall Correction Factor (RCF) based on prior rainfall conditions (Table 5.11). When only isolated showers or thundershowers are expected, it may be assumed that some areas will not receive any rain and the RCF is set to 1 (i.e. effectively not used) (Laing, 1978). Since isolated dry (non-precipitating) thundershowers again pose the risk of fire ignition by lightning, Laing (1978) suggested that forecasters consult the decision diagram presented in Figure 5.28 when determining the risk of lightning ignition risk during convective outbreaks.

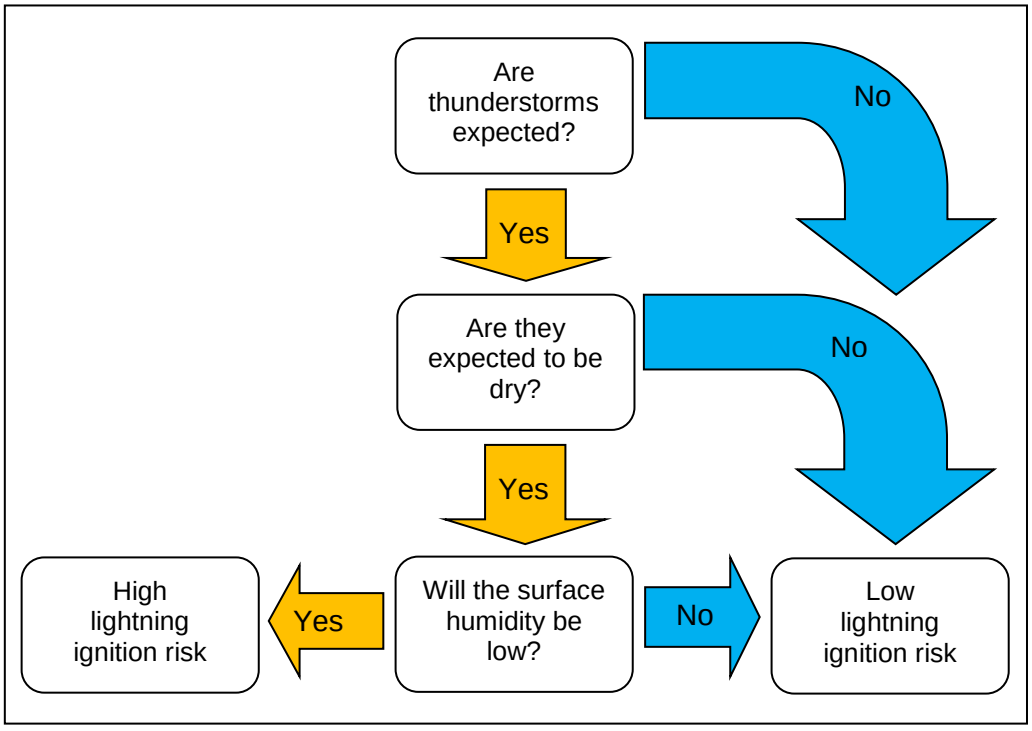

Figure 5.28 Decision diagram for gauging the risk of lightning (adapted from Laing, 1978).

According to Willis *et al*. (2001) a modification was made to the RCF in an attempt to recognise that fine fuels will dry faster than usual under warm, dry and windy conditions. This adjustment entails pushing back the latest rainfall event one day (for every hour the air temperature exceeds 23°C, the relative humidity falls below 50% and the wind speed exceeds 20 km h^{-1}). Such an adjustment, however, entails the use of hourly measurements and complicates its operationalisation. No mention is made of such an adjustment in the recent notice in the Government Gazette (Notice 1099 of

2013), nor is there any knowledge of its application by the SAWS forecasters (personal experience, 1998 – 2003).

Table 5.11 Determination of the Rainfall Correction Factor (RCF) to be used in the calculation of the Lowveld Fire Danger Index (LFDI) (Laing, 1978; Notice 1099 of 2013)

Rainfall (mm)	Number of days since last rainfall occurrence											
	1	2	3	4	5	6	7 – 8	9 – 10	11 – 12	13 – 15	16 – 20	21+
0.1 – 2.6	0.7	0.9	1	1	1	1	1	1	1	1	1	1
2.7 – 5.2	0.6	0.8	0.9	1	1	1	1	1	1	1	1	1
5.3 – 7.6	0.5	0.7	0.9	0.9	1	1	1	1	1	1	1	1
7.7 – 10.2	0.4	0.6	0.8	0.9	0.9	1	1	1	1	1	1	1
10.3 – 12.8	0.4	0.6	0.7	0.8	0.9	0.9	1	1	1	1	1	1
12.9 – 15.3	0.3	0.5	0.7	0.8	0.8	0.9	1	1	1	1	1	1
15.4 – 20.5	0.2	0.5	0.6	0.7	0.8	0.8	0.9	1	1	1	1	1
20.6 – 25.5	0.2	0.4	0.5	0.7	0.7	0.8	0.9	1	1	1	1	1
25.6 – 38.4	0.1	0.3	0.4	0.6	0.6	0.7	0.8	0.9	1	1	1	1
38.5 – 51.1	0.1	0.2	0.4	0.5	0.5	0.6	0.7	0.8	0.9	1	1	1
51.2 – 63.8	0.1	0.2	0.3	0.4	0.5	0.6	0.7	0.7	0.8	0.9	1	1
63.9 – 76.5	0.1	0.1	0.2	0.3	0.4	0.5	0.6	0.7	0.8	0.8	0.9	1
76.6 +	0.1	0.1	0.1	0.2	0.4	0.5	0.6	0.6	0.7	0.8	0.9	1

Table 5.12 Modified Rainfall Correction Factor (RCF) used in the calculation of the Lowveld Fire Danger Index (LFDI)

Rainfall (mm)	Number of days since last rainfall occurrence												
	0	1	2	3	4	5	6	7 – 8	9 – 10	11 – 12	13 – 15	16 – 20	21+
0.1 – 2.6	0.5	0.7	0.9	1	1	1	1	1	1	1	1	1	1
2.7 – 5.2	0.4	0.6	0.8	0.9	1	1	1	1	1	1	1	1	1
5.3 – 7.6	0.3	0.5	0.7	0.9	0.9	1	1	1	1	1	1	1	1
7.7 – 10.2	0.2	0.4	0.6	0.8	0.9	0.9	1	1	1	1	1	1	1
10.3 – 12.8	0.2	0.4	0.6	0.7	0.8	0.9	0.9	1	1	1	1	1	1
12.9 – 15.3	0.1	0.3	0.5	0.7	0.8	0.8	0.9	1	1	1	1	1	1
15.4 – 20.5	0.1	0.2	0.5	0.6	0.7	0.8	0.8	0.9	1	1	1	1	1
20.6 – 25.5	0.1	0.2	0.4	0.5	0.7	0.7	0.8	0.9	1	1	1	1	1
25.6 – 38.4	0.1	0.1	0.3	0.4	0.6	0.6	0.7	0.8	0.9	1	1	1	1
38.5 – 51.1	0.1	0.1	0.2	0.4	0.5	0.5	0.6	0.7	0.8	0.9	1	1	1
51.2 – 63.8	0.1	0.1	0.2	0.3	0.4	0.5	0.6	0.7	0.7	0.8	0.9	1	1
63.9 – 76.5	0.1	0.1	0.1	0.2	0.3	0.4	0.5	0.6	0.7	0.8	0.8	0.9	1
76.6 +	0.1	0.1	0.1	0.1	0.2	0.4	0.5	0.6	0.6	0.7	0.8	0.9	1

Table 5.11 is applied without difficulties during operational weather forecasting (e.g. forecasting today or tomorrow's LFDI). However, a problem is encountered when determining the RCF in a research setting using historical climate data. Since Table 5.11 does not make any mention of what to do when rainfall was encountered on the day in question, a modification was made by introducing a new column for such occurrences in Table 5.12 (viz. 0 days since last rainfall occurrence).

Trollope (2005; cited by Steenkamp, 2013) adapted the LFDI for field use during controlled burning, replacing the RCF with a curing factor. More details on this adapted field version of the LFDI can be found at the end of this section.

LOWVELD FIRE DANGER INDEX

The LFDI can be calculated as follows (Willis *et al*., 2001; Notice 1099 of 2013):

$$LFDI = (BI + WF) \times RCF$$

where: *LFDI* is the Lowveld Fire Danger Index (unitless)
BI is the Burning Index determined from Figure 5.27 (unitless)
WF is the Wind Factor determined from Table 5.10 (unitless)
RCF is the Rainfall Correction Factor determined from Table 5.11 or Table 5.12 (unitless)

The LFDI is a positive quantity that increases with increasing fire danger and has no upper bound, although values above 100 are very unlikely. This prompted some (including Laing himself) to advocate an upper limit of 100, but it can easily be shown how extreme weather conditions can result in LFDI values that will exceed this artificial ceiling. Worked examples of the LFDI calculation is provided in Table 5.13. Interpretation of the LFDI values are in accordance with Table 5.14, which provides information regarding the danger rating, colour coding, expected fire behaviour, the difficulty of suppression as well as aspects of fire prevention. Again, the threshold values provided in Table 5.14 differ from what was initially proposed by Laing (1978) for Zimbabwe, presumably in order to align better with fire front intensities. Table 5.15 contains information on the legal implications of the various LFDI categories as well as the relationship with disaster management at all three tiers of Government (i.e.

Local, Provincial and National). A final step proposed by Laing (1978) involves the assessment of local fire danger by fire managers or estate managers based on fuel condition.

Table 5.13 Calculation of the Lowveld Fire Danger Index (LFDI) from daily observed weather variables at Hazyview, South Africa

Date	Observations	BI	WF	RCF	LFDI	Colour Code
1992-09-20	T_{max} = 39°C RH_{min} = 13% Wind speed = 4 km h^{-1} Time since last rainfall = 4 days Rainfall amount = 1 mm	72	5	1.0	**77**	Red
1992-09-28	T_{max} = 24.5°C RH_{min} = 46% Wind speed = 3.4 km h^{-1} Time since last rainfall = 1 day Rainfall amount = 3.5 mm	39.5	5	0.6	**27**	Green
1992-09-30	T_{max} = 35.5°C RH_{min} = 24% Wind speed = 4.1 km h^{-1} Time since last rainfall = 3 days Rainfall amount = 3.5 mm	60.5	5	0.9	**59**	Yellow

Laing (1978) warned of the spatial validity of the LFDI, especially in hilly terrain. This is due to the representativeness of standard meteorological observations and the considerable natural variation that the relevant climatic element exhibit (e.g. vertical profiles in temperature, relative humidity and wind, lee effects and wind channelling as well as erratic rainfall distribution due to showers). These problems highlighted by Laing (1978), however severe, are in fact common to all FDRSs. It is interesting to note that in the same year as Laing's publication, Turner and Lawson (1978) elaborated on these same aspects in terms of interpreting the FWI.

Table 5.14 Interpretation of the Lowveld Fire Danger Index (LFDI) (SAWS, 2002; Willis *et al*., 2001; Notice 1099 of 2013; KZN FPA, 2015)

LFDI values	0 – 20	21 – 45	46 – 60	61 – 75	≥ 76
Colour category	**BLUE**	**GREEN**	**YELLOW**	**ORANGE**	**RED**
Danger rating	**Low**	**Moderate**	**Dangerous**	**Very dangerous**	**Extremely dangerous**
Fire behaviour	Fires are not likely to ignite. If they do, they are likely to go out without suppression action. There is little flaming combustion. Flame lengths in grassland and plantation forest litter lower than 0.5 m and rates of forward spread less than 0.15 km h^{-1}.	Fires likely to ignite readily but spread slowly. Flame lengths in grassland and plantation forest litter lower than 1 m and rates of forward spread less than 0.3 km h^{-1}.	Fires ignite readily and spread rapidly, burning in the surface layers below trees. Flame lengths in grasslands and plantation forests between 1 and 2 m, and rates of forward spread between 0.3 and 1.5 km h^{-1}.	Fires ignited readily and spread very rapidly, with local crowning and short-range spotting. Flame lengths between 2 and 5 m, and rates of forward spread between 1.5 and 2 km h^{-1}.	Conflagrations are likely in plantation forests, stands of alien invasive trees and shrubs, sugar cane plantations, and fynbos. Long range fire spotting is likely in these fuel types. Rates of forward spread of head fires can exceed 4 km h^{-1} and flame lengths will be in the order of 5 – 15 m or more.
Fire suppression difficulty	Direct attack feasible: one or a few field crew teams with basic firefighting tools easily suppresses any fire that may occur.	Direct attack feasible: fires safely approached on foot. Suppression is readily achieved by direct manual attack methods.	Direct attack constrained: fires not safe to approach on foot for more than very short periods. Best forms of control should combine water tankers and back burning from fire control lines.	Direct attack not feasible: fires cannot be approached at all and back burning, combined with aerial support are the only effective means to combat fires. Equipment such as water tankers should concentrate efforts on the protection of houses.	Any form of fire control is likely to be precluded until the weather changes. Back burning dangerous and best avoided.
Fire prevention and preparedness measures	No precaution is needed	Fires including prescribed burns may be lit, used or maintained in the open air on the condition that persons making fires take reasonable precautions against the fires spreading.	No fires may be allowed in the open air except those that are authorized by the Chief Fire Officer of the local fire service.	No fires may be allowed under any circumstances in the open air.	No fires may be allowed under any circumstances in the open air and Fire Protection Associations and municipal Disaster Management Centres must invoke contingency fire emergency and disaster management plans including extraordinary readiness and response plans. All operations likely to ignite fires halted. Householders placed on alert.

Table 5.15 Legal implications of the Lowveld Fire Danger Index (LFDI) categories and the relationship with disaster management (Notice 1099 of 2013)

LFDI values	0 – 20	21 – 45	46 – 60	61 – 75	≥ 76
Colour category	BLUE	GREEN	YELLOW	ORANGE	RED
Danger rating	Low	Moderate	Dangerous	Very dangerous	Extremely dangerous
Application of the act	Not applicable	Not applicable	Above precautionary measure to be prescribed and made applicable nationally on days rated moderate.	Section 10(1) (b) applies: no person may light, use or maintain a fire in the open air.	Section 10(1) (b) applies: no person may light, use or maintain a fire in the open air.
Relationship with disaster management	Not applicable	Not applicable	Not applicable	The threat of disastrous wildfires exists at municipal level under these conditions. Municipal Disaster Management Centres must invoke contingency plans and inform National and Provincial Disaster Management Centre (Section 49 of the Disaster Management Act of 2002).	The threat of disastrous wildfires at provincial level exists under these conditions. Municipal Disaster Management Centres must invoke contingency plans and inform National and Provincial Disaster Management Centres (Section 49 of the Disaster Management Act 0f 2002).

MODIFIED LOWVELD FIRE DANGER INDEX

As stated previously (Section 4.1.4), the degree of curing of plant material has a substantial influence on its flammability and should therefore be included in any FDRS. The RCFs provided in Table 5.11 were intended to reassess FMC, but were flawed to some extent for the same reason highlighted by the following publications:

a) soil water content had no significant influence on the intensity of grassland fires a day or more after a rainfall event (Trollope & Tainton, 1986);
b) field trials conducted in the Eastern Cape showed that grass fuels, which constitute the majority of the plant fuel load in African savannas, were in equilibrium with atmospheric humidity within one hour (Trollope *et al*., 2007); and
c) the RCFs documented by Laing (1978) were based on heavy fuels rather than fine fuels and were therefore not very representative of grasslands (Meikel *et al*., 2012).

Trollope (2005; cited by Steenkamp, 2013) consequently modified the LFDI for providing guidance to prescribed burning in African grasslands and savannas. This modification mainly involved substituting the RCF with a Grass Curing Factor (GCF) that describes the condition of the grass fuel at the time of burning (Trollope *et al*., 2007; Meikel *et al*., 2012):

$$LFDI_{Field} = (BI + WF) \times GCF$$

where: *LFDI*$_{Field}$ is the LFDI adapted for use in the field (unitless)
BI is determined with the use of Figure 5.27 (unitless)
WF is determined with the use of Table 5.10 (unitless)
GCF is the grass curing (GC) divided by 100

Based on burn trials conducted in October 2006 in the Kruger National Park, Trollope *et al*. (2007) calibrated the following regression equation (R^2 = 0.92) to provide guidance during controlled burning:

$$LFDI_{Field} = [3.76432 + 1.8062T - 0.219905RH + 0.646309W] \times GCF$$

where: *LFDI*$_{Field}$ is the LFDI adapted for use in the field (unitless)
T is the air temperature (°C) at time of burn
RH is the relative humidity (%) at time of burn
W is the wind speed (km h^{-1}) at time of burn
GCF is the grass curing (GC) at time of burn divided by 100

In essence values derived from the two modified versions of the LFDI differ with less than one. A simple procedure for determining grass curing for use in the modified LFDI within southern African grassland and savanna communities was described by Trollope *et al*. (2010). This procedure involves determining the FMC and then converting to GC using:

$$\mathrm{GC} = 108 - 0.78\mathrm{FMC}$$

where: *GC* is the grass curing (%)
FMC is the fuel moisture content (%)

The modified LFDI is used in the field in conjunction with the guidelines in Table 5.16 for conducting prescribed burning (Trollope *et al*., 2007; Meikel *et al*., 2012). The first $LFDI_{Field}$ equation is also used in conjunction with Table 5.16 in AFIS.

Table 5.16 Prescribed burning guidelines in relation to the modified Lowveld Fire Danger Index ($LFDI_{Field}$) (Meikel *et al*., 2012)

LFDI values	0 – 20	21 – 45	46 – 60	61 – 75	≥ 76
Colour category	BLUE	GREEN	YELLOW	ORANGE	RED
Danger rating	Low	Moderate	Dangerous	Very dangerous	Extremely dangerous
Fire intensity ($kJ\ s^{-1}\ m^{-1}$)	< 500	500 – 1 000	1 001 – 2 000	2 000 – 3 000	> 3 000
Prescribed burning	Too cold, humid or wet for prescribed burning.	Suitable for prescribed burning to remove moribund and/or unpalatable grass material, or to construct burnt firebreaks.	Suitable for prescribed burning to remove moribund and/or unpalatable grass material up to a maximum index value of 55.	Suitable for prescribed burning to control and/or prevent the encroachment of undesirable plants (e.g. bush encroachment).	Too dangerous and unsuitable for prescribed burning.

5.5 COMPARISON OF FIRE DANGER RATING SYSTEMS

In a study by Viegas *et al*. (1999) the performance of the following FDRSs were evaluated across six different regions in France, Italy and Portugal:

a) the Canadian Fire Weather Index (FWI; Section 5.1);
b) the French or numerical risk method;
c) the Italian method;
d) the Portuguese or modified Nesterov method; and
e) the Spanish method.

These five FDRSs were tested for overall performance during both summer and winter seasons over a 3 – 9 year period against observed daily number of fires and burned area. By making use of the so-called Mahalonobis distance to assess the relative performance of each method for a given region and fire season, Viegas *et al*. (1999) concluded that the Canadian FWI fared better in summer, while the modified Nesterov method performed best in winter and reasonably well in summer across all regions.

Cruz and Plucinski (2007) evaluated the rate of fire spread from the following FDRSs as applied to large wildfires in radiata pine (*Pinus radiata*) plantations in New South Wales, Australia:

a) the McArthur Forest Fire Danger Index (FFDI; Section 5.3) and predicted rate of spread by the Forest Fire Danger Meter (FFDM);
b) the Forest Fire Behaviour Tables (FFBT) for Western Australia (Sneeuwjagt & Peet, 1985; cited by Cruz & Plucinski, 2007); and
c) the Canadian Forest Fire Behaviour Prediction (FBP) system (Section 5.1).

The study was motivated by fire suppression personnel noting that the observed fire behaviour not matching the predictions. The results showed that both the FBP and FFBT systems outperformed the FFDI and FFDM in providing a better indication of extreme fire behaviour. It was most notably the ISI of the Canadian system that captured fire spread potential anomalies which the McArthur system failed to identify (Cruz & Plucinski, 2007).

Steenkamp *et al*. (2013) performed a quantitative comparison of fire danger index performance over South Africa. The four indices in the comparison included:

a) the Lowveld Fire Danger Index (LFDI);
b) the Canadian Fire Weather Index (FWI);
c) the McArthur Forest Fire Danger Index (FFDI); and
d) the McArthur Grassland Fire Danger Index (GFDI).

No changes were made to the models' fuel components (Steenkamp *et al*., 2013). Meteorological input variables to these indices were provided for the period June 2007 to October 2010 by assimilation fields of the UK Met Office's Unified Model (UM). The UM has been configured by the South African Weather Service (SAWS) to run at a 0.11° grid spacing. Historical fire activity was determined by using burned area data as well as active fire detections (1 km resolution) from the MODIS sensors on board the Terra and Aqua satellite platforms. Fire activity was defined in terms of (i) a fire-day; and (ii) a large fire-day with more than four burned area pixels (100 ha) recorded. For statistical reasons only grid boxes wherein a minimum of 20 large fire events occurred were included in analyses.

Following the approach put forward by Andrews *et al*. (2003), the individual ranking of each FDI included in the comparison was determined for the following four criteria and summarised per individual cell:

1) the R^2 obtained from logistic regression;
2) the range of the predicted values from the logistic model;

3) the percentile shifts; and
4) the Bhatthacharyya coefficient.

The overall ranking with the lowest value indicated the best ranking FDI. Mapping these overall rankings also provided regional analyses of their effectiveness. A diagrammatical presentation of the process description is given in Figure 5.29.

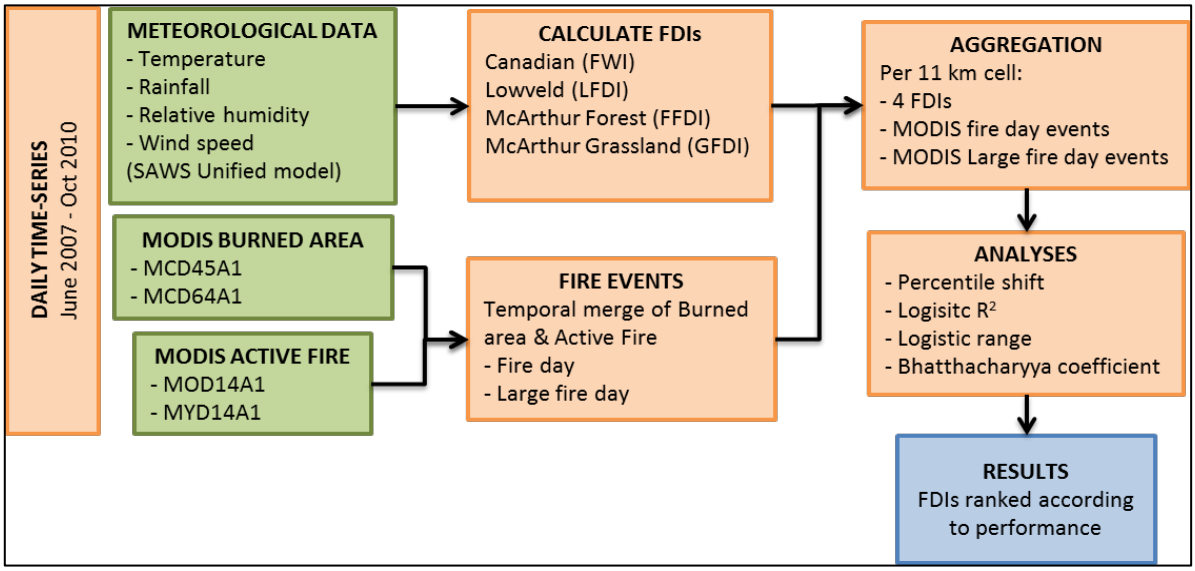

Figure 5.29 **Data sources and processing steps applied in the comparison of fire danger index performance over South Africa (Steenkamp *et al*., 2013).**

The general results could be summarised by Table 5.17 and Figure 5.30. The FWI ranked in first position in 90.3% of all the cells, making it the best performing index over South Africa by a large margin. The LFDI ranked in second position in 54.8% of the cells, while the two McArthur models, the FFDI and GFDI, were respectively ranked third and fourth.

Table 5.17 **Performance of four fire danger indices over South Africa (overall ranks expressed in percentages) (after Steenkamp *et al*., 2013)**

Rank	FWI	LFDI	FFDI	GFDI
1	90.3	6.5	5.5	2.6
2	5.6	54.8	30.1	21.4
3	2.7	33.4	32.3	30.3
4	1.3	5.4	32.2	45.7

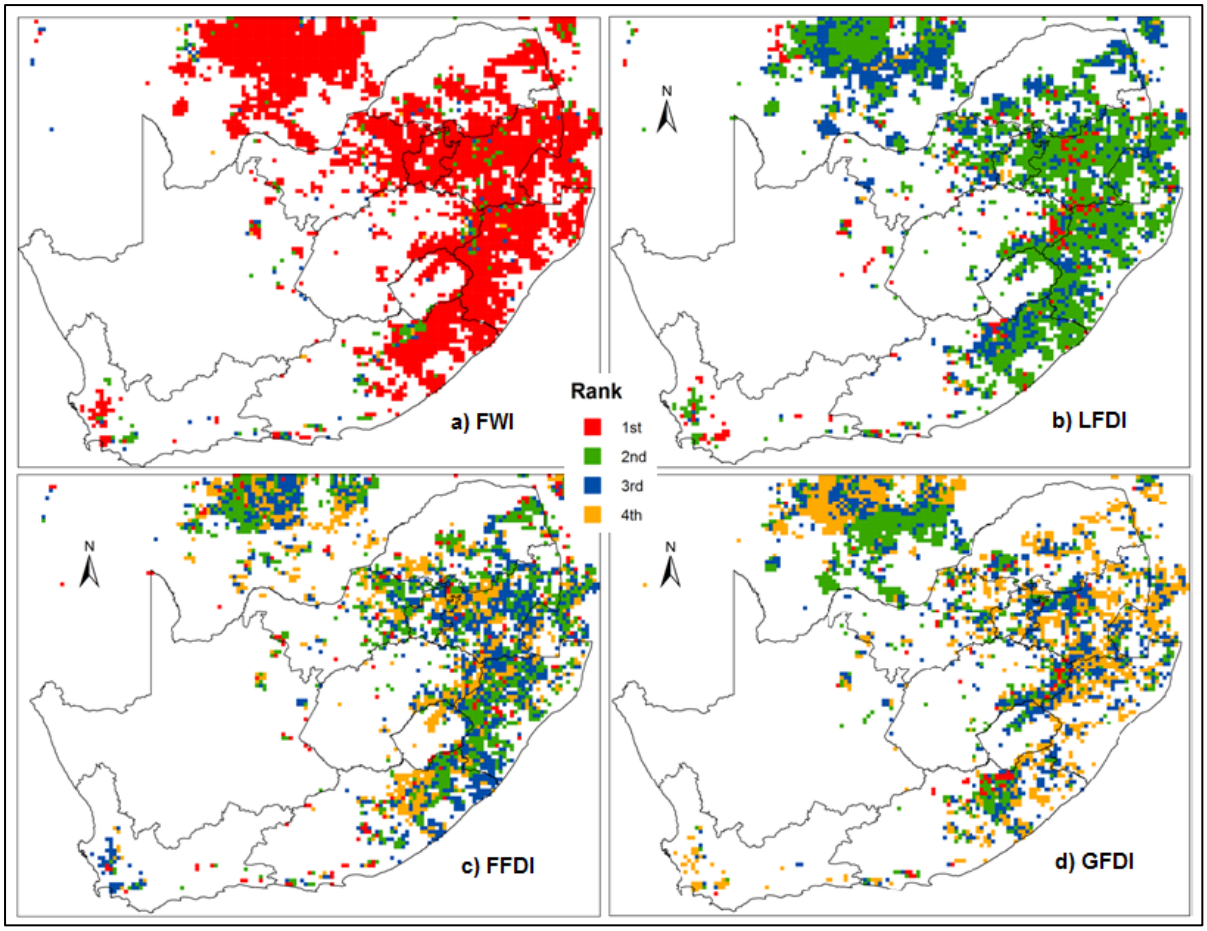

Figure 5.30 **Spatial performances of four fire danger indices over South Africa (Steenkamp *et al*., 2013). Ranking per grid box for: a) Fire Weather Index; b) Lowveld Fire Danger Index; c) McArthur Forest Fire Danger Index; and d) McArthur Grassland Fire Danger Index. Note that the white areas indicate grid boxes that were excluded because either the minimum requirement of 20 fire events were not met, or a negative correlation was observed between the specific index and fire activity.**

The CSIR consequently decided to include the FWI along with the LFDI on their Advanced Fire Information System (AFIS) website. The only calibration was to align the scale of the FWI to that of the LFDI (WAMIS, 2015). These findings were presented in February 2013 to a meeting of the Department of Agriculture, Forestry and Fisheries (DAFF), SAWS and other stakeholders. At the time the US FDRS was gazetted to be the national fire danger rating system (Notice 1054 of 2005), but SAWS experienced problems in its implementation (Frost, 2013, personal communication). The decision was subsequently made not to adopt the McArthur system as proposed by SAWS at the time, but to keep using the LFDI instead. As pointed out by Sharples *et al*. (2009) any change in a FDRS has important implications for “the fire management industry and the community at large”. It was motivated that the LFDI is entrenched in local

communities and there is a clear understanding of resources required to suppress fires based on the LFDI colour coding. The adoption of the LFDI as the official South African National Fire Danger Rating System was gazetted later that year (Notice 1099 of 2013). This was widely communicated to the end-user community (Pool, 2013).

CHAPTER 6

DESCRIPTION OF THE STUDY AREA

Biomes are defined as “the world’s major communities, classified according to the predominant vegetation and characterized by adaptations of organisms to that particular environment” (Campbell, 1996). Mucina *et al*. (2006) described grasslands as comprising of “herbaceous vegetation of relatively short and simple structure that is dominated by graminoids, usually of the family *Poaceae*” with a distinct lack of woody plants, which may be rare or confined to gullies or the slopes of ridges or rocky outcrops. Grasslands, including sown pasture and rangeland, cover about 3.5 billion ha globally (more than double the total cropped area), which amounts to about 26% of the world land surface and 70% of the world agricultural area (Solh, 2005; FAO, 2013). Worldwide, the livelihoods of over 800 million people are linked to this major biome. Grasslands are a principal feed source for livestock and provide various ecosystem services such as constituting a habitat for wildlife, nutrient cycling, storage for carbon and water as well as watershed protection for numerous large river systems (Solh, 2005; FAO, 2013). Grasslands are also important for local conservation of plant genetic resources since many uncultivated plant species hold potential for sustainable agriculture or medicinal use. Despite occupying only a small fraction of the world’s surface, burning in grasslands accounts for almost half the global carbon emissions from fire (Daniau *et al*., 2013).

In South Africa, grasslands comprise the second largest biome after savanna, covering about 20% of the country (Gibson *et al*., 2007) and extending into some of the other major neighbouring biomes such as Nama-karoo, savanna, thicket or forest (Palmer & Ainslie, 2005). The bulk of South Africa’s grasslands are located on the high central plateau (locally referred to as the Highveld), while some inland patches are also found in the Eastern Cape and KwaZulu-Natal (Mucina *et al*., 2006). This study focused on the central grassland biome of South Africa, for which a detailed description is provided in this chapter.

6.1 PHYSICAL AND ECONOMICAL DESCRIPTION

The study area covers the grassland of the central interior plateau to the west of the Drakensberg escarpment and the Drakensberg escarpment itself. Politically, it comprises the south-eastern part of the North West province and small, isolated patches of the extreme south-eastern corner of the Northern Cape, central and southern Gauteng, the Free State (excluding the extreme north-west), the Highveld region of Mpumalanga, the kingdom of Lesotho as well as the bordering Drakensberg escarpment of the Eastern Cape, KwaZulu-Natal and the kingdom of Swaziland (shaded area in Figure 6.1a). Strategic urban centres within the study area include:

- Gauteng – Johannesburg, southern part of Pretoria, towns of the East Rand (e.g. Benoni, Boksburg, Germiston, Kempton Park) and West Rand (e.g. Randburg, Roodepoort, Krugersdorp), Vereeniging, Vanderbijlpark;
- Mpumalanga – Witbank (eMalahleni), Secunda (eMbalenhle), Bethal, Ermelo, Piet Retief, Standerton;
- North West – Carletonville, Klerksdorp, Potchefstroom;
- Free State – Bloemfontein, Welkom, Kroonstad, Bethlehem;
- Lesotho – Maseru; and
- Swaziland – Mbabane.

The topography is predominantly flat to rolling, occasionally incised by river valleys or broken by small mountains, but also includes steep slopes and buttresses of the mountainous regions of the continental divide (Mucina *et al*., 2006). The land rises from about 1 200 m in the west towards the Great Escarpment in the east where altitudes vary between 1 800 and 3 200 m (Figure 6.1b), with the highest peak in southern Africa, Thabana Ntlenyana, reaching 3 482 m above mean sea-level. The Highveld is predominantly drained by tributaries of the Orange River, which flows westwards towards the Atlantic Ocean, while the northern and eastern extremities are drained by tributaries of the Limpopo and other smaller rivers (e.g. Komati and Great Usutu rivers) that flow towards the Indian Ocean.

The underground wealth of the central grassland is world renown. Coal, gold, uranium, manganese, vanadium, chrome and a host of less important minerals are mined in the north, while diamonds are also found in parts of the Free State and Lesotho.

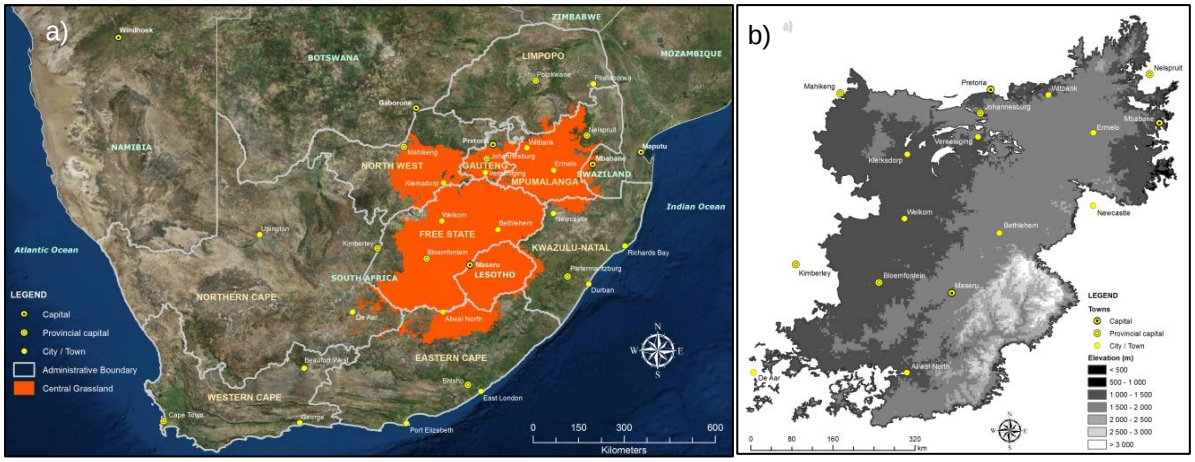

Figure 6.1 **a) Map of southern Africa highlighting the central grassland biome, for which elevations above mean sea level are shown in (b).**

Agriculturally, this area may be considered the most productive in South Africa (Ellery, 1992). Natural grassland supports livestock farming, with beef production the most important livestock-related activity, followed by small-stock (sheep and goat) production (Palmer & Ainslie, 2005). Poultry production (mainly broilers) are mostly concentrated near urban centres, while a number of farmers also derive some or all of their income from commercial hunting or ecotourism (Palmer & Ainslie, 2005). Large portions of the grasslands have been ploughed and converted into mostly dryland cultivation for the production of maize, sunflower, soybeans, sorghum, groundnut, potatoes, dry beans and wheat along with a variety of vegetable crops (DAFF, 2017). Silviculture is also practiced along the eastern mountain regions, where mainly exotic *Pinus* and *Eucalyptus* species are grown for timber and paper (Mucina *et al*., 2006).

The combination of ample mineral, fossil fuel and agricultural resources makes the central grassland a hub of industrialization and economic growth, centred on Gauteng. The associated urban development and large human population has exerted a lot of pressure on the surrounding grasslands, bringing about changes in species composition and production potential (Palmer & Ainslie, 2005).

6.2 ECOLOGICAL DESCRIPTION

Olson *et al*. (2001) classified this area under the “montane grass- and shrublands” biome, with similarly classified regions occurring in high-elevation areas of east Africa (e.g. Ethiopian Highlands), central Asia (e.g. Tibetan Plateau) and South America (e.g. Andean Plateau). According to Acocks (1953) the study area comprises the so-called

“climatic climax and fire climax grasslands of the central interior plateau and eastern escarpment region”. An updated and more spatially detailed classifications of the vegetation types of South Africa, Lesotho and Swaziland was provided by Mucina and Rutherford (2006) (Figure 6.2). According to the latter classification the study area comprises the dry and mesic Highveld grasslands as well as the Drakensberg grassland, indicated respectively by the light, dark and bright green shaded areas in Figure 6.2. Due to the potential impact on the synoptic weather typing associated with enhanced fire danger (Chapter 8), the sub-escarpment grassland (turquoise shaded areas in Figure 6.2) were excluded from this study along with small pockets of the above-mentioned bioregions in Limpopo and the central parts of the Eastern Cape.

6.2.1 Vegetation

To a large degree the Drakensberg and dry Highveld grasslands (Mucina & Rutherford, 2006) coincide with the climatic climax grassland (Acocks, 1953), which comprises the bulk of the study area. This area is alleged to be either too arid or too cold to allow an escalation to woody communities, even in the absence of fire (Acocks, 1953; Tainton, 1999). At lower elevations the most important graminoid species include *B. serrata*, *C. plurinodis*, *E. chloromelas*, *E. curvula*, *E. muticus*, *E. racemosa*, *H. contortus*, *M. caffra*, *S. sphacelata*, *T. leucothrix* and *T. triandra* (Figure 3.27), while at higher elevations the stand may also include *B. firmior*, *C. marginatus*, *D. filifolius*, *F. caprina*, *F. costata*, *F. scabra*, *H. hirtulum*, *K. cristata*, *M. caprina*, *M. disticha*, *M. macowanii*, *P. binata*, *P. microphylla*, *T. dregei* and *T. spicatus* (Tainton, 1999). The open grassland has an abundance of geophytic herbs and is frequented by patches of karroid scrub (e.g. *D. austro-africana*, *R. burchellii*, *R. ciliate* and *R. erosa*), while small trees (e.g. *E. crispa*, *C. spicata*) are sparsely distributed and mainly confined to river banks or rocky outcrops. At high elevations the short scrubby vegetation is structurally related to Nama Karoo and often dominated by chamaephytes and hemicryptophytes (Ellery, 1992). Most of the grasses are perennial and form a basal coverage that ranges from about 6 – 15%, while a reduction in basal cover is common in degraded areas. Bush encroachment, particularly by *A. karroo*, is also fairly common in the north-west.

Although the temperate grasses and some of the geophytes remain active where soil water is available, conditions are generally too dry and cold for growth during the winter

months. Therefore, the growing season usually commences in September, when the temperature of the upper 5 cm of soil reaches about 12°C, and concludes in April (Tainton, 1999). Growth during the spring and midsummer period is often limited by water stress, so that the most rapid growth occurs during the late summer and autumn (Tainton, 1999).

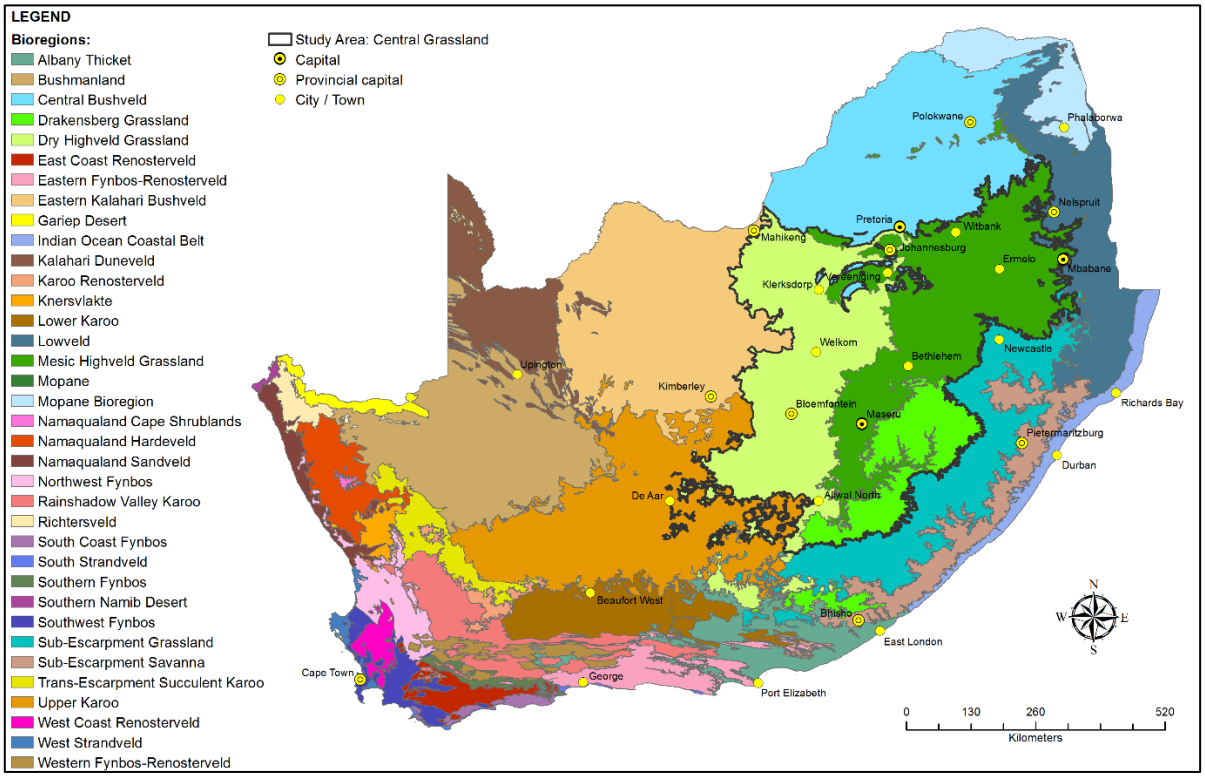

Figure 6.2 **Vegetation types of South Africa, Lesotho and Swaziland (after Mucina & Rutherford, 2006), highlighting the study area in the central grassland.**

The dry Highveld grassland is also locally referred to as the sweetveld as it is dominated by the so-called sweet grasses (Figure 6.3), which have a lower fibre content, remain palatable to herbivores and provide year-round grazing (Tainton, 1999; Palmer & Ainslie, 2006; van Oudtshoorn, 2012). The sweetveld is typically 0.75 m to 1.6 m tall and forms a fairly uniform stand interspersed by a number of forbs and cool season grasses, while shrubs are generally only located along rocky ridges and hill-slopes (Tainton, 1999). According to Mucina *et al*. (2006) the stand is dominated by C_4 grasses, mostly belonging to the subfamily *Chloridoideae*.

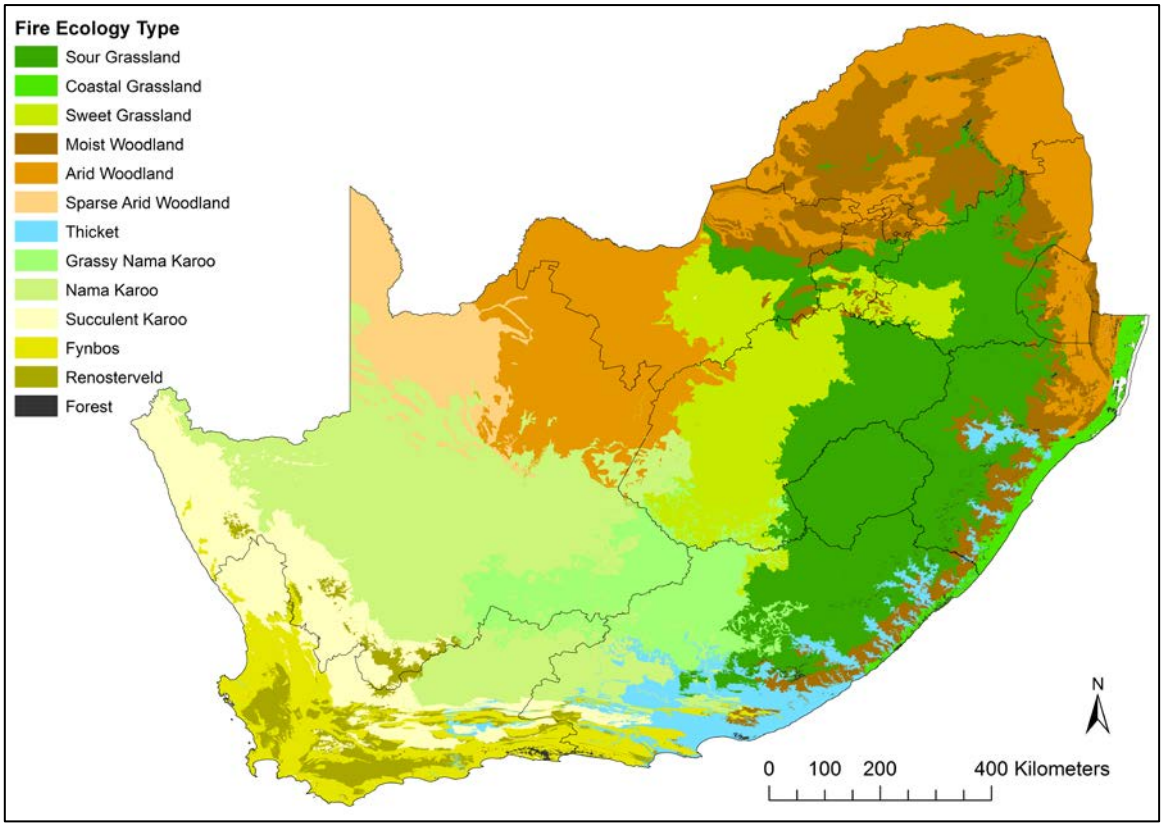

Figure 6.3 **Distribution of fire-ecology types based on Mucina and Rutherford (2006) vegetation types (Forsyth *et al*., 2010).**

The mesic Highveld grassland (Mucina & Rutherford, 2006) roughly coincides with the fire climax grassland of potential forest or savanna areas (Acocks, 1953) in the east and north of the study area (Figure 6.2). These grasslands are normally intermixed with patches of forest or bush and developed where Acocks (1953) believed these vegetation types to be the natural climax if not for the restricting influence of fire, frost or grazing (Low & Rebelo, 1996; Tainton, 1999). Although it is generally accepted that fire plays an essential role in the maintenance of grasslands (van Wilgen & Scholes, 1997; Bond *et al*., 2005; Mucina *et al*., 2006; Archibald *et al*., 2008), Acocks' classification of this part of the grassland biome as "false" (i.e. not climatically determined) was successfully dismissed by Ellery (1992) who listed evidence from a variety of disciplines to prove that the entire area has been covered by grassland for millennia. Grass species found in potential forest areas at high elevations include, among others, *A. junciformis*, *A. semialata*, *D. filifolius*, *E. muticus*, *E. racemosa*, *H. contortus*, *H. dissoluta*, *M. ceresiiforme*, *R. altera*, *T. triandra*, *T. leucothrix* and *T. spicatus* (Tainton, 1999). Similar grass species are found in potential savanna areas, which boasts a better representation of *H. hirta*, while the woody component is

composed of bushveld rather than forest species (Tainton, 1999). Most of these grasses are perennial and form a basal coverage that ranges from about 8 – 16% in potential savanna areas and 10 – 20% in potential forest areas. Degradation is associated with changes in species composition (most significantly a reduction in the *Themeda*-dominated sward), while a loss of basal cover may also occur in fire climax grassland of potential savanna areas (Tainton, 1999).

Parts of the eastern Highveld are dominated by sour grasses (Figure 6.3), which are higher in fibre content and unpalatable during the dry season as plants tend to withdraw nutrients from their leaves (Tainton, 1999; Palmer & Ainslie, 2006; van Oudtshoorn, 2012). Sourveld typically occur at higher altitudes in high rainfall (> 650 mm per annum) areas (Forsyth *et al*., 2010). According to Mucina *et al*. (2006), sour grasses mostly belong to the subfamily *Panicoideae* (*Andropogoneae*), which all use the C_4 photosynthetic pathway. However, C_3 grasses become more prominent in the higher altitude Drakensberg grassland (Mucina *et al*., 2006).

6.2.2 Veld Production Potential and Structural Transformations

The central grasslands are fairly productive, yielding 1 t ha^{-1} y^{-1} in the drier western parts to 3.5 t ha^{-1} y^{-1} in the wetter eastern parts where soil fertility plays a determining factor (Tainton, 1999). Stocking rates, which vary considerably from year to year mainly due to rainfall variability, are relatively high over grasslands and easily 3 – 4 times the recommended rate on communal grazing lands (Mucina *et al*., 2006). The carrying capacity range between 1 and 5 ha AU^{-1} y^{-1} (hectares per animal unit per year) across the dry Highveld and Drakensberg grassland, and between 1 and 3 ha AU^{-1} y^{-1} over the mesic Highveld grassland.

Acocks (1953) warned of large scale structural transformations occurring in the grassland biome due to the invasion of dwarf shrubs from the neighbouring semi-arid Karoo to the southwest. However, observations reveal that this did not take place as envisaged (Palmer & Ainslie, 2006). On the contrary, a study by Masubelele *et al*. (2014) suggests a general increase in the cover of native grass species in lieu of shrubs in the adjacent Grassy Nama Karoo over the period 1962 – 2009. Du Toit *et al*. (2015) also provided photographic evidence of an increase in grass cover after the occurrence of several wildfires in the Grassy Nama Karoo. This increase in grass-

dominated vegetation is clearly not supported by the popular hypothesis of degradation due to an expanding Karoo Shrubland (Acocks, 1953), nor does it fit the proposed effects of CO_2 fertilization. Although the drivers of change is very complex, possible explanations for the observed transition include an increase in annual total precipitation for this region with grasses replacing shrubs as moisture stress decreases (Moncrieff *et al*., 2015), as well as reduced grazing pressure due to a reduction in stocking rate over the last few decades (Masubelele *et al*., 2014). Further increases in grass cover will result in escalated fire risk which is likely to further alter vegetation structure, species composition and grazing capacity in this region (Masubelele *et al*., 2014; du Toit *et al*., 2015). A south-westward expansion of the grassland biome into the Nama Karoo, its south-western neighbour, cannot be overruled. According to Moncrieff *et al*. (2015) CO_2 fertilization may also result in the projected expansion of woodlands at the expense of grasslands, although such changes may be countered through management practices (e.g. veld burning).

6.2.3 Fauna

The central grassland provides a rich habitat for fauna. Historically, it was home to large numbers of wild ungulate herbivores like the black wildebeest (*Connochaetes gnou*), blesbok (*Damaliscus dorcas phillipsi*), red hartebeest (*Alcelaphus buselaphus caama*), springbok (*Antidorcas marsupialis*), impala (*Aepyceros melampus melampus*), Burchell's zebra (*Equus quagga burchelli*), eland (*Taurotragus oryx*), Cape buffalo (*Syncerus caffer*), black rhinoceros (*Diceros bicornis*) and southern white rhinoceros (*Ceratotherium simum simum*), but these animals are now mainly restricted to game farms and nature reserves (Ellery, 1992; Palmer & Ainslie, 2006). Other prominent herbivores include porcupine (*Hystrix africaeaustralis*) and several species of hare, tortoise, grasshoppers and harvester termites (e.g. *Hodotermes mossambicus*). Although their influence is very local, the latter can seriously deplete grass stands, particularly during periods of drought (Mucina *et al*., 2006).

Grassland avifauna include some 350 species of which 10 are endemic and as many as 40 are specialists that depend exclusively on grassland habitat (BirdLife SA, 2017). Threatened, rare or endangered grassland bird species include the African grass owl (*Tyto capensis*), blue korhaan (*Eupodotis caerulescens*), Botha's lark (*Spizocorys fringillaris*), Rudd's lark (*Heteromirafra ruddi*), blue swallow (*Hirundo atrocaerulea*),

ground woodpecker (*Geocolaptes olivaceus*), secretary bird (*Sagittarius serpentarius*), southern bald ibis (*Geronticus calvus*) and yellow-breasted pipit (*Anthus chloris*).

6.2.4 Soil

Soils are variable and largely related to parent material, geomorphology and climate (Ellery, 1992). The soils of the sweetveld (Section 6.2.1) are eutrophic (i.e. not highly leached) and commonly derived from parent material that gave rise to a high base status (e.g. sandstones, mudstones and shales of the Karoo Supergroup). In contrast, the soils of the sourveld are dystrophic (i.e. predisposed to leaching) and generally more acidic, typically of quartzite and andesitic origin (Mucina *et al*., 2006; Palmer & Ainslie, 2006). From the 14 broad soil groups reported in South Africa by Fey (2010), duplex and oxidic soils generally dominate in the western half, plinthic and vertic soils are found across the central and northern parts and humic soils in the extreme east. Lithic soils are distributed across the whole region. Texturally, the soils across the study region range from sandy-loam to sandy-clay (Figure 6.4), but can be quite shallow and stony on rocky slopes and outcrops.

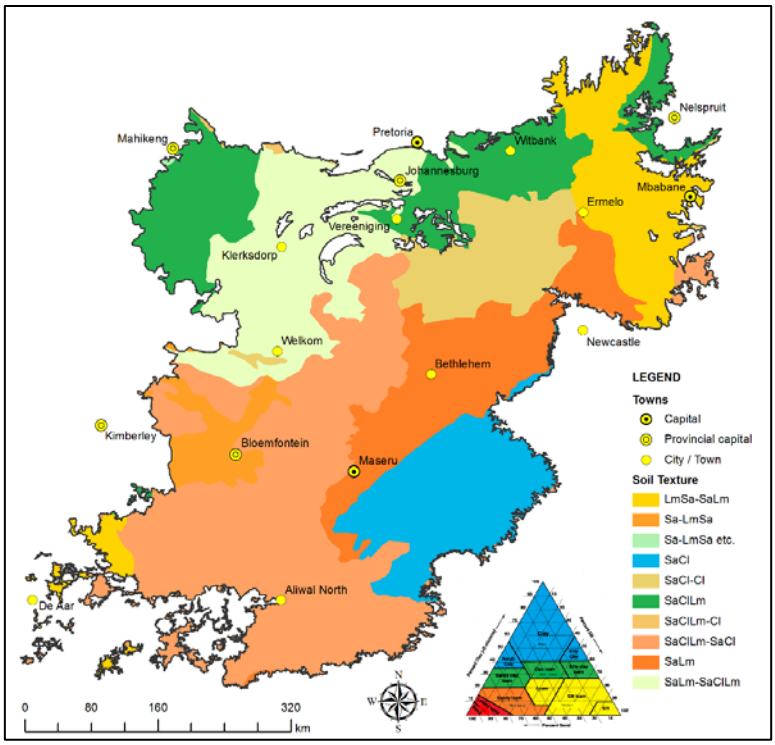

Figure 6.4 **Variation in soil texture types across the central grassland biome with Cl = Clay; Lm = Loam; Sa = Sand and Si = Silt (data obtained from Midgley *et al*., 1994). The region corresponds to the shaded area in Figure 6.1a.**

6.3 CLIMATOLOGICAL DESCRIPTION

The climate of an area is largely determined by climatic controls such as the intensity of solar radiation and its variation with latitude, continentality (i.e. distribution of land and water surfaces), the modifying effects of major sea currents, prevailing winds, the position of high- and low-pressure areas and the seasonal variation of these positions, as well as the general exposure of the locality (i.e. elevation, location of mountain barriers etc.) (Lowry, 1972). While the topography and continentality became evident from the previous discussions (Section 6.1), this section will focus on the typical synoptic scale pressure patterns in the vicinity of the study area and attempt to describe the most important aspects of the observed (historical) climate.

6.3.1 Typical Near-surface Synoptic Scale Weather Patterns over Southern Africa

Although pressure, wind and rainfall patterns are constantly changing, there are certain basic patterns in the pressure and wind fields that occur regularly. Seasonal variations exist in the southern Atlantic Ocean high-pressure cell (AOH) and southern Indian Ocean high-pressure cell (IOH). The variation in both the latitudinal (N-S) and longitudinal (E-W) movement of the AOH are half-annually. The IOH is subjected to a half-annual variation in its latitudinal movement, but an annual variation in its longitudinal movement. On average the AOH is located 3° further north than the IOH but both cells shift 5 - 6° northwards in the winter (van Heerden & Hurry, 1998). The annual longitudinal shift of the AOH is 7 - 13°, while the IOH is subject to a considerably larger longitudinal shift of 24 – 30° (van Heerden & Hurry, 1998). The latter, therefore, has a much larger effect on the weather and climate of South Africa.

During the summer months the following weather conditions prevail as depicted in Figure 6.5a (adapted from van Heerden & Hurry, 1998):

i) The IOH and AOH move further southwards, causing westerly winds to occur well to the south of the country.

ii) The IOH is centred further out to sea. Wind blowing from this high-pressure cell then has a longer sea track over the warm Indian Ocean – where lots of moisture is accumulated – before it moves in over the eastern parts of the subcontinent. This often results in cloudy conditions over these eastern areas with drizzle along the eastern escarpment and adjacent Lowveld.

iii) Moisture laden south-easterly trade winds invade the eastern (and especially north-eastern) parts of the subcontinent. These winds sometimes recurve southwards, influencing the northern provinces; on occasion they move further northwards and influence Zimbabwe and Zambia.

iv) When moist air is in circulation (as imported by the south-easterly trades), uplift thereof will result in condensation, cloud formation and precipitation.

v) The AOH is a source of subsiding air, having its centre fairly near the west coast of South Africa. The winds blowing from it have a much shorter sea track and thus carry little moisture.

vi) Where the cooler, drier air coming from the AOH meets that from the IOH, a moisture boundary (also referred to as a moisture front or dry-line) forms. Uplift occurs along this moisture front due to the undercutting effect of the colder, drier air, often affecting the rainfall distribution over the entire region.

vii) Sometimes the AOH lies further south and then the south-westerly winds have a longer sea track and contain more moisture. General rain may then occur over the south-eastern parts.

viii) Due to strong surface heating, a heat low normally develops over the north-western interior with convergence in and to the east of it.

ix) South-easterly trades blow to the north of the AOH. These winds accumulate moisture and recurve clockwise around a tropical low – which typically develops over northern Angola or the Congo – and invades Angola and the Congo from the southwest. These winds are then known as the south-westerly monsoon. A convergence zone, known as the Congo Air Boundary (CAB), develops where these winds meet the south-easterly trades from the Indian Ocean.

x) North-easterly trades blow across the equator (to become the north-easterly monsoon) and where they meet the south-easterly trades a convergence zone is formed, which is known as the Inter-Tropical Convergence Zone (ITCZ).

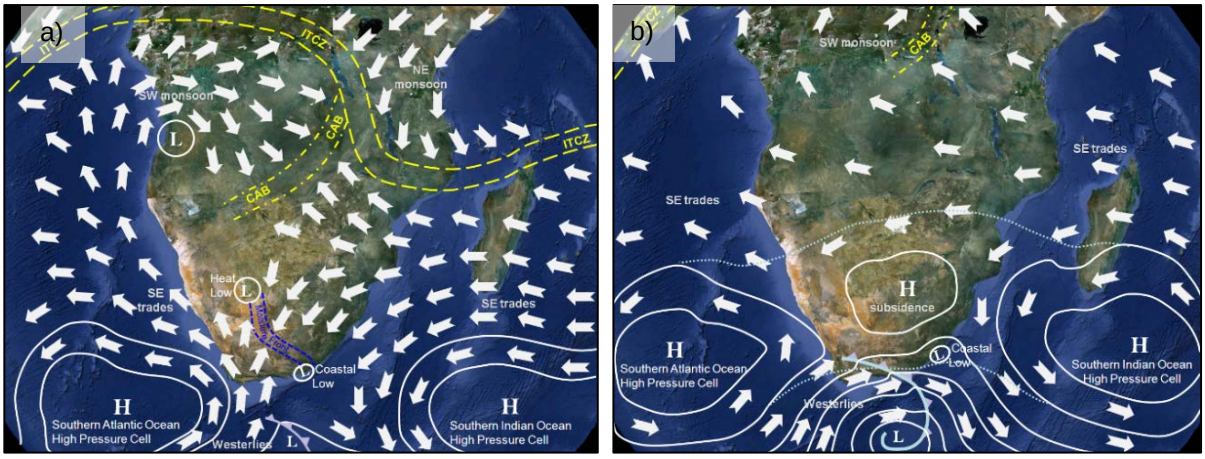

Figure 6.5 **Basic weather patterns over southern Africa during (a) summer, and (b) winter (adapted from van Heerden & Hurry, 1998).**

During the winter months the following weather conditions prevail as depicted in Figure 6.5b (adapted from van Heerden & Hurry, 1998):

i) The IOH and AOH move further northwards, bringing westerly winds to the southern and south-western coastal regions of South Africa.

ii) Generally cool to cold conditions prevail and in the absence of heat lows over the interior, the AOH and IOH are linked across the land.

iii) A separate high-pressure cell usually forms over the north-eastern interior. The associated subsiding air results in clear skies and calm conditions over large parts of the interior.

iv) With the northwards movement of the Indian and Atlantic high-pressure systems, mid-latitude cyclones, which are accompanied by cold fronts and develop over the Atlantic Ocean, invade the southern regions of South Africa. On occasions these cold fronts have influenced regions as far north as Zambia when a strong high-pressure system ridges closely behind the cold front.

v) Cloudy conditions associated with rain influence the southern, south-western and eastern coasts. Uplift is mainly due to cyclonic or frontal action, but orographic uplift does occur over the escarpment where snowfalls may occur. Interior snowfalls usually occur with the presence of a strong high, following closely behind a cold front, thus pushing the cold air into the interior. A strong upper air flow aids with the uplift, and thus enables condensation and cloud formation to take place.

vi) The north-easterly monsoon disappears completely and the ITCZ shifts far north of the equator (between 5°N and 20°N). The south-easterly trades still

blow to the north of the high-pressure belt and moves across the equator and recurve north-eastwards, becoming part of the great summer Monsoon of India.

vii) The south-westerly monsoon also moves further north, crossing the coast well north of Angola. This results in the CAB moving much further north.

6.3.2 Description of Common Climatic Elements

Mean annual precipitation (Figure 6.6a) increases from about 400 mm in the lower lying west to around 1 000 mm in the east, while topographical effects give rise to values of up to 1 900 mm in places against the Drakensberg (Schulze, 1994). Concomitantly, the coefficient of variation decreases from 30 – 35% in the west to less than 20% on the escarpment (Schulze, 2007). The number of days per year with recorded rainfall exceeding 10 mm varies from only about 15 in the west to 25 in the east (Tyson, 1986; SAWS, 2012). More than 80% of the precipitation occurs during the austral summer from October to March (Tyson, 1986), with the peak rainfall month shifting from January in the east to February in the west (Schulze, 1994). Evaporation and transpiration rates are also high during this period on account of the high temperatures. Mean annual potential evaporation (Figure 6.6b) decreases from about 2 500 mm in the warmer, dryer west to around 1 000 mm in the east.

Precipitation is almost exclusively in the form of showers and thundershowers, which can be heavy on occasion and exceed 50 mm in a single day (Schulze, 1994). A strong diurnal cycle in rainfall is thus also evident as afternoon and early evening convective development is largely driven by surface heating and atmospheric instability (Tyson, 1986). The average number of thunderstorms in a year varies spatially from around 60 in the west, 70 in the north and 100 in Lesotho (Schulze, 1994; SAWS, 2012). Lightning flash densities increase from between 5 – 10 flashes per km^2 in the west to 15 – 20 in Mpumalanga (SAWS, 2011). Due to the convective nature of the rainfall, infiltration rates are low and runoff rates high (Tainton, 1996). Annually, about 2 – 8 hail occurrences (depending largely on altitude) may be expected at any one spot (Tyson, 1986). The winters are usually dry and sunny, but unsettled weather may result on average in 5 – 8 snow days per year (mainly in midwinter) in the south, while the frequency decreases sharply northwards (Schulze, 1994).

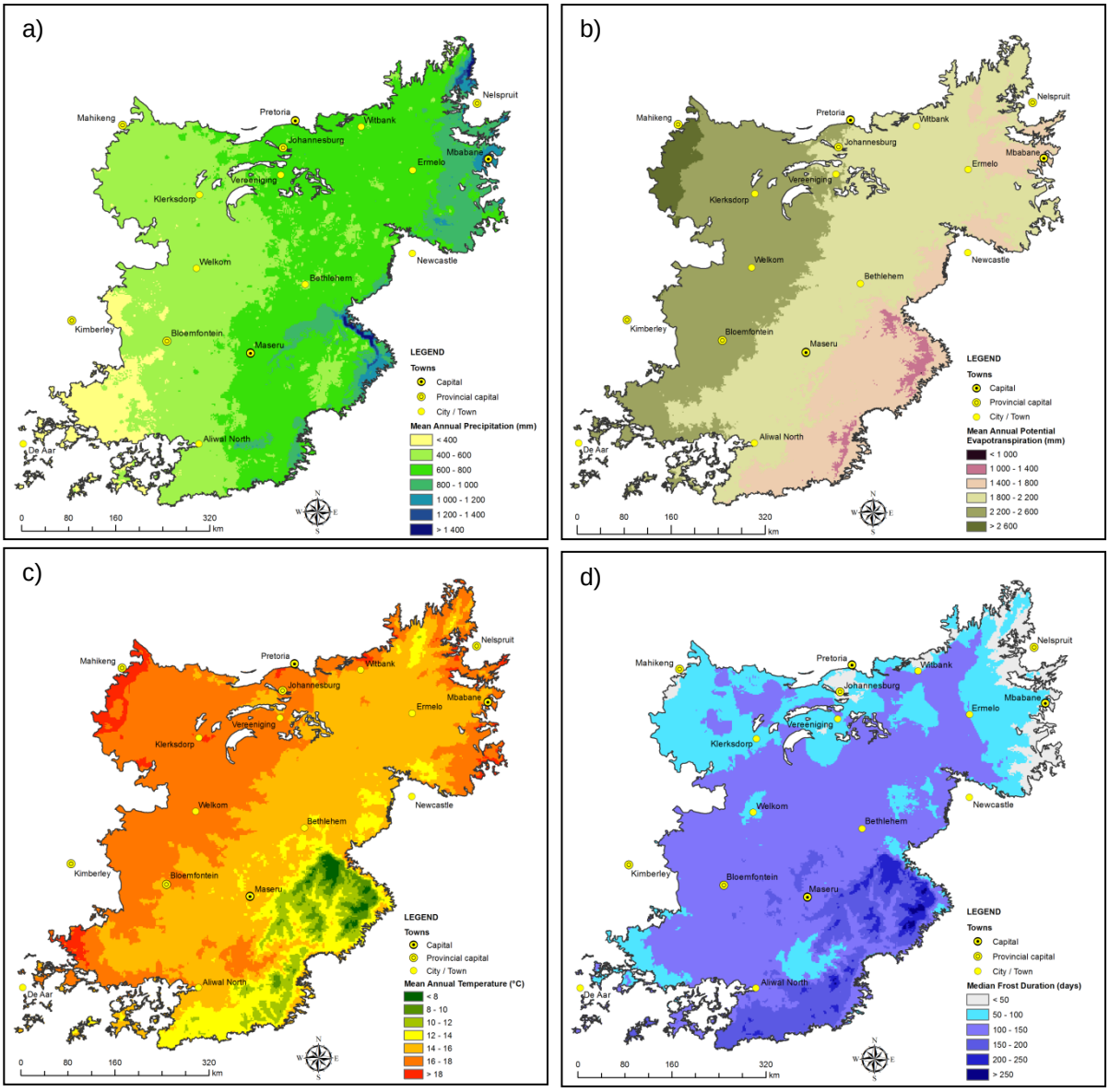

Figure 6.6 **Long-term climate summary for the period 1950 to 2000 of the central grassland biome, showing: (a) mean annual precipitation; (b) mean annual potential evapotranspiration; (c) mean annual temperature; and (d) median frost duration (data obtained from Schulze, 2007). The region corresponds to the shaded area in Figure 6.1a.**

Mean daylight hours across the study area range from a minimum of 9.9 – 10.5 hours in June to 13.5 – 14.1 hours in December (Allan *et al*., 1998). At the same time the daily extraterrestrial radiation may range from about 17.4 – 21.9 MJ m^{-2} per day in June to 43.0 – 44.1 MJ m^{-2} per day in December (Allan *et al*., 1998). Actual sunshine duration remains between 70 and 80% of the possible in winter, but decreases to about 60% of the possible in summer during the peak of the cloudy (or rainy) season over the eastern parts (Schulze, 1994).

The relatively high elevation of the central grassland (Figure 6.1b) gives rise to relative cooler conditions than the surrounding areas. This also gives rise to fairly large diurnal and seasonal temperature ranges, as attested by the climate summary provided in Table 6.1. Mean annual temperatures (Figure 6.6c) decrease from around 18°C on the western boundary to less than 10°C on the higher lying parts of the Drakensberg mountains (i.e. Lesotho Highlands). Annually, the frequency of days with maximum temperatures exceeding 30°C drops from about 60 in the west to less than 10 days over the higher elevations in the east (Tyson, 1986). Median frost duration (Figure 6.6d; with frost days defined as days having a minimum temperature below 0°C) decreases from more than 150 days per annum over the southern mountains to less than 50 in the extreme north and north-east (Schulze, 2007; SAWS, 2012). Table 6.1 attempts to summarise some of the main climatic elements for strategic centres located within the central grassland biome.

Table 6.1 Summary of a selection of climatic elements for strategic centres located within the central grassland biome (data obtained from FAO, 2006; SAWS, 2012; Windfinder, 2018)

Station	Coordinates	Altitude (m)	Total annual rainfall (mm)	Average maximum temperature (°C) January / July		Average minimum temperature (°C) January / July		Prevailing wind (direction, knots) January / July		Köppen-Geiger climate class
Aliwal North	30° 48' S 26° 53' E	1 347	569	31.1	17.0	14.5	-0.8	NNW 6	NNW 6	BSk
Bethlehem	28° 15' S 28° 20' E	1 680	680	27.2	16.4	13.2	-2.0	NE 7	WSW 7	Cwb
Bloemfontein	29° 06' S 26° 18' E	1 351	559	30.8	17.4	15.3	-1.9	NNE 8	NW 6	BSk
Ermelo	26° 30' S 29° 59' E	1 769	689	23.8	16.3	13.5	3.1	E 9	W 9	Cwb
Johannesburg	26° 09' S 28° 11' E	1 695	750	25.7	17.1	14.9	3.7	E 8	NNW 9	Cwb
Klerksdorp	26° 48' S 26° 38' E	1 350	545	29.8	19.3	16.6	4.1	NNW 4	NNW 7	BSh
Maseru	29° 18' S 27° 30' E	1 530	676	28.3	17.0	14.1	-1.9	N 7	N 6	Cwb
Mbabane	26° 19' S 31° 06' E	1 163	1 422	24.7	19.1	15.0	5.5	E 5	W 5	Cwb
Pretoria	25° 44' S 28° 11' E	1 330	674	28.6	19.6	17.5	4.5	ENE 5	NNE 4	Cwa
Vereeniging	26° 41' S 27° 55' E	1 440	671	27.9	18.5	15.9	0.2	NE 6	NW 6	Cwa
Welkom	28° 00' S 26° 40' E	1 338	561	30.0	18.1	16.7	1.9	NNE 8	NNW 7	BSk
Witbank	25° 50' S 29° 11' E	1 545	672	26.0	18.2	15.1	4.0	E 7	NNW 6	Cwb

In accordance with the longitudinal shift in the IOH (Section 6.3.1) winds blow mainly from the north-east during summer and north-west during winter (Table 6.1), when occasional cold snaps are accompanied by southerly winds for a day or two. During thunderstorms strong and gusty south-westerly winds of short duration are also a

common feature (Schulze, 1994). In general, autumn is the windiest season, when dust storms sporadically occur in the drier west (depending on denudation of the surface due to prolonged drought). Thermal gradients usually result in a diurnal cycle in the wind direction, producing a backing of the wind from north-east to north-west during the day (Tyson & Preston-Whyte, 2000), while mountain/valley breezes typically develop in hilly terrain (Section 4.3.3). On the whole winds tend to be light in the morning and attain their maximum speed in the afternoon as the stability profile of the lower atmosphere changes and the depth of the mixing layer increases (Section 4.2.6).

6.3.3 Köppen-Geiger Climate Classification

Each station's Köppen-Geiger climate classification is provided in Table 6.1 According to Kottek *et al*. (2006) the western part of the study area (primarily sweet veld) falls mostly under BSk, while the eastern portion (transitioning to sour veld) falls under Cwb. A narrow strip of Cwa is nestled in between, with small intrusions of BSh in the north-west and Cfb in the far south (Figure 6.7). BSk is branded as semi-arid cold steppe with the accumulated annual precipitation exceeding five times the dryness threshold ($P_{ann} > 5^{x}P_{th}$; with $P_{th} = 2^{x}|T_{ann}|+28$ and $|T_{ann}|$ the absolute value of the annual mean temperature in °C), and the annual mean temperature falling below 18°C ($T_{ann} < 18$°C). Cwb is classed as a mesothermal climate with dry winters and long and warm summers. Here dry winters imply that $Pw_{min} < Ps_{min}$ and $Ps_{max} > 10^{x}Pw_{min}$ (where Pw and Ps denote winter and summer precipitation in mm, respectively), whereas at least four months should have a mean temperature of 10°C or more in order for the summer to be classed as long and warm (Kottek *et al*., 2006).

Beck *et al*. (2005) detected an expansion of dry B climates in the Köppen-Geiger classification during the second half of the 20th century (i.e. 1951 – 2000) that might be amplified should global warming continue unabated. This conclusion is supported by climate model simulations performed by Kunz and Schulze (2010) and Rubel and Kottek (2010), which showed a future eastward shift of the BS/Cw boundary over the study area.

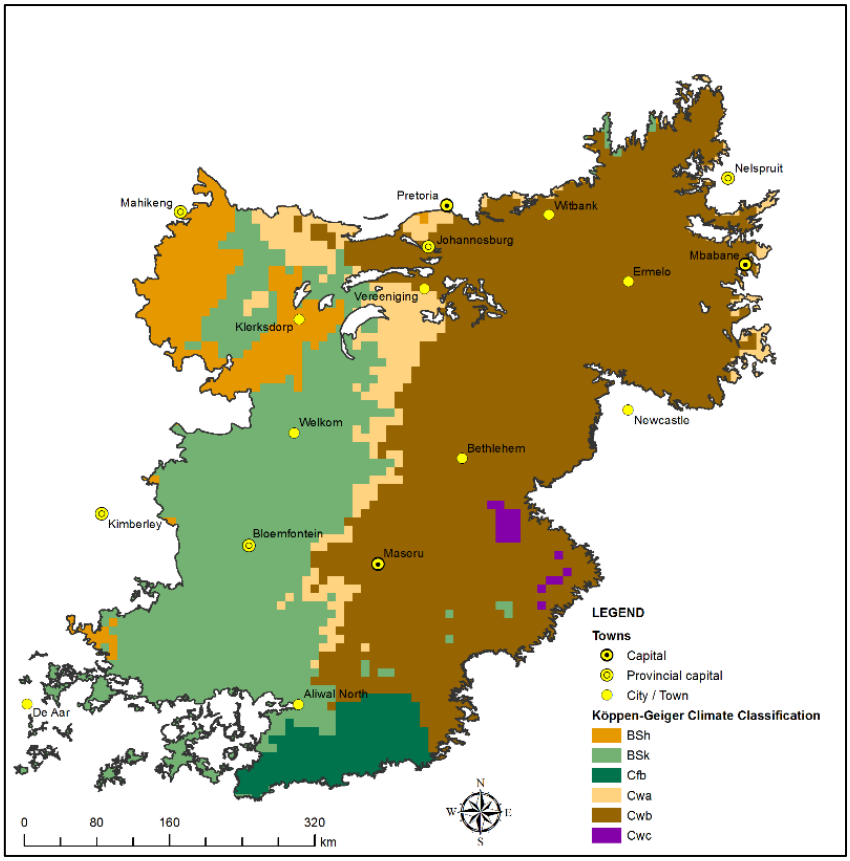

Figure 6.7 **Köppen-Geiger climate classification of the central grassland biome, based on gridded climate data for the period 1951 to 2000 (data obtained from Kottek *et al*., 2006).**

CHAPTER 7

HISTORICAL FIRE REGIME OF THE CENTRAL GRASSLAND BIOME OF SOUTH AFRICA

Knowledge of the historical fire regime, and the contemporary fire-climate relationship in particular, is of paramount importance in order to make informed strategic management decisions and to assess the potential impacts of projected future changes in climate. Such knowledge is not always readily available at a regional level and for a particular biome. Fire statistics pertaining directly to the study area are either difficult to access or do not readily exist. For example, not all of the local fire protection associations function at the same level of efficiently and submit fire reports regularly. Reporting efficiency also differs markedly across provincial boundaries. The aim of this chapter was to summarise the existing information on the fire regime of the central grassland biome or surrounding region, where available, and to augment the description of its fire regime where possible.

7.1 CURRENT KNOWLEDGE OF THE FIRE REGIME

7.1.1 Prehistoric Fires

Paleoenvironmental reconstruction of fire activity has been performed for only a handful of sites in southern Africa (Scott, 2002; Power *et al*., 2010; Marlon *et al*., 2016). Such paleofire records enable modern changes in biomass burning to be evaluated in a longer-term context (Marlon *et al*., 2016). Scott (2002) analysed microscopic charcoal trapped in sediments in order to provide a fire history of the grassland and savanna regions in South Africa. Only a few locations fell within the study area, namely:

- Elim and Craigrossie, near Clarens in the eastern Free State; and
- Rietvlei Dam and Moreletta River, near Pretoria, on the northern edge of the study area.

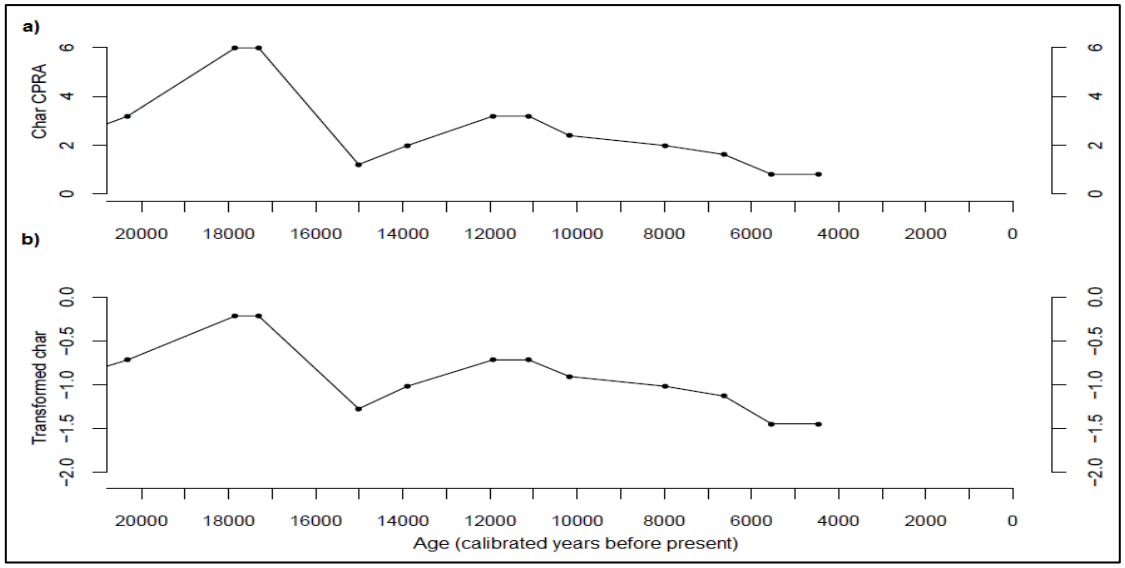

Figure 7.1 **Charcoal sequence from lacustrine deposits at Elim in the eastern Free State, showing the a) untransformed charcoal influx, and b) transformed charcoal influx (using the Box-Cox transformation) (GPWG, 2017).**

Table 7.1 **Charcoal influx z-scores, calculated for a reference period of 21 000 – 200 calibrated years before present, reflecting biomass burning at Elim (after Marlon *et al*., 2016)**

Age (calibrated years before present)	Charcoal Influx (z-score sign)
0 − 100	+
100 − 200	+
200 − 300	+
300 − 400	~0
400 − 500	~0
500 − 1500	~0
1500 − 2500	~0
2500 − 3500	-
3500 − 4500	~0
4500 − 5500	-
5500 − 6500	-
6500 − 7500	~0
7500 − 8500	-
8500 − 9500	-
9500 − 10500	~0
10500 − 11500	~0
11500 − 12500	~0
12500 − 13500	~0
13500 − 14500	~0
14500 − 15500	~0
15500 − 16500	-
16500 − 17500	+
17500 − 18500	+
18500 − 19500	n/a
19500 − 20500	+
20500 − 21500	+

Burning seems to have occurred regularly in the study area since the last glacial maximum (~ 21 ka), with no clear evidence of periods of increased fire activity on a regional scale (Scott, 2002). Only Elim (28.5°S; 28.5°E) seems to be adopted into the Global Charcoal Database (GCD) (GPWG, 2017). Analysis of the charcoal record at

Elim revealed a local increase in burning between 21 ka and 16.5 ka before present (Figure 7.1). This was confirmed by Marlon *et al*. (2016), who further found higher levels of biomass burning during the past 300 years (Table 7.1).

7.1.2 Fire Ignition

Although lightning is the main natural source of ignition for grassland fires, it tends to correspond more with the onset of the rainy season which often brings scattered thunderstorms with dry lightning (Pyne *et al*., 2004). Thus, the overwhelming majority of ignitions during the dry season (Section 6.3.2) are anthropogenic in origin (Archibald *et al*., 2008). This also holds true for the savanna of the Kruger National Park (KNP) to the north-east of the study area (van Wilgen *et al*., 2000; 2014). According to Archibald *et al*. (2010a) ignitions increase in accordance with human population density to reach a turning point at about 25 people per square kilometre.

7.1.3 Fire Season and Fire Recurrence

In South Africa, fires are observed in all months of the year, while the central and eastern parts exhibit a winter fire season due to summer rainfall (Strydom & Savage, 2016). Here only a small fraction (<0.6%) of the burning occurs from January through March (Archibald *et al*., 2010a). The fire season in various parts of the summer rainfall region of southern Africa was reported to be from June to September by Scholes *et al*. (1996), August to October by Everson *et al*. (2004), May to September by Heinl *et al*. (2007), July to October by Archibald *et al*. (2010a), May to November by Liu *et al*. (2010), and May to October by Pricope & Binford (2012). Strydom and Savage (2016) presented monthly fire frequencies for each province in South Africa (Figure 7.2), which highlights a winter fire season that commences about a month earlier in the north-east (Gauteng and Mpumalanga provinces). Since natural fires usually occur later in the season (Pyne *et al*., 2004; de Ronde *et al*., 2004a; Archibald *et al*., 2010a), urban areas tend to burn earlier when compared to other land use types.

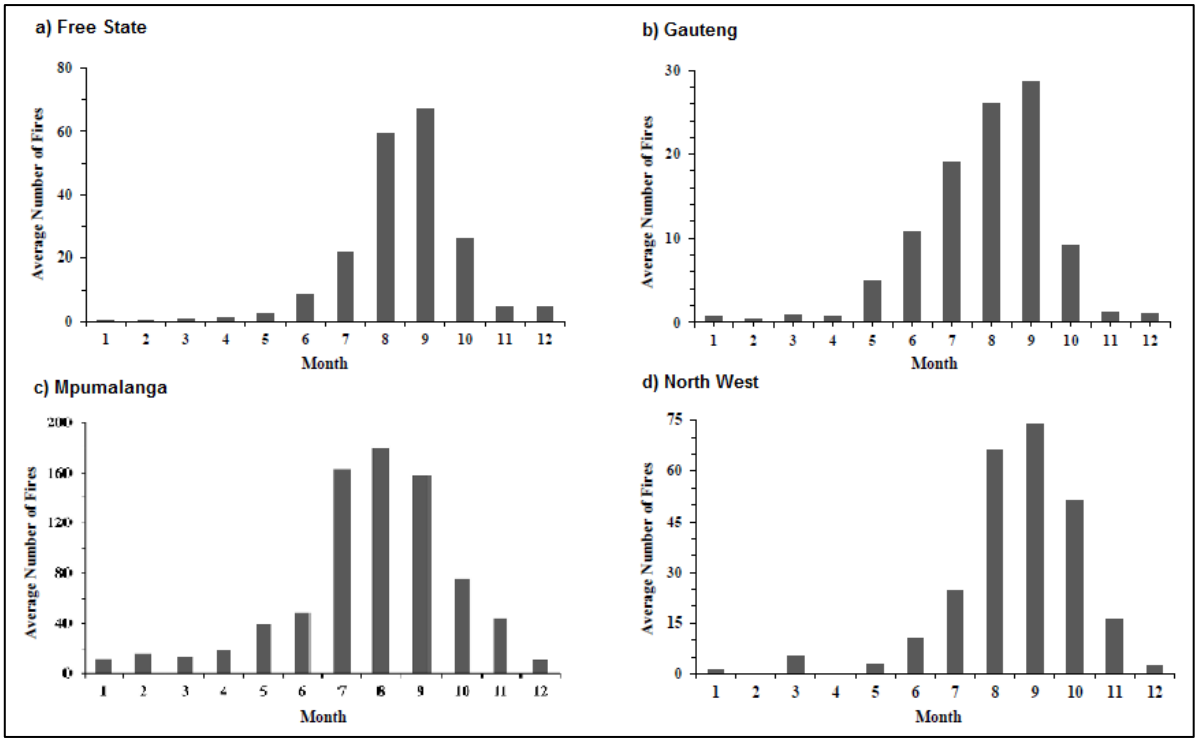

Figure 7.2 **Monthly fire frequencies for a) Free State, b) Gauteng, c) Mpumalanga, and d) North West Provinces, averaged over the period 2003 – 2011 (Strydom & Savage, 2016). Note that the ranges of the vertical scales are not the same and that the land areas are not of comparable sizes.**

Overall, the median fire-return interval was estimated at about 2 – 6 years for those parts of the landscape that do burn, but should be closer to the bottom-end of this scale for uncultivated land which made up the bulk of the area (Table 7.2). This is in line with the mean fire-return interval of 4.5 years (ranging from 1 – 34 years) reported in the 11 major land systems of the KNP (van Wilgen *et al*., 2000; Govender *et al*., 2006). Prichard *et al*. (2017) purported African savannas and grasslands to burn every 1 – 5 years, while Mucina *et al*. (2006) cited 1 – 4 years in grasslands. By implication the region has one of the shortest fire-return intervals on Earth, which can easily be motivated by the strong seasonality of the rainfall. Higher cumulative precipitation and hence soil moisture conditions during the antecedent growing seasons (i.e. a year or two before the fire season), stimulates vegetative productivity in this biome resulting in more fine fuels (Heinl *et al*., 2007; Archibald *et al*., 2008; Krawchuk & Moritz, 2011; Pricope & Binford, 2012). Once the dry season commences, these fine fuels cure rapidly and condition the area to extensive surface fires (Archibald *et al*., 2010a; Bedia *et al*., 2015). Strydom and Savage (2016) found no significant trend in the frequency of fires over South Africa.

Table 7.2 **Fire statistics of different land-use categories for South African grasslands based on remotely sensed data for the period 2001 – 2008 (Archibald *et al*., 2010a)**

Land use	Area (10^3 km^2)	Portion burnt (%)	Median fire-return interval of all pixels* (years)	Median fire-return interval of burnt pixels* (years)	Peak month
Protected	8	17	8.3 (6.1 – 11.0)	3.2 (2.6 – 3.8)	Aug
Uncultivated	187	9	14.0 (8.8 – 21.0)	2.5 (2.0 – 3.1)	Aug
Cultivated	63	11	23.0 (11.0 – 47.0)	6.4 (4.2 – 9.5)	Aug
Settlements	4	4	113.0 (20.0 – 626.0)	5.6 (3.1 – 10)	Jun

*confidence intervals are presented in brackets

7.1.4 Fire Intensity

Attempts to quantitatively measure the intensity of fires in South Africa appear to be restricted to the fynbos (van Wilgen *et al*., 1985), montane grasslands of KwaZulu-Natal (Everson *et al*., 1985) and savannah areas (Trollope, 2005; cited by Steenkamp, 2013; Govender *et al*., 2006). Archibald *et al*. (2010a) could not determine any noteworthy trends in fire size or fire intensity with a progression in fire season as remotely sensed Fire Radiative Power (FRP), a proxy for fireline intensity, showed little variation throughout the year over grasslands. Once again a human influence was detected by Archibald *et al*. (2010a), who pointed out that the grassland fire regime varies across a gradient of human land use intensity, ranging from protected land, uncultivated (but grazed) land and cultivated land to settlements. As shown in Figure 7.3, median FRP was generally observed to increase as human land use intensity decreased.

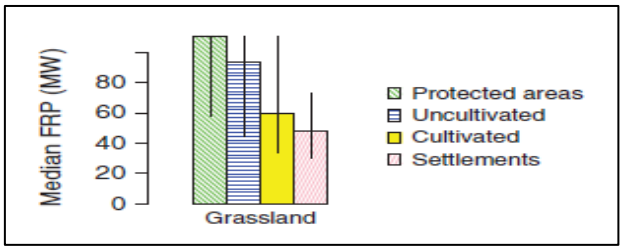

Figure 7.3 **Median Fire Radiative Power (FRP) (in MW per 5×5 km pixel; whiskers indicate ±25 percentiles) for southern African grasslands, across a gradient of human land use types ranging from protected land (green), uncultivated land (blue), cultivated land (yellow) and settlements (pink) (Archibald *et al*., 2010a).**

7.1.5 Fire Size, Density and Area Burned

Akin to many climatic elements (e.g. daily rainfall totals, hourly wind speeds etc.), fire size exhibit a positively skew distribution with a specific area experiencing numerous small fires and only a few large ones. According to Archibald *et al*. (2010a) the mean and maximum fire size decreases with an increase in human population density, while

fires exceeding 20 km^2 (2 000 ha) seldom occur in areas with more than 10 people per square kilometre. Figure 7.4a confirms that the larger fires tend to occur in areas with lower population densities, while maximum fire size (defined by the 95th percentile) ranged from 5 – 50 km^2 over the period 2001 – 2008.

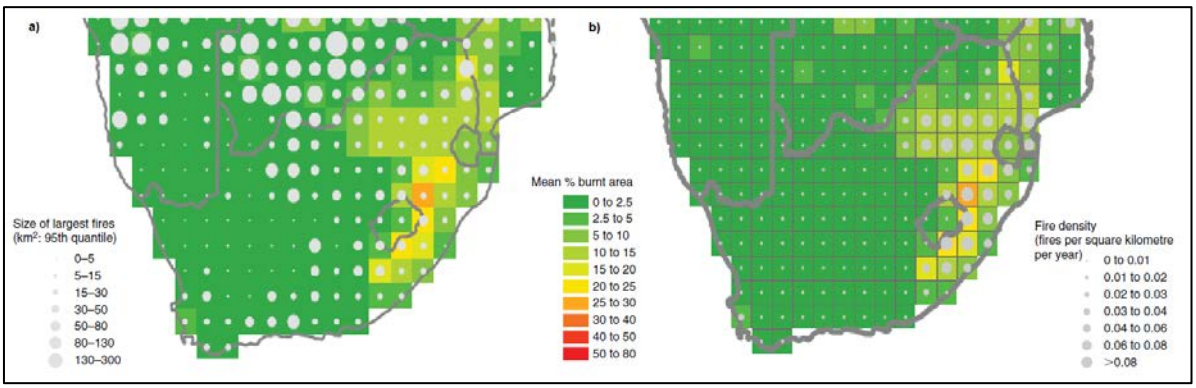

Figure 7.4 **Results of an 8-year remote sensing study for southern Africa showing a) maximum fire size, and b) fire density. The background shading depicts the mean percentage burnt area for southern Africa (Archibald *et al*., 2010a).**

Fire densities decreased from more than 0.08 fires km^{-2} y^{-1} in the east to 0.02 fires km^{-2} y^{-1} in the west (Figure 7.4b). Higher fire counts over the mountain grasslands in the east of the study area were also confirmed by satellite remote sensing studies conducted by Krawchuk *et al*. (2009b) and Strydom and Savage (2016). The average monthly number of fires ranged from a minimum of 10 to a maximum of roughly 180 at the peak of the fire season in Mpumalanga (Figure 7.2c), while the other provinces displayed similar minima of about 1 and maxima ranging between 30 and 75 fires per month (Strydom & Savage, 2016).

Area burned is primarily determined by fuel continuity (Prichard *et al*., 2017). This results in much smaller fires near settlements and cultivated areas, mainly due to the highly fragmented landscape, numerous manmade barriers to fire spread and the large numbers of domestic grazers in the region (Archibald *et al*., 2010a). Using the MODIS burned area product, which was shown to detect about 75% of the burned area by Roy and Boschetti (2009), Archibald *et al*. (2010a) observed very little burning (<5%) in urban areas (Table 7.2), while a larger portion of protected land surfaces (>15%) burned during an 8-year study period. Hence the largest contribution to the total burned area in southern Africa is not made by occasional large fires that occur under extreme conditions, but rather by the cumulative effect of several small- to

medium-sized fires (Archibald *et al*., 2010a). This correspondence between fire density and burned area can be noted in Figure 7.4b.

Figure 7.5 depicts the annual burned area from 1995 to 2017 for all South African grasslands (blue line), constructed from data obtained from FAOSTAT (2019). The long-term mean burned area was 1.4×10^4 km^2 (1.4×10^6 ha), an area smaller than Gauteng, with a standard deviation of about 3.4×10^3 km^2 (3.4×10^5 ha). The most fire prone years (in terms of burned area) occurred in 2003 (1.7×10^6 ha), 2005 (2.2×10^6 ha), 2007 (1.8×10^6 ha) and 2010 (1.9×10^6 ha), while the lowest fire activity occurred between 1996 and 2000 (averaging 1.1×10^6 ha), in 2004 (1.3×10^6 ha), 2012 (1.3×10^6 ha) and 2016 (6.3×10^5 ha). It is also clear from Figure 7.5 that these years corresponded, respectively, to the highest and lowest amounts of biomass burned (red line) and GHG fire emissions (green line). The amount of biomass burned in 2005 was estimated at 9.23 Tg (compared to an average value of 5.85 Tg), while the associated GHG emissions amounted to about 1 030 Gg (with an average long-term value of approximately 655 Gg).

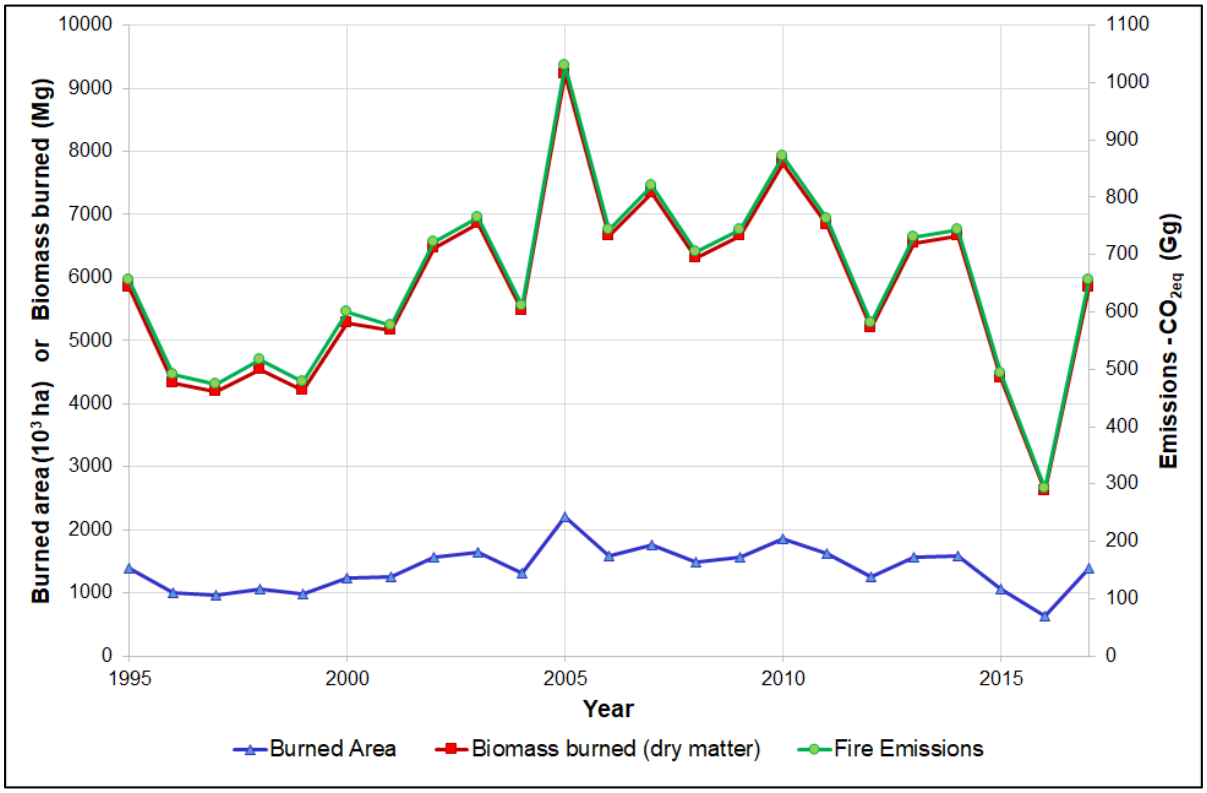

Figure 7.5 **Annual burned area, amount of biomass consumed and greenhouse gas emissions (CO_2 equivalent) for grassland fires in South Africa for the period 1995 – 2017 (data from FAOSTAT, 2019).**

7.1.6 Fire Losses

The majority of fires in South Africa originate from open flames during grass, bush or waste burnings (FPASA, 2019), which resulted in 449 reported fatalities and close to ZAR 349 million in damages during the 10-year period spanning 2009 – 2018 (Figure 7.6). It is also evident from Figure 7.6 that such financial losses exhibit a large inter-annual variability and increased dramatically during 2014, 2015 and 2017. The lower financial loss in 2016 corresponds to a reduction in biomass consumption and area burned (Figure 7.5).

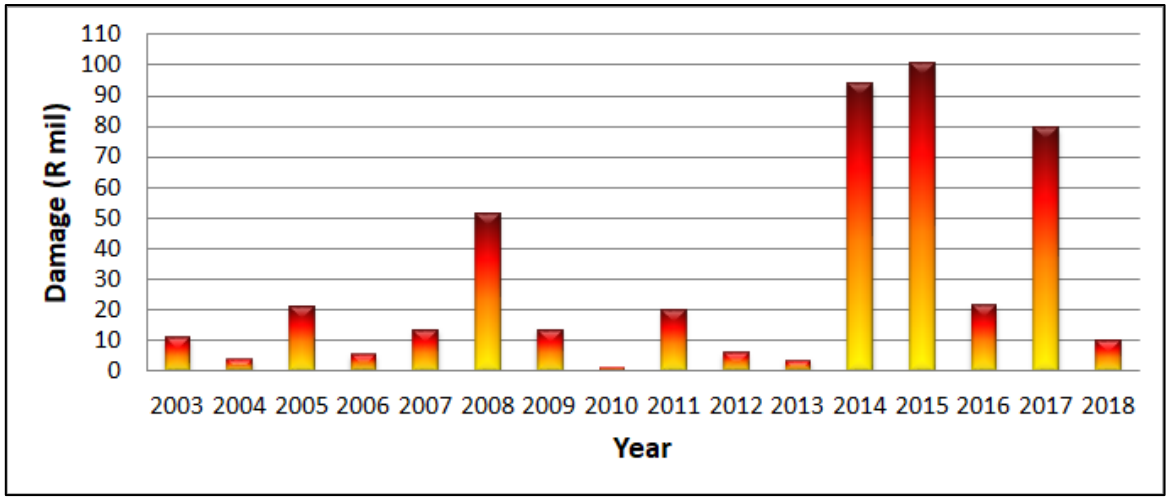

Figure 7.6 **Annual damage (in millions of Rands) resulting from fires in the "rubbish, grass and bush" category (information provided by FPASA, 2019).**

7.2 PROBLEM STATEMENT AND RESEARCH OBJECTIVES

A comprehensive description of the fire regime of the summer rainfall region of South Africa was provided by previous studies, but knowledge gaps remain as some of this information was applicable to a much larger area. These pertain to (i) setting the fire season for the central grassland, (ii) assessing the amount of (and trends in) total burned area, and (iii) describing the historical distribution of (and shifts in) fire danger across the area.

Interpreting historical fire data can be problematic since trends in the number of fires and burned area are not solely determined by meteorological conditions. Ignition source, fire management practices and technological advances in fire detection and reporting could hold a hefty sway on such analyses (Wastl *et al*., 2012). For this reason most research studies rather consider the potential climate-related fire risk by

calculating various fire danger indices (FDIs) from historical climatological observations (Wastl *et al*., 2012) or the outputs of global climate models (Chapter 9).

As highlighted in Chapter 5, fire danger rating is the cornerstone of modern-day fire management programs as it pertains to staffing levels, the deployment of preparedness resources as well as the introduction of fire restrictions on public lands (Interagency Standards for Fire and Fire Aviation Operations Group, 2019). In South Africa, even on private land there are legal consequences to the owner if a fire that was started on days classed as very dangerous got out of control. Since such assessments are used by and impact a range of stakeholders, their acceptance of a recognized fire danger rating system (FDRS) and the consistent application of fire danger rating is important. In order to identify high fire danger, the local fire danger continuum is divided into discrete classes based on historical fire danger conditions (Jolly *et al*., 2019). Although the fire danger categories (also referred to as staffing levels) for a selection of FDIs were reported in Chapter 5, the appropriateness of these classification thresholds to southern Africa, and the central grassland biome in particular, may be questioned. This is especially true for those indices that were developed with a different climate and fuel structure in mind.

Therefore, with specific reference to the central grassland biome of South Africa (shaded area in Figure 6.1a), the research objectives of this chapter were:

1) To define the fire season at the hand of actual fires;
2) To assess the damage done in terms of burned area by wildland fires and identify possible trends;
3) To test the appropriateness and, where necessary, adjust the classification thresholds of a selection of FDIs in order to better suit the local climate and fire danger conditions;
4) To evaluate the climate-related fire danger against a selection of FDIs for the historical base period of 1981 – 2010; and
5) To identify possible trends in the mean FDI-values over the historical period.

7.3 MATERIALS AND METHODS

7.3.1 Defining the Fire Season and Evaluating Burned Area

MODIS MCD64A1.006 burned area data (Giglio *et al*., 2015) were used by the Council for Scientific and Industrial Research (CSIR) – Meraka Institute to construct monthly burned area data for each municipal area in South Africa. These data were obtained from the CSIR for the period 2002 – 2017. Only those municipal areas that fell within the central grassland biome were subsequently used to determine the monthly mean and annual total burned areas for each province and the study area as a whole. The fire season was subsequently defined as all months having a long-term mean burned area of greater or equal to 20 000 ha. Regression analysis was performed on the annual total burned area and the linear trend tested for significance using Genstat.

7.3.2 Calculating the Fire Danger Indices

The climate variables required for calculating the FDIs include:

- 14:00 LST air temperature at a height of 2 m (T in °C);
- 14:00 LST relative humidity at a height of 2 m (RH in %);
- 14:00 LST wind speed at a height of 10 m (WS in km h^{-1}); and
- 24-hour accumulated precipitation (P in mm).

These variables are thought to represent the afternoon conditions when fire danger is at its highest during the course of a typical cloudless day (Section 4.2).

While historically observed climate data from SAWS was used in the climatological description of the study area (Table 6.1), the station data had a lot of gaps and its representativeness of the entire central grassland debateable. Daily gridded reanalysis data provide a single consistent, near-homogeneous set of data (Tennant, 2004; Beck & Philipp, 2010). However, one major issue is the reduced quality of such data sets before the advent of satellite data around 1979 and affects the Southern Hemisphere in particular (Kistler *et al*., 2001; Tennant, 2004). Tennant (2004) thus advises against using pre-1979 reanalyses from longer data sets such as NCEP/NCAR (Kalnay *et al*., 1996) and ERA5 (C3S, 2019; Hersbach *et al*., 2018).

For this study ERA5 reanalysis data, dating back to 1979, was used for the surface climatic variables required for calculating the various FDIs over the historical period. A comprehensive description of ERA5 reanalysis data can be found in ECMWF (2016) and Hersbach *et al*. (2018). The data was downloaded from the Copernicus Climate Change Service Climate Data Store (C3S, 2019). A spatial resolution of 0.25° × 0.25° was chosen when downloading the climate variables listed in Table 7.3 for the historical period spanning 1979 to 2018. Daily 12:00 GMT (corresponding to 14:00 LST) wind components at a height of 10 m, air temperature and dewpoint temperature were downloaded in GRIB format. A bash script called "gribconvert_glob.sc" (Appendix A) employed the Perl script "grib2ctl.pl" (Ebisuzaki, 2017) and the Grid Analysis and Display System (GrADS) (COLA, 2018) in order to convert the GRIB files to a data format that could be ingested in Fortran.

Table 7.3 Climate variables obtained from ERA5 through direct download (D) or subsequent calculations (C)

Source	Variable	Level	Units	Time	Interval	Abbreviation
D	Zonal wind component[a]	10 m	ms^{-1}	12:00 GMT	Daily	U_{10}
	Meridional wind component[a]	10 m	ms^{-1}	12:00 GMT	Daily	V_{10}
	Air temperature[a]	2 m	K	12:00 GMT	Daily	T
	Dewpoint temperature[a]	2 m	K	12:00 GMT	Daily	Td
	24-hour accumulated total precipitation[b]	Surface	mm	00:00 – 12:00 GMT	Daily	P
C	Resultant wind speed	10 m	ms^{-1}	12:00 GMT	Daily	WS_{10}
	Relative humidity	2 m	%	12:00 GMT	Daily	RH

[a] downloaded from C3S (2019)
[b] downloaded from KNMI (2019)

Daily 24-hour accumulated total precipitation was calculated from the hourly totals and the units converted from m to mm (C3S, 2019). Such calculations were already performed for each gridpoint from 1 January 1979 to 30 June 2019 and made available for downloaded in NetCDF format via the KNMI Climate Explorer (KNMI, 2019). A bash script called "rainconvert_glob.sc" (Appendix B) used GrADS to convert the daily precipitation from to data files that could be ingested in Fortran. It also created a self-describing file for each data file that is required for displaying it in GrADS. A Fortran program called "rpoint2grid.f" (Appendix C) was subsequently used to create daily gridded data files for each month, similar in format to those containing the other near-surface variables. The program "klimcal.f" (Appendix D) was then used to calculate the long-term rainfall climatology for each gridpoint from this data. The output of "klimcal.f" was required by "fire4era.f" (Appendix E) when calculating the FFDI.

The zonal and meridional wind components were used to determine the resultant wind speed using Pythagoras' Theorem (page 399 of Appendix E):

$$WS_{10} = \sqrt{{U_{10}}^2 + {V_{10}}^2}$$

The dewpoint temperature was used in combination with the air temperature to calculate relative humidity, all at a screen height of 2 m (page 399 of Appendix E). The following equations were used to calculate the near-surface relative humidity (Campbell & Norman, 1998):

$$RH = 100\frac{e_a}{e_s}$$

$$e_s = a\ exp\left(\frac{\mathrm{b}T}{\mathrm{c} + T}\right)$$

where: RH = relative humidity (%)

e_a = actual vapour pressure or vapour pressure at dewpoint temperature (Pa);

e_s = saturation vapour pressure or vapour pressure at air temperature (Pa);

T = air temperature (°C); and

Coefficients a = 611.21 (Pa), b = 17.502 (unitless), c = 240.97 (°C).

The above equations yield the exact same RH values as those obtained using the formulas in ECMWF (2016) without the need to involve surface pressures. Lawrence (2005) proposed using the same formulas as Campbell and Norman (1998) but with slightly different coefficients, resulting in RH values that differ with less than 0.1% for a wide range of temperatures and dewpoint temperatures (not shown). Although the coefficients are used to estimate e_s over water (as opposed to ice), Lawrence (2005) indicated that this method provides values for e_s with a relative error less than 0.4% over the temperature range of -40°C to 50°C.

The Fortran program "fire4era.f" (Appendix E) was used to calculate the following FDIs (which were discussed in Chapter 5) at a daily interval for each gridpoint within the study area (shaded area in Figure 6.1a):

a) Canadian Fire Weather Index (CFWI);

b) Canadian Daily Severity Rating (CDSR);
c) Lowveld Fire Danger Index (LFDI); and
d) McArthur Forest Fire Danger Index (FFDI).

The modified RCF in Table 5.12 was used in the calculation of the LFDI. Daily spatial maxima, means and long-term mean annual and fire season frequencies of each fire danger category was also calculated within "fire4era.f". Meticulous care was taken to test the calculated FDI values. The CFWI- and CDSR-values were tested against sample data from Wang *et al*. (2015), while the LFDI-values were tested against manual calculations provided in Table 5.13. The FFDI-values were tested against output from a mobile app named "Calc-F.D.I." (Taranenko & Wiese, 1997) and an online calculator available from https://cfsres.com/ffdi (although these did not consider previous rainfall events).

7.3.3 Defining Fire Danger Levels

Average and extreme conditions for an area are normally defined in terms of climatologically-based percentile points (WMO, 2017). Percentiles have the ability to capture incremental changes along the entire fire danger continuum (Jolly *et al*., 2019) and are thus commonly used to determine the classification thresholds (also referred to as climatological breakpoints or cut-off levels) associated with a FDI or its component indices. However, there is no general agreement on which percentile breakpoints to use in defining the classification thresholds (Table 7.5). For example, the National Veld and Forest Fire Act of South Africa (Act 101 of 1998) advocated using the 25th, 84th, 96th and 98th percentiles as climatological breakpoints for the LFDI (Table 7.5). The US NFDRS generally employ the 90th and 97th percentiles for the two highest breakpoints, while half and quarter the value of the 90th percentile are used as the two lowest breakpoints (Helfman *et al*., 1987; Heinsch *et al*., 2009). Imposing the 90th percentile as a breakpoint dictates that over the 30-year climatology only 10% of the daily FDI-values across all gridpoints within the study area fell in the higher danger category.

Some studies use annual climate data when determining category thresholds, while others only employ the local fire season data. Heinsch *et al*. (2009) and Bedia *et al*. (2015) cautions against using annual data because the higher fire danger rating

thresholds may be lower when months outside the fire season are included. However, such concerns are probably more valid for regions where the fire-season falls in mid-summer to autumn as opposed to the winter and spring as is the case over the central grassland biome of South Africa (Section 6.4.3). In addition, including all months in determining the category thresholds allows for possible changes in the length of the fire season.

Table 7.5 Percentile points used to define fire danger classification thresholds from the literature

Reference	Percentile used as climatological breakpoint			
	Low / Moderate	Moderate / High	High / Very High	Very High / Extreme
Act 101 of 1998	25	84	96	98
Helfman *et al*. (1987); Heinsch *et al*. (2009)	¼ of 90	½ of 90	90	97
Andrews *et al*. (2003)*; Sirca *et al*. (2018)	25	50	75	90
de Jong et al. (2016)	75	90	95	99
Pérez-Sánchez *et al*. (2017)	10	50	90	97
Jolly *et al*. (2019)	60	80	90	97

* excluding 75th percentile (only used three breakpoints)

In Section 5.5 it was argued that the LFDI is better adapted for use within the study area, while there is a clear understanding of resources required to suppress fires based on the danger rating and associated colour coding. In fact, historical attempts to introduce a different FDRS in South Africa was met with quite some resistance from the end-user community. For this reason, it was decided that although the LFDI were to be included in the analysis, no attempts were made to alter the original category thresholds. In fact, given the discrepancy in which set of percentile breakpoints to be used, the decision was made to select that combination that corresponded best with the original LFDI category thresholds. To be clear, depending on the climatological distribution of the LFDI-values obtained here, the combination of percentile breakpoints to be used when classifying the other FDIs may differ from those advocated by the National Veld and Forest Fire Act of South Africa (Act 101 of 1998).

After running “fire4era.f” for each FDI for the climatological standard normal base period of 1981 – 2010 (WMO, 2017), the Fortran program “fcdf4era.f” (similar to “fcdf4gcm.f” in Appendix F) was used to sort all the daily FDI-values over the entire study area and calculate the corresponding 99 percentiles. For each index, with the exception of the LFDI (for reasons explained above), the FDI-values corresponding to

the chosen climatological breakpoints were then used to alter the category thresholds within “fire4era.f” before running it again. These same thresholds were later used in “fire4gcm.f” (Section 9.4).

7.3.4 Spatio-temporal Distribution of Fire Danger

Time series of the fire season spatial maximum and mean LFDI was visually inspected for peak recurrence intervals. For each FDI, maps were constructed with the aid of GrADS to depict the spatial distribution of long-term mean occurrences within each of the five fire danger rating classes (the “extreme” and “catastrophic” classes of the FFDI were combined for this analysis). For ease of comparison, these maps were constructed for the fire season as well as the whole year (all months included).

7.3.5 Assessing Recent Changes in Fire Danger

In order to identify the potential impact of recent climate change on fire danger over the central grassland biome of South Africa the cumulative distribution function (CDF) for each fire season FDI was constructed for four consecutive 10-year periods (viz. 1979 – 1988, 1989 – 1998, 1999 – 2008 and 2009 – 2018) and visually compared to each other.

Daily spatial maximum LFDIs comprised the highest LFDI-value occurring across the entire study area for each day, whereas the daily spatial mean LFDIs consisted of one mean LFDI-value representative of the entire study area per day. Both daily spatial maximum and mean LFDIs were calculated by “fire4era.f” and tested statistically for differences using the non-parametric Mann-Whitney U test in Genstat. In each test the pairs consisted of two 10-year periods (e.g. 1979 – 1988 vs. 2009 – 2018) of corresponding fire season daily spatial maximum or mean LFDI-values.

Maps were constructed using GrADS in order to depict the spatial distribution of changes in the decadal mean fire season occurrences within the highest two fire danger rating categories (“very high” and “extreme” combined) for each FDI. As an example of the changes occurring at a single gridpoint, the frequencies within each fire danger class were compared for the gridpoint matching the geographical location of Bloemfontein (any of the 410 gridpoints could have been chosen).

7.4 RESULTS AND DISCUSSION

7.4.1 Defining the Fire Season and Evaluating Burned Area

Satellite data confirmed that fires are observed in all months of the year over the study area, with the long-term (2002 – 2017) monthly mean burned area ranging from a minimum of about 4 700 ha in February to a maximum of 341 800 ha in September (Figure 7.7). Fires occur predominantly during the cool, dry months when grass is either dead or dormant, with the peak burning shifting from August in the north and east (viz. North West, Gauteng, Mpumalanga, KwaZulu Natal and Lesotho) to September over the remainder of the study area (viz. Free State and Eastern Cape). Applying a minimum threshold of 20 000 ha identified the months of May through November as constituting the fire season for the central grassland biome. This result is generally supported by Scholes *et al*. (1996), Everson *et al*. (2004), Archibald *et al*. (2010a), Liu *et al*. (2010), Pricope & Binford (2012) and Strydom and Savage (2016), with the possible omission of a month at the start or end of the period.

Annual total burned area across the entire study area ranged from a maximum of 1.6 million ha in 2002 and 2011 to a minimum of 478 000 ha in 2016 (Figure 7.8). To a large extent the years with the highest (viz. 2002, 2005, 2010 and 2011) and lowest total burned area (viz. 2004, 2009, 2012 and 2016) correspond well with the FAOSTAT data depicted in Figure 7.5, although the latter was not limited to the grasslands of the study area. Not surprisingly, Mpumalanga (maximum of 679 000 ha in 2002) and the Free State (maximum of 456 000 ha in 2002) had a much higher total burned area during the analysis period as these two provinces comprised the largest portion of the study area. Surprising though, was that all provinces and the study area as a whole revealed a (albeit weak) negative linear trend in annual total burned area (shown by the dashed trend line and corresponding R^2 value in each graph in Figure 7.8). The linear trends for Mpumalanga and the central grassland as a whole were found to be statistically highly significant at the 5% significance level (probability values of 0.011 and 0.017, respectively). It is to be expected that the simple linear regressions employed here would not produce high coefficients of determination (e.g. $R^2 = 0.35$ for the central grassland as a whole) in an area subjected to large climate variability. For the study area as a whole the regression equation indicated a decline in total burned area of about 34 000 ha per annum over the period 2002 – 2017.

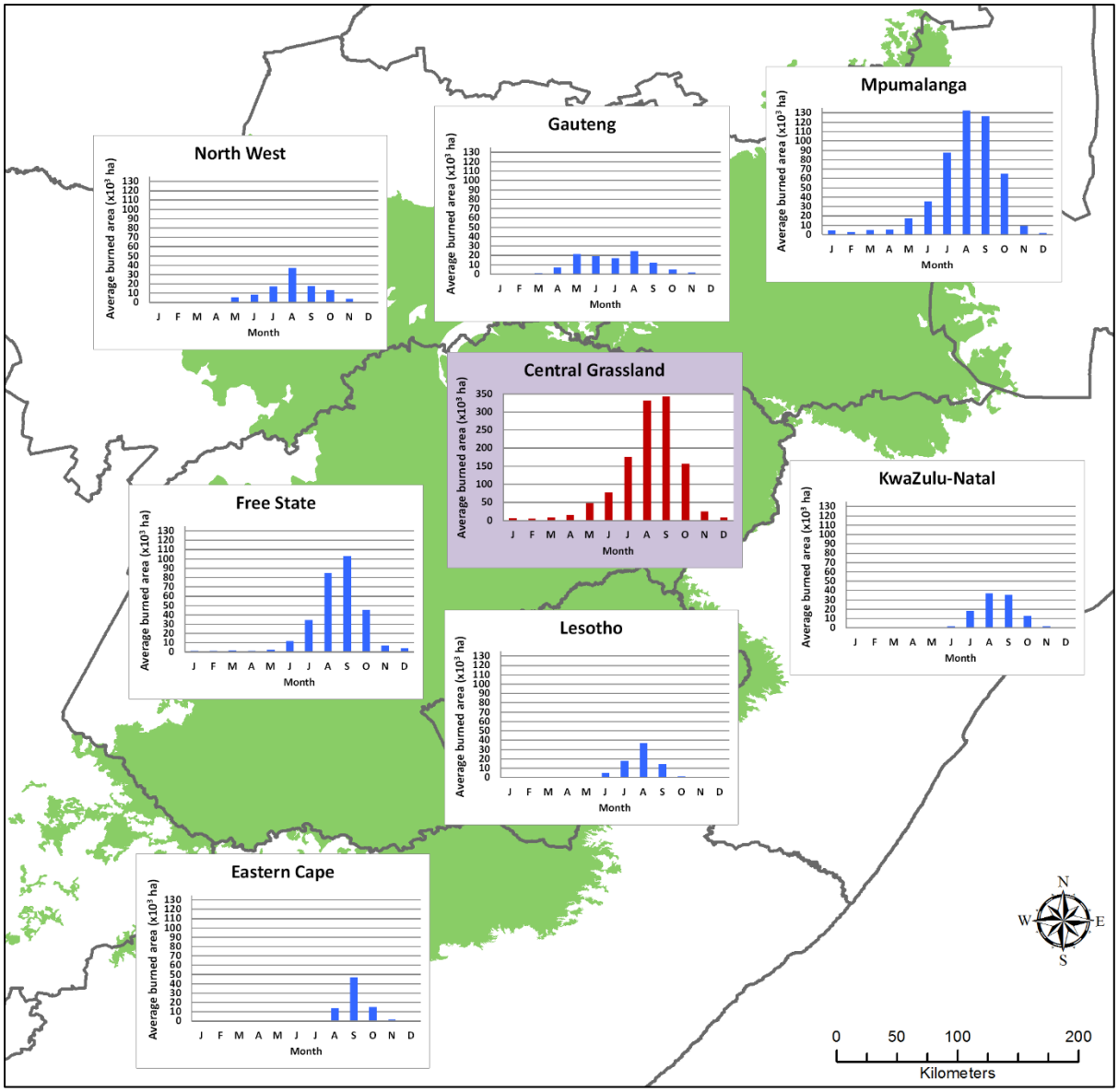

Figure 7.7 **Variation in monthly mean burned area across the central grassland biome (green shaded area), constructed using MODIS MCD64A1.006 burned area data for the period 2002 – 2017.**

High rainfall years (or several years of fuel accumulation during normal conditions) result in increased fuel availability and more burning during subsequent dry years (Heinl *et al*., 2007; Pricope & Binford, 2012). On the other hand, recurring droughts reduce fuel production and resultant burning. This theory is reinforced when noting the antecedent rainfall leading up to the seasons of maximum and minimum burning. For example, the mid-summer rainfall during the 2004/2005, 2005/2006 and 2009/2010, 2010/2011 seasons was above-normal over large portions of the study area, resulting in higher fuel loads. In contrast, the bulk of the central grassland was dominated by

below-normal mid-summer rainfall during the 2003/2004, 2011/2012 and 2015/2016 seasons, which were subsequently marked by a much lower burned area.

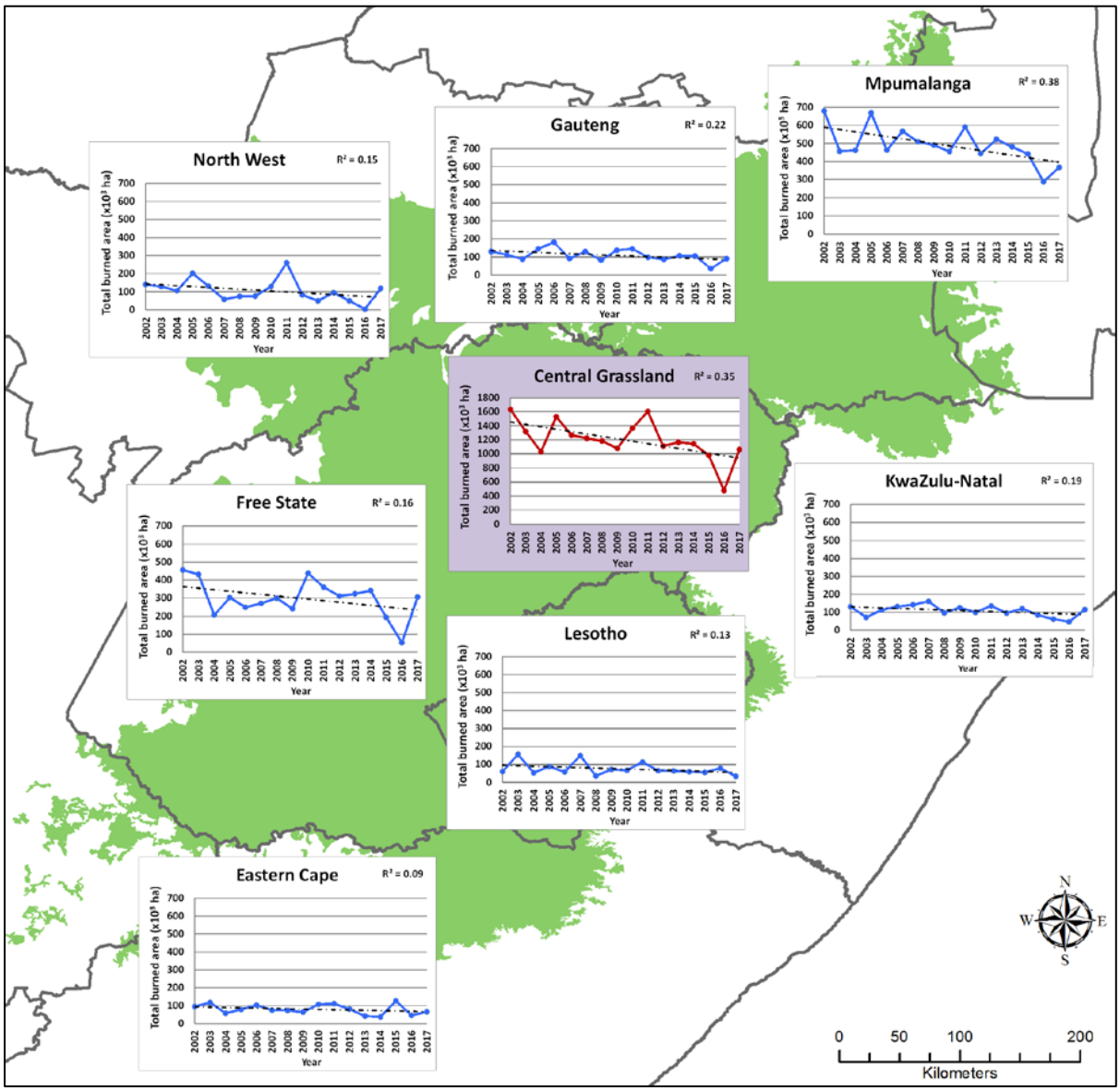

Figure 7.8 **Variation in annual total burned area across the central grassland biome (green shaded area), constructed using MODIS MCD64A1.006 burned area data for the period 2002 – 2017.**

7.4.2 Classifying Fire Danger

Figure 7.9 depicts the CDFs of the CFWI, CDSR, LFDI and FFDI for the central grassland biome, constructed using index values for all months during the 1981 – 2010 climatological base period. Neither of these have a normal distribution, which have bearing on the use of statistical testing later on. It is also evident that the FFDI- and CDSR-values are generally lower than those of the other FDIs.

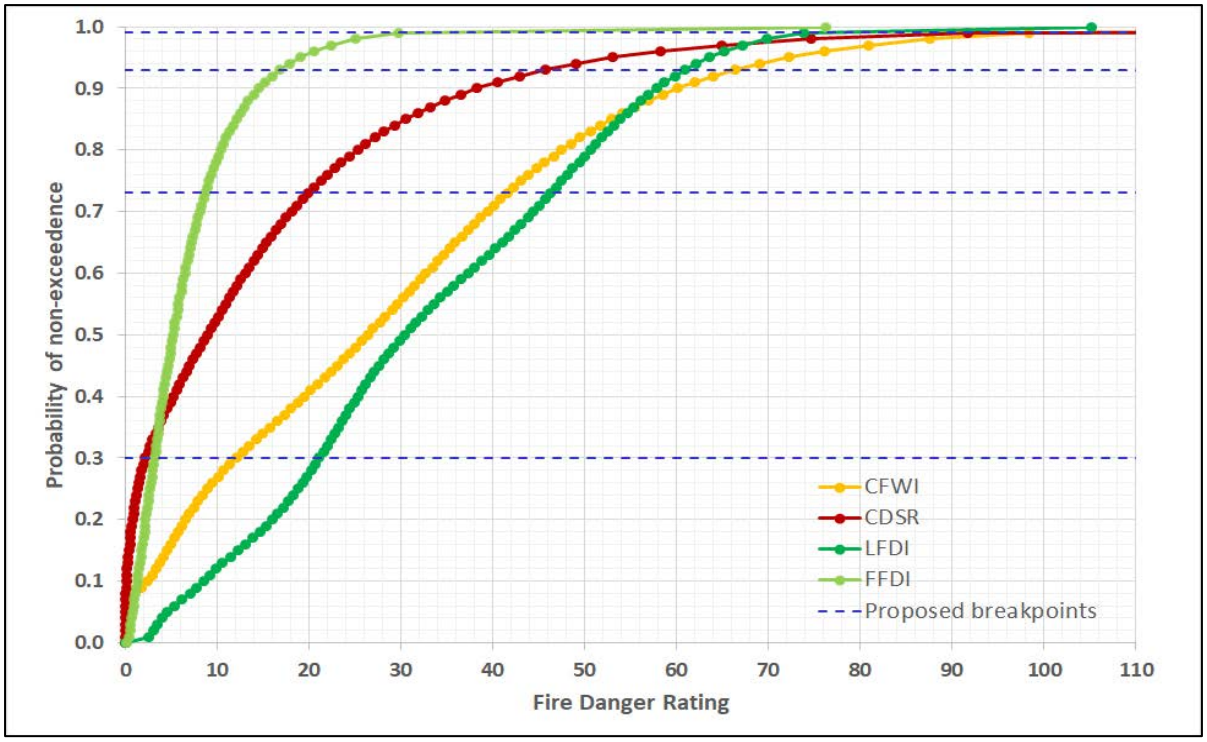

Figure 7.9 **Cumulative distribution functions of the CFWI, CDSR, LFDI and FFDI for the period 1981 – 2010 over the central grassland biome of South Africa (all gridpoints combined).**

The original recommended fire danger category threshold values from Chapter 5 and those corresponding to the various sets of percentile breakpoints referenced in Table 7.5 (labelled Ref. A – F), are given for each FDI in Table 7.6 for the 1981 – 2010 climatological base period (all months included). For each reference set, the average difference between the four newly calculated (using ERA5 data) and original thresholds are presented in grey in Table 7.6. For the locally used LFDI it was reassuring to see that the differences between the original threshold values and those calculated using the percentile breakpoints proposed by Act 101 of 1998 (Ref. A in Table 7.6) were very small (average difference of 1). In contrast, the differences between the original LFDI threshold values and those calculated using the percentile breakpoints proposed by De Jong *et al*. (2016; Ref. D in Table 7.6) and Pérez-Sánchez *et al*. (2017; Ref. E in Table 7.6) were substantial (average difference of ±10). It was also clear that the original fire danger levels conveyed in Chapter 5 for the CFWI, CDSR and FFDI were notably different from all the calculated thresholds.

Table 7.6 **Fire danger classification thresholds for the central grassland biome, determined using various recommended percentile breakpoints for the period 1981 – 2010 (all months included)**

Index	Fire Danger Classification Thresholds							
	Original	**Ref. A**	**Ref. B**	**Ref. C**	**Ref. D**	**Ref. E**	**Ref. F**	**Proposed[b]**
CFWI	**30**	88	81	60	98	81	81	98
	20	76	60	43	72	60	60	66
	10	52	30	26	60	26	48	42
	5	10	15	9	43	2	33	12
	Average difference[a]	+40	+30	+18	+52	+26	+39	+38
CDSR	**15**	75	65	38	92	65	65	92
	5	58	38	21	53	38	38	46
	3	29	19	9	38	9	25	20
	1	2	10	1	21	0	13	2
	Average difference[a]	+35	+27	+11	+45	+22	+29	+34
LFDI	**76**	70	67	58	74	67	67	74
	61	65	58	48	64	58	58	61
	46	53	29	30	58	30	51	46
	21	19	14	19	48	9	37	21
	Average difference[a]	+1	-9	-12	+10	-10	+2	0
FFDI	**75**	25	22	15	30	22	22	30
	50	21	15	9	19	15	15	17
	25	12	7	5	15	5	10	9
	12	3	4	3	9	1	7	3
	Average difference[a]	-25	-29	-33	-22	-30	-27	-26
Reference	Ref. A = Act 101 of 1998 Ref. B = Helfman *et al*. (1987); Heinsch *et al*. (2009) Ref. C = Andrews *et al*. (2003); Sirca *et al*. (2018) Ref. D = de Jong et al. (2016) Ref. E = Pérez-Sánchez *et al*. (2017) Ref. F = Jolly *et al*. (2019) [a] average of four thresholds differences (proposed minus original threshold) [b] correspond to the 30th, 73rd, 93rd and 99th percentiles							

The breakpoints that corresponded best with the original LFDI category thresholds (viz. 21, 46, 61 and 76) were the 30th, 73rd, 93rd and 99th percentiles (represented by the blue dashed lines in Figure 7.9 and the last column in Table 7.6). In all cases, the recommended category thresholds were considerably higher than the original ones for the Canadian indices (i.e. CFWI and CDSR), and much lower for the Australian index (i.e. FFDI), suggesting that the original thresholds were not appropriate for the climate of the study area. This became even more apparent when noting the mean annual occurrences within each fire danger category for these FDIs. As an example, the mean annual occurrences at a single gridpoint, corresponding to the geographical position of Bloemfontein, are presented in Table 7.7. Under the original threshold schemes an exorbitant high number of days fell in the “extreme” category according to the CFWI (65%) and CDSR (56%), while this class seemed to be redundant in the case of the FFDI where the long-term mean annual occurrence was zero. In comparison, the original LFDI threshold scheme and that proposed for use with the other FDIs (blue dashed lines in Figure 7.9 and the last column in Table 7.6) presented a more

acceptable spread dominated by the “moderate” and “high” categories in accordance with other studies (e.g. Heinsch *et al*., 2009; Jolly *et al*., 2019).

Table 7.7 **Mean annual number of days during the 1981 – 2010 period falling in each fire danger category for the gridpoint corresponding to the geographical location of Bloemfontein (29.00°S 26.25°E)**

Index	Percentile Breakpoint Scheme	Fire Danger Rating				
		1 Low	2 Moderate	3 High	4 Very High	5 Extreme
CFWI	Original	20.0	28.2	33.0	46.1	237.9
	Proposed	53.8	149.1	113.1	43.7	5.5
CDSR	Original	36.2	26.4	15.3	82.8	204.5
	Proposed	46.7	152.9	118.9	41.5	5.2
LFDI	Original	65.3	155.2	96.4	43.3	5.0
FFDI	Original	247.5	96.7	20.9	0.1	0.0
	Proposed	38.1	153.4	111.7	51.8	10.2

7.4.3 Spatio-temporal Distribution of Fire Danger

Analysis of the spatial mean LFDI time series revealed a clear annual peak in fire danger. This result was not surprising and already highlighted in Section 7.4.1 – hence the whole reason for a fire season. Of greater interest was the fairly regular occurring peaks in mean LFDI values within the fire season. The recurrence of these peaks were determined to range from about 7 to 14 days, with and overall average interval of approximately 10 days across the historical period. The spatial maximum LFDI time series yielded a similar result. An example of the variation in spatial maximum LFDI (red line) and mean LFDI (blue line) within a single fire season is presented in Figure 7.10 for 2010.

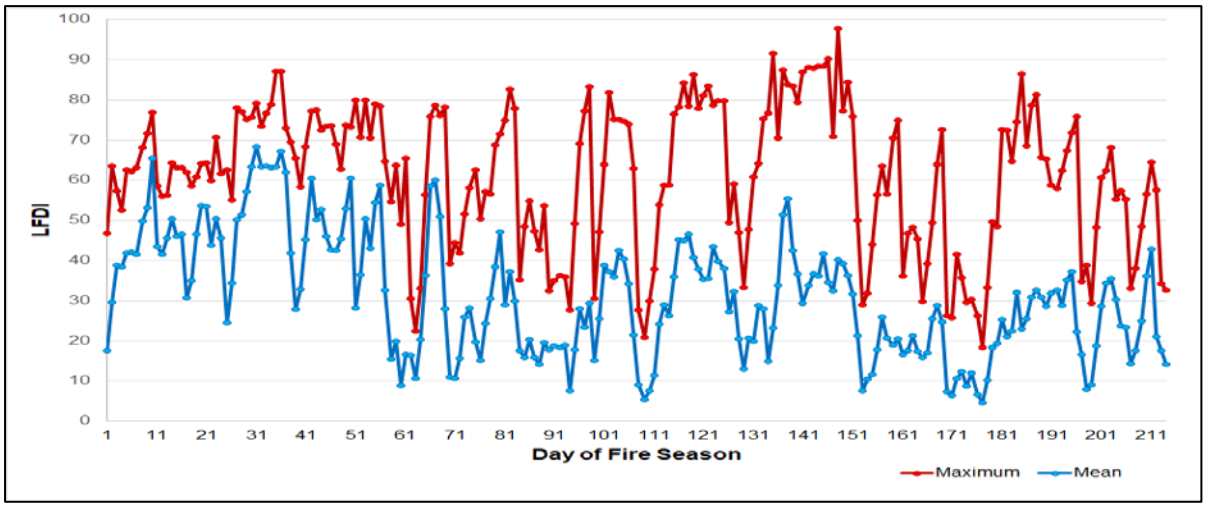

Figure 7.10 **Time series of the spatial daily maximum (red line) and mean (blue line) LFDI for the central grassland biome of South Africa during the 2010 fire season (May – November).**

The long-term annually averaged severity rating (CLSR) ranged from less than 10 over the eastern escarpment up to 35 in the extreme southwest of the central grassland biome (not shown). Maps depicting the spatial distribution of the long-term mean fire season (Figure 7.11) and annual (Figure 7.12) occurrences in each LFDI fire danger rating category, confirmed a notable variation in fire danger across the study area. For both averaging periods, the highest frequency of very dangerous (i.e. “very high” and “extreme”) days, with a commensurate minimal incidence of “low” fire danger days, occurred towards the warmer and drier southwest. The lowest frequency of very dangerous days, with a matching maximum incidence of “low” fire danger days, occurred over the cooler and wetter escarpment regions in the east. On average, “extreme” conditions occurred on about 5 – 9 (i.e. 2 – 4%) of the possible 214 days in the fire season (May – November) in the southwest and almost never in the far northeast and east (Figure 7.11). Annually, “extreme” conditions occurred on 10 – 16 days (i.e. 3 – 4%) in the southwest (Figure 7.12). Very dangerous conditions during the fire season accounted for approximately half of the annual frequency in the southwest, but nearly all of these occurrences over the escarpment regions in the east. Similar patterns, but with slightly different frequencies, were observed for the CFWI, CDSR and FFDI (not shown).

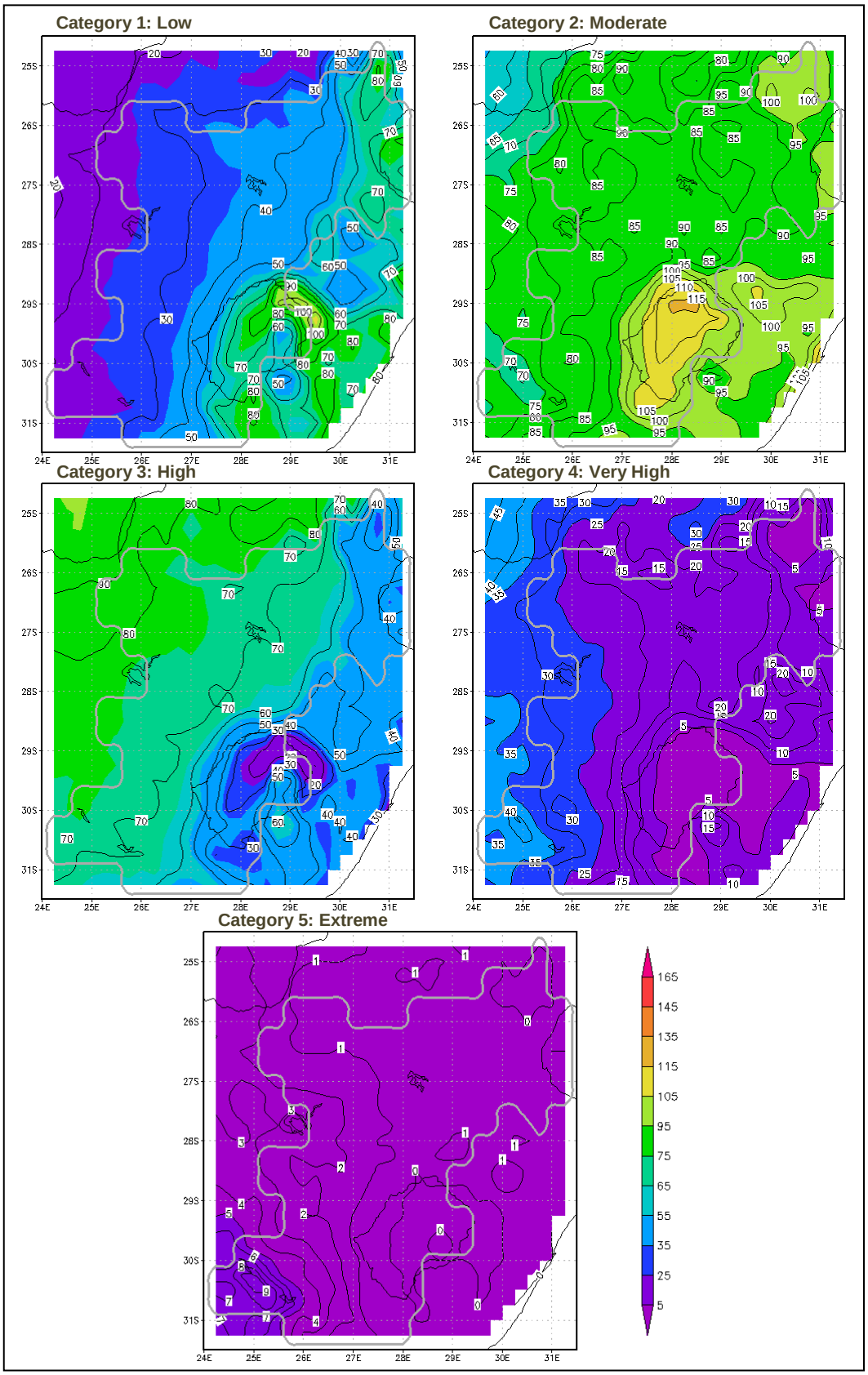

Figure 7.11 **Spatial distribution of mean fire season number of days during the 1981 – 2010 period falling in each LFDI fire danger rating category. The grey polygon delineates the central grassland biome.**

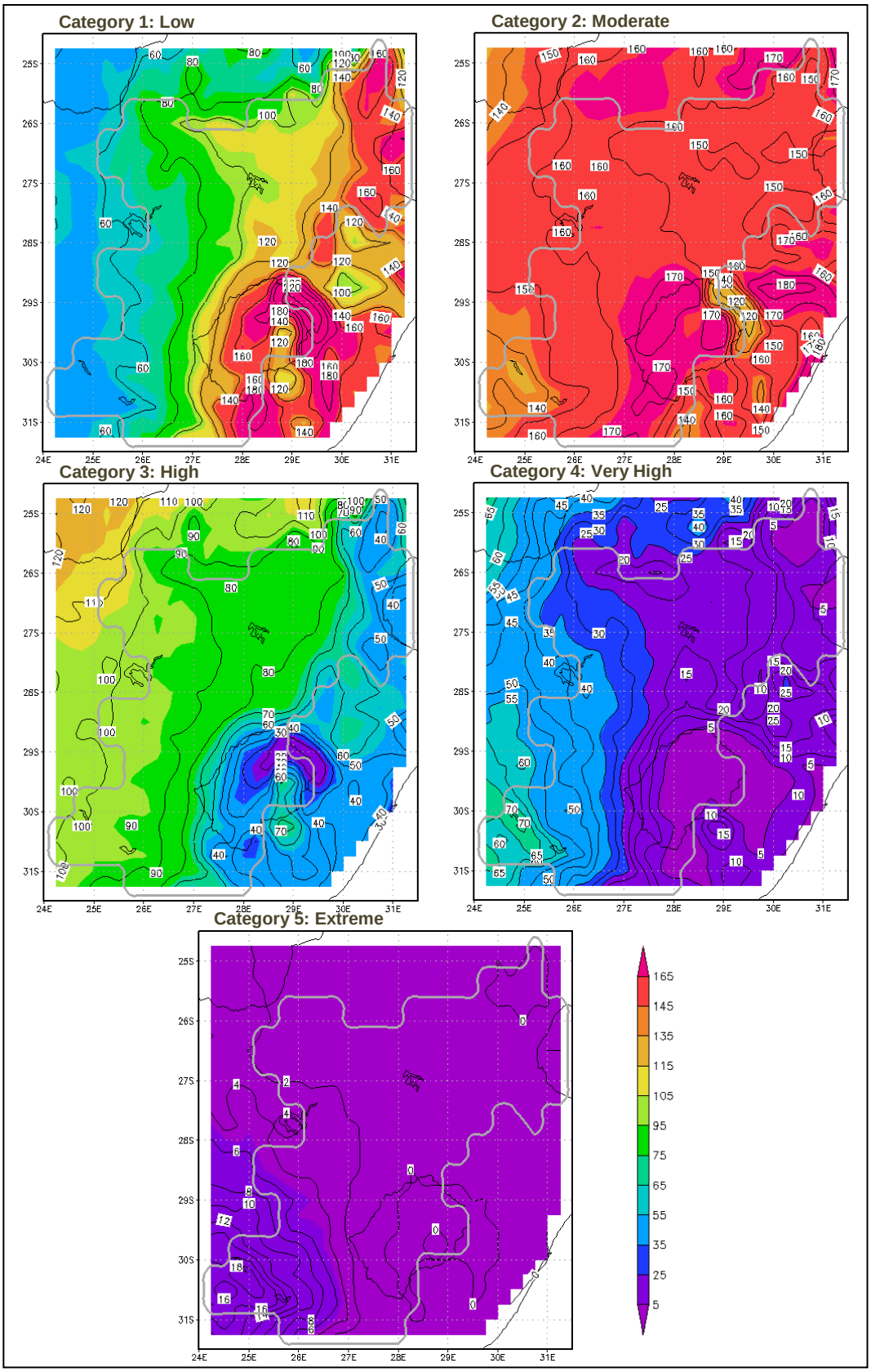

Figure 7.12 **Spatial distribution of mean annual number of days during the 1981 – 2010 period falling in each LFDI fire danger rating category. The grey polygon delineates the central grassland biome.**

7.4.4 Recent Changes in Fire Danger

Figure 7.13 presents the fire season CDF for each FDI for four consecutive 10-year periods (viz. 1979 – 1988, 1989 – 1998, 1999 – 2008 and 2009 – 2018). For the central grassland biome, all index values have been increasing since the 1979 – 1988 period as indicated by a shift of the CDFs towards the right for each successive decade. The shift towards higher fire danger seemed to be more pronounced in the most recent decade. Comparing the 93rd percentile breakpoint for different periods, it also became evident that conditions that used to be rare may now be more common. For example, with the LFDI (bottom-left panel in Figure 7.13) the threshold value associated with the 93rd percentile was 59 in 1979 – 1988, but this value corresponded to a probability of non-exceedance of 86% (occurring 14% of the time) in 2009 – 2018. Hence, the frequency of occurrence of very dangerous (i.e. “very high” and “extreme”) conditions doubled in four decades. Similar findings hold for the other indices.

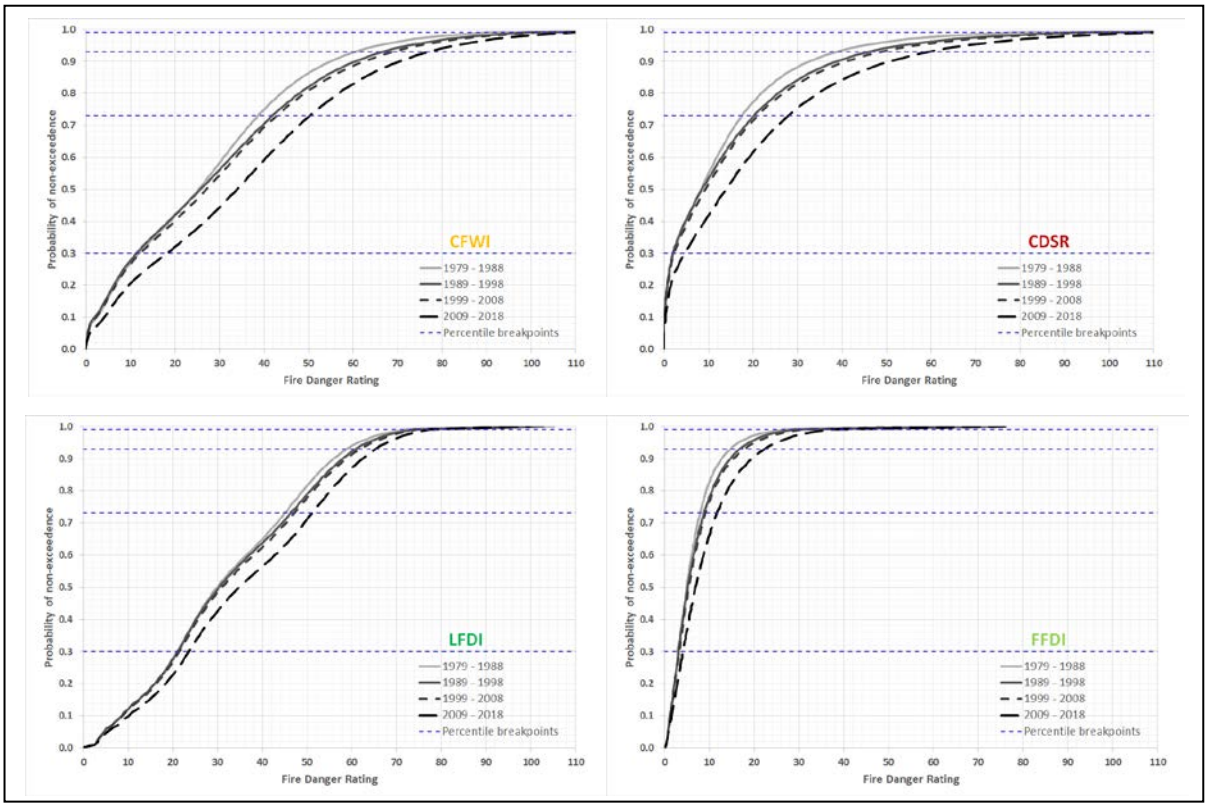

Figure 7.13 Cumulative distribution functions of the fire season CFWI, CDSR, LFDI and FFDI for four consecutive decades over the central grassland biome of South Africa.

The non-parametric Mann-Whitney U test revealed that the daily spatial maximum and mean LFDIs of the two middle decades (i.e. 1989 – 1998 and 1999 – 2008) did not differ significantly from each other (Table 7.8). This is in agreement with the minor shift

between these two decades in the LFDI-values presented in the bottom-left panel of Figure 7.13. Both the spatial maximum and mean LFDI values of the first and second decades (i.e. 1979 – 1988 and 1989 – 1998) and first and third decades (i.e. 1979 – 1988 and 1999 – 2008) differed significantly ($p < 0.05$). The differences between the first and fourth decades (i.e. 1979 – 1988 and 2009 – 2018) and third and fourth decades (i.e. 1999 – 2008 and 2009 – 2018) were deemed highly significant ($p < 0.001$ in Table 7.8). The latter finding reinforced the theory of accelerated change during the latter part of the historical period highlighted by the CDFs in Figure 7.13.

Table 7.8 **Results of testing for statistical significant differences between the fire season spatial maximum and mean LFDIs of four historical 10-year periods**

Decades Compared	p-values	
	Maximum LFDI	Mean LFDI
1979 – 1988 and 1989 – 1998	0.031	0.011
1979 – 1988 and 1999 – 2008	0.011	< 0.001
1979 – 1988 and 2009 – 2018	< 0.001	< 0.001
1989 – 1998 and 1999 – 2008	0.656	0.166
1989 – 1998 and 2009 – 2018	< 0.001	< 0.001
1999 – 2008 and 2009 – 2018	< 0.001	< 0.001

Figure 7.14 portrays the frequency of occurrence within each fire danger rating class according to the CFWI, CDSR, LFDI and FFDI for a single gridpoint matching the geographical location of Bloemfontein. Also at this scale, the number of occurrences falling within the lower two classes (i.e. “low” and “moderate”) generally decreased, while those in the two higher categories (i.e. “very high” and “extreme”) increased. For example, according to the LFDI (bottom-left graph in Figure 7.14) the number of days falling within the “extreme” category increased from 4.1 in 1979 – 1988 to 4.8 in 1989 – 1998, 5.4 in 1999 – 2008, and 11.3 in 2009 – 2018. Once again, the largest shift occurred in the last decade (represented by the golden bars in Figure 7.14). In addition, the long-term severity rating (CLSR, obtained by averaging the CDSR values) was also calculated for this gridpoint and yielded 20.1 in 1979 – 1988, 26.5 in 1989 – 1998, 27.2 in 1999 – 2008, and 34.6 in 2009 – 2018. The increasing CLSR also pointed to an increasing fire danger with time.

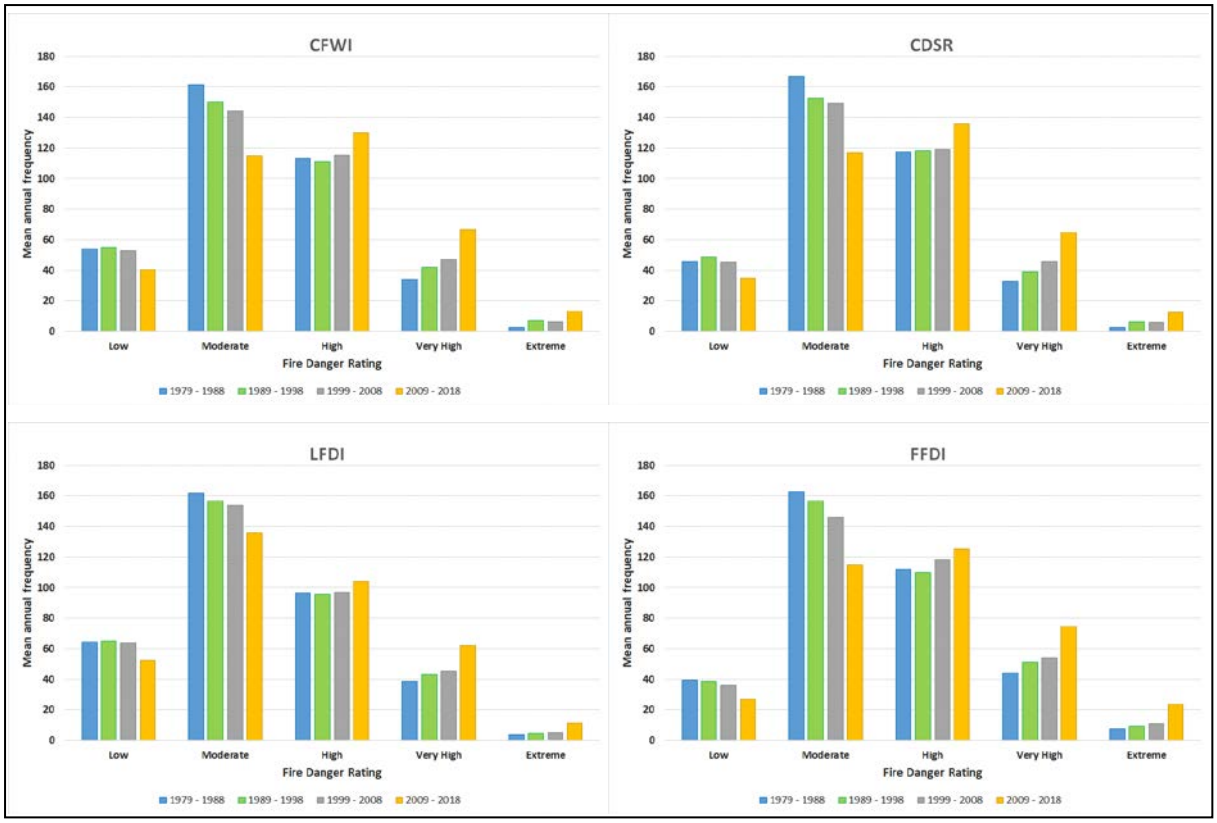

Figure 7.14 **Mean annual occurrences in each fire danger category calculated for four consecutive decades for the gridpoint falling over Bloemfontein (29.00°S 26.25°E).**

Maps depicting the spatial distribution of decadal mean occurrence of very dangerous days within the fire season, calculated for each of the FDIs for the period 1979 – 1988, and the subsequent changes during the ensuing three decades, are presented in Figures 7.15 – 7.18. A similar spatial variation in fire danger was observed across the study area for the decade 1979 – 1988 (top left panels in Figures 7.15 – 7.18) as for the 30-year period presented in Figure 7.11 for the LFDI. For all four FDIs, there were about 30 or more days in the two highest fire danger rating categories towards the warmer and drier southwest, with only a few (generally less than 5) occurrences over the cooler and wetter escarpment regions in the east.

There was a strong agreement among FDIs that there was an unprecedented increase in the number of very dangerous days over large portions of the study area, particularly over the western half and during the last decade. It was only along the eastern extremities that little to no changes were observed up to 2008. Compared to the 1979 – 1988 means, very dangerous occurrences over the far western parts increased by between 10 – 15 days by 1989 – 1998 (top right panels in Figures 7.15 – 7.18), 15 –

20 days by 1999 – 2008 (bottom left panels in Figures 7.15 – 7.18), and 30 – 40 days by 2009 – 2018 (bottom right panels in Figures 7.15 – 7.18). The FFDI yielded even larger changes, up to 65 days, during the last decade (bottom right panel in Figure 7.18).

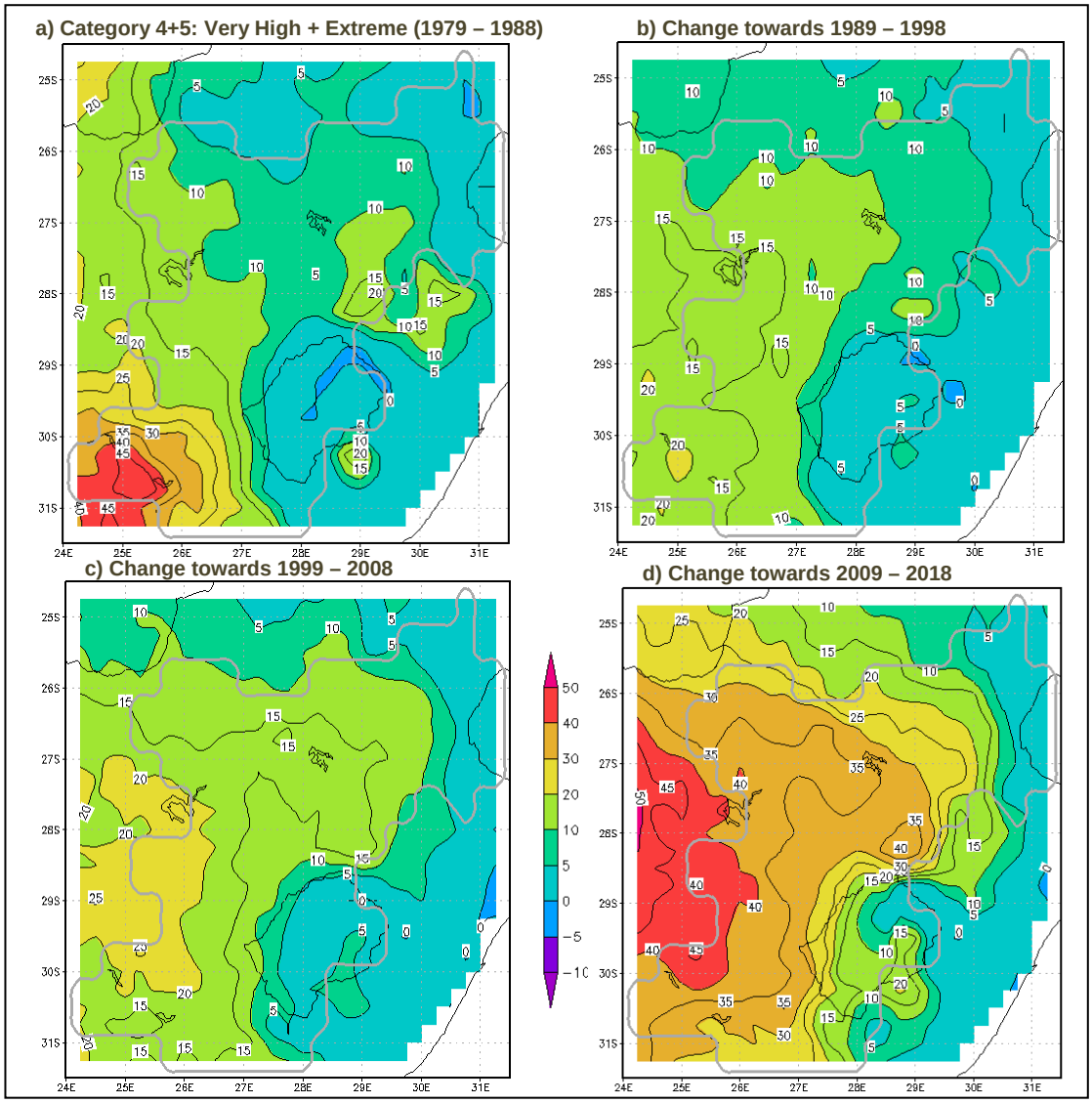

Figure 7.15 **Spatial distribution of a) mean fire season number of days during the 1979 – 1988 period falling in the very high and extreme categories according to the CFWI, and differences in occurrence between b) 1979 – 1988 and 1989 – 1998, c) 1979 – 1988 and 1999 – 2008, and d) 1979 – 1988 and 2009 – 2018. The grey polygon delineates the central grassland biome.**

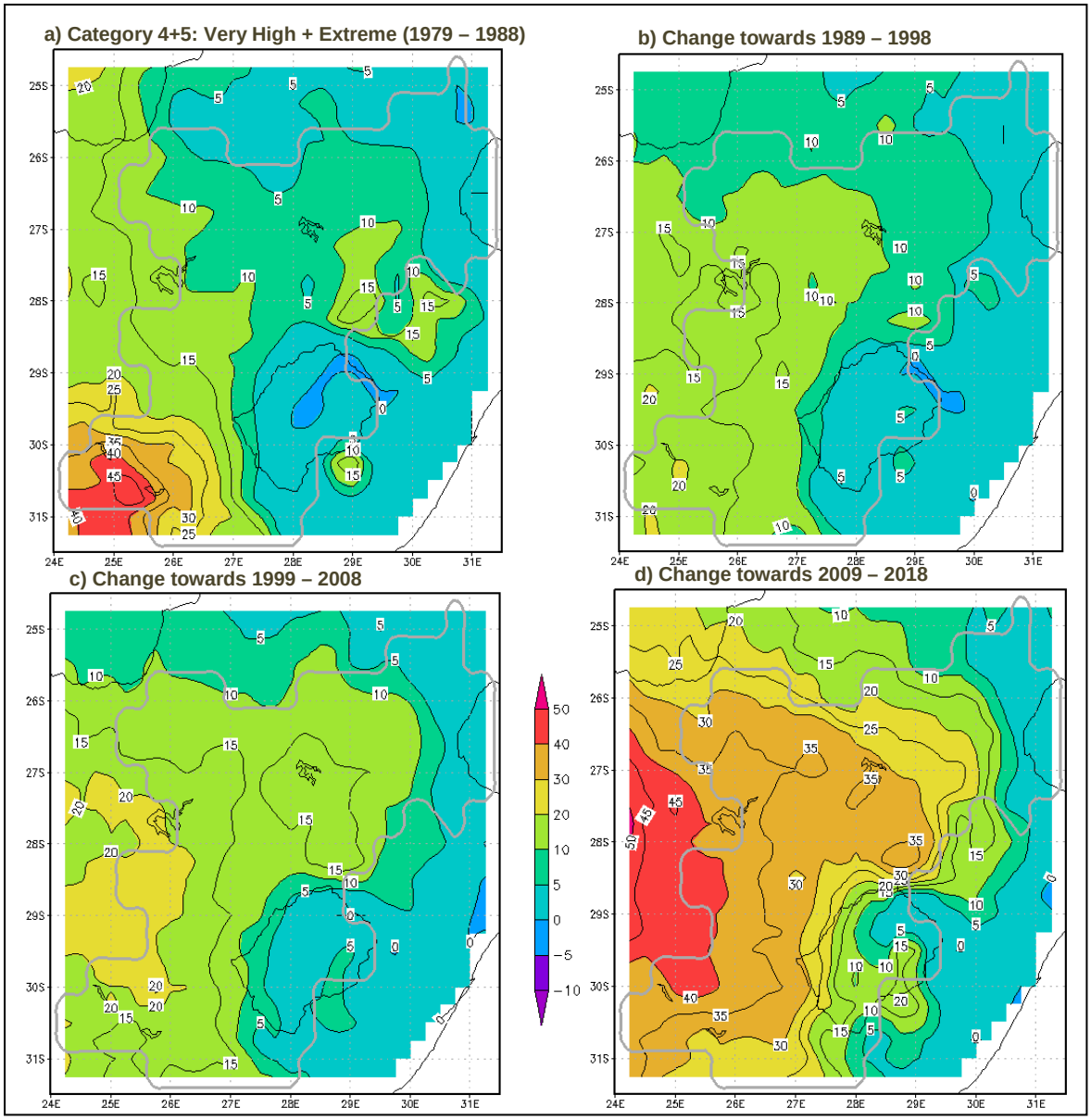

Figure 7.16 **Spatial distribution of a) mean fire season number of days during the 1979 – 1988 period falling in the very high and extreme categories according to the CDSR, and differences in occurrence between b) 1979 – 1988 and 1989 – 1998, c) 1979 – 1988 and 1999 – 2008, and d) 1979 – 1988 and 2009 – 2018. The grey polygon delineates the central grassland biome.**

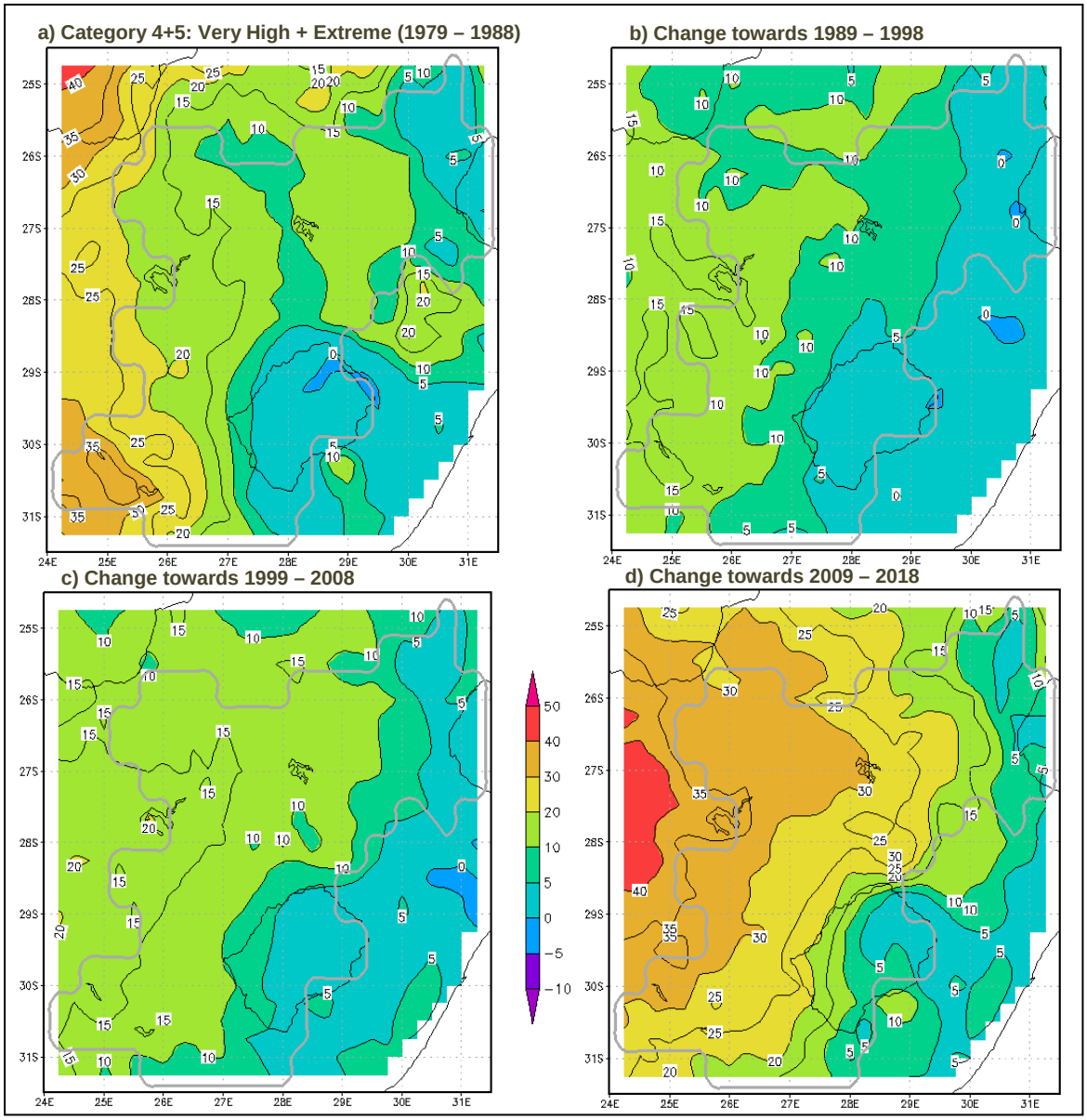

Figure 7.17 **Spatial distribution of a) mean fire season number of days during the 1979 – 1988 period falling in the very high and extreme categories according to the LFDI, and differences in occurrence between b) 1979 – 1988 and 1989 – 1998, c) 1979 – 1988 and 1999 – 2008, and d) 1979 – 1988 and 2009 – 2018. The grey polygon delineates the central grassland biome.**

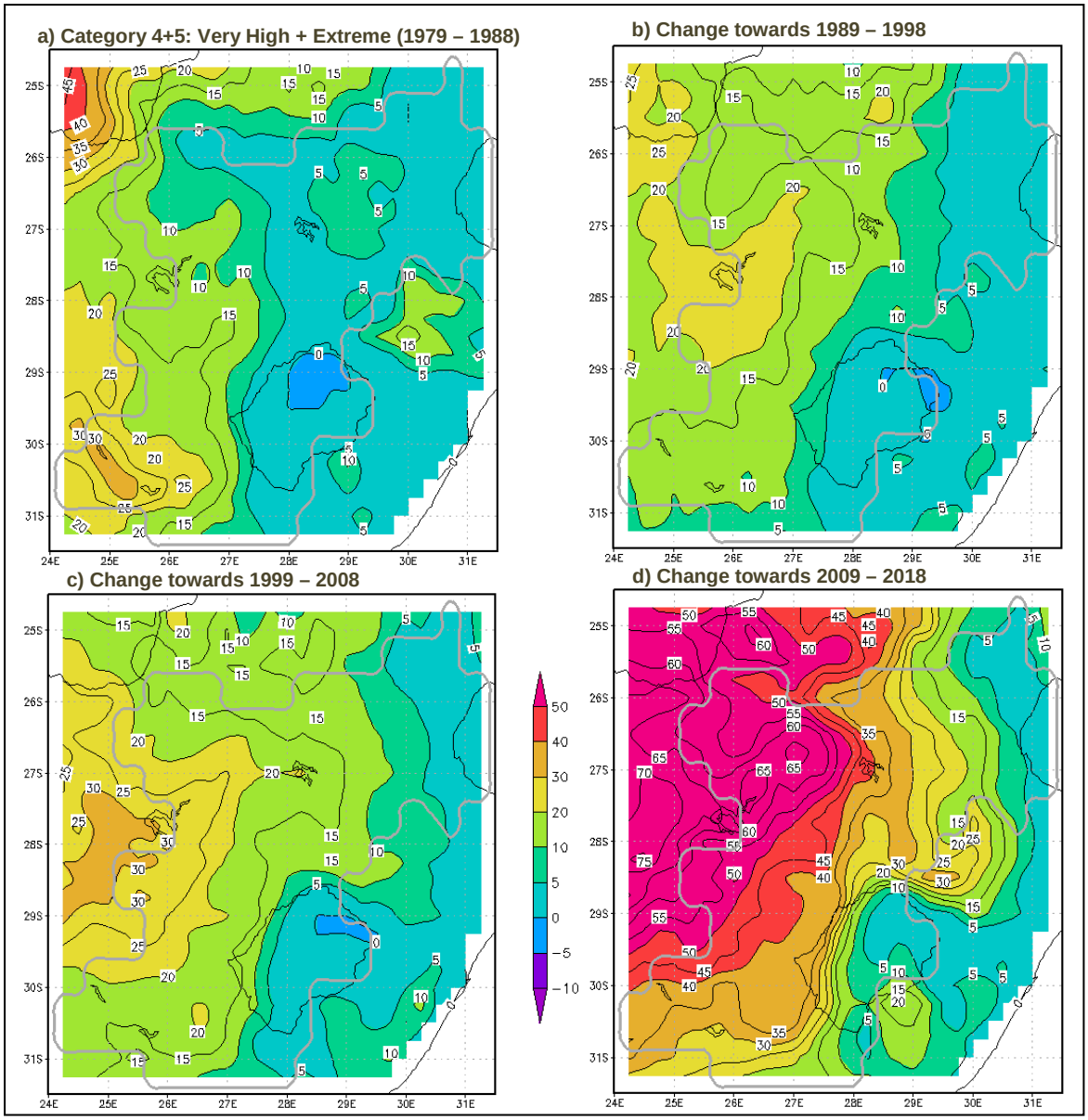

Figure 7.18 **Spatial distribution of a) mean fire season number of days during the 1979 – 1988 period falling in the very high and extreme categories according to the FFDI, and differences in occurrence between b) 1979 – 1988 and 1989 – 1998, c) 1979 – 1988 and 1999 – 2008, and d) 1979 – 1988 and 2009 – 2018. The grey polygon delineates the central grassland biome.**

7.5 CONCLUDING REMARKS

Fire has always been a key abiotic factor influencing the vegetation dynamics over the central grassland biome of South Africa. Although previous studies described the fire regime in the region, not all of it is directly applicable to the central grassland biome of South Africa. Knowledge gaps around the recent characteristics and trends in this area's fire regimes can be addressed by employing satellite remote sensing to estimate burned area (e.g. MODIS MCD64A1.006) and using reanalysis climate data (e.g. ERA5) to calculate climatological fire danger.

A range of FDIs is used worldwide and has been calculated here, but without proper calibration of the fire danger rating category thresholds to local climate conditions these are of little use. This was particularly true for the CFWI, CDR and FFDI. Before embarking on a description of the historical distribution of fire danger (and the potential impacts of future changes in climate thereon), climatological percentile breakpoints were used to bring their performance more in line with the locally developed LFDI.

The study defined the fire season of the central grassland biome as ranging from May to November, with peak burning shifting from August in the north and east to September in the south and west. Climatological fire danger was shown to be considerably higher in the south-western part of the central grassland biome than over the eastern escarpment region and has been increasing during the recent historical period, with the biggest shift occurring during the most recent decade (i.e. 2009 – 2018). Unprecedented increases in very dangerous days occurred during this time period, particularly over the western half of the study area.

This has, however, not culminated in a commensurate increase in remotely sensed burned area. This incongruity can probably be ascribed to veld management practices including fire suppression and avoidance techniques, as well as fuel continuity and availability. The last decade has been marked by prolonged droughts, particularly over the southern and western parts of the central grassland region, while stocking rates remained relatively high. This may also have resulted in reduced fuel loads and hence a reduction in observed burned area at a time when the climatological fire danger has been increasing.

CHAPTER 8

SYNOPTIC WEATHER PATTERNS RELATED TO INCREASED FIRE DANGER

Weather conditions, in combination with local topography and fuel characteristics, influence fire behaviour (Chapter 4). For this reason climatic elements such as air temperature, relative humidity, precipitation and wind speed, measured on a daily (and in some cases hourly) basis, are required as input to several FDRS (Chapter 5). These daily weather characteristics observed over a specific area are, however, controlled by the large-scale or synoptic atmospheric state (Lennard & Hegerl, 2014). As stated by Castellnou *et al*. (2010), "every wildfire can be related to a certain meteorological condition and a synoptic situation of the parameters which define the fire… these determine fire spread pattern and fire behaviour". Knowledge of the synoptic circulation patterns that have historically resulted in increased surface fire-weather conditions furthers the understanding of the interactions between wildfire and climate variability over a particular region (Crimmins, 2006). Such knowledge is therefore beneficial in both understanding and predicting the conditions leading to devastating wildfires. Fire-weather climatology can also form a valuable component in the training of aspirant weather forecasters, fire managers and fire suppression personnel in basic fire-weather concepts (Crimmins, 2006). The main objective of this chapter is to examine the relationship between synoptic-scale circulation and fire danger rating over the central grassland biome of South Africa. At the same time it should be acknowledged that overall wildfire activity is also influenced by precursor conditions, while large wildfires can burn for several days.

8.1 SYNOPTIC CLASSIFICATION OR TYPING

Synoptic climatology can be defined as the study of "the relationships between the atmospheric circulation and the surface environment of a region" (Yarnal, 1993), although Lee and Sheridan (2015) suggested that the term "surface environment" be replaced by "climate-related outcome" as these need not be at the surface. Classification or typing of synoptic patterns is thus regarded as the most common

approach to synoptic climatology and provides insight into the influence of large-scale processes on local environmental conditions (Smithson, 1987; Yarnal, 1993; Barry & Perry, 2001; Hewitson & Crane, 2002; Pearce *et al*., 2011). Classification in itself attempts to group individuals either according to similarities of properties (i.e. synoptic types) or by relationships between objects (i.e. map-pattern classifications) (Yarnal, 1993), with the main aim to minimise internal variability in groups and maximise differences between them (Barry & Perry, 2001; Hewitson & Crane, 2002).

Two fundamental approaches to synoptic classification exist (Yarnal, 1993; Lee & Sheridan, 2015), namely circulation-to-environment (where environmental data are evaluated in relation to circulation patterns) or environment-to-circulation (where inclusion of circulation patterns are based on environmental variable criteria). In addition, both manual, subjective approaches and automated, objective classifications exist, which in turn may be applied at nearly any spatial or temporal scale (Wilby & Wigley, 1997; Barry & Perry, 2001; Lee & Sheridan, 2015). Such classification schemes have been applied to a variety of meteorological or environmental problems such as the statistical downscaling of climatic elements (e.g. daily precipitation at a point station), air quality, acid rain, streamflow, water quality etc. (Smithson, 1987; Yarnal, 1993; Barry & Perry, 2001).

The first attempt at objective weather map classification for South Africa was made by Longley (1976; cited by Taljaard, 1995a), who identified the most frequently recurring summer and winter 850 hPa geopotential height patterns over the land during a three-year period. Taljaard (1995a) proposed a subjective manual classification (Figure 8.1) for both summer and winter surface circulation patterns over southern Africa, comprising the conventional standard types of pressure distribution (i.e. high pressure systems, high pressure ridges, low pressure systems, low pressure troughs and zonal flow). This classification was very useful as it related temperature and rainfall patterns to each synoptic circulation pattern. Since the position of these synoptic weather systems is key in determining the associate weather, this initial classification was altered to include nine summer and 16 winter patterns (Taljaard, 1995b).

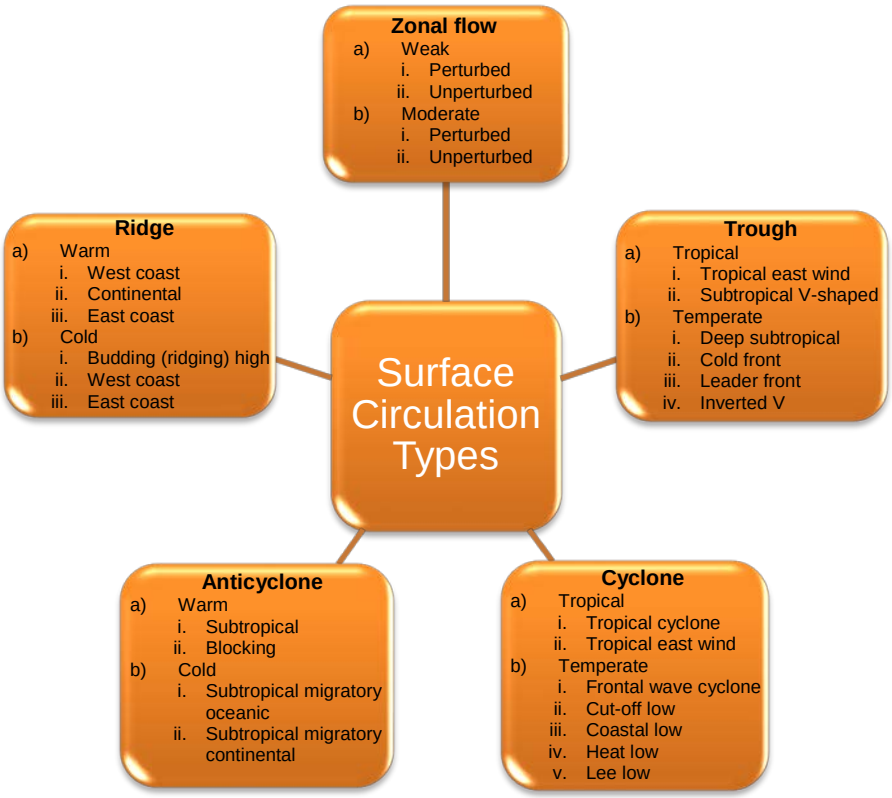

Figure 8.1 **The five main surface (sea-level and 850 hPa) circulation types over southern Africa south of 17°S proposed by Taljaard (1995a).**

Tyson and Preston-Whyte (2000) also provided a broad subjective classification of synoptic patterns over southern Africa into fine-weather and mildly disturbed conditions (e.g. fine-weather continental high, coastal low and Berg winds), tropical disturbances associated with tropical easterly airflow (e.g. easterly wave, easterly low) and temperate mid-latitude disturbances associated with westerly airflow (e.g. westerly wave, cut-off low, southerly meridional flow, ridging anticyclone, west-coast trough, cold snap). It should be noted that the purpose of their classification was perhaps more aimed at the development of conceptual models for educational purposes (author's opinion), while in practice several of these circulation types are likely to occur simultaneously in complex, composite situations which makes them challenging to categorise.

Subjective manual classification schemes such as those mentioned above, pose a problem as they are very time consuming and cannot be reproduced exactly as some circulation patterns are undeniably difficult to classify, while different analysts may not reach similar decisions when considering borderline cases (Barry & Perry, 1973;

2001). “Internal drift” may also occur when even a single analyst turns out to be inconsistent with the classification of weak or transitional patterns when working with a relatively long time period (Barry & Perry, 2001). The advent of high-speed computers and digital datasets resulted in the proliferation of automated, objective classification methods that are able to generate reproducible categories. These methods include (Yarnal, 1993; Barry & Perry, 2001):

- correlation-based classification (e.g. Lund, 1963; Kirchhofer, 1974; Key & Crane, 1986);
- eigenvector-based classifications (e.g. Key & Crane, 1986; Preisendorfer, 1988; Jiang *et al*., 2009);
- compositing (e.g. Pereira *et al*., 2005; Seluchi & Chou, 2009), indexing (e.g. Kutiel *et al*., 1996) and specification (e.g. Kidson, 1997); and
- artificial neural networks (e.g. Hewitson & Crane, 2002; Michaelides *et al*., 2010; Sheridan & Lee, 2011).

Ironically, all classifications are innately subjective to some degree as the outcomes are still influenced by human decisions (e.g. choice of predictor variable(s), domain size and number of classes) (Lee & Sheridan, 2015). One consideration that detracts from the application of all synoptic classification schemes is “the fact that atmospheric modes are continuous so that the delimitation of any boundary between classes must be arbitrary and therefore somewhat unsatisfactory” (Barry & Perry, 1973). This view is echoed by Taljaard (1995a), Yarnal (1993) and Hewitson and Crane (2002). Upon considering the daily circulation patterns over the southern African region, it will be next to impossible to identify two days with the exact same weather conditions (Taljaard, 1995a). As pointed out by Hewitson and Crane (2002) the internal variability in a group may also result in the same synoptic type being associated with different local responses, while different synoptic types could very well induce similar responses.

Even though circulation patterns display a range of modes, the variety of possible configurations is not infinite over a specific geographical area (Barry & Perry, 2001). There is also definitely some correlation between certain easily recognisable synoptic circulation patterns and distinctive weather occurrences such as cloudy or clear, wet

or dry, windy or calm, cold or warm conditions, all of which have been shown to influence wildfire behaviour (Section 4.2). Without such correlation, forecaster experience would hardly have existed (Taljaard, 1995a). Inevitably, the following assumptions are common to all synoptic classifications (Yarnal, 1993):

a) atmospheric circulation is a critical determinant of the surface environment;
b) all the important patterns/types are identified;
c) within group variability is acceptable; and
d) agreement between the temporal and spatial scales of the surface variables and atmospheric circulation processes.

It does, however, remain desirable from a global modelling context to relate the surface climate response to the driving synoptic state as Global Climate Models (GCMs) are able to simulate the latter reasonably well, while struggling to capture certain local climatic elements (e.g. rainfall) accurately, especially in regions of complex topography (Hewitson & Crane, 2005; Tennant & Reason, 2005; Lennard & Hegerl, 2014). GCMs may also differ in terms of the projected future response of some or other local climatic element, but are more likely to agree on simulated circulation states (Hewitson & Crane, 2006; Lennard & Hegerl, 2014). In addition to being used as a data reduction technique, synoptic classification has also been used to extend data records (where the circulation record is considerably longer than that of the local environmental parameter) or to downscale coarse-grid GCM circulation data to local scale environmental data (Hewitson & Crane, 2006).

8.2 STATISTICAL DOWNSCALING

GCMs are the main source of climate predictions at various time scales. These dynamical models represent the world as an array of grid-points. However, the spatial resolution of GCMs is often too coarse to resolve regional scale effects (Hessami *et al*., 2008). Consequently, sub-grid processes, such as convection and precipitation, are particularly difficult to reproduce, necessitating the parameterisation of these important processes. This implies that locations and variables for which forecasts are required may not be represented explicitly by these models (Maini *et al*., 2004). In addition, the GCMs have systematic errors and are deterministic. Non-linear responses and the inherently chaotic nature of the climate system renders climate prediction even more challenging (MacKellar *et al*., 2007). It is apparent that – complex

and sophisticated as GCMs are – these models are by no means perfect representations of the climate system (MacKellar *et al*., 2007).

Downscaling approaches have subsequently emerged as a means of relating large-scale atmospheric predictor variables (such as 850 hPa geopotential heights) to station-scale meteorological series (Wigley *et al*., 1990; Hay *et al*., 1991; Wilby & Wigley, 1997). Variables such as rainfall, which are not always accurately represented by these models, can be derived using statistical approaches to build relationships between the required forecast parameter and variables that are simulated more accurately (Steyn, 2009). Owing to model imperfections, systematic errors may occur. The statistical interpretation of numerical climate predictions possesses an inbuilt accounting capability for the local topographic and environmental conditions that control the precipitation and other surface weather parameters and can compensate for any model biases (Landman *et al*., 2001, Maini *et al*., 2004). Even if GCMs are run at high resolution the need will still remain to downscale the results from such models to individual sites or localities for impact studies (Wilby & Wigley, 1997).

Downscaling activities are normally either spatial or temporal in nature. This spatial or temporal nature usually stems directly from the application of the downscaling procedure. Spatial downscaling refers to “techniques used to derive finer resolution climate information from coarser GCM output”, while temporal downscaling involves “the derivation of finer-scale temporal data from coarser-scale temporal information e.g. daily data from monthly or seasonal information” (CICS, 2016). Certain studies require the use of either high resolution gridded data or the use of site-specific data, while other studies may require the use of hourly or daily data, neither of which is catered for by large-scale GCMs (Steyn, 2009).

Statistical downscaling is based on the fundamental assumption that regional climate is conditioned by both the local physiographic features as well as the large scale atmospheric state (Hessami *et al*., 2008). On this basis, large scale atmospheric fields are related to local variables through a statistical model in which GCM simulations are used as input for the large scale atmospheric variables (or “predictors”) to downscale the local climate variables (or “predictands”) with the use of observed climatic data. Most statistical downscaling work has concentrated on predicting the rainfall and

temperature at a single site as these are the most important input variables for many natural systems models (Wilby *et al*., 2004). The choice of downscaling method is governed by the application and to some extent the nature of the local predictand. According to Wilby *et al*. (2004) issues that need to be considered when attempting statistical downscaling are the choice of downscaling method, the choice of predictors, whether or not extremes should be modelled, whether or not tropical areas are included and possible feedbacks from other climate subsystems. Drawing from reviews by Hewitson and Crane (1996), Wilby and Wigley (1997), Murphy (1999), Wilby *et al*. (2002), the Canadian Institute for Climate Studies (CICS, 2016), Wilby and Dawson (2007) and Hessami *et al*. (2008), statistical downscaling techniques may be grouped into the following categories:

- Empirical methods (e.g. Benestad (2004));
- Weather pattern-based approaches (e.g. Hewitson and Crane (2002; 2006));
- Stochastic weather generators (e.g. Oelschlägel (1995)); and
- Regression-based methods (e.g. Steyn and Walker (2010).

Table 8.1 Advantages and disadvantages of weather pattern-based statistical downscaling (after Wilby *et al*. (2004) and CICS (2016))

Advantages	Disadvantages
a) Provides more realistic scenarios of climate change at individual sites than the direct application of GCM-derived scenarios. b) Is computationally much less demanding than dynamical downscaling using numerical models. c) Based on sensible physical linkages between climate on the large scale and weather on the local scale. d) Quite versatile as it can be applied to a wide variety of studies e.g. surface climate, air quality, flooding, etc. e) Overlaying (compositing) can be employed for the analysis of extreme events.	a) Requires the additional task of weather classification. b) Large amounts of observational data may be required to establish statistical relationships for the current climate. c) Specialist knowledge may be required to apply the technique correctly. d) The relationships may not be valid under future climate forcing. e) It may not capture intra-type variations (i.e. variations that occur in a specific synoptic type) in surface climate. f) Different relationships between the weather types and local climate may have occurred at some sites during the observed record.

Of particular interest to this study is the weather pattern-based approaches (also referred to as weather typing or the use of analogues). These approaches are based on a classification scheme which is subsequently used to simulate the local surface variables, such as precipitation, from the corresponding (daily) weather patterns (Wilby & Wigley, 1997). Wilby *et al*. (2004) and CICS (2016) list some of the advantages and disadvantages common to weather pattern-based approaches (Table 8.1).

8.3 SELF-ORGANIZING MAPS

Yin (2007) defines self-organisation as “a fundamental pattern recognition process, in which intrinsic inter- and intra-pattern relationships in the data set are learnt without the presence of a potentially biased or subjective external influence”. The self-organizing map (SOM), also referred to as a “Kohonen Neural Network”, was originally proposed by Kohonen (1982; 1990; 2001) as a form of ANN that uses unsupervised-learning algorithms. It is a data visualisation and analysis technique that reduces high-dimensional data space nonlinearly to a low-dimensional (usually 2D) discrete array of nodes without any prior knowledge about the clusters in the input data (Kohonen, 2001; Hewitson & Crane, 2006; Yin, 2007; Yin, 2011). The discrete lattice of nodes or data archetypes produced is referred to as a Kohonen map or master SOM (Sheridan & Lee, 2011; Yin, 2011). Essentially, SOMs are used to reduce dimensions and extracting patterns from many types of data, especially large and complex high-dimensional data sets (Germano, 1999; Richardson *et al*., 2003).

Whereas other ANNs apply error-correction learning, SOMs use competitive learning and a neighbourhood function in order to combine clustering and ordering processes to preserve the topological properties of the input data space (Yin, 2011). It is this unique topology preserving property of SOMs that allows for the visualisation of the relative mutual relationships among the data (Yin, 2007). Perhaps the most significant difference between SOMs and other contemporary ANNs is that the latter consider spatial organisation of the processing units as a secondary aspect, while the former places emphasis on “creating a localised, structured arrangement of representations in the basic network module” (Kohonen, 1990). As a classification method SOMs are very popular as the data are treated as a continuum, while most classical techniques rely on some form of correlation, specification and/or empirical orthogonal functions (Barry & Perry, 1973; Lennard & Hegerl, 2014). In addition, SOMs don’t require the data to conform to a particular distribution or underlying model (Hewitson & Crane, 2002). A study by Peña *et al*. (2007) revealed that SOM compared well, and in certain aspects outperformed, other contemporary topology preserving mapping techniques like Topographic Product of Experts (ToPoE), Harmonic Topographic Map (HaToM), Topographic Neural Gas (ToNeGas) and Inverse-weighted K-Means Topology-Preserving Map (IKToM).

For demonstrative purposes, Figure 8.2 depicts the result of a hypothetical SOM trained using the characteristics of animals (e.g. size, likes to swim). In this case the SOM grouped all the animals that like to swim at the bottom and those that prefer to dwell on land at the top, while larger animals were clustered on the left and smaller ones to the right. It should be noted that the map was trained purely on the animals' qualities as it had no real sense of a "giraffe" or a "crab". Data is organised spatially by grouping similar data items together, while adjacent areas share some of these similarities (Bação & Lobo, 2010).

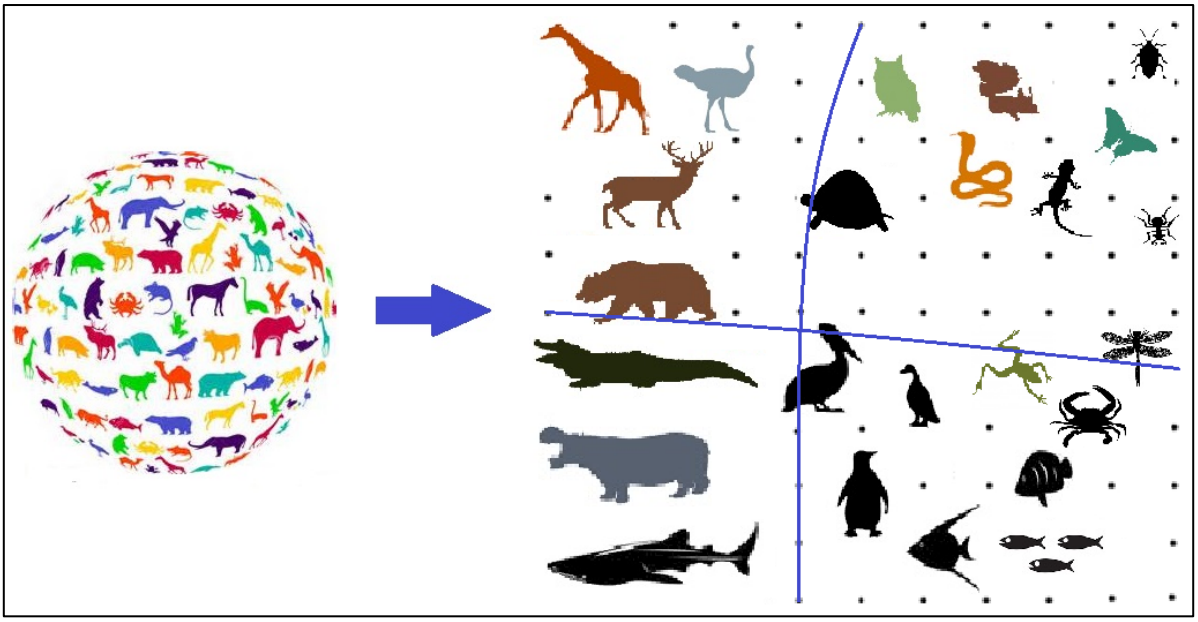

Figure 8.2 Hypothetical example of an animal data set trained using SOM analysis.

SOMs have found application in numerous fields of science and technology, with more than 7 700 scientific articles either applying this method or otherwise benefitting from it (CIS, 2017). Its relative simplicity and computational efficiency renders it a trendy data analysis technique (Gorban *et al*., 2007; Yin, 2007). SOM analyses have been used in a wide variety of climate applications, particularly to characterise inter-annual, seasonal and event-scale variability all over the world (e.g. Cavazos, 1999; 2000; Hewitson & Crane, 2002; 2005; 2006; Hewitson *et al*., 2004; Crimmins, 2006; Hope *et al*., 2006; Schuenemann *et al*., 2009; Cassano *et al*., 2011; Pearce *et al*., 2011; Yin, 2011; Chattopadhyay *et al*., 2013; Oettli *et al*., 2014). SOMs have also been employed in several climatological studies over southern Africa (e.g. Richardson *et al*., 2003; Tennant, 2003; Hewitson *et al*., 2004; Hewitson & Crane, 2005; 2006; Tadross *et al*.,

2005; Tennant & Reason, 2005; Sang *et al*., 2008; MacKellar *et al*., 2010; van Schalkwyk & Dyson, 2013; Lennard & Hegerl, 2014; Dyson, 2015; Engelbrecht *et al*., 2015; Stander *et al*., 2016, Mogale & Dyson, 2017).

A comprehensive description of the SOM algorithm is provided by Yin (2007), Yin (2011) and Oettli *et al*. (2014). SOMs operate in two modes, training and mapping, whereas the typical structure consists of one input and one output layer. An early decision involves setting up the array or network size (i.e. number of nodes or neurons) of the SOM and how it is initially distributed amid the multidimensional data (Yin, 2011; Lennard & Hegerl, 2014). The size of the master SOM is given by the product of the number of nodes in the abscissa and ordinate directions in accordance with the notation used by Tennant & Hewitson, 2002; Tadross *et al*., 2005; Tennant & Reason, 2005 and Schuenemann *et al*., 2009. Hewitson & Crane (2002; 2006) uses the reverse notation, while Yin (2011) agrees in wording with the above-mentioned notation but then fails to adhere to it. The SOM size impinges on the resolution of variability and is chosen subjectively according to the desired degree of generalisation (Hewitson & Crane, 2002; Yin, 2011). In the case of synoptic-scale circulation a smaller number of nodes would necessarily result in more generalised circulation patterns over the study area, while a larger number would portray a broader range of circulation archetypes (Lennard & Hegerl, 2014). It is also to be expected that the standard deviation of the downscaled variable (e.g. fire danger rating) will decrease for each class as the number of nodes are increased (Barry & Perry, 2001). To ensure the stability of the calculations, Reusch *et al*. (2007) advised using an asymmetric grid, although square SOMs have been employed (e.g. 3 × 3 by Chattopadhyay *et al*., 2008; 7 × 7 by Tozuka *et al*., 2008).

Training commences as the reference vectors of the master SOM is first initialised with either linear values (derived from PCA) or values randomly extracted from the input data (Yin, 2011). According to Lennard and Hegerl (2014) both types are equally effective, though linear initialization requires more preparation. Training the SOM against a given input data set involves an iterative, competitive process referred to as vector quantization (Yin, 2011). During vector quantization, the coefficients (i.e. weights) on a node vector (also referred to as neurons) are budged in the direction of the training vectors such that they span the variation in the data space. This is done

by choosing the node vector with the smallest Euclidian distance to the data vector (i.e. whose coefficients closest match the input vector) as the best-matching unit or 'winning' node for that specific input vector (Yin, 2011; Lennard & Hegerl, 2014; Oettli *et al*., 2014). The winning node is subsequently updated by effectively nudging it in the direction of the data vector (Sheridan & Lee, 2011). At the same time, the coefficients of the neighbouring nodes are also adjusted (inversely proportionate to their distance from the winning node) so that each vector converges to the input pattern (Figure 8.3). An update neighbourhood is thus created with the winning node at its centre. It should be noted that the data vector doesn't form part of a group at this time but is merely used to fine-tune the location of the reference node vector in the data space (Hewitson & Crane, 2002).

By employing an iterative training process the node vectors are gradually adjusted to span the whole data space (Lennard & Hegerl, 2014), while the speed of adjustment is governed by the 'radius of influence' and the 'learning rate'. The former determines the number of surrounding nodes to be updated, while the latter controls how quickly the coefficients shift towards the data points (Hewitson & Crane, 2002; Lennard & Hegerl, 2014). According to Lennard & Hegerl (2014) the best practice is to choose a relatively large initial value for the radius of influence and to allow it to decrease slowly to unity with each iteration. Hewitson and Crane (2002) suggested setting the value to the smallest of the array dimensions for the first pass, progressively decreasing it with each iteration. This will maintain the topology of the map while it aligns itself with the data and eventually allow each node the freedom to attain an ultimate stable position in the data space. The learning rate is usually set to a small value as a large number of iterations are made, gradually decreasing it linearly to almost zero (Sheridan & Lee, 2011; Lennard & Hegerl, 2014). Hewitson and Crane (2002) suggested keeping the learning rate at the software (i.e. SOM-PAK; Section 8.4) default for the first pass and using a value half of that for the second pass. Unfortunately, little or no attention is afforded to the exact choice of these parameters in most publications. Generally, the number of iterations must be at least 500 times the number of nodes in the network (Haykin, 1994; cited by Yin, 2011). Normally training is performed in two successive passes in order to first develop the broad mapping and then to refine it further by using the reference vectors obtained at the end of the first pass (Hewitson & Crane, 2002; Tennant & Hewitson, 2002; Sheridan & Lee, 2011).

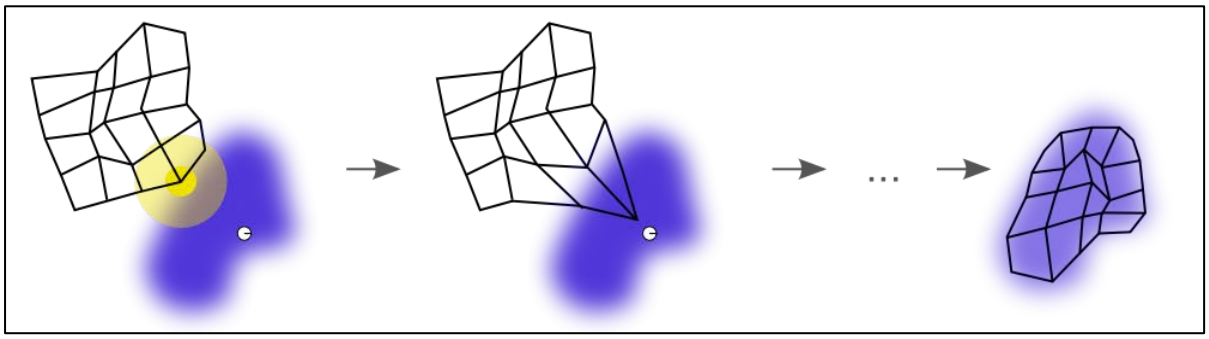

Figure 8.3 **Training of a hypothetical self-organizing map (SOM). The blue shading represents the input data space and the small white circle the current input vector drawn from that distribution. Left: Initially the nodes are randomly positioned in the data space and the nearest node vector (highlighted in yellow) to the current input vector is chosen. Middle: The winning node is shifted towards the input vector while its neighbouring ones are also adjusted to a lesser extent. Right: Following numerous iterations the grid tends to approximate the data distribution (Wikipedia, 2017).**

The result of the training process is a two-dimensional Kohonen or 'self-organised' map consisting of a regular grid of nodes or neurons. The node vectors constitute a representative pattern of the data space continuum as each node position represents the approximate mean of the nearby data samples (Yin, 2011; Lennard & Hegerl, 2014). The map thus attempts to represent all the available input vectors with optimal accuracy using a restricted set of patterns (CIS, 2017). A higher number of nodes are allocated where the data is more dense, thereby allowing for greater discrimination in such regions (Hewitson & Crane, 2002; Sheridan & Lee, 2011). The map can be either in a hexagonal or rectangular grid, although the choice of lattice has little bearing on the end result (Openshaw, 1994; cited by Lennard & Hegerl, 2014). At the same time the patterns become ordered on the grid so that similar nodes are located close to one another, while the most unrelated ones are placed furthest apart (Hewitson & Crane, 2002; Sheridan & Lee, 2011; CIS, 2017). It should be noted, however, that the arrangement does not constitute a quantitative measure of similarity (Hewitson & Crane, 2002). For example, the difference between the beetle and butterfly in the top right corner of Figure 8.2 is not necessarily similar to that between the shark and hippopotamus in the bottom left corner. According to Hewitson and Crane (2002) the two diagonals of the master SOM are comparable to the first two principal components of the data (though they are not necessarily orthogonal to each other), with the transitional states sandwiched between them. At this point the SOM procedure has achieved the equivalent of the typing phase in a traditional synoptic climatological

analysis (Hewitson & Crane, 2002), with each node representing “a range of states in the continuum described by the original data space”.

During the mapping procedure (Figure 8.4) the distances between any input vector and the reference node vectors of the trained master SOM are calculated in order to assign each case to the best matching or most related pattern (Sheridan & Lee, 2011; Yin, 2011). The very fact that an input vector can be mapped to an archetype pattern implies that its features should be similar to the identified pattern (Yin, 2011). For the purpose of frequency analysis the same data used for training can also be mapped to the trained SOM (Yin, 2011).

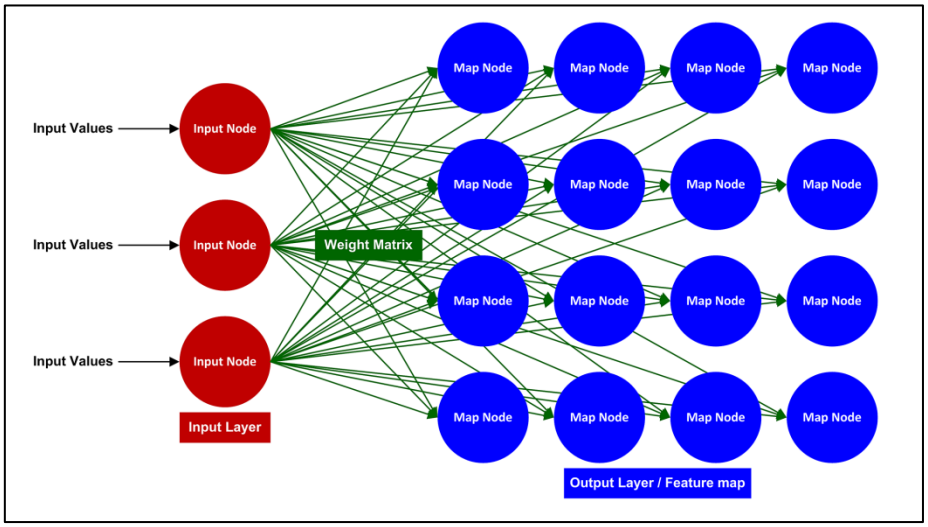

Figure 8.4 **Mapping of input vectors to a self-organizing map (SOM) in a rectangular neural layout (Vantaram & Saber, 2012).**

8.4 PROBLEM STATEMENT AND RESEARCH OBJECTIVE

From the foregoing discussion it is clear that synoptic typing, and in particular the SOM methodology, can be a useful tool in highlighting those large-scale weather patterns associated with extreme weather events. However, the only published studies remotely relating to this was by Juhnke and Fuggle (1987) for the South-Western Cape of South Africa, Pereira *et al*. (2005) for Portugal and Annas *et al*. (2007) for Southeast Asia.

The research objective of this chapter was thus to employ SOM analysis in order to identify those synoptic weather patterns that lead to increased fire danger over the

central grassland biome of South Africa. Such a study would aid novice weather forecasters in particular in predicting hazardous fire weather conditions.

8.5 MATERIALS AND METHODS

Monthly means of climatic elements (such as those provided in Section 7.3) are insufficient in rendering the nature of the controlling weather processes, while the volume of data generated by three or six-hourly observations is generally too much for an appropriate synopsis (Barry & Perry, 2001). Most of the studies referenced in the previous section rather employed daily time intervals, using climate variables sourced from either meteorological observation stations or reanalysis data interpolated to a regularly spaced grid, or both.

ERA5 reanalysis data was used for the surface climatic variables required for calculating the various fire danger indices (viz. CFWI, CDSR, LFDI and FFDI). The methods used for calculating these were discussed in Section 7.5.1.1. The program "fire4era.f" (Appendix E) were used to calculate the spatial mean and maximum FDI value over the study area at a daily interval. The decision was made to use the LFDI in the synoptic typing exercise for brevity and because its suitability to the study area has already been established (Sections 5.5 and 7.5.2.1). ERA reanalysis data, assimilated and reinterpreted to the CCAM grid of 0.5° × 0.5° (Section 9.4), was also used for the classification variable (z_{850}).

SOM analysis was used to categorise 30 years of daily fire season climate data over southern Africa into a number of archetypal circulation modes. The climatological standard reference period of 1981 – 2010 was chosen in accordance with WMO (2017). The SOM-PAK program (Kohonen *et al*., 1996; CIS, 2017) was used to perform a synoptic typing on the daily (12:00 GMT) gridded ERA data in order to assist in the identification of the main nodes that are associated with higher fire danger at a daily time scale. SOM-PAK was downloaded from http://www.cis.hut.fi/research/som_lvq_pak.shtml. The use of SOM-PAK involves four steps, namely map initialisation, map training, evaluation of quantisation error and visualisation.

There is no simple way of determining beforehand what domain will yield the best results (Barry & Perry, 2001). While it is fair to assume that the diagnostic features on

a daily synoptic analysis also operate on time scales of days, care should be taken that the horizontal dimensions of the grid are smaller than the size of the atmospheric features commonly found in the circulation patterns (Yarnal, 1993). The chosen domain must be representative of relevant behaviour – if it is too large the circulation patterns may be dominated by atmospheric features far from the region of interest and if it is too small relevant large-scale systems may not be adequately depicted (Gutowski & Cassano, 2014). The domain used to produce the Kohonen map or master SOM thus covered southern Africa and the surrounding ocean from 15 to 45°S and 0 to 45°E (henceforth referred to as domain A). This larger domain made it possible to identify large-scale synoptic systems from both subtropical and temperate latitudes that would influence the fire weather over the study area. FDI values were calculated over the central-eastern part of southern Africa, while only those values that fell within the central grassland biome (henceforth referred to as domain B; shaded area in Figure 6.1a) were used in the mapping procedure.

After experimenting with different shapes of the SOM grid, the final choice fell on a 5 × 4 shape (i.e. 5 columns and 4 rows), analogous in effect to clustering to 20 nodes. Other synoptic studies involving SOMs have used a relatively smaller number of nodes (e.g. 12 by Tennant & Reason, 2005; 12 by Crimmins, 2006; 9 by Chattopadhyay *et al*., 2008; 12 by Jiang, 2010; 20 by Yin, 2011; 8 by Chattopadhyay *et al*., 2013; 12 by Lennard & Hegerl, 2014; 12 by Dyson, 2015). A 7 × 5 shape, resulting in 35 nodes similar to that used by Hewitson and Crane (2002), Tennant & Hewitson (2002), van Schalkwyk and Dyson (2013) and Engelbrecht *et al*. (2015), was deemed excessive for the purpose of this study as the 20 node SOM could adequately describe the variation in the synoptic circulation that occurred during the burning season (viz. May – November). A 35-node SOM produced similar classification in pattern but with a slightly higher level of detail than the 20-node one used (not shown). A rectangular lattice was used as it simplified visual display and analysis.

A multivariate clustering procedure such as SOM will experience difficulties in identifying smaller-scale synoptic features (Yin, 2011) such as cut-off lows, heat lows or coastal lows. Another consideration which may detract from the application of this classification scheme is the fact that the weather experienced at the surface is not only governed by low-level air masses and their motions. Although SOM-analysis is an

objective classification method, a remaining source of subjectivity is the choice of predictor (training) variable(s). Choosing a good predictor variable that controls the surface environment and is represented accurately by GCMs is crucial in capturing the climatic variation (Yarnal *et al*., 2001; Wilks, 2006; Cavazos & Hewitson, 2005).

Most synoptic climatological analyses rely on mean sea-level pressures (MSLP) to depict the large-scale atmospheric circulation characteristics (Yarnal *et al*., 2001; van Schalkwyk and Dyson, 2013; Lee & Sheridan, 2015). Motivated by the unique topography of the interior plateau and eastern escarpment region of South Africa, with the bulk of the study area located between 1 200 and 3 400 m above mean sea level (see Section 6.1 for a more detailed physical description of the study area), it was decided to rather use the 850 hPa geopotential heights (z_{850}). The inherent flaws related to using pressure reduced to sea level over this area have been highlighted by Taljaard (1995a) and Tennant and Hewitson (2002). Using z_{850} proves beneficial as it remains representative of surface conditions without being contaminated by local effects (Pereira *et al*., 2005). The suitability of z_{850} was further underpinned by its use in previous studies as a predictor of daily precipitation and temperature (e.g. Wetterhall *et al*., 2009; Lazenby *et al*., 2014; Shrestha *et al*., 2014), while it is also closely related to the wind speed and direction by virtue of the geostrophic approximation (Holton, 1992). Each node thus constituted a 91 × 61 array (in accordance with the notation used by Sang *et al*., 2008), representing a pattern of 12:00 GMT z_{850} over domain A. The 12:00 GMT reanalysis time was selected to correspond with the afternoon peak in fire weather conditions (Section 4.2).

Training of the SOM was achieved by random initialisation of the node vectors and applying two consecutive passes of 10^6 iterations each. For the duration of the first pass the learning rate was kept at the SOM-PAK software default (0.01) and the second pass 0.04. The initial update radius was set to 3.0 and progressively decreased for subsequent training passes with a rate half that of the initial one. One diagonal axis of the resultant master SOM was expected to capture the dominating high pressure to low pressure systems and the second the spatial variation in geopotential heights across the region (Lennard & Hegerl, 2014).

Evaluation of the quantisation error (i.e. the shortest distance between nodes) was performed for each day in the 30-year period in order to achieve the best SOM (i.e. presenting the smallest average quantization error). A Sammon map (Sammon, 1969) depicts the approximate Euclidean distances between node vectors while preserving the inherent data structure. Such a map was subsequently used to detect error in the SOM. A Sammon map that folds over itself is indicative of an unstable learning process and could result in spurious results and non-robust interpretation of nodal relationships (Sammon, 1969; Sheridan & Lee, 2011; Lennard & Hegerl, 2014). In the final visualisation step it should also be evident from the master SOM that similar circulation types are grouped close to each other while dissimilar ones are placed in opposite corners.

The final step involved counting the number of very dangerous days (i.e. falling in the "very high" and "extreme" categories) under each node and ranking them in order to identify the archetypal patterns corresponding to increased fire danger.

8.6 RESULTS AND DISCUSSION

8.6.1 Synoptic Regimes during the Fire Season

A set of 20 SOM patterns (5 × 4) was attained after training the ERA gridded daily z_{850} data over domain A for the period of 1981 – 2010. The Sammon map in Figure 8.5 depicts the two-dimensional distribution of nodes within the data space after training of the SOM. From Figure 8.5 it is evident that the nodes along the far right column of the Sammon map are more similar (due to the smaller distances between them) than those along the left. Since the Sammon map did not fold over itself, the results should be fairly robust.

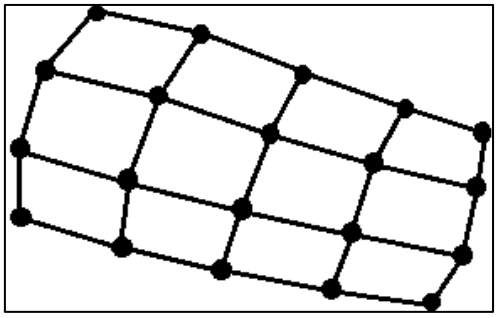

Figure 8.5 Sammon map depicting the distortion surface for the 20-node SOM.

The 20 archetype patterns are presented in Figure 8.6 and span the range of synoptic conditions that influence the weather of southern Africa during the course of the fire season (i.e. May – November). Concise descriptions of each archetypal synoptic pattern are provided in Table 8.2.

Table 8.2 Description of the archetype patterns contained in the master SOM (node numbers correspond with those presented in Figure 8.6)

Node	Description of synoptic weather pattern
1	A trough along the Namibian coast with high pressure dominating the entire region as a strong AOH ridges south of the country and extends a ridge of high pressure coastwise to the east
2	A trough along the Namibian coast with high pressure dominating the entire region as a fairly strong AOH extends a ridge across the southern interior
3	A trough stretching diagonally across the central interior with a moderately-developed westerly wave and associated cold front to the south-east of the country
4	A trough stretching diagonally across the interior with a moderately-developed westerly wave and associated cold front extending over the eastern interior
5	A well-developed westerly wave and associated cold front extending over the eastern interior
6	A trough along the Namibian coast with high pressure dominating the entire region as a fairly strong AOH ridges south of the country and a bulge of high pressure develops on the east coast
7	A trough of lower pressure over the western interior, wedged between the AOH and IOH
8	A marked trough over Namibia and a weak-developed westerly wave and associated cold front over the central southern interior
9	A marked trough over Namibia and a moderately-developed westerly wave and associated cold front over the central interior
10	A marked trough over Namibia and a well-developed westerly wave and associated cold front over the central interior
11	A broad band of high pressure over the bulk of the area with a strong high pressure cell centred on the east coast and adjacent interior and a trough located along the Namibian coast
12	A weak west-coast trough, while the IOH extends a ridge over the north-eastern parts
13	A west-coast trough with a broad westerly wave and associated cold front off the south-west coast, while the IOH extends a ridge over the north-eastern parts
14	A west-coast trough with moderately-developed westerly wave and associated cold front off the south-west coast, while the IOH extends a ridge over the north-eastern parts
15	A pre-frontal trough over the western interior with a well-developed westerly wave and associated cold front along the south-west coast
16	A strong high pressure cell, centred in the north-east, dominates the entire region, with a broad westerly wave far to the west over the south Atlantic Ocean
17	A fairly strong IOH centred over the north-eastern interior, while a broad westerly wave is located over the south Atlantic Ocean
18	A broad westerly wave and associated cold front to the west of the country, while the IOH extends a well-developed ridge over the north-eastern parts
19	A moderately-developed westerly wave and associated cold front to the west of the country, while the IOH extends a ridge over the north-eastern parts
20	A well-developed westerly wave and associated cold front located to the west of the country, while the IOH extends a ridge over the north-eastern parts

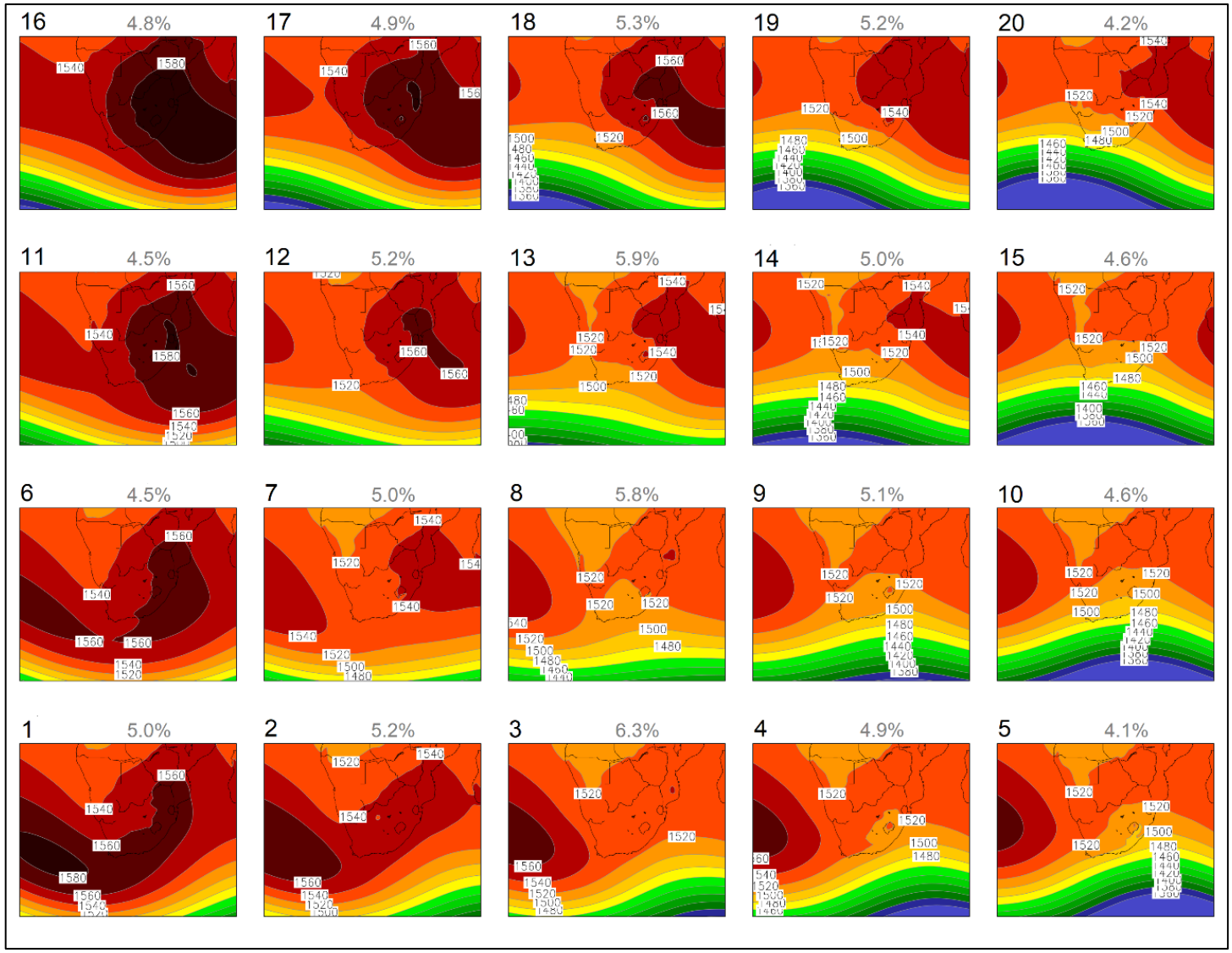

Figure 8.6 **Kohonen map or master SOM depicting fire season archetypal 850 hPa geopotential height patterns for the period 1981 – 2010. Nodes are numbered from 1 to 20, while frequencies of occurrence are indicated as percentages above each node.**

Similar archetypes are grouped together with the most unrelated types located at opposite corners of the master SOM (Figure 8.6). The archetypes on the left-hand side are dominated by broad regions of high pressure that progressively builds over the eastern parts of the subcontinent when moving towards the top corner. In contrast, the archetypes displaying deep troughs are clustered on the right of the SOM and become stronger whilst propagating eastwards when scrolling towards the bottom and right of the master SOM. A classic synoptic sequence would see the retreat of the South Indian Ocean High Pressure Cell (IOH) with the eastward propagation of a westerly wave accompanied by a surface cold front, followed by a ridging South Atlantic Ocean High Pressure Cell (AOH). This sequence takes about 7 – 14 days and is illustrated by following the outer panels in Figure 8.6 in clockwise fashion, commencing at node 16. The central panels represent the cases for an established west-coast trough or weaker troughs (or troughs passing far to the south of the country). Although well-developed easterly waves (V-troughs) over Namibia and connections with the middle latitudes in the form of a tropical-temperate trough (TTT) are important synoptic patterns over southern Africa, such systems are not common during the fire season. With the exception of the latter, the 12 archetype pattern SOM attained for MSLP over southern Africa by Lennard and Hegerl (2014) correspond fairly well with the master SOM presented in Figure 8.6.

The frequency of each archetype was determined by mapping the daily z_{850} data to the trained SOM. An even distribution across the whole training data set would result in a node frequency of occurrence of $\frac{1}{20}$ or 5.0%. Although most of the frequencies in Figure 8.6 are not considerably different from the anticipated 5.0%, it can be seen that the most frequently occurring archetype is node 3 (6.3%). This node is dominated by an AOH anchored off the west coast, weak high pressure over the subcontinent, and a frontal trough south-east of the country. The least frequent archetypes are nodes 5 and 20 (4.1 and 4.2%, respectively), associated with different stages of frontal passage.

8.6.2 Synoptic Patterns related to Increased Fire Danger

Results of classifying the daily maximum and mean fire season LFDIs over domain B according to the accepted fire danger rating thresholds (Sections 5.4 and 7.4.2), and recording the number of very dangerous days pertaining to each node in the master SOM for the period 1981 – 2010 are presented in Table 8.3. Note that the spatial mean LFDI values were considerably lower than the maximum values due to the size of the study area and the marked spatial distribution in fire danger found in it (Section 7.4.3). In either case, the ranking shows that the 12 highest ranked nodes occurred along and to the right of the central column in Figure 8.6. These nodes are associated with different intensities and stages of progression in the passage of a westerly wave (and accompanying surface cold front).

This result agrees with the author's experience in the forecasting office. Typically, warm, dry conditions with strong, gusty north-westerly winds are experienced over the south-western part of the study area when a cold front is located over the south-west coast or adjacent interior. Precipitation from air mass thunderstorms ahead of the advancing trough seldom occur during the fire season due to limited moisture. These conditions, which have already been shown to result in extreme fire danger (Section 4.4), gradually shift north- and eastwards as the frontal trough moves east in its passage across the country. Nodes 10 and 15 resulted in the single highest occurrence of very dangerous fire danger days over the central grassland biome according to the spatial mean LFDI, accounting for 28 cases each. These two nodes fit the above scenario and represent well-developed troughs to the west of (node 15), or over the western part of, the study area (domain B). Corresponding results were found by Stipaničev *et al*. (2008) and Vučetić *et al*. (2019) along the Croatian coast where an approaching cold front accompanied by a low level jet was recognized as favourable for the beginning and spread of wildfires.

Table 8.3 **Number of very dangerous fire danger days over the central grassland biome (using the spatial maximum and mean fire season LFDI) pertaining to each node in the master SOM for the period 1981 – 2010. For ease of comparison the nodes are ranked in order of descending number of occurrences.**

Node	Maximum		Mean	
	Occurrences	Rank	Occurrences	Rank
1	93	17	1	17.5
2	124	15	5	12.5
3	223	2	14	6
4	188	9	11	8
5	186	10	11	8
6	91	18	0	19.5
7	137	14	1	17.5
8	205	6	8	10.5
9	216	4	17	5
10	220	3	28	1.5
11	72	20	4	14
12	150	13	2	15.5
13	198	7	8	10.5
14	209	5	20	4
15	225	1	28	1.5
16	75	19	0	19.5
17	115	16	2	15.5
18	172	12	5	12.5
19	197	8	11	8
20	182	11	22	3

8.7 CONCLUDING REMARKS

SOMs have been employed successfully by numerous researchers to link noteworthy weather phenomena to specific synoptic weather patterns. Knowledge of the large-scale weather systems that typically give rise to hazardous conditions is a crucial part of the weather forecasting endeavour. This methodology was applied in this chapter to determine the archetypal synoptic patterns of the 850 hPa geopotential heights over southern Africa from reanalysis data. Subsequently, spatial means and maxima of the fire season LFDI over the central grassland biome were classified according to the accepted climatological thresholds and the number of occurrences of very dangerous (i.e. “very high” and “extreme”) fire danger days pertaining to each SOM node determined for the climatological standard normal base period of 1981 – 2010.

The results revealed a pattern of archetypical synoptic patterns ranging from well-developed westerly waves (and accompanying surface cold fronts) to high pressure systems dominating the subcontinent during the fire season. The highest number of very dangerous days were clearly linked to the warm, dry and windy

conditions typically experienced ahead (i.e. east) of a well-developed frontal trough that is making its way across the country. This finding concurs and formalises local forecaster experience and will allow aspirant fire weather forecasters to better predict hazardous fire weather conditions over the central grassland.

CHAPTER 9

PROJECTED IMPACTS OF CLIMATE CHANGE ON THE FIRE REGIME

Climate change and variability is expected to have a profound impact on wildland fire regimes. This view is echoed by several researchers (e.g. Williams *et al*., 2001; Flannigan *et al*., 2000; 2013; Kitzberger & Veblen, 2003; Moriondo *et al*., 2006; Krawchuk *et al*., 2009a; Mori & Johnson, 2013; Dennison *et al*., 2014; Huang *et al*., 2015; Wu *et al*., 2015). The scale of impact may vary regionally in accordance with the direction and magnitude of change or relative importance of the individual factors (Bedia *et al*., 2015), while their interplay may sometimes obscure the link with climate and fire weather (Wu *et al*., 2015). From the literature (Fosberg *et al*., 1993; Lindesay, 1997; Flannigan *et al*., 2000, 2005; Hoffmann *et al*., 2003; Vučetić *et al*., 2006; Podur & Wotton, 2010; Litschert *et al*., 2012; Wastl *et al*., 2012; de Groot *et al*., 2013; Matthews *et al*., 2014; Mitchell *et al*., 2014; Wu *et al*., 2015) it seems that the main issues pertaining to climate change - fire interactions are:

- Changes in fire weather due to climate change;
- Effects of climate change on biomes / ecoregions (and by implication, fuels);
- Changes in fire regimes due to climate change; and
- Effects of biomass burning on the regional or global climate due to local changes to the land surface characteristics (e.g. albedo and fluxes of heat and moisture), vegetation-climate feedbacks and/or alterations to the atmospheric chemistry (e.g. pyrogenic emissions of CO_2 or BC).

While some of the issues mentioned above were already dealt with in Chapter 3, this section will attempt to summarise the main impacts of climate change on wildland fires from the available literature. The discussion will be split according to historically observed impacts (Section 9.1.1) and those projected for future time periods (Section 9.1.2).

9.1 HISTORICAL IMPACTS OF CLIMATE CHANGE ON WILDLAND FIRES FROM THE LITERATURE

There is broad consensus that the area, frequency and intensity of wildland fire has generally been increasing over all vegetated continents during the last few decades (e.g. Kasischke & Turetsky, 2006; Westerling & Bryant, 2008; Bowman *et al*., 2009; Goldammer *et al*., 2009; Hu *et al*., 2010; Montiel & Herrero, 2010; Carvalho *et al*., 2011; Dennison *et al*., 2014; Calder *et al*., 2015; Jolly *et al*., 2015; Liu *et al*., 2015; Prichard *et al*., 2017). There is, however, considerable spatial variability with certain areas indicating no detectable changes or even slight decreases (e.g. Bergeron & Flannigan, 1995; Flannigan *et al*., 2000; 2001; 2009; Krawchuk *et al*., 2009a). When considering the more recent past (i.e. last 100 years or so), some regions have a unique history of fire suppression and land-use land cover (LULC) changes which may conceal interpretations of fire-climate interactions (Hessl, 2011). Therefore, paleo-environmental data are also considered.

Any changes in fire regime may correspond with noteworthy and far-reaching impacts to local ecosystems, atmospheric chemistry and air quality as well as human safety, livelihoods and local economies (Chapter 3). The perceived worldwide changes in wildland fire activity can be attributed to the following factors (Amiro *et al*., 2001; Pausas *et al*., 2008; Flannigan *et al*., 2009; Goldammer *et al*., 2009; Krawchuk *et al*., 2009a; Montiel & Herrero, 2010; Kloster *et al*., 2012; Flato *et al*., 2013; Liu *et al*., 2014):

- LULC changes and landscape fragmentation, which could have resulted from increased land clearing for croplands or pastures (e.g. slash-and-burn agriculture or the establishment of sugarcane, palm oil and other cash crops in South America, sub-Saharan Africa and Southeast Asia), urbanization and rural abandonment (e.g. increased wildland-urban interface (WUI), decreased land cultivation, reduced utilization of vegetation resources, increased fuel loads and hence more severe and often uncontrollable fires in Iberia), or encroachment by invasive plant species;
- Factors affecting ignition agents and probabilities (e.g. population density);

- Advances in fire prevention and/or suppression;
- Shifts in policy paradigms related to wildfire management (e.g. fire exclusion), including political and socio-economic turmoil which drives ecosystem impoverishment and inhibits certain countries' capacities to employ efficient wildland fire management (e.g. central Asia); and
- Climate change which includes both increased climate variability and a shift towards conditions more favourable for wildfire occurrence, as well as climate-induced changes in vegetation characteristics.

Studies suggesting that historical changes in wildland fire regimes can be attributed to observed changes in the climate abound, with Table 9.1 attempting to summarise some of these. The fire history records used in these studies came from a variety of sources, including:

a) Charcoal, black carbon or chemical tracers of fires preserved in lake and ocean sediment cores (e.g. Lynch *et al*., 2007; Bal *et al*., 2011; Fletcher & Moreno, 2012);
b) Charcoal, black carbon or chemical tracers of fires deposited in soils and other depositional environments such as loess and paleosols (e.g. Wang *et al*., 2012) or ice cores (e.g. Eichler *et al*., 2011; Wang *et al*., 2010; 2015);
c) Fire-scarred tree rings (e.g. Kharuk *et al*., 2008; Swetnam *et al*., 2009; Meunier *et al*., 2014);
d) Documented fires (e.g. Lara *et al*., 2003; Forsyth & Van Wilgen, 2008; Moreno *et al*., 2014);
e) Remotely sensed satellite observations (e.g. Heinl *et al*., 2007; Dennison *et al*., 2014; Alvarado *et al*., 2017); and
f) FDIs calculated from standard meteorological observations or reanalysis data (e.g. Wastl *et al*., 2012; Fernandes *et al*., 2014; Jolly *et al*., 2015).

These sources of historical information on wildland fire activity cover a whole range of spatial and temporal scales. Time series obtained from sediment cores offer the opportunity to study regional fires on centennial to multi-millennial time scales,

dendrochronological reconstructions provide annually resolved information over the last few centuries in particular forests, while satellite observations document global fire activity on hourly to monthly time scales over the last few decades (Power *et al*., 2010; Kehrwald *et al*., 2013).

Common themes that emerged from the studies that focused on historical wildland fire-climate interactions across the globe (Table 9.1) included:

a) Fire activity is not universally higher today than in the distant past (e.g. Bergeron *et al*., 2004; Whitlock *et al*., 2006; Calder *et al*., 2015; Bal *et al*., 2011; Eichler *et al*., 2011);
b) Fire regimes respond rapidly to abrupt changes in climate (e.g. Grissino-Mayer & Swetnam, 2000; Lynch *et al*., 2007; Wang *et al*., 2012; Calder *et al*., 2015);
c) Climate change has the potential to influence the frequency, severity, extent and seasonal duration of wildfires (e.g. Moreno *et al*., 2014; Marlon *et al*., 2013; Jolly *et al*., 2015);
d) Fire activity exhibits strong inter-annual variability, while changes in fire regime vary considerably from one region to another (e.g. Mouillot & Field, 2005; Groisman *et al*., 2007; Marlon *et al*., 2013);
e) The most dominant climatic elements affecting historical fire activity are air temperature and precipitation (e.g. Huber & Markgraf, 2003; Higuera *et al*., 2010; Pechony & Shindell, 2010; Daniau *et al*., 2012; Litschert *et al*., 2012; Jolly *et al*., 2015; Carter *et al*., 2017); and
f) Fire has an important role to play in vegetation-climate feedbacks (e.g. Whitlock *et al*., 2006; Kharuk *et al*., 2008; Higuera *et al*., 2010).

It is worthwhile to elaborate here on the second last point (e) listed above. Historical records revealed an increase in fire activity during warm periods and reduced activity in cold ones (Bowman *et al*., 2009). In boreal and alpine environments increased temperatures have resulted in a prolonged growing season with higher fuel accumulation, a longer snow-free season, drier fuels and subsequently larger burned areas (Westerling *et al*., 2006; Heyerdahl *et al*., 2008; Hessl, 2011). In

some regions (e.g. parts of Canada and northern Europe) warming was probably offset by enhanced precipitation so that fire frequency remained relatively unchanged or actually decreased (Van Wagner, 1988; Bergeron *et al*., 2004; Hessl, 2011; Wallenius *et al*., 2011). Although warmer and drier conditions are generally considered to lead to increased fire activity (Section 4.2), the immense spatial variability of climate change and of fire environment types prevents such generalisations (Williams *et al*., 2001).

Precipitation seems to play a larger role than temperature in determining global fire activity (Pechony & Shindell, 2010). A mounting body of evidence supports a varying sensitivity of fire occurrence (i.e. frequency) to moisture-related variables along a vegetation productivity gradient (e.g. Meyn *et al*., 2007; Nitschke & Innes, 2008; Prasad *et al*., 2008; Van der Werf *et al*., 2008; Westerling & Bryant, 2008; Krawchuk & Moritz, 2011; Daniau *et al*., 2012; Batllori *et al*., 2013; Flannigan *et al*., 2013). In relatively wet subtropical or tropical biomes with medium to high long-term net primary productivity, the abundance of biomass is always sufficient for large fires to spread (Krawchuk & Moritz, 2011). In such biomass-rich areas the foremost constraint during the fire season is the fuel flammability which is a function of fuel moisture content, so that dry periods become a strong driver of wildfire activity (Meyn *et al*., 2007; Van der Werf *et al*., 2008; Krawchuk & Moritz, 2011). Such fire regimes are also referred to as energy-limited as large fires can only occur once enough energy is available to dry out the abundant fuels (Westerling & Bryant, 2008). Conversely, in biomass-poor regions where resources are more limited or variable (e.g. deserts, xeric shrublands or grasslands), the importance of fuel moisture on wildfire activity is eclipsed by the availability and continuity of burnable fuels (Meyn *et al*., 2007; Krawchuk & Moritz, 2011). Cumulative precipitation during the growing season preceding the fire season therefore becomes a stronger driver of wildfire activity in fuel-limited areas (Swetnam & Baisan, 1994; Crimmins & Comrie, 2004; Pausas, 2004; Van der Werf *et al*., 2008; Krawchuk & Moritz, 2011). Such fire regimes are also referred to as moisture-

limited as large fires can only be sustained once antecedent moisture has resulted in increased fuel loads (Westerling & Bryant, 2008).

This implies that fire regimes are governed by both the direct effects of climate on fire weather conditions and fuel moisture linked to scales of days to months, as well as indirect effects on fuel accumulation and continuity associated with a longer climate memory (Swetnam & Baisan, 1994; Heyerdahl *et al*., 2008; Hessl, 2011; Krawchuk & Moritz, 2011). This explains the large spatial variability and sometimes contradicting findings emanating from wildland fire - climate change studies. Under relatively wet conditions, an increase in precipitation will result in decreased fire activity, whereas prolonged dry spells would have the opposite effect. At the same time, under relatively dry conditions, an increase in precipitation could result in increased fire activity as excess moisture leads to the growth of additional vegetation that can quickly dry out during the fire season (Turner *et al*., 2008; Westerling & Bryant, 2008; Daniau *et al*., 2012; 2013). It is also suggested that the timing of precipitation during the fire season (affecting fuel moisture) is just as important as the actual amount (affecting fuel load) (Flannigan *et al*., 2009; Archibald *et al*., 2010b). In some instances, minor increases in precipitation amounts could be offset by enhanced evapotranspiration over land owing to rising air temperatures (Stocks *et al*., 1998).

Jolly *et al*. (2015) provided a global analysis of trends in fire season length from 1979 to 2013 (Figure 9.1). Noteworthy increases in fire season length and a commensurate proliferation in long fire weather seasons (red shading in Figure 9.1) were found in parts of Alaska, the western U.S.A. and Florida, western Mexico, north-east Brazil, parts of Argentina (Gran Chaco and Patagonia), the western Mediterranean region, East Africa, Persia, eastern Asia and parts of Australia (Cape York and Eyre Peninsulas). At the same time fire weather seasons have shortened and became less frequent (blue shading in Figure 9.1) in parts of Canada (western Cordillera, Manitoba and Ontario), the Andes region of western

South America, parts of Scandinavia, West Africa, the Kalahari, central Asia, southern India (Tamil Nadu) and northern Western Australia.

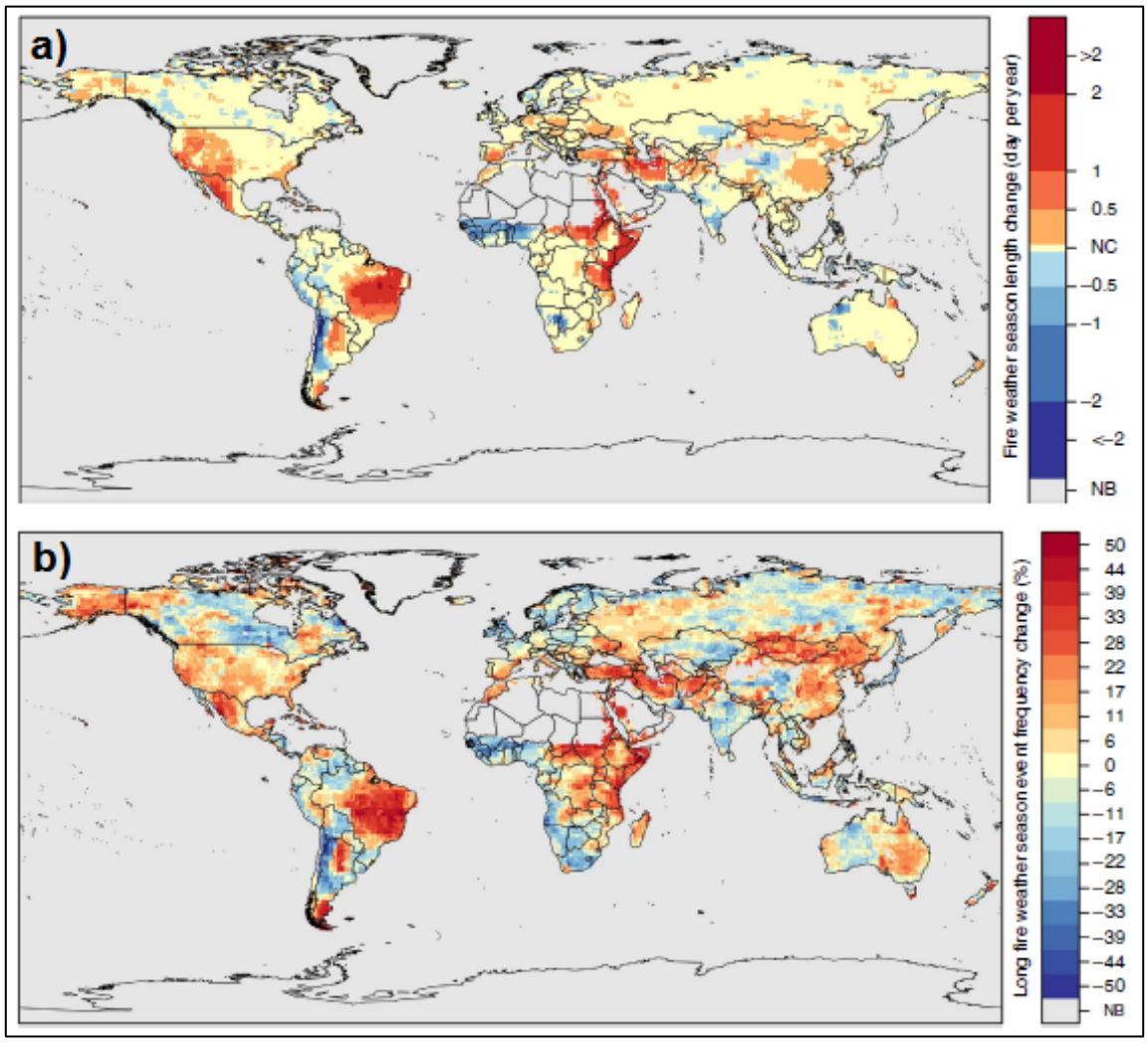

Figure 9.1 **Global pattern of (a) trends in fire season length for the period 1979 – 2013; and (b) changes in the number of long fire weather seasons (> 1σ above historical mean) during the second half of the study period (1996 – 2013) relative to the first half (1979 – 1996). NC denotes areas with no significant change and NB those with little or no burnable vegetation (Jolly *et al*., 2015).**

Table 9.1 Summary of key findings from studies that focused on perceived historical wildland fire-climate interactions across the globe (ordered according to world region and date of publication)

Area	Period	Relevant key findings	Reference
Africa			
Sub-Saharan western Africa	past million years	fire incidence was low until about 400 000 years ago; since then intense fire episodes occurred with climate changing from interglacial to glacial; a peak in the present interglacial is unique in the past million years suggesting human influence	Bird & Cali (1998)
Africa	1981 – 1991	time period too short for any realistic findings	Barbosa *et al*. (1999)
Kruger National Park, South Africa	1941 – 1996	median fire return interval under prescribed burning of 3.1 (1.8 – 4.6) years, with longer returns in drier areas and becoming much longer after adopting a lightning fire policy; most fires occurred from September to November; significant relationship between burnt area and preceding 5 year annual rainfall	Van Wilgen *et al*. (2000)
Grassland and savanna regions, South Africa	past 190 000 years	no particular period during which fires were regionally more prevalent, although burning occurred commonly	Scott (2002)
Southern Okavango Delta, Botswana	1989 – 2003	annual extent of burned area fluctuated considerably; no increase in fire activity was detected	Heinl *et al*. (2007)
Tropical Africa	1981 – 1999	lagged SOI is a good predictor for burned area	Riaño *et al*. (2007)
Table Mountain National Park, South Africa	1970 – 2007	decrease in mean fire return interval from 31.6 to 13.5 years; in the last two decades the area subjected to short (≤ six years) intervals between fires covered > 16% of the park	Forsyth & Van Wilgen (2008)
Southern Africa	2000 – 2008	increase of 6.9% in the area burnt for every 10 mm change in monthly accumulated rainfall index; increase in annual burned area by 2.3% for a 10% increase in seasonality of rainfall; effect of climate in driving variation is limited by human impact	Archibald *et al*. (2010b)
Northern Kruger National Park, South Africa, and Limpopo National Park, Mozambique	past 1 500 years	peaks in fire activity at Mapimbi about every 200 years between 1440 and 1860, every 20 – 30 years during the last 140 years and a fire return interval of 10 years in the last 50 years; peak intervals at Chixuludzi of about 20 years before 1000 and 130 – 200 years thereafter; return intervals at Chinyangani of 20 years since the 1950s and 80 years before then	Ekblom & Gillson (2010)
Kavango-Zambezi Transfrontier Conservation Area	2000 – 2010	increase in fire frequency of eastern Caprivi and north-eastern Botswana (particularly in September), across all land-use categories and irrespective of the fire management policy; significant change in fire seasonality in Caprivi due to an altered burn program	Pricope & Binford (2012)
Cederberg Mountains, South Africa	past 15 600 years	decrease in fire activity between 15 400 – 14 500 years ago (highest fire frequency), and increase after 1 900 years ago; fire frequency might have triggered shifts in fynbos species composition	Valsecchi *et al*. (2013)
South Africa	2003 – 2013	increase in annual fire frequency in all provinces except for a slight decrease in Mpumalanga; highest fire frequency occurs in grasslands	Strydom & Savage (2016)
Mount Kenya, central Kenya	2000 – 2015	increase in inter-annual variability but no clear trend in burned area; seasonality appears to have shifted from a bimodal to a unimodal pattern	Downing *et al*. (2017)
KwaZulu-Natal midlands, South Africa	1960 – 2015	decrease in annual average LFDI over the last two decades at two of the three sites considered (viz. Cedara and Ukulinga); overall earlier onset to the fire season and an attendant increase in fire season duration	Strydom & Savage (2017)

Area	Period	Relevant key findings	Reference
Asia			
Northern Eurasia	1936 – 2000	significant increases in fire danger over the eastern half of northern Eurasia and a decrease to the west of the Urals	Groisman *et al*. (2007)
Central Siberia, Russia	1800 – 2000	increasing number of fires in the 20th century; decrease in fire return intervals (FRI) in 20th century (compared to 19th century) with larger reductions in the south; fire number deviation is strongly correlated with summer temperature anomaly; wildfires cause a 3 to 5 fold increase in seasonal thawing depth of permafrost	Kharuk *et al*. (2008)
Belukha glacier, southern Siberia, Russia	past 750 years	exceptionally high forest-fire activity between 1600 – 1680 following an extremely dry period; no significant increase in biomass burning during the last 300 years	Eichler *et al*. (2011)
Loess Plateau, China	past 27 500 years	decrease in fire frequency since the Last Glacial Maximum (22.3 to 14.6 ka ago) with an increase after 4 ka ago; high fire activities coincide with the Younger Dryas, Older Dryas, Heinrich events and Greenland stadials, suggesting a rapid response of regional fires to abrupt climate changes; periodicities of 1 620 and 1 040 years match the cyclicity of the East Asian monsoon	Wang *et al*. (2012)
Mt. Muztagh Ata, Eastern Pamirs, China	1875 – 2000	levoglucosan/rBC ratio revealed a substantial increase in wildfires in western Siberia and/or Central Asia in 1940s – 1950s	Wang *et al*. (2015)
Australasia			
Southeast Australia	1970 – 2007	rapid increase in annual cumulative FFDI of 10 – 40% between 1980 – 2000 and 2001 – 2007 at many locations, with associated jumps in the number of very high and extreme fire danger days	Lucas *et al*. (2007)
Australia	past 250 000 years	on a glacial timescale burning is facilitated during periods of climate change and environmental instability; burning has increased progressively over the past few hundred thousand years with major accelerations around the time of first human settlement of the continent and with the arrival of Europeans	Lynch *et al*. (2007)
Europe			
Eastern Spain	1941 – 1994	increase in mean fire hazard index values and in the number of very high risk days; increase in number of wildfires and burned area	Piñol *et al*. (1998)
Eastern Iberian Peninsula	1874 – 2000	increase in annual number of fires and area burned during the last century; area burned is positively correlated with summer rainfall of two years earlier	Pausas (2004)
Eastern Mediterranean	past 20 000 years	the main factor controlling the timing of regional fire activity during the Mid-Holocene and the last Glacial-Interglacial climatic transition, was climatically-induced variation in biomass availability; periodicity of ~1500 years	Turner *et al*. (2008)
Southern Europe	1986 – 2005	average annual number of forest fires increased by 34%, while the average area burnt annually decreased by 19%	Miranda *et al*. (2009)
Central Pyrenees, Spain	past 3 300 years	higher frequencies of fire occurrence between 2900 – 2650 and 1850 – 1550 years ago, generally decreasing thereafter	Bal *et al*. (2011)
Spain	1968 – 2010	upward changes were detected in both the number of fires and burned area in all regions and seasons in the 1970s, while downward changes were mostly observed from the 1990s to the present in the Mediterranean region and in the vegetative season of the northwest and the interior regions	Moreno *et al*. (2014)
European Alps	1951 – 2010	increase in fire danger in the Western and Southern Alps; decrease in return period of extraordinarily high index values, especially in the Western and Southern Alps	Wastl *et al*. (2012)

Area	Period	Relevant key findings	Reference
Public forests, Portugal	1943 – 2011	increase in fire weather (i.e. FWI); upward shifts in burned area in 1952 and 1973	Fernandes *et al*. (2014)
North America			
Canada	1918 – 1986	a decreasing trend in annual area burned at the beginning of the period, followed by a sharp rise since the mid-1970s	Van Wagner (1988)
Yellowstone National Park, U.S.A.	1895 – 1990	significant correlation between observed variations in burn area and variations in climate; increased aridity (due to higher temperature and reduced precipitation) suggests a trend toward conditions that favour more wildfires	Balling *et al*. (1992)
South-western U.S.A.	1700 – 1900	variation in fire regime patterns determined by gradients of elevation, forest type and drought fluctuations; shorter fire return periods at drier sites	Swetnam & Baisan (1994)
El Malpais National Monument, south-western U.S.A.	1700 – 1992	fire frequency was high during a relatively dry period from 1700 – 1790 and decreased in the wetter period thereafter with a shift in fire season from mainly midsummer to late spring	Grissino-Mayer & Swetnam (2000)
Central Yellowstone National Park, U.S.A.	past 17 000 years	fire frequency was moderate (4 fires/ka) during the last glacial period, reached highest values in the early Holocene (>10 fires/ka) and decreased after 7 000 years ago	Millspaugh *et al*. (2000)
Boreal forest, Canada	1700s – 1999	decrease in fire frequency from the pre-industrial era to the present for many sites	Bergeron *et al*. (2004)
Canada	1920 – 1999	pronounced upward trend in area burned by large fires since 1970s	Gillett *et al*. (2004)
Boreal region, North America	1959 – 1999	increase in large fire (>1 000 km^2) events and annual burned area, particularly in the west; decrease in fraction of total burned area attributed to human-ignited fires; increased burning during the early and late growing season	Kasischke & Turetsky (2006)
Western U.S.A.	1970 – 2003	large wildfire activity increased considerably in the mid-1980s, becoming more frequent and lasting longer with an increase in fire season length	Westerling *et al*. (2006)
Pacific Northwest, U.S.A.	1905 – 2000	increased tendency for forest fires in warm-phase Pacific Decadal Oscillation years, which is then correlated to annual burn area; little relationship to ENSO; Palmer Drought Severity Index correlated with burn area	Keeton *et al*. (2007)
Boreal forest, North America	1918 – 2005	increase in frequency of large fire years and area burned in Canada during the last four decades of 20^{th} century; large-scale climatic patterns (ENSO/PDO and/or AO) are strongly related to the area burned	Fauria & Johnson (2008)
Interior Oregon, Washington, U.S.A. and southern British Columbia, Canada	1651 – 1900	more than half of the highly synchronous fire years transpired under a northwest-southwest dipole in summer PDSI; ENSO and PDO were weak drivers of regionally synchronous fires	Heyerdahl *et al*. (2008)
Sequoia National Park, U.S.A.	past 3 000 years	maximum fire frequency during the warm and drought-prone period from 800 – 1300; significant multi-decadal association between fire and the Palmer Drought Severity Index (PDSI)	Swetnam *et al*. (2009)
Yellowstone National Park, U.S.A.	1240 – 1975	area burned was significantly higher during periods of extreme annual drought; widespread burning occurred in 1240, 1540 and 1700, at 150 – 300 year intervals	Higuera *et al*. (2010)
Alaskan tundra, U.S.A.	past 5 000 years	large fires are rare in tundra, yet several large fires occurred during the late glacial period and the past 60 years; climatic conditions linked to the unprecedented 2007 fire were exceptional; 95% of the inter-annual variability in area burned is explained by June – September temperature and precipitation	Hu *et al*. (2010)
Northwest Canada	1630 – 2000	decrease in the occurrence of forest fires; decrease in average annual burned area from 2.0% in the first half of the 19^{th} century to 0.33% in the latter half of the 20^{th} century	Wallenius *et al*. (2011)

Area	Period	Relevant key findings	Reference
Seney National Wildlife Refuge, Michigan, U.S.A.	1700 – 1983	increase in fire activity at the turn of 20th century	Drobyshev *et al*. (2012)
Southern Rockies Ecoregion, U.S.A.	1930 – 2006	overall increase by two orders of magnitude in the annual number of fires recorded and in the number of large fires since 1970	Litschert *et al*. (2012)
Western U.S.A.	1984 – 2011	increase in number of large fires (7 p.a.) and total large fire area (355 km^2 p.a.), notably in the southern and mountain ecoregions and in accordance with increasing drought severity	Dennison *et al*. (2014)
Northern Mexico	1650 – 2010	from 1 650 to 1 886 fires occurred during drought years, with little influence of climate in antecedent years; from 1887 to 2003 drought in the year of fire became generally unimportant and fires instead occurred following wet years	Meunier *et al*. (2014)
Northern Quebec, Canada	past 7 000 years	increase in fire occurrence from 7 000 to reach a maximum between 4 000 – 3 000 years before present, and decreasing thereafter	Oris *et al*. (2014)
Montane forests of the Colorado Front Range, Western U.S.A.	1597 – 1995	merely 16% of the study area showed a shift towards more severe fires; recent large wildfires in the Front Range are not fundamentally different from similar events that occurred historically under extreme weather conditions	Sherriff *et al*. (2014)
Mogollon Rim, south-western USA	1940 – 2011	increasing number of wind driven fires and maximum run lengths, especially since the 1980s	Swetnam (2014)
Western U.S.A.	1984 – 2012	increasing trends in area burned by high-severity fires found in only 4 of 43 analysis regions	Baker (2015)
Colorado Rockies, western U.S.A.	past 2 000 years	a dramatic increase in fire activity during the Medieval Climate Anomaly (MCA) compared to the period before and after	Calder *et al*. (2015)
Continental U.S.A.	1980 – 2013	overall increase in the length of fire seasons in 11 western states, as well as Texas, Oklahoma and Alaska	Hamilton (2015)
Rocky Mountains, U.S.A.	past 1 500 years	elevated fire occurrence around 1 350 and 900 years ago, as well as the 20th century, linked to periods of protracted drought and higher temperature; greatest increase in wildfire activity at mid-elevations during the 20th century; increase in number of large wildfires and area burned over the last few decades	Carter *et al*. (2017)
South America			
Central Chile	1976 – 1999	increase in number of wildfires, but large fluctuation in area burned annually	Aravena *et al*. (2003)
Rio Rubens Bog, southern Argentina	past 12 700 years	abrupt increase in fire occurrence between 11 700 – 7 500 years ago, and again after 400 years ago	Huber & Markgraf (2003)
Northern Patagonia, Argentina	1599 – 1989	increase in the mean number of sites recording fire during the five driest years, with little or no fire occurrence during the five wettest single years; increase of about 3x in the rate of lightning ignitions after 1978; years in which the southeast Pacific subtropical anticyclone is more intense and located further south are years of greater drought and fire	Kitzberger & Veblen (2003)
Lake Region, Chile	1979 – 1999	no significant trend in forest area burned annually, with drier summers during fire years	Lara *et al*. (2003)
Eastern side of the Andes, Argentina	past 16 000 years	increase in fire activity between 13 250 – 11 400 years ago; a shift to a surface-fire regime occurred between 7 500 – 4 400 years ago; decrease in fire frequency in recent centuries	Whitlock *et al*. (2006)
Laguna San Pedro, southern Chile	past 1 500 years	increase in fire activity between 1 500 – 1 300 and 1 000 – 725 years ago	Fletcher & Moreno (2012)
Cordón Serrucho Norte, Argentina	past 17 500 years	increase in fire frequency between 11 200 – 7 000 and after 3 000 years ago	Markgraf *et al*. (2013)

Area	Period	Relevant key findings	Reference
Isla Grande de Chiloé, Chile	past 17 800 years	enhanced fire activity between 0.8 – 2, 4 – 4.3, 8 – 11 and 16.1 –17.8 ka	Pesce & Moreno (2014)
Chile	1984 – 2016	significant increase in the number of fires at the national level, but no statistically significant changes in burnt area	Úbeda & Sarricolea (2016)
Serra do Cipó region, south-eastern Brazil	1984 – 2014	strong inter-annual variation in burned area; general decrease in burned area and the frequency of very short return intervals	Alvarado *et al*. (2017)
Global			
Global	1900 – 2000	general decrease in burned area at higher latitudes (with some evidence of an increase in temperate forests near the end of the 20th century), but increases in the tropics	Mouillot & Field (2005)
Global	1996 – 2006	high sensitivity of global fire activity to ENSO events, particularly in tropical forests	Le Page *et al*. (2008)
Global	past 21 000 years	less-than-present fire activity during the last deglaciation (21 – 11 ka) in North America, Europe and southern South America; greater-than-present fire activity from 19 – 17 ka in tropical latitudes of South America and Africa; greater-than-present fire activity from 16 – 13 ka in Indochina and Australia	Power *et al*. (2008)
Global	1960 – 2000	significant increase in emissions from wildfires due to the increasing importance of forest and peat soil burning	Schultz *et al*. (2008)
Global	850 – 2003	until the late 18th century global fire activity was primarily climate-driven (i.e. little anthropogenic influence); changes in global precipitation played a larger role than those in temperature in determining global fire activity variations; sharp increases in biomass burning from the 19th century, mainly due to direct anthropogenic activities; sharp downturn in global fire activity around 1900 due to increased fire suppression and decreased vegetation density	Pechony & Shindell (2010)
Southern Hemisphere	past 650 years	biomass burning decreased by roughly 50% in the 1600s, increased by roughly 100% by the late 1800s, and decreased again by about 70% from the late 1800s to present day	Wang *et al*. (2010)
Global	past 22 000 years	general rapid increase in biomass burning during the last deglaciation (14 – 10 ka), where after it continued to increase more slowly in the NH throughout the Holocene, while initially decreasing in the SH	Daniau *et al*. (2012)
Global	past 12 000 years	general global increase in fire activity during the Holocene; neither changes in human populations nor changes in land use are sufficient to explain the biomass burning record at regional and continental scales during the Holocene; widespread increase in fire from 3 – 2 ka ago (except Australasia); general decrease in burning during the past century in many areas, but there were also large increases (e.g. Australia and parts of Europe)	Marlon *et al*. (2013)
Global	1979 – 2013	fire season length increased by ~19% across 25% of the Earth's vegetated surface, while the global burnable area affected by long fire weather seasons doubled	Jolly *et al*. (2015)
Global	past 22 000 years	general increase in biomass burning during last 21 ka, consistent with warming, increasing CO_2 concentrations and fuel availability; sharp increase in global fire activity during the past several decades, with higher charcoal fluxes in the northern hemisphere than during the past 22 ka	Marlon *et al*. (2016)

9.2 FUTURE IMPACTS OF CLIMATE CHANGE ON WILDLAND FIRES FROM THE LITERATURE

To date, research on the potential future impact of climate change on fire activity is fairly unevenly distributed across the world with a relative abundance of literature focusing on North America, Europe and Boreal Asia, with a scarcity of studies concentrating on Africa, Australasia, South America and the remainder of Asia (Table 9.2). Such studies generally appeared around 1990 (Brown *et al*., 2004; Hessl, 2011) and typically employ GCMs to simulate contemporary and future climate states under various GHG emission scenarios at scales ranging from regional to global (Section 6.3). Occasionally GCM outputs are used in combination with a Climate Fire Modelling System (CFMS; e.g. Torn & Fried, 1992), carbon-nitrogen biogeochemical model (e.g. Kloster *et al*., 2012), Community Atmosphere Model (CAM; e.g. Ward *et al*., 2012), Fire Economics Simulator (FES; e.g. Fried *et al*., 2008), Dynamic Global Vegetation Model (DGVM; e.g. Balshi *et al*., 2008), Land Surface Model (LSM; e.g. Hoffmann *et al*., 2003) or a multivariate statistical Generalized Additive Model (GAM; e.g. Krawchuk *et al*., 2009b) to help estimate specific features of future fire regimes or their projected impacts.

As pointed out by some of the key findings summarized in Table 9.2, there is considerable spatial variability in the projected worldwide deviations in wildland fire activity, while some of these changes have the potential to occur relatively quickly and be extreme. This is particularly true under the mid-high GHG emission scenarios, emphasizing the need for mitigation and adaptation strategies. Overall, changes in future fire weather play the principal role in altering future fire regimes (Huang *et al*., 2015). The projected warming for the 21st century is expected to increase fuel dryness, reduce relative humidity and create climatic conditions that promote frequent and extensive wildfires, possibly over a lengthened fire season, particularly in those energy-limited regions where precipitation is expected to decrease (Moriondo *et al*., 2006; Aldersley *et al*., 2011). There is a widely held belief that climate variability should increase with climate change, yielding more frequent extreme fire weather events (Moriondo *et al*., 2006; Pearce *et al*., 2011).

Natural ignition probabilities may also escalate in a warmer climate due to more cloud-to-ground lightning discharges (Price & Rind, 1994). In addition, increasing fire activity as a response to climate change constitutes a positive feedback mechanism and will thus result in further changes in climate (Section 3.5).

Climate-driven vegetation change also plays a large role in determining characteristics of future fire regimes, particularly in the spatial fuel distribution and burn pattern, total burned area and rate of spread (Liu & Wimberly, 2016). The effects of climate change on fire occurrence may be overshadowed by the direct effects of human influence in certain geographic regions (Liu *et al*., 2012; Huang *et al*., 2015), particularly where fire suppression becomes very effective in protecting an increasing population and expanding WUI. However, growing pressures on natural resources and accompanying LULC changes also suggest a potential future increase in anthropogenic ignitions (Kloster *et al*., 2012).

Pechony and Shindell (2010) considered the trends in global fire activity projected by the Goddard Institute for Space Studies (GISS) GCM for the period 2004 to 2100 under three different SRES scenarios, relative to a base period spanning 844 to 2000 (Figure 9.2). From their analysis it is clear that there is no uniform global trend in future fire activity. However, the general spatial patterns of changes in biomass burning trends are fairly consistent across emission scenarios, where decreases were shown to be linked primarily to enhanced precipitation. Surprisingly, greater biomass burning is predicted under the milder A1B and B1 scenarios (as opposed to the warmer A2 scenario). This can probably be attributed to the declining population (and hence fire suppression) along with a reversal of land conversion which forms part of these SRES storylines (Pechony & Shindell, 2010). For southern Africa, these projections show a general increase in fire activity over the region with the exception of the A2 scenario which predicts a decrease over the south-eastern parts (Figure 9.2).

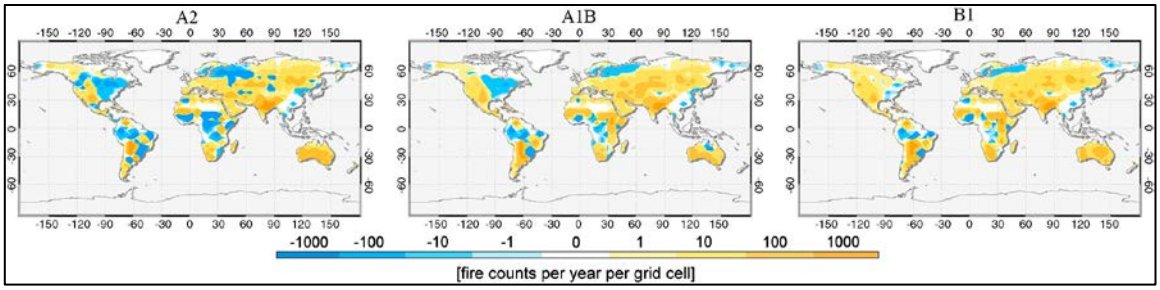

Figure 9.2 **Projected changes in global fire activity over the 21st century under three greenhouse gas emission scenarios (Pechony & Shindell, 2010).**

To highlight the uncertainty associated with such climate predictions, it might be prudent to compare some of the projections for southern Africa obtained by other researchers:

- Scholze *et al*. (2006) also found a weak pattern of decreased fire activity over the south-eastern part and increases over the remainder with a warming of 3°C;
- Krawchuk *et al*. (2009b) found a general decrease in fire-prone pixels under the A2 scenario towards the end of the century, with little/no change over the eastern part of South Africa;
- Liu *et al*. (2010) found a general increase in wildfire potential towards the end of the century under the A2 scenario;
- Moritz *et al*. (2012) indicated a likely increase in fire probability over the south-eastern parts, a likely decrease in the north and south-west, and low model agreement over the central and western parts by the end of the century under the A2 scenario;
- Flannigan *et al*. (2013) found no change in Cumulative Severity Rating (CSR) over the central parts and a general increase over the remainder by 2050, and an increase across the whole region by the end of the century under the A2 scenario;
- Bedia *et al*. (2015) found a general increase in FWI by 2045 under RCP8.5, with the exception of the south-eastern part; and
- Huang *et al*. (2015) found a general decrease in fire activity by 2050, with the exception of the western interior.

Table 9.2 Summary of key findings from studies that focused on projected future wildland fire-climate interactions across the globe (ordered according to world region and date of publication)

Area	Projections used*	Relevant key findings	Reference
Africa			
West Africa	ECHAM (A1B)	under fire suppression: increase in area covered by woodlands / forests in lieu of savannas / grasslands; frequent fires reduce biomass, maintaining it close to current levels	Scheiter & Savadogo (2014)
Asia			
Russia and Canada	CGCM2 HadCM ECHAM CCSM ($1\times CO_2$, $2\times CO_2$)	large increases in areal extent of extreme fire danger; earlier start to the fire season; increases in area experiencing high to extreme fire danger, particularly in June and July	Stocks *et al*. (1998)
Boreal forest, Russia	CGCM2 CCSM 1.4 ECHAM4 / OPYC3 MPI GFDL-R30-c HADCM3 CSIRO Mk2 (all B2)	increase in fire danger by the end of the 21st century; doubling in areas of maximum fire danger risk by middle of the century; maximum changes at the southern forest zone boundary	Malevsky-Malevich *et al*. (2008)
Boreal forest, northeast China	CGCM3 (B1) HadCM3 (A2)	increase in fire occurrence density by 30% (B1) to under 230% (A2) in 2081 – 2100; predicted change in overall fire occurrence density is positively related to the degree of temperature and precipitation change	Liu *et al*. (2012)
Russia	CCSM3 (A2)	decreased mean total biomass across the south-western parts and increases in north-eastern Siberia and along the Amur River border; warming climate and fire create a more complex pattern of height and stand age distribution	Shuman *et al*. (2017)
Australasia			
Australia	CSIRO4 CSIRO9 ($1\times CO_2$, $2\times CO_2$)	widespread increase in fire danger of more than 10%, with smaller changes or even decreases over parts of the northern interior	Beer & Williams (1995)
Australia	CSIRO9 ($1\times CO_2$, $2\times CO_2$)	general increase in fire danger, which is largest on the north-east coast (~30%) and northern NSW and south-east WA (~40%); regional variation in changes in fire season length	Williams *et al*. (2001)
Southeast Australia	CCAM (Mark2, Mark3)	increase in ΣFFDI of 0 – 4% by 2020 under the low scenario and 0 – 10% under the high scenario; by 2050 the increase is 0 – 8% (low) and 10 – 30% (high)	Lucas *et al*. (2007)
Australia	RAMS & CSIRO Mk2 (B2, A2)	general increase in fire risk with probabilities of far higher FDI values under the A2 scenario by 2100	Pitman *et al*. (2007)
Sydney region, Australia	CCAM (Mark2, Mark3)	increase of 20 – 84% in potential large-fire (≥1 000 ha) ignition days by 2050	Bradstock *et al*. (2009)

Area	Projections used*	Relevant key findings	Reference
New Zealand	CGMR CNCM3 CSMK3 ECHOG GFMC20 GFMC21 HADCM3 HADGEM MIHR MPEH5 MRCGCM (all A1B)	increase in fire danger in the east and south of the South Isl. and the west of the North Isl.; unchanged or decreased fire danger across the West Coast of the South Isl. And parts of the North Isl. by the 2080s; a general rapid increase in fire danger to the 2050s, where after it levels off or decrease by the 2080s	Pearce *et al*. (2011)
Tasmania, Australia	CCAM & ECHAM5/MPI-OM GFDL-CM2.0 GFDL-CM2.1 MIROC3.2 UKMO-HadCM3 CSIRO-Mk3.5 (A2)	increase in fire danger, especially in spring and in the east; increase in days of elevated fire danger; overall lengthening of the fire season; highest fire danger days associated with a lee low-pressure system ahead of a cool change	Fox-Hughes *et al*. (2014)
Europe			
Southern Europe (Mediterranean)	HadRM3P (A2, B2)	general increase in fire risk (in terms of number of extreme events and length of fire season) under both scenarios over entire area	Moriondo *et al*. (2006)
Peak District, England	HadCM3 (A1FI, B1)	little change in wildfire incidence in the near future, but an overall increase in summer wildfires from 2070	Albertson *et al*. (2010)
Portugal	HIRHAM (A2 = 2×CO_2)	increase of 478% in area burned (from 1.4% to 7.8% of available burnable area); increase of 279% in fire occurrence; largest increases in northern and central districts	Carvalho *et al*. (2010)
Portugal	MUGCM-MM5 (1×CO_2, 2×CO_2)	increase in length of fire season; increase in FWI values in beginning of summer; increase in total area burned	Carvalho *et al*. (2011)
Iberian Peninsula and Greece	ECHAM5 (A1B)	fire season (JJAS) increases in SSR and FWI90 for the periods 2011 – 2040 (slight) and 2041 – 2070 (large); unrealistic spatial variability, especially for Greece, for the period 2071 – 2100	Bedia *et al*. (2013)
Portugal	MIROC (B1)	increasing risk of fire under future climate conditions, with an increase in mean burnt area of 7% by 2051 – 2080 and 11% by 2071 – 2100; increasing inter-annual variability of the fire regime	Pereira *et al*. (2013)
Europe	MPI-ESM-LR IPSL-CM5A-MR HadGEM2-ES CCSM4 (all RCP2.6, RCP8.5)	increase in burned area at the continental scale with biggest increases under RCP8.5 (~1.8 to 3.6 times) and for eastern Europe	Wu *et al*. (2015)
Corsica, France	seem to have used IPCC's AR5 ensemble mean (RCP6.0)	increase in wildland fire risk due to the possible expansion of xeric and thermophilic vegetation	Garbolino *et al*. (2016)
North America			
Canada	GFDL GISS OSU (1×CO_2, 2×CO_2)	increase of ~46% in SSR and burned area	Flannigan & Van Wagner (1991)

Area	Projections used*	Relevant key findings	Reference
Yellowstone National Park, U.S.A.	GFDL GISS HadCM OSU ($1\times CO_2$, $2\times CO_2$)	increased aridity (due to higher temperature and higher evapotranspiration) suggests a climate-induced increase in fire hazard	Balling *et al*. (1992)
Northern California, U.S.A.	CCFMS & GFDL GISS HadCM ($1\times CO_2$, $2\times CO_2$)	increase in area burned and the frequency of escaped fires; biggest increase in fire severity in grasslands	Torn & Fried (1992)
U.S.A.	GISS GCM 2 ($1\times CO_2$, $2\times CO_2$)	increase of 44% in lightning-caused fires and 78% in area burned	Price & Rind (1994)
Canada	CGCM ($1\times CO_2$, $2\times CO_2$)	decrease in FWI over much of the eastern parts (probably due to a decrease in drought periods), with increases elsewhere	Bergeron & Flannigan (1995)
North America	HADCM2 CGCM ($1\times CO_2$, $2\times CO_2$)	increase of 10 – 50% in SSR over most areas	Flannigan *et al*. (2000)
Boreal forest, Canada	CRCM ($1\times CO_2$, $2\times CO_2$)	increase of more than 20% in fire weather severity in some parts; increase in area burned	Amiro *et al*. (2001)
Canada	CRCM ($1\times CO_2$, $2\times CO_2$)	decrease in fire danger for some eastern areas, but increase for the remainder of the country	Flannigan *et al*. (2001)
Boreal forest, western Canada	CGCM1 ($1\times CO_2$, $3\times CO_2$)	more severe burning conditions (greater intensity, depth of burn and total fuel consumption) and shorter fire cycles in future; accompanied shift in forest composition with decline in species with no direct fire survival traits	de Groot *et al*. (2003)
Boreal forest, Canada	CGCM1 ($2\times CO_2$, $3\times CO_2$)	decrease in fire frequency compared to pre-industrial level for most sites; increase in burn rate for most sites under both scenarios, but no change or a decrease over some eastern and western parts	Bergeron *et al*. (2004)
Western U.S.A.	PCM IS92a	increase in the number of days with high fire danger by 2089, particularly in the northern Rockies, Great Basin and the Southwest	Brown *et al*. (2004)
Southern California, U.S.A.	GFDLv2 PCM (A2, B1)	end-of-century shift in coastal föhn winds to later (Nov – Dec) in the season, suggesting an increase in extreme fire weather	Miller & Schlegel (2006)
Alberta, Canada	CRCM ($1\times CO_2$, $2\times CO_2$, $3\times CO_2$)	increase in area burned of 12.9% ($2\times CO_2$) and 29.4% ($3\times CO_2$)	Tymstra *et al*. (2007)
Boreal North America (north of 45°N)	DGVM & CGCM2 (A2, B2)	increase in area burned of ~2x western boreal area by 2041 – 2050 and between 3.5 – 5.5x by the end of the 21st century	Balshi *et al*. (2008)
California, U.S.A.	CFES2 & GFDL CM2.1 PCM (A2, B1)	considerable increase in the number of fires that escape initial attack during the 21st century due to subtle shifts in fire behaviour induced by changes in the climate	Fried *et al*. (2008)

Area	Projections used*	Relevant key findings	Reference
California, U.S.A.	GFDL-CM2.1 (B1, A2) PCM (A2)	increase of 9 – 15% in total annual area burned by the end of the century under all scenarios; increase of ~18% in annual biomass consumption by fire under PCM-A2, but under GFDL-A2 and GFDL-B1 it increased initially but then levelled off or even decreased by the end of the century	Lenihan *et al*. (2008)
North Okanagan area, Canada	CGCM1 (IS92a) CGCM2 (A2) HadCM3 (A2)	increase in fire season length (~30%) and fire weather severity (~95%) during summer months by 2070	Nitschke & Innes (2008)
California, U.S.A.	GFDL PCM (A2, B1)	mixed results in the south, but increase of between 12 – 53% in large fire risk over the remainder by the end of the 21st century; GFDL and A2 scenarios exhibited greater increases	Westerling & Bryant (2008)
Boreal forest, Canada	CGCM1 ($1\times CO_2$, $2\times CO_2$, $3\times CO_2$)	increase in area burned by ~33% under $2\times CO_2$ and ~50% under $3\times CO_2$; increase in fuel consumption density by ~34% under $2\times CO_2$ and ~94% under $3\times CO_2$	Amiro *et al*. (2009)
Central-eastern Alberta, Canada	CRCM ($1\times CO_2$, $2\times CO_2$, $3\times CO_2$)	increase of 1.5x and 1.8x in lightning fire initiation and corresponding 1.9x and 2.6x increase in area burned by 2040 – 2049 and 2080 – 2089, respectively	Krawchuk *et al*. (2009a)
Western U.S.A.	GISS GCM 3 (A1B)	increase of 54% in annual mean burned area by the 2050s; largest increases in forested areas	Spracklen *et al*. (2009)
Ontario, Canada	CGCM3 HADCM3 (A1B, A2, B1)	increase in area burned of ~2x by 2040 and ~8x by the end of the 21st century under A2, with smaller increases under A1B and B1 scenarios	Podur & Wotton (2010)
Canada	CGCM1 HADCM3 (A2)	increase in fire occurrence of 25% by 2030 and between 75% (CGCM3) and 140% (HADCM3) by the end of the 21st century across all forested regions	Wotton *et al*. (2010)
Greater Yellowstone, Wyoming, U.S.A.	CCSM3.0 CNRM-CM3.0 GFDL-CM2.1 (A2)	increases in annual area burned and the frequency of regionally synchronous fires; decrease in fire rotation (the time to burn an area equal to the landscape area) from the historical 100 – 300 years to less than 30 years	Westerling *et al*. (2011)
Southern Rockies Ecoregion, U.S.A.	HadCM3 ECHAM5 (A2, B1)	increase in median burned area, particularly under the B1 scenario	Litschert *et al*. (2012)
Contiguous U.S.A.	CCSM-CRCM CCSM-MM5I CCSM-WRFG CGCM3-CRCM CGCM3-RCM3 CGCM3-WRFG GFDL-HRM3 GFDL-RSM GFDL-WRFG HadCM3-HRM3 (all A2)	increase in fire potential in the Pacific coast, Southwest, Rocky Mountains, northern Great Plains and Southeast; increase in inter-seasonal and inter-annual fire potential variability in coastal regions	Liu *et al*. (2013)

Area	Projections used*	Relevant key findings	Reference
Columbia Montane Cordillera Ecoprovince, Canada	HadGEM1 HadCM3 CCSM3.0 MRI-CGCM ECHAM5 MIROC3.2 IPSL-CM4 GISS-EH GFDL-CM2.1 CSIRO-Mk3.0 CGCM3 BCCR-BCM2.0 (all A1B, A2, B1)	increase in the probability of large-scale fires; probability of experiencing catastrophic fires under "average" summer conditions by 2080	Mori & Johnson (2013)
South-eastern U.S.A.	HadCM3-MM5 CCSM-MM5 GFDL-RCM3 (A2, B2)	increase in wildfire danger; increase in high or mixed severity fire occurrences	Mitchell *et al*. (2014)
Longleaf pine ecosystem, south-eastern U.S.A.	CCSM3 GFDL-CM2.1 HadCM3 PCM (all A1FI, B1)	decrease in burned area due to urban growth; urbanization is likely a bigger threat than climate change	Costanza *et al*. (2015)
Western U.S.A.	BCCR-BCM2.0 CGCM3.1(T47) CNRM-CM3 CSIRO-Mk3.0 GFDL-CM2.0 GFDL-CM2.1 GISS-ER INM-CM3.0 IPSL-CM4 MIROC3.2 ECHO-G ECHAM5/MPI-OM MRI-CGCM2.3.2 CCSM3 PCM HadCM3 (all A1B, A2, B2)	indirect climate-driven vegetation change amplify direct climate-driven increase in fire frequency and size and has a larger overall effect on future total burned area	Liu & Wimberly (2016)
South America			
Amazonia	HadCM3 (A1B, A2)	large increase in areas of moderate, high and very high fire danger across entire region, with greatest changes in eastern and central parts	Golding & Betts (2008)
Savanna and shrubland areas, Brazil	RCA4 (RCP4.5)	increase in extreme levels of fire danger, largely due to an increase in maximum temperature	Silva *et al*. (2016)
Amazonia	CARLUC & 35 CMIP5 GCMs (RCP2.6, RCP8.5)	increase in fire intensity, primarily due to increased temperature and secondarily due to reduced precipitation in east; increase in carbon losses of up to 90% per unit area burned	De Faria *et al*. (2017)
Global			
Tropical savannas (Africa, Australia, South America)	LSM (unmodified & modified vegetation) & CCM3.2	increase in fire frequency by 42% due to climatic effects (i.e. warming and positive feedback due to conversion of tropical savanna to grassland)	Hoffmann *et al*. (2002)
Tropical forests (Amazon, Congo, Indonesia/New Guinea)	LSM (undisturbed, 50% clearing, 100% clearing) & CCM3.2	increase in FFDI by 41, 56 and 58%, and increase in fire frequency of 44, 80 and 123% in the Amazon, Congo and Indonesia, respectively	Hoffmann *et al*. (2003)

Area	Projections used*	Relevant key findings	Reference
Global	CNRM-CM3 CSIRO-Mk3.0 GFDL-CM2.0 GFDL-CM2.1 GISS-ER INM-CM3.0 IPSL-CM4 MIROC3.2 ECHAM5/MPI-OM MRI-CGCM2.3.2 PCM HadCM3 (all A1B, A2, B1) GISS-EH (A1B) CGCM3.1 (B1) GISS-AOM (A1B, B1) CCSM3 (A1B, B1)	increased wildfires in most semi-arid regions (including southern Africa, the Sahel, central Australia, central Asia, western U.S.A), south-eastern U.S.A., much of South America and high elevation areas (e.g. Tibetan plateau); reduced fire frequency for some boreal regions (e.g. north-east Canada), tropical west and central Africa and parts of Amazonia	Scholze *et al*. (2006)
Global	GAM & GFDL CM2.1 (A2, B1)	widespread impact of climate change on wildfire with considerable invasion and withdrawal of fire across large areas due to the interplay of temperature and precipitation variables	Krawchuk *et al*. (2009b)
Global	HadCM3 CGCM2 CSIRO NIES (A1FI, A2, B1, B2)	increase in wildfire potential in the U.S.A., South America, central Asia, southern Europe, southern Africa and Australia, especially under A1FI and A2 scenarios; increase in length of fire season by a few months	Liu *et al*. (2010)
Global	GISS (A1B, A2, B1)	rapid increase in fire activity after about 2050 under all three scenarios; the increase is smaller under A2 due to the continued population growth (and increased suppression) and to a lesser extent LULC change	Pechony & Shindell (2010)
Global	CLM-CN & ECHAM5/MPI-OM CCSM (A1B)	increase in fire carbon emissions of 17 – 62% by the end of the century, particularly in SH South America	Kloster *et al*. (2012)
Global	16 GCMs from CMIP3 (A2)	great uncertainty (~54% of the terrestrial globe) in near-term changes in fire probability, particularly at higher latitudes; by the end of the 21st century increases in fire probability over ~62% of the terrestrial globe, while ~20% shows decreases mainly in the tropics	Moritz *et al*. (2012)
Mediterranean-type ecosystems (California and Baja California, Mediterranean Basin, central Chile, Western Cape, southwest and south Australia)	BCCR-BCM2.0 CCSM3 CNRM-CM3 CSIRO-MK3.0 ECHAM5/MPI ECHO-G GFDL-CM2.1 GISS-AOM HadCM3 INM-CM3.0 IPSL-CM4 MIROC3.2 MRI-CGCM2.3.2 PCM (all A2)	substantial variation both among and in regions, while relatively small changes in future climates could translate into drastic and divergent shifts in fire activity; decrease in fire activity over more than half the biome by 2070 – 2099 when warmer, drier conditions are predicted, while increases are expected under a warmer, wetter future	Batllori *et al*. (2013)

Area	Projections used*	Relevant key findings	Reference
Boreal forests of central Russia, western Canada	CGCM3.1 HadCM3 IPSLCM4 (all A1B, A2, B1)	increase in severity of fire weather conditions, particularly in Canada and under the IPSL A2 scenario; changes in the fire regime will affect forest composition	de Groot *et al*. (2013)
Global	CGCM3.1 T47 HadCM3 IPSL-CM4 (all A1B, A2, B1)	worldwide increase in Cumulative Severity Rating (CSR) for all models and scenarios, particularly for the northern hemisphere and towards the end of the 21st century	Flannigan *et al*. (2013)
Global	ACCESS-1.0 GFDL-ESM2G IPSL-CM5A-MR MIROC-ESM MRI-CGCM3 (all RCP4.5, RCP8.5)	highest sensitivity to FWI variability found in areas with historical low mean values; most biomes show very weak positive or even negative anomalies in FWI for both RCPs; increase in FWI over most of southern Africa for both RCPs	Bedia *et al*. (2015)
Global	GISS GCM 3 (A1B, A2, B1)	increase in fire frequencies by ~27% globally; increases in fire occurrence over Amazonia, Australia and Central Russia, while south-east Africa shows a large decreasing trend owing to significant increases in land use and population	Huang *et al*. (2015)

* GCM used with emission scenario(s) in brackets

9.3 PROBLEM STATEMENT AND RESEARCH OBJECTIVE

A probability density function (PDF) can be used to describe the probability of occurrence of values of a climatic variable (e.g. the Gaussian curve in Figure 9.3 for temperature). It is easy to see from Figure 9.3 that a relatively small shift in the PDF can bring about considerable changes in the frequency of extreme events. In light of the discussions in Section 4.2 it is not difficult to imagine how such changes in certain key climatic variables (e.g. temperature, rainfall and wind) can modify the fire regime for some area. Thus, whether driven by natural or human forcings, present and future climate change will result in changes in the probability of the occurrence or severity of wildfires.

From the foregoing literature review it is evident that very few studies have focused on the projected future impacts of climate change on wildland fire in Africa, and southern Africa in particular. A handful of global studies do exist, but they do not focus on a specific biome and their spatial scales are too coarse to paint a clear picture of the possible future changes in the fire regime at a regional scale.

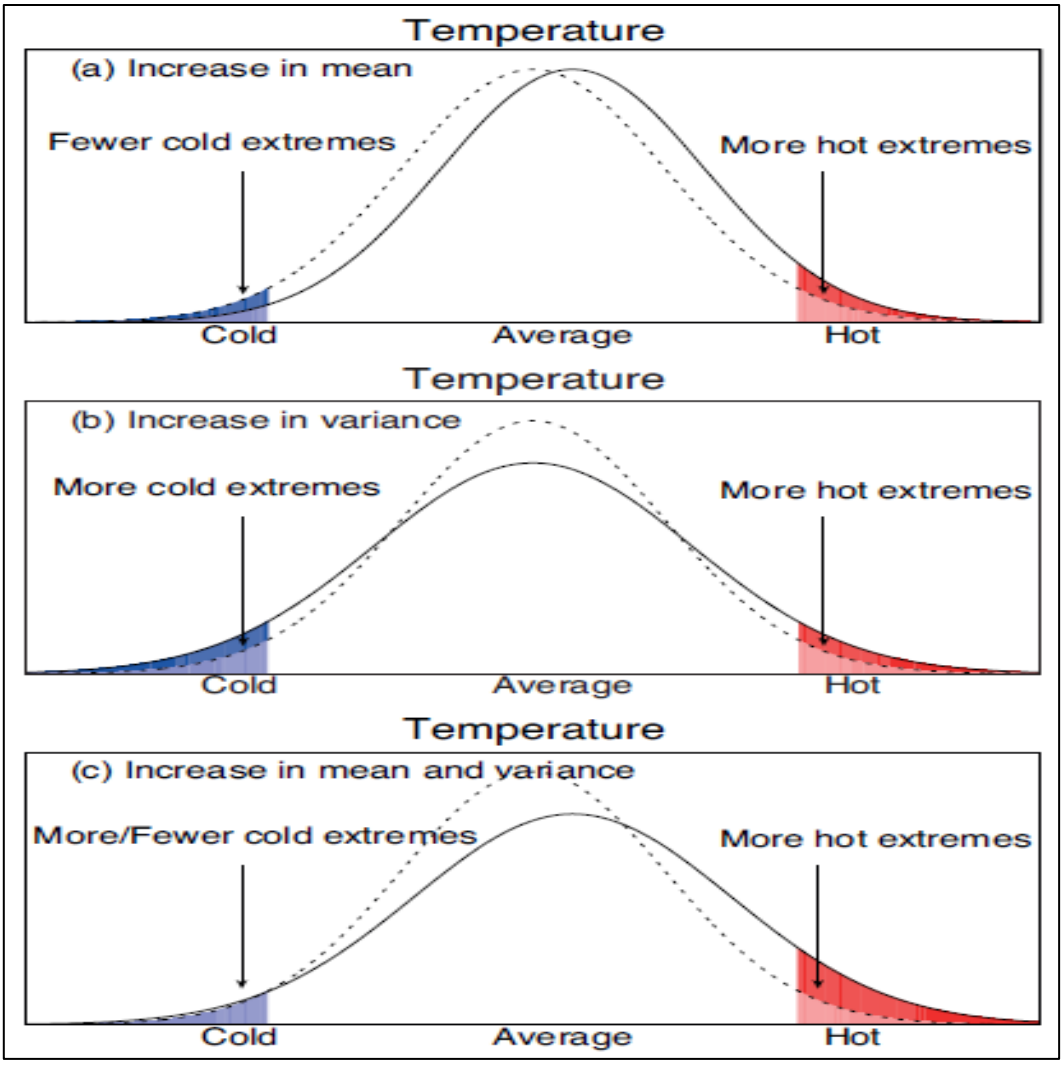

Figure 9.3 **Schematic representation of the probability density functions of daily temperature, which tends to be normally distributed. Dashed lines represent the historical distribution and solid lines a changed future distribution. The shaded areas indicate the probability of occurrence of extremes due to an (a) increase in the mean; (b) increase in variance; (c) increase in both the mean and variance or (d) a change in skewness (Cubasch *et al*., 2013).**

The research objective of this chapter was thus to use dynamically downscaled climate simulations over the central grassland biome of South Africa to assess the projected impacts of climate change on the climatological fire danger. This information will facilitate strategic decision-making around future fire suppression needs and resource allocation, which is crucial in a water scarce, developing country such as South Africa.

9.4 MATERIALS AND METHODS

The future climate projections used in this study was obtained from the conformal-cubic atmospheric model (CCAM), described by McGregor (1996, 2005a, 2005b) and McGregor and Dix (2001; 2008). CCAM was developed by the Commonwealth Scientific and Industrial Research Council (CSIRO) in Australia, while a locally modified version was maintained and run by the Climate Studies, Modeling and Environmental Health Research Group of the Council for Scientific and Industrial Research (CSIR) in South Africa. CCAM employs a conformal-cubic grid that covers the globe but has the capacity to run in a variable resolution stretched-grid mode, i.e. shrinking the grid intervals over the area of interest, whilst gradually decreasing the resolution as one moves away from the area of interest (McGregor & Dix, 2001; Engelbrecht *et al*., 2009). This allows more flexibility to downscaling experiments. CCAM has been verified against the present-day climate and was used in several climate projection studies over southern Africa (e.g. Engelbrecht *et al*., 2002; Engelbrecht, 2005; Olwoch *et al*., 2008; Engelbrecht *et al*., 2009; Potgieter, 2009; Engelbrecht *et al*., 2011). In order to explore the uncertainty in simulations and overcome some of the barriers to confidence in prediction, ensembles are employed (Flato *et al*., 2013; McGuffie & Henderson-Sellers, 2014) informed by similar assumptions around future GHG emissions.

CCAM was run in stand-alone mode (i.e. no atmospheric nudging) and forcing it at the lower boundary on a monthly basis with bias-corrected sea-surface temperatures (SSTs) and sea-ice from coupled global climate model (CGCM) (Engelbrecht *et al*., 2009; 2011). A set of six CGCMs were used, each employing the same GHG forcings (viz. A2, which is very similar to RCP8.5). The A2 emission scenario is described in detail by Nakićenović *et al*. (2000), while its similarities to RCP8.5 is pointed out by Vuuren *et al*. (2011) and Cubasch *et al*. (2013). The A2 scenario matches anthropogenic GHG emission trends over recent decades more closely (Westerling *et al*., 2011) and has been employed by the majority of studies listed in Table 9.2. It can be thought of as the “business as usual” scenario, representing a future climate state under no mitigation strategies.

CCAM was used to simulate both present-day and future climate over southern Africa and surrounding oceans at a spatial resolution of about 0.5° × 0.5° (Engelbrecht *et al*., 2011). The six CGCMs that were used to provide the lower boundary forcing data, also contributed to coordinated climate model experiments such as CMIP5 (Taylor *et al*., 2012) and the IPCC's AR5, and include CSIRO Mk3.5, ECHAM5/MPI-OM, GFDL-CM2.0, GFDL-CM2.1, MIROC3.2 and UKMO HADCM3. For ease of reference, the abbreviation allocated to each ensemble member (EMa to EMf in Figure 9.4) will be used from here onwards. The output comprised of daily gridded minimum and maximum temperatures, minimum and maximum relative humidity at screen height, 24-hour accumulated precipitation, and 10 m wind speed at 14:00 LST for the period 1981 to 2100.

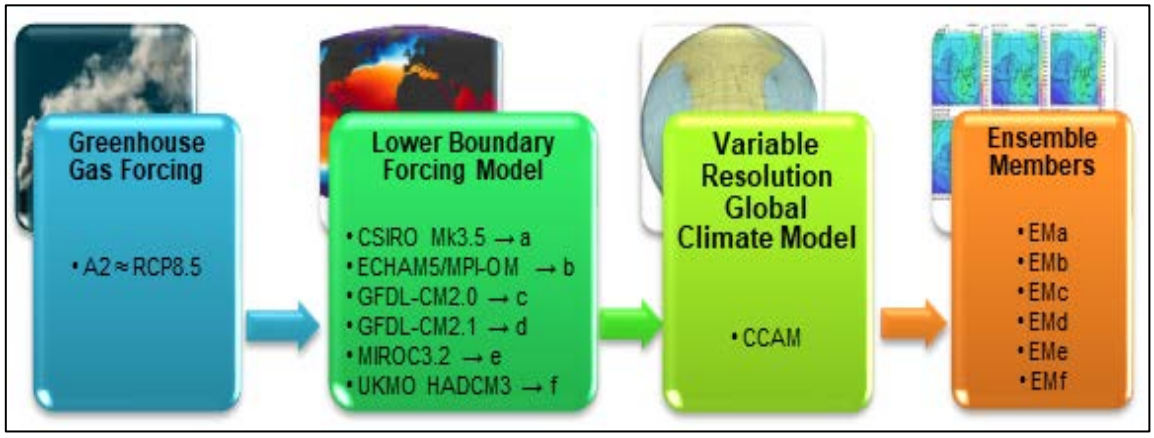

Figure 9.4 Development of the six ensemble members used to predict the future climate.

While several methods have been used to determine the potential impacts of climate change on fire activity, most studies used FDIs to focus on changes in fire weather and associated fire season severity (e.g. Stocks *et al*., 1998; Flannigan *et al*., 2001; Hoffmann *et al*., 2003; Lucas *et al*., 2007; Malevsky-Malevich *et al*., 2008; Pearce *et al*., 2011; Pereira *et al*. 2013; Liu *et al*., 2014; Bedia *et al*., 2015). The Fortran program "fire4gcm.f" (not included) was used to calculate the following FDIs (which were discussed in Chapter 5) at a daily interval for each gridpoint within the study area (delineated in Figure 6.1):

a) Canadian Fire Weather Index (CFWI);
b) Canadian Daily Severity Rating (CDSR);
c) Lowveld Fire Danger Index (LFDI); and
d) McArthur Forest Fire Danger Index (FFDI).

Daily spatial maxima, means and long-term mean annual and fire season frequencies of each fire danger category was also calculated in “fire4gcm.f” using the climatological breakpoints determined in Section 7.4.2. “fire4gcm.f” is similar to “fire4era.f” (Appendix E), but uses a 0.5° × 0.5° grid and the daily maximum temperature and minimum relative humidity at screen height. In order to determine future changes, the various fire statistics were calculated for the following four consecutive 30-year periods:

a) the climatological standard normal base period of 1981 – 2010 (WMO, 2017);
b) the current climate epoch of 2011 – 2040;
c) the near-future climate epoch of 2041 – 2070; and
d) the distant future climate epoch of 2071 – 2100.

Similar 30-year time slices were considered by Lines *et al*. (2005) and Wilby *et al*. (2006).

For each FDI and ensemble member, the CDF were constructed for the four consecutive 30-year periods and compared to each other. Maps were constructed with the aid of GrADS to depict the spatial distribution of changes in long-term mean occurrences in the highest two fire danger rating categories (“very high” and “extreme” combined). This “delta method” was also employed by Winkler *et al*., (2011) and Bedia *et al*. (2015), in order to extract the climate change signal from GCM simulations while meaningfully diminishing the problems related to model bias. These maps were constructed for the whole year (all months included) and fire season only. Finally, the frequencies in each class were compared for a single gridpoint matching the geographical location of Bloemfontein (any of the 119 gridpoints could have been chosen).

9.5 RESULTS AND DISCUSSION

9.5.1 Current Climate Epoch (2011 – 2040)

With the exception of EMd (notable decrease) and EMe (notable increase), there was no clear change in overall fire danger when comparing the CDFs for the fire season CFWI (Appendix G) for the 30-year period spanning 2011 – 2040 to that of the climatological base period (1981 – 2010). Similar findings hold for the CDSR (Appendix H), LFDI (Appendix I) and FFDI (Appendix J).

The spatial distribution of projected changes in long-term mean fire season number of days falling in the highest two fire danger rating categories (i.e. “very high” and “extreme”) between the base period and 2011 – 2040 are presented in Figures 9.5 – 9.8 for the CFWI, CDSR, LFDI and FFDI, respectively. Each figure contains the predictions of the six ensemble members, indicated as EMa – Emf (refer to Figure 9.4 for a complete description).

Noteworthy decreases (> 10 days, primarily in the south) in the number of very dangerous days were projected for the CFWI, CDSR and FFDI by EMd. One ensemble member, EMe, consistently predicted notable increases (> 10 days, primarily in the south and west) for the CFWI, CDSR and LFDI, but across the entire region for the FFDI. The largest projected increase in very dangerous days was 25 for the FFDI simulated by EMe in the north-west (bottom-left panel in Figure 9.8). Generally small changes (< 5 days) were indicated over the central grassland biome for this climate epoch by the reaming ensemble members for all FDIs.

Similar maps depicting the spatial distribution of projected changes in the occurrence of very dangerous days for the same time period, but for the entire year, are provided in Appendix K. In terms of annual changes, the pattern is fairly similar to that of the fire season but with larger increments, particularly for FFDI. The largest projected increase in very dangerous days was 40 in the north-west for the FFDI simulated by EMe (bottom-left panel in the 4th figure in Appendix K).

Table 9.3 **Changes in the mean annual (Ann) and fire season (FS) number of days falling in each fire danger category for the period 2011 – 2040 relative to 1981 – 2010 for the gridpoint in Bloemfontein (29.25°S 26.25°E)**

FDI	Fire Danger Rating	Ensemble Member											
		EMa		EMb		EMc		EMd		EMe		EMf	
		Ann	FS	Ann	FS	Ann	FS	Ann	FS	Ann	FS	Ann	FS
CFWI	Low	-0.2	3.9	-8.4	1.8	0.9	0.5	8.7	8.1	-9.8	-5.6	2.1	3.8
	Moderate	6.6	2.5	-2.4	-3.3	-7.7	-8.8	15.8	12.1	-19.4	-18.0	2.6	1.1
	High	1.0	1.1	9.8	3.6	3.9	4.9	-10.4	-7.2	15.3	11.3	-2.1	-0.8
	Very High	-5.0	-5.3	1.5	-1.2	1.4	2.3	-12.0	-10.8	12.0	10.5	-2.0	-3.2
	Extreme	-2.4	-2.2	-0.5	-0.9	1.6	1.1	-2.1	-2.2	1.9	1.7	-0.5	-0.9
CDSR	Low	-2.4	2.8	-7.8	1.7	1.2	0.3	6.2	5.8	-9.6	-5.6	1.3	2.2
	Moderate	8.9	3.7	-2.8	-3.0	-8.6	-9.0	18.9	14.7	-19.9	-18.6	2.8	2.4
	High	0.6	0.9	9.7	3.6	4.3	5.4	-11.7	-7.8	17.0	12.2	-0.7	-0.1
	Very High	-4.8	-5.4	1.4	-1.4	1.7	2.3	-11.4	-10.6	10.7	9.6	-2.7	-3.5
	Extreme	-2.3	-2.1	-0.5	-0.8	1.4	0.9	-2.0	-2.1	1.8	1.7	-0.6	-1.0
LFDI	Low	-2.1	1.0	-3.5	1.5	-3.4	-3.6	8.1	7.9	-13.6	-9.9	0.4	1.8
	Moderate	2.7	-0.2	-4.1	-3.5	-5.1	-4.3	4.9	4.5	-12.3	-11.6	0.5	-0.2
	High	2.3	2.1	3.7	1.9	6.3	5.9	-8.6	-7.9	14.2	12.9	0.2	-0.5
	Very High	-3.1	-2.8	3.0	0.0	1.2	1.5	-5.4	-4.4	10.9	8.2	-1.8	-1.2
	Extreme	0.2	-0.1	0.8	0.0	1.1	0.5	1.1	-0.1	0.8	0.4	0.7	0.1
FFDI	Low	-1.7	1.4	-6.6	1.2	-6.4	-4.6	12.1	11.0	-18.3	-13.3	0.6	0.6
	Moderate	8.1	5.4	-5.0	-1.8	0.2	-2.2	10.7	9.5	-12.9	-10.9	-0.6	3.3
	High	0.7	0.9	6.4	2.3	2.2	3.2	-11.1	-9.4	10.4	9.0	1.2	-0.4
	Very High	-6.5	-5.2	1.9	-1.7	-1.0	1.9	-12.5	-9.9	14.7	11.2	-2.3	-2.1
	Extreme	-0.6	-2.5	3.3	0.0	5.2	1.7	0.8	-1.2	6.1	4.1	1.1	-1.4

A comparison of the frequencies in each fire danger rating class was performed for a single gridpoint matching the geographical location of Bloemfontein. Table 9.3 contains the absolute changes in the long-term mean number of days falling in a particular category between the current climate era and the historical base period. Such changes are presented for both the entire year (column marked Ann) and the fire season (column marked FS) for each of the six ensemble members. Negative values are marked in blue. EMc and EMe were the only ensemble members that predicted increases in the number of “very high” and “extreme” days for all fire season FDIs. EMa, EMb, EMd and EMf generally projected decreases in these two highest categories during the fire season, but with negligible small changes for LFDI and FFDI under EMb and EMf. The strongest disagreement was between EMd and EMe. The largest projected changes in “very high” and “extreme” days was -10.8 and -2.2 for the CFWI simulated by EMd, and +11.2 and +4.1 for the FFDI under EMe, respectively (Table 9.3). The reason for this discrepancy can probably be attributed to the contrasting predictions of precipitation and temperature (Appendix L). Under EMd the mean total fire season rainfall is

projected to increase by 22 mm and the mean maximum temperature with about 0.1°C. Under EMe the mean total fire season rainfall is projected to decrease by 2 mm and the mean maximum temperature to increase by 1.6°C.

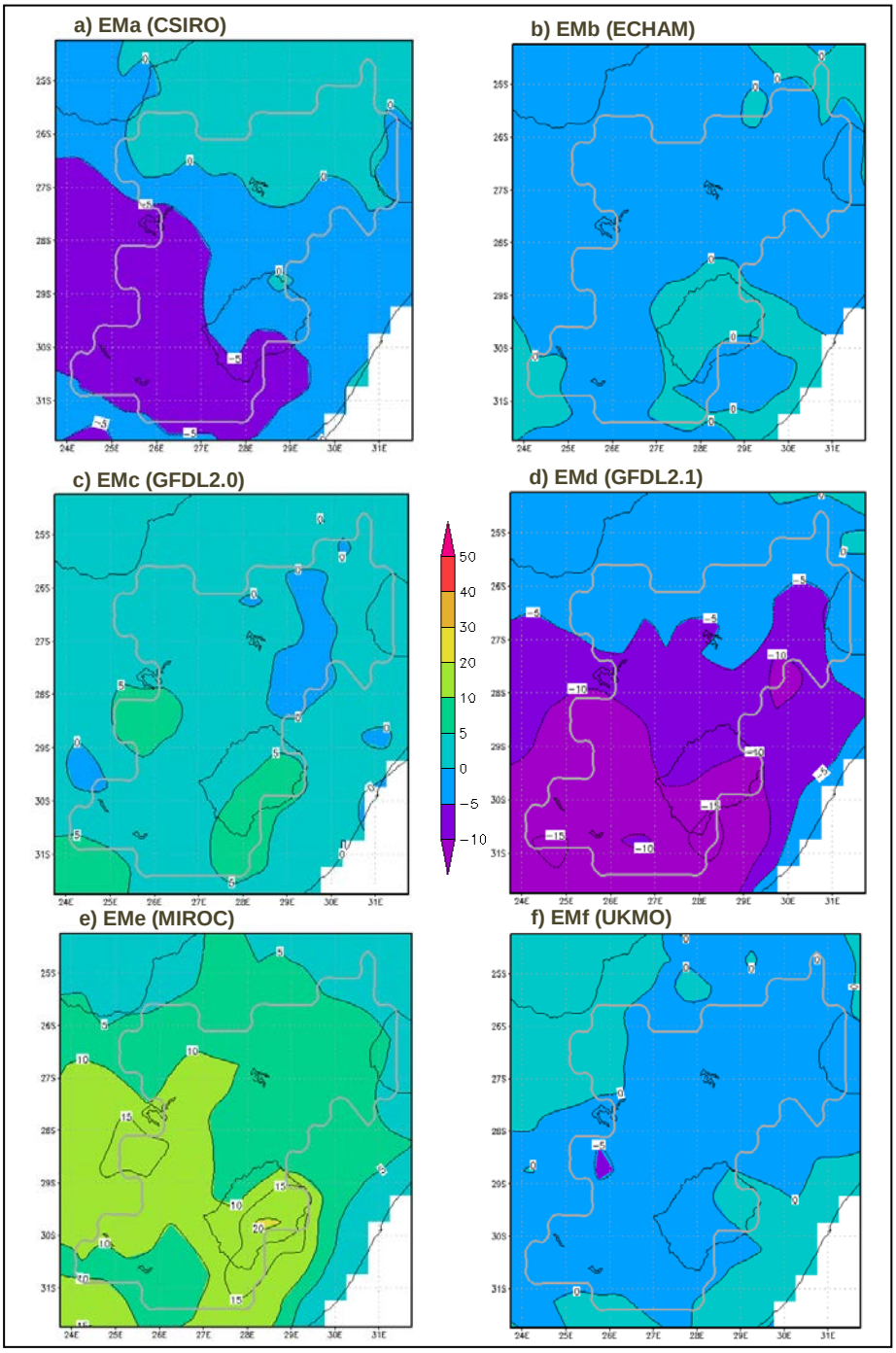

Figure 9.5 **Spatial distribution of changes in mean fire season occurrences of very high and extreme danger days combined according to the CFWI for the period 2011 – 2040 relative to the climatological base period (1981 – 2010). The grey polygon delineates the central grassland biome.**

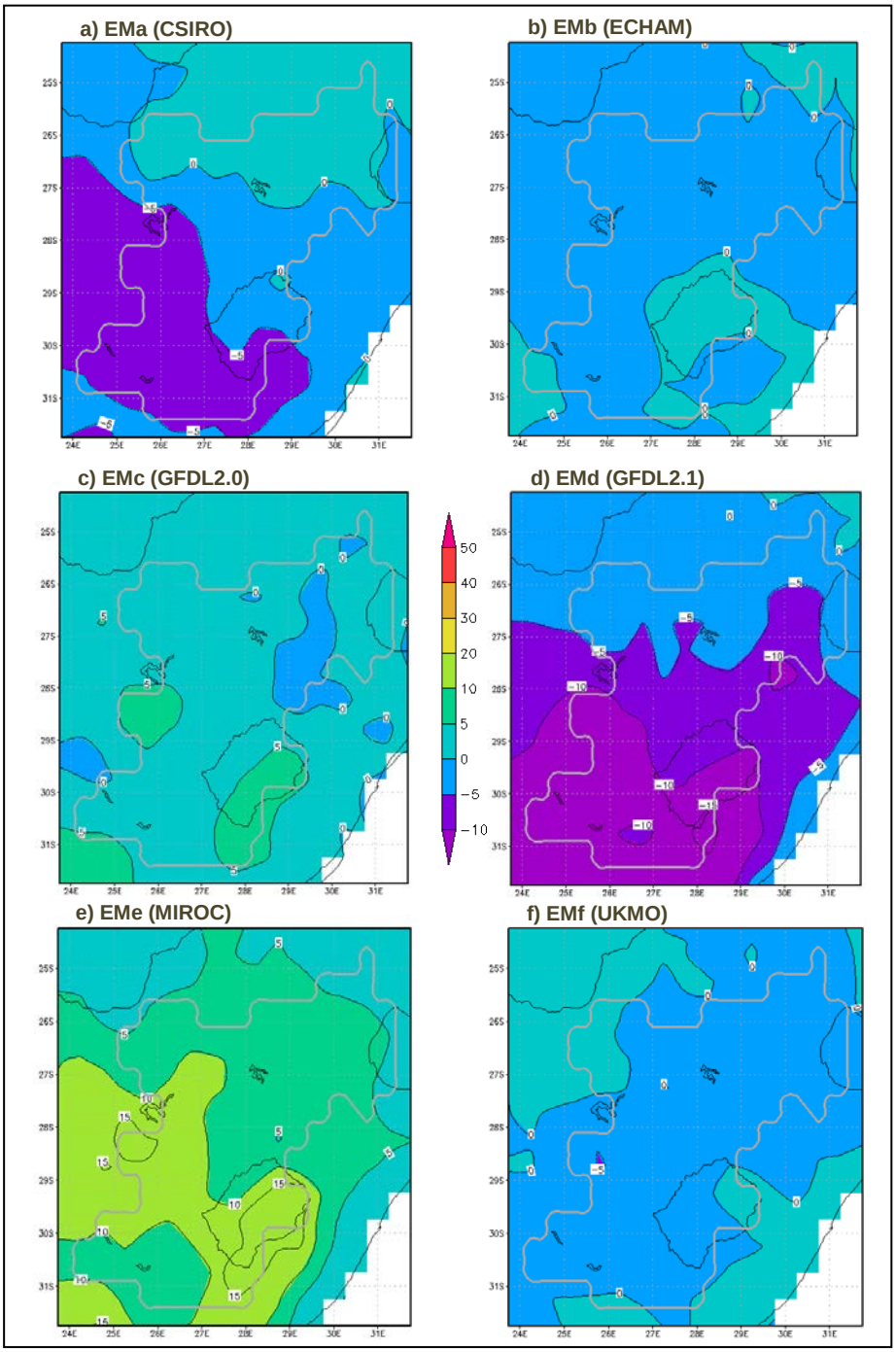

Figure 9.6 **Spatial distribution of changes in mean fire season occurrences of very high and extreme danger days combined according to the CDSR for the period 2011 – 2040 relative to the climatological base period (1981 – 2010). The grey polygon delineates the central grassland biome.**

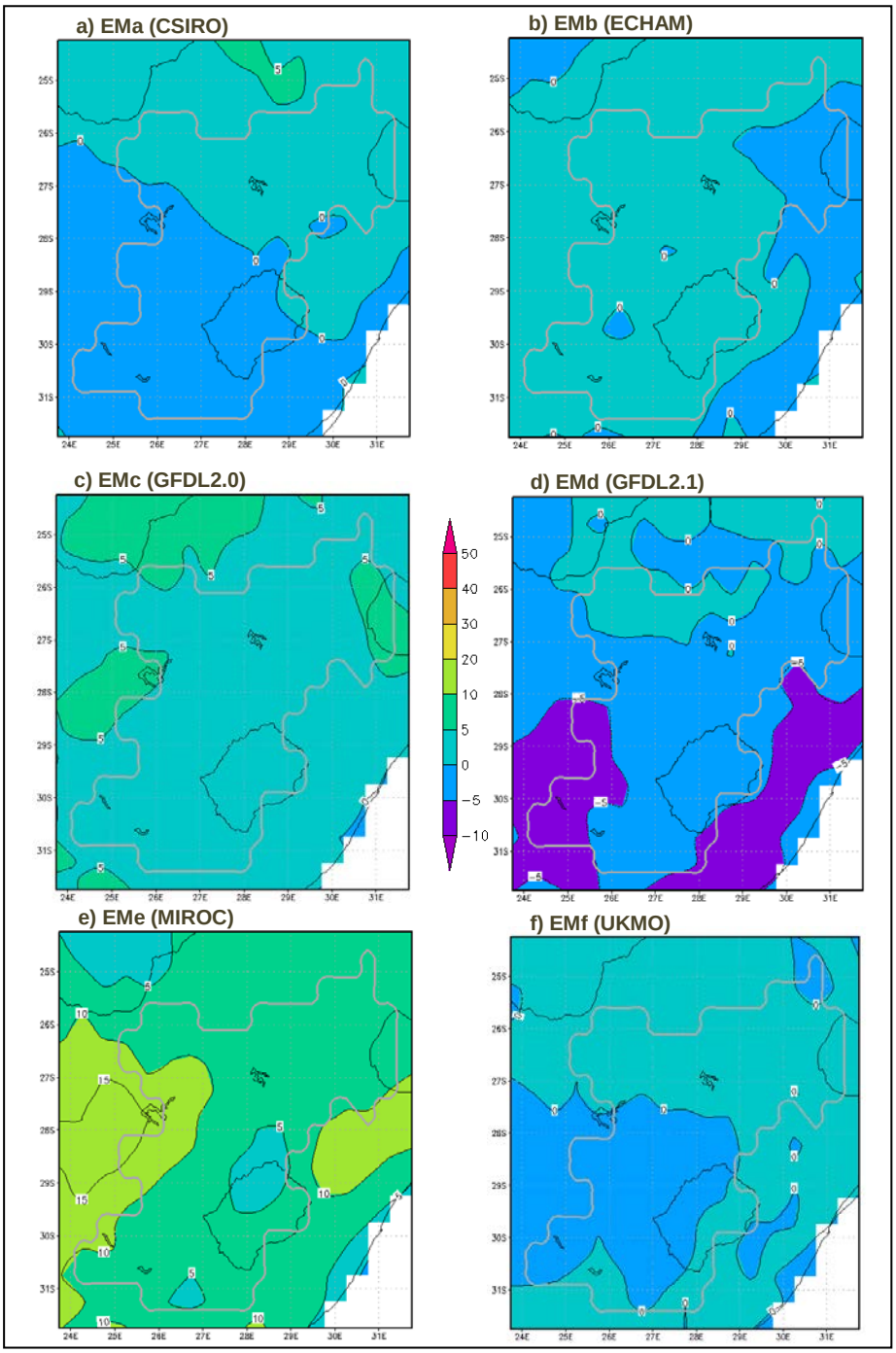

Figure 9.7 **Spatial distribution of changes in mean fire season occurrences of very high and extreme danger days combined according to the LFDI for the period 2011 – 2040 relative to the climatological base period (1981 – 2010). The grey polygon delineates the central grassland biome.**

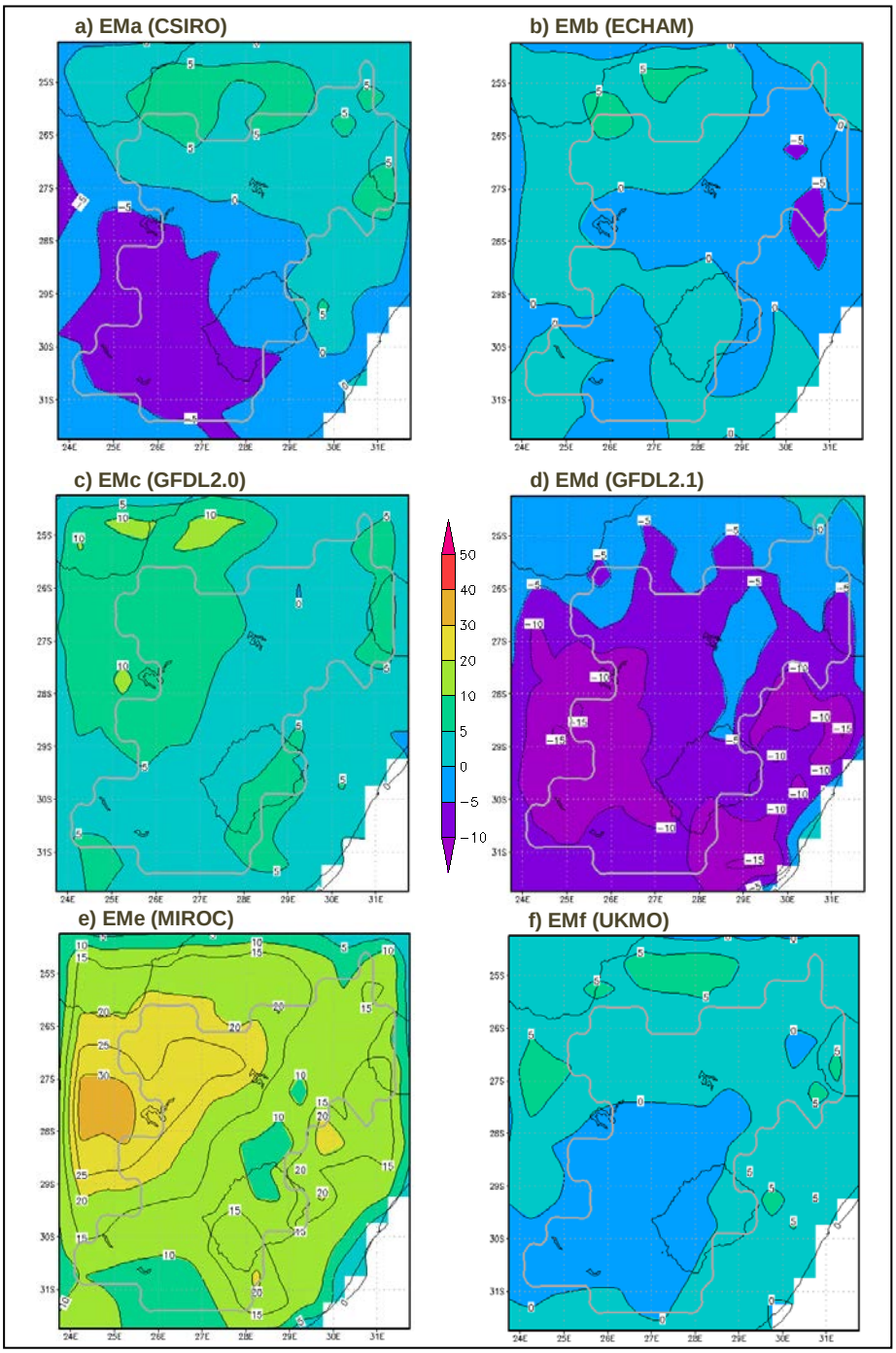

Figure 9.8 **Spatial distribution of changes in mean fire season occurrences of very high and extreme danger days combined according to the FFDI for the period 2011 – 2040 relative to the climatological base period (1981 – 2010). The grey polygon delineates the central grassland biome.**

9.5.2 Near-future Climate Epoch (2041 – 2070)

Compared to the climatological base period (1981 – 2010), there was a slight decrease in overall fire danger as depicted by the leftward shift in the CDFs for the fire season CFWI (Appendix G) under EMa and EMd for the period spanning 2041 – 2070. However, the shift from 2011 – 2040 was undetectable under EMd. The other ensemble members predicted a notable increase in fire danger. Similar findings hold for the CDSR (Appendix H) and LFDI (Appendix I), while all ensemble members predicted an overall increase in fire danger (albeit slight in some cases) for the FFDI (Appendix J).

Figures 9.9 – 9.12 provide the spatial distribution of projected changes in the long-term mean fire season occurrence of very dangerous days between the climatological base period (1981 – 2010) and the 30-year period spanning 2041 – 2070 for the CFWI, CDSR, LFDI and FFDI, respectively. Each panel in Figures 9.9 – 9.12 represents one of the six ensemble members (viz. EMa – Emf). Although the various ensemble members did not predict the same pattern of change for this climate epoch, some general patterns did emerge. Relatively smaller changes were predicted over the southern Highveld (i.e. Eastern Free State) for all FDIs by all ensemble members. Two of the ensemble members (viz. EMa and EMd) predicted decreases for all FDIs, centred over the central and southern parts of the study area, respectively. Although all ensemble members agreed in terms of warming, the decrease in fire danger under EMa and EMd can probably be attributed to the corresponding projected increase in mean total fire season precipitation these areas (Appendix N). In the case of EMd, the indicated decreases were only very slight when compared to that which were already projected for the preceding 30-year time period. The remaining ensemble members (viz. EMb, EMc, EMe and EMf) consistently predicted increases in the number of very dangerous days during the fire season over the entire central grassland biome for all four FDIs, particularly in the west to north-west and southern Lesotho. These increments were smaller for the LFDI and largest for FFDI. The highest projected increase in very dangerous days (up to 40 in the north-west) was for the FFDI

simulated by EMe (bottom-left panel in Figure 9.12). This corresponded with EMe drying the most and presenting the strongest warming (Appendix N). The annual changes presented in Appendix M are similar in pattern, differing in magnitude only.

Table 9.4 **Changes in the mean annual (Ann) and fire season (FS) number of days falling in each fire danger category for the period 2041 – 2070 relative to 1981 – 2010 for the gridpoint in Bloemfontein (29.25°S 26.25°E)**

FDI	Fire Danger Rating	Ensemble Member											
		EMa		EMb		EMc		EMd		EMe		EMf	
		Ann	FS	Ann	FS	Ann	FS	Ann	FS	Ann	FS	Ann	FS
CFWI	Low	-12.7	0.4	-17.8	-2.3	-6.0	-3.1	6.4	7.6	-18.1	-4.5	-23.6	-5.2
	Moderate	7.3	3.5	-14.1	-15.1	-12.9	-13.8	17.4	14.8	-19.9	-13.5	-24.4	-19.6
	High	8.3	2.8	17.5	8.5	7.3	6.9	-8.0	-7.4	13.9	6.0	24.9	15.9
	Very High	-1.6	-5.1	11.3	7.2	8.3	7.5	-14.0	-12.8	19.7	9.8	20.5	7.6
	Extreme	-1.3	-1.5	3.0	1.7	3.4	2.5	-1.7	-2.3	4.4	2.3	2.5	1.2
CDSR	Low	-11.5	0.5	-16.6	-2.2	-6.3	-3.2	4.0	5.1	-16.3	-4.6	-21.2	-5.1
	Moderate	5.9	3.5	-15.2	-15.2	-12.8	-13.8	20.2	17.4	-22.0	-13.5	-27.7	-20.2
	High	8.7	2.7	17.8	8.6	7.8	7.1	-8.9	-7.9	15.1	6.3	26.7	16.7
	Very High	-2.0	-5.5	11.0	7.0	8.1	7.5	-13.7	-12.5	18.9	9.7	20.0	7.5
	Extreme	-1.1	-1.2	3.0	1.8	3.2	2.3	-1.6	-2.1	4.2	2.1	2.2	1.1
LFDI	Low	-10.4	-3.0	-18.0	-8.1	-8.8	-8.2	6.5	6.5	-17.5	-6.7	-26.1	-10.1
	Moderate	1.2	-1.1	-6.1	-8.0	-11.0	-9.0	1.7	4.4	-12.6	-12.0	-9.4	-4.2
	High	7.4	5.2	10.3	8.2	7.6	7.0	-6.3	-6.8	12.8	10.1	17.9	13.8
	Very High	0.0	-1.3	11.5	7.1	9.0	8.8	-3.7	-4.0	12.6	7.3	13.6	6.9
	Extreme	1.8	0.2	2.4	0.7	3.3	1.4	1.8	-0.1	4.7	1.3	4.0	0.5
FFDI	Low	-13.2	-0.8	-19.0	-6.7	-12.5	-8.6	11.1	11.5	-20.2	-9.2	-28.9	-12.8
	Moderate	0.3	3.7	-20.3	-12.4	-10.5	-8.7	11.1	11.2	-26.8	-11.4	-30.8	-14.6
	High	4.9	1.2	14.6	6.9	3.4	4.9	-12.5	-11.2	9.2	4.3	22.8	16.6
	Very High	-0.7	-4.4	9.6	5.3	3.8	3.9	-12.6	-10.8	16.2	9.4	16.5	8.1
	Extreme	8.7	0.3	15.0	6.9	15.9	8.5	2.9	-0.6	21.6	6.9	20.4	2.8

Table 9.4 provides the absolute changes in the long-term mean number of days falling in a particular fire danger category between the near-future climate era and the historical base period for the Bloemfontein gridpoint. With the exception of EMa and EMd, the fire season days falling in the two highest categories are projected to increase for all FDIs. For the LFDI, only small changes of between 0.1 to 1.4 is predicted in the long-term mean number of “extreme” days during the fire season. Annual changes are slightly larger in magnitude (viz. 1.8 – 4.7). The slight decrease under EMd can probably be attributed to the projected increase in mean total fire season precipitation by 34 mm in combination with a relatively small increase of about 0.9°C in the mean maximum temperature. Under EMe the mean total fire season rainfall is projected to increase by only 6 mm, which is largely offset by the expected rise of 2.3°C in the mean maximum temperature.

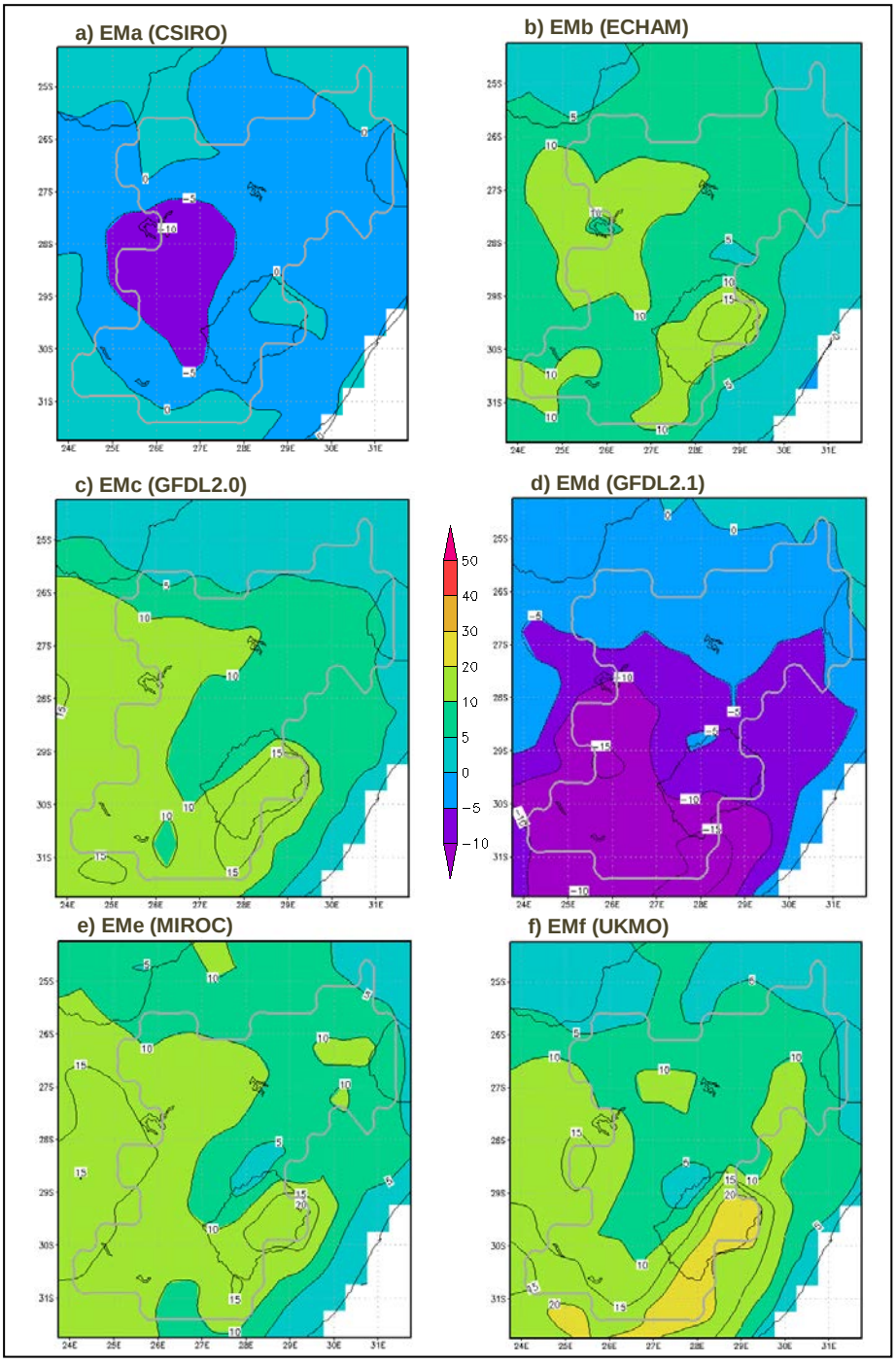

Figure 9.9 **Spatial distribution of changes in mean fire season occurrences of very high and extreme danger days combined according to the CFWI for the period 2041 – 2070 relative to the climatological base period (1981 – 2010). The grey polygon delineates the central grassland biome.**

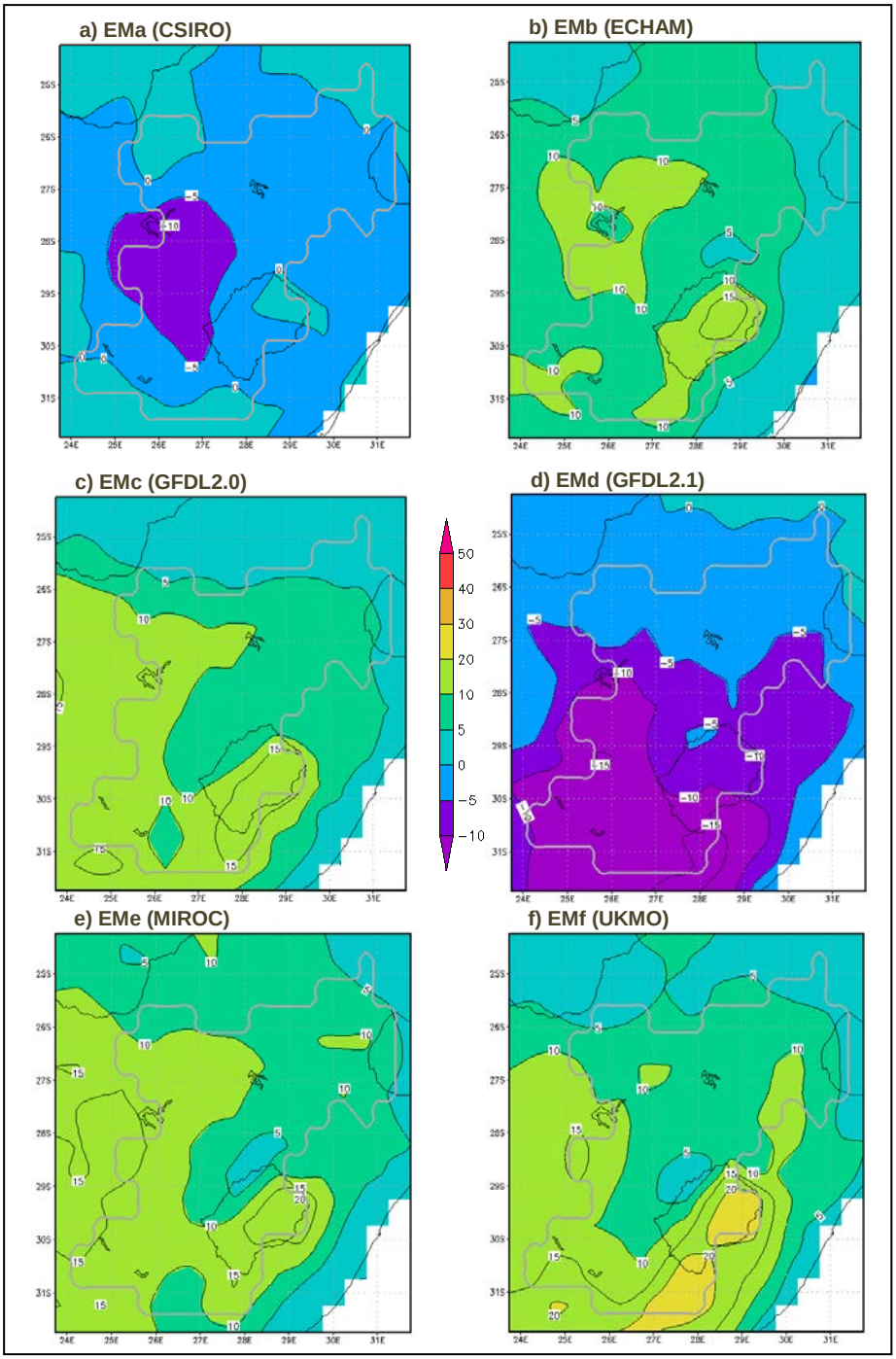

Figure 9.10 **Spatial distribution of changes in mean fire season occurrences of very high and extreme danger days combined according to the CDSR for the period 2041 – 2070 relative to the climatological base period (1981 – 2010). The grey polygon delineates the central grassland biome.**

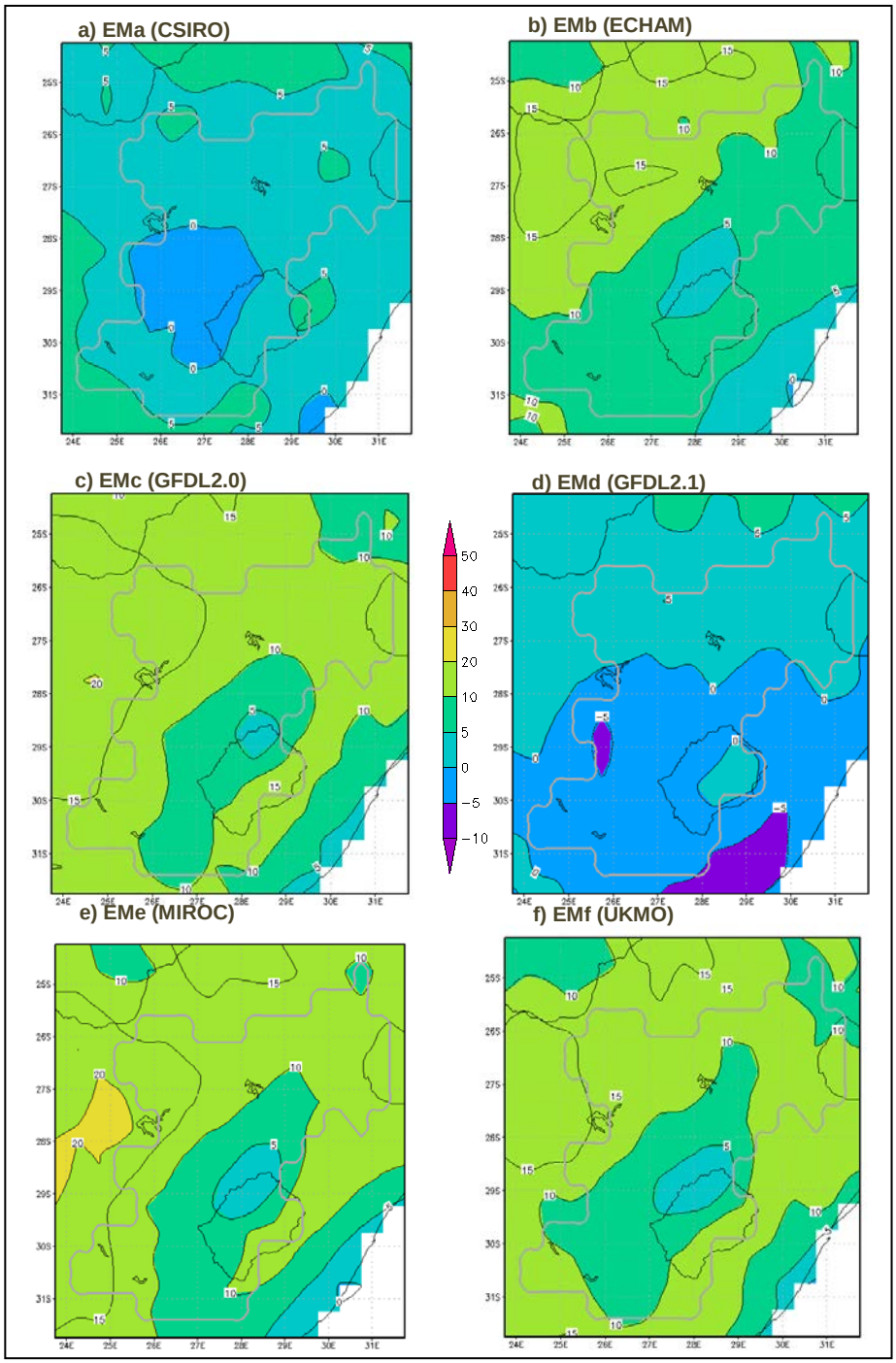

Figure 9.11 **Spatial distribution of changes in mean fire season occurrences of very high and extreme danger days combined according to the LFDI for the period 2041 – 2070 relative to the climatological base period (1981 – 2010). The grey polygon delineates the central grassland biome.**

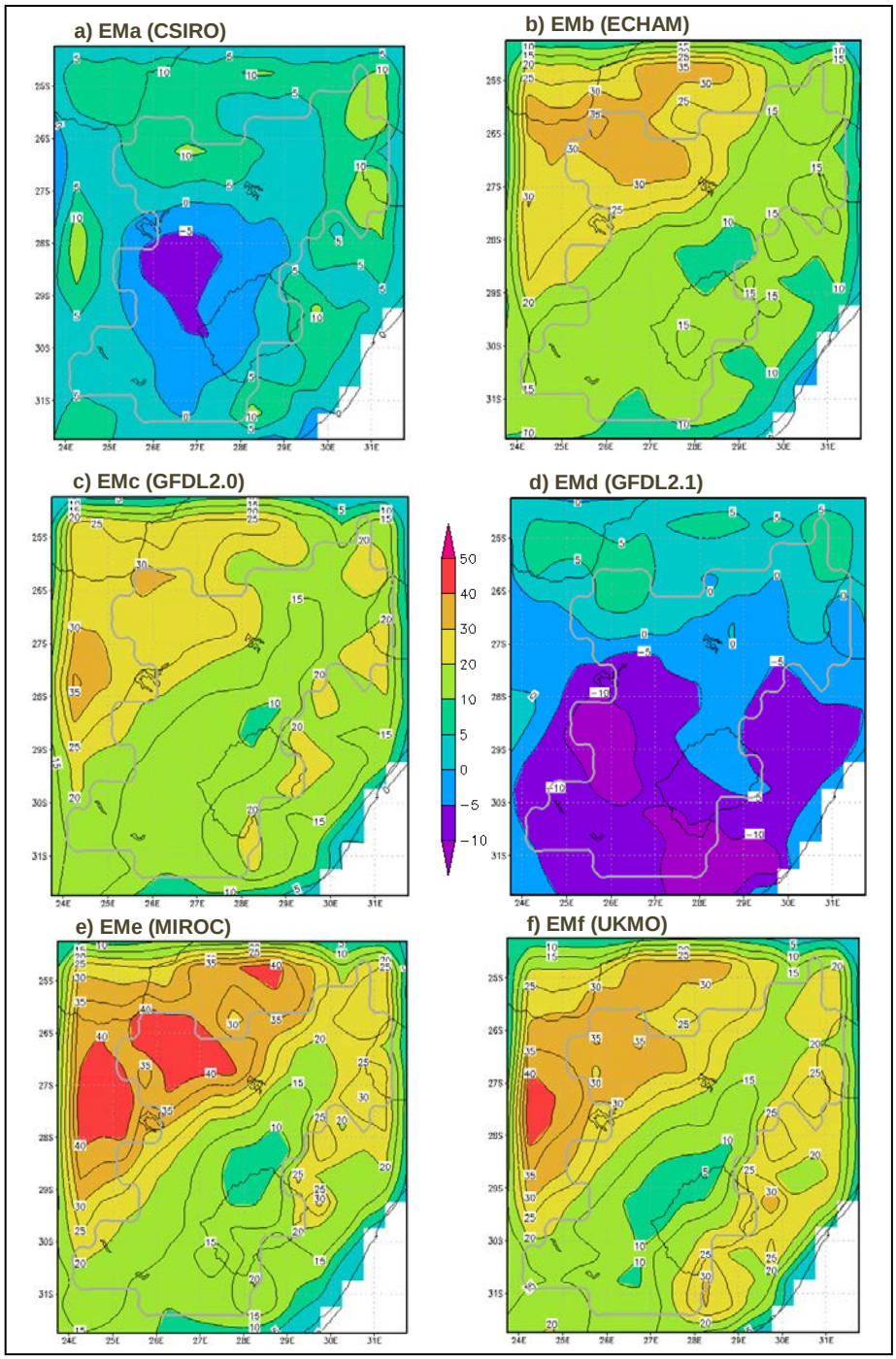

Figure 9.12 **Spatial distribution of changes in mean fire season occurrences of very high and extreme danger days combined according to the FFDI for the period 2041 – 2070 relative to the climatological base period (1981 – 2010). The grey polygon delineates the central grassland biome.**

9.5.3 Distant Future Climate Epoch (2071 – 2100)

A pattern of generally increasing fire danger emerged when comparing the CDFs for the fire season FDIs for the period 2071 – 2100 to that of the climatological base period (1981 – 2010). This was true for the CFWI (Appendix G), CDSR (Appendix H), LFDI (Appendix I) and FFDI (Appendix J) under EMa, EMb, EMc, EMe and EMf. The exception was the predictions under EMd for the CFWI, CDSR and LFDI, which showed negligible changes over the base period. Although the EMd projection for fire season FFDI did indicate a slight increase in fire danger (as depicted by the rightward shift in the CDF in the middle-right panel of Appendix J) compared to the base period, there was no detectable change over the preceding 30-year period (2041 – 2070). The most notable changes in overall fire danger were projected by EMe, which corresponded with a general pattern of drying and strong warming (Appendix P).

Figures 9.13 – 9.16 present the changes in long-term mean number of very dangerous days during the fire season between the climatological base period and the 30-year period spanning 2071 – 2100. EMa and EMd (top-left and middle-right panels in Figures 9.13 and 9.14, respectively) presented only minor increases and in some cases even negative changes over the southern and central parts of the study area. In the case of the Canadian indices (i.e. CFWI and CDSR), these negative changes were, however, smaller than for the 2041 – 2070 period, thus marking a slight increase from the preceding climate epoch. For each FDI, the spatial pattern of change was more or less consistent between EMb, EMc, EMe and EMf, while the magnitude of change differed markedly from one ensemble member to another. Notable increases in very dangerous days were predicted across the central grassland biome by EMb, EMc and EMe, especially towards the south and west. Generally, EMb and EMe predicted the largest increases for all FDIs, while the largest increments (~ 90) were projected for the FFDI in the north-west (Figure 9.16). This area also had the largest projected increases in long-term mean fire season maximum temperature (Appendix P).

Considering the annual changes relative to the climatological base period (Appendix O), the largest discrepancies occurred between EMa and EMe. With the CFWI and CDSR the frequency of very dangerous days were shown to decrease by up to 5 in the south-west under EMa, while increases of about 65 – 75 were predicted by EMe over this area. For the LFDI, slight increases of less than 5 were predicted under EMa over the south-west, while EMe purported much larger increases of more than 60. In the case of the FFDI, the number of days falling in the “very high” and “extreme” categories were shown to increase by less than 10 under EMa and by more than 100 under EMe over the south-western part of the study area. The largest projected increase in very dangerous days was 165 for the FFDI simulated by EMe in the north-west (bottom-left panel in the 4th figure in Appendix O).

The absolute changes in the long-term mean number of days falling in a particular fire danger category between the distant future climate era and the historical base period for the Bloemfontein gridpoint are provided in Table 9.5. It is surprising that even with the projected warming of close to 3°C towards the end of the century, EMa and EMd simulated a decrease in the number of “extreme” days (both seasonally and annually) for CFWI and CDSR. Both of these ensemble members simulate a wetter future (under EMd the mean total fire season rainfall is projected to increase by 31 mm). There is agreement between the remaining ensemble members that the number of “very high” and “extreme” days will increase for all FDIs with respect to the historical base period. The largest increases are projected for the FFDI under EMe, with the number of “extreme” cases expected to soar with about 39 days during the fire season (81 days annually). This dramatic increase under EMe is probably due to the projected negligible change in the mean total fire season rainfall (decrease by 6 mm) in combination with a large increase of approximately 5°C in the seasonal mean maximum temperature. Keep in mind that the increased warming will not only aid combustion, but will result in tremendous drying due to enhanced evapotranspiration.

Table 9.5 **Changes in the mean annual (Ann) and fire season (FS) number of days falling in each fire danger category for the period 2071 – 2100 relative to 1981 – 2010 for the gridpoint in Bloemfontein (29.25°S 26.25°E)**

FDI	Fire Danger Rating	Ensemble Member											
		EMa		EMb		EMc		EMd		EMe		EMf	
		Ann	FS	Ann	FS	Ann	FS	Ann	FS	Ann	FS	Ann	FS
CFWI	Low	-3.8	1.9	-19.6	-4.9	-17.8	-7.9	-12.7	-2.4	-36.4	-12.4	-26.0	-6.1
	Moderate	9.2	1.9	-11.5	-14.0	-24.4	-23.6	9.1	6.9	-56.5	-39.2	-20.3	-15.4
	High	1.2	2.3	14.4	6.8	16.2	11.0	4.3	-0.3	21.3	10.7	23.7	12.7
	Very High	-5.8	-5.3	13.9	10.2	19.8	15.4	-0.4	-3.2	56.4	31.2	19.2	7.9
	Extreme	-0.9	-0.8	2.8	1.9	6.2	5.1	-0.3	-1.0	15.3	9.7	3.4	1.0
CDSR	Low	-5.5	1.1	-17.1	-3.6	-15.4	-6.7	-13.0	-3.6	-32.2	-10.4	-22.9	-5.3
	Moderate	10.7	2.8	-13.7	-15.3	-27.0	-25.1	10.0	8.4	-61.1	-41.4	-24.2	-16.6
	High	1.4	2.1	14.5	7.1	16.8	11.3	4.0	-0.5	23.6	11.8	25.3	13.5
	Very High	-5.9	-5.2	13.4	9.9	19.7	15.6	-0.5	-3.2	54.7	30.5	18.7	7.6
	Extreme	-0.7	-0.7	2.9	1.9	5.9	4.8	-0.4	-1.0	15.0	9.4	3.0	0.8
LFDI	Low	-7.1	-4.3	-14.4	-8.9	-20.8	-16.6	-8.7	-3.0	-35.5	-17.9	-26.9	-10.3
	Moderate	-3.0	-5.0	-16.8	-15.5	-16.6	-14.8	-2.2	-0.7	-38.5	-29.5	-7.5	-9.8
	High	9.2	8.9	12.2	10.5	16.9	15.1	2.5	1.1	19.0	14.9	15.5	11.6
	Very High	-1.4	-0.6	14.5	11.6	15.6	13.7	4.0	1.1	40.4	26.7	13.3	7.6
	Extreme	2.3	0.9	4.5	2.4	4.9	2.6	4.3	1.4	14.5	5.8	5.6	0.9
FFDI	Low	-10.5	-4.2	-24.3	-10.9	-26.4	-17.6	-14.8	-4.3	-40.4	-21.5	-30.3	-11.9
	Moderate	4.9	3.2	-21.2	-14.7	-29.3	-19.6	-0.6	3.5	-75.7	-47.5	-30.9	-13.5
	High	1.7	1.8	9.9	6.7	7.1	6.8	0.3	-0.4	1.2	4.3	13.2	7.3
	Very High	-5.4	-4.2	10.6	5.4	19.1	13.5	0.3	-4.3	34.2	25.5	19.4	9.3
	Extreme	9.1	3.3	25.0	13.4	29.4	16.9	14.8	5.5	80.7	39.3	28.6	8.8

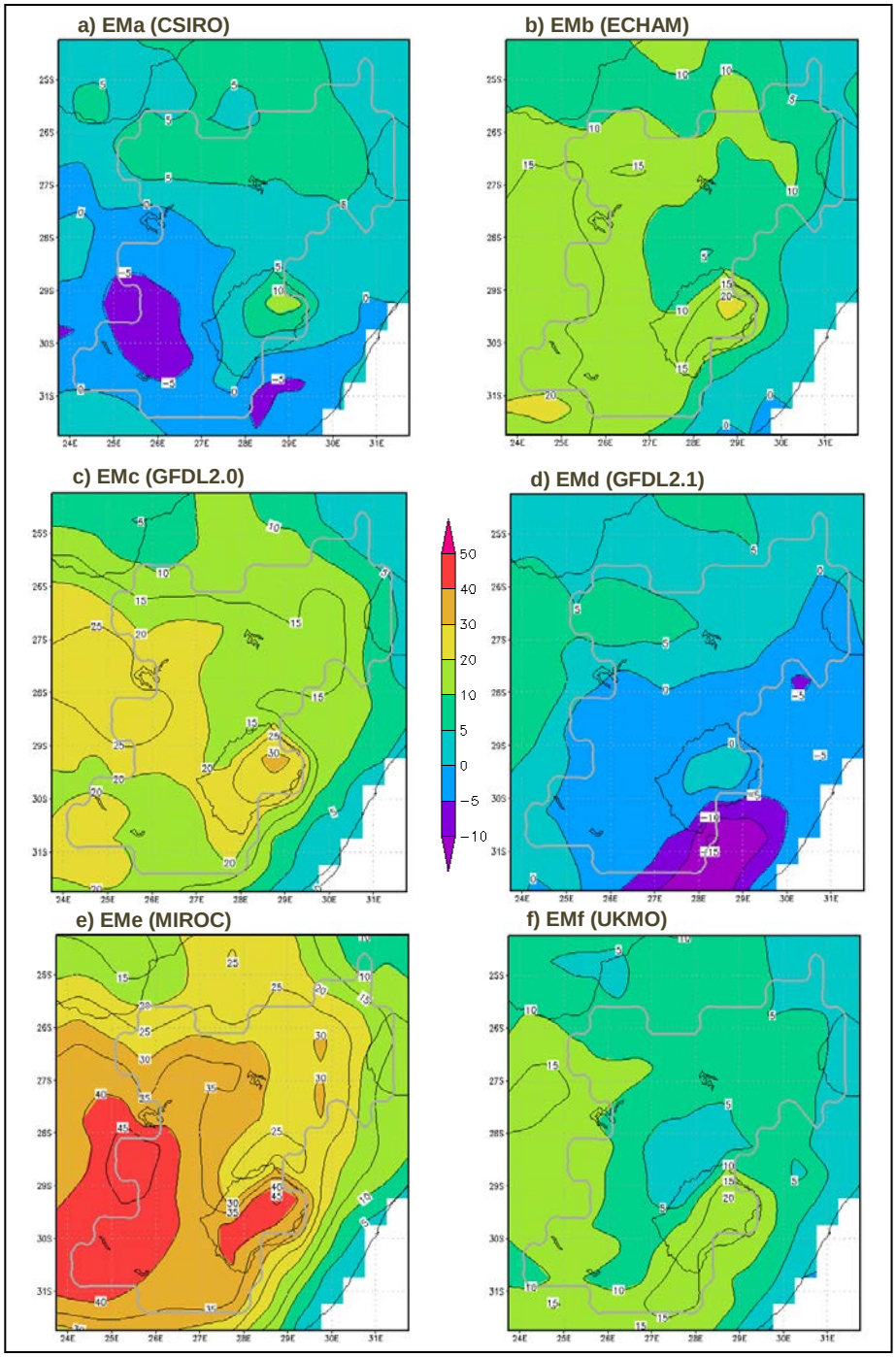

Figure 9.13 **Spatial distribution of changes in mean fire season occurrences of very high and extreme danger days combined according to the CFWI for the period 2071 – 2100 relative to the climatological base period (1981 – 2010). The grey polygon delineates the central grassland biome.**

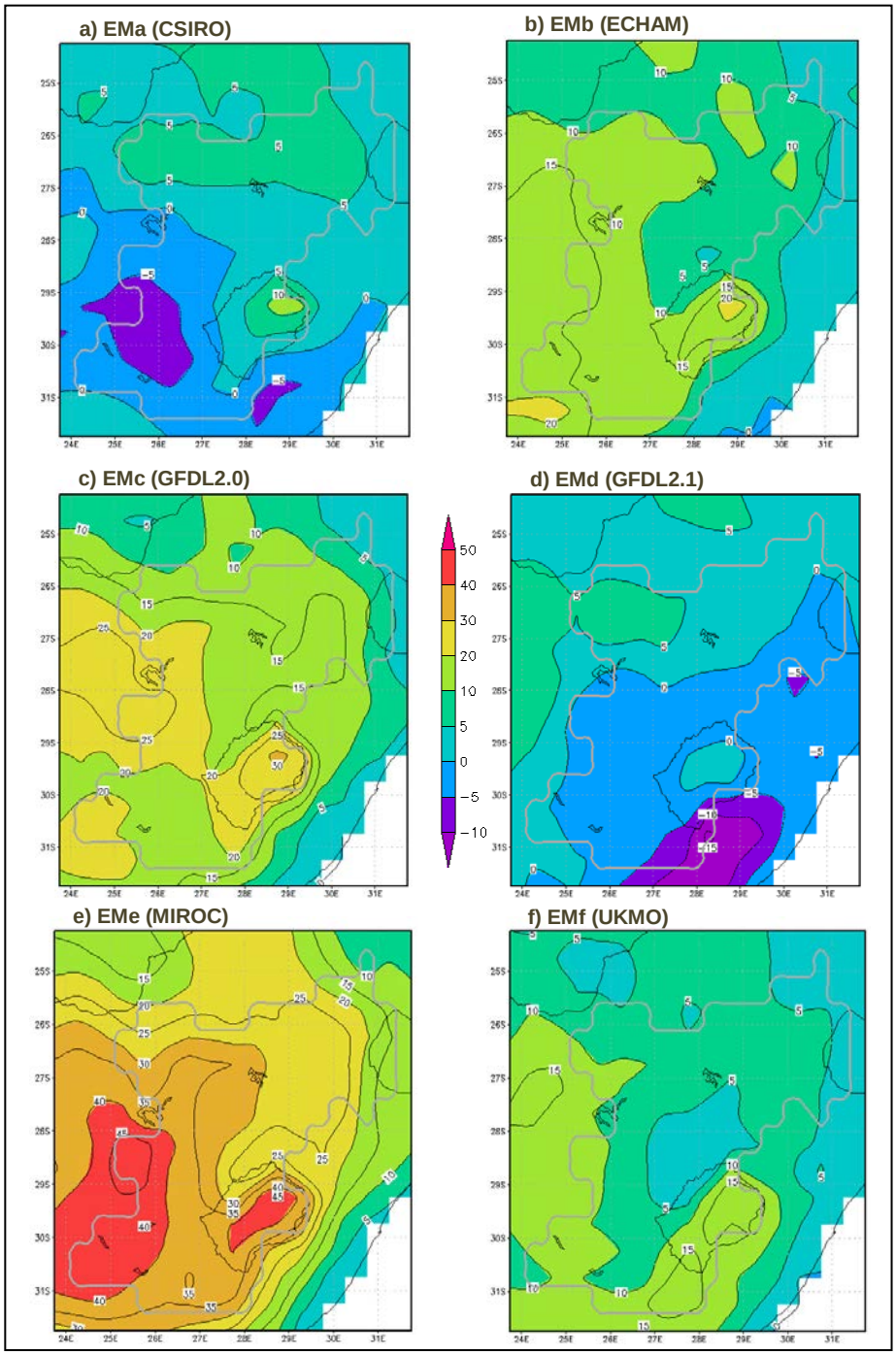

Figure 9.14 **Spatial distribution of changes in mean fire season occurrences of very high and extreme danger days combined according to the CDSR for the period 2071 – 2100 relative to the climatological base period (1981 – 2010). The grey polygon delineates the central grassland biome.**

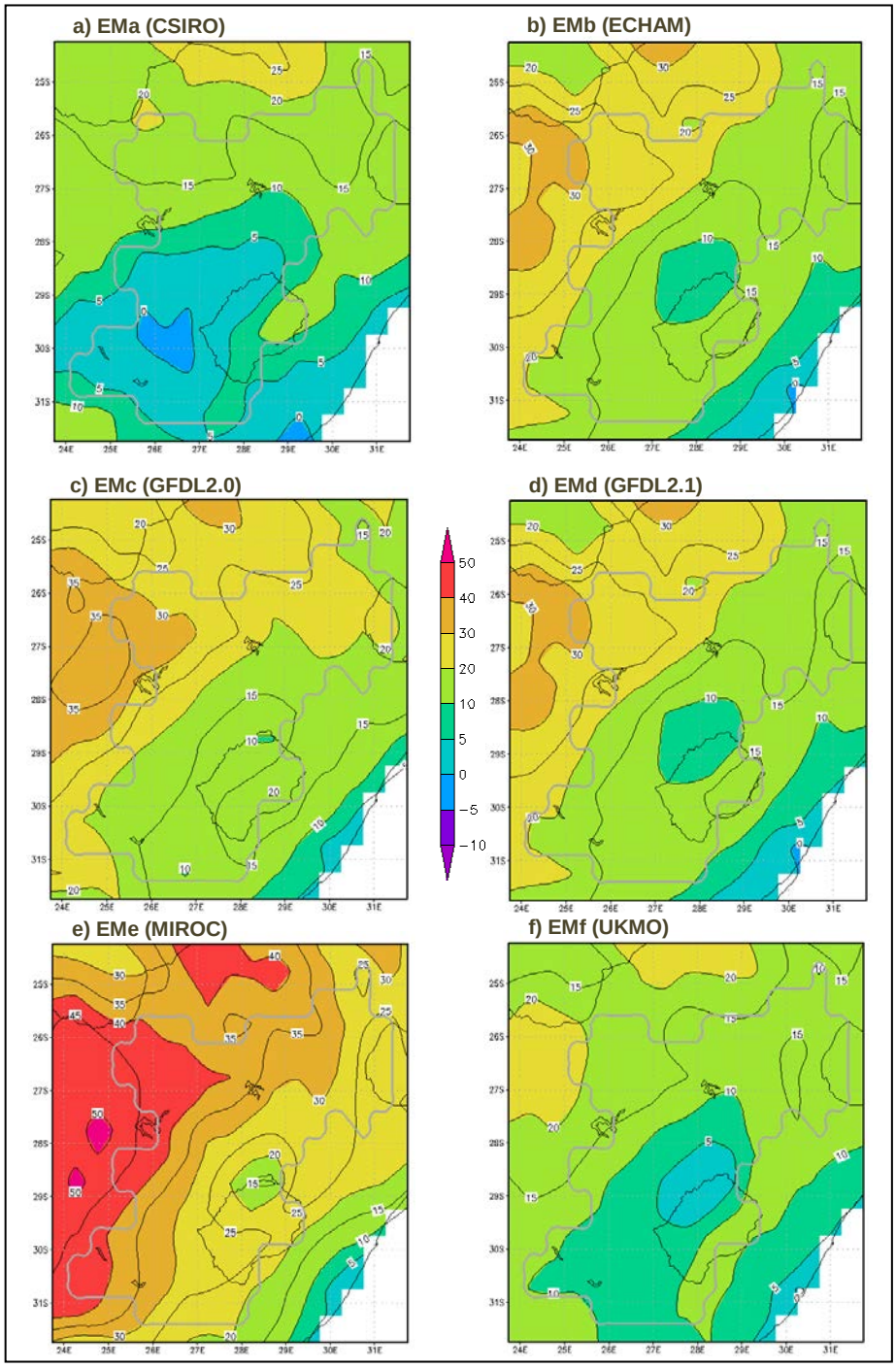

Figure 9.15 **Spatial distribution of changes in mean fire season occurrences of very high and extreme danger days combined according to the LFDI for the period 2071 – 2100 relative to the climatological base period (1981 – 2010). The grey polygon delineates the central grassland biome.**

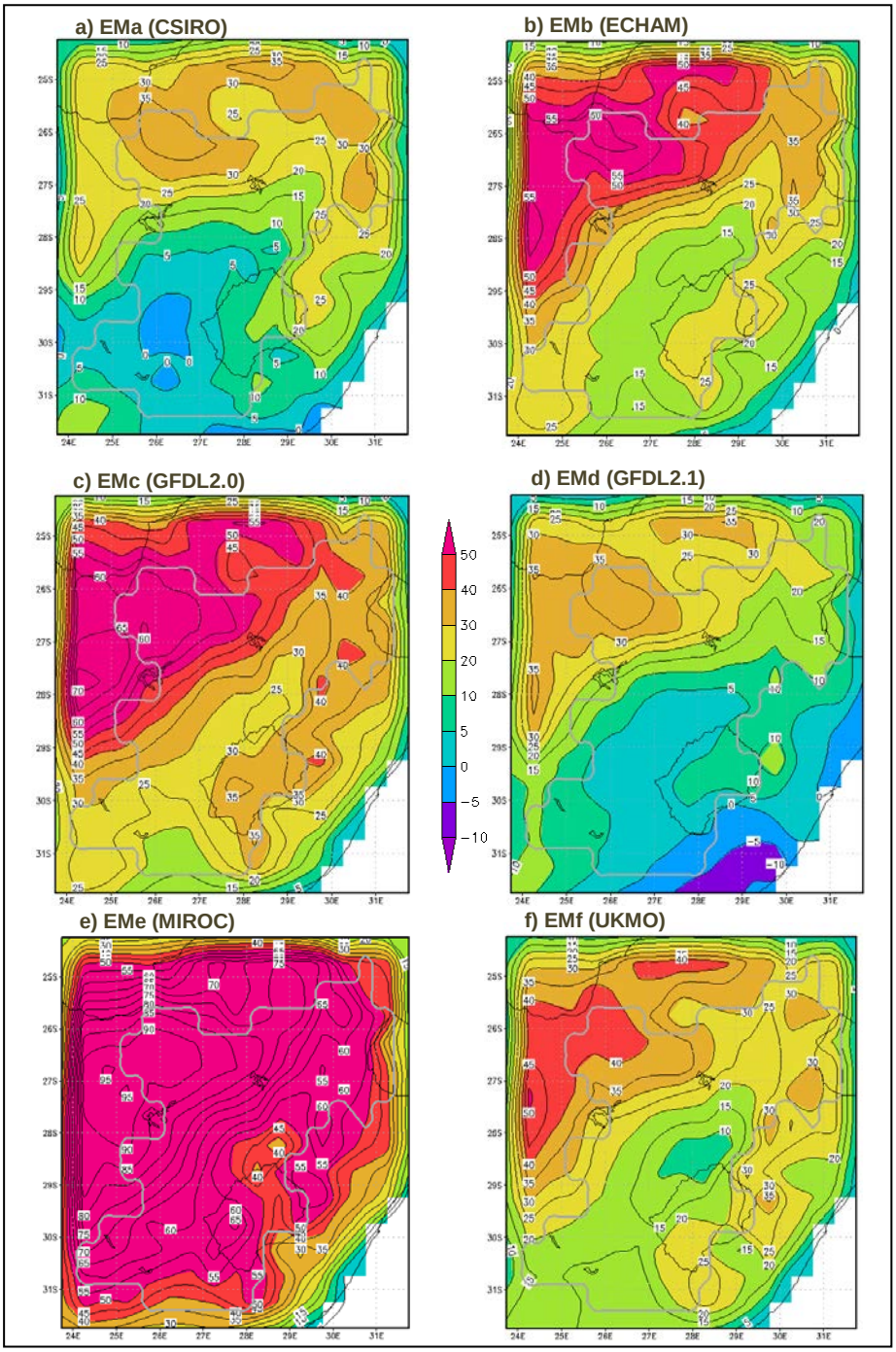

Figure 9.16 **Spatial distribution of changes in mean fire season occurrences of very high and extreme danger days combined according to the FFDI for the period 2071 – 2100 relative to the climatological base period (1981 – 2010). The grey polygon delineates the central grassland biome.**

9.6 CONCLUDING REMARKS

Projections from the various ensemble members, employing a similar GHG emission scenario, did not reveal a clear change in overall fire danger when comparing the CDFs for the fire season FDIs between the current climate epoch (2011 – 2040) and that of the climatological base period. This is in agreement with findings by Bedia *et al*. (2015) for a similar period (i.e. 2026 – 2045). Broadly inconsistent spatial patterns of change in very dangerous occurrences matched this finding for the current climate epoch. Although the highest frequency of very dangerous days were located in the warmer and drier southwest (Section 7.4.3), half of the ensemble members (viz. CSIRO Mk3.5, GFDL-CM2.1 and UKMO HADCM3) predicted decreases of up to 15 days for all four FDIs across the southern parts of the study area. Such decreases can probably be attributed to increased rainfall offsetting the slight warming predicted by these ensemble members.

With the exception of two ensemble members (viz. CSIRO Mk3.5 and GFDL-CM2.1), a more comparable pattern of change in the number of “very high” and “extreme” days emerged for the near-future climate epoch (2041 – 2070), but with different magnitudes corresponding to different degrees of warming. Smaller changes were predicted over the southern Highveld by all ensemble members and FDIs, while the largest increases occurred in the north-west situated at a lower altitude.

The occurrence of very dangerous days further increased in the distant future climate epoch (2071 – 2100) across the central grassland biome, especially towards the west, with MIROC3.2 predicting the largest increases on account of strong warming. Projections of changes for the FFDI were consistently larger than for the other FDIs. Again, the projections from CSIRO Mk3.5 and GFDL-CM2.1 differed considerably from the others. Both the spatial distribution maps and the CDFs concurred that the shift towards higher fire danger seemed to be more

pronounced from mid-century onwards. This finding is in agreement with that of Pechony and Shindell (2010).

Note that no biotic effects were included in these projections, though future trends in fire activity will be regulated not only by climate, but also by vegetation and fire suppression practices. It is further assumed that land use practices will continue in a manner familiar today and that there will be no escalation to woody communities in the study area (although some of the FDIs are already used in a similar way in both grassland and forested areas). As pointed out by Brown *et al*. (2004), by focusing on climatological fire danger a number of these complicating factors are eliminated.

CHAPTER 10

CONCLUSIONS

The central grassland biome of South Africa is subject to seasonal wildfires that play a pivotal role in the ecology and distribution of grassland vegetation, while the attendant occasional damage to livestock production systems, infrastructure, air quality and human health and safety can be severe. The area is the source of several major rivers in the region, has a rich biodiversity, is agriculturally highly productive, and harbours a hub of industrialization and the economic powerhouse of South Africa. But what justifies the distinctiveness of the central grassland biome of South Africa is its anthropogenic fire antiquity. Since it is home to the “cradle of mankind”, hominids have played a progressively important role in the fire regime, either directly (e.g. by acting as a major ignition source) or indirectly (e.g. by influencing fuel loads and continuity). Fire is also an important aspect of rangeland management, particularly in the moist sourveld in the east of the study area.

However, man’s capacity to manage fire remains imperfect, particularly in the face of an altered fire regime under a changing climate. In a water scarce, developing country with limited resources, the importance of planning with such changes cannot be overstressed. It is thus important to evaluate recent historical and projected future changes to the region’s fire regime. Knowledge of the large-scale weather patterns that have historically resulted in increased fire risk will also aid aspirant weather forecasters in fire weather prediction.

The effects of changes in climate vary quite dramatically from one geographical region to another. It is precisely due to such spatial variations that local or regional studies are required to understand the local effects of climate change. Climate change does not merely involve an adjustment of a single climatic element (e.g.

temperature), but rather a change in several interlinked climate variables (e.g. temperature, rainfall, humidity and fire danger).

10.1 HISTORICAL EVALUATION OF THE FIRE REGIME

Knowledge gaps relating to fire regime characteristics and trends of the central grassland biome of South Africa were identified in Chapter 7. These pertain to the time and amount of actual burning and the spatio-temporal distribution of fire danger across the region. Because fire behaviour responds to an ever-fluctuating combination of fuel characteristics, weather conditions and topographical features, incorporating all potential factors pertaining to the fire regime into a single metric was seemingly impossible. This study thus considered both actual observed fire (i.e. total burned area obtained through satellite remote sensing) and climatological fire danger (i.e. FDIs calculated with historical climate data).

An accurate working definition of the central grassland's fire season was imperitive as it informed the methodology of the study. Using MODIS burned area data the fire season of the central grassland biome was defined as ranging from May to November, with peak burning shifting from August in the north and east to September in the south and west. This result was in agreement with other studies with a larger regional focus (e.g. Archibald *et al*., 2010a; Strydom and Savage, 2016). The earlier start and peak of the fire season in the east can probably be ascribed to:

- a combination of higher fuel loads and an earlier onset (and incidence) of frost;
- the enhanced ignition that accompany a higher population density, supported by noting that most fires are started near access roads and places of dwelling over weekends; and
- the use of fire as a veld management practice in the sourveld.

There was a large inter-annual variability in the total burned area, which ranged from 0.48 to 1.6 million ha per annum. Annual burning seemed to be linked to

precipitation during the antecedent summer season. Enhanced mid-summer rainfall resulted in increased burning, as excess moisture leads to additional biomass that can quickly dry out during the fire season. This is in accordance with the theory proposed by Krawchuk and Moritz (2011) that the importance of fuel moisture on wildfire activity is eclipsed by the availability and continuity of burnable fuels in xeric grasslands. Thus, all indications are that we are dealing with a "moisture-limited fire regime" as defined by Westerling and Bryant (2008).

The perceived increase in wildland fire activity in various world regions does not apply to the central grassland biome of South Africa. A statistically significant negative trend in annual total burned area was observed over the study area, corresponding to a decline of about 34 000 ha per annum over the period 2002 – 2017. This occurred during a time that the climatological fire danger has been increasing. This inconsistency can probably be ascribed to:

- veld management practices, including efficient fire suppression and avoidance techniques; and
- fuel continuity and availability in a moisture-limited fire regime.

The latter point is supported by noting that the prolonged drought during the last decade, particularly over the southern and western parts of the central grassland region, has resulted in lower fuel loads and enhanced competition between fire and livestock for grass fibre.

While the locally developed fire danger index (LFDI) is widely accepted by the end-user community, it is not well-known internationally and virtually non-existant in scientific journal publications. For this reason, LFDI was compared with the internationally better known indices CFWI, CDSR and FFDI to evaluate climatological fire danger. The fire danger rating category thresholds employed by these indices required calibration to local conditions. This was achieved by introducing climatological breakpoints based on the 30^{th}, 73^{rd}, 93^{rd} and 99^{th} percentiles.

Climatological fire danger was shown to be considerably higher in the south-western part of the central grassland biome than over the eastern escarpment region during the climatological standard normal base period (1981 – 2010). This can be attributed to the generally warmer and drier conditions towards the west. On average, “very high” fire danger conditions occurred on 5 – 15 days on the eastern escarpment as opposed to 15 – 40 days in the south-west according to the LFDI. While the number of “extreme” days ranged from 5 – 9 in the south-west, such days were very rare over the eastern escarpment. This is in contradiction to higher fire activity (as presented by the higher fire counts portrayed in Figure 1.2) over the eastern escarpment region. This incongruity can probably be ascribed to:

- the increased risk of anthropogenic ignitions in the eastern escarpment region;
- rangeland management practices in the moist sourveld where fire is used to improve forage quality (by removing excess litter accumulation) and to prevent encroachment by woody plants; and
- the influence of topography on fire behaviour.

A significant increase in climate-related fire danger was found during the recent historical period (1979 – 2018), with the largest shift occurring during the most recent decade (i.e. 2009 – 2018). All FDIs pointed to unprecedented increases in very dangerous (i.e. “very high” and “extreme”) conditions during this time period, particularly over the western half of the study area. Compared to the 1979 – 1988 means, very dangerous occurrences over the western parts increased by more than 30 days during the fire season by 2009 – 2018, and even more according to the FFDI. These findings reinforced the theory of accelerated change during the latter part of the historical period.

10.2 SYNOPTIC WEATHER PATTERNS THAT HAVE HISTORICALLY RESULTED IN INCREASED FIRE DANGER

Knowledge of the large-scale weather systems that typically give rise to hazardous conditions is a crucial part of weather forecasting. The SOM methodology was successfully applied in Chapter 8 to objectively determine the archetypal synoptic patterns of the 850 hPa geopotential heights over southern Africa for the period 1981 – 2010. These ranged from well-developed westerly waves (and accompanying surface cold fronts) to high pressure systems dominating the subcontinent during the fire season. Mapping the number of occurrences of very dangerous days to each SOM node revealed a clustering around well-developed frontal troughs at different stages of progression over the subcontinent. It is believed that the warm, dry and windy conditions typically experienced ahead (i.e. east) of a well-developed frontal trough is conducive to runaway wildfires over this area. Leewards of the escarpment conditions are usually exasperated by bergwinds. This finding was supported by the fire season average peak recurrence interval in spatial mean LFDIs of about 10 days (Section 7.4.3), as such systems are generally found to frequent the region at a similar time interval. These finding were in line with local forecaster experience, and demonstrated the soundness of SOM analysis in similar studies.

10.3 PROJECTED IMPACTS OF CLIMATE CHANGE ON THE FIRE REGIME

Projections from various ensemble members, employing a similar GHG emission scenario (viz. A2), were used to calculate FDIs for the following three consecutive periods and compared against the climatological base period (1981 – 2010):

- the current climate epoch (2011 – 2040);
- the near-future climate epoch (2041 – 2070); and
- the distant future climate epoch (2071 – 2100).

Although a significant increase in climate-related fire danger was found during the recent historical period (Chapter 7), the projections did not support a continued increase over the current climate epoch (2011 – 2040) (Chapter 9). Moreover,

broadly inconsistent spatial patterns of change in very dangerous occurrences matched this finding for the current climate epoch.

For ECHAM5/MPI-OM, GFDL-CM2.0 and UKMO HADCM3A a more consistent pattern, but with different magnitudes of change in the number of very dangerous days during the fire season, emerged for the near-future and distant-future climate epochs. Generally, smaller changes were predicted over the southern Highveld by all ensemble members and FDIs, while the largest increases occurred in the north-west, particularly for FFDI. An increase of between 5 – 15 very dangerous days was predicted for the near-future climate epoch, and 5 – 45 days for the distant future epoch. MIROC3.2 consistently projected larger increases (about double those presented above).

The pattern and magnitude of change generally corresponded to different degrees of warming. The shift towards higher fire danger seemed to be more prominent from mid-century onwards. This finding is in agreement with that of Pechony and Shindell (2010). The projections from two ensemble members, CSIRO Mk3.5 and GFDL-CM2.1, differed considerably from the others. They predicted a decrease of between 5 – 15 very dangerous days over the central and southern parts of the study area for the current and near-future climate epochs, and decreases of less than 5 days for the distant future epoch. In light of the warming predicted by all ensemble members, it is difficult to explain why the projections of CSIRO Mk3. and GFDL-CM2.1 could be realised, even if they show an increase in rainfall over these areas. Is the enhanced rainfall really enough to offset the warming? Any rationale involving fuel loads are futile (if not contradictory to the conclusions in Section 10.1) as such feedbacks are not well presented in GCMs.

Uncertainty stemming from discrepancies among future climate scenarios and unrepresented processes (e.g. vegetation dynamics), create uncertainty about the accuracy of predictions of the future. Nonetheless, the results of this study

underscore the potentially large impacts of climate change on the central grassland biome.

10.4 LIMITATIONS AND KEY ASSUMPTIONS

The following caveats were identified in assessing fire danger at a regional scale:

a) It is extremely difficult to incorporate anthropogenic factors pertaining to fire ignition and management practices into fire danger predictions.

b) The FDI-values are representative of the general climatological fire danger over a relatively large area and may misrepresent conditions where fires actually occur, particularly in hilly terrain. Potential fuels may be completely exposed to solar radiation, implying that air temperature and relative humidity would be more extreme. Winds at the ground may be notably different from the average wind speeds at a single level, and rainfall measurements (and predictions) are subjected to issues pertaining to spatial and temporal representivity, especially when the bulk of the rainfall occurs in the form of showers and thundershowers.

c) Predictions of future fire danger are sensitive to the choice of GCM and emission scenario used. GCMs focus primarily on GHG emissions as a climate forcing while potential changes in the composition of the biome are under-represented. Climate projections by GCMs, especially rainfall predictions, are surrounded by uncertainty. The results reported in this study were based on a “worst case scenario”, and could have been significantly different if a high mitigation GHG emission scenario was also condidered.

The assumption was made that land use practices will continue in a manner familiar today and that there will be no escalation to woody communities within the study area. The limitations listed above were not overcome, but by shifting the focus to climate-related fire danger a number of these complicating factors were eliminated and the validity of the results strengthened.

10.5 RECOMMENDATIONS AND FUTURE RESEARCH

Irrespective of fuel characteristics and ignition probabilities, climatological fire danger over the central grassland biome of South Africa has been increasing in recent history. Future projections also indicate further increases in climatological fire danger, with extreme fire danger conditions becoming more rampant. Future fire suppression requirements are thus likely to impose greater demands on fire fighting and exceed the current capacity. Policy makers should be aware of this and strategize accordingly.

Although wildfires are an important and necessary abiotic factor in the grassland biome, land managers, particularly livestock farmers, need to be more vigilant if they want to effectively control the timing and extend of burning in order to prevent unplanned costly wildfires. Fuel management (e.g. fuel reduction and isolation) training should be provided to commercial, communal and emerging farmers alike. All tiers of government and all potential stakeholders should invest in fuel management and fire suppression infrastrastructure. For example, government must aid in establishing fire breaks along roads and railroads at the onset of the fire season. Furthermore, rural land owners should no longer have a choice in joining their local fire protection agency – the collective cost of one land owner failing to implement adequate measures could simply be too high.

This study assessed the historical and future climate-related fire danger across the central grassland biome of South Africa. In the process some interesting possibilities for future research were identified in order to further understand the linkages between wildland fires and climate variability and change. These include:

a) Incorporating topography in the fire danger assessment.
b) Incorporating fuel characteristics in the fire danger assessment.
    - The use of seasonal weather forecasts to empirically predict fuel loads during the ensuing fire season.

- The use of a grassland production model to simulate fuel loads and using the current season's observations or future climate projections as input. However, a suitable biophysical model could not be identified yet and must first be subjected to validation against limited production data. The interdisciplinary nature of such an endeavour necessitates collaboration with a team of experts.

c) Expanding this type of research to all grasslands or other biomes in the region (e.g. savanna or fynbos).

GLOSSARY

Back fire

That part of the fire perimeter that propagates against the wind (or down-slope) with the flames leaning over already burnt material (CSIRO, 2013; Trollope *et al*., 2004).

Back burning

A technique used in controlled burning and wildfire suppression which entails starting small fires along a manmade or natural firebreak in front of a main fire front. The small fires will burn “back towards the main fire front” against the wind direction. The rationale behind back burning is to remove the fuel in front of the main fire line.

Chimney

A topographic feature with three walls that form a steep, narrow chute through which airflow can be channelled (The COMET Program, 2009e).

Climate feedback

An internal climate process that amplifies or dampens the climate response to an initial forcing (NRC, 2005).

Climate forcing

An energy imbalance imposed on the climate system by either natural or manmade influences (NRC, 2005).

Curing

Either refers to the process whereby the fuel (dead plant material) loses moisture over time, or the proportional weight of dead plant material to live plant material. A curing factor of 80% means that of the total grass biomass, 80% of the grass is

dead (Willis *et al*., 2001). The percentage curing of grassland is used to estimate fuel availability.

Draped fuels

Aerial fuels in the form of needles, leaves, twigs, etc. that fell from the forest canopy and have lodged on lower branches and brush (Schlobohm & Brain, 2002).

Duff

Partially decomposed organic material of the forest floor located below any recently fallen twigs, needles and leaves (Schlobohm & Brain, 2002).

Ensemble members

Sets of model simulations typically stemming either from different GCMs (referred to as Multi-model Ensembles, MMEs), or from a single GCM with slight modifications in either the initial conditions or in its physical or chemical description (referred to as Perturbed Parameter (or Physics) Ensembles, PPEs) (Flato *et al*., 2013; McGuffie & Henderson-Sellers, 2014).

Equilibrium Moisture Content (EQMC)

Represents the moisture content a dead fuel would have if it were allowed to gain or lose moisture for a sufficiently long period at a constant temperature and humidity (Laing, 1978).

Fire behaviour

Refers to “the release of heat energy during combustion as described by fire intensity, rate of spread of the fire front, flame characteristics and other related phenomena” (Trollope, 1981).

Firebrand

A mobile ignition source such as a flying ember or flaming rolling log or pine cone that may result in spotting. Firebrands enhance the ability of a fire to cross potential

barriers and less combustible areas (Hargrove *et al*., 2000; The COMET Program, 2009b).

Fire ecology

Defined by Trollope (1981) as “the study of the response of the biotic and abiotic components of the ecosystem to the season, frequency, type and intensity of fire”.

Fire effects

Designates both direct (e.g. fuel consumption, mortality of flora and fauna, smoke generation) and indirect (e.g. plant succession and soil erosion) consequences of a fire on ecosystem components.

Fire intensity

Refers to “the release of heat energy per unit time per unit length of fire front” and is expressed in $kJs^{-1}m^{-1}$ (Byram, 1959; cited by de Ronde *et al*., 2004b; Moreira *et al*., 2011).

Fire regime

A term given to the general pattern in which fires naturally occur in a particular ecosystem over an extended period of time (Weston, 2010). It encompasses a number of factors including frequency, intensity, severity (comprising physical and ecological aspects), season of burn, type of fire (crown, surface, ground) and size (including shape or pattern) (Weber & Flannigan, 1997 and Gill & Allan, 2008; cited by de Groot *et al*., 2013; Scott *et al*., 2014).

Fire season

The fire season commences when the fuel moisture content drops to the point where it becomes potentially combustible (Laing, 1978). Its onset is the result of pre-season influences which may stretch backwards for several months. In the grasslands of southern Africa the fire season extends from mid-winter to early summer (de Ronde *et al*., 2004b), prior to the arrival of the main rains.

Fire severity

Fire severity refers to the loss or damage to vegetation that may be determined through either ground observations or by satellite data (Scott *et al*., 2014). Although Moreira *et al*. (2011) defined it as a measure of the impact of the fire on soil and vegetation as measured by indicators such as plant mortality, the degree of canopy damage or the amount of surface litter consumed, Scott *et al*. (2014) would rather allocate those aspects to “burn severity”.

Firestorm

A conflagration which attains such intensity that it creates and sustains its own wind circulation as the rising hot air draws in more of the surrounding air. The strong updraft creates severe turbulence and erratic winds, while the pronounced wind shear is capable of producing tornado-like features called fire whirls (ScienceDaily, 2015).

Fire weather

The weather variables (climatic elements) that influence fire behaviour, starts, and suppression (e.g. temperature, precipitation, humidity and wind) (Flannigan *et al*., 2009).

Fire whirl

A tornado-like feature comprising a moving, vertically oriented vortex of rapidly rising air that lifts smoke, debris and fire. Fire whirls range in size from a few centimetres to over 150 m in diameter while wind speeds in the centre can exceed 80 knots (The COMET Program, 2010b).

Flame height

The average vertical distance measured from the tip of the flame to a position on the ground directly below it. This value may be significantly smaller than the flame

length when flames are tilted due to the effects of wind and slope (The COMET Program, 2009a).

Flame length

The distance measured (at an angle when the flames are tilted in windy conditions or on terrain with an acute slope) from the middle of the flaming zone at base of the fire to the tip of the flame (The COMET Program, 2009a).

Flank fire

That part of the fire perimeter that is generally aligned parallel to the wind direction with the flames more or less leaning along the flank (CSIRO, 2013).

Fuel moisture content

The amount of water in a fuel – usually expressed as a percentage of dry weight of the plant material (Bianci & Defosse, 2014). It affects the ease of ignition, the fraction of fuel consumed as well as the combustion rate thereof.

Head fire

The most rapidly spreading part of the fire perimeter where the flames are driven by wind (or assisted by sloping terrain) towards unburnt fuel (CSIRO, 2013; Trollope *et al*., 2004).

Ladder fuels

Vertically continuous fuels which enable the advancement from surface to crown fires (The COMET Program, 2009b).

Radiative forcing (RF)

Often used as a measure of climate impacts and their relative importance, RF is defined as “a perturbation to the net radiative flux at the top of the atmosphere or the tropopause relative to the pre-industrial state” (Ward *et al*., 2012)

Slope reversal

When a fire crosses over a ridge line or drainage to a slope with a different orientation.

Sourveld

Veld in which the grasses are only palatable in the growing season, typically found in high rainfall areas (van Oudtshoorn, 2012).

Spot fire

A new fire started some distance ahead of the main fire front by burning embers carried with the wind (Trollope *et al*., 2004) or firebrands rolling downhill.

Sweetveld

Veld in which most of the grasses are palatable throughout the year, typically found in low rainfall areas (van Oudtshoorn, 2012).

Wildfire

An unplanned vegetation fire. A generic term which includes grass, forest and shrub fires.

REFERENCES

ACOCKS, J.P.H., 1953. *Veld Types of South Africa. Botanical Survey Memoir No. 28*. Pretoria: Government Printer. 192pp.

ACT NO. 101 of 1998. National Veld and Forest Fire Act, 1998. *Government Gazette of the Republic of South Africa* No. 19515.

ADAB, H., KANNIAH, K.D. and SOLAIMANI, K., 2013. Modeling forest fire risk in the northeast of Iran using remote sensing and GIS techniques. *Natural Hazards* 65, 1723-1743.

AHRENS, C.D., 2003. *Meteorology Today: An Introduction to Weather, Climate, and the Environment*. 7th Ed. Pacific Grove: Brooks/Cole.

ALBERTSON, K., AYLEN, J., CAVAN, G. and MCMORROW, J., 2010. Climate change and the future occurrence of moorland wildfires in the Peak District of the UK. *Climate Research* 45(24), 105-118.

ALDERSLEY, A., MURRAY, S.J. and CORNELL, S.E., 2011. Global and regional analysis of climate and human drivers of wildfire. *Science of the Total Environment* 409, 3472-3481.

ALEXANDER, M.E., 1990. Computer calculation of the Keetch-Byram drought index – Programmers beware! *Fire Management Notes* 51(4), 23-24.

ALLEN, O.E., 1988. *Planet Earth: Atmosphere*. Amsterdam: Time-Life Books. 176pp.

ALLEN, R.G., PEREIRA, L.S., RAES, D. and SMITH, M., 1998. *Crop Evaporation – Guidelines for Computing Crop Water Requirements – FAO Irrigation and Drainage Paper 56*. Rome: FAO.

ALMASY, S. and GALLMAN, S., 2015. Canada wildfires: Thousands flee homes in Saskatchewan, British Columbia. *Cable News Network (CNN)*, 9 July 2015.

ALVARADO, S.T., FORNAZARI, T., CÓSTOLA, A., MORELLATO, L.P.C. and SILVA, T.S.F., 2017. Drivers of fire occurrence in a mountainous Brazilian

cerrado savanna: Tracking long-term fire regimes using remote sensing. *Ecological Indicators* 78, 270-281.

AMIRO, B.D., CANTIN, A., FLANNIGAN, M.D. and DE GROOT, W.J., 2009. Future emissions from Canadian boreal forest fires. *Canadian Journal of Forest Research* 39, 383-395.

AMIRO, B.D., STOCKS, B.J., ALEXANDER, M.E., FLANNIGAN, M.D. and WOTTON, B.M., 2001. Fire, climate change, carbon and fuel management in the Canadian boreal forest. *International Journal of Wildland Fire* 10, 405-413.

ANDERSON, K.R. and ENGLEFIELD, P., 2001. Quantile characteristics of forest fires in Saskatchewan. *Proceedings of the 4th Symposium on Fire and Forest Meteorology, 13 – 15 November 2001, Reno, Nevada, USA*. p9-16.

ANDREAE, M.O., 1997. Emissions of Trace Gases and Aerosols from South African Savanna Fires. In: B.W. van Wilgen, M.O. Andreae, J.G. Goldammer & J.A. Lindesay (eds.). *Fire in Southern African Savannas. Ecological and Atmospheric Perspectives*. Cape Town: Witwatersrand University Press. p161-177.

ANDREAE, M.O. and MERLET, P., 2001. Emission of trace gases and aerosols

ANDREWS, P.L., LOFTSGAARDEN, D.O. and BRADSHAW, L.S., 2003. Evaluation of fire danger rating indexes using logistic regression and percentile analysis. *International Journal of Wildland Fire* 12(2), 213-226.

ANNAS, S., KANAI, T. and KOYAMA, S., 2007. Principal Component Analysis and Self-Organizing Map for visualizing and classifying fire risks in forest regions. *Agricultural Information Research* 16(2), 44-51.

ANTHES, R.A., PANOFSKY, H.A., CAHIR, J.J. and RANGO, A., 1975. *The Atmosphere*. Charles E. Columbus: Merrill Publishing Co. 339pp.

ARAVENA, J.C., LEQUESNE, C., JIMENEZ, H., LARA, A. and ARMESTO, J.J., 2003. Fire History in Central Chile: Tree-Ring Evidence and Modern Records. In: T.T. Veblen, W.L. Baker, G. Montenegro & T.W. Swetnam (eds.). *Ecological Studies, Vol. 160: Fire and Climatic Change in Temperate Ecosystems of the Western Americas*. New York: Springer-Verlag. 444pp.

ARCHIBALD, S., 2008. “Where there is a spark is there fire?: The importance of ignitions in determining fire regimes in southern Africa”. *South African Journal of Botany* 74(2), 360, doi:10.1016/j.sajb.2008.01.028.

ARCHIBALD, S., NICKLESS, A., GOVENDER, N., SCHOLES, R.J. and LEHSTEN, V., 2010b. Climate and the inter-annual variability of fire in southern Africa: a meta-analysis using long-term field data and satellite-derived burnt area data. *Global Ecology and Biogeography* 19, 794-809.

ARCHIBALD, S., SCHOLES, R.J., ROY, D.P., ROBERTS, G. and BOSCHETTI, L., 2010a. Southern African fire regimes as revealed by remote sensing. *International Journal of Wildland Fire* 19, 861-878.

ARYA, A.P., 2001. *Introduction to Micrometeorology*. 2nd Ed. London: Academic Press. 420pp.

ATKINS, N., 2014. *London State College Survey of Meteorology* [Online]. Retrieved from http://apollo.lsc.vsc.edu/classes/met130/ (Accessed 11/02/2014).

AYRES, J., MAYNARD, R. and RICHARDS, R., 2006. *Air Pollution Reviews: Air Pollution and Health*. Singapore: Imperial College Press. 249pp.

BAÇÃO, F. and LOBO, V., 2010. *Introduction to Kohonen’s Self-Organizing Maps*. Lisbon: Instituto Superior de Estatística e Gestão de Informação. 22pp.

BAKER, W.L., 2015. Are high-severity fires burning at much higher rates recently than historically in dry-forest landscapes of the western USA? *PLoS One* 10(9), e0136147, doi:10.1371/journal.pone.0136147.

BAL, M.-C., PELACHS, A., PEREZ-OBIOL, R., JULIA, R. and CUNILL, R., 2011. Fire history and human activities during the last 3300 cal yr BP in Spain's Central Pyrenees: The case of the Estany de Burg. *Palaeogeography, Palaeoclimatology, Palaeoecology* 300, 179-190.

BALFOUR, D.A. and MIDGLEY, J.J., 2006. Fire induced stem death in an African acacia is not caused by canopy scorching. *Austral Ecology* 31, 892-896.

BALLING, R.C., MEYER, G.A. and WELLS, S.G., 1992. Climate change in Yellowstone National Park: Is the drought-related risk of wildfires increasing? *Climatic Change* 22, 35-45.

BALOG, J., 2010. Birthday Canyon, Greenland Ice Sheet [Online]. Retrieved from https://ncmns.wordpress.com/2013/06/12/when-glaciers-get-dirty/ (Accessed 21/10/2016).

BALSHI, M.S., MCGUIRE, A.D., DUFFY, P., FLANNIGAN, M., WALSH, J. and MELILLO, J., 2008. Assessing the response of area burned to changing climate in western boreal North America using a Multivariate Adaptive Regression Splines (MARS) approach. *Global Change Biology* 15, 578-600.

BARBOSA, P.M., STROPPIANA, D. and GRÉGOIRE, J.-M., 1999. An assessment of vegetation fire in Africa (1981 – 1991): Burned areas, burned biomass, and atmospheric emissions. *Global Biogeochemical Cycles* 13(4), 933-950.

BARLOW, J. and PERES, C.A., 2004. Ecological responses to El Niño-induced surface fires in central Brazilian Amazonia: management implications for flammable tropical forests. *Philosophical Transactions of the Royal Society of London. Series B: Biological Sciences* 359(1443), 367-380.

BARROS, A.M.G., PEREIRA, J.M.C., and LUND, U.J., 2012. Identifying geographical patterns of wildfire orientation: A watershed-based analysis. *Forest Ecology and Management* 264, 98-107.

BARRY, R.G., 2008. *Mountain Weather and Climate*. 3rd Ed. Cambridge: Cambridge University Press. 506pp.

BARRY, R.G. and CARLETON, A.M., 2001. *Synoptic and Dynamic Climatology*. London: Routledge. 620pp.

BARRY, R.G. and PERRY, A.H., 1973. *Synoptic Climatology: Methods and Applications*. London: Methuen & Co. 555pp.

BARRY, R.G. and PERRY, A.H., 2001. *Synoptic climatology and its applications*. In: R.G. Barry & A.M. Carleton (eds.). *Synoptic and Dynamic Climatology*. London: Routledge.

BATLLORI, E., PARISIEN, M.-A., KRAWCHUK, M.A. and MORITZ, M.A., 2013. Climate change-induced shifts in fire for Mediterranean ecosystems. *Global Ecology and Biogeography* 22, 1118-1129.

BAUMBACH, G. and VOGT, U., 1999. Experimental determination of the effect of mountain-valley breeze circulation on air pollution in the vicinity of Freiburg. *Atmospheric Environment* 33, 4019-4027.

BECK, C., GRIESER, J., KOTTEK, M., RUBEL, F. and RUDOLF, B., 2005. Characterizing Global Climate Change by means of Köppen Climate Classification. *DWD Klimastatusbericht* 2005, 139-149.

BECK, C. and PHILIPP, A., 2010. Evaluation and comparison of circulation type classifications for the European domain. *Physics and Chemistry of the Earth* 35, 374- 387.

BECK, P.A., GOETZ, S.J., MACK, M.C., ALEXANDER, H.D., JIN, Y., RANDERSON, J.T. and LORANTY, M.M., 2011. The impacts and implications of an intensifying fire regime on Alaskan boreal forest composition and albedo. *Global Change Biology* 17, 2853-2866.

BEDIA, J., HERRERA, S., GUTIÉRREZ, J.M., BENALI, A., BRANDS, S., MOTA, B. and MORENO, J.M., 2015. Global patterns in the sensitivity of burned area to fire-weather: Implications for climate change. *Agricultural and Forest Meteorology* 214-215, 369-379.

BEDIA, J., HERRERA, S., SAN MARTÍN, D., KOUTSIAS, N. and GUTIÉRREZ, J.M., 2013. Robust projections of Fire Weather Index in the Mediterranean using statistical downscaling. *Climatic Change* 120, 229-247.

BEER, T., 1990. The Australian national bushfire model project. *Mathematical and Computer Modelling* 13(12), 49-56.

BEER, T. and WILLIAMS, A., 1995. Estimating Australian forest fire danger under conditions of doubled carbon dioxide concentrations. *Climatic Change* 29, 169-188.

BELL, T. and ADAMS, M., 2009. Smoke from Wildfires and Prescribed Burning in Australia: Effects on Human Health and Ecosystems. In: A. Bytnerowicz, M. Arbaugh, A. Riebau & C. Andersen (eds.). *Wildland Fires and Air Pollution*. Amsterdam: Elsevier. p289-316.

BELL, T.L., ROSENFELD, D., KIM, K.-M., YOO, J.-M., LEE, M.-I. and HAHNENBERGER, M., 2008. Midweek increase in U.S. summer rain and

storm heights suggests air pollution invigorates rainstorms. *Journal of Geophysical Research* 113, D02209, doi:10.1029/2007JD008623.

BENESTAD, R.E., 2004. Empirical-statistical downscaling in climate modeling. *Eos Transactions of the American Geophysical Union* 85(42), 417-422.

BERGERON, Y. and FLANNIGAN, M.D., 1995. Predicting the effects of climate change on fire frequency in the southeastern Canadian boreal forest. *Water, Air and Soil Pollution* 82, 437-444.

BERGERON, Y., FLANNIGAN, M., GAUTHIER, S., LEDUC, A. and PATRICK LEFORT, P., 2004. Past, current and future fire frequency in the Canadian boreal forest: Implications for sustainable forest management. *Ambio* 33(6), 356-360.

BIERLY, E.W. and HEWSON, E.W., 1962. Some restrictive meteorological conditions to be considered in the design of stacks. *Journal of Applied Meteorology* 1, 383-390.

BINKLEY, D., BECKER-HEIDMANN, P., CLARK, J.S., CRUTZEN, P.J., FROST, P., GILL, A.M., GRANSTRÖM, A., MACK, F., MENAUT, J.-C., WEIN, R.W. and VAN WILGEN, B., 1993. Group Report: Impacts of Fires on Ecosystems. In: P.J. Crutzen & J.G. Goldammer (eds.). *Fire in the Environment. The Ecological, Atmospheric, and Climatic Importance of Vegetation Fires*. Chichester: John Wiley & Sons. p360-372.

BIRD, M.I. and CALI, J.A., 1998. A million-year record of fire in sub-Saharan Africa. *Nature* 394, 767-769.

BIRDLIFE SOUTH AFRICA, 2017. The Grassland Biome [Online]. Retrieved from https://www.birdlife.org.za/conservation/terrestrial-bird-conservation/the-grassland-biome (Accessed 15/12/2017).

BOND, T.C., DOHERTY, S.J., FAHEY, D.W., FORSTER, P.M., BERNTSEN, T., DEANGELO, B.J., FLANNER, M.G., GHAN, S., KÄRCHER, B., KOCH, D., KINNE, S., KONDO, Y., QUINN, P.K., SAROFIM, M.C., SCHULTZ, M.G., SCHULZ, M., VENKATARAMAN, C., ZHANG, H., ZHANG, S., BELLOUIN, N., GUTTIKUNDA, S.K., HOPKE, P.K., JACOBSON, M.Z., KAISER, J.W., KLIMONT, Z., LOHMANN, U., SCHWARZ, J.P., SHINDELL, D.,

STORELVMO, T., WARREN, S.G. and ZENDER, C.S., 2013. Bounding the role of black carbon in the climate system: A scientific assessment. *Journal of Geophysical Research: Atmospheres* 118, 5380-5552.

BOND, W.J., GELDENHUYS, C.J., EVERSON, T.M., EVERSON, C.S. and CALVIN, M.F., 2004. Fire Ecology: Characteristics of some Important Biomes of sub-Sahara Africa. In: J.G. Goldammer & C. de Ronde (eds.). *Wildland Fire Management Handbook for sub-Sahara Africa*. Stellenbosch: comPress. p11-26.

BOND, W.J. and VAN WILGEN, B.W., 1996. *Fire and Plants*. London: Chapman & Hall. 262pp.

BOND, W.J., WOODWARD, F.I. and MIDGLEY, G.F., 2005. The global distribution of ecosystems in a world without fire. *New Phytologist* 165, 525-538.

BORGHETTI, M., DE ANGELIS, P., RASCHI, A., SCARASCIA-MUGNOZZA, G.E., TOGNETTI, R. and VALENTINI, R., 1993. Relations between sap velocity and cavitation in broad-leaved trees. In: M. Borghetti, J. Grace & A. Raschi (eds.). *Water Transport in Plants under Climatic Stress*. Cambridge: Cambridge University Press. p114-139.

BOWMAN, D.M.J.S., BALCH, J.K., ARTAXO, P., BOND, W.J., CARLSON, J.M., COCHRANE, M.A., D'ANTONIO, C.M., DE FRIES, R.S., DOYLE, J.C., HARRISON, S.P., JOHNSTON, F.H., KEELEY, J.E., KRAWCHUK, M.A., KULL, C.A., MARSTON, J.B., MORITZ, M.A., PRENTICE, I.C., ROOS, C.I., SCOTT, A.C., SWETNAM, T.W., VAN DER WERF, G.R. and PYNE, S.J., 2009. Fire in the Earth System. *Science* 324(5926), 481-484.

BOX, G.E.P. and DRAPER, N.R., 1987. *Empirical Model-Building and Response Surfaces*. Chichester: John Wiley & Sons.

BRADSTOCK, R.A., 2010. A biogeographic model of fire regimes in Australia: current and future implications. *Global Ecology and Biogeography* 19, 145-158.

BRADSTOCK, R.A., COHN, J.S., GILL, A.M., BEDWARD, M. and LUCAS, C., 2009. Prediction of the probability of large fires in the Sydney region of

south-eastern Australia using fire weather. *International Journal of Wildland Fire* 18, 932-943.

BRANSBY, D.I. and TAINTON, N.M., 1977. The disc pasture meter: possible applications in grazing management. *African Journal of Range & Forage Science* 12(1), 115-118.

BROWN, T.J., HALL, B.L. and WESTERLING, A.L., 2004. The impact of twenty-first century climate change on wildland fire danger in the western United States: An applications perspective. *Climatic Change* 62, 365-388.

BUCKLE, C., 1996. *Weather and Climate in Africa*. Edinburgh Gate: Longman.

BYTNEROWICZ, A., ARBAUGH, M.J., ANDERSEN, C. and RIEBAU, A.R., 2009. Integrating Research on Wildland Fires and Air Quality: Needs and Recommendations. In: A. Bytnerowicz, M.J. Arbaugh, A.R. Riebau & C. Andersen (eds.). *Wildland Fires and Air Pollution*. Amsterdam: Elsevier. p585-602.

CALDER, W.J., PARKE, D., STOPKA, C.J., JIMÉNEZ-MORENO, G., and SHUMAN, B.N., 2015. Medieval warming initiated exceptionally large wildfire outbreaks in the Rocky Mountains. *Proceedings of the National Academy of Sciences* 112(43), 13261-13266.

CAMPBELL, G.S. and NORMAN, J.M., 1998. An Introduction to Environmental Biophysics. 2nd Ed. New York: Springer. 286pp.

CAMPBELL, N.A., 1996. *Biology*. 4th Ed. Menlo Park: Benjamin/Cummings.

CARTER, V.A., POWER, M.J., LUNDEEN, Z.J., MORRIS, J.L., PETERSEN, K.L., BRUNELLE, A., ANDERSON, R.S., SHINKER, J.J., TURNEY, L., KOLL, R. and BARTLEIN, P.J., 2017. A 1,500-year synthesis of wildfire activity stratified by elevation from the U.S. Rocky Mountains. *Quaternary International*, in press, doi:10.1016/j.quaint.2017.06.051.

CARVALHO, A.C., CARVALHO, A., MARTINS, H., MARQUES, C., ROCHA, A., BORREGO, C., VIEGAS, D.X. and MIRANDA, A.I., 2011. Fire weather risk assessment under climate change using a dynamical downscaling approach. *Environmental Modelling & Software* 26, 1123-1133.

CARVALHO, A.C., FLANNIGAN, M.D., LOGAN, K.A., GOWMAN, L.M., MIRANDA, A.I. and BORREGO, C., 2010. The impact of spatial resolution on area burned and fire occurrence projections in Portugal under climate change. *Climatic Change* 98, 177-197.

CASSANO, E.N., CASSANO, J.J. and NOLAN, M., 2011. Synoptic weather pattern controls on temperature in Alaska. *Journal of Geophysical Research* 116, D11108, doi:10.1029/2010JD015341.

CASTELLNOU, M., LARRAÑAGA, A., MIRALLES, M., VILALTA, O. and MOLINA, D., 2010. Wildfire Scenarios: Learning from Experience. In: J.S. Silva, F. Rego, P. Fernandes & E. Rigolot (eds.). *Towards Integrated Fire Management – Outcomes of the European Project Fire Paradox*. European Forest Institute Research Report 23. Retrieved from http://www.efi.int/files/attachments/publications/efi_rr23.pdf (Accessed 10/07/2016).

CASTRO, R. and CHUVIECO, E., 1998. Modeling forest fire danger from geographic information systems. *Geocarto International* 13(1), 15-23.

CATRY, F.X., REGO, F.C., SILVA, J.S., MOREIRA, F., CAMIA, A., RICOTTA, C. and CONEDERA, M., 2010. Fire Starts and Human Activities. In: J.S. Silva, F. Rego, P. Fernandes & E. Rigolot (eds.). *Towards Integrated Fire Management – Outcomes of the European Project Fire Paradox*. European Forest Institute Research Report 23. Retrieved from http://www.efi.int/files/attachments/publications/efi_rr23.pdf (Accessed 10/07/2016).

CAUSLEY C.L., FOWLER, W.M., LAMONT, B.B. and HE, T., 2016. Fitness benefits of serotiny in fire- and drought-prone environments. *Plant Ecology* 217(6), 773-779.

CAVAZOS, T., 1999. Large-scale circulation anomalies conducive to extreme precipitation events and derivation of daily rainfall in northeastern Mexico and southeastern Texas. *Journal of Climate* 12, 1506-1523.

CAVAZOS, T., 2000. Using self-organizing maps to investigate extreme climate events: An application to wintertime precipitation in the Balkans. *Journal of Climate* 13, 1718-1732.

CAVAZOS, T. and HEWITSON, B.C., 2005. Performance of NCEP-NCAR reanalysis variables in statistical downscaling of daily precipitation. *Climatic Research* 28, 95-107.

CERTINI, G., 2005. Effects of Fire on Properties of Forest Soils: A Review. *Oecologia* 143(1), 1-10.

CHATTOPADHYAY, R., SAHAI, A.K. and GOSWAMI, B.N., 2008. Objective identification of nonlinear convectively coupled phases of monsoon intraseasonal oscillation: Implications for prediction. *Journal of the Atmospheric Sciences* 65, 1549-1569.

CHATTOPADHYAY, R., VINTZILEOS, A. and ZHANG, C., 2013. A description of the Madden-Julian Oscillation based on a self-organizing map. *Journal of Climate* 26, 1716-1732.

CHENEY, N.P., GOULD, J.S. and CATCHPOLE, W.R., 1993. The influence of fuel, weather and fire-shape variables on fire-spread in grasslands. *International Journal of Wildland Fire* 3(1), 31-44.

CHENEY, N.P. and SULLIVAN, A., 1997. *Grassfires, fuel, weather and fire behaviour*. Melbourne: CSIRO. 102pp.

CHOCZYNSKA, J. and JOHNSON, E.A., 2009. A soil heat and water transfer model to predict belowground grass rhizome bud death in a grass fire. *Journal of Vegetation Science* 20, 277-287.

CHRISTENSEN, N.L., 1993. Fire Regimes and Ecosystem Dynamics. In: P.J. Crutzen & J.G. Goldammer (eds.). *Fire in the Environment. The Ecological, Atmospheric, and Climatic Importance of Vegetation Fires*. Chichester: John Wiley & Sons. p233-244.

CHRISTIAN, T.J., KLEISS, B., YOKELSON, R.J., HOLZINGER, R., CRUTZEN, P.J., HAO, W.M., SAHARJO, B.H. and WARD, D.E., 2003. Comprehensive laboratory measurements of biomass-burning emissions: 1. Emissions from Indonesian, African, and other fuels. *Journal of Geophysical Research* 108(D23), 4719, doi:10.1029/2003JD003704.

CHRUST, M.F., WHITEMAN, C.D. and HOCH, S.W., 2013. Observations of thermally driven wind jets at the exit of Weber Canyon, Utah. *Journal of Applied Meteorology and Climatology* 52:5, 1187-1200.

CHUBAROVA, N.Y., PRILEPSKY, N.G., RUBLEV, A.N. and RIEBAU, A.R., 2009. A Mega-Fire Event in Central Russia: Fire Weather, Radiative, and Optical Properties of the Atmosphere, and Consequences for Subboreal Forest Plants. In: A. Bytnerowicz, M. Arbaugh, A. Riebau & C. Andersen (eds.). *Wildland Fires and Air Pollution*. Amsterdam: Elsevier. p247-264.

CHUVIECO, E., 2003. *Wildland Fire Danger Estimation and Mapping: The Role of Remote Sensing Data. Series in Remote Sensing Vol. 4*. Singapore: World Scientific.

CICS (Canadian Institute for Climate Studies), 2016. Canadian Climate Impacts and Scenarios FAQ: Downscaling Background. Retrieved from http://web.archive.org/web/20150922174716/http:/www.cics.uvic.ca/scenarios/ (Accessed 10/07/2016).

CIS (Laboratory of Computer and Information Science), 2017. Bibliography of SOM papers [Online]. Retrieved from http://www.cis.hut.fi/research/som-bibl/ (Accessed 10/12/2016).

COLA (Center for Ocean-Land-Atmosphere Studies), 2018. The Grid Analysis and Display System (GrADS). [Online]. Retrieved from http://cola.gmu.edu/grads/ (Accessed 13/08/2018).

COLEMAN, T.W. and RIESKE, L.K., 2006. Arthropod response to prescription burning at the soil-litter interface in oak-pine forests. *Forest Ecology and Management* 233, 52-60.

COLLINS, M., KNUTTI, R., ARBLASTER, J., DUFRESNE, J.-L., FICHEFET, T., FRIEDLINGSTEIN, P., GAO, X., GUTIWSKI, W.J., JOHNS, T., KRINNER, G., SHONGWE, M., TEBALDI, A., WEAVER, A.J. and WEHNER, M., 2013. Long-term Climate Change: Projections, Commitments and Irreversibility. In: T.F. Stocker, D. Qin, G.-K. Plattner, M. Tignor, S.K. Allen, J. Boschung, A. Nauels, Y. Xia, V. Bex & P.M. Midgley (eds.). *Climate Change 2013: The Physical Science Basis. Contribution of Working Group I to the Fifth*

Assessment Report of the Intergovernmental Panel on Climate Change. Cambridge: Cambridge University Press.

COSTANZA, J.K., TERANDO, A.J., MCKERROW, A.J. and COLLAZO, J.A., 2015. Modeling climate change, urbanization, and fire effects on *Pinus palustris* ecosystems of the southeastern U.S. *Journal of Environmental Management* 151, 186-199.

COTTON, W.R. and PIELKE, R.A., 2007. *Human Impacts on Weather and Climate. 2nd Ed*. Cambridge: Cambridge University Press.

COUNTRY FIRE AUTHORITY (CFA), 2016. Fire Danger Rating Brochure [Online]. Retreived from http://www.cfa.vic.gov.au/warnings-restrictions/about-fire-danger-ratings/fire_danger_rating.pdf (Accessed 07/12/2016).

CRIMMINS, M.A., 2006. Synoptic climatology of extreme fire-weather conditions across the southwest United States. *International Journal of Climatology* 26, 1001-1016.

CRIMMINS, M.A. and COMRIE, A.C., 2004. Interactions between antecedent climate and wildfire variability across south-eastern Arizona. *International Journal of Wildland Fire* 13, 455-466.

CROSBY, J.S. and CHANDLER, C.C., 2009. NC Fire Weather Tech Note 01 – Getting the most from your wind speed observation [Online]. Retrieved from http://ncforestservice.gov/fire_control/fc_technotes.htm (Accessed 08/08/2014).

CRUZ, M.G. and PLUCINSKI, M.P., 2007. *Billo road fire: report on fire behaviour and suppression activities*. Report no. A.07.02. Yarralumla: Bushfire Cooperative Research Centre.

CSIRO, 2013. Bushfire behaviour and the fire environment [Online]. Retrieved from http://www.csiro.au/Outcomes/Safeguarding-Australia/Bushfire Behaviour-2.aspx (Accessed 11/12/2013).

CUBASCH, U., WUEBBLES, D., CHEN, D., FACCHINI, M.C., FRAME, D., MAHOWALD, N. and WINTHER, J.-G., 2013. Introduction. In: Stocker, T.F., D. Qin, G.-K. Plattner, M. Tignor, S.K. Allen, J. Boschung, A. Nauels, Y. Xia, V. Bex & P.M. Midgley (eds.). *Climate Change 2013: The Physical Science*

Basis. Contribution of Working Group I to the Fifth Assessment Report of the Intergovernmental Panel on Climate Change. Cambridge: Cambridge University Press. p119-158.

CURT, T., BORGNIET, L. and BOUILLON, C., 2013. Wildfire frequency varies with the size and shape of fuel types in southeastern France: Implications for environmental management. *Journal of Environmental Management* 117, 150-161.

CURT, T., SCHAFFHAUSER, A., BORGNIET, L., DUMAS, C., ESTEVE, R., GANTEAUME, A., JAPPIOT, M., MARTIN, W., N'DIAYE, A. and POILVET, B., 2011. Litter flammability in oak woodlands and shrublands of southeastern France. *Forest Ecology and Management* 261, 2214-2222.

CWFIS (Canadian Wildland Fire Information System), 2015. Canadian Wildland Fire Information System [Online]. Retrieved from http://cwfis.cfs.nrcan.gc.ca/home (Accessed 01/07/2015).

C3S (Copernicus Climate Change Service), 2019. ERA5: Fifth generation of ECMWF atmospheric reanalyses of the global climate. Copernicus Climate Change Service Climate Data Store (CDS) [Online]. Retrieved from https://cds.climate.copernicus.eu/cdsapp#!/home (Accessed 02/06/2019).

DAFF (Department of Agriculture, Forestry and Fisheries), 2017. Crop Estimates [Online]. Retrieved from www.daff.gov.za/statistics (Accessed 11/11/2017).

DANIAUA, A.-L., BARTLEIN, P.J., HARRISON, S.P., PRENTICE, I.C., BREWER, S., FRIEDLINGSTEIN, P., HARRISON-PRENTICE, T.I., INOUE, J., IZUMI, K., MARLON, J.R., MOONEY, S., POWER, M.J., STEVENSON, J., TINNER, W., ANDRIČ, M., ATANASSOVA, J., BEHLING, H., BLACK, M., BLARQUEZ, O., BROWN, K.J., CARCAILLET, C., COLHOUN, E.A., COLOMBAROLI, D., DAVIS, B.A.S., D'COSTA, D., DODSON, J., DUPONT, L., ESHETU, Z., GAVIN, D.G., GENRIES, A., HABERLE, S., HALLETT, D.J., HOPE, G., HORN, S.P., KASSA, T.G., KATAMURA, F., KENNEDY, L.M., KERSHAW, P., KRIVONOGOV, S., LONG, C., MAGRI, D., MARINOVA, E., MCKENZIE, G.M., MORENO, P.I., MOSS, P., NEUMANN, F.H., NORSTRÖM, E., PAITRE, C., RIUS, D., ROBERTS, N., ROBINSON,

G.S., SASAKI, N., SCOTT, L., TAKAHARA, H., TERWILLIGER, V., THEVENON, F., TURNER, R., VALSECCHI, V.G., VANNIÈRE, B., WALSH, M., WILLIAMS, N. and ZHANG, Y., 2012. Predictability of biomass burning in response to climate changes. *Global Biogeochemical Cycles* 26, GB4007, doi:10.1029/2011GB004249.

DANIAUA, A.-L., GOÑI, M.F.S., MARTINEZ, P., URREGO, D.H., BOUT-ROUMAZEILLES, V., DESPRAT, S. and MARLON, J.R., 2013. Orbital-scale climate forcing of grassland burning in southern Africa. *Proceedings of the National Academy of Sciences* 110(13), 5069-5073.

DEBANO, L.F., 2000. The role of fire and soil heating on water repellency in wildland environments: a review. *Journal of Hydrology* 231-232, 195-206.

DEE, D.P., UPPALA, S.M., SIMMONS, A.J., BERRISFORD, P., POLI, P., KOBAYASHI, S., ANDRAE, U., BALMASEDA, M.A., BALSAMO, G., BAUER, P., BECHTOLD, P., BELJAARS, A.C.M., VAN DE BERG, L., BIDLOT, J., BORMANN, N., DELSOL, C., DRAGANI, R., FUENTES, M., GEER, A.J., HAIMBERGER, L., HEALY, S.B., HERSBACH, H., HÓLM, E.V., ISAKSEN, L., KÅLLBERG, P., KÖHLER, M., MATRICARDI, M., MCNALLY, A.P., MONGE-SANZ, B.M., MORCRETTE, J-J., PARK, B-K., PEUBEY, C., DE ROSNAY, P., TAVOLATO, C., THÉPAUT, J-N. and VITART, F., 2011. The ERA-Interim reanalysis: configuration and performance of the data assimilation system. *Quarterly Journal of the Royal Meteorological Society* 137, 553-597.

DE FARIA, B.L., BRANDO, P.M., MACEDO, M.N., PANDAY, P.K., SOARES-FILHO, B.S. and COE, M.T., 2017. Current and future patterns of fire-induced forest degradation in Amazonia. *Environmental Research Letters* 12, 095005, doi:10.1088/1748-9326/aa69ce.

DE GROOT, W.J., BOTHWELL, P.M., CARLSSON, D.H. and LOGAN, K.A., 2003. Simulating the effects of future fire regimes on western Canadian boreal forests. *Journal of Vegetation Science* 14, 355-364.

DE GROOT, W.J., FIELD, R.D., BRADY, M.A., ROSWINTIARTI, O. and MOHAMAD, M., 2007. Developing of the Indonesian and Malaysian Fire

Danger Rating Systems. *Mitigation and Adaptation Strategies for Global Change* 12, 165-180.

DE GROOT, W.J., FLANNIGAN, M.D. and CANTIN, A.S., 2013. Climate change impacts on future boreal fire regimes. *Forest Ecology and Management* 294, 35-44.

DE GROOT, W.J., GOLDAMMER, J.G., JUSTICE, C.O., LYNHAM, T.J., CSISZAR, I.A. and SAN-MIGUEL-AYANZ, J., 2010. Implementing a global early warning system for wildland fire. In: D.X. Viegas (ed.). *Abstracts of the VI International Conference on Forest Fire Research*, 15 – 18 November 2010, ADAI/CEIF Univ. Coimbra, Portugal.

DE GROOT, W.J., GOLDAMMER, J.G., KEENAN, T., BRADY, M.A., LYNHAM, T.J., JUSTICE, C.O., CSISZAR, I.A. and O'LOUGHLIN, K., 2006. Developing a global early warning system for wildland fire. In: D.X. Viegas (ed.). *Abstracts of the V International Conference of Forest Fire Research*, 27 – 30 November 2006, Figueira da Foz (Coimbra), Portugal. *Forest Ecology and Management* 234S, S10, doi:10.1016/j.foreco.2006.08.25.

DE GROOT, W.J., WARDATI and WANG, Y., 2005. Calibrating the fine fuel moisture code for grass ignition potential in Sumatra, Indonesia. *International Journal of Wildland Fire* 14(2), 161-168.

DE JONG, M.C., WOOSTER, M.J., KITCHEN, K., MANLEY, C., GAZZARD, R. and MCCALL, F.F., 2016. Calibration and evaluation of the Canadian Forest Fire Weather Index (FWI) System for improved wildland fire danger rating in the United Kingdom. *Natural Hazards and Earth System Sciences* 16, 1217-1237.

DELFINO, R.J., BRUMMEL, S., WU, J., STERN, H., OSTRO, B., LIPSETT, M., WINER, A., STREET, D.H., ZHANG, L., TJOA, T. and GILLEN, D.L., 2009. The relationship of respiratory and cardiovascular hospital admissions to the southern California wildfires of 2003. *Occupational and Environmental Medicine* 66(3), 189-197.

DENNEKAMP, M. and ABRAMSON, M.J., 2011. The effects of bushfire smoke on respiratory health. *Respirology* 16, 198-209.

DENNISON, P.E., BREWER, S.C., ARNOLD, J.D. and MORITZ, M.A., 2014. Large wildfire trends in the western United States, 1984 – 2011. *Geophysical Research Letters* 41(8), 2928-2933.

DE RONDE, C., TROLLOPE, W.S.W., BAILEY, A.B., BROCKETT, B.H., EVERSON, T.M. and EVERSON, C.S., 2004a. Application of Prescribed Burning. In: J.G. Goldammer & C. de Ronde (eds.). *Wildland Fire Management Handbook for sub-Sahara Africa*. Stellenbosch: comPress. p285-323.

DE RONDE, C., TROLLOPE, W.S.W., PARR, C.L., BROCKETT, B.H. and GELDENHUYS, C.J., 2004b. Fire Effects on Flora and Fauna. In: J.G. Goldammer & C. de Ronde (eds.). *Wildland Fire Management Handbook for sub-Sahara Africa*. Stellenbosch: comPress. p60-87.

DIAZ, J.M., 2012. Economic Impacts of Wildfire. Southern Fire Exchange Fact Sheet 2012-7 [Online]. Retrieved from http://fireadaptednetwork.org/wp-content/uploads/2014/03/economic_costs_of_wildfires.pdf (Accessed 09/10/2016).

DIMITRAKOPOULOS, A.P., BEMMERZOUK, A.M. and MITSOPOULOS, I.D., 2011. Evaluation of the Canadian fire weather index system in an eastern Mediterranean environment. *Meteorological Applications* 18, 83-93.

DIXON, K.W., ROCHE, S. and PATE, J.S., 1995. The promotive effect of smoke derived from burnt native vegetation on seed germination of Western Australian plants. *Oecologia* 101(2), 185-192.

DOERR, S.H., SHAKESBY, R.A., BLAKE, W.H., CHAFER, C.J., HUMPHREYS, G.S. and WALLBRINK, P.J., 2006. Effects of differing wildfire severities on soil wettability and implications for hydrological response. *Journal of Hydrology* 319, 295-311.

DOWDY, A.J., MILLS, G.A., FINKELE, K. and DE GROOT, W.J., 2009. *Australian fire weather as represented by the McArthur Forest Fire Danger Index and the Canadian Forest Fire Weather Index. CAWCR Technical Report No. 10.* Melbourne: Centre for Australian Weather and Climate Research. 84pp.

DOWDY, A.J., MILLS, G.A., FINKELE, K. and DE GROOT, W.J., 2010. Index sensitivity analysis applied to the Canadian Forest Fire Weather Index and the McArthur Forest Fire Danger Index. *Meteorological Applications* 17, 298-312.

DOWNING, T.A, IMO, M. and KIMANZI, J., 2017. Fire occurrence on Mount Kenya and patterns of burning. *GeoResJ* 13, 17-26.

DROBYSHEV, I., GOEBEL, P.C., BERGERON, Y. and CORACE III, R.G., 2012. Detecting changes in climate forcing on the fire regime of a North American mixed-pine forest: A case study of Seney National Wildlife Refuge, Upper Michigan. *Dendrochronologia* 30, 137-145.

DUFFEY, E., MORRIS, M.G., SHEAIL, J., WARD, L.K., WELLS, D.A. and WELLS, T.C.E., 1974. *Grassland ecology and wildlife management*. London: Chapman & Hall.

DUPUY, J.-L. and ALEXANDRIAN, D., 2010. Fire Modelling and Simulation Tools. In: J.S. Silva, F. Rego, P. Fernandes & E. Rigolot (eds.). *Towards Integrated Fire Management – Outcomes of the European Project Fire Paradox*. European Forest Institute Research Report 23. Retrieved from http://www.efi.int/files/attachments/publications/efi_rr23.pdf (Accessed 10/07/2016).

DU TOIT, J.C.O., O'CONNOR, T.G. and VAN DEN BERG, L., 2015. Photographic evidence of fire-induced shifts from dwarf-shrub- to grass-dominated vegetation in Nama-Karoo. *South African Journal of Botany* 101, 148-152.

DYSON, L.L. 2015. A heavy rainfall sounding climatology over Gauteng, South Africa, using self-organising maps. *Climate Dynamics* 45(11-12), 3051-3065.

EASTAUGH, C.S., 2012. *Impacts of Extant Climate Change on Forest Growth and Forest Fire Hazard in Austria*. PhD Thesis, University of Natural Resources and Life Sciences, Austria.

EBISUZAKI, W., 2017. Grib2ctl documentation and download [Online]. Retrieved from https://www.cpc.ncep.noaa.gov/products/wesley/grib2ctl.html (Accessed 12/09/2019).

ECMWF (European Centre for Medium-Range Weather Forecasts), 2007. IFS Documentation CY31R1 [Online]. Retrieved from http://www.ecmwf.int/search/elibrary/part?solrsort=sort_label%20asc&title=part&secondary_title=31r1 (Accessed 22/11/2016).

ECMWF (European Centre for Medium-Range Weather Forecasts), 2016. IFS Documentation Cy41r2. Part IV: Physical Processes [Online]. Retrieved from http://www.ecmwf.int/sites/default/files/elibrary/2016/16648-part-iv-physical-processes.pdf (Accessed 05/01/2017).

EFFIS (European Forest Fire Information System), 2015. European Forest Fire Information System [Online]. Retrieved from http://forest.jrc.ec.europa.eu/effis/ (Acessed 07/072015).

EICHLER, A., TINNER, W., BRÜTSCH, S., OLIVIER, S., PAPINA, T. and SCHWIKOWSKI, M., 2011. An ice-core based history of Siberian forest fires since AD 1250. *Quaternary Science Reviews* 30, 1027-1034.

EKBLOM, A. and GILLSON, L., 2010. Fire history and fire ecology of Northern Kruger (KNP) and Limpopo National Park (PNL), southern Africa. *The Holocene* 20(7), 1063-1077.

ELLERY, W.N., 1992. *Classification of Vegetation of the South African Grassland Biome*. PhD Thesis. University of the Witwatersrand, Johannesburg. pp211.

ENGELBRECHT, F.A., LANDMAN, W.A., ENGELBRECHT, C.J., LANDMAN, S., BOPAPE, M.M., ROUX, B., MCGREGOR, J.L. and THATCHER, M., 2011. Multi-scale climate modelling over Southern Africa using a variable-resolution global model. *Water SA* 37(5), 647-658.

ENGELBRECHT, C.J., LANDMAN, W.A., ENGELBRECHT, F.A. and MALHERBE, J., 2015. A synoptic decomposition of rainfall over the Cape south coast of South Africa. *Climate Dynamics* 44, 2589-2607.

ENGSTROM, R.T., 2010. First-order fire effects on animals: review and recommendations. *Fire Ecology* 6(1), 115-130.

EPIFANIO, C.C., 2015. Lee Vortices. In: G. North, F. Zhang & J. Pyle (eds.). *The Encyclopedia of the Atmospheric Sciences* (2nd Ed). London: Elsevier.

EUMETSAT (European Organisation for the Exploitation of Meteorological Satellites), 2014. Stop of McArthur Forest Fire Danger Index (FFDI) from CSIR [Online]. Retrieved from https://www.eumetsat.int/website/home/News/DAT_2041733.html (Accessed 21/01/2014).

EVANGELIOU, N., BALKANSKI, Y., COZIC, A., HAOB, W.M. and MØLLER, A.P., 2014. Wildfires in Chernobyl-contaminated forests and risks to the population and the environment: A new nuclear disaster about to happen? *Environment International* 73, 346-358.

EVERSON, T.M., EVERSON, C.S., DICKS, H.M. and POULTER, A.G., 1988. Curing rates in the grass sward of the highland sourveld in the Natal Drakensberg. *Southern African Forestry Journal* 145, 1-8.

EVERSON, T.M., EVERSON, C.S., DE RONDE, C. and TROLLOPE, W.S.W., 2004. Regional Fire Management: Objectives, Practices and Prescribed Burning Application. In: J.G. Goldammer & C. de Ronde (eds.). *Wildland Fire Management Handbook for sub-Sahara Africa*. Stellenbosch: comPress. p114-143.

EVERSON, T.M., SMITH, F.R. and EVERSON, C.S., 1985. Characteristics of fire behaviour in the montane grasslands of natal. *Journal of the Grassland Society of Southern Africa*, 2:3, 13-21.

FAO (Food and Agriculture Organization of the United Nations), 2006. Local Climate Estimator [Online]. Retrieved from http://www.fao.org/nr/climpag/locclim/locclim_en.asp (Accessed 15/07/2018).

FAO (Food and Agriculture Organization of the United Nations), 2013. Sustainable Grasslands Working Paper [Online]. Retrieved from http://www.fao.org/fileadmin/templates/nr/sustainability_pathways/docs/Working_Paper_Sustainable_Grasslands.pdf (Accessed 13/12/2017). *E-Conference on Sustainable Grasslands, 2 – 30 September 2013*.

FAOSTAT, 2019. Food and agriculture data [Online]. Retrieved from http://www.fao.org/faostat/en/#home (Accessed 30/12/2019).

FAURIA, M.M. and JOHNSON, E.A., 2008. Climate and wildfires in the North American boreal forest. *Philosophical Transactions of the Royal Society B* 363, 2317-2329.

FELZER, B.S., CRONIN, T., REILLY, J.M., MELILLO, J.M. and WANG, X., 2007. Impacts of ozone on trees and crops. *Comptes Rendus Geoscience* 339, 784-798.

FENG, Z., PAOLETTI, E., BYTNEROWICZ, A. and HARMENS, H., 2015. Ozone and plants. *Environmental Pollution* 202, 215-216.

FERNANDES, P., 2010. Scientific Knowledge and Operational Tools to Support Prescribed Burning: Recent Developments. In: J.S. Silva, F. Rego, P. Fernandes & E. Rigolot (eds.). *Towards Integrated Fire Management – Outcomes of the European Project Fire Paradox*. European Forest Institute Research Report 23. Retrieved from http://www.efi.int/files/attachments/publications/efi_rr23.pdf (Accessed 10/07/2016).

FERNANDES, P.M., LOUREIRO, C., GUIOMAR, N., PEZZATTI, G.B., MANSO, F.T. and LOPES, L., 2014. The dynamics and drivers of fuel and fire in the Portuguese public forest. *Journal of Environmental Management* 146, 373-382.

FEY, M.V., 2010. *Soils of South Africa*. Cape Town: Cambridge University Press. pp287.

FISCHER, M.A., DI BELLA, C.M. and JOBBÁGY, E.G., 2015. Influence of fuel conditions on the occurrence, propagation and duration of wildland fires: A regional approach. *Journal of Arid Environments* 120, 63-71.

FLANNIGAN, M.D., AMIRO, B.D., LOGAN, K.A., STOCKS, B.J. and WOTTON, B.M., 2005. Forest fires and climate change in the 21st century. *Mitigation and Adaptation Strategies for Global Change* 11, 847-859.

FLANNIGAN, M.D., CAMPBELL, I., WOTTON, M., CARCAILLET, C., RICHARD, P. and BERGERON, Y., 2001. Future fire in Canada's boreal forest: paleoecology results and general circulation model – regional climate model simulations. *Canadian Journal of Forest Research* 31, 854-864.

FLANNIGAN, M.D., CANTIN, A.S., DE GROOT, W.J., WOTTON, M., NEWBERY, A. and GOWMAN, L.M., 2013. Global wildland fire season severity in the 21st century. *Forest Ecology and Management* 294, 54-61.

FLANNIGAN, M.D., KRAWCHUK, M.A., DE GROOT, W.J., WOTTON, B.M. and GOWMAN, L.M., 2009. Implications of changing climate for global wildland fire. *International Journal of Wildland Fire* 18, 483-507.

FLANNIGAN, M.D., STOCKS, B.J. and WOTTON, B.M., 2000. Climate change and forest fires. *The Science of the Total Environment* 262, 221-229.

FLANNIGAN, M.D. and VAN WAGNER, C.E., 1991. Climate change and wildfire in Canada. *Canadian Journal of Forest Research* 21, 66-72.

FLANNIGAN, M.D and WOTTON, B.M., 2001. Climate, weather and area burned. In: E.A. Johnson & K. Miyanishi (eds.). *Forest fires: behavior and ecological effects*. San Diego: Academic Press.

FLATO, G., MAROTZKE, J., ABIODUN, B., BRACONNOT, P., CHOU, S.C., COLLINS, W., COX, P., DRIOUECH, F., EMORI, S., EYRING, V., FOREST, C., GLECKLER, P., GUILYARDI, E., JAKOB, C., KATTSOV, V., REASON, C. and RUMMUKAINEN, M., 2013. Evaluation of Climate Models. In: T.F. Stocker, D. Qin, G.-K. Plattner, M. Tignor, S.K. Allen, J. Boschung, A. Nauels, Y. Xia, V. Bex & P.M. Midgley (eds.). *Climate Change 2013: The Physical Science Basis. Contribution of Working Group I to the Fifth Assessment Report of the Intergovernmental Panel on Climate Change.* Cambridge: Cambridge University Press.

FLETCHER, M.-S. and MORENO, P.I., 2012. Vegetation, climate and fire regime changes in the Andean region of southern Chile (38°S) covaried with centennial-scale climate anomalies in the tropical Pacific over the last 1500 years. *Quaternary Science Reviews* 46, 46-56.

FORSYTH, G.G., KRUGER, F.J. and LE MAITRE, D.C., 2010. *National Veldfire Risk Assessment: Analysis of Exposure of Social, Economic and Environmental Assets to Veldfire Hazards in South Africa*. Pretoria: CSIR.

FORSYTH, G.G. and VAN WILGEN, B.W., 2008. The recent fire history of the Table Mountain National Park and implications for fire management. *Koedoe: African Protected Area Conservation* 50(1), 3-9.

FOSBERG, M.A., MEARNS, L.O. and PRICE, C., 1993. Climate Change – Fire Interactions at the Global Scale: Predictions and Limitations of Methods. In: P.J. Crutzen & J.G. Goldammer (eds.). *Fire in the Environment. The Ecological, Atmospheric, and Climatic Importance of Vegetation Fires*. Chichester: John Wiley & Sons. p123-137.

FOWLER, C.T., 2003. Human health impacts of forest fires in the southern United States: a literature review. *Journal of Ecological Anthropology* 7, 39-63.

FOX-HUGHES, P., HARRIS, R.M.B., LEE, G., GROSE, M. and BINDOFF, N., 2014. Future fire danger climatology for Tasmania, Australia, using a dynamically downscaled regional climate model. *International Journal of Wildland Fire* 23(3), 309-321.

FPASA (Fire Protection Association of Southern Africa), 2019. SA National Fire Statistics [Online]. Retrieved from http://www.fpasa.co.za/index.php/journals/sa-national-fire-statistics (Accessed 20/12/2019).

FRIED, J.S., GILLESS, J.K., RILEY, W.J., MOODY, T.J., DE BLAS, C.S., HAYHOE, K., MORITZ, M., STEPHENS, S. and TORN, M., 2008. Predicting the effect of climate change on wildfire behavior and initial attack success. *Climatic Change* 87(Suppl 1), S251-S264.

FROMM, M., TUPPER, A., ROSENFELD, D., SERVRANCKX, R. and MCRAE, R., 2006. Violent pyro-convective storm devastates Australia's capital and pollutes the stratosphere, *Geophysical Research Letters* 33, L05815, doi:10.1029/2005GL025161.

GAŁEK, G., SOBIK, M., BŁAŚ, M., POLKOWSKA, Ż, CICHAŁA–KAMROWSKA, K. and WAŁASZEK, K., 2015. Dew and hoarfrost frequency, formation efficiency and chemistry in Wroclaw, Poland. *Atmospheric Research* 151, 120-129.

GANATSAS, P., ANTONIS, M. and MARIANTHI, T., 2011. Development of an adapted empirical drought index to the Mediterranean conditions for use in forestry. *Agricultural and Forest Meteorology* 151, 241-250.

GARBOLINO, E., SANSEVERINO-GODFRIN, V. and HINOJOS-MENDOZA, G., 2016. Reprint of: Describing and predicting of the vegetation development of Corsica due to expected climate change and its impact on forest fire risk evolution. *Safety Science* 97, 81-87.

GARCIA-PRATS, A., DEL CAMPO, A., TARCÍSIO, F.J.G. and ANTONIO, M.J., 2015. Development of a Keetch and Byram-based drought index sensitive to forest management in Mediterranean conditions. *Agricultural and Forest Meteorology* 205, 40-50.

GEDZELMAN, S.D., 1980. *The Science and Wonders of the Atmosphere*. New York: John Wiley & Sons. 535pp.

GELDENHUYS, C.J., 1994. Bergwind fires and the location pattern of forest patches in the southern Cape landscape. *South African Journal of Biogeography* 21, 49-62.

GELDENHUYS, C.J., VAN WILGEN, B.W., BOND, W.J., VAN DE VIJVER, C.A.D.M. and DE RONDE, C., 2004. Fire Effects on the Maintenance of Biodiversity, Soil and Nutrients. In: J.G. Goldammer & C. de Ronde (eds.). *Wildland Fire Management Handbook for sub-Sahara Africa*. Stellenbosch: comPress. p88-113.

GERMANO, T., 1999. Self-organizing maps [Online]. Retrieved from http://davis.wpi.edu/~matt/courses/soms/ (Accessed 23/11/2016).

GFMC (Global Fire Monitoring Center), 2016. Wildland Fire and Tourism [Online]. Retrieved from http://www.fire.uni-freiburg.de/Manag/TUI_1.htm (Accessed 09/10/2016).

GIBSON, D., PATERSON, G, NEWBY, T., LAKER, M. and HOFFMAN, T., 2007. Land. In: E. Lickindorf & R. Clark (eds.). *South Africa Environmental Outlook: A report on the state of the environment*. Pretoria: Department of Environmental Affairs and Tourism.

GIGLIO, L., JUSTICE, C., BOSCHETTI, L. and ROY, D., 2015. MCD64A1 MODIS/Terra+Aqua Burned Area Monthly L3 Global 500m SIN Grid V006. Data set supplied by NASA EOSDIS Land Processes DAAC [Online]. Retrieved from https://doi.org/10.5067/MODIS/MCD64A1.006 (Accessed 18/01/2019).

GIGLIO, L., RANDERSON, J.T. and VAN DER WERF, G.R., 2013. Analysis of daily, monthly, and annual burned area using the fourth-generation global fire emissions database (GFED4). *Journal of Geophysical Research: Biogeosciences* 118, 317-328.

GIGLIO, L., VAN DER WERF, G.R., RANDERSON, J.T., COLLATZ, G.J. and KASIBHATLA, P., 2006. Global estimation of burned area using MODIS active fire observations. *Atmospheric Chemistry and Physics* 6, 957-974.

GIGNOUX, J., CLOBERT, J. and MENAUT, J.C., 1997. Alternative fire resistance strategies in savanna trees. *Oecologia* 110(4), 576-583.

GILLETT, N.P., WEAVER, A.J., ZWIERS, F.W. and FLANNIGAN, M.D., 2004. Detecting the effect of climate change on Canadian forest fires. *Geophysical Research Letters* 31, L18211, doi:10.1029/2004GL020876.

GIRARDIN, M-P., TARDIF, J., FLANNIGAN, M.D., WOTTON, B.M. and BERGERON, Y., 2004. Trends and periodicities in the Canadian Drought Code and their relationships with atmospheric circulation for the southern Canadian boreal forest. *Canadian Journal of Forest Research* 34(1), 103-119.

GLOBAL EWS, 2015. A Global Early Warning System for Wildland Fires [Online]. Retrieved from http://www.fire.uni-freiburg.de/gwfews/partners.html (Accessed 07/07/2015).

GOLDAMMER, J.G. and CRUTZEN, P.J., 1993. Fire in the Environment: Scientific Rationale and Summary of Results of the Dahlem Workshop. In: P.J. Crutzen & J.G. Goldammer (eds.). *Fire in the Environment. The Ecological, Atmospheric, and Climatic Importance of Vegetation Fires*. Chichester: John Wiley & Sons. p1-14.

GOLDAMMER, J.G., STATHEROPOULOS, M. and ANDREAE, M.O., 2009. Impacts of Vegetation Fire Emissions on the Environment, Human Health, and Security: A Global Perspective. In: A. Bytnerowicz, M.J. Arbaugh, A.R. Riebau & C. Andersen (eds.). *Wildland Fires and Air Pollution*. Amsterdam: Elsevier. p3-36.

GOLDING, N. and BETTS, R., 2008. Fire risk in Amazonia due to climate change in the HadCM3 climate model: Potential interactions with deforestation. *Global Biogeochemical Cycles* 22, GB4007, doi:10.1029/2007GB003166.

GONZÁLEZ-PÉREZ, J.A., GONZÁLEZ-VILA, F.J., ALMENDROSB, G. and KNICKER, H., 2004. The effect of fire on soil organic matter – a review. *Environment International* 30, 855-870.

GOOSSE, H., ARZEL, O., LUTERBACHER, J., MANN, M.E., RENSSEN, H., RIEDWYL, N., TIMMERMANN, A., XOPLAKI, E. and WANNER, H., 2006. The origin of the European “Medieval Warm Period”. *Climate of the Past* 2, 99-113.

GORBAN, A.N., KÉGL, B., WUNSCH, D.C. and ZINOVYEV, A.Y., 2007. Preface. In: A.N. Gorban, B. Kégl, D.C. Wunsch & A.Y. Zinovyev (eds.). *Lecture Notes in Computational Science and Engineering: Principal Manifolds for Data Visualization and Dimension Reduction*. Berlin: Springer.

GOSLING, M., 2017. Knysna fires: Tally of destruction grows. *The Citizen*, 29 June 2017.

GOUBITZ, S., WERGER, M. and NE'EMAN, G., 2002. Germination response to fire-related factors of seeds from non-serotinous and serotinous cones. *Plant Ecology* 169(2), 195-204.

GOVENDER, N., TROLLOPE, W.S.W. and VAN WILGEN, B.W., 2006. The effect of fire season, fire frequency, rainfall and management on fire intensity in savanna vegetation in South Africa. *Journal of Applied Ecology* 43, 748-758.

GPWG (Global Paleofire Working Group), 2017. Global Charcoal Database [Online]. Retrieved from http://www.paleofire.org/index.php (Accessed 20/12/2017).

GREENE, J., 2012. Looking east towards a brush fire in Azusa Canyon from Mount Wilson Red Box Road where numerous cabins were burned in the fire on 18 March 2012 [Online]. Retrieved from https://commons.wikimedia.org/wiki/File:Pyrocumulus_cloud_in_the_Angeles_National_Forest_California.JPG (Accessed 11/02/2016).

GRESSWELL, R.E., 1999. Fire and aquatic ecosystems in forested biomes of North America. *Transactions of the American Fisheries Society* 128, 193-221.

GRIFFITHS, D. 1999. Improved formula for the drought factor in McArthur's forest fire danger meter. *Australian Forestry* 62(2), 202-206.

GRISSINO-MAYER, H.D. and SWETNAM, T.W., 2000. Century-scale climate forcing of fire regimes in the American Southwest. *The Holocene* 10(2), 213-220.

GROISMAN, P.Y., SHERSTYUKOV, B.G., RAZUVAEV, V.N., KNIGHT, R.W., ENLOE, J.G., STROUMENTOVA, N.S., WHITFIELD, P.H., FØRLAND, E., HANNSEN-BAUER, I., TUOMENVIRTA, H., ALEKSANDERSSON, H., MESCHERSKAYA, A.V. and KARL, T.R., 2007. Potential forest fire danger over Northern Eurasia: Changes during the 20th century. *Global and Planetary Change* 56, 371-386.

GUTNIKOV, S., 2010. Задымленность аэропорта Шереметьево (Москва, Россия) от дыма лесных пожаров в августе 2010 года [Online]. Retrieved from https://commons.wikimedia.org/wiki/File:Smoke_from_forest_fires_Sheremetyevo_20100807_01.JPG (Accessed 17/08/2016).

GUTOWSKI, W.J. and CASSANO, J.J., 2014. Self-Organizing Maps: A method for analysing Large-Scale Meteorological Patterns associated with extreme events. *US CLIVAR Variations* 12(1), 7-10.

HADLEY, O.L. and KIRCHSTETTER, T.W., 2012. Black-carbon reduction of snow albedo. *Nature Climate Change* 2, 437-440.

HAGLER, G.S.W., BERGIN, M.H., SMITH, E.A. and DIBB, J.E., 2007. A summer time series of particulate carbon in the air and snow at Summit, Greenland.

Journal of Geophysical Research 112, D21309, doi:10.1029/2007JD008993.

HAINES, D.A., 1988. A lower atmospheric severity index for wildland fire. *National Weather Digest* 13(2), 23-27.

HAMILTON, B.A., 2015. *2014 Quadrennial Fire Review Final Report*. Washington: USDA Forest Service & Department of the Interior. 80pp.

HANSEN, E.M., JOHNSON, M.C., BENTZ, B.J., VANDYGRIFF, J.C. and MUNSON. A.S., 2015. Fuel loads and simulated fire behavior in “old stage” beetle-infested ponderosa pine of the Colorado Plateau. *Forest Science* 61, 644-664.

HANTSON, S., PUEYO, S. and CHUVIECO, E., 2014. Global fire size distribution is driven by human impact and climate. *Global Ecology and Biogeography* 24, 77-86.

HAO, W.M., BONDARENKO, O.O., ZIBTSEV, S. and HUTTON, D., 2009. Vegetation Fires, Smoke Emissions, and Dispersion of Radionuclides in the Chernobyl Exclusion Zone. In: A. Bytnerowicz, M. Arbaugh, A. Riebau & C. Andersen (eds.). *Wildland Fires and Air Pollution*. Amsterdam: Elsevier. p265-275.

HARDY, C.C. and HARDY, C.E., 2007. Fire danger rating in the United States of America: an evolution since 1916. *International Journal of Wildland Fire* 16, 217-231.

HARGROVE, W.W., GARDNER, R.H., TURNER, M.G., ROMME, W.H. and DESPAIN, D.G., 2000. Simulating fire patterns in heterogeneous landscapes. *Ecological Modelling* 135, 243-263.

HAY, L.E., MCCABE, G.J., WOLOCK, D.M. and AYERS, M.A., 1991. Simulation of precipitation by weather type analyses. *Water Resource Research* 27, 493-501.

HEINL, M., FROST, P., VANDERPOST, C. and SLIVA, J., 2007. Fire activity on drylands and floodplains in the southern Okavango Delta, Botswana. *Journal of Arid Environments* 68, 77-87.

HEINSCH, F.A., ANDREWS, P.L. and KURTH, L.L., 2009. Implications of using percentiles to define fire danger levels. Extended Abstract P1.5. *Proceedings of the 8th Symposium on Fire and Forest Meteorology, 12 – 15 October 2009, Kalispell, U.S.A*.

HELFMAN, R.S., STRAUB, R.J. and DEEMING, J.E., 1987. User's Guide to AFFIRMS: Time-share Computerized Processing for Fire Danger Rating. INT-82. Boise: USDA Forest Service.

HERSBACH, H., DE ROSNAY, P., BELL, B., SCHEPERS, D., SIMMONS, A., SOCI, C., ABDALLA, S., BALMASEDA, A.M., BALSAMO, G., BECHTOLD, P., BERRISFORD, P., BIDLOT, J., DE BOISSÉSON, E., BONAVITA, M., BROWNE, P., BUIZZA, R., DAHLGREN, P., DEE, D., DRAGANI, R., DIAMANTAKIS, M., FLEMMING, J., FORBES, R., GEER, A., HAIDEN, T., HÓLM, E., HAIMBERGER, L., HOGAN, R., HORÁNYI, A., JANISKOVÁ, M., LALOYAUX, P., LOPEZ, P., MUÑOZ-SABATER, J., PEUBEY, C., RADU, R., RICHARDSON, D., THÉPAUT, J-N, VITART, F., YANG, X., ZSÓTÉR, E. and ZUO, H., 2018. Operational global reanalysis: progress, future directions and synergies with NWP. ERA Report Series 27. Reading: European Centre for Medium Range Weather Forecasts.

HESSAMI, M., GACHON, P., OUARDA, T.B.M.J. and ST-HILAIRE, A., 2008. Automated regression-based statistical downscaling tool. *Environmental Modelling and Software* 23(6), 813-834.

HESSL, A.E., 2011. Pathways for climate change effects on fire: models, data, and uncertainties. *Progress in Physical Geography* 35(3), 393-407.

HEWITSON, B.C. and CRANE, R.G., 1996. Climate downscaling: techniques and application. *Climate Research* 7, 85-95.

HEWITSON, B.C. and CRANE, R.G., 2002. Self-organizing maps: Application to synoptic climatology. *Climate Research* 1(22), 13-26.

HEWITSON, B.C. and CRANE, R.G., 2005. Gridded area-averaged daily precipitation via conditional interpolation. *Journal of Climate* 18, 41-57.

HEWITSON, B.C. and CRANE, R.G., 2006. Consensus between GCM climate change projections with empirical downscaling: Precipitation downscaling over South Africa. *International Journal of Climatology* 26, 1315-1337.

HEWITSON, B.C., TENNANT, W. and WALAWEGE, R., 2004. Atmospheric Moisture Transport and Sources for Southern Africa. WRC Report No. 1012/1/04. Pretoria: Water Research Commission. 76pp.

HEYERDAHL, E.K., MCKENZIE, D., DANIELS, L.D., HESSL, A.E., LITTELL, J.S. and MANTUA, N.J., 2008. Climate drivers of regionally synchronous fires in the inland Northwest (1651 – 1900). *International Journal of Wildland Fire* 17, 40-49.

HIGUERA, P.E., 2015. Taking time to consider the causes and consequences of large wildfires. *Proceedings of the National Academy of Sciences* 112(43), 13137-13138.

HIGUERA, P.E., WHITLOCK, C. and GAGE, J.A., 2010. Linking tree-ring and sediment-charcoal records to reconstruct fire occurrence and area burned in subalpine forests of Yellowstone National Park, USA. *The Holocene* 21(2), 327-341.

HOFFMANN, W.A., ADASME, R., HARIDASAN, M., DE CARVALHO, M.T., GEIGER, E.L., PEREIRA, M.A., GOTSCH, S.G. and FRANCO, A.C., 2009. Tree topkill, not mortality, governs the dynamics of savanna forest boundaries under frequent fire in central Brazil. *Ecology* 90, 1326-1337.

HOFFMANN, W.A., SCHROEDER, W. and JACKSON, R.B., 2002. Positive feedbacks of fire, climate, and vegetation and the conversion of tropical savanna. *Geophysical Research Letters* 29(22), 2052, doi:10.1029/2002GL015424.

HOFFMANN, W.A., SCHROEDER, W. and JACKSON, R.B., 2003. Regional feedbacks among fire, climate, and tropical deforestation. *Geophysical Research Letters* 108(D23), 4721, doi:10.1029/2003JD003494.

HOLTON, J.R., 1992. *An Introduction to Dynamic Meteorology*. 3rd Ed. San Diego: Academic Press. 511pp.

HOPE, P.K., DROSDOWSKY, W. and NICHOLLS, N., 2006. Shifts in the synoptic systems influencing southwest Western Australia. *Climate Dynamics* 26, 751-764.

HU, F.S., HIGUERA, P.E., WALSH, J.E., CHAPMAN, W.L., DUFFY, P.A., BRUBAKER, L.B. and CHIPMAN, M.L., 2010. Tundra burning in Alaska: Linkages to climatic change and sea ice retreat. *Journal of Geophysical Research* 115, G04002, doi:10.1029/2009JG001270.

HUANG, Y., WU, S. and KAPLAN, J.O., 2015. Sensitivity of global wildfire occurrences to various factors in the context of global change. Atmospheric Environment, doi:10.1016/j.atmosenv.2015.06.002.

HUBER, U.M. and MARKGRAF, V., 2003. Holocene Fire Frequency and Climate Change at Rio Rubens Bog, Southern Patagonia. In: T.T. Veblen, W.L. Baker, G. Montenegro & T.W. Swetnam (eds.). *Ecological Studies, Vol. 160: Fire and Climatic Change in Temperate Ecosystems of the Western Americas*. New York: Springer-Verlag. 444pp.

HYSTAD, P. and KELLER, C.P., 2005. Experience of a tourism industry impacted by a forest fire disaster. In: T. Delamere, C. Randall & D. Robinson (eds.). *Proceedings of the 11th Canadian Congress on Leisure Research, 17 – 20 May 2005, Nanaimo, British Columbia, Canada*.

IFSTA (International Fire Service Training Association), 2008. *Essentials of Fire Fighting and Fire Department Operations*. 5th Ed. New York: Pearson. 1440pp.

ILIOPOULOS, N., PAPADOPOULOS, A. GOUVAS, M. and DASIOU, Z., 2010. Study of fire danger index and its possibility of application in the Greek area. In: A.A. Argiriou & A.J. Kazantzidis (eds.). *Proceedings of the 10th International Conference on Meteorology, Climatology and Atmospheric Physics (COMECAP), 25 – 28 May 2010, Patras, Greece*. p 329-336.

INTERAGENCY STANDARDS FOR FIRE AND FIRE AVIATION OPERATIONS GROUP, 2019. Interagency Standards for Fire and Fire Aviation Operations. NFES 2724 [Online]. Retrieved from https://www.nifc.gov/PUBLICATIONS/redbook/2019/RedBookAll.pdf (Accessed 21/11/2019).

IPCC (Intergovernmental Panel on Climate Change), 2013a. Summary for Policymakers. In: T.F. Stocker, D. Qin, G.-K. Plattner, M. Tignor, S.K. Allen, J. Boschung, A. Nauels, Y. Xia, V. Bex & P.M. Midgley (eds.). *Climate Change 2013: The Physical Science Basis. Contribution of Working Group I to the Fifth Assessment Report of the Intergovernmental Panel on Climate Change.* Cambridge: Cambridge University Press.

IPCC (Intergovernmental Panel on Climate Change), 2013b. Annex III: Glossary [S. Planton (ed.)]. In: T.F. Stocker, D. Qin, G.-K. Plattner, M. Tignor, S.K. Allen, J. Boschung, A. Nauels, Y. Xia, V. Bex & P.M. Midgley (eds.). *Climate Change 2013: The Physical Science Basis. Contribution of Working Group I to the Fifth Assessment Report of the Intergovernmental Panel on Climate Change.* Cambridge: Cambridge University Press.

JACOBI, H.-W., LIM, S., MÉNÉGOZ, M., GINOT, P., LAJ, P., BONASONI, P., STOCCHI, P., MARINONI, A. and ARNAUD, Y., 2015. Black carbon in snow in the upper Himalayan Khumbu Valley, Nepal: observations and modeling of the impact on snow albedo, melting, and radiative forcing. *The Cryosphere* 9, 1685-1699.

JEMISON, G.M., 1935. Influence of weather factors on moisture content of light fuels in forests of the northern Rocky Mountains. *Journal of Agricultural Research* 51(10), 885-906.

JIANG, N., 2010. *Application of Two Different Weather Typing Procedures*. Sydney: Verlag. 148pp.

JIANG, N., HAY, J.E. and FISHER, G.W., 2009. Classification of New Zealand synoptic weather types and relation to the Southern Oscillation Index. *Weather and Climate* 25, 43-70.

JIMÉNEZ, M.A, SIMÓ, G., WRENGER, B., TELISMAN-PRTENJAK, M., GUIJARRO, J.A. and CUXART, J., 2016. Morning transition case between the land and the sea breeze regimes. *Atmospheric Research* 172-173, 95-108.

JIN, Y.F., RANDERSON, J.T., GOULDEN, M.L. and GOETZ, S.J., 2012. Post-fire changes in net shortwave radiation along a latitudinal gradient in boreal

North America. *Geophysical Research Letters* 39, L13403, doi:10.1029/2012GL051790.

JOHNSTON, F.H., HENDERSON, S.B., CHEN, Y., RANDERSON, J.T., MARLIER, M., DEFRIES, R.S., KINNEY, P., BOWMAN, D.M.S. and BRAUER, M., 2012. Estimated global mortality attributable to smoke from landscape fires. *Environmental Health Perspectives* 120, 695-701.

JOLLY, W.M., BRADSHAW, L. and WALLACE, J., 2016. Updating the National Fire Danger Rating System: NFDRS2016. Presentation to S590: Advanced Fire Behavior Interpretation [Online]. Retrieved from http://www.wfas.net/nfdrs2016/index.php/en/downloads (Accessed 30/10/2016).

JOLLY, W.M., COCHRANE, M.A., FREEBORN, P.H., HOLDEN, Z.A., BROWN, T.J., WILLIAMSON, G.J. and BOWMAN, D.M.J.S., 2015. Climate-induced variations in global wildfire danger from 1979 to 2013. *Nature Communications* 6(7537), doi:10.1038/ncomms8537.

JOLLY, W.M., FREEBORN, P.H., PAGE, W.G. and BUTLER, B.W., 2019. Severe fire danger index: a forecastable metric to inform firefighter and community wildfire risk management. *Fire* 2(47), doi:10.3390/fire2030047.

JOUBERT, D.F., SMIT, G.N. and HOFFMAN, M.T., 2012. The role of fire in preventing transitions from a grass dominated state to a bush thickened state in arid savannas. *Journal of Arid Environments* 87, 1-7.

JUHNKE, S.R. and FUGGLE, R.F., 1987. Predicting weather for prescribed burns in the South-Western Cape, Republic of South Africa. *South African Forestry Journal* 142, 41-46.

KAISER, J.W., HEIL, A., ANDREAE, M.O., BENEDETTI, A., CHUBAROVA, N., JONES, L., MORCRETTE, J.-J., RAZINGER, M., SCHULTZ, M.G., SUTTIE, M. and VAN DER WERF, G.R., 2012. Biomass burning emissions estimated with a global fire assimilation system based on observed fire radiative power. *Biogeosciences* 9, 527-554.

KALNAY, E., KANAMITSU, M., KISTLER, R., COLLINS, W., DEAVEN, D., GANDIN, L., IREDELL, M., SAHA, S., WHITE, G., WOOLLEN, J., ZHU, Y., CHELLIAH, M., EBISUZAKI, W., HIGGINS, W., JANOWIAK, J. MO, K.C.,

ROPELEWSKI, C., WANG, J., LEETMAA, A., REYNOLDS, R., JENNE, R. and JOSEPH, D., 1996. The NCEP/NCAR 40-year reanalysis project. *Bulletin of the American Meteorological Society* 77, 437-471.

KALOGNOMOU, E.-A., LENNARD, C., SHONGWE, M., PINTO, I., FAVRE, A., KENT, M., HEWITSON, B., DOSIO, A., NIKULIN, G., PANITZ, H.-J. and BÜCHNER, M., 2013. A diagnostic evaluation of precipitation in CORDEX models over southern Africa. *Journal of Climate* 26(23), 9477-9506.

KA-MPHEZULU, M.M., 2016. Facebook status update. Retrieved from https://www.facebook.com/mtjhatjhanambusi.mgwezani/posts/1795072460725669?pnref=story (Accessed 27/07/2016).

KANG, C.-M., GOLD, D. and KOUTRAKIS, P., 2014. Downwind O_3 and PM2.5 speciation during the wildfires in 2002 and 2010. *Atmospheric Environment* 95, 511-519.

KARNOSKY, D.F., SKELLY, J.M., PERCY, K.E. and CHAPPELKA, A.H., 2007. Perspectives regarding 50 years of research on effects of tropospheric ozone air pollution on US forests. *Environmental Pollution* 147(3), 489-506.

KASISCHKE, E.S. and TURETSKY, M.R., 2006. Recent changes in the fire regime across the North American boreal region – Spatial and temporal patterns of burning across Canada and Alaska. *Geophysical Research Letters* 33, L09703, doi:10.1029/2006GL025677.

KAUFFMAN, J.B., CUMMINGS, D.L. and WARD, D.E., 1994. Relationships of fire, biomass and nutrient dynamics along a vegetation gradient in the Brazilian cerrado. *Journal of Ecology* 82(3), 519-531.

KEANE, R.E., 2015. *Wildland Fuel Fundamentals and Applications*. Heidelberg: Springer. 191pp.

KEETCH, J.J. and BYRAM, G.M., 1968. *A Drought Index for Forest Fire Control*. Research Paper SE-38. (Revised 1988). Asheville: United States Department of Agriculture – Forest Service. 32pp.

KEETON, W.S., MOTE, P.W. and FRANKLIN, J.F., 2007. Climate Variability, Climate Change, and Western Wildfire with Implications for the Urban-Wildland Interface. In: A. Troy & R.G. Kennedy (eds.). *Advances in the*

Economics of Environmental Resources, Volume 6: Living on the Edge: Economic, Institutional and Management Perspectives on Wildfire Hazard in the Urban Interface. Bingley: Emerald Group. 206pp.

KEHRWALD, N.M., WHITLOCK, C., BARBANTE, C., BROVKIN, V., DANIAU, A.-L., KAPLAN, J.O., MARLON, J.R., POWER, M.J., THONICKE, K. and VAN DER WERF, G.R., 2013. Fire research: Linking past, present, and future data. *Eos Transactions of the American Geophysical Union* 94(46), 421-423.

KEY, J. and CRANE, R.G., 1986. A comparison of synoptic classification schemes based on objective procedures. *Journal of Climatology* 6, 375-388.

KHARUK, V.I., RANSON, K.J. and DVINSKAYA, M.L., 2008. Wildfires dynamic in the larch dominance zone. *Geophysical Research Letters* 35, L01402, doi:10.1029/2007GL032291.

KIDSON, J.W., 1997. The utility of surface and upper air data in synoptic climatological specification of surface climatic variables. *International Journal of Climatology* 17, 399-413.

KIRCHHOFER, W., 1974. *Classification of European 500 mb Patterns*. Arbeitsberichte der Schweizerischen Meteorologischen Zentralanstalt 43. Zurich: Swiss Meteorological Institute. 19pp.

KIRKMAN, K.P., 2002. The influence of various types and frequencies of rest on the production and condition of sourveld grazed by sheep or cattle. 2. Vigour. *African Journal of Range & Forage Science* 19(2), 93-105.

KISTLER, R., KALNAY, E., COLLINS, W., SAHA, S., WHITE, G., WOOLLEN, J., CHELLIAH, M., EBISUZAKI, W., KANAMITSU, M., KOUSKY, V., VAN DEN DOOL, H., JENNE, R. and FIORINO, M., 2001. The NCEP-NCAR 50-year reanalysis: Monthly means CD-ROM and documentation. *Bulletin of the American Meteorological Society* 82, 247-267.

KITZBERGER, T. and VEBLEN, T.T., 2003. Influences of Climate on Fire in Northern Patagonia, Argentina. In: T.T. Veblen, W.L. Baker, G. Montenegro & T.W. Swetnam (eds.). *Ecological Studies, Vol. 160: Fire and Climatic*

Change in Temperate Ecosystems of the Western Americas. New York: Springer-Verlag. 444pp.

KLOSTER, S., MAHOWALD, N.M., RANDERSON, J.T. and LAWRENCE, P.J., 2012. The impacts of climate, land use, and demography on fires during the 21st century simulated by CLM-CN. *Biogeosciences* 9, 509-525.

KNMI (Koninklijk Nederlands Meteorologisch Instituut), 2019. Climate Explorer: European Climate Assessment & Data [Online]. Retrieved from https://climexp.knmi.nl/start.cgi (Accessed 20/11/2019).

KNUTSON, T.R., MCBRIDE, J.I., CHAN, J., EMANUEL, E., HOLLAND, G., LANDSEA, C., HELD, I., KOSSIN, J.P., SRIVASTAVA, K. and SUGI, M., 2010. Tropical cyclones and climate change. *Nature Geoscience*, doi:10.1038/ngeo779.

KOCHI, I., DONOVAN, G.H., CHAMP, P.A. and LOOMIS, J.B., 2010. The economic cost of adverse health effects from wildfire-smoke exposure: a review. *International Journal of Wildland Fire* 19, 803-817.

KOHONEN, T., 1982. Self-organized formation of topologically correct feature maps. *Biological Cybernetics* 43, 59-69.

KOHONEN, T., 1990. The self-organizing map. *Proceedings of the Institute of Electrical and Electronics Engineers* 78(9), 1464-1480.

KOHONEN, T., 2001. *Self-Organizing Maps*. 3rd Ed. Berlin: Springer. 501pp.

KOHONEN, T. HYNNINEN, J., KANGAS, J. and LAAKSONEN, J., 1996. *SOM_PAK: The Self-Organizing Map Program Package*. Technical Report A31. Espoo: Helsinki University of Technology, Laboratory of Computer and Information Science.

KOTTEK, M., GRIESER, J., BECK, C., RUDOLF, B. and RUBEL, F., 2006. World Map of the Köppen-Geiger climate classification updated. *Meteorologische Zeitschrift* 15(3), 259-263.

KRAWCHUK, M.A. and MORITZ, M.A., 2011. Constraints on global fire activity vary across a resource gradient. *Ecology* 92(1), 121-132.

KRAWCHUK, M.A., CUMMING, S.G. and FLANNIGAN, M.D., 2009a. Predicted changes in fire weather suggest increases in lightning fire initiation and

future area burned in the mixedwood boreal forest. *Climatic Change* 92, 83-97.

KRAWCHUK, M.A., MORITZ, M.A., PARISIEN, M.-A., VAN DORN, J. and HAYHOE, K., 2009b. Global pyrogeography: the current and future distribution of wildfire. *PLoS ONE* 4(4), e5102, doi:10.1371/journal.pone.0005102.

KUNZ, R.P. and SCHULZE, R.E., 2010. Climate Change 2010 and Climatic Zones in South Africa. In: R.E. Schulze (ed.). *Atlas of Climate Change and the South African Agricultural Sector: A 2010 Perspective*. Pretoria: Department of Agriculture, Forestry and Fisheries. p143-149.

KUTIEL, H., MAHERAS, P. and GUIKA, S., 1996. Circulation and extreme rainfall conditions in the eastern Mediterranean during the last century. *International Journal of Climatology* 16(1), 73-92.

KZN FPA (KwaZulu-Natal Fire Protection Association), 2015. KwaZulu-Natal Fire Protection Association, Firestop [Online]. Retrieved from http://www.firestop.co.za/ (Accessed 13/07/2015).

LAING, M.V., 1978. *Forecasting bush and forest fire weather in Rhodesia. Meteorological Notes, Series B, No. 60*. Salisbury: Department of Meteorological Services. 29pp.

LAMONT, B.B. and DOWNES, K.S., 2011. Fire-stimulated flowering among resprouters and geophytes in Australia and South Africa. *Plant Ecology* 212(12), 2111-2125.

LAMPIN-MAILLET, C., MANTZAVELAS, A., GALIANA, L., JAPPIOT, M., LONG, M., HERRERO, G., KARLSSON, O., IOSSIFINA, A., THALIA, L. and THANASSIS, P., 2010. Wildland Urban Interfaces, Fire Behaviour and Vulnerability: Characterization, Mapping and Assessment. In: J.S. Silva, F. Rego, P. Fernandes & E. Rigolot (eds.). *Towards Integrated Fire Management – Outcomes of the European Project Fire Paradox*. European Forest Institute Research Report 23. Retrieved from http://www.efi.int/files/attachments/publications/efi_rr23.pdf (Accessed 10/07/2016).

LANDMAN, W.A., MASON, S.J., TYSON, P.D. and TENNANT, W.J., 2001. Statistical downscaling of GCM simulations to Streamflow. *Journal of Hydrology* 252, 221-236.

LANG, Y., 2014. Dark Snow Spells Doom for Glacial Melt Rates [Online]. Retrieved from http://glacierhub.org/2014/11/06/dark-snow-spells-doom-for-glacial-melt-rates/ (Accessed 16/10/2016).

LARA, A., WOLODARSKY-FRANKE, A., ARAVENA, J.C., CORTÉS, M., FRAVER, S. and SILLA, F., 2003. Fire Regimes and Forest Dynamics in the Lake Region of South-Central Chile. In: T.T. Veblen, W.L. Baker, G. Montenegro & T.W. Swetnam (eds.). *Ecological Studies, Vol. 160: Fire and Climatic Change in Temperate Ecosystems of the Western Americas*. New York: Springer-Verlag. 444pp.

LAWES, M.J., ADIE, H., RUSSELL-SMITH, J., MURPHY, B. and MIDGLEY, J.J., 2011. How do small savanna trees avoid stem mortality by fire? The roles of stem diameter, height and bark thickness. *Ecosphere* 2(4), 1-13.

LAWRENCE, M.G., 2005. The relationship between relative humidity and the dewpoint temperature in moist air: a simple conversion and applications. *Bulletin of the American Meteorological Society* 86, 225-233.

LAWSON, B.D. and ARMITAGE, O.B., 2008. *Weather Guide for the Canadian Forest Fire Danger Rating System*. Edmonton: Natural Resources Canada. 73pp.

LÁZARO, A. and MONTIEL, C., 2010. Overview of Prescribed Burning Policies and Practices in Europe and Other Countries. In: J.S. Silva, F. Rego, P. Fernandes & E. Rigolot (eds.). *Towards Integrated Fire Management – Outcomes of the European Project Fire Paradox*. European Forest Institute Research Report 23. Retrieved from http://www.efi.int/files/attachments/publications/efi_rr23.pdf (Accessed 10/07/2016).

LAZENBY, M.J., LANDMAN, W.A., GARLAND, R.M. and DeWitt, D.G., 2014. Seasonal temperature prediction skill over Southern Africa and human health. *Meteorological Applications* 21, 963-974.

LEARNING ESSENTIALS. 2004. *Mapping Environmental Disasters: Bushfires and Threatened Species*. (DVD). New York: Insight Media.

LEE, C.C. and SHERIDAN, S.C., 2015. Synoptic climatology: An overview. *Reference Module in Earth Systems and Environmental Sciences*, doi: 10.1016/B978-0-12-409548-9.09421-5.

LEFPA, 2014. Lowveld & Escarpment Fire Protection Association [Online]. Retrieved from http://www.lefpa.co.za/ (Accessed 30/01/2014).

LENIHAN, J.M., BACHELET, D., NEILSON, R.P. and DRAPEK, R., 2008. Response of vegetation distribution, ecosystem productivity, and fire to climate change scenarios for California. *Climatic Change* 87(Suppl 1), S215-S230.

LENNARD, C. and HEGERL, G., 2014. Relating changes in synoptic circulation to the surface rainfall response using self-organising maps. *Climate Dynamics*, doi 10.1007/s00382-014-2169-6.

LE PAGE, Y., PEREIRA, J.M.C., TRIGO, R., DA CAMARA, C., OOM, D. and MOTA, B., 2008. Global fire activity patterns (1996 – 2006) and climatic influence: an analysis using the World Fire Atlas. *Atmospheric Chemistry and Physics* 8, 1911-1924.

LEVITOV, M., 2010. Moscow Smoke Pollution Delays Flights as Fires Spread. *Bloomberg*, 7 August 2010.

LI, Q., YANG, Y., BAO, X., LIU, F., LIANG, W., ZHU, J., BEZEMER, T.M. and VAN DER PUTTEN, W.H., 2015. Legacy effects of elevated ozone on soil biota and plant growth. *Soil Biology & Biochemistry* 91, 50-57.

LIN, N.-H., TSAY, S.-C., MARING, H.B., YEN, M.-C., SHEU, G.-R., WANG, S.-H., CHI, K.H., CHUANG, M.-T., OU-YANG, C.-F., FU, J.S., REID, J.S., LEE, C.-T., WANG, L.-C., WANG, J.-L., HSU, C.N., SAYER, A.M., HOLBEN, B.N., CHU, Y.-C., NGUYEN, X.A., SOPAJAREE, K., CHEN, S.-J., CHENG, M.-T., TSUANG, B.-J., TSAI, C.-J., PENG, C.-M., SCHNELL, R.C., CONWAY, T., CHANG, C.-T., LIN, K.-S., TSAI, Y.I., LEE, W.-J., CHANG, S.-C., LIU, J.-J., CHIANG, W.-L., HUANG, S.-J., LIN, T.-H. and LIU, G.-R., 2013. An overview of regional experiments on biomass burning aerosols and related

pollutants in Southeast Asia: From BASE-ASIA and the Dongsha Experiment to 7-SEAS. *Atmospheric Environment* 78, 1-19.

LINDESAY, J.A., 1997. African Savanna Fires, Global Atmospheric Chemistry and the Southern Tropical Atlantic Regional Experiment. In: B.W. van Wilgen, M.O. Andreae, J.G. Goldammer & J.A. Lindesay (eds.). *Fire in Southern African Savannas. Ecological and Atmospheric Perspectives*. Cape Town: Witwatersrand University Press. p1-16.

LINES, G.S., PANCURA, M. and LANDER, C., 2005. *Building Climate Change Scenarios of Temperature and Precipitation in Atlantic Canada using the Statistical Downscaling Model (SDSM)*. Dartmouth: Meteorological Service of Canada. 41pp.

LITSCHERT, S.E., BROWN, T.C. and THEOBALD, D.M., 2012. Historic and future extent of wildfires in the Southern Rockies Ecoregion, USA. *Forest Ecology and Management* 269, 124-133.

LIU, J.C., PEREIRA, G., UHL, S.A., BRAVO, M.A. and BELL, M.L., 2015. A systematic review of the physical health impacts from non-occupational exposure to wildfire smoke. *Environmental Research* 136, 120-132.

LIU, Y., GOODRICK, S.L. and HEILMAN, W., 2014. Wildland fire emissions, carbon, and climate: Wildfire–climate interactions. *Forest Ecology and Management* 317, 80-96.

LIU, Y., GOODRICK, S.L. and STANTURF, J.A., 2013. Future U.S. wildfire potential trends projected using a dynamically downscaled climate change scenario. *Forest Ecology and Management* 294, 120-135.

LIU, Y., STANTURF, J.A. and GOODRICK, S.L., 2010. Trends in global wildfire potential in a changing climate. *Forest Ecology and Management* 259, 685-697.

LIU, Z. and WIMBERLY, M.C., 2016. Direct and indirect effects of climate change on projected future fire regimes in the western United States. *Science of the Total Environment* 542, 65-75.

LIU, Z., YANG, J., CHANG, Y., WEISBERG, P.J. and HE, H.S., 2012. Spatial patterns and drivers of fire occurrence and its future trend under climate

change in a boreal forest of Northeast China. *Global Change Biology* 18, 2041-2056.

LIVINGSTONE, D., 1905. *Livingstone's Travels and Researches in South Africa*. Philidelphia: J.W. Bradley. 460pp.

LOHMANN, D., TIETJEN, B., BLAUM, N., JOUBERT, D.F. and JELTSCH, F., 2014. Prescribed fire as a tool for managing shrub encroachment in semi-arid savanna rangelands. *Journal of Arid Environments* 107, 49-56.

LOTAN, J.E., 1976. Cone Serotiny – Fire Relationships in Lodgepole Pine. *Proceedings of the 14th Tall Timbers Fire Ecology Conference, 8 – 10 October 1974, Tall Timbers Research Center, Tallahassee, U.S.A*. pp. 267-278.

LOUPPE, D., OUATTARA, N. and COULIBALY, A., 1995. The effect of brush fires on vegetation: the Aubreville fire plots after 60 years. *Commonwealth Forestry Review* 74, 288-292.

LOWRY, W., 1972. *WMO – No. 327 Compendium of Lecture Notes in Climatology for Class IV Meteorological Personnel*. Geneva: World Meteorological Organisation.

LUCAS, C., HENNESSEY, K., MILLS, G.A. and BATHOLS, J., 2007. *Bushfire Weather in Southeast Australia: Recent Trends and Projected Climate Change Impacts*. *Bushfire CRC Consultancy Report to the Climate Institute of Australia*. Melbourne: Bushfire Cooperative Research Centre. 80pp.

LUI, Y. and WEISBERG, R.H., 2011. A Review of Self-Organizing Map Applications in Meteorology and Oceanography. In: J.I. Mwasiagi (ed.). *Self Organizing Maps – Applications and Novel Algorithm Design*. Rijeka: InTech.

LUND, I.A., 1963. Map-pattern classification by statistical methods. *Journal of Applied Meteorology* 2, 56-65.

LUNDQUIST, J.E., 2007. The relative influence of diseases and other small-scale disturbances on fuel loading in the Black Hills. *Plant Disease* 91, 147-152.

LYNCH, A.H., BERINGER, J., KERSHAW, P., MARSHALL, A., MOONEY, S., TAPPER, N., TURNEY, C. and VAN DER KAARS, S., 2007. Using the

paleorecord to evaluate climate and fire interactions in Australia. *Annual Review of Earth and Planetary Sciences* 35, 215-239.

MACKELLAR, N.C., HEWITSON, B.C. and TADROSS, M.A., 2007. Namaqualand's climate: Recent historical changes and future scenarios. *Journal of Arid Environments* 70(4), 604-614.

MACKELLAR, N.C., TADROSS, M.A. and HEWITSON, B.C., 2010. Synoptic-based evaluation of climatic response to vegetation change over southern Africa. *International Journal of Climatology* 30, 774-789.

MACKIE, B., 2013. *Warning Fatigue: Insights from the Australian Bushfire Context*. PhD Thesis, University of Canterbury, New Zealand.

MAGHAMI, M.R., HIZAM, H., GOMES, C., RADZI, M.A., REZADAD, M.I. and HAJIGHORBANI, S., 2016. Power loss due to soiling on solar panel: A review. *Renewable and Sustainable Energy Reviews* 59, 1307-1316.

MAINI, P., KUMAR, A., SINGH, S.V. and RATHORE, L.S., 2004. Operational model for forecasting location specific quantitative precipitation and probability of precipitation over India. *Journal of Hydrology* 288, 170-188.

MALEVSKY-MALEVICH, S.P., MOLKENTIN, E.K., NADYOZHINA, E.D. and SHKLYAREVICH, O.B., 2008. An assessment of potential change in wildfire activity in the Russian boreal forest zone induced by climate warming during the twenty-first century. *Climatic Change* 86, 463-474.

MALILAY, J., 1999. A Review of Factors Affecting the Human Health Impacts of Air Pollutants from Forest Fires. In: K.T. Gsoh, D. Schwela & J.G. Goldammer (eds.). *Health Guidelines for Vegetation Fire Events – Background Papers*. Geneva: World Health Organisation.

MARIĆ, T. and DURRAN, D.R., 2009. Observations of gap flow in the Wipp Valley on 20 October 1999: Evidence of subsidence. *Journal of the Atmospheric Sciences* 66, 984-1001.

MARKGRAF, V., IGLESIAS, V. and WHITLOCK, C., 2013. Late and postglacial vegetation and fire history from Cordón Serrucho Norte, northern Patagonia. *Palaeogeography, Palaeoclimatology, Palaeoecology* 371, 109-118.

MARLON, J.R., BARTLEIN, P.J., DANIAU, A.-L., HARRISON, S.P., MAEZUMI, S.Y., POWER, M.J., TINNER, W. and VANNIÉRE, B., 2013. Global biomass burning: a synthesis and review of Holocene paleofire records and their controls. *Quaternary Science Reviews* 65, 5-25.

MARLON, J.R., KELLY, R., DANIAU, A.-L., VANNIÉRE, B., POWER, M.J., BARTLEIN, P.J., HIGUERA, P., BLARQUEZ, O., BREWER, S., BRÜCHER, T., FEURDEAN, A., ROMERA, G.G., IGLESIAS, V., MAEZUMI, S.Y., MAGI, B., MUSTAPHI, C.J.C. and ZHIHAI, T., 2016. Reconstructions of biomass burning from sediment-charcoal records to improve data-model comparisons. *Biogeosciences* 13, 3225-3244.

MASUBELELE, M.L., HOFFMAN, M.T., BOND, W.J. and GAMBIZA, J., 2014. A 50 year study shows grass cover has increased in shrublands of semi-arid South Africa. *Journal of Arid Environments* 104, 43-51.

MATAIX-SOLERA, J., GUERRERO, C., GARCÍA-ORENES, F., BÁRCENAS, G.M. and TORRES, P., 2009. Forest Fire Effects on Soil Microbiology. In: A. Cerdà & P.R. Robichaud (eds.). *Fire Effects on Soils and Restoration Strategies*. Enfield: Science Publishers.

MATHEWSON, T., KEAVY, C., MORGAN, P., ELLIS, M., LANGE-NAVARO, R., DUNN, N., PARRISH, D. and HICKMAN, S., 2008. *Introduction to Wildland Fire Behavior, S-190*. National Wildfire Coordination Group. Available online from http://training.nwcg.gov/pre-courses/s290/S-290%20Student%20CD/S-190_Student%20Workbook.pdf.

MATTHEWS, S., WATSON, P., BRUCE, J., SULLIVAN, A., PINKARD, L. and WILLIAMS, D., 2014. Fuels, fire, and climate change. *Proceedings of 4th Fire Behavior and Fuels Conference, 1 to 4 July 2013, St. Petersburg, Russia*.

MAURIN, O., DAVIES, T.J., BURROWS, J.E., DARU, B.H., YESSOUFOU, K., MUASYA, A.M., VAN DER BANK, M. and BOND, W.J., 2014. Savanna fire and the origins of the 'underground forests' of Africa. *New Phytologist* 204, 201-214.

MCGREGOR, J.L., 2005. C-CAM: Geometric aspects and dynamical formulation. CSIRO Atmospheric Research Tech. Paper No. 70, 43.

MCGREGOR, J.L. and DIX, M.R., 2001. The CSIRO conformal-cubic atmospheric GCM. In: P. F. Hodnett (ed.). *IUTAM Symposium on Advances in Mathematical Modeling of Atmosphere and Ocean Dynamics*. Dordrecht: Kluwer. p197-202.

MCGREGOR, J.L. and DIX, M.R., 2008. An updated description of the Conformal-Cubic Atmospheric Model. In: K. Hamilton & W. Ohfuchi (eds.). *High Resolution Simulation of the Atmosphere and Ocean*. New York: Springer. p 51 – 76.

MCGUFFIE, K. and HENDERSON-SELLERS, A., 2014. *The Climate Modelling Primer*. 4th Ed. Chichester: John Wiley & Sons. 439pp.

MCGUIRE, R., 2015. Thick smoke from U.S. hampers efforts to fight local fires. *Osoyoos Times*, 26 August 2015.

MCRAE, R. and SHARPLES, J., 2012. Turn and burn: the strange world of fire tornadoes [Online]. Retrieved from http://theconversation.com/turn-and-burn-the-strange-world-of-fire-tornadoes-11193 (Accessed 10/02/2016).

MEIKEL, S. and HEINE, J., 1987. A fire index system for the Transvaal Lowveld and adjoining escarpment areas. *South African Forestry Journal* 143, 55 - 57.

MEIKEL, S., HEINE, J., HEINE, L. and TROLLOPE, W.S.W., 2012. Special Report: Fire Danger Rating System for Prescribed Burning. *Working on Fire International*, 8 March 2012.

MENAUT, J.-C., ABBADIE, L. and VITOUSEK, P.M., 1993. Nutrient and Organic Matter Dynamics in Tropical Ecosystems. In: P.J. Crutzen & J.G. Goldammer (eds.). *Fire in the Environment. The Ecological, Atmospheric, and Climatic Importance of Vegetation Fires*. Chichester: John Wiley & Sons. p213-231.

MERCER, D.E., PYE, J.M., PRESTEMON, J.P., BUTRY, D.T. and HOLMES, T.P., 2000. Economic effects of catastrophic wildfires: Assessing the effectiveness of fuel reduction programs for reducing the economic impacts

of catastrophic forest fire events [Online]. Retrieved from http://freshfromflorida.s3.amazonaws.com/economic_effects.pdf (Accessed 09/10/2016).

MEUNIER, J., ROMMEA, W.H. and BROWN, P.M., 2014. Climate and land-use effects on wildfire in northern Mexico, 1650 – 2010. *Forest Ecology and Management* 325, 49-59.

MEYN, A., WHITE, P.S., BUHK, C. and JENTSCH, A., 2007. Environmental drivers of large, infrequent wildfires: the emerging conceptual model. *Progress in Physical Geography* 31(3), 287-312.

MICHAELIDES, S., TYMVIOS, F. and CHARALAMBOUS, D., 2010. Investigation of trends in synoptic patterns over Europe with artificial neural networks. *Advances in Geosciences* 23, 107-112.

MICHALETZ, S.T., JOHNSON, E.A. and TYREE, M.T., 2012. Moving beyond the cambium necrosis hypothesis of post-fire tree mortality: cavitation and deformation of xylem in forest fires. *New Phytologist* 194, 254-263.

MIDGLEY, D.C., PITMAN, W.V. and MIDDLETON, B.J., 1994. *Surface water resources of South Africa (WR90). Volumes I-VI (Appendices) and Volume I-VI (Maps), WRC Reports 298/1.1/94, 298/1.2/94, 298/2.1/94, 298/2.2/94, 298/3.1/94, 298/3.2/94, 298/4.1/94, 298/4.22/94, 298/5.1/94, 298/5.2/94, 298/6.1/94, 298/6.2/94*. Pretoria: Water Research Commission.

MIEVILLE, A., GRANIER, C., LIOUSSE, C., GUILLAUME, B., MOUILLOT, F., LAMARQUE, J.-F., GRÉGOIRE, J.-M. AND PÉTRON, G., 2010. Emissions of gases and particles from biomass burning during the 20th century using satellite data and an historical reconstruction. *Atmospheric Environment* 44, 1469-1477.

MILLER, N. L. and SCHLEGEL, N.J., 2006. Climate change projected fire weather sensitivity: California Santa Ana wind occurrence. *Geophysical Research Letters* 33, L15711, doi:10.1029/2006GL025808.

MILLS, A.J. and FEY, M.V., 2004. Frequent fires intensify soil crusting: physicochemical feedback in the pedoderm of long-term burn experiments in South Africa. *Geoderma* 121, 45-64.

MILLSPAUGH, S.H., WHITLOCK, C. and BARTLEIN, P.J., 2000. Variations in fire frequency and climate over the past 17 000 yr in central Yellowstone National Park. *Geology* 28(3), 211-214.

MIRANDA, A.I., MARCHI, E., FERRETTI, M. and MILLÁN, M.M., 2009. Forest Fires and Air Quality Issues in Southern Europe. In: A. Bytnerowicz, M. Arbaugh, A. Riebau & C. Andersen (eds.). *Wildland Fires and Air Pollution*. Amsterdam: Elsevier. p209-232.

MISHRA, D.D., 2014. *Fundamental Concepts in Environmental Studies*. Revised Ed. New Delhi: S. Chand & Company.

MITCHELL, R.J., LIU, Y., O'BRIEN, J.J., ELLIOTT, K.J., STARR, G., MINIAT, C.F. and HIERS, J.K., 2014. Future climate and fire interactions in the southeastern region of the United States. *Forest Ecology and Management* (in press).

MOELTNER, K., KIM, M.-K., ZHU, E. and YANG, W., 2013. Wildfire smoke and health impacts: A closer look at fire attributes and their marginal effects. *Journal of Environmental Economics and Management* 66, 476-496.

MOGALE, M. and DYSON, L.L., 2017. Continental tropical low-pressure systems and their associated rainfall over the Highveld of South Africa using self-organizing maps. *Proceedings of the 33rd annual conference of the South African Society for Atmospheric Sciences, 21 – 22 September 2017, Polokwane, South Africa*.

MÖLDERS, N., 2010. Comparison of Canadian Forest Fire Danger Rating System and National Fire Danger Rating System fire indices derived from Weather Research and Forecasting (WRF) model data for the June 2005 Interior Alaska wildfires. *Atmospheric Research* 95, 290-306.

MONCRIEFF, G.R., SCHEITER, S., SLINGSBY, J.A. and HIGGINS, S.I., 2015. Understanding global change impacts on South African biomes using Dynamic Vegetation Models. *South African Journal of Botany* 101, 16-23.

MONTIEL, C. and HERRERO, G., 2010. An Overview of Policies and Practices Related to Fire Ignitions at the European Union Level. In: J.S. Silva, F. Rego, P. Fernandes & E. Rigolot (eds.). *Towards Integrated Fire Management –*

Outcomes of the European Project Fire Paradox. European Forest Institute Research Report 23. Retrieved from http://www.efi.int/files/attachments/publications/efi_rr23.pdf (Accessed 10/07/2016).

MOOLA, F.M. and VASSEUR, L., 2009. The importance of clonal growth to the recovery of *Gaultheria procumbens* L. (Ericaceae) after forest disturbance. *Plant Ecology* 201(1), 319-337.

MOREIRA, F., VIEDMA, O., ARIANOUTSOU, M., CURT, T., KOUTSIAS, N., RIGOLOT, E., BARBATI, A., CORONA, P., VAZ, P., XANTHOPOULOS, G., MOUILLOT, F. and BILGILI, E., 2011. Landscape - wildfire interactions in southern Europe: Implications for landscape management. *Journal of Environmental Management* 92, 2389-2402.

MORENO, M.V., CONEDERA, M., CHUVIECO, E. and PEZZATTI, G.B., 2014. Fire regime changes and major driving forces in Spain from 1968 to 2010. *Environmental Science & Policy* 37, 11-22.

MORGAN, P., KEANE, R.E., DILLON, G.K., JAIN, T.B., HUDAK, A.T., KARAU, E.C., SIKKINK, P.G., HOLDEN, Z.A. and STRAND, E.K., 2014. Challenges of assessing fire and burn severity using field measures, remote sensing and modelling. *International Journal of Wildland Fire* 23, 1045-1060.

MORI, A.S. and JOHNSON, E.A., 2013. Assessing possible shifts in wildfire regimes under a changing climate in mountainous landscapes. *Forest Ecology and Management* 310, 875-886.

MORIONDO, M., GOOD, P., DURAO, R., BINDI, M., GIANNAKOPOULOS, C. and CORTE-REAL, J., 2006. Potential impact of climate change on fire risk in the Mediterranean area. *Climate Research* 31, 85-95.

MORITZ, M.A., PARISIEN, M.-A., BATLLORI, E., KRAWCHUK, M.A., VAN DORN, J., GANZ, D.J. and HAYHOE, K., 2012. Climate change and disruptions to global fire activity. *Ecosphere* 3(6), 49, doi:10.1890/ES11-00345.1.

MOUILLOT, F. and FIELD, C.B., 2005. Fire history and the global carbon budget: a 1°×1° fire history reconstruction for the 20th century. *Global Change Biology* 11, 398-420.

MUCINA, L., HOARE, D.B., LÖTTER, M.C., DU PREEZ, P.J., RUTHERFORD, M.C., SCOTT-SHAW, C.R., BREDENKAMP, G.J., POWRIE, L.W., SCOTT, L., CAMP, K.G.T., CILLIERS, S.S., BEZUIDENHOUT, H., MOSTERT, T.H., SIEBERT, S.J., WINTER, P.J.D., BURROWS, J.E., DOBSON, L., WARD, R.A., STALMANS, M., OLIVER, E.G.H., SIEBERT, F., SCHMIDT, E., KOBISI, K. and KOSE, L., 2006. Grassland biome. *Strelitzia* 19, 348-437.

MUCINA, L. and RUTHERFORD, M.C., 2006. The vegetation of South Africa, Lesotho and Swaziland. *Strelitzia* 19. Pretoria: South African National Biodiversity Institute.

MURPHY, B.P. and BOWMAN, D.M.J.S., 2012. What controls the distribution of tropical forest and savanna? *Ecology Letters* 15, 748-758.

MURPHY, J., 1999. An evaluation of statistical and dynamical techniques for downscaling local climate. *Journal of Climate* 12, 2256-2284.

MURPHY, M., 2016. Wildfire cripples tourism in California's scenic Big Sur. *Marketwatch*, 31 August 2016.

MYDANS, S., 1997. Southeast Asia Chokes on Indonesia's Forest Fires. *The New York Times*, 25 September 1997.

MYHRE, G., GOVAERTS, Y., HAYWOOD, J.M., BERNTSEN, T.K. and LATTANZIO, A., 2005. Radiative effect of surface albedo change from biomass burning. *Geophysical Research Letters* 32, L20812, doi:10.1029/2005GL022897.

NAEHER, L.P., BRAUER, M., LIPSETT, M., ZELIKOFF, J.T., SIMPSON, C.D., KOENIG, J.Q. and SMITH, K.R., 2007. Woodsmoke health effects: a review. *Inhalation Toxicology* 19(1), 67-106.

NAKIĆENOVIĆ, N., DAVIDSON, O., DAVIS, G., GRÜBLER, A., KRAM, T., LA ROVERE, E.L., METZ, B., MORITA, T., PEPPER, W., PITCHER, H., SANKOVSKI, A., SHUKLA, P., SWART, R., WATSON, R. and DADI, Z., 2000. *Emission Scenarios: A Summary of Working Group III of the Intergovernmental Panel on Climate Change*. Cambridge: Cambridge University Press.

NASA-EOS (National Aeronautics and Space Administration's Earth Observatory System), 2010. Smoke over Moscow [Online]. Retrieved from http://earthobservatory.nasa.gov/NaturalHazards/view.php?id=45089&eocn=image&eoci=related_image (Accessed 17/08/2016).

NASA-OMPS (National Aeronautics and Space Administration – Ozone Mapping and Profiler Suite), 2015. Smoke from Northern Canada to the Southeastern US [Online]. Retrieved from http://ozoneaq.gsfc.nasa.gov/omps/blog/2015/06/smoke-northern-canada-southeastern-us (Accessed 05/07/2015).

NEARY, D.G., 2002. A flood of ash and sediment fills the washes in the White Mountains after the fire [Online]. Retrieved from http://ncfp.files.wordpress.com/2013/02/ash-flow.jpg?w=595 (Accessed 29/09/2016).

NIELSEN, T.T. and RASMUSSEN, K., 2001. Utilization of NOAA AVHRR for assessing the determinants of savannah fire distribution of Burkina Faso. *International Journal of Wildland Fire* 10, 129-135.

NIMMO, D. 2014. Pyrodiversity vs biodiversity. *Australasian Science*, December 2014, 16-19. Retrieved from http://www.australasianscience.com.au/article/issue-december-2014/pyrodiversity-vs-biodiversity.html (Accessed on 08/08/2016).

NITSCHKE, C.R. and INNES, J.L., 2008. Climatic change and fire potential in South-Central British Columbia, Canada. *Global Change Biology* 14, 841-855.

NOBLE, I.R., BARY, G.A.V. and GILL, A.M., 1980. McArthur's fire-danger meters expressed as equations. *Australian Journal of Ecology* 5, 201-203.

NOTICE 1054 of 2005. The National Fire Danger Rating System in terms of the National Veld and Forest Fire Act, 1998 (Act No. 101 of 1998). *Government Gazette of the Republic of South Africa* No. 27735.

NOTICE 1099 of 2013. Publication of the Fire Danger Rating System for General Information in terms of Section 9(1) on the National Veld and Forest Fire Act, 1998 (Act No. 101 of 1998). *Government Gazette of the Republic of South Africa* No. 37014.

NRC (National Research Council), 2005. *Radiative Forcing of Climate Change: Expanding the Concept and Addressing Uncertainties*. Washington: National Academies Press.

O'CONNOR, T.G., PUTTICK, J.R. and HOFFMAN, M.T., 2014. Bush encroachment in southern Africa: changes and causes. *African Journal of Range & Forage Science* 31(2), 67-88.

OELSCHLÄGEL, B., 1995. A method for downscaling global climate model calculations by a statistical weather generator. *Ecological Modelling* 82, 199-204.

OETTLI, P., TOZUKA, T., IZUMO, T., ENGELBRECHT, F.A. and YAMAGATA, T., 2014. The self-organizing map, a new approach to apprehend the Madden-Julian Oscillation influence on the intraseasonal variability of rainfall in the southern African region. *Climate Dynamics* 43, 1557-1573.

OHASHI, Y., TERAO, T., SHIGETA, Y. and OHSAWA, T., 2015. In situ observational research of the gap wind "Hijikawa-Arashi" in Japan. *Meteorology and Atmospheric Physics* 127, 33-48.

OKE, T.R., 1978. *Boundary Layer Climates*. London: Methuen & Co.

OKE, T.R., 1987. *Boundary Layer Climates*. 2nd Ed. London: Methuen & Co.

OLORUNFEMI, I.E., OGUNRINDE, T.A. and FASINMIRIN, J.T., 2014. Soil Hydrophobicity: An Overview. *Journal of Scientific Research & Reports* 3(8), 1003-1037.

OLSON, D.M., DINERSTEIN, E., WIKRAMANAYAKE, E.D., BURGESS, N.D., POWELL, G.V.N., UNDERWOOD, E.C., D'AMICO, J.A., ITOUA, I., STRAND, H.E., MORRISON, J.C., LOUCKS, C.J., ALLNUTT, T.F., RICKETTS, T.H., KURA, Y., LAMOREUX, J.F., WETTENGEL, W.W., HEDAO, P. and KASSEM, K.R., 2001. Terrestrial ecoregions of the world: a new map of life on Earth. *BioScience* 51(11), 933-938.

ORIS, F., ASSELIN, H., FINSINGER, W., HELY, C., BLARQUEZ, O., FERLAND, M.-E., BERGERON, Y. and ALI, A.A., 2014. Long-term fire history in northern Quebec: implications for the northern limit of commercial forests. *Journal of Applied Ecology* 51, 675-683.

PALMER, A.R. and AINSLIE, A.M., 2005. Grasslands of South Africa. In: J.M. Suttie, S.G. Reynolds & C. Batello (eds.). *Grasslands of the World.* Rome: FAO. p77-120.

PALMER, A.R. and AINSLIE, A.M., 2006. Arid rangeland production systems of Southern Africa. *Sécheresse* 17(1-2), 98-104.

PARISE, M. and CANNON, S.H., 2012. Wildfire impacts on the processes that generate debris flows in burned watersheds. *Natural Hazards* 61, 217-227.

PATON-WALSH, C., LOUISA K. EMMONS, L.K. and WIEDINMYER, C., 2012. Australia's Black Saturday fires - Comparison of techniques for estimating emissions from vegetation fires. *Atmospheric Environment* 60, 262-270.

PAUSAS, J., 2004. Changes in fire and climate in the Eastern Iberian Peninsula (Mediterranean Basin). *Climatic Change* 63, 337-350.

PAUSAS, J.G., LLOVET, J., RODRIGO, A. and VALLEJO, R., 2008. Are wildfires a disaster in the Mediterranean basin? – A review. *International Journal of Wildland Fire* 17, 713-723.

PEARCE, H.G., KERR, J., CLARK, A., MULLAN, B., ACKERLEY, D., CAREY-SMITH, T. and YANG, E., 2011. *Improved estimates of the effect of climate change on NZ fire danger*. Scion Client Report No. 18087. Christchurch: Scion Rural Fire Research Group in conjunction with NIWA. 84pp.

PEARCE, J.L., BERINGER, J., NICHOLLS, N., HYNDMAN, R.J, UOTILA, P. and TAPPER, N.J., 2011. Investigating the influence of synoptic-scale meteorology on air quality using self-organizing maps and generalized additive modelling. *Atmospheric Environment* 45, 128-136.

PECHONY, O. and SHINDELL, D.T., 2010. Driving forces of global wildfires over the past millennium and the forthcoming century. *Proceedings of the National Academy of Sciences* 107(45), 19167-19170.

PEÑA, M., BARBAKH, W. and FYFE, C., 2007. Topology-Preserving Mappings for Data Visualisation. In: A.N. Gorban, B. Kégl, D.C. Wunsch & A.Y. Zinovyev (eds.). *Lecture Notes in Computational Science and Engineering: Principal Manifolds for Data Visualization and Dimension Reduction*. Berlin: Springer.

PEREIRA, M.G., CALADO, T.J., DACAMARA, C.C. and CALHEIROS, T., 2013. Effects of regional climate change on rural fires in Portugal. *Climate Research* 57, 187-200.

PEREIRA, M.G., TRIGO, R.M., DA CAMARA, C.C., PEREIRA, J.M.C. and LEITE, S.M., 2005. Synoptic patterns associated with large summer forest fires in Portugal. *Agricultural and Forest Meteorology* 129, 11-25.

PÉREZ-SÁNCHEZ, J., SENENT-APARICIO, J., DÍAZ-PALMERO, J.M. and CABEZAS-CEREZO, J. DE D., 2017. A comparative study of fire weather indices in a semiarid south-eastern Europe region. Case of study: Murcia (Spain). Science of the Total Environment 590-591, 761-774.

PESAVA, P., AKSU, R., TOPRAK, S., HORVATH, H. and SEIDL, S., 1999. Dry deposition of particles to building surfaces and soiling. *The Science of the Total Environment* 235, 25-35.

PESCE, O.H. and MORENO, P.I., 2014. Vegetation, fire and climate change in central-east Isla Grande de Chiloé (43°S) since the Last Glacial Maximum, northwestern Patagonia. *Quaternary Science Reviews* 90, 143-157.

PIÑOL, J., TERRADAS, J. and LLORET, F., 1998. Climate warming, wildfire hazard, and wildfire occurrence in coastal eastern Spain. *Climatic Change* 38, 345-357.

PITMAN, A.J., NARISMA, G.T. and MCANENEY, J., 2007. The impact of climate change on the risk of forest and grassland fires in Australia. *Climatic Change* 84, 383-401.

PODUR, J. and WOTTON, M., 2010. Will climate change overwhelm fire management capacity? *Ecological Modelling* 221, 1301-1309.

POOL, T., 2013. Fire update: 8th Fire Management Symposium. *Wood Southern Africa & Timber Times* 38(7), 8-13.

POTTER, B.E. and MARTIN, J.E., 2001. Accuracy of 24- and 48-hour forecasts of Haines' Index. *National Weather Digest* 25(3,4), 38-46.

POWER, M.J., MARLON, J., ORTIZ, N., BARTLEIN, P.J., HARRISON, S.P., MAYLE, F.E., BALLOUCHE, A., BRADSHAW, R.H.W., CARCAILLET, C., CORDOVA, C., MOONEY, S., MORENO, P.I., PRENTICE, I.C.,

THONICKE, K., TINNER, W., WHITLOCK, C., ZHANG, Y., ZHAO, Y., ALI, A.A., ANDERSON, R.S., BEER, R., BEHLING, H., BRILES, C., BROWN, K.J., BRUNELLE, A., BUSH, M., CAMILL, P., CHU, G.Q., CLARK, J., COLOMBAROLI, D., CONNOR, S., DANIAU, A.-L., DANIELS, M., DODSON, J., DOUGHTY, E., EDWARDS, M.E., FINSINGER, W., FOSTER, D., FRECHETTE, J., GAILLARD, M.-J., GAVIN, D.G., GOBET, E., HABERLE, S., HALLETT, D.J., HIGUERA, P., HOPE, G., HORN, S., INOUE, J., KALTENRIEDER, P., KENNEDY, L., KONG, Z.C., LARSEN, C., LONG, C.J., LYNCH, J., LYNCH, E.A., MCGLONE, M., MEEKS, S., MENSING, S., MEYER, G., MINCKLEY, T., MOHR, J., NELSON, D.M., NEW, J., NEWNHAM, R., NOTI, R., OSWALD, W., PIERCE, J., RICHARD, P.J.H., ROWE, C., SANCHEZ GOÑI, M.F., SHUMAN, B.N., TAKAHARA, H., TONEY, J., TURNEY, C., URREGO-SANCHEZ, D.H., UMBANHOWAR, C., VANDERGOES, M., VANNIERE, B., VESCOVI, E., WALSH, M., WANG, X., WILLIAMS, N., WILMSHURST, J. and ZHANG, J.H., 2008. Changes in fire regimes since the Last Glacial Maximum: an assessment based on a global synthesis and analysis of charcoal data. *Climate Dynamics* 30, 887-907.

POWER, M.J., MARLON, J.R., BARTLEIN, P.J. and HARRISON, S.P., 2010. Fire history and the Global Charcoal Database: A new tool for hypothesis testing and data exploration. *Palaeogeography, Palaeoclimatology, Palaeoecology* 291, 52-59.

PRASAD, V.K., BADARINATH, K.V.S. and EATURU, A., 2008. Biophysical and anthropogenic controls of forest fires in the Deccan Plateau, India. *Journal of Environmental Management* 86, 1-13.

PREISENDORFER, R.W., 1988. *Principal component analysis in meteorology and oceanography*. Amsterdam: Elsevier. 425pp.

PRICE, C. and RIND, D., 1994. The impact of a 2 × CO_2 climate on lightning-caused fires. *Journal of Climate 7*, 1484-1494.

PRICHARD, S.J., STEVENS-RUMANN, C.S. and HESSBURG, P.F., 2017. Tamm Review: Shifting global fire regimes: Lessons from reburns and research needs. *Forest Ecology and Management* 396, 217-233.

PRICOPE, N.G. and BINFORD, M.W., 2012. A spatio-temporal analysis of fire recurrence and extent for semi-arid savanna ecosystems in southern Africa using moderate-resolution satellite imagery. *Journal of Environmental Management* 100, 72-85.

PROJECT NIGHTJAR, 2016. Bronze-winged courser chicks [Online]. Retrieved from http://nightjar.exeter.ac.uk/story/coursers (Accessed 29/10/2016).

PYNE, S.J., 1997. *World Fire: The Culture of Fire on Earth*. Seattle: University of Washington Press.

RAHAYU, J.T., 2015. More Indonesia airports affected by haze from land fires. *Antara News*, 11 September 2015.

RAHN, M., 2009. Wildfire Impact Analysis. *Fire Impact Analysis*, Spring 2009. Retrieved from http://universe.sdsu.edu/sdsu_newscenter/images/rahn2009fireanalysis.pdf (Accessed 09/10/2016).

RAÍNHA, M. and FERNANDES, P.M., 2002. Using the Canadian Fire Weather Index (FWI) in the Natural Park of Montesinho, NE Portugal: Calibration and Application to Fire Management. In: D.X. Viegas (ed.). *Forest Fire Research & Wildland Fire Safety.* Rotterdam: Millpress.

RAMANATHAN, V. and CARMICHAEL, G., 2008. Global and regional climate changes due to black carbon. *Nature Geoscience* 1, 221-227.

RAMANATHAN, V. and FENG, Y., 2008. On avoiding dangerous anthropogenic interference with the climate system: Formidable challenges ahead. *Proceedings of the National Academy of Sciences* 105(38), 14245-14250.

RAMANATHAN, V. and FENG, Y., 2009. Air pollution, greenhouse gases and climate change: Global and regional perspectives. *Atmospheric Environment* 43, 37-50.

REUSCH, D.B., ALLEY, R.B. and HEWITSON, B.C., 2007. North Atlantic climate variability from a self-organizing map perspective. *Journal of Geophysical Research* 112, D02104 doi:10.1029/2006JD007460.

RIAÑO, D., RUIZ, J.A.M., MARTÍNEZ, J.B. and USTIN, S.L., 2007. Burned area forecasting using past burned area records and Southern Oscillation Index for tropical Africa (1981 – 1999). *Remote Sensing of Environment* 107, 571-581.

RICHARDSON, A.J., RISIEN, C. and SHILLINGTON, F.A., 2003. Using self-organizing maps to identify patterns in satellite imagery. *Progress in Oceanography* 59, 223- 239.

ROBINSON, P.J. and HENDERSON-SELLERS, A., 1999. *Contemporary Climatology*. 2nd Ed. Singapore: Pearson.

ROSENFELD, D., FROMM, M., TRENTMANN, J., LUDERER, G., ANDREAE, M.O. and SERVRANCKX, R., 2007. The Chisholm firestorm: observed microstructure, precipitation and lightning activity of a pyro-cumulonimbus. *Atmospheric Chemistry and Physics* 7, 645-659.

ROSENFELD, D., LOHMANN, U., RAGA, G.B., O'DOWD, C.D., KULMALA, M., FUZZI, S., REISSELL, A. and ANDREAE, M.O., 2008. Flood or drought: How do aerosols affect precipitation? *Science* 321, 1309-1313.

ROSENFELD, D. and WOODLEY, W., 2001. Pollution and clouds. *Physics World*, February 2001, 34-37.

ROY, D.P. and BOSCHETTI, L., 2009. Southern Africa validation of the MODIS, L3JRC and GlobCarbon burned-area products. *Transactions on Geoscience and Remote Sensing* 47(4), 1032-1044.

RUBEL, F., and KOTTEK, M., 2010. Observed and projected climate shifts 1901 – 2100 depicted by world maps of the Köppen-Geiger climate classification. *Meteorologische Zeitschrift* 19(2), 135-141.

SAMMON, J.W., 1969. A nonlinear mapping for data structure analysis. *IEEE Transactions on Computers* C-18, 401-409.

SANDBERG, D.V., OTTMAR, R.D., PETERSON, J.L. and CORE, J., 2002. Wildland Fire in Ecosystems: Effects of Fire on Air. General Technical Report RMRS-GTR-42-V5. Fort Collins, USDA Forest Service. 79pp.

SANDERS, D., LAING, J. and HOUGHTON, M., 2008. *Tourism Recovery: The Impact of Bushfires on Tourism end Visitation in Alpine National Parks*.

Sustainable Tourism Cooperative Research Centre [Online]. Retrieved from http://www.crctourism.com.au/ (Accessed 05/01/2015).

SANG, H., GELFAND, A.E., LENNARD, C., HEGERL, G. and HEWITSON, B., 2008. Interpreting self-organizing maps through space-time data models. *The Annals of Applied Statistics* 2(4), 1194-1216.

SAN-MIGUEL-AYANZ, J., CARLSON, J.D., ALEXANDER, M., TOLHURST, K., MORGAN, G., SNEEUWJAGT, R., and DUDLEY, M., 2003. Current methods to assess fire danger potential. In: E. Chuvieco (ed.). *Wildland Fire Danger Estimation and Mapping: The Role of Remote Sensing Data.* Singapore: World Scientific.

SAWS (South African Weather Service), 2002. *Alignment chart and tables used by the operational weather forecasters in calculating the Lowveld Fire Danger Index*. Pretoria: SAWS.

SAWS (South African Weather Service), 2012. Climate data supplied by South African Weather Service. Climate databank. Pretoria: SAWS.

SCHAFFHAUSER, A., CURT, T. and TATONI, T., 2011. Fire-vegetation interplay in a mosaic structure of *Quercus suber* woodlands and Mediterranean maquis under recurrent fires. *Forest Ecology and Management* 262, 730-738.

SCHEITER, S. and SAVADOGO, P., 2014. Ecosystem management can mitigate vegetation shifts induced by climate change in West Africa. *Ecological Modelling* 332, 19-27.

SCHLOBOHM, P. and BRAIN, J., 2002. *Gaining an Understanding of the National Fire Danger Rating System*. Boise: National Wildfire Coordinating Group. 72pp.

SCHMIDT-NIELSON, K., 1997. *Animal Physiology: Adaptation and Environment*. 5th Ed. Cambridge: Cambridge University Press. 613pp.

SCHOLES, R.J., KENDALL, J. and JUSTICE, C.O., 1996. The quantity of biomass burned in southern Africa. *Journal of Geophysical Research* 101, 23667-23676.

SCHOLZE, M., KNORR, W., ARNELL, N.W. and PRENTICE, I.C., 2006. A climate-change risk analysis for world ecosystems. *Proceedings of the National Academy of Sciences* 103(35), 13116-13120.

SCHUENEMANN, K.C., CASSANO, J.J. and FINNIS, J., 2009. Forcing of precipitation over Greenland: Climatology for 1961–99. *Journal of Hydrometeorology* 10, 60-78.

SCHULTZ, M.G., HEIL, A., HOELZEMANN, J.J., SPESSA, A., THONICKE, K., GOLDAMMER, J.G., HELD, A.C., PEREIRA, J.M.C. and VAN HET BOLSCHER, M., 2008. Global wildland fire emissions from 1960 to 2000. *Global Biogeochemical Cycles* 22, GB2002, doi:10.1029/2007GB003031.

SCHULZE, R.R., 1994. *Climate of South Africa. Part 8: general survey*. Pretoria: Government Printer.

SCHULZE, R.E., 2007. *South African Atlas of Climatology and Agrohydrology. WRC Report 1489/1/06*. Pretoria: Water Research Commission. pp276.

SCHWELA, D., 2001. Fire disasters: The WHO-UNEP-WMO health guidelines for vegetation fire events. *Annals of Burns and Fire Disasters* 14(4), 1-5.

SCIENCEDAILY, 2015. Reference Terms: Firestorm [Online]. Retrieved from http://www.sciencedaily.com/terms/firestorm.htm (Accessed 11/01/2015).

SCOTT, A.C., BOWMAN, D.M.J.S., BOND, W.J., PYNE, S.J. and ALEXANDER, M.E., 2014. *Fire on Earth: An Introduction*. Chichester: John Wiley & Sons. 435p.

SCOTT, L., 2002. Microscopic charcoal in sediments: Quaternary fire history of the grassland and savanna regions in South Africa. *Journal of Quaternary Science* 17, 77-86.

SEEMA, S., 2016. U'khand fires: Smoke hampers IAF op. *The Times of India (Mumbai edition)*, 2 May 2016.

SELUCHI, M.E. and CHOU, S.C., 2009. Synoptic patterns associated with landslide events in the Serra do Mar, Brazil. *Theoretical and Applied Climatology* 98, 67-77.

SHARP, J. and MASS, C.F., 2002. Columbia Gorge gap flow: Insights from observational analysis and ultra-high-resolution simulation. *Bulletin of the American Meteorological Society* 83, 1757-1762.

SHARPLES, J.J., MCRAE, R.H.D., WEBER, R.O. and GILL, A.M., 2009. A simple index for assessing fire danger rating. *Environmental Modelling & Software* 24, 764-774.

SHERIDAN, S.C. and LEE, C.C., 2011. The self-organizing map in synoptic climatological research. *Progress in Physical Geography* 35(1), 109-119.

SHERRIFF, R.L., PLATT, R.V., VEBLEN, T.T., SCHOENNAGEL, T.L. and GARTNER, M.H., 2014. Historical, observed, and modeled wildfire severity in montane forests of the Colorado Front Range. *PLoS One* 9(9), e106971, doi:10.1371/journal.pone.0106971.

SHI, Y., MATSUNAGA, T., SAITO, M., YAMAGUCHI, Y. and CHEN, X., 2015. Comparison of global inventories of CO_2 emissions from biomass burning during 2002 – 2011 derived from multiple satellite products. *Environmental Pollution* 206, 479-487.

SHONGWE, M.E., LENNARD, C., LIEBMANN, B., KALOGNOMOU, E.-A., NTSANGWANE, L. and PINTO, I., 2014. An evaluation of CORDEX regional climate models in simulating precipitation over Southern Africa. *Atmospheric Science Letters*, doi:10.1002/asl2.538.

SHRESTHA, S., THIN, N.M.M. and DEB, P., 2014. Assessment of climate change impacts on irrigation water requirement and rice yield for Ngamoeyeik Irrigation Project in Myanmar. In: S. Shresta (ed.). *Climate Change Impacts and Adaptation in Water Resources and Water Use Sectors: Case studies from Southeast Asia*. Cham: Springer. 119pp.

SHUMAN, J.K., FOSTER, A.C., SHUGART, H.H., HOFFMAN-HALL, A., KRYLOV, A., LOBODA, T., ERSHOV, D. AND SOCHILOVA, E., 2017. Fire disturbance and climate change: implications for Russian forests. *Environmental Research Letters* 12, 035003, doi:10.1088/1748-9326/aa5eed.

SILVA, P., BASTOS, A., DACAMARA, C.C. and LIBONATI, R., 2016. Future Projections of Fire Occurrence in Brazil Using EC-Earth Climate Model. *Revista Brasileira de Meteorologia* 31(3), 288-297.

SIRCA, C., SALIS, M., ARCA, B., DUCE, P. and SPANO, D., 2018. Assessing the performance of fire danger indexes in a Mediterranean area. *iForest - Biogeosciences and Forestry* 11, 563-571. doi:10.3832/ifor2679-011.

SIWELE, N.D., 2011. *A Review and Assessment for Thaba Chweu Local Municipality Veldfire Management in Mpumalanga Province*. M. Thesis, University of the Free State, South Africa.

SMIT, G.N., RICHTER, C.G.F. and AUCAMP, A.J., 1999. Bush encroachment: An approach to understanding and managing the problem. In: N.M. Tainton (ed.). *Veld Management in South Africa.* Pietermaritzburg: University of Natal Press.

SMITHSON, P.A., 1987. Developments in synoptic and dynamic climatology. *Progress in Physical Geography* 11, 121-132.

SNYMAN, H.A., 2003. Fire and the dynamics of a semi-arid grassland: (2) Influence on soil characteristics. *African Journal of Range & Forage Science* 20(1), 1-26.

SNYMAN, H.A., 2005. Influence of fire on litter production and root and litter turnover in a semi-arid grassland of South Africa. *South African Journal of Botany* 71(2), 145-153.

SNYMAN, H.A., 2006. Short-term response of burnt grassland to defoliation in a semi-arid climate of South Africa. *African Journal of Range & Forage Science* 23(1), 1-11.

SOLH, M., 2005. Foreword. In: J.M. Suttie, S.G. Reynolds & C. Batello (eds.). *Grasslands of the World*. Rome: FAO. pxiii-xiv.

SPRACKLEN, D.V., MICKLEY, L.J., LOGAN, J.A., HUDMAN, R.C., YEVICH, R., FLANNIGAN, M.D. and WESTERLING, A.L., 2009. Impacts of climate change from 2000 to 2050 on wildfire activity and carbonaceous aerosol concentrations in the western United States. *Journal of Geophysical Research* 114, D20301, doi:10.1029/2008JD010966.

STANDER, J.H., DYSON, L. and ENGELBRECHT, C.J., 2016. A snow forecasting decision tree for significant snowfall over the interior of South Africa. *South African Journal of Science* 112(9/10), Art. #2015-0221, 10pp.

STEENKAMP, K., WESSELS, K., FROST, P. and MCFERREN, G., 2013. *Quantitative Comparison of Performance of Fire Danger Indices in South Africa. Report to Department of Agriculture, Forestry and Fisheries (DAFF)*. Pretoria: CSIR Meraka Institute. 47p.

STETLER, K.M., VENN, T.J. and CALKIN, D.E., 2010. The effects of wildfire and environmental amenities on property values in northwest Montana, USA. *Ecological Economics* 69, 2233-2243.

STEYN, A.S., 2009. *Downscaling of Global Circulation Model Predictions to Daily Rainfall over the Upper Olifants River Catchment*. MSc Thesis. University of the Free State, South Africa. 112pp.

STEYN, A.S. and WALKER, S., 2010. Die afskaling van globale sirkulasiemodelvoorspellings na daaglikse reënval oor die Bo-Olifantsrivieropvanggebied. *South African Journal of Science and Technology* 29(3), 163-164.

STIPANIČEV, D., ŠPANJOL, Ž., VUČETIĆ, M., VUČETIĆ, V., ROSAVEC, R. and BODROZIĆ, L., 2008. The Kornati fire accident facts and figures – configuration, vegetation and meteorology. *WIT Transactions on Ecology and the Environment* 119, 387-396. doi:10.2495/FIVA080381.

STOCKS, B.J., FOSBERG, M.A., LYNHAM, T.J., MEARNS, L., WOTTON, B.M., YANG, Q., JIN, J-Z., LAWRENCE, K., HARTLEY, G.R., MASON, J.A. and McKENNEY, D.W., 1998. Climate change and forest fire potential in Russian and Canadian boreal forests. *Climatic Change* 38, 1-13.

STOCKS, B.J., LAWSON, B.D., ALEXANDER, M.E., VAN WAGNER, C.E., MCALPINE, R.S., LYNHAM, T.J. and DUBE, D.E., 1989. The Canadian Forest Fire Danger Rating System: An overview. *Forestry Chronicle* 65, 450-457.

STOCKS, B.J. and TROLLOPE, W.S.W., 1993. Fire Management: Principles and Options in the Forested and Savanna Regions of the World. In: P.J. Crutzen

& J.G. Goldammer (eds.). *Fire in the Environment. The Ecological, Atmospheric, and Climatic Importance of Vegetation Fires*. Chichester: John Wiley & Sons. p 315-326.

STRYDOM, S. and SAVAGE, M.J., 2016. A spatio-temporal analysis of fires in South Africa. *South African Journal of Science* 112(11/12), Art. #2015-0489, doi:0.17159/sajs.2016/20150489.

STRYDOM, S. and SAVAGE, M.J., 2017. Observed variability and trends in the microclimate of the midlands of KwaZulu-Natal and its influence on fire danger. *International Journal of Climatology*, doi:10.1002/joc.5207.

SWETNAM, T.W., 2014. Reaping the Whirlwind: Wildfire and Climate Change in the Western United States. *Public lecture held on 4 March 2014 at the UCSB Bren School, U.S.A.* [Online]. Retrieved from https://www.youtube.com/watch?v=RdjHRMizE3A (Accessed 17/01/2016).

SWETNAM, T.W. and BAISAN, C.H., 1994. Historical fire regime patterns in the southwestern United States since AD 1700. *Proceedings of the 2nd La Mesa Fire Symposium, 29 to 31 March 1994, Los Alamos, New Mexico, U.S.A*.

SWETNAM, T.W., BAISAN, C.H., CAPRIO, A.C., BROWN, P.M., TOUCHAN, R., ANDERSON, R.S. and HALLETT, D.J., 2009. Multi-millennial fire history of the Giant Forest, Sequoia National Park, California, USA. *Fire Ecology* 5(3), 120-150.

TADROSS, M.A., HEWITSON, B.C. and USMAN, M.T., 2005. The Interannual variability of the onset of the maize growing season over South Africa and Zimbabwe. *Journal of Climate* 18, 3356-3372.

TAINTON, N.M., 1999. The ecology of the main grazing lands of South Africa. In: N.M. Tainton (ed.). *Veld Management in South Africa.* Pietermaritzburg: University of Natal Press.

TALJAARD, J.J., 1995a. *Technical Paper No. 30. Atmospheric Circulation Systems, Synoptic Climatology and Weather Phenomena of South Africa. Part 4: Surface Pressure and Wind Phenomena in South Africa.* Pretoria, Government Printer. 42pp.

TALJAARD, J.J., 1995b. *Technical Paper No. 29. Atmospheric Circulation Systems, Synoptic Climatology and Weather Phenomena of South Africa. Part 3: The Synoptic Climatology of South Africa in January and July.* Pretoria: Government Printer. 64pp.

TANSKANEN, H., 2007. *Fuel Conditions and Fire Behavior Characteristics of Managed Picea Abies and Pinus Sylvestris Forests in Finland*. PhD Thesis, University of Helsinki, Finland.

TANSKANEN, H. and VENÄLÄINEN, A., 2008. The relationship between fire activity and fire weather indices at different stages of the growing season in Finland. *Boreal Environment Research* 13, 285-302.

TARANENKO, O. and WIESE, R., 1997. Calc-F.D.I. [Mobile application software].

TAYLOR, S.W. and ALEXANDER, M.E., 2006. Science, technology, and human factors in fire danger rating: the Canadian experience. *International Journal of Wildland Fire* 15, 121–135.

TAYLOR, K.E., STOUFFER, R.J. and MEEHL, G.A., 2012. An overview of CMIP5 and the experiment design. *BAMS* 93(4), 485-498.

TENNANT, W., 2003. An assessment of intraseasonal variability from 13-yr GCM simulations. *Monthly Weather Review* 131, 1975-1991.

TENNANT, W., 2004. Considerations when using pre-1979 NCEP/NCAR reanalyses in the southern hemisphere. *Geophysical Research Letters* 31, L11112.

TENNANT, W.J. and HEWITSON, B.C., 2002. Intra-seasonal rainfall characteristics and their importance to the seasonal prediction problem. *International Journal of Climatology* 22, 1033-1048.

TENNANT, W.J. and REASON, C.J., 2005. Associations between the global energy cycle and regional rainfall in South Africa and Southwest Australia. *Journal of Climate* 18, 3032-3047.

THE COMET PROGRAM, 2007a. THE PBL in regions of complex terrain – Part 1 [Online]. Retrieved from http://www.meted.ucar.edu/ (Accessed 12/01/2016).

THE COMET PROGRAM, 2007b. THE PBL in regions of complex terrain – Part 2 [Online]. Retrieved from http://www.meted.ucar.edu/ (Accessed 14/01/2016).

THE COMET PROGRAM, 2008a. Assessing fire danger [Online]. Retrieved from http://www.meted.ucar.edu/ (Accessed 11/01/2016).

THE COMET PROGRAM, 2008b. Fire behavior [Online]. Retrieved from http://www.meted.ucar.edu/ (Accessed 19/01/2016).

THE COMET PROGRAM, 2008c. S-290 Unit 4: Basic Weather Processes [Online]. Retrieved from http://www.meted.ucar.edu/ (Accessed 25/11/2014).

THE COMET PROGRAM, 2008d. S-290 Unit 5: Temperature and Relative Humidity Relationships [Online]. Retrieved from http://www.meted.ucar.edu/ (Accessed 25/11/2014).

THE COMET PROGRAM, 2008e. Stability, smoke management and fire weather forecasting [Online]. Retrieved from http://www.meted.ucar.edu/ (Accessed 18/01/2016).

THE COMET PROGRAM, 2008f. Mesoscale meteorology effects on fire behavior [Online]. Retrieved from http://www.meted.ucar.edu/ (Accessed 03/02/2016).

THE COMET PROGRAM, 2008g. Fire weather climatology [Online]. Retrieved from http://www.meted.ucar.edu/ (Accessed 17/01/2016).

THE COMET PROGRAM, 2009a. S-290 Unit 1: The fire environment [Online]. Retrieved from http://www.meted.ucar.edu/ (Accessed 18/01/2015).

THE COMET PROGRAM, 2009b. S-290 Unit 3: Fuels [Online]. Retrieved from http://www.meted.ucar.edu/ (Accessed 25/11/2014).

THE COMET PROGRAM, 2009c. S-290 Unit 7: Wind Systems [Online]. Retrieved from http://www.meted.ucar.edu/ (Accessed 23/08/2015).

THE COMET PROGRAM, 2009d. S-290 Unit 9: Observing the Weather [Online]. Retrieved from http://www.meted.ucar.edu/ (Accessed 18/12/2015).

THE COMET PROGRAM, 2009e. S-290 Unit 2: Topographic influences on wildland fire behaviour [Online]. Retrieved from http://www.meted.ucar.edu/ (Accessed 05/11/2013).

THE COMET PROGRAM, 2010a. S-290 Unit 10: Fuel Moisture [Online]. Retrieved from http://www.meted.ucar.edu/ (Accessed 21/12/2015).

THE COMET PROGRAM, 2010b. S-290 Unit 11: Extreme wildland fire behavior [Online]. Retrieved from http://www.meted.ucar.edu/ (Accessed 04/01/2016).

THE COMET PROGRAM, 2010c. S-290 Unit 6: Atmospheric Stability [Online]. Retrieved from http://www.meted.ucar.edu/ (Accessed 25/11/2014).

THE COMET PROGRAM, 2010d. S-290 Unit 12: Gauging fire behavior and guiding fireline decisions [Online]. Retrieved from http://www.meted.ucar.edu/ (Accessed 07/01/2016).

THOMPSON, W.R., 1937. *Veld Burning: Its History and Importance in South Africa*. Pretoria: University of Pretoria.

TIAN, X., MCRAE, D.J., JIN, J., SHU, L., ZHAO, F. and WANG, M., 2011. Wildfires and the Canadian Forest Fire Weather Index system for the Daxing'anling region of China. *International Journal of Wildland Fire* 20, 963-973.

TODD, T.C., 1996. Effects of management practices on nematode community structure in tallgrass prairie. *Applied Soil Ecology* 3, 235-246.

TORN, M.S. and FRIED, J.S., 1992. Predicting the impacts of global warming on wildland fire. *Climatic Change* 21(3), 257-274.

TOSCA, M.G., RANDERSON, J.T. and ZENDER, C.S., 2013. Global impact of smoke aerosols from landscape fires on climate and the Hadley circulation. *Atmospheric Chemistry and Physics* 13, 5227-5241.

TOZUKA, T., LUO, J-J., MASSON, S. and YAMAGATA, T., 2008. Tropical Indian Ocean variability revealed by self-organizing maps. *Climate Dynamics* 31, 333-343.

TROLLOPE, W.S.W., 1981. Recommended terms, definitions and units to be used in fire ecology in South Africa. *Proc. Grassld. Soc. Sth. Afr*. 16, 107-109.

TROLLOPE, W.S.W., 1989. Veld burning as a Management Practice in Livestock Production. In: J.E. Danckwerts & W.R. Teague (eds.). *Veld Management in the Eastern Cape.* Pretoria: Government Printer. p 67-73.

TROLLOPE, W.S.W., 1999. Veld burning. In: N.M. Tainton (ed.). *Veld Management in South Africa.* Pietermaritzburg: University of Natal Press.

TROLLOPE, W.S.W., 2007. Fire – a key factor in the ecology and management of African grasslands and savannas. In: R.E. Masters & K.E.M. Galley (eds.). *Proceedings of the 23rd Tall Timbers Fire Ecology Conference: Fire in Grassland and Shrubland Ecosystems*. Tallahassee: Tall Timbers Research Center. p 2-14.

TROLLOPE, W.S.W., DE RONDE, C. and GELDENHUYS, C.J., 2004. Fire Behaviour. In: J.G. Goldammer & C. de Ronde (eds.). *Wildland Fire Management Handbook for sub-Sahara Africa*. Stellenbosch: comPress. p 27-59.

TROLLOPE, W.S.W., GOVENDER, N., AUSTIN, C.D., HELD, A.C., STEYN, B., VAN DIYK, E., TROLLOPE, L.A., HOFFMANN, A., KRAUS, D. and POTGIETER, A., 2007. *SavFIRE burning trial – effect of point vs. perimeter ignitions on fire mosaics in the Kruger National Park* [Online]. Retrieved from http://www.fire.uni-freiburg.de/GlobalNetworks/Africa/Afrifirenet_6f.html (Accessed 12/07/2015).

TROLLOPE, W.S.W., TROLLOPE, L.A. and HARTNETT, D.C., 2002. Fire behaviour a key factor in the fire ecology of African grasslands and savannas. In: D.X. Viegas (ed.). Forest Fire Research & Wildland Fire Safety. Rotterdam: Millpress.

TUI, 2016. Like the Phoenix from the Ashes: Forest fires in the Mediterranean and neighbouring regions – natural environmental factor or ecological risk? [Online]. Retrieved from http://www.fire.uni-freiburg.de/Manag/Waldbrandflyer-TUI-GFMC-German.pdf (Accessed 09/10/2016).

TURNER, J.A. and LAWSON, B.D., 1978. *Weather in the Canadian Forest Fire Danger Rating System: A User Guide to National Standards and Practices*. Victoria: Canadian Forestry Service. 40pp.

TURNER, R., ROBERTS, N. and JONES, M.D., 2008. Climatic pacing of Mediterranean fire histories from lake sedimentary microcharcoal. *Global and Planetary Change* 63, 317-324.

TYMSTRA, C., FLANNIGAN, M.D., ARMITAGE, O.B. and LOGAN, K., 2007. Impact of climate change on area burned in Alberta's boreal forest. *International Journal of Wildland Fire* 16, 153-160.

TYSON, P.D. and PRESTON-WHYTE, R.A., 2000. *The Weather and Climate of Southern Africa*. 2nd Ed. Cape Town: Oxford.

ÚBEDA, X. and OUTEIRO, L.R., 2009. Physical and Chemical Effects of Fire on Soil. In: A. Cerdà & P.R. Robichaud (eds.). *Fire Effects on Soils and Restoration Strategies*. Enfield: Science Publishers.

ÚBEDA, X. and SARRICOLEA, P., 2016. Wildfires in Chile: A review. *Global and Planetary Change* 146, 152-161.

UBYSZ, B. and VALETTE, J-C., 2010. Flammability: Influence of Fuel on Fire Initiation. In: J.S. Silva, F. Rego, P. Fernandes & E. Rigolot (eds.). *Towards Integrated Fire Management – Outcomes of the European Project Fire Paradox*. European Forest Institute Research Report 23. Retrieved from http://www.efi.int/files/attachments/publications/efi_rr23.pdf (Accessed 10/07/2016).

URBANSKI, S.P., HAO, W.M. and BAKER, S., 2009. Chemical Composition of Wildland Fire Emissions. In: A. Bytnerowicz, M. Arbaugh, A. Riebau & C. Andersen (eds.). *Wildland Fires and Air Pollution*. Amsterdam: Elsevier. p79-107.

VAN HEERDEN, J. and HURRY, L., 1998. *Southern Africa's Weather Patterns: An Introductory Guide*. 2nd Ed. Pretoria: Collegium. 95pp.

VALACHOVIC, Y.S., LEE, C.A., SCANLON, H., VARNER, J.M., GLEBOCKI, R., GRAHAM, B.D. and RIZZO, D.M., 2011. Sudden oak death-caused changes to surface fuel loading and potential fire behavior in Douglas-fir-tanoak forests. *Forest Ecology and Management* 261, 1973-1986.

VALSECCHI, V., CHASE, B.M., SLINGSBY, J.A., CARR, A.S., QUICK, L.J., MEADOWS, M.E., CHEDDADI, R. and REIMER, P.J., 2013. A high resolution 15,600-year pollen and microcharcoal record from the Cederberg Mountains, South Africa. *Palaeogeography, Palaeoclimatology, Palaeoecology* 387, 6-16.

VAN DE VIJVER, C.A.D.M., 1999. *Fire and life in Tarangire: effects of burning and herbivory on an east African Savanna system*. PhD Thesis, Wageningen University, The Netherlands.

VAN DER WERF, G.R., DEMPEWOLF, J., TRIGG, S.N., RANDERSON, J.T., KASIBHATLA, P.S., GIGLIO, L., MURDIYARSO, D., PETERS, W., MORTON, D.C., COLLATZ, G.J., DOLMAN, A.J. and DEFRIES, R.S., 2008. Climate regulation of fire emissions and deforestation in equatorial Asia. *Proceedings of the National Academy of Sciences* 105(51), 20350-20355.

VAN DER WERF, G.R., RANDERSON, J.T., GIGLIO, L., COLLATZ, G.J., MU, M., KASIBHATLA, P.S., MORTON, D.C., DEFRIES, R.S., JIN, Y. and VAN LEEUWEN, T.T., 2010. Global fire emissions and the contribution of deforestation, savanna, forest, agricultural, and peat fires (1997 – 2009). *Atmospheric Chemistry and Physics* 10, 11707-11735.

VAN OUDTSHOORN, F., 2012. *Guide to Grasses of Southern Africa*. 3rd Ed. Pretoria: Briza.

VAN SCHALKWYK, L. and DYSON, L.L., 2013. Climatological characteristics of fog at Cape Town International Airport. *Weather and Forecasting* 28(3), 631-646.

VANTARAM, S.R. and SABER, E., 2012. Survey of contemporary trends in color image segmentation. *Journal of Electronic Imaging* 21(4), 040901-1-040901-28 doi: 10.1117/1.JEI.21.4.040901.

VAN WAGNER, C.E., 1974. *Structure of the Canadian forest fire weather index. Publ. No. 1333*. Ottawa: Department of the Environment, Canadian Forestry Service.

VAN WAGNER, C.E., 1987. *Development and structure of the Canadian forest fire weather index system. Technical Report 35*. Ottawa: Canadian Forestry Service.

VAN WAGNER, C.E., 1988. The historical pattern of annual burned area in Canada. *The Forestry Chronicle* 64, 182-185.

VAN WILGEN, B.W., BIGGS, H.C., O'REGAN, S. and MARE, N., 2000. A fire history of the savanna ecosystems in the Kruger National Park, South Africa between 1941 and 1996. *South African Journal of Science* 96, 167-178.

VAN WILGEN, B.W., GOVENDER, N., SMIT, I.P.J. and MACFADYEN, S., 2014. The ongoing development of a pragmatic and adaptive fire management policy in a large African savanna protected area. *Journal of Environmental Management* 132, 358-368.

VAN WILGEN, B.W., LE MAITRE, D.C. and KRUGER, F.J., 1985. Fire behaviour in South African fynbos (Macchia) vegetation and predictions from Rothermel's fire model. *Journal of Applied Ecology* 22, 207-216.

VCAA (Victorian Curriculum and Assessment Authority), 2016. *Bushfire Education* [Online]. Retrieved from http://bushfireeducation.vic.edu.au/resources.html (Accessed 04/07/2016).

VIEGAS, D.X., BOVIO, G., FERREIRA, A., NOSENZO, A. and SOL, B., 1999. Comparative study of various methods of fire danger evaluation in southern Europe. *International Journal of Wildland Fire* 9(4), 235-246.

VUČETIĆ, M., VUČETIĆ, V., ŽELJKO, Š., BARČIĆ, D., ROSAVEC, R. AND MANDIĆ, A., 2006. Secular variations of monthly severity rating on the Croatian Adriatic coast during the forest fire season. In: D.X. Viegas (ed.). *Proceedings of the V International Conference on Forest Fire Research, 27 – 30 November 2006, Figueira da Foz, Portugal*.

VUČETIĆ, V., ČAVLINA TOMAŠEVIĆ, I. and MIFKA, B., 2019: Low level jet and large wildfires in Croatia. *Proceedings of the 6th International Fire Behavior and Fuels Conference, 29 April – 3 May 2019, Marseille, France*. http://albuquerque.firebehaviorandfuelsconference.com/wp-content/uploads/sites/13/2019/04/Visnjica-Vucetic-Marseille.pdf

WALKER, A., 2015. So many fires are burning in Alaska the Midwest is covered in smoke [Online]. Retrieved from http://gizmodo.com/so-many-fires-are-burning-in-alaska-and-canada-theres-s-1715010214 (Accessed 05/07/2015).

WALLENIUS, T. H., PENNANEN, J. and BURTON, P.J., 2011. Long-term decreasing trend in forest fires in northwestern Canada. *Ecosphere* 2(5), art53, doi:10.1890/ES11-00055.1.

WAMIS (Wide Area Monitoring Information System), 2014. Wide Area Monitoring Information System [Online]. Retrieved from http://wamis.meraka.org.za/ (Accessed 30/01/2014).

WANG, X., DING, Z. and PENG, P., 2012. Changes in fire regimes on the Chinese Loess Plateau since the last glacial maximum and implications for linkages to paleoclimate and past human activity. *Palaeogeography, Palaeoclimatology, Palaeoecology* 315-316, 61-74.

WANG, X. and LI, Y., 2016. Predicting urban heat island circulation using CFD. *Building and Environment* 99, 82-97.

WANG, Y., ANDERSON, K.R. and SUDDABY, R.M., 2015. *Updated source code for calculating fire danger indices in the Canadian Forest Fire Weather Index System*. Information Report NOR-X-424. Edmonton: Canadian Forest Service – Northern Forestry Centre. 26pp.

WANG, Z., CHAPPELLAZ, J., PARK, K. and MAK, J.E., 2010. Large variations in Southern Hemisphere biomass burning during the last 650 years. *Science* 330, 1663-1666.

WARD, D.S., KLOSTER, S., MAHOWALD, N.M., ROGERS, B.M., RANDERSON, J.T. and HESS, P.G., 2012. The changing radiative forcing of fires: global model estimates for past, present and future. *Atmospheric Chemistry and Physics* 12, 10857-10886.

WASTL, C., SCHUNK, C., LEUCHNER, M., PEZZATTI, G.B. and MENZEL, A., 2012. Recent climate change: Long-term trends in meteorological forest fire danger in the Alps. *Agricultural and Forest Meteorology* 162-163, 1-13.

WATT, J., JARRETT, D. and HAMILTON, R., 2008. Dose-response functions for the soiling of heritage materials due to air pollution exposure. *Science of the Total Environment* 400, 415-424.

WELZ, A. 2013. The surprising role of CO_2 in changes on the African Savanna. *Grassroots* 13(3), 31-35.

WESTERLING, A.L. and BRYANT, B.P., 2008. Climate change and wildfire in California. *Climatic Change* 87(Suppl 1), S231-S249.

WESTERLING, A.L., HIDALGO, H.G., CAYAN, D.R. and SWETNAM, T.W., 2006. Warming and earlier spring increase western U.S. forest wildfire activity. *Science* 313(5789), 940-943.

WESTERLING, A.L., TURNER, M.G., SMITHWICK, E.A.H., ROMME, W.H. and RYAN, M.G., 2011. Continued warming could transform Greater Yellowstone fire regimes by mid-21st century. *Proceedings of the National Academy of Sciences* 108(32), 13165-13170.

WESTON, D., 2010. What is a fire regime? [Online]. Retrieved from http://oregonexplorer.info/wildfire/WildfireRisk/FireRegimeDefinition (Accessed 31/01/2014).

WETTERHALL, F., BÁRDOSSY, A., CHEN, D., HALLDIN, S. and XU, C.Y., 2009. Statistical downscaling of daily precipitation over Sweden using GCM output. *Theoretical and Applied Climatology* 96, 95-103.

WHITLOCK, C., BIANCHI, M.M., BARTLEIN, P.J., MARKGRAF, V., MARLON, J., WALSH, M. and MCCOY, N., 2006. Postglacial vegetation, climate, and fire history along the east side of the Andes (lat 41–42.5°S), Argentina. *Quaternary Research* 66, 187-201.

WIEDINMYER, C., AKAGI, S.K., YOKELSON, R.J., EMMONS, L.K., AL-SAADI, J.A., ORLANDO, J.J. and SOJA, A.J., 2011. The Fire INventory from NCAR (FINN): a high resolution global model to estimate the emissions from open burning. *Geoscientific Model Development* 4, 625-641.

WIGDER, N.L., JAFFE, D.A. and SAKETA, F.A., 2013. Ozone and particulate matter enhancements from regional wildfires observed at Mount Bachelor during 2004 – 2011. *Atmospheric Environment* 75, 24-31.

WIGLEY, T.M.L., JONES, P.D., BRIFFA, K.R. and SMITH, G., 1990. Obtaining sub-grid scale information from coarse resolution general circulation model output. *Journal of Geophysical Research* 95, 1943-1953.

WIKIPEDIA, 2017. Somtraining [Online]. Retrieved from https://commons.wikimedia.org/wiki/File%3ASomtraining.svg (Accessed 05/01/2017).

WILBY, R.L., CHARLES, S.P., ZORITA, E., TIMBAL, B., WHETTON, P. and MEARNS, L.O., 2004. *Guidelines for Use of Climate Scenarios Developed from Statistical Downscaling Methods*. IPCC Task Group on Scenarios for Climate Impact Assessment (TGCIA). 27pp.

WILBY, R.L. and DAWSON, C.W., 2007. SDSM 4.2 User Manual [Online]. Retrieved from https://co-public.lboro.ac.uk/cocwd/SDSM/ (Accessed 01/11/2007).

WILBY, R.L., DAWSON, C.W. and BARROW, E.M., 2002. SDSM – a decision support tool for the assessment of regional climate change impacts. *Environmental Modelling and Software* 17(2), 145-157.

WILBY, R.L., WHITEHEAD, P.G., WADE, A.J., BUTTERFIELD, D., DAVIS, R.J. and WATTS, G., 2006. Integrated modelling of climate change impacts on water resources and quality in a lowland catchment: River Kennet, UK. *Journal of Hydrology* 330, 204-220.

WILBY, R.L. and WIGLEY, T.M.L., 1997. Downscaling general circulation model output: a review of methods and limitations. *Progress in Physical Geography* 21(4), 530-548.

WILKS, D.S., 2006. *Statistical Methods in the Atmospheric Sciences*. San Diego: Academic Press.

WILLIAMS, A.A.J., KAROLY, D.J. and TAPPER, N., 2001. The sensitivity of Australian fire danger to climate change. *Climatic Change* 49, 171-191.

WILLIAMS, R.J., BRADSTOCK, R.A., CARY, G.J., GILL, A.M., LIEDLOFF, A.C., LUCAS, C., WHELAN, R.J., ANDERSEN, A.A., BOWMAN, D.J.M.S., CLARKE, P., COOK, G.J., HENNESSY, K. and YORK, A., 2009. *Interactions between Climate, Fire Regimes and Biodiversity in Australia: A Preliminary Assessment*. Canberra: Department of Climate Change and Department of Environment, Water, Heritage and the Arts. 196pp.

WILLIS, C., VAN WILGEN, B., TOLHURST, K., EVERSON, C., D'ABRETON, P., PERO, L. and FLEMING, G., 2001. *The Development of a National Fire Danger Rating System for South Africa*. Pretoria: CSIR Environmentek. 76pp.

WINDFINDER, 2018. Windfinder spot wind statistics [Online]. Retrieved from https://www.windfinder.com/ (Accessed 18/07/2018).

WMO (World Meteorological Organisation), 2011. World Meteorological Organisation press release of January 2011 [Online]. Retrieved from http://www.wmo.int. (Accessed on 12/07/2014).

WMO (World Meteorological Organisation), 2017. WMO Guidelines on the Calculation of Climate Normals. WMO No. 1203 [Online]. Retrieved from https://library.wmo.int/doc_num.php?explnum_id=4166 (Accessed 18/01/2019).

WOOD, S.M., MURPHY, B.P. and BOWMAN, D.M.J.S., 2011. Firescape ecology: how topography determines the contrasting distribution of fire and rain forest in the south-west of the Tasmanian Wilderness World Heritage Area. *Journal of Biogeography* 38, 1807-1820.

WOTTON, B., 2009. Interpreting and using outputs from the Canadian Forest Fire Danger Rating System in research applications. *Environmental and Ecological Statistics* 16, 107-131.

WOTTON, B.M., NOCK, C.A. and FLANNIGAN, M.D., 2010. Forest fire occurrence and climate change in Canada. *International Journal of Wildland Fire* 19, 253-271.

WOW, 2016. Bushfires in Australia [Online]. Retreived from http://www.wow.com/wiki/Bushfires#cite_note-12 (Accessed 07/12/2016).

WU, M., KNORR, W., THONICKE, K., SCHURGERS, G., CAMIA, A. and ARNETH, A., 2015. Sensitivity of burned area in Europe to climate change, atmospheric CO_2 levels, and demography: A comparison of two fire-vegetation models. *Journal of Geophysical Research: Biogeosciences* 120, 2256-2272.

XU, Y., SUN, J., LIN, Q., MA, J., SHI, Y. and LOU, K., 2012. Effects of a surface wildfire on soil nutrient and microbial functional diversity in a shrubbery. *Acta Ecologica Sinica* 32, 258-264.

YARNAL, B. 1993. *Synoptic climatology in environmental analysis: A primer*. London: Belhaven. 195pp.

YARNAL, B., COMRIE, A.C., FRAKES, B. and BROWN, D.P., 2001. Developments and prospects in synoptic climatology. *International Journal of Climatology* 21, 1923-1950.

YASUNARI, T.J., KOSTER, R.D., LAU, W.K.M. and KIM, K.-M., 2015. Impact of snow darkening via dust, black carbon, and organic carbon on boreal spring climate in the Earth system. *Journal of Geophysical Research: Atmospheres* 120, 5485-5503.

YIN, C., 2011. *Applications of Self-Organizing Maps to Statistical Downscaling of Major Regional Climate Variables*. PhD Thesis, University of Waikato, New Zealand. 240pp.

YIN, H., 2007. Learning Nonlinear Principal Manifolds by Self-Organising Maps. In: A.N. Gorban, B. Kégl, D.C. Wunsch & A.Y. Zinovyev (eds.). *Lecture Notes in Computational Science and Engineering: Principal Manifolds for Data Visualization and Dimension Reduction*. Berlin: Springer.

ZÄNGL, G., 2004. A reexamination of the valley wind system in the Alpine Inn Valley with numerical simulations. *Meteorology and Atmospheric Physics* 87, 241-256.

ZIELINSKI, S., 2014. What do wild animals do in a wildfire? *National Geographic*, 22 July 2014. Retrieved from http://news.nationalgeographic.com/news/2014/07/140721-animals-wildlife-wildfires-nation-forests-science/ (Accessed on 08/08/2016).

APPENDIX A

```
#!/bin/bash
#####################################################################
# gribconvert_glob.sc     This is a bash script to convert ERA5 reanalysis      #
# data from grib format to a data format that can be displayed by GrADS      #
# and ingested by FORTRAN. It also creates the ctl files and                 #
# tests whether the date in the filename matches that of the                 #
# file content.                                                              #
#####################################################################
#    Stephan Steyn   (steynas@ufs.ac.za)              2019                  #
#####################################################################

set -xv

# Set period: begin & end year, begin & end month ##########
iyrbeg=1979
iyrend=2018
imthbeg=1
imthend=12

# Edit the following line to match location of data ########
  mydir="/run/media/stephan/SS_Transcend/ERA5"

iyr=$iyrbeg
z="0"
m=11
n=4

while [ $iyr -le $iyrend ]; do
 leap=0
 let leapa=$iyr/4
 let leapa=$leapa*4
 let leapb=$iyr/100
 let leapb=$leapb*100
 let leapc=$iyr/400
 let leapc=$leapc*400
 if [ $leapa -eq $iyr ]; then
  leap=1
  if [[ $leapb -eq $iyr ]] && [[ $leapc -ne $iyr ]]; then
   leap=0
  fi
 fi
 imth=$imthbeg
 while [ $imth -le $imthend ]; do
  if [ $imth -le 9 ]; then
   mth=$z$imth
  else
   mth=$imth
  fi
  if [ $imth -eq 1 ]; then
   maand="jan"
   ndays=31
  fi
  if [ $imth -eq 2 ]; then
   maand="feb"
   ndays=28
    if [ $leap -eq 1 ]; then
     ndays=29
    fi
  fi
  if [ $imth -eq 3 ]; then
```

```
 maand="mar"
 ndays=31
fi
if [ $imth -eq 4 ]; then
 maand="apr"
 ndays=30
fi
if [ $imth -eq 5 ]; then
 maand="may"
 ndays=31
fi
if [ $imth -eq 6 ]; then
 maand="jun"
 ndays=30
fi
if [ $imth -eq 7 ]; then
 maand="jul"
 ndays=31
fi
if [ $imth -eq 8 ]; then
 maand="aug"
 ndays=31
fi
if [ $imth -eq 9 ]; then
 maand="sep"
 ndays=30
fi
if [ $imth -eq 10 ]; then
 maand="oct"
 ndays=31
fi
if [ $imth -eq 11 ]; then
 maand="nov"
 ndays=30
fi
if [ $imth -eq 12 ]; then
 maand="dec"
 ndays=31
fi
# Convert GRIB to GrADS data format ########################
 grib2ctl.pl $mydir/ERA5_sfcvar12_$iyr$mth.grib > $mydir/ERA5_sfcvar12_$iyr$mth.ctl
 gribmap -i $mydir/ERA5_sfcvar12_$iyr$mth.ctl -0
 cat << END1 > convert.gs
 function main()
 'reinit'
 rname1='ERA5_sfcvar12_'
 rname2='ERA5_sfc12_'
 ext1='.ctl'
 ext2='.dat'
 jaar=$iyr
 mnth=$mth
 fname1=rname1%jaar%mnth%ext1
 fname2=rname2%jaar%mnth%ext2
 tlabel=$maand$iyr
 'open $mydir/'fname1''
 'set x 1 1440'
** set lon 0.00 359.75
 'set y 1 721'
** set lat -90.00 90.00
 'set time 'tlabel''
 'set gxout fwrite'
 'set fwrite $mydir/'fname2''
 tyd=1
 while (tyd <= $ndays)
  'set t 'tyd
*** surface 10 metre U wind component [m/s]
```

```
  'd no10Usfc'
*** surface 10 metre V wind component [m/s]
  'd no10Vsfc'
*** surface 2 metre dewpoint temperature [K]
  'd no2Dsfc'
*** surface 2 metre temperature [K]
  'd no2Tsfc'
  tyd=tyd+1
 endwhile
 'close 1'
 'reinit'
 'quit'
END1
 grads -lbc "run convert.gs"

# Compare date of filename with date of ctl file ###########
 dname="12Z01$maand$iyr"
 fn="$mydir/ERA5_sfcvar12_$iyr$mth.ctl"
 dctl=$(awk -v line="$m" -v field="$n" 'NR==line{print $field}' $fn)
 if [ $dctl != $dname ]; then
  echo "contents of $dname did NOT match date in filename" >> progress.txt
 fi

# Create ctl file ##########################################
 cat << END2 > $mydir/ERA5_sfc12_$iyr$mth.ctl
DSET ^ERA5_sfc12_$iyr$mth.dat
TITLE ERA5 reanalysis
UNDEF -9999
XDEF 1440 linear 0.00 0.25
YDEF 721 linear -90.00 0.25
ZDEF 1 levels 1
TDEF 31 linear 12z01$maand$iyr 01DY
VARS 4
no10Usfc 1 99 u10
no10Vsfc 1 99 v10
no2Dsfc 1 99 dewpoint
no2Tsfc 1 99 temp
ENDVARS
END2

 echo "$iyr$mth converted" >> progress.txt
 let imth+=1
done
 let iyr+=1
done
cat progress.txt
```

APPENDIX B

```
#!/bin/bash
######################################################################
# rainconvert_glob.sc     This is a bash script to convert ERA5 reanalysis     #
# rainfall data from netCDF format (as retrieved from the KNMI Climate     #
# Explorer website) to a data format that can be displayed by              #
# GrADS and ingested by FORTRAN. It also creates the ctl files             #
# and tests whether the date in the filename matches that of               #
# the file content.                                                        #
######################################################################
#    Stephan Steyn  (steynas@ufs.ac.za)          2019                     #
######################################################################

set -xv

# Set domain window ##########
latstart=-35.00
latend=-15.00
lonstart=10.00
lonend=42.00
res=0.25

maxxn=$(echo "scale=2;($lonend-$lonstart)"|bc)
maxx=$(echo "scale=2;($maxxn/$res+1)"|bc)
xmax=$(echo ${maxx%%.*})
maxyn=$(echo "scale=2;($latend-($latstart))"|bc)
maxy=$(echo "scale=2;($maxyn/$res+1)"|bc)
ymax=$(echo ${maxy%%.*})

# Edit the following line to match location of data ########
  mydir="/home/steynas/ERA5/ERA5DailyRain"
# mydir="/run/media/stephan/SS_Transcend/ERA5/ERA5DailyRain"
  rname1="igridera5_prcp_daily_af_"
  rname2="ERA5_rain_"
  ext1=".ctl"
  ext2=".dat"
  ext3=".nc"
  z="0"
  u="_"
  n="_n"

echo "STATUS OF ERA5 RAINFALL netCDF CONVERSION:" > rprogress.txt
echo $xmax "longitudinal grids," $ymax "latitudinal grids" >> rprogress.txt

y=0
while [ $y -lt $ymax ]; do
 ylat=$(echo "scale=2;($latstart+($y*$res))"|bc)
 x=0
 while [ $x -lt $xmax ]; do
  xlon=$(echo "scale=2;($lonstart+($x*$res))"|bc)
  x10=$(echo ${xlon%%.*})
  if [ $x10 -lt 10 ]; then
   long=$z$z$z$xlon
   lonn=$z$xlon
  else
   long=$z$z$xlon
   lonn=$z$xlon
  fi

  fname1_c=$rname1$long$u$ylat$n$ext1
  fname1_n=$rname1$long$u$ylat$n$ext3
```

```
  fname2_c=$rname2$lonn$u$ylat$ext1
  fname2_d=$rname2$lonn$u$ylat$ext2
  FILE=$mydir/$fname1_n

# Test if file exists (don't create .ctl & .dat if no .nc file)
  if [ -s "$FILE" ]; then

#  Create ctl file for original .nc file ######################
   cat << END1 > $mydir/$fname1_c
DSET ^$fname1_n
DTYPE netcdf
TITLE era5_prcp_daily_af
UNDEF -9999.
XDEF 1 linear $xlon 0.25
YDEF 1 linear $ylat 0.25
ZDEF 1 linear 1 1
TDEF 14791 linear 00z01JAN1979 01DY
VARS 1
tp 0 t,z,y,x Daily Rainfall [mm/day]
ENDVARS
END1

#  Convert netCDF to GrADS data format ########################
   cat << END2 > rainconvert.gs
  function main()
  'reinit'
  'open $mydir/$fname1_c'
  'set t 1 14791'
** set time from 1JAN1979 to 30JUN2019
  'set gxout fwrite'
  'set fwrite $mydir/$fname2_d'
  'd tp'
  'close 1'
  'reinit'
  'quit'
END2
   grads -lbc "run rainconvert.gs"

#  Create ctl file for newly created .dat file #################
  cat << END3 > $mydir/$fname2_c
DSET ^$fname2_d
TITLE ERA5 reanalysis
UNDEF -9999.
XDEF 1 linear $xlon 0.25
YDEF 1 linear $ylat 0.25
ZDEF 1 levels 1
TDEF 14791 linear 00z01JAN1979 01DY
VARS 1
tp 1 99 Daily Rainfall [mm/day]
ENDVARS
END3

   echo "$xlon$ylat converted" >> rprogress.txt
  fi
# End of file exist test
  let x+=1
 done
 let y+=1
done
cat rprogress.txt
```

APPENDIX C

```
    program rpoint2grid

!######################################################################
!# This FORTRAN program reads point series of daily accumulated       #
!# precipitation and writes it to a monthly gridded ERA5 format.      #
!# It is typically run before 'fire4era.f' or 'fire_v4.f' as these programs require  #
!# monthly gridded values.                                            #
!# Before running this program make sure that the parameters          #
!# defined in 'par_rpoint2grid.h' is correct.                         #
!# To compile: gfortran rpoint2grid.f                                 #
!#   an error message might be received when the data array is        #
!#   too big (depending on period) - in such cases the module         #
!#   and main program should be compiled as:                          #
!#      gfortran -c -mcmodel=large rpoint2grid.f                      #
!#      gfortran rpoint2grid.o                                        #
!# To run: ./a.out                                                    #
!# Output written to:                                                 #
!#  /home/steynas/ERA5/ERA5DailyRain/                                 #
!#  'ERA5_drain_198101.dat'       (substitute year & month)           #
!######################################################################
!#    Stephan Steyn   (steynas@ufs.ac.za)          2019               #
!######################################################################
!
! Brief description of variables used:
! i = counter for longitude (W-E points)
! j = counter for latitude (N-S points)
! k = counter for days
! m = counter for months (m=13 is annual, m=14 is fire season)
! n = calendar year
! nn = counter for years
! rec1,rec2,irec = record number to be read from/written to file
! leap1a ... leap1c, leapn = criteria to determine whether
!                    current year is a leap year
! mdays = number of days in a month
! ydays = number of days in a year
! nyears = length of analysis period (in years)
! fsn = length of fire season (in months)
! sarea = indicator for grid inclusion in study area (1=in;0=out)
! darea = indicator for grid inclusion in display window (1=in)
! rain, rain_d = daily (24h accumulated) rainfall (in mm)
!######################################################################

 ! Declarations ***************************************************
 implicit none
 include 'par_rpoint2grid.h'    ! parameter file
 integer :: i,j,k,l,m,n,nn,t,leapa,leapb,leapc,leapn,filestat,
&         rec1,rec2,irec
 integer, dimension(12) :: mdays
 integer, dimension(AX,AY) :: darea,sarea
 real :: x,y,ydays,nyears,fsn
 real, dimension(ATT) :: rain
 real, dimension(AX,AY,31,12,AT) :: rain_d
 character :: path*33,fname1*5,fname2*3,nname*5,rname*6,
&           yyear*4,mmonth*2,ext1*4,ext2*4,u*1,lat*6,lon*6,xlon*5

 ! Data statements and defining characters ************************
 data mdays/31,28,31,30,31,30,31,31,30,31,30,31/   ! Days in month
 ydays=365.                              ! Days in year
 nyears=real(AT)         ! Analysis period (in years)
 fsn=real(fs)            ! Length of fire season (in months)
```

```
path="/home/steynas/ERA5/ERA5DailyRain/" ! Path to data directory
! on cluster - use path*33 under declarations
!path="/run/media/stephan/SS_Transcend/ERA5/ERA5DailyRain/" ! Path
! to data directory on external - use path*51
fname1="ERA5_"              ! Folder where data is located #1
nname="rain_"               ! Input filename (generic part)
rname="drain_"              ! Output filename (generic part)
u="_"
ext1=".dat"
ext2=".txt"
print*,"Period selected:",startyr,"-",endyr,"=",AT,"years total"

! Initialising the climatological averages/totals
rain_d=-9999.
rain=0.                     ! whole array initialising
darea=0                     ! whole array initialising
sarea=0                     ! whole array initialising
leapa=0
leapb=0
leapc=0
leapn=0

! Start looping through gridpoints ******************************
do j=222,301    ! 34.75S to 15.00S in ERA5 grid
  y=(latstart-res)+(j*res)
  open(101,file='coordinates.txt')
  write(101,100) y    ! might become problematic for NH
  close(101)
  open(101,file='coordinates.txt')
  read(101,200) lat
  close(101)
  do i=41,169    ! 10.00E to 42.00E ine ERA5 grid
    x=(lonstart-res)+(i*res)
    open(101,file='coordinates.txt')
    write(101,100) x
    close(101)
    open(101,file='coordinates.txt')
    read(101,200) xlon    ! might become problematic for lon>=100
    close(101)
    lon="0"//xlon
    ! Delineate calculation and display area (includes study area)
    ! according to ERA5 grid (0.25 x 0.25 resolution)
    ! Gridpoint included if darea = 1
    if (j.ge.236.and.j.le.262) then
      if (i.ge.98.and.i.le.126) then
        darea(i,j)=1
      endif
    endif
    ! Delineate study area: Central Grassland Biome
    ! Gridpoint included if sarea = 1
    if (j.ge.236.and.j.le.237) then
      if (i.ge.104.and.i.le.113) then
        sarea(i,j)=1
      endif
    elseif (j.ge.238.and.j.le.240) then
      if (i.ge.98.and.i.le.114) then
        sarea(i,j)=1
      endif
    elseif (j.eq.241) then
      if (i.ge.100.and.i.le.114) then
        sarea(i,j)=1
      endif
    elseif (j.eq.242) then
      if (i.ge.100.and.i.le.118) then
        sarea(i,j)=1
      endif
```

```
      elseif (j.ge.243.and.j.le.244) then
       if (i.ge.104.and.i.le.118) then
        sarea(i,j)=1
       endif
      elseif (j.eq.245) then
       if (i.ge.104.and.i.le.116) then
        sarea(i,j)=1
       endif
      elseif (j.ge.246.and.j.le.247) then
       if (i.ge.102.and.i.le.116) then
        sarea(i,j)=1
       endif
      elseif (j.eq.248) then
       if (i.ge.102.and.i.le.118) then
        sarea(i,j)=1
       endif
      elseif (j.eq.249) then
       if (i.ge.106.and.i.le.118) then
        sarea(i,j)=1
       endif
      elseif (j.eq.250) then
       if (i.ge.106.and.i.le.120) then
        sarea(i,j)=1
       endif
       if (i.eq.124) then
        sarea(i,j)=1
       endif
      elseif (j.eq.251) then
       if (i.ge.106.and.i.le.120) then
        sarea(i,j)=1
       endif
       if (i.ge.123.and.i.le.124) then
        sarea(i,j)=1
       endif
      elseif (j.ge.252.and.j.le.253) then
       if (i.ge.104.and.i.le.126) then
        sarea(i,j)=1
       endif
      elseif (j.ge.254.and.j.le.256) then
       if (i.ge.102.and.i.le.126) then
        sarea(i,j)=1
       endif
      elseif (j.ge.257.and.j.le.258) then
       if (i.ge.104.and.i.le.108) then
        sarea(i,j)=1
       endif
       if (i.ge.114.and.i.le.126) then
        sarea(i,j)=1
       endif
      elseif (j.ge.259.and.j.le.260) then
       if (i.ge.120.and.i.le.124) then
        sarea(i,j)=1
       endif
      elseif (j.ge.261.and.j.le.262) then
       if (i.eq.124) then
        sarea(i,j)=1
       endif
      else
       sarea(i,j)=0
      endif
      ! Reading daily rainfall data from file **********************
      open(102,file=path//fname1//nname//lon//u//lat//ext1,
     &  form='unformatted',access='direct',recl=ATT*4,iostat=filestat,
     &  status='old')
      if (filestat.eq.0) then     ! only execute if file exists
       read(102,rec=1)(rain(t),t=1,14610)
```

```
      print*,"Reading daily rain for lat=",lat," long=",lon
      if (startyr==1979) then
       t=1    ! Counter for time steps (days) in analysis period
      elseif (startyr==1980) then
       t=366
      elseif (startyr==1981) then
       t=732
      else
       print*,"Need to set start time if YYYY > 1981"
       goto 300
      endif
      do n=startyr,endyr    ! Start looping through years --------
       write(yyear,'(i4.4)')n
       nn=n-startyr+1
       ! Test for leap years
       leapa=mod(n,4)
       leapb=mod(n,100)
       leapc=mod(n,400)
       if (leapa==0) then
        if (leapb==0) then
         if (leapc==0) then
          leapn=1
         else
          leapn=0
         endif
        else
         leapn=1
        endif
       else
        leapn=0
       endif
       if (leapn==1) then
        mdays(2)=29
        ydays=366.
       else
        mdays(2)=28
        ydays=365.
       endif
       do m=1,12    ! Start looping through months ----------
        write(mmonth,'(i2.2)')m
        ! Allocate daily rainfall values and calculate monthly
        ! totals for each year *********************************
        do k=1,mdays(m)
         rain_d(i,j,k,m,nn)=rain(t)
         t=t+1
        enddo    ! k-loop (days) ends
       enddo    ! m-loop (months) ends -------------------------
      enddo    ! n-loop (years) ends ----------------------------
     endif    ! file exists if
     close(102)
    enddo     ! i-loop ends
   enddo     ! j-loop ends

100  FORMAT (' ',f6.2)
200  FORMAT (a7)

    ! Writing daily rainfall to grid for each month to file
    ! (same format as other ERA5 climate variables) ******************
    leapa=0
    leapb=0
    leapc=0
    leapn=0
    do n=startyr,endyr    ! Start looping through years ----------
     write(yyear,'(i4.4)')n
     nn=n-startyr+1
     ! Test for leap years
```

```
      leapa=mod(n,4)
      leapb=mod(n,100)
      leapc=mod(n,400)
      if (leapa==0) then
       if (leapb==0) then
        if (leapc==0) then
         leapn=1
        else
         leapn=0
        endif
       else
        leapn=1
       endif
      else
       leapn=0
      endif
      if (leapn==1) then
       mdays(2)=29
       ydays=366.
      else
       mdays(2)=28
       ydays=365.
      endif
      do m=1,12    ! Start looping through months ----------
       write(mmonth,'(i2.2)')m
       ! Writing daily data to file ********************************
       print*,"Writing rainfall data for ",n,mmonth
       open(103,file=path//fname1//rname//yyear//mmonth//ext1,
     &      access='direct',recl=AX*AY*4)
       irec=1
       do k=1,mdays(m)    ! Start looping through days ----------
        write(103,rec=irec)((rain_d(i,j,k,m,nn),i=1,AX),j=1,AY)
        irec=irec+1
       enddo    ! k-loop (days) ends
       close(103)
      enddo    ! m-loop (months) ends --------------------------
     enddo    ! n-loop (years) ends -----------------------------
     print*,'<>=<>=<>=<>=<>=<>=<>=<>=<>=<>=<>=<>=<>=<>=<>=<>=<>=<>=<>=<>=<>=<>'
300   continue

      end program rpoint2grid
```

Below the required parameter file “par_rpoint2grid.h”:

```
      integer AX,AY,startyr,endyr,AT,ATT,fstart,fend,fs
      real latstart,lonstart,res
      character pperiod*9,GCM*4
      parameter(AX=1440,AY=721)   ! dim of ERA global array
      parameter(ATT=14791)        ! dim of ERA rain array
      parameter(startyr=1979,endyr=2018,AT=endyr-startyr+1,
     &         pperiod="1979_2018")
      parameter(fstart=05,fend=11,fs=fend-fstart+1)
      parameter(GCM="ERA5")
      parameter(latstart=-90.0,lonstart=0.0,res=0.25)
```

APPENDIX D

```
    program klimcal

!######################################################################
!# This FORTRAN program calculates the long-term precipitation        #
!# climatology from gridded ERA5 data.                                #
!# Long-term annual and seasonal means are calculated in              #
!# accordance with WMO-No.1203 (2017).                                #
!# It is typically run before 'fire4era.f' or 'fire4gcm.f' as         #
!# these programs require the mean total annual precipitation         #
!# over a reference climatological period for further                 #
!# calculations.                                                      #
!# Before running this program make sure that the parameters          #
!# defined in 'par_klimcal.h' is correct.                             #
!# To compile: gfortran klimcal.f                                     #
!#    an error message might be received when the data array is       #
!#    too big (depending on period) - in such cases the module        #
!#    and main program should be compiled as:                         #
!#       gfortran -c -mcmodel=large klimcal.f                         #
!#       gfortran klimcal.o                                           #
!# To run: ./a.out                                                    #
!# Output written to:                                                 #
!#   /home/steynas/ERA5/ERA5DailyRain/                                #
!#   'rklim_ERA5_1981_2010.dat'         (or substitute period)        #
!######################################################################
!#    Stephan Steyn   (steynas@ufs.ac.za)            2019             #
!######################################################################
!# some of the code for ingesting gridded data was adapted from       #
!# a program provided by F. Engelbrecht (fengelbrecht@csir.co.za)     #
!######################################################################
!
! Brief description of variables used:
! i = counter for longitude (W-E points)
! j = counter for latitude (N-S points)
! k = counter for days
! m = counter for months
! n = calendar year
! nn = counter for years
! rec1, rec2, irec = record number to be read from/written to file
! leapa ... leapc, leapn = criteria to determine whether
!                     current year is a leap year
! mdays = number of days in a month
! ydays = number of days in a year
! nyears = length of analysis period (in years)
! fsn = length of fire season (in months)
! sarea = indicator for grid inclusion in study area (1=in;0=out)
! darea = indicator for grid inclusion in display window (1=in)
! rain_d = daily (24h accumulated) rainfall (in mm)
! rain_e = monthly total rainfall for each year (in mm)
! rain_g = monthly total rainfall over all years (in mm)
! rain_h = monthly mean total rainfall over all years (in mm)
! rain_a = annual mean total rainfall over all years (in mm)
! rain_s = fire season mean total rainfall over all years (in mm)
!######################################################################

! Declarations ******************************************************
implicit none
include 'par_klimcal.h'    ! parameter file
integer :: i,j,k,m,n,nn,leapa,leapb,leapc,leapn,rec1,rec2,irec
integer, dimension(12) :: mdays
integer, dimension(AX,AY) :: darea,sarea
```

```
real :: ydays,nyears,fsn
real, dimension(AX,AY) :: rain_a,rain_s
real, dimension(AX,AY,12) :: rain_g,rain_h
real, dimension(AX,AY,31,12,AT) :: rain_d
real, dimension(AX,AY,12,AT) :: rain_e
character :: ipath*33,opath*27,fname1*5,rname*6,yyear*4,mmonth*2,
&           ext1*4

! Data statements and defining characters ************************
data mdays/31,28,31,30,31,30,31,31,30,31,30,31/   ! Days in month
ydays=365.                    ! Days in year
nyears=real(AT)               ! Analysis period (in years)
fsn=real(fs)                  ! Length of fire season (in months)
ipath="/home/steynas/ERA5/ERA5DailyRain/" ! Path to input rain
! data directory on cluster - use ipath*33 under declarations
!ipath="/run/media/stephan/SS_Transcend/ERA5/ERA5DailyRain/"
! Path to input rain data directory on external - use ipath*51
!opath="/run/media/stephan/SS_Transcend/ERA5prep/" !Path to output
! data directory on external - use opath*41 under declarations
opath="/home/steynas/Results4ERA5/" ! Path to output
! data directory on cluster - use opath*27 under declarations
fname1="ERA5_"              ! Folder where data is located #1
rname="drain_"              ! Input filename (daily rainfall)
ext1=".dat"
print*,"Period selected:",startyr,"-",endyr,"=",AT,"years total"

! Initialising the climatological averages/totals
rain_e=0.    ! (whole array initialising)
rain_g=0.    ! (whole array initialising)
rain_h=0.    ! (whole array initialising)
rain_a=0.    ! (whole array initialising)
rain_s=0.    ! (whole array initialising)
leapa=0
leapb=0
leapc=0
leapn=0

! Read daily data from ERA ***************************************
do n=startyr,endyr    ! Start looping through years ----------
  write(yyear,'(i4.4)')n
  nn=n-startyr+1
  ! Test for leap years
  leapa=mod(n,4)
  leapb=mod(n,100)
  leapc=mod(n,400)
  if (leapa==0) then
    if (leapb==0) then
      if (leapc==0) then
        leapn=1
      else
        leapn=0
      endif
    else
      leapn=1
    endif
  else
    leapn=0
  endif
  if (leapn==1) then
    mdays(2)=29
    ydays=366.
  else
    mdays(2)=28
    ydays=365.
  endif
  do m=1,12    ! Start looping through months ----------
```

```
      write(mmonth,'(i2.2)')m
      ! Reading daily data from file ******************************
      print*,"Reading data for ",n,mmonth
      open(101,file=ipath//fname1//rname//yyear//mmonth//ext1,
     &       access='direct',recl=AX*AY*4)
      irec=1
      do k=1,mdays(m)    ! Start looping through days ----------
       read(101,rec=irec)((rain_d(i,j,k,m,nn),i=1,AX),j=1,AY)
       irec=irec+1
      enddo    ! k-loop (days) ends
      close(101)

      ! Delineate calculation and display area (includes study area)
      ! according to ERA5 grid (0.25 x 0.25 resolution)
      ! Gridpoint included if darea = 1
      darea=0                       ! whole array initialising
      do j=1,AY
       do i=1,AX
        if (j.ge.236.and.j.le.262) then
         if (i.ge.98.and.i.le.126) then
          darea(i,j)=1
         endif
        endif
       enddo     ! i-loop ends
      enddo     ! j-loop ends
      ! Delineate study area: Central Grassland Biome
      ! Gridpoint included if sarea = 1
      sarea=0                       ! whole array initialising
      do j=1,AY
       do i=1,AX
        if (j.ge.236.and.j.le.237) then
         if (i.ge.104.and.i.le.113) then
          sarea(i,j)=1
         endif
        elseif (j.ge.238.and.j.le.240) then
         if (i.ge.98.and.i.le.114) then
          sarea(i,j)=1
        endif
        elseif (j.eq.241) then
         if (i.ge.100.and.i.le.114) then
          sarea(i,j)=1
         endif
        elseif (j.eq.242) then
         if (i.ge.100.and.i.le.118) then
          sarea(i,j)=1
         endif
        elseif (j.ge.243.and.j.le.244) then
        if (i.ge.104.and.i.le.118) then
         sarea(i,j)=1
        endif
        elseif (j.eq.245) then
         if (i.ge.104.and.i.le.116) then
          sarea(i,j)=1
         endif
        elseif (j.ge.246.and.j.le.247) then
         if (i.ge.102.and.i.le.116) then
          sarea(i,j)=1
         endif
        elseif (j.eq.248) then
         if (i.ge.102.and.i.le.118) then
          sarea(i,j)=1
         endif
        elseif (j.eq.249) then
         if (i.ge.106.and.i.le.118) then
          sarea(i,j)=1
         endif
```

```
      elseif (j.eq.250) then
       if (i.ge.106.and.i.le.120) then
        sarea(i,j)=1
       endif
       if (i.eq.124) then
        sarea(i,j)=1
       endif
      elseif (j.eq.251) then
       if (i.ge.106.and.i.le.120) then
        sarea(i,j)=1
       endif
       if (i.ge.123.and.i.le.124) then
        sarea(i,j)=1
       endif
      elseif (j.ge.252.and.j.le.253) then
       if (i.ge.104.and.i.le.126) then
        sarea(i,j)=1
       endif
      elseif (j.ge.254.and.j.le.256) then
       if (i.ge.102.and.i.le.126) then
        sarea(i,j)=1
       endif
      elseif (j.ge.257.and.j.le.258) then
       if (i.ge.104.and.i.le.108) then
        sarea(i,j)=1
       endif
       if (i.ge.114.and.i.le.126) then
        sarea(i,j)=1
       endif
      elseif (j.ge.259.and.j.le.260) then
       if (i.ge.120.and.i.le.124) then
        sarea(i,j)=1
       endif
      elseif (j.ge.261.and.j.le.262) then
       if (i.eq.124) then
        sarea(i,j)=1
       endif
      else
       sarea(i,j)=0
      endif
     enddo    ! i-loop ends
    enddo    ! j-loop ends

    ! Calculate monthly totals for each year **********************
    do k=1,mdays(m)
     do j=1,AY
      do i=1,AX
       if (darea(i,j).eq.1.and.rain_d(i,j,k,1,1).ne.-9999.)
&       then
       ! only use non-missing values within display area
        rain_e(i,j,m,nn)=rain_e(i,j,m,nn)+rain_d(i,j,k,m,nn)
       else    ! missing value if
        rain_e(i,j,m,nn)=-9999.
       endif    ! missing value if ends
      enddo    ! i-loop ends
     enddo    ! j-loop ends
    enddo    ! k-loop (days) ends
    ! Calculate monthly means for each year **********************
    do j=1,AY
     do i=1,AX
      if (darea(i,j).eq.1.and.rain_d(i,j,1,1,1).ne.-9999.) then
      ! only use non-missing values within display area
       ! Calculate accumulated monthly means over all years *****
       rain_g(i,j,m)=rain_g(i,j,m)+rain_e(i,j,m,nn)    ! total
      else    ! missing value if
       rain_g(i,j,m)=-9999.
```

```
      endif    ! missing value if ends
     enddo    ! i-loop ends
    enddo    ! j-loop ends
   enddo    ! m-loop (months) ends ---------------------------------
  enddo    ! n-loop (years) ends -----------------------------------

  ! Calculate monthly means over all years ************************
  do m=1,12
   do j=1,AY
    do i=1,AX
     if (darea(i,j).eq.1.and.rain_d(i,j,1,1,1).ne.-9999.) then
     ! only use non-missing values within display area
      rain_h(i,j,m)=rain_g(i,j,m)/nyears    ! mean total
      rain_a(i,j)=rain_a(i,j)+rain_h(i,j,m)
      if (m.ge.fstart.and.m.le.fend) then
       rain_s(i,j)=rain_s(i,j)+rain_h(i,j,m)
      endif    ! fire season if ends
     else    ! missing value if
      rain_h(i,j,m)=-9999.
     endif    ! missing value if ends
    enddo    ! i-loop ends
   enddo    ! j-loop ends
  enddo    ! m-loop (months) ends

  ! Calculate long-term annual and seasonal means ******************
  do j=1,AY
   do i=1,AX
    if (darea(i,j).eq.1.and.rain_d(i,j,1,1,1).ne.-9999.) then
    ! only use non-missing values within display area
     ! rain_a(i,j) and rain_s(i,j) was already calculated
    else    ! missing value if
     rain_a(i,j)=-9999.
     rain_s(i,j)=-9999.
    endif    ! missing value if ends
   enddo    ! i-loop ends
  enddo    ! j-loop ends
  print*,'All fields have been calculated'
  print*,' '
  print*,'Printing some test values:'
  print*,"Long-term annual rain for FABL =",rain_a(106,245)
  print*,"Long-term fire season rain for FABL =",rain_s(106,245)

  ! Writing climatology to file ***********************************
  open(102,file=opath//'rklim_'//fname1//pperiod//ext1,
 &       form='unformatted',access='direct',recl=AX*AY*4)
  rec1=1
  rec2=2
  write(102,rec=rec1)((rain_a(i,j),i=1,AX),j=1,AY)
  write(102,rec=rec2)((rain_s(i,j),i=1,AX),j=1,AY)
  close(102)
  print*,'Output written to: ',opath//'rklim_'//fname1//pperiod//
 &      ext1,'               (mean annual & fire season totals)'
  print*,'<>=<>=<>=<>=<>=<>=<>=<>=<>=<>=<>=<>=<>=<>=<>=<>=<>=<>=<>=<>'

  end program klimcal
```

Below the required parameter file “par_klimcal.h”:

```
  integer AX,AY,startyr,endyr,AT,fstart,fend,fs
  character pperiod*9
  parameter(AX=1440,AY=721)   ! dim of ERA global array
  parameter(startyr=1981,endyr=2010,AT=endyr-startyr+1,
 &        pperiod="1981_2010")
  parameter(fstart=05,fend=11,fs=fend-fstart+1)
```

APPENDIX E

```
      program fire4era

!######################################################################
!# This FORTRAN program calculates various fire danger indices        #
!# from gridded ERA data. It is similar to 'fire4gcm.f' except        #
!# that it uses ERA5 reanalysis data on a higher resolution grid.     #
!# It is typically run after 'klimcal.f' as it requires the           #
!# reference period rainfall climatology in further calculations.     #
!# Before running this program make sure that the parameters          #
!# defined in 'par_fire4era.h' is correct.                            #
!# To compile: gfortran fire4era.f                                    #
!#   an error message might be received when the data array is        #
!#   too big (depending on period) - in such cases the module         #
!#   and main program should be compiled as:                          #
!#      gfortran -c -mcmodel=large fire4era.f                         #
!#      gfortran fire4era.o                                           #
!# To run: ./a.out                                                    #
!# Output written to:                                                 #
!#  /home/steynas/Results4ERA5/                                       #
!#  'all_CFWI.ERA5.txt'            (or substitute CFWI)               #
!#  'all_fs_CFWI.ERA5.txt'         (or substitute CFWI)               #
!#  'max_CFWI.ERA5.txt'            (or sub. CFWI)                     #
!#  'max_fs_CFWI.ERA5.txt'         (or sub. CFWI)                     #
!#  'mean_CFWI.ERA5.txt'           (or sub. CFWI)                     #
!#  'mean_fs_CFWI.ERA5.txt'        (or sub. CFWI)                     #
!#  'klima_CFWI.ERA5_1981_2010.dat'  (or sub. CFWI, period)           #
!#  'klims_CFWI.ERA5_1981_2010.dat'  (or sub. CFWI, period)           #
!######################################################################
!#    Stephan Steyn  (steynas@ufs.ac.za)          2019                #
!######################################################################
!
! Brief description of variables used:
! i = counter for longitude (W-E points)
! j = counter for latitude (N-S points)
! k = counter for days
! m = counter for months (m=13 is annual, m=14 is fire season)
! n = calendar year
! nn = counter for years
! tel = counter for number of FDI-values in study area
! bak = counter for number of days since last rainfall event
! bp = breakpoints used to categorise FDIs
! irec, rec1 ... rec12 = record number used in input/output
! leap1a ... leap1c, leapn = criteria to determine whether
!                      current year is a leap year
! mdays = number of days in a month
! ydays = number of days in a year
! nyears = length of analysis period (in years)
! fsn = length of fire season (in months)
! sarea = indicator for grid inclusion in study area (1=in;0=out)
! darea = indicator for grid inclusion in display window (1=in)
! rain_d = daily (24h accumulated) rainfall (in mm)
! rain1 = yesterday's accumulated 24 hour rainfall (mm)
!       (with observed data, measured this morning at 8am
!        but with GCM data this would be yesterdays rainfall)
! rain2 = accumulated 24 hour rainfall for the day before
!       yesterday (i.e. 2 days ago) (mm)
! rmean, aklim = reference period mean annual precipitation (mm)
! sklim = reference period mean fire season precipitation (mm)
! rain_e = monthly total rainfall for each year (in mm)
! rain_g = monthly total rainfall over all years (in mm)
```

```
! rain_h = monthly mean total rainfall over all years (in mm)
! rain_a = annual mean total rainfall over all years (in mm)
! rain_s = fire season mean total rainfall over all years (in mm)
! u10_d = u10 = daily 12Z zonal wind speed at 10 m (in m/s)
! v10_d = v10 = daily 12Z meridional wind speed at 10 m (in m/s)
! w10_d = daily 12Z (resultant) wind speed at 10 m (in m/s)
! w10 = daily 12Z (resultant) wind speed at 10 m (in km/h)
! w10_e = monthly total 12Z wind speed for each year (in m/s)
! w10_f = monthly mean 12Z wind speed for each year (in m/s)
! w10_g = accumulated monthly 12Z mean wind speed over all years
! w10_h = monthly mean 12Z wind speed over all years
! w10_a = annual mean 12Z wind speed over all years (in m/s)
! w10_s = fire season mean 12Z wind speed over all years (in m/s)
! tair_d = daily 12Z (drybulb) temperature (in K)
! tair = daily 12Z (drybulb) temperature (in oC)
! tair_e = monthly total 12Z temperature for each year (in K)
! tair_f = monthly mean 12Z temperature for each year (in K)
! tair_g = accumulated monthly mean 12Z temperature over all
!        years
! tair_h = monthly mean 12Z temperature over all years
! tair_a = annual mean 12Z temperature over all years (in K)
! tair_s = fire season mean 12Z temperature over all years (in K)
! tdew_d = daily 12Z dewpoint temperature (in K)
! tdew = daily 12Z dewpoint temperature (in oC)
! ea = daily 12Z vapour pressure (in hPa)
! es = daily 12Z saturation vapour pressure (in hPa)
! rhum_d = rhum = daily 12Z relative humidity (as %)
! rhum_e = monthly total 12Z relative humidity for each year
! rhum_f = monthly mean 12Z relative humidity for each year
! rhum_g = accumulated monthly mean 12Z relative humidity
!        over all years
! rhum_h = monthly mean 12Z relative humidity over all years
! rhum_a = annual mean 12Z relative humidity over all years
! rhum_s = fire season mean 12Z relative humidity over all years
! CFWI_d = daily value of the Canadian Fire Weather Index (CFWI)
! CDSR_d = daily value of the Canadian Daily Severity Rating (CDSR)
! LFDI_d = daily value of the Lowveld Fire Danger Index (LFDI)
! FFDI_d = daily value of the Forest Fire Danger Index (FFDI)
! CFWImax_d = daily maximum value of CFWI across the entire area
! CDSSmax_d = daily maximum value of CDSR across the entire area
! LFDImax_d = daily maximum value of LFDI across the entire area
! FFDImax_d = daily maximum value of FFDI across the entire area
! CFWImean_d = daily mean value of CFWI across the entire area
! CDSSmean_d = daily mean value of CDSR across the entire area
! LFDImean_d = daily mean value of LFDI across the entire area
! FFDImean_d = daily mean value of FFDI across the entire area
! ****_cat1e ... ****_cat5e = monthly total occurrences of each fire
!                  danger index category for each year
!                  (**** = CFWI, CDSR, LFDI or FFDI)
! ****_cat1g ... ****_cat5g = accumulated monthly total occurrences
!                  per category over all years
! ****_cat1h ... ****_cat5h = monthly mean occurrences per
!                  category over all years
! ****_cat1a ... ****_cat5a = annual mean occurrences per
!                  category over all years
! ****_cat1s ... ****_cat5s = fire season mean occurrence per
!                  category over all years
!                  (**** = CFWI, CDSR, LFDI or FFDI)
! CMSR = Canadian Monthly Severity Rating (MSR)
!      (MSR = Acc.DSR/days in month)
! CSSR = Canadian Seasonal Severity Rating (SSR)
!   (Acc.MSR/months in fire season)~(Acc.DSR/days in fire season)
! CLSR = fire season long-term severity rating (Acc.SSR/years)
! CAN = index used for writing out either CFWI or CDSR values
!#################################################################
```

```
! Declarations ************************************************
implicit none
include 'par_fire4era.h'    ! parameter file
integer :: i,j,k,l,m,n,nn,leapa,leapb,leapc,leapn,bak,Julian,jday,
&         rec1,rec2,rec3,rec4,rec5,rec6,rec7,rec8,rec9,rec10,irec
integer :: tel
integer, dimension(12) :: dmon,mdays
integer, dimension(AX,AY) :: darea,sarea
real :: ydays,nyears,fsn,El,Fl,ffmc,ffmc1,dmc,dmc1,dc,dc1,isi,bui,
&       CFWI,CDSR,tair,tdew,rmean,rain,rain1,rain2,ea,es,rhum,u10,
&       v10,w10,y,ymax,KBDI,KBDI1,FFDI,RCF0,RCFmin,BI,WF,LFDI
real :: M1,Rf,Ed,Ew,Ma,Kl,Kw,Ky,Pr,Re,B,Mr,V,Rd,Dr,Q1,Fw,Ff,Qr,Kd,
&       Ko,Fd,x,dtr,decl,T,dl,lat,dQ,Pn,D
real, parameter :: pi = 3.141592654
real, dimension(4) :: bp
real, dimension(20) :: raint,RCF
real, dimension(AX,AY) :: prev_ffmc,prev_dmc,prev_dc,prev_KBDI,
&                   rain_a,rain_s,tair_a,tair_s,
&                   rhum_a,rhum_s,w10_a,w10_s,CFWI_cat1a,
&                   CFWI_cat1s,CFWI_cat2a,CFWI_cat2s,
&                   CFWI_cat3a,CFWI_cat3s,CFWI_cat4a,
&                   CFWI_cat4s,CFWI_cat5a,CFWI_cat5s,
&                   CDSR_cat1a,CDSR_cat1s,CDSR_cat2a,
&                   CDSR_cat2s,CDSR_cat3a,CDSR_cat3s,
&                   CDSR_cat4a,CDSR_cat4s,CDSR_cat5a,
&                   CDSR_cat5s,LFDI_cat1a,LFDI_cat1s,
&                   LFDI_cat2a,LFDI_cat2s,LFDI_cat3a,
&                   LFDI_cat3s,LFDI_cat4a,LFDI_cat4s,
&                   LFDI_cat5a,LFDI_cat5s,FFDI_cat1a,
&                   FFDI_cat1s,FFDI_cat2a,FFDI_cat2s,
&                   FFDI_cat3a,FFDI_cat3s,FFDI_cat4a,
&                   FFDI_cat4s,FFDI_cat5a,FFDI_cat5s,
&                   CLSR,aklim,sklim
real, dimension(AX,AY,12) :: rain_g,rain_h,tair_g,tair_h,rhum_g,
&                     rhum_h,w10_g,w10_h,CFWI_cat1g,
&                     CFWI_cat1h,CFWI_cat2g,CFWI_cat2h,
&                     CFWI_cat3g,CFWI_cat3h,CFWI_cat4g,
&                     CFWI_cat4h,CFWI_cat5g,CFWI_cat5h,
&                     CDSR_cat1g,CDSR_cat1h,CDSR_cat2g,
&                     CDSR_cat2h,CDSR_cat3g,CDSR_cat3h,
&                     CDSR_cat4g,CDSR_cat4h,CDSR_cat5g,
&                     CDSR_cat5h,LFDI_cat1g,LFDI_cat1h,
&                     LFDI_cat2g,LFDI_cat2h,LFDI_cat3g,
&                     LFDI_cat3h,LFDI_cat4g,LFDI_cat4h,
&                     LFDI_cat5g,LFDI_cat5h,FFDI_cat1g,
&                     FFDI_cat1h,FFDI_cat2g,FFDI_cat2h,
&                     FFDI_cat3g,FFDI_cat3h,FFDI_cat4g,
&                     FFDI_cat4h,FFDI_cat5g,FFDI_cat5h
real, dimension(AX,AY,AT) :: CSSR
real, dimension(31,12,AT) :: CFWImax_d,CDSRmax_d,LFDImax_d,
&                     FFDImax_d,CFWImean_d,CDSRmean_d,
&                     LFDImean_d,FFDImean_d
real, dimension(AX,AY,31,12,AT) :: tair_d,tdew_d,rain_d,rhum_d,
&                       u10_d,v10_d,w10_d,CFWI_d,
&                       CDSR_d,LFDI_d,FFDI_d
real, dimension(AX,AY,12,AT) :: rain_e,w10_e,w10_f,tair_e,tair_f,
&                       rhum_e,rhum_f,CMSR,CFWI_cat1e,
&                       CFWI_cat2e,CFWI_cat3e,CFWI_cat4e,
&                       CFWI_cat5e,CDSR_cat1e,CDSR_cat2e,
&                       CDSR_cat3e,CDSR_cat4e,CDSR_cat5e,
&                       LFDI_cat1e,LFDI_cat2e,LFDI_cat3e,
&                       LFDI_cat4e,LFDI_cat5e,FFDI_cat1e,
&                       FFDI_cat2e,FFDI_cat3e,FFDI_cat4e,
&                       FFDI_cat5e
character :: ipath1*19,ipath2*33,opath*27,fname1*5,nname*6,ext1*4,
&          rname*6,finx*5,yyear*4,mmonth*2,kperiod*9,ext2*4
```

```
! Data statements and defining characters ************************
data mdays/31,28,31,30,31,30,31,31,30,31,30,31/   ! Days in month
data dmon/0,31,59,90,120,151,181,212,243,273,304,334/
ydays=365.                                ! Days in year
nyears=real(AT)              ! Analysis period (in years)
fsn=real(fs)                 ! Length of fire season (in months)
kperiod="1981_2010"          ! Period used for climatology
ipath1="/home/steynas/ERA5/" ! Path to input surface variable
! data directory on cluster - use ipath*19 under declarations
!ipath1="/run/media/stephan/SS_Transcend/ERA5/" ! Path to input
! surface variable data directory on external - use ipath*37
ipath2="/home/steynas/ERA5/ERA5DailyRain/" ! Path to input rain
! data directory on cluster - use ipath*33 under declarations
!ipath2="/run/media/stephan/SS_Transcend/ERA5/ERA5DailyRain/"
! Path to input rain data directory on external - use ipath*51
opath="/home/steynas/Results4ERA5/" ! Path to output data
! directory and rainfall climatology on cluster - use opath*27
!opath="/run/media/stephan/SS_Transcend/Results4ERA5/" !Path to
! output data directory on external - use opath*45
fname1="ERA5_"               ! Folder where data is located
nname="sfc12_"               ! Input filename (generic part)
rname="drain_"               ! Input filename (daily rainfall)
ext1=".dat"
ext2=".txt"
select case(ind)
 case (1)
  if (CAN.eq.1) then
   finx="CFWI."           ! Fire danger index indicator
   if (cbp.eq.1) then
   ! CFWI categories - CFWIS (2015); Global EWS (2015)
    bp(1)=5.0; bp(2)=10.0; bp(3)=20.0; bp(4)=30.0
   else
   ! CFWI categories - climatological 99,93,73,30 percentiles
    bp(1)=11.5; bp(2)=41.5; bp(3)=65.5; bp(4)=97.5
   endif
  else
   finx="CDSR."           ! Fire danger index indicator
   if (cbp.eq.1) then
   ! CDSR categories - CFWIS (2015)
    bp(1)=1.0; bp(2)=3.0; bp(3)=5.0; bp(4)=15.0
   else
   ! CDSR categories - climatological 99,93,73,30 percentiles
    bp(1)=1.5; bp(2)=19.5; bp(3)=45.5; bp(4)=91.5
   endif
  endif
 case (2)
  finx="LFDI."             ! Fire danger index indicator
  ! LFDI categories - Notice 1099 (2013)
   bp(1)=20.5; bp(2)=45.5; bp(3)=60.5; bp(4)=75.5
  ! Rather keep using above breakpoints as opposed to
  ! following climatological 99,93,73,30 percentiles:
  ! bp(1)=20.5; bp(2)=45.5; bp(3)=60.5; bp(4)=73.5
 case (3)
  finx="FFDI."             ! Fire danger index indicator
  if (cbp.eq.1) then
  ! FFDI categories - CFA (2016)
   bp(1)=11.5; bp(2)=24.5; bp(3)=49.5; bp(4)=74.5
  else
  ! FFDI categories - climatological 99,95,75,25 percentiles
   bp(1)=2.5; bp(2)=8.5; bp(3)=16.5; bp(4)=29.5
  endif
end select
print*,"Period selected:",startyr,"-",endyr,"=",AT,"years total"
print*,"Index selected: ",finx
print*,"Breakpoints used:",bp(1),bp(2),bp(3),bp(4)
```

```
! Read rainfall climatology ************************************
print*,"Reading rainfall climatology"
open(101,file=opath//'rklim_'//fname1//kperiod//ext1,
&    form='unformatted',access='direct',recl=AX*AY*4)
rec1=1
rec2=2
read(101,rec=rec1)((aklim(i,j),i=1,AX),j=1,AY)
read(101,rec=rec2)((sklim(i,j),i=1,AX),j=1,AY)
close(101)

! Initialising the climatological averages/totals
! (whole array initialising)
prev_ffmc=85.0       ! Fine Fuel Moisture Code (FFMC)
prev_dmc=6.0         ! Duff Moisture Code (DMC)
prev_dc=15.0         ! Drought Code (DC)
prev_KBDI=25.4       ! Keetch-Byram Drought Index (KBDI)
rhum_d=0.            ! Relative humidity
CFWI_cat1e=0.        ! Canadian Fire Weather Index (CFWI)
CFWI_cat2e=0.
CFWI_cat3e=0.
CFWI_cat4e=0.
CFWI_cat5e=0.
CFWI_cat1g=0.
CFWI_cat2g=0.
CFWI_cat3g=0.
CFWI_cat4g=0.
CFWI_cat5g=0.
CFWI_cat1h=0.
CFWI_cat2h=0.
CFWI_cat3h=0.
CFWI_cat4h=0.
CFWI_cat5h=0.
CFWI_cat1a=0.
CFWI_cat1s=0.
CFWI_cat2a=0.
CFWI_cat2s=0.
CFWI_cat3a=0.
CFWI_cat3s=0.
CFWI_cat4a=0.
CFWI_cat4s=0.
CFWI_cat5a=0.
CFWI_cat5s=0.
CFWImax_d=0.
CFWImean_d=0.
CDSR_cat1e=0.        ! Canadian Daily Severity Rating (CDSR)
CDSR_cat2e=0.
CDSR_cat3e=0.
CDSR_cat4e=0.
CDSR_cat5e=0.
CDSR_cat1g=0.
CDSR_cat2g=0.
CDSR_cat3g=0.
CDSR_cat4g=0.
CDSR_cat5g=0.
CDSR_cat1h=0.
CDSR_cat2h=0.
CDSR_cat3h=0.
CDSR_cat4h=0.
CDSR_cat5h=0.
CDSRmax_d=0.
CDSRmean_d=0.
CMSR=0.
CSSR=0.
CLSR=0.
LFDI_cat1e=0.        ! Lowveld Fire Danger Index (LFDI)
```

```
LFDI_cat2e=0.
LFDI_cat3e=0.
LFDI_cat4e=0.
LFDI_cat5e=0.
LFDI_cat1g=0.
LFDI_cat2g=0.
LFDI_cat3g=0.
LFDI_cat4g=0.
LFDI_cat5g=0.
LFDI_cat1h=0.
LFDI_cat2h=0.
LFDI_cat3h=0.
LFDI_cat4h=0.
LFDI_cat5h=0.
LFDI_cat1a=0.
LFDI_cat1s=0.
LFDI_cat2a=0.
LFDI_cat2s=0.
LFDI_cat3a=0.
LFDI_cat3s=0.
LFDI_cat4a=0.
LFDI_cat4s=0.
LFDI_cat5a=0.
LFDI_cat5s=0.
LFDImax_d=0.
LFDImean_d=0.
FFDI_cat1e=0.        ! McArthur Forest Fire Danger Index (FFDI)
FFDI_cat2e=0.
FFDI_cat3e=0.
FFDI_cat4e=0.
FFDI_cat5e=0.
FFDI_cat1g=0.
FFDI_cat2g=0.
FFDI_cat3g=0.
FFDI_cat4g=0.
FFDI_cat5g=0.
FFDI_cat1h=0.
FFDI_cat2h=0.
FFDI_cat3h=0.
FFDI_cat4h=0.
FFDI_cat5h=0.
FFDI_cat1a=0.
FFDI_cat1s=0.
FFDI_cat2a=0.
FFDI_cat2s=0.
FFDI_cat3a=0.
FFDI_cat3s=0.
FFDI_cat4a=0.
FFDI_cat4s=0.
FFDI_cat5a=0.
FFDI_cat5s=0.
FFDImax_d=0.
FFDImean_d=0.
leapa=0
leapb=0
leapc=0
leapn=0
tel=0
! Delineate calculation and display area (includes study area)
! according to ERA5 grid (0.25 x 0.25 resolution)
! Gridpoint included if darea = 1
darea=0                    ! whole array initialising
do j=1,AY
 do i=1,AX
  if (j.ge.236.and.j.le.262) then
   if (i.ge.98.and.i.le.126) then
```

```
      darea(i,j)=1
     endif
    endif
  enddo    ! i-loop ends
enddo    ! j-loop ends
! Delineate study area: Central Grassland Biome
! Gridpoint included if sarea = 1
sarea=0                    ! whole array initialising
do j=1,AY
 do i=1,AX
  if (j.ge.236.and.j.le.237) then
   if (i.ge.104.and.i.le.113) then
    sarea(i,j)=1
   endif
  elseif (j.ge.238.and.j.le.240) then
   if (i.ge.98.and.i.le.114) then
    sarea(i,j)=1
   endif
  elseif (j.eq.241) then
   if (i.ge.100.and.i.le.114) then
    sarea(i,j)=1
   endif
  elseif (j.eq.242) then
   if (i.ge.100.and.i.le.118) then
    sarea(i,j)=1
   endif
  elseif (j.ge.243.and.j.le.244) then
   if (i.ge.104.and.i.le.118) then
    sarea(i,j)=1
   endif
  elseif (j.eq.245) then
   if (i.ge.104.and.i.le.116) then
    sarea(i,j)=1
   endif
  elseif (j.ge.246.and.j.le.247) then
   if (i.ge.102.and.i.le.116) then
    sarea(i,j)=1
   endif
  elseif (j.eq.248) then
   if (i.ge.102.and.i.le.118) then
    sarea(i,j)=1
   endif
  elseif (j.eq.249) then
   if (i.ge.106.and.i.le.118) then
    sarea(i,j)=1
   endif
  elseif (j.eq.250) then
   if (i.ge.106.and.i.le.120) then
    sarea(i,j)=1
   elseif (i.eq.124) then
    sarea(i,j)=1
   endif
  elseif (j.eq.251) then
   if (i.ge.106.and.i.le.120) then
    sarea(i,j)=1
   elseif (i.ge.123.and.i.le.124) then
    sarea(i,j)=1
   endif
  elseif (j.ge.252.and.j.le.253) then
   if (i.ge.104.and.i.le.126) then
    sarea(i,j)=1
   endif
  elseif (j.ge.254.and.j.le.256) then
   if (i.ge.102.and.i.le.126) then
    sarea(i,j)=1
   endif
```

```
    elseif (j.ge.257.and.j.le.258) then
      if (i.ge.104.and.i.le.108) then
        sarea(i,j)=1
      elseif (i.ge.114.and.i.le.126) then
        sarea(i,j)=1
      endif
    elseif (j.ge.259.and.j.le.260) then
      if (i.ge.120.and.i.le.124) then
        sarea(i,j)=1
      endif
    elseif (j.ge.261.and.j.le.262) then
      if (i.eq.124) then
        sarea(i,j)=1
      endif
    else
      sarea(i,j)=0
    endif
  enddo    ! i-loop ends
enddo    ! j-loop ends

! Output files for all months in year
open(102,file=opath//'all_'//finx//GCM//pperiod//ext2) ! file to
              ! which all daily FDIs are written
open(103,file=opath//'max_'//finx//GCM//pperiod//ext2) ! file to
              ! which daily spatial maximum FDIs are written
open(104,file=opath//'mean_'//finx//GCM//pperiod//ext2) ! file to
              ! which daily spatial mean FDIs are written
! Output files for fire season months only
open(105,file=opath//'all_fs_'//finx//GCM//pperiod//ext2)
open(106,file=opath//'max_fs_'//finx//GCM//pperiod//ext2)
open(107,file=opath//'mean_fs_'//finx//GCM//pperiod//ext2)

! Read daily data from ERA ***************************************
do n=startyr,endyr    ! Start looping through years ----------
  write(yyear,'(i4.4)')n
  nn=n-startyr+1
  ! Test for leap years
  leapa=mod(n,4)
  leapb=mod(n,100)
  leapc=mod(n,400)
  if (leapa==0) then
    if (leapb==0) then
      if (leapc==0) then
        leapn=1
      else
        leapn=0
      endif
    else
      leapn=1
    endif
  else
    leapn=0
  endif
  if (leapn==1) then
    mdays(2)=29
    ydays=366.
  else
    mdays(2)=28
    ydays=365.
  endif
  do m=1,12    ! Start looping through months ----------
    write(mmonth,'(i2.2)')m
    ! Reading daily data from file ******************************
    print*,"Reading data for ",n,mmonth
    open(108,file=ipath1//fname1//nname//yyear//mmonth//ext1,
&       access='direct',recl=AX*AY*4)
```

```
    do k=1,mdays(m)    ! Start looping through days ----------
     rec1=(k-1)*4+1
     rec2=(k-1)*4+2
     rec3=(k-1)*4+3
     rec4=(k-1)*4+4
     read(108,rec=rec1)((u10_d(i,j,k,m,nn),i=1,AX),j=1,AY)
     read(108,rec=rec2)((v10_d(i,j,k,m,nn),i=1,AX),j=1,AY)
     read(108,rec=rec3)((tdew_d(i,j,k,m,nn),i=1,AX),j=1,AY)
     read(108,rec=rec4)((tair_d(i,j,k,m,nn),i=1,AX),j=1,AY)
    enddo    ! k-loop (days) ends
    close(108)
    open(109,file=ipath2//fname1//rname//yyear//mmonth//ext1,
&       access='direct',recl=AX*AY*4)
    irec=1
    do k=1,mdays(m)    ! Start looping through days ----------
     read(109,rec=irec)((rain_d(i,j,k,m,nn),i=1,AX),j=1,AY)
     irec=irec+1
    enddo    ! k-loop (days) ends
    close(109)

    ! Calculate fire danger indices ******************************
    do k=1,mdays(m)    ! Start looping through days ----------
     do j=1,AY
      do i=1,AX
       if (darea(i,j).eq.1.and.rain_d(i,j,k,1,1).ne.-9999.)
&        then
        ! only use non-missing values within display area
         ! Allocating last 20 days' rainfall
         do bak=20,1,-1
          if (k.le.bak.and.m.eq.1.and.nn.eq.1) then
            raint(bak)=0. ! assume no rain fell previously as
                    ! its the start of the analysis period
          else if (k.le.bak.and.m.eq.1.and.nn.ne.1) then
            l=mdays(12)
            raint(bak)=rain_d(i,j,l-(bak-k),12,nn-1)
          else if (k.le.bak.and.m.ne.1) then
            l=mdays(m-1)
            raint(bak)=rain_d(i,j,l-(bak-k),m-1,nn)
          else
            raint(bak)=rain_d(i,j,k-bak,m,nn)
          endif
         enddo    ! bak-loop ends
         rmean=aklim(i,j)
         rain1=raint(1)
         rain2=raint(2)
         rain=rain_d(i,j,k,m,nn)
         tdew=tdew_d(i,j,k,m,nn)-273.16 ! convert to oC
         tair=tair_d(i,j,k,m,nn)-273.16 ! convert to oC
         ! calculate relative humidity (Campbell & Norman,
         ! 1998)
         ea=611.21*exp(17.502*tdew/(240.97+tdew))
         es=611.21*exp(17.502*tair/(240.97+tair))
         rhum=100.*(ea/es)
         if (rhum.gt.100.) then
          rhum=100.    ! ensuring RH <= 100%
         endif
         rhum_d(i,j,k,m,nn)=rhum
         ! calculate resultant wind
         u10=u10_d(i,j,k,m,nn)
         v10=v10_d(i,j,k,m,nn)
         w10_d(i,j,k,m,nn)=sqrt(u10**2.+v10**2.)
         w10=w10_d(i,j,k,m,nn)*3.6    ! convert to km/h
         select case(ind)
```

```
!%%%%%%%%%%%%%%%%%%%%%%%%%%%%%%%%%%%%%%%%%%%%%%%%%
case(1)    ! Canadian Fire Weather Index (CFWI)      %
!%%%%%%%%%%%%%%%%%%%%%%%%%%%%%%%%%%%%%%%%%%%%%%%%%
!% This section calculates the Canadian Fire Weather %
!% Index, based on code and tested against sample    %
!% input/output data from:                           %
!% Wang, Y., Anderson, K.R. and Suddaby, R.M., 2015. %
!% Updated source code for calculating fire danger   %
!% indices in the Canadian Forest Fire Weather Index %
!% System. Nat. Resour. Can., Can. For. Serv., North.%
!% For. Cent., Edmonton.                             %
!% The formulae for calculating solar declination    %
!% and daylength was obtained from Bear Giles        %
!% (bear@fsl.noaa.gov) and Joseph Bartlo             %
!% (jabartlo@delphi.com).                            %
!%%%%%%%%%%%%%%%%%%%%%%%%%%%%%%%%%%%%%%%%%%%%%%%%%
! Brief description of interim variables used:
! Rf = Effective rainfall for calculating FFMC
! Re = Effective rainfall for calculating DMC
! Rd = Effective rainfall for calculating DC
! ffmc = Fine Fuel Moisture Code
! ffmc1 = Previous day's FFMC
! M1 = Fine Fuel Moisture Content from previous day
! Mr = Fine Fuel Moisture Content after rain
! Ma = Fine Fuel Moisture Content after drying
! Ed = Fine Fuel equilibrium moisture content (EMC)
! Ew = Fine Fuel EMC for wetting
! Ko = Intermediate step in calculation of Kd
! Kd = Log drying rate, FFMC drying rate, FFMC ln (M)/day
! Kl = Intermediate step in calculation of Kw
! Kw = Natural log wetting rate, ln (M)/day
! dmc = Duff Moisture Content
! dmc1 = Previous day's DMC
! Pr = DMC after rain
! DM1 = Duff Moisture Content from previous day
! DMr = Duff moisture content after rain
! DM = Duff moisture content after drying
! Ky = Log drying rate in DMC, ln (M)/day
! Le = Effective day length in DMC, hours
! B = Slope variable in DMC rain effect
! Q = Moisture equivalent of DC, units of 0.254 mm
! Q1 = Moisture equivalent of previous day's DC
! Qr = Moisture equivalent after rain
! V = Potential evapotranspiration, units of
!    0.254 mm water/day
! dc = Drought Code
! dc1 = Previous day's Drought Code
! Dr = Drought Code after rain
! Lf = Day-length adjustment in Drought Code
! Fw = Wind function
! Ff = Fine fuel moisture function
! Fd = Duff moisture function
! isi = Initial spread index
! bui = Buildup index
! B = Intermediate fire weather index

ffmc1=prev_ffmc(i,j)       ! use yesterday's values
dmc1=prev_dmc(i,j)
dc1=prev_dc(i,j)

! Determine Daylength *********************************
! Convert calendar date to Julian Day
Julian=dmon(m)+k
if (leapn==1.and.m>1) then
  Julian=Julian+1
endif
```

```
      jday=Julian
      ! Calculate solar declination and daylength
      ! lat=-40.25+.5*real(j-1)    ! for GCMs
      lat=-90.00+.25*real(j-1)     ! for ERA5
      if (lat<-80..or.lat>80.) then
       print *, "latitude out of acceptable bounds"
      else
       dtr=pi/180.                 ! degrees to radians
       x=dtr*360./366.*jday        ! fraction of a year
       decl=dtr*(0.33029-22.9717*cos(x)+3.8346*sin(x)-
     &      0.3495*cos(2.*x)+0.0261*sin(2.*x)-
     &      0.1392*cos(3.*x)+0.0727*sin(3.*x)) ! sol declination
       T=-tan(dtr*(lat))*tan(decl)-sin(dtr*0.8)/
     &    (cos(dtr*(lat))*cos(decl)) ! fraction day in sunlight
       if (T<-1..or.T>1.) then
        print *, "Problem with daylength calculation"
       else
        dl=2.*(12./pi)*acos(T)
        El=dl-3.1
       endif
      endif
      ! Daylength factor according to Lawson & Armitage (2008):
      if (m==1) then
       if (lat>10.) then              ! NH
        Fl=-1.6
       elseif (lat<-10.) then         ! SH
        Fl=6.4
       else                           ! EQ
        Fl=1.4
       endif
      elseif (m==2) then
       if (lat>10.) then              ! NH
        Fl=-1.6
       elseif (lat<-10.) then         ! SH
        Fl=5.
       else                           ! EQ
        Fl=1.4
       endif
      elseif (m==3) then
       if (lat>10.) then              ! NH
        Fl=-1.6
       elseif (lat<-10.) then         ! SH
        Fl=2.4
       else                           ! EQ
        Fl=1.4
       endif
      elseif (m==4) then
       if (lat>10.) then              ! NH
        Fl=0.9
       elseif (lat<-10.) then         ! SH
        Fl=0.4
       else                           ! EQ
        Fl=1.4
       endif
      elseif (m==5) then
       if (lat>10.) then              ! NH
        Fl=3.8
       elseif (lat<-10.) then         ! SH
        Fl=-1.6
       else                           ! EQ
        Fl=1.4
       endif
      elseif (m==6) then
       if (lat>10.) then              ! NH
        Fl=5.8
       elseif (lat<-10.) then         ! SH
```

```
        Fl=-1.6
       else                              ! EQ
        Fl=1.4
       endif
      elseif (m==7) then
       if (lat>10.) then                 ! NH
        Fl=6.4
       elseif (lat<-10.) then            ! SH
        Fl=-1.6
       else                              ! EQ
        Fl=1.4
       endif
      elseif (m==8) then
       if (lat>10.) then                 ! NH
        Fl=5.0
       elseif (lat<-10.) then            ! SH
        Fl=-1.6
       else                              ! EQ
        Fl=1.4
       endif
      elseif (m==9) then
       if (lat>10.) then                 ! NH
        Fl=2.4
       elseif (lat<-10.) then            ! SH
        Fl=-1.6
       else                              ! EQ
        Fl=1.4
       endif
      elseif (m==10) then
       if (lat>10.) then                 ! NH
        Fl=-1.6
       elseif (lat<-10.) then            ! SH
        Fl=0.9
       else                              ! EQ
        Fl=1.4
       endif
      elseif (m==11) then
       if (lat>10.) then                 ! NH
        Fl=-1.6
       elseif (lat<-10.) then            ! SH
        Fl=3.8
       else                              ! EQ
        Fl=1.4
       endif
      elseif (m==12) then
       if (lat>10.) then                 ! NH
        Fl=-1.6
       elseif (lat<-10.) then            ! SH
        Fl=5.8
       else                              ! EQ
        Fl=1.4
       endif
      endif

      ! Determine Fine Fuel Moisture Code ******************
      M1=(147.2*(101.-ffmc1))/(59.5+ffmc1)        ! Eq. 1
      if (rain1>0.5) then
       rf=rain1-0.5                               ! Eq. 2
       if (M1<=150.) then
        Mr=M1+42.5*Rf*exp(-100./(251.-M1))*
&          (1.-exp(-6.93/Rf))                    ! Eq. 3a
       else
        Mr=(M1+42.5*Rf*exp(-100./(251.-M1))*
&          (1.-exp(-6.93/Rf)))+
&          (.0015*(M1-150.)**2.)*sqrt(Rf)        ! Eq. 3b
       endif
```

```
        if (Mr>250.) then
          Mr=250.
        endif
        M1=Mr
      endif
      Ed=.942*(rhum**.679)+(11.*exp((rhum-100.)/10.))+
     &    .18*(21.1-tair)*(1.-1./exp(.1150*rhum))    ! Eq. 4
      if (M1>Ed) then
        Ko=.424*(1.-(rhum/100.)**1.7)+(.0694*sqrt(w10))*
     &      (1.-(rhum/100.)**8.)                     ! Eq. 6a
        Kd=Ko*(.581*exp(.0365*tair))                 ! Eq. 6b
        Ma=Ed+(M1-Ed)/10.**Kd                        ! Eq. 8
      else
        Ew=.618*(rhum**.753)+(10.*exp((rhum-100.)/10.))+
     &      .18*(21.1-tair)*(1.-1./exp(.115*rhum))   ! Eq. 5
        if (M1<Ew) then
          Kl=.424*(1.-((100.-rhum)/100.)**1.7)+      ! Eq. 7a
     &       (.0694*sqrt(w10))*(1.-((100.-rhum)/100.)**8.)
          Kw=Kl*(.581*exp(.0365*tair))               ! Eq. 7b
          Ma=Ew-(Ew-M1)/10.**Kw                      ! Eq. 9
        else
          Ma=M1
        endif
      endif
      ffmc=(59.5*(250.-Ma))/(147.2+Ma)               ! Eq. 10
      if (ffmc>101.) then
        ffmc=101.
      endif
      if (ffmc<=0.) then
        ffmc=0.
      endif

      ! Determine Duff Moisture Code **********************
      if (rain1<=1.5) then
        Pr=dmc1
      else
        Re=.92*rain1-1.27                            ! Eq. 11
        M1=20.+280./exp(0.023*dmc1)                  ! Eq. 12
        if (dmc1<=33.) then
          B=100./(0.5+0.3*dmc1)                      ! Eq. 13a
        else
          B=62*log(dmc1)-17.2                        ! Eq. 13c
          if (dmc1-65.<=0.) then
            B=14.-1.3*log(dmc1)                      ! Eq. 13b
          endif
        endif
        Mr = M1+(1000.*Re)/(48.77+B*Re)              ! Eq. 14
        Pr=43.43*(5.6348-log(Mr-20.))                ! Eq. 15
      endif
      if (tair>=-1.1) then
        Ky=1.894*(tair+1.1)*(100.-rhum)*(El*0.0001) ! Eq. 16
      else
        Ky=0.                                        ! Eq. 17
      endif
      if (Pr<0.) then
        Pr=0.
      endif
      dmc=Pr+Ky
      if (dmc<=0.) then
        dmc=0.
      endif

      ! Determine Drought Code ****************************
      if (rain1>2.8) then
        Rd=0.83*rain1-1.27                           ! Eq. 18
        Q1=800.*exp(-dc1/400.)                       ! Eq. 19
```

```
  Qr=Q1+3.937*Rd                              ! Eq. 20
  Dr=400.*log(800./Qr)                        ! Eq. 21
  if (Dr>0.) then
   dc1=Dr
  else
   dc1=0.
  endif
 endif
 if (tair<-2.8) then
  V=Fl
 else
  V=(0.36*(tair+2.8)+Fl)                      ! Eq. 22
 endif
 if (V<=0.) then
  V=0.
 endif
 dc=dc1+0.5*V

 ! Determine Initial Spread Index *********************
 M1=(147.2*(101.-ffmc))/(59.5+ffmc)           ! Eq. 1
 Fw=exp(0.05039*w10)                          ! Eq. 24
 Ff=91.9*exp(-0.1386*M1)*(1.+(M1**5.31)/4.93e7) ! Eq. 25
 isi=0.208*Fw*Ff                              ! Eq. 26

 ! Determine Build Up Index ***************************
 if (dmc<=0.4*dc) then
  bui=(0.8*dmc*dc)/(dmc+0.4*dc)               ! Eq. 27a
 else
  bui=dmc-(1.-0.8*dc/(dmc+0.4*dc))*
&     (0.92+(0.0114*dmc)**1.7)                ! Eq. 27b
 endif
 if (bui<0.) then
  bui=0.
 endif

 ! Determine Fire Weather Index & Daily Severity Rating
 if (bui<=80.) then
  Fd=0.626*bui**0.809+2.                      ! Eq. 28a
 else
  Fd=1000./(25.+108.64*exp(-0.023*bui))       ! Eq. 28b
 endif
 B=0.1*isi*Fd                                 ! Eq. 29
 if (B>1.) then
  CFWI=exp(2.72*(0.434*log(B))**0.647)        ! Eq. 30a
 else
  CFWI=B                                      ! Eq. 30b
 endif
 CDSR=0.0272*CFWI**1.77                       ! Eq. 41

 CFWI_d(i,j,k,m,nn)=CFWI
 CDSR_d(i,j,k,m,nn)=CDSR
 prev_ffmc(i,j)=ffmc                ! use today's values
 prev_dmc(i,j)=dmc                  ! for tomorrow's
 prev_dc(i,j)=dc                    ! calculation

 !%%%%%%%%%%%%%%%%%%%%%%%%%%%%%%%%%%%%%%%%%%%%%%%%%%%%%%%%
 case(2)   ! Lowveld Fire Danger Index (LFDI)                  %
 !%%%%%%%%%%%%%%%%%%%%%%%%%%%%%%%%%%%%%%%%%%%%%%%%%%%%%%%%
 !% This section calculates the Lowveld Fire Danger            %
 !% Index. It is based on Notice 1099 of 2013, though          %
 !% a slight adaptation was made to the RCF in order           %
 !% to accommodate historical data where rain could            %
 !% have occurred on the day in question (i.e. 0 days          %
 !% since last rainfall event). It was tested against          %
 !% sample data provided in my thesis.                         %
 !%%%%%%%%%%%%%%%%%%%%%%%%%%%%%%%%%%%%%%%%%%%%%%%%%%%%%%%%
```

```
! Brief description of interim variables used:
! BI = Burning Index (unitless)
! WF = Wind Factor (unitless)
! RCFmin = Rainfal Correction Factor (unitless)
! LFDI = Lowveld Fire Danger Index (unitless)

! Calculate Burning Index (BI)
!BI=30.834+1.0333*tair-0.37*rhum
BI=(tair-35.)-((35.-tair)/30.)+((100.-rhum)*.37)+30.

! Calculate Wind Factor (WF)
if (w10.lt.2.5) then
  WF=0.
elseif (w10.ge.2.5 .and. w10.lt.8.5) then
  WF=5.
elseif (w10.ge.8.5 .and. w10.lt.16.5) then
  WF=10.
elseif (w10.ge.16.5 .and. w10.lt.25.5) then
  WF=15.
elseif (w10.ge.25.5 .and. w10.lt.32.5) then
  WF=20.
elseif (w10.ge.32.5 .and. w10.lt.36.5) then
  WF=25.
elseif (w10.ge.36.5 .and. w10.lt.41.5) then
  WF=30.
elseif (w10.ge.41.5 .and. w10.lt.45.5) then
  WF=35.
elseif (w10.ge.45.5) then
  WF=40.
endif

! Calculate Rainfall Correction Factor (RCF)
RCF=1.
RCF0=1.
RCFmin=1.
do bak=20,1,-1
  if (bak.ge.16) then
    if (raint(bak).ge.63.9) then
      RCF(bak)=.9
    endif
  else if (bak.ge.13.and.bak.lt.16) then
    if (raint(bak).ge.51.2) then
      RCF(bak)=.9
    endif
    if (raint(bak).ge.63.9) then
      RCF(bak)=.8
    endif
  else if (bak.ge.11.and.bak.lt.13) then
    if (raint(bak).ge.38.5) then
      RCF(bak)=.9
    endif
    if (raint(bak).ge.51.2) then
      RCF(bak)=.8
    endif
    if (raint(bak).ge.76.6) then
      RCF(bak)=.7
    endif
  else if (bak.ge.9.and.bak.lt.11) then
    if (raint(bak).ge.25.6) then
      RCF(bak)=.9
    endif
    if (raint(bak).ge.38.5) then
      RCF(bak)=.8
    endif
    if (raint(bak).ge.51.2) then
      RCF(bak)=.7
```

```
  endif
  if (raint(bak).ge.76.6) then
    RCF(bak)=.6
  endif
 else if (bak.ge.7.and.bak.lt.9) then
  if (raint(bak).ge.15.4) then
    RCF(bak)=.9
  endif
  if (raint(bak).ge.25.6) then
    RCF(bak)=.8
  endif
  if (raint(bak).ge.38.5) then
    RCF(bak)=.7
  endif
  if (raint(bak).ge.63.9) then
    RCF(bak)=.6
  endif
 else if (bak.eq.6) then
  if (raint(bak).ge.10.3) then
    RCF(bak)=.9
  endif
  if (raint(bak).ge.15.4) then
    RCF(bak)=.8
  endif
  if (raint(bak).ge.25.6) then
    RCF(bak)=.7
  endif
  if (raint(bak).ge.38.5) then
    RCF(bak)=.6
  endif
  if (raint(bak).ge.63.9) then
    RCF(bak)=.5
  endif
 else if (bak.eq.5) then
  if (raint(bak).ge.7.7) then
    RCF(bak)=.9
  endif
  if (raint(bak).ge.12.9) then
    RCF(bak)=.8
  endif
  if (raint(bak).ge.20.6) then
    RCF(bak)=.7
  endif
  if (raint(bak).ge.25.6) then
    RCF(bak)=.6
  endif
  if (raint(bak).ge.38.5) then
    RCF(bak)=.5
  endif
  if (raint(bak).ge.63.9) then
    RCF(bak)=.4
  endif
 else if (bak.eq.4) then
  if (raint(bak).ge.5.3) then
    RCF(bak)=.9
  endif
  if (raint(bak).ge.10.3) then
    RCF(bak)=.8
  endif
  if (raint(bak).ge.15.4) then
    RCF(bak)=.7
  endif
  if (raint(bak).ge.25.6) then
    RCF(bak)=.6
  endif
  if (raint(bak).ge.38.5) then
```

```
    RCF(bak)=.5
   endif
   if (raint(bak).ge.51.2) then
    RCF(bak)=.4
   endif
   if (raint(bak).ge.63.9) then
    RCF(bak)=.3
   endif
   if (raint(bak).ge.76.6) then
    RCF(bak)=.2
   endif
  else if (bak.eq.3) then
   if (raint(bak).ge.2.7) then
    RCF(bak)=.9
   endif
   if (raint(bak).ge.7.7) then
    RCF(bak)=.8
   endif
   if (raint(bak).ge.10.3) then
    RCF(bak)=.7
   endif
   if (raint(bak).ge.15.4) then
    RCF(bak)=.6
   endif
   if (raint(bak).ge.20.6) then
    RCF(bak)=.5
   endif
   if (raint(bak).ge.25.6) then
    RCF(bak)=.4
   endif
   if (raint(bak).ge.51.2) then
    RCF(bak)=.3
   endif
   if (raint(bak).ge.63.9) then
    RCF(bak)=.2
   endif
   if (raint(bak).ge.76.6) then
    RCF(bak)=.1
   endif
  else if (bak.eq.2) then
   if (raint(bak).ge.0.1) then
    RCF(bak)=.9
   endif
   if (raint(bak).ge.2.7) then
    RCF(bak)=.8
   endif
   if (raint(bak).ge.5.3) then
    RCF(bak)=.7
   endif
   if (raint(bak).ge.7.7) then
    RCF(bak)=.6
   endif
   if (raint(bak).ge.12.9) then
    RCF(bak)=.5
   endif
   if (raint(bak).ge.20.6) then
    RCF(bak)=.4
   endif
   if (raint(bak).ge.25.6) then
    RCF(bak)=.3
   endif
   if (raint(bak).ge.38.5) then
    RCF(bak)=.2
   endif
   if (raint(bak).ge.63.9) then
    RCF(bak)=.1
```

```
    endif
  else if (bak.eq.1) then
    if (raint(bak).ge.0.1) then
      RCF(bak)=.7
    endif
    if (raint(bak).ge.2.7) then
      RCF(bak)=.6
    endif
    if (raint(bak).ge.5.3) then
      RCF(bak)=.5
    endif
    if (raint(bak).ge.7.7) then
      RCF(bak)=.4
    endif
    if (raint(bak).ge.12.9) then
      RCF(bak)=.3
    endif
    if (raint(bak).ge.15.4) then
      RCF(bak)=.2
    endif
    if (raint(bak).ge.25.6) then
      RCF(bak)=.1
    endif
  endif
  if (RCFmin.gt.RCF(bak)) then
    RCFmin=RCF(bak)    ! ensure using smallest RCF
  endif
enddo     ! bak-loop ends
if (rain.ge.0.1) then ! check today's rain as well
  RCF0=.5
endif
if (rain.ge.2.7) then
  RCF0=.4
endif
if (rain.ge.5.3) then
  RCF0=.3
endif
if (rain.ge.7.7) then
  RCF0=.2
endif
if (rain.ge.12.9) then
  RCF0=.1
endif
if (RCFmin.gt.RCF0) then
    RCFmin=RCF0    ! ensure using smallest RCF
endif

! Calculate Lowveld Fire Danger Index (LFDI)
LFDI=(BI+WF)*RCFmin
if (LFDI.lt.0.) then
  LFDI=0.      ! ensuring LFDI is not negative
endif
LFDI_d(i,j,k,m,nn)=LFDI

!%%%%%%%%%%%%%%%%%%%%%%%%%%%%%%%%%%%%%%%%%%%%%%%%%%%%%%
case(3)   ! McArthur Forest Fire Danger Index (FFDI)                                   %
!%%%%%%%%%%%%%%%%%%%%%%%%%%%%%%%%%%%%%%%%%%%%%%%%%%%%%%
!% This section calculates McArthur's Forest Fire                                      %
!% Danger Index Mk5 based on formulas listed by:                                       %
!% Noble et al. (1980), Griffiths (1999), Willis et                                    %
!% al. (2001), Schlobohm & Brain (2002), Sharples et                                   %
!% al. (2009), Williams et al. (2009), Garcia-Prats                                    %
!% et al. (2015). It was tested against sample                                         %
!% input/output data from an app named 'Calc-F.D.I.'                                   %
!% and an online FFDI calculator available from                                        %
!% https://cfsres.com/ffdi although these did not                                      %
```

```
!% consider previous rainfall events.                                                    %
!%%%%%%%%%%%%%%%%%%%%%%%%%%%%%%%%%%%%%%%%%%%%%%%%%%%%%%%%%%%%%%%%%%%%%%%%%%%%%%%%%%%%
! Brief description of interim variables used:
! Pn = net 24 hour rainfall (mm)
! ymax = rainfall factor based on a screening of the
!       past 20 days' rain (unitless)
! dQ = actual evapotranspiration or daily addition to
!     soil water deficiency (mm)
! KBDI = today's Keetch-Byram Drought Index or
!       accumulated soil water deficit (mm)
! KBDI1 = yesterday's KBDI
! D = drought factor (unitless)

KBDI1=prev_KBDI(i,j)        ! use yesterday's value

! Screening last 20 days' rainfall to determine ymax
ymax=0.
do bak=20,1,-1
  if (raint(bak).gt.2.) then
    y=(raint(bak)-2.)/(bak**1.3)
  else
    y=0.
  endif
  if (y.gt.ymax) then
    ymax=y
  endif
enddo
if (rain.gt.2.) then ! 0 days since last rain event
  y=(rain-2.)/(.8**1.3)
endif
if (y.gt.ymax) then
  ymax=y    ! ensuring that largest y is used
endif

! Calculating Keetch-Byram Drought Index (KBDI)
dQ=(203.2-KBDI1)*(0.968*exp(0.0875*tair+1.552)-8.3)/
&       (1000.*(1.+10.88*exp(-0.001736*rmean)))   ! Eq. 5.12
! Alternative dQ for Meditterranean (Ganatsas et al.,
! 2011): then also change DUL=200mm and rain threshold
! to 3mm (from 5.08)
c       dQ=(200.-KBDI1)*(1.713*exp(0.0875*tair+1.552)-14.59)/
c &       (10E3*(1.+10.88*exp(-0.001736*rmean)))    ! Eq. 5.15
if (rain2.eq.0.) then
  Pn=max((rain1-5.08),0.)
elseif (rain2.gt.5.08) then
  Pn=rain1                          ! Eq. 5.13
else
  Pn=max((5.08-rain1),0.)
endif
KBDI=(KBDI1-Pn)+dQ                  ! Eq. 5.14
if (KBDI.lt.0.) then
  KBDI=0.           ! ensuring KBDI is not negative
endif

! Calculating Drought Factor (DF)
D=(10.5*(1.-exp((KBDI+30.)/-40.))*
&       ((ymax+42.)/(ymax+3.*ymax+42.)))        ! Eq. 5.??
if (D.gt.10.) then
  D=10.             ! ensuring DF < 10
elseif (D.le.0.) then
  D=.01             ! ensuring DF > 0
endif

! Calculating the FFDI Mark5
FFDI=2.*exp(-.45+.987*log(D)-.0345*rhum+.0338*tair+
&       .0234*w10)
```

```
          if (FFDI.lt.0.) then
            FFDI=0.            ! ensuring FFDI is not negative
          endif

          FFDI_d(i,j,k,m,nn)=FFDI
          prev_KBDI(i,j)=KBDI                    ! use today's values for
                                                 ! tomorrow's calculation
          !%%%%%%%%%%%%%%%%%%%%%%%%%%%%%%%%%%%%%%%%%%%%%%%%%%%%%%%%%%%%%%%%%%%%%%%%
          end select
        else    ! missing value if
          select case(ind)
          case(1)    ! CFWI
           CFWI_d(i,j,k,m,nn)=-9999.
           CDSR_d(i,j,k,m,nn)=-9999.
          case(2)    ! LFDI
            LFDI_d(i,j,k,m,nn)=-9999.
          case(3)    ! FFDI
            FFDI_d(i,j,k,m,nn)=-9999.
          end select
        endif    ! missing value if ends
      enddo    ! i-loop ends
    enddo    ! j-loop ends
  enddo    ! k-loop (days) ends
  ! Determining daily spatial maximimum and mean FDIs
  do k=1,mdays(m)
    do j=1,AY
      do i=1,AX
        if (sarea(i,j).eq.1.and.rain_d(i,j,k,1,1).ne.-9999.)
&       then
        ! only use non-missing values within study area
          select case(ind)
            case(1)    ! CFWI
              ! Writing daily CFWI-value to file (all grids)
              write(102,100) CFWI_d(i,j,k,m,nn),
&                            CDSR_d(i,j,k,m,nn)
              if (m.ge.fstart.and.m.le.fend) then ! fire season
                write(105,100) CFWI_d(i,j,k,m,nn),
&                              CDSR_d(i,j,k,m,nn)
              endif
              ! Allocating spatial maximum CFWI-value per day
              if (CFWImax_d(k,m,nn).lt.CFWI_d(i,j,k,m,nn)) then
                CFWImax_d(k,m,nn)=CFWI_d(i,j,k,m,nn)
              endif
              ! Allocating spatial maximum CDSR-value per day
              if (CDSRmax_d(k,m,nn).lt.CDSR_d(i,j,k,m,nn)) then
                CDSRmax_d(k,m,nn)=CDSR_d(i,j,k,m,nn)
              endif
              ! Accumulating daily spatial total CFWI/CDSR-value
              CFWImean_d(k,m,nn)=CFWImean_d(k,m,nn)+
&                                CFWI_d(i,j,k,m,nn)
              CDSRmean_d(k,m,nn)=CDSRmean_d(k,m,nn)+
&                                CDSR_d(i,j,k,m,nn)
            case(2)    ! LFDI
              ! Writing daily LFDI-value to file (all grids)
              write(102,200) LFDI_d(i,j,k,m,nn)
              if (m.ge.fstart.and.m.le.fend) then ! fire season
                write(105,200) LFDI_d(i,j,k,m,nn)
              endif
              ! Allocating spatial maximum LFDI-value per day
              if (LFDImax_d(k,m,nn).lt.LFDI_d(i,j,k,m,nn)) then
                LFDImax_d(k,m,nn)=LFDI_d(i,j,k,m,nn)
              endif
              ! Accumulating daily spatial total LFDI-value
              LFDImean_d(k,m,nn)=LFDImean_d(k,m,nn)+
&                                LFDI_d(i,j,k,m,nn)
            case(3)    ! FFDI
```

```
            ! Writing daily FFDI-value to file (all grids)
            write(102,200) FFDI_d(i,j,k,m,nn)
            if (m.ge.fstart.and.m.le.fend) then ! fire season
              write(105,200) FFDI_d(i,j,k,m,nn)
            endif
            ! Allocating spatial maximum FFDI-value per day
            if (FFDImax_d(k,m,nn).lt.FFDI_d(i,j,k,m,nn)) then
              FFDImax_d(k,m,nn)=FFDI_d(i,j,k,m,nn)
            endif
            ! Accumulating daily spatial total FFDI-value
            FFDImean_d(k,m,nn)=FFDImean_d(k,m,nn)+
&                         FFDI_d(i,j,k,m,nn)
          end select
          tel=tel+1
        endif    ! missing value if ends
      enddo    ! i-loop ends
    enddo    ! j-loop ends
    ! Writing spatial max and mean FDIs to file (all months)
    select case(ind)
     case(1)   ! CFWI     (choose between FWI/DSR)
      if (CAN.eq.1) then
      ! Write out for all months of year
       write (103,200) CFWImax_d(k,m,nn)
       ! Calculate daily spatial mean CFWI-value
       CFWImean_d(k,m,nn)=CFWImean_d(k,m,nn)/gnum
       write (104,200) CFWImean_d(k,m,nn)
      else
       write (103,200) CDSRmax_d(k,m,nn)
       ! Calculate daily spatial mean CDSR-value
       CDSRmean_d(k,m,nn)=CDSRmean_d(k,m,nn)/gnum
       write (104,200) CDSRmean_d(k,m,nn)
      endif
     case(2)   ! LFDI
      write (103,200) LFDImax_d(k,m,nn)
      ! Calculate daily spatial mean LFDI-value
      LFDImean_d(k,m,nn)=LFDImean_d(k,m,nn)/gnum
      write (104,200) LFDImean_d(k,m,nn)
     case(3)   ! FFDI
      write (103,200) FFDImax_d(k,m,nn)
      ! Calculate daily spatial mean FFDI-value
      FFDImean_d(k,m,nn)=FFDImean_d(k,m,nn)/gnum
      write (104,200) FFDImean_d(k,m,nn)
    end select
    if (m.ge.fstart.and.m.le.fend) then ! fire season
     select case(ind)
      case(1)   ! CFWI     (choose between FWI/DSR)
       if (CAN.eq.1) then
        write (106,200) CFWImax_d(k,m,nn)
        ! Calculate daily spatial mean CFWI-value
        CFWImean_d(k,m,nn)=CFWImean_d(k,m,nn)/gnum
        write (107,200) CFWImean_d(k,m,nn)
       else
        write (106,200) CDSRmax_d(k,m,nn)
        ! Calculate daily spatial mean CDSR-value
        CDSRmean_d(k,m,nn)=CDSRmean_d(k,m,nn)/gnum
        write (107,200) CDSRmean_d(k,m,nn)
       endif
      case(2)   ! LFDI
       write (106,200) LFDImax_d(k,m,nn)
       ! Calculate daily spatial mean LFDI-value
       LFDImean_d(k,m,nn)=LFDImean_d(k,m,nn)/gnum
       write (107,200) LFDImean_d(k,m,nn)
      case(3)   ! FFDI
       write (106,200) FFDImax_d(k,m,nn)
       ! Calculate daily spatial mean FFDI-value
       FFDImean_d(k,m,nn)=FFDImean_d(k,m,nn)/gnum
```

```
            write (107,200) FFDImean_d(k,m,nn)
          end select
         endif   ! month selection if ends
        enddo    ! k-loop (days) ends
100     FORMAT (f5.1,3X,f5.1)
200     FORMAT (f5.1)
        ! Calculate monthly totals for each year **********************
        ! Tally monthly occurrences per FDI category ******************
        do k=1,mdays(m)
         do j=1,AY
          do i=1,AX
           if (darea(i,j).eq.1.and.rain_d(i,j,k,1,1).ne.-9999.)
     &      then
           ! only use non-missing values within display area
            rain_e(i,j,m,nn)=rain_e(i,j,m,nn)+rain_d(i,j,k,m,nn)
            w10_e(i,j,m,nn)=w10_e(i,j,m,nn)+w10_d(i,j,k,m,nn)
            tair_e(i,j,m,nn)=tair_e(i,j,m,nn)+tair_d(i,j,k,m,nn)
            rhum_e(i,j,m,nn)=rhum_e(i,j,m,nn)+
     &                       rhum_d(i,j,k,m,nn)
            select case(ind)
             case(1)    ! CFWI
              if (CAN.eq.1) then   ! CFWI categories
               if (CFWI_d(i,j,k,m,nn).lt.bp(1)) then
                CFWI_cat1e(i,j,m,nn)=CFWI_cat1e(i,j,m,nn)+1.
               else if (CFWI_d(i,j,k,m,nn).ge.bp(1).and.
     &                  CFWI_d(i,j,k,m,nn).lt.bp(2)) then
                CFWI_cat2e(i,j,m,nn)=CFWI_cat2e(i,j,m,nn)+1.
               else if (CFWI_d(i,j,k,m,nn).ge.bp(2).and.
     &                  CFWI_d(i,j,k,m,nn).lt.bp(3)) then
                CFWI_cat3e(i,j,m,nn)=CFWI_cat3e(i,j,m,nn)+1.
               else if (CFWI_d(i,j,k,m,nn).ge.bp(3).and.
     &                  CFWI_d(i,j,k,m,nn).lt.bp(4)) then
                CFWI_cat4e(i,j,m,nn)=CFWI_cat4e(i,j,m,nn)+1.
               else if (CFWI_d(i,j,k,m,nn).ge.bp(4)) then
                CFWI_cat5e(i,j,m,nn)=CFWI_cat5e(i,j,m,nn)+1.
               endif
              else   ! CDSR categories
               if (CDSR_d(i,j,k,m,nn).lt.bp(1)) then
                CDSR_cat1e(i,j,m,nn)=CDSR_cat1e(i,j,m,nn)+1.
               else if (CDSR_d(i,j,k,m,nn).ge.bp(1).and.
     &                  CDSR_d(i,j,k,m,nn).lt.bp(2)) then
                CDSR_cat2e(i,j,m,nn)=CDSR_cat2e(i,j,m,nn)+1.
               else if (CDSR_d(i,j,k,m,nn).ge.bp(2).and.
     &                  CDSR_d(i,j,k,m,nn).lt.bp(3)) then
                CDSR_cat3e(i,j,m,nn)=CDSR_cat3e(i,j,m,nn)+1.
               else if (CDSR_d(i,j,k,m,nn).ge.bp(3).and.
     &                  CDSR_d(i,j,k,m,nn).le.bp(4)) then
                CDSR_cat4e(i,j,m,nn)=CDSR_cat4e(i,j,m,nn)+1.
               else if (CDSR_d(i,j,k,m,nn).gt.bp(4)) then
                CDSR_cat5e(i,j,m,nn)=CDSR_cat5e(i,j,m,nn)+1.
               endif
              endif
              CMSR(i,j,m,nn)=CMSR(i,j,m,nn)+CDSR_d(i,j,k,m,nn)
             case(2)    ! LFDI categories
              if (LFDI_d(i,j,k,m,nn).lt.bp(1)) then
               LFDI_cat1e(i,j,m,nn)=LFDI_cat1e(i,j,m,nn)+1.
              else if (LFDI_d(i,j,k,m,nn).ge.bp(1).and.
     &                 LFDI_d(i,j,k,m,nn).lt.bp(2)) then
               LFDI_cat2e(i,j,m,nn)=LFDI_cat2e(i,j,m,nn)+1.
              else if (LFDI_d(i,j,k,m,nn).ge.bp(2).and.
     &                 LFDI_d(i,j,k,m,nn).lt.bp(3)) then
               LFDI_cat3e(i,j,m,nn)=LFDI_cat3e(i,j,m,nn)+1.
              else if (LFDI_d(i,j,k,m,nn).ge.bp(3).and.
     &                 LFDI_d(i,j,k,m,nn).lt.bp(4)) then
               LFDI_cat4e(i,j,m,nn)=LFDI_cat4e(i,j,m,nn)+1.
              else if (LFDI_d(i,j,k,m,nn).ge.bp(4)) then
```

```
            LFDI_cat5e(i,j,m,nn)=LFDI_cat5e(i,j,m,nn)+1.
           endif
          case(3)    ! FFDI categories
           if (FFDI_d(i,j,k,m,nn).lt.bp(1)) then
            FFDI_cat1e(i,j,m,nn)=FFDI_cat1e(i,j,m,nn)+1.
           else if (FFDI_d(i,j,k,m,nn).ge.bp(1).and.
&                  FFDI_d(i,j,k,m,nn).lt.bp(2)) then
            FFDI_cat2e(i,j,m,nn)=FFDI_cat2e(i,j,m,nn)+1.
           else if (FFDI_d(i,j,k,m,nn).ge.bp(2).and.
&                  FFDI_d(i,j,k,m,nn).lt.bp(3)) then
            FFDI_cat3e(i,j,m,nn)=FFDI_cat3e(i,j,m,nn)+1.
           else if (FFDI_d(i,j,k,m,nn).ge.bp(3).and.
&                  FFDI_d(i,j,k,m,nn).lt.bp(4)) then
            FFDI_cat4e(i,j,m,nn)=FFDI_cat4e(i,j,m,nn)+1.
           else if (FFDI_d(i,j,k,m,nn).ge.bp(4)) then
            FFDI_cat5e(i,j,m,nn)=FFDI_cat5e(i,j,m,nn)+1.
           endif
         end select
        else    ! missing value if
         rain_e(i,j,m,nn)=-9999.
         w10_e(i,j,m,nn)=-9999.
         tair_e(i,j,m,nn)=-9999.
         rhum_e(i,j,m,nn)=-9999.
         select case(ind)
          case(1)    ! CFWI
           CFWI_cat1e(i,j,m,nn)=-9999.
           CFWI_cat2e(i,j,m,nn)=-9999.
           CFWI_cat3e(i,j,m,nn)=-9999.
           CFWI_cat4e(i,j,m,nn)=-9999.
           CFWI_cat5e(i,j,m,nn)=-9999.
           CDSR_cat1e(i,j,m,nn)=-9999.
           CDSR_cat2e(i,j,m,nn)=-9999.
           CDSR_cat3e(i,j,m,nn)=-9999.
           CDSR_cat4e(i,j,m,nn)=-9999.
           CDSR_cat5e(i,j,m,nn)=-9999.
          case(2)    ! LFDI
           LFDI_cat1e(i,j,m,nn)=-9999.
           LFDI_cat2e(i,j,m,nn)=-9999.
           LFDI_cat3e(i,j,m,nn)=-9999.
           LFDI_cat4e(i,j,m,nn)=-9999.
           LFDI_cat5e(i,j,m,nn)=-9999.
          case(3)    ! FFDI
           FFDI_cat1e(i,j,m,nn)=-9999.
           FFDI_cat2e(i,j,m,nn)=-9999.
           FFDI_cat3e(i,j,m,nn)=-9999.
           FFDI_cat4e(i,j,m,nn)=-9999.
           FFDI_cat5e(i,j,m,nn)=-9999.
         end select
        endif     ! missing value if ends
       enddo    ! i-loop ends
      enddo    ! j-loop ends
     enddo    ! k-loop (days) ends
     ! Calculate monthly means for each year **********************
     do j=1,AY
      do i=1,AX
       if (darea(i,j).eq.1.and.rain_d(i,j,1,1,1).ne.-9999.) then
       ! only use non-missing values within display area
        w10_f(i,j,m,nn)=w10_e(i,j,m,nn)/mdays(m)
        tair_f(i,j,m,nn)=tair_e(i,j,m,nn)/mdays(m)
        rhum_f(i,j,m,nn)=rhum_e(i,j,m,nn)/mdays(m)
        ! Calculate accumulated monthly means over all years *****
        rain_g(i,j,m)=rain_g(i,j,m)+rain_e(i,j,m,nn)     ! total
        w10_g(i,j,m)=w10_g(i,j,m)+w10_f(i,j,m,nn)
        tair_g(i,j,m)=tair_g(i,j,m)+tair_f(i,j,m,nn)
        rhum_g(i,j,m)=rhum_g(i,j,m)+rhum_f(i,j,m,nn)
        select case(ind)
```

```
          case(1)    ! CFWI
           CFWI_cat1g(i,j,m)=CFWI_cat1g(i,j,m)+
&                    CFWI_cat1e(i,j,m,nn) ! total
           CFWI_cat2g(i,j,m)=CFWI_cat2g(i,j,m)+
&                    CFWI_cat2e(i,j,m,nn) ! total
           CFWI_cat3g(i,j,m)=CFWI_cat3g(i,j,m)+
&                    CFWI_cat3e(i,j,m,nn) ! total
           CFWI_cat4g(i,j,m)=CFWI_cat4g(i,j,m)+
&                    CFWI_cat4e(i,j,m,nn) ! total
           CFWI_cat5g(i,j,m)=CFWI_cat5g(i,j,m)+
&                    CFWI_cat5e(i,j,m,nn) ! total
           CDSR_cat1g(i,j,m)=CDSR_cat1g(i,j,m)+
&                    CDSR_cat1e(i,j,m,nn) ! total
           CDSR_cat2g(i,j,m)=CDSR_cat2g(i,j,m)+
&                    CDSR_cat2e(i,j,m,nn) ! total
           CDSR_cat3g(i,j,m)=CDSR_cat3g(i,j,m)+
&                    CDSR_cat3e(i,j,m,nn) ! total
           CDSR_cat4g(i,j,m)=CDSR_cat4g(i,j,m)+
&                    CDSR_cat4e(i,j,m,nn) ! total
           CDSR_cat5g(i,j,m)=CDSR_cat5g(i,j,m)+
&                    CDSR_cat5e(i,j,m,nn) ! total
           CMSR(i,j,m,nn)=CMSR(i,j,m,nn)/mdays(m)
           if (m.ge.fstart.and.m.le.fend) then  ! for SSR
            CSSR(i,j,nn)=CSSR(i,j,nn)+CMSR(i,j,m,nn)
           endif
          case(2)    ! LFDI
           LFDI_cat1g(i,j,m)=LFDI_cat1g(i,j,m)+
&                    LFDI_cat1e(i,j,m,nn) ! total
           LFDI_cat2g(i,j,m)=LFDI_cat2g(i,j,m)+
&                    LFDI_cat2e(i,j,m,nn) ! total
           LFDI_cat3g(i,j,m)=LFDI_cat3g(i,j,m)+
&                    LFDI_cat3e(i,j,m,nn) ! total
           LFDI_cat4g(i,j,m)=LFDI_cat4g(i,j,m)+
&                    LFDI_cat4e(i,j,m,nn) ! total
           LFDI_cat5g(i,j,m)=LFDI_cat5g(i,j,m)+
&                    LFDI_cat5e(i,j,m,nn) ! total
          case(3)    ! FFDI
           FFDI_cat1g(i,j,m)=FFDI_cat1g(i,j,m)+
&                    FFDI_cat1e(i,j,m,nn) ! total
           FFDI_cat2g(i,j,m)=FFDI_cat2g(i,j,m)+
&                    FFDI_cat2e(i,j,m,nn) ! total
           FFDI_cat3g(i,j,m)=FFDI_cat3g(i,j,m)+
&                    FFDI_cat3e(i,j,m,nn) ! total
           FFDI_cat4g(i,j,m)=FFDI_cat4g(i,j,m)+
&                    FFDI_cat4e(i,j,m,nn) ! total
           FFDI_cat5g(i,j,m)=FFDI_cat5g(i,j,m)+
&                    FFDI_cat5e(i,j,m,nn) ! total
         end select
        else    ! missing value if
         rain_g(i,j,m)=-9999.
         w10_g(i,j,m)=-9999.
         tair_g(i,j,m)=-9999.
         rhum_g(i,j,m)=-9999.
         select case(ind)
          case(1)    ! CFWI
           CFWI_cat1g(i,j,m)=-9999.
           CFWI_cat2g(i,j,m)=-9999.
           CFWI_cat3g(i,j,m)=-9999.
           CFWI_cat4g(i,j,m)=-9999.
           CFWI_cat5g(i,j,m)=-9999.
           CDSR_cat1g(i,j,m)=-9999.
           CDSR_cat2g(i,j,m)=-9999.
           CDSR_cat3g(i,j,m)=-9999.
           CDSR_cat4g(i,j,m)=-9999.
           CDSR_cat5g(i,j,m)=-9999.
           CMSR(i,j,m,nn)=-9999.
```

```
          case(2)    ! LFDI
            LFDI_cat1g(i,j,m)=-9999.
            LFDI_cat2g(i,j,m)=-9999.
            LFDI_cat3g(i,j,m)=-9999.
            LFDI_cat4g(i,j,m)=-9999.
            LFDI_cat5g(i,j,m)=-9999.
          case(3)    ! FFDI
            FFDI_cat1g(i,j,m)=-9999.
            FFDI_cat2g(i,j,m)=-9999.
            FFDI_cat3g(i,j,m)=-9999.
            FFDI_cat4g(i,j,m)=-9999.
            FFDI_cat5g(i,j,m)=-9999.
          end select
        endif    ! missing value if ends
      enddo    ! i-loop ends
    enddo    ! j-loop ends
  enddo    ! m-loop (months) ends --------------------------------
  ! Calculate seasonal severity index (SSR) for fire season only
  if (ind.eq.1) then    ! Calculate seasonal severity index (SSR)
    do j=1,AY
      do i=1,AX
        if (darea(i,j).eq.1.and.rain_d(i,j,1,1,1).ne.-9999.) then
        ! only use non-missing values within display area
          CSSR(i,j,nn)=CSSR(i,j,nn)/fsn
          CLSR(i,j)=CLSR(i,j)+CSSR(i,j,nn)
        else
          CSSR(i,j,nn)=-9999.
        endif    ! missing value if ends
      enddo    ! i-loop ends
    enddo    ! j-loop ends
  endif    ! index if ends
enddo    ! n-loop (years) ends ----------------------------------
close(102)
close(103)
close(104)
close(105)
close(106)
close(107)

! Calculate monthly means over all years *************************
do m=1,12
  do j=1,AY
    do i=1,AX
      if (darea(i,j).eq.1.and.rain_d(i,j,1,1,1).ne.-9999.) then
      ! only use non-missing values within display area
        rain_h(i,j,m)=rain_g(i,j,m)/nyears    ! mean total
        rain_a(i,j)=rain_a(i,j)+rain_h(i,j,m)
        w10_h(i,j,m)=w10_g(i,j,m)/nyears
        w10_a(i,j)=w10_a(i,j)+w10_h(i,j,m)
        tair_h(i,j,m)=tair_g(i,j,m)/nyears
        tair_a(i,j)=tair_a(i,j)+tair_h(i,j,m)
        rhum_h(i,j,m)=rhum_g(i,j,m)/nyears
        rhum_a(i,j)=rhum_a(i,j)+rhum_h(i,j,m)
        select case(ind)
          case(1)    ! CFWI
            CFWI_cat1h(i,j,m)=CFWI_cat1g(i,j,m)/nyears !mean total
            CFWI_cat1a(i,j)=CFWI_cat1a(i,j)+CFWI_cat1h(i,j,m)
            CFWI_cat2h(i,j,m)=CFWI_cat2g(i,j,m)/nyears !mean total
            CFWI_cat2a(i,j)=CFWI_cat2a(i,j)+CFWI_cat2h(i,j,m)
            CFWI_cat3h(i,j,m)=CFWI_cat3g(i,j,m)/nyears !mean total
            CFWI_cat3a(i,j)=CFWI_cat3a(i,j)+CFWI_cat3h(i,j,m)
            CFWI_cat4h(i,j,m)=CFWI_cat4g(i,j,m)/nyears !mean total
            CFWI_cat4a(i,j)=CFWI_cat4a(i,j)+CFWI_cat4h(i,j,m)
            CFWI_cat5h(i,j,m)=CFWI_cat5g(i,j,m)/nyears !mean total
            CFWI_cat5a(i,j)=CFWI_cat5a(i,j)+CFWI_cat5h(i,j,m)
            CDSR_cat1h(i,j,m)=CDSR_cat1g(i,j,m)/nyears !mean total
```

```
    CDSR_cat1a(i,j)=CDSR_cat1a(i,j)+CDSR_cat1h(i,j,m)
    CDSR_cat2h(i,j,m)=CDSR_cat2g(i,j,m)/nyears !mean total
    CDSR_cat2a(i,j)=CDSR_cat2a(i,j)+CDSR_cat2h(i,j,m)
    CDSR_cat3h(i,j,m)=CDSR_cat3g(i,j,m)/nyears !mean total
    CDSR_cat3a(i,j)=CDSR_cat3a(i,j)+CDSR_cat3h(i,j,m)
    CDSR_cat4h(i,j,m)=CDSR_cat4g(i,j,m)/nyears !mean total
    CDSR_cat4a(i,j)=CDSR_cat4a(i,j)+CDSR_cat4h(i,j,m)
    CDSR_cat5h(i,j,m)=CDSR_cat5g(i,j,m)/nyears !mean total
    CDSR_cat5a(i,j)=CDSR_cat5a(i,j)+CDSR_cat5h(i,j,m)
   case(2)    ! LFDI
    LFDI_cat1h(i,j,m)=LFDI_cat1g(i,j,m)/nyears !mean total
    LFDI_cat1a(i,j)=LFDI_cat1a(i,j)+LFDI_cat1h(i,j,m)
    LFDI_cat2h(i,j,m)=LFDI_cat2g(i,j,m)/nyears !mean total
    LFDI_cat2a(i,j)=LFDI_cat2a(i,j)+LFDI_cat2h(i,j,m)
    LFDI_cat3h(i,j,m)=LFDI_cat3g(i,j,m)/nyears !mean total
    LFDI_cat3a(i,j)=LFDI_cat3a(i,j)+LFDI_cat3h(i,j,m)
    LFDI_cat4h(i,j,m)=LFDI_cat4g(i,j,m)/nyears !mean total
    LFDI_cat4a(i,j)=LFDI_cat4a(i,j)+LFDI_cat4h(i,j,m)
    LFDI_cat5h(i,j,m)=LFDI_cat5g(i,j,m)/nyears !mean total
    LFDI_cat5a(i,j)=LFDI_cat5a(i,j)+LFDI_cat5h(i,j,m)
   case(3)    ! FFDI
    FFDI_cat1h(i,j,m)=FFDI_cat1g(i,j,m)/nyears !mean total
    FFDI_cat1a(i,j)=FFDI_cat1a(i,j)+FFDI_cat1h(i,j,m)
    FFDI_cat2h(i,j,m)=FFDI_cat2g(i,j,m)/nyears !mean total
    FFDI_cat2a(i,j)=FFDI_cat2a(i,j)+FFDI_cat2h(i,j,m)
    FFDI_cat3h(i,j,m)=FFDI_cat3g(i,j,m)/nyears !mean total
    FFDI_cat3a(i,j)=FFDI_cat3a(i,j)+FFDI_cat3h(i,j,m)
    FFDI_cat4h(i,j,m)=FFDI_cat4g(i,j,m)/nyears !mean total
    FFDI_cat4a(i,j)=FFDI_cat4a(i,j)+FFDI_cat4h(i,j,m)
    FFDI_cat5h(i,j,m)=FFDI_cat5g(i,j,m)/nyears !mean total
    FFDI_cat5a(i,j)=FFDI_cat5a(i,j)+FFDI_cat5h(i,j,m)
  end select
  if (m.ge.fstart.and.m.le.fend) then
   rain_s(i,j)=rain_s(i,j)+rain_h(i,j,m)
   w10_s(i,j)=w10_s(i,j)+w10_h(i,j,m)
   tair_s(i,j)=tair_s(i,j)+tair_h(i,j,m)
   rhum_s(i,j)=rhum_s(i,j)+rhum_h(i,j,m)
   select case(ind)
    case(1)    ! CFWI
     CFWI_cat1s(i,j)=CFWI_cat1s(i,j)+CFWI_cat1h(i,j,m)
     CFWI_cat2s(i,j)=CFWI_cat2s(i,j)+CFWI_cat2h(i,j,m)
     CFWI_cat3s(i,j)=CFWI_cat3s(i,j)+CFWI_cat3h(i,j,m)
     CFWI_cat4s(i,j)=CFWI_cat4s(i,j)+CFWI_cat4h(i,j,m)
     CFWI_cat5s(i,j)=CFWI_cat5s(i,j)+CFWI_cat5h(i,j,m)
     CDSR_cat1s(i,j)=CDSR_cat1s(i,j)+CDSR_cat1h(i,j,m)
     CDSR_cat2s(i,j)=CDSR_cat2s(i,j)+CDSR_cat2h(i,j,m)
     CDSR_cat3s(i,j)=CDSR_cat3s(i,j)+CDSR_cat3h(i,j,m)
     CDSR_cat4s(i,j)=CDSR_cat4s(i,j)+CDSR_cat4h(i,j,m)
     CDSR_cat5s(i,j)=CDSR_cat5s(i,j)+CDSR_cat5h(i,j,m)
    case(2)    ! LFDI
     LFDI_cat1s(i,j)=LFDI_cat1s(i,j)+LFDI_cat1h(i,j,m)
     LFDI_cat2s(i,j)=LFDI_cat2s(i,j)+LFDI_cat2h(i,j,m)
     LFDI_cat3s(i,j)=LFDI_cat3s(i,j)+LFDI_cat3h(i,j,m)
     LFDI_cat4s(i,j)=LFDI_cat4s(i,j)+LFDI_cat4h(i,j,m)
     LFDI_cat5s(i,j)=LFDI_cat5s(i,j)+LFDI_cat5h(i,j,m)
    case(3)    ! FFDI
     FFDI_cat1s(i,j)=FFDI_cat1s(i,j)+FFDI_cat1h(i,j,m)
     FFDI_cat2s(i,j)=FFDI_cat2s(i,j)+FFDI_cat2h(i,j,m)
     FFDI_cat3s(i,j)=FFDI_cat3s(i,j)+FFDI_cat3h(i,j,m)
     FFDI_cat4s(i,j)=FFDI_cat4s(i,j)+FFDI_cat4h(i,j,m)
     FFDI_cat5s(i,j)=FFDI_cat5s(i,j)+FFDI_cat5h(i,j,m)
   end select
  endif    ! fire season if ends
 else    ! missing value if
  rain_h(i,j,m)=-9999.
  w10_h(i,j,m)=-9999.
```

```
      tair_h(i,j,m)=-9999.
      rhum_h(i,j,m)=-9999.
      select case(ind)
       case(1)    ! CFWI
        CFWI_cat1h(i,j,m)=-9999.
        CFWI_cat2h(i,j,m)=-9999.
        CFWI_cat3h(i,j,m)=-9999.
        CFWI_cat4h(i,j,m)=-9999.
        CFWI_cat5h(i,j,m)=-9999.
        CDSR_cat1h(i,j,m)=-9999.
        CDSR_cat2h(i,j,m)=-9999.
        CDSR_cat3h(i,j,m)=-9999.
        CDSR_cat4h(i,j,m)=-9999.
        CDSR_cat5h(i,j,m)=-9999.
       case(2)    ! LFDI
        LFDI_cat1h(i,j,m)=-9999.
        LFDI_cat2h(i,j,m)=-9999.
        LFDI_cat3h(i,j,m)=-9999.
        LFDI_cat4h(i,j,m)=-9999.
        LFDI_cat5h(i,j,m)=-9999.
       case(3)    ! FFDI
        FFDI_cat1h(i,j,m)=-9999.
        FFDI_cat2h(i,j,m)=-9999.
        FFDI_cat3h(i,j,m)=-9999.
        FFDI_cat4h(i,j,m)=-9999.
        FFDI_cat5h(i,j,m)=-9999.
      end select
     endif    ! missing value if ends
    enddo    ! i-loop ends
  enddo    ! j-loop ends
enddo    ! m-loop (months) ends
! Calculate long-term annual and seasonal means in accordance with
! WMO-No.1203 (2017) *********************************************
do j=1,AY
 do i=1,AX
  if (darea(i,j).eq.1.and.rain_d(i,j,1,1,1).ne.-9999.) then
  ! only use non-missing values within display area
   ! rain_a(i,j) and rain_s(i,j) was already calculated
   w10_a(i,j)=w10_a(i,j)/12.
   w10_s(i,j)=w10_s(i,j)/fsn
   tair_a(i,j)=tair_a(i,j)/12.
   tair_s(i,j)=tair_s(i,j)/fsn
   rhum_a(i,j)=rhum_a(i,j)/12.
   rhum_s(i,j)=rhum_s(i,j)/fsn
   select case(ind)
    case(1)    ! CFWI
     ! CFWI_catXa(i,j) and CFWI_catXs(i,j) and
     ! CDSR_catXa(i,j) and CDSR_catXs(i,j) was
     ! already calculated
     CLSR(i,j)=CLSR(i,j)/nyears
    case(2)    ! LFDI
     ! LFDI_catXa(i,j) and LFDI_catXs(i,j) was
     ! already calculated
    case(3)    ! FFDI
     ! FFDI_catXa(i,j) and FFDI_catXs(i,j) was
     ! already calculated
   end select
  else    ! missing value if
   rain_a(i,j)=-9999.
   rain_s(i,j)=-9999.
   tair_a(i,j)=-9999.
   tair_s(i,j)=-9999.
   rhum_a(i,j)=-9999.
   rhum_s(i,j)=-9999.
   w10_a(i,j)=-9999.
   w10_s(i,j)=-9999.
```

```
      select case(ind)
       case(1)    ! CFWI
         CFWI_cat1a(i,j)=-9999.
         CFWI_cat1s(i,j)=-9999.
         CFWI_cat2a(i,j)=-9999.
         CFWI_cat2s(i,j)=-9999.
         CFWI_cat3a(i,j)=-9999.
         CFWI_cat3s(i,j)=-9999.
         CFWI_cat4a(i,j)=-9999.
         CFWI_cat4s(i,j)=-9999.
         CFWI_cat5a(i,j)=-9999.
         CFWI_cat5s(i,j)=-9999.
         CDSR_cat1a(i,j)=-9999.
         CDSR_cat1s(i,j)=-9999.
         CDSR_cat2a(i,j)=-9999.
         CDSR_cat2s(i,j)=-9999.
         CDSR_cat3a(i,j)=-9999.
         CDSR_cat3s(i,j)=-9999.
         CDSR_cat4a(i,j)=-9999.
         CDSR_cat4s(i,j)=-9999.
         CDSR_cat5a(i,j)=-9999.
         CDSR_cat5s(i,j)=-9999.
         CLSR(i,j)=-9999.
       case(2)    ! LFDI
         LFDI_cat1a(i,j)=-9999.
         LFDI_cat1s(i,j)=-9999.
         LFDI_cat2a(i,j)=-9999.
         LFDI_cat2s(i,j)=-9999.
         LFDI_cat3a(i,j)=-9999.
         LFDI_cat3s(i,j)=-9999.
         LFDI_cat4a(i,j)=-9999.
         LFDI_cat4s(i,j)=-9999.
         LFDI_cat5a(i,j)=-9999.
         LFDI_cat5s(i,j)=-9999.
       case(3)    ! FFDI
         FFDI_cat1a(i,j)=-9999.
         FFDI_cat1s(i,j)=-9999.
         FFDI_cat2a(i,j)=-9999.
         FFDI_cat2s(i,j)=-9999.
         FFDI_cat3a(i,j)=-9999.
         FFDI_cat3s(i,j)=-9999.
         FFDI_cat4a(i,j)=-9999.
         FFDI_cat4s(i,j)=-9999.
         FFDI_cat5a(i,j)=-9999.
         FFDI_cat5s(i,j)=-9999.
      end select
    endif    ! missing value if ends
  enddo    ! i-loop ends
 enddo    ! j-loop ends
 print*,'All fields have been calculated'
 print*,' '
 print*,'Printing some test values:'
 print*,"Long-term annual rain for point(106,245)=",rain_a(106,245)
 print*,"Long-term annual Tmax for point(106,245)=",tair_a(106,245)
&-273.15
 select case(ind)
  case(1)    ! CFWI
    print*,"Annual fequency of CFWI,CDSR in cat1 at point(106,245)
&         =", CFWI_cat1a(106,245),CDSR_cat1a(106,245)
    print*,"Annual fequency of CFWI,CDSR in cat2 at point(106,245)
&         =", CFWI_cat2a(106,245),CDSR_cat2a(106,245)
    print*,"Annual fequency of CFWI,CDSR in cat3 at point(106,245)
&         =", CFWI_cat3a(106,245),CDSR_cat3a(106,245)
    print*,"Annual fequency of CFWI,CDSR in cat4 at point(106,245)
&         =", CFWI_cat4a(106,245),CDSR_cat4a(106,245)
    print*,"Annual fequency of CFWI,CDSR in cat5 at point(106,245)
```

```
&          =", CFWI_cat5a(106,245),CDSR_cat5a(106,245)
    print*,"Long-term severity index CLSR at point(106,245)="
&         , CLSR(106,245)
  case(2)    ! LFDI
    print*,"Annual fequency of LFDI in cat1 at point(106,245)=",
&         LFDI_cat1a(106,245)
    print*,"Annual fequency of LFDI in cat2 at point(106,245)=",
&         LFDI_cat2a(106,245)
    print*,"Annual fequency of LFDI in cat3 at point(106,245)=",
&         LFDI_cat3a(106,245)
    print*,"Annual fequency of LFDI in cat4 at point(106,245)=",
&         LFDI_cat4a(106,245)
    print*,"Annual fequency of LFDI in cat5 at point(106,245)=",
&         LFDI_cat5a(106,245)
  case(3)    ! FFDI
    print*,"Annual fequency of FFDI in cat1 at point(106,245)=",
&         FFDI_cat1a(106,245)
    print*,"Annual fequency of FFDI in cat2 at point(106,245)=",
&         FFDI_cat2a(106,245)
    print*,"Annual fequency of FFDI in cat3 at point(106,245)=",
&         FFDI_cat3a(106,245)
    print*,"Annual fequency of FFDI in cat4 at point(106,245)=",
&         FFDI_cat4a(106,245)
    print*,"Annual fequency of FFDI in cat5+ at point(106,245)=",
&         FFDI_cat5a(106,245)
 end select

 ! Writing climatology to file ***********************************
 open(110,file=opath//'klima_'//finx//GCM//pperiod//ext1,
&        form='unformatted',access='direct',recl=AX*AY*4)
        ! file to which annual means/totals are written
 open(111,file=opath//'klims_'//finx//GCM//pperiod//ext1,
&        form='unformatted',access='direct',recl=AX*AY*4)
        ! file to which fire season means/totals are written
 rec1=1
 rec2=2
 rec3=3
 rec4=4
 rec5=5
 rec6=6
 rec7=7
 rec8=8
 rec9=9
 rec10=10
 write(110,rec=rec1)((rain_a(i,j),i=1,AX),j=1,AY)
 write(111,rec=rec1)((rain_s(i,j),i=1,AX),j=1,AY)
 write(110,rec=rec2)((tair_a(i,j),i=1,AX),j=1,AY)
 write(111,rec=rec2)((tair_s(i,j),i=1,AX),j=1,AY)
 write(110,rec=rec3)((rhum_a(i,j),i=1,AX),j=1,AY)
 write(111,rec=rec3)((rhum_s(i,j),i=1,AX),j=1,AY)
 write(110,rec=rec4)((w10_a(i,j),i=1,AX),j=1,AY)
 write(111,rec=rec4)((w10_s(i,j),i=1,AX),j=1,AY)
 select case(ind)
  case(1)    ! CFWI
    if (CAN.eq.1) then
      write(110,rec=rec5)((CFWI_cat1a(i,j),i=1,AX),j=1,AY)
      write(111,rec=rec5)((CFWI_cat1s(i,j),i=1,AX),j=1,AY)
      write(110,rec=rec6)((CFWI_cat2a(i,j),i=1,AX),j=1,AY)
      write(111,rec=rec6)((CFWI_cat2s(i,j),i=1,AX),j=1,AY)
      write(110,rec=rec7)((CFWI_cat3a(i,j),i=1,AX),j=1,AY)
      write(111,rec=rec7)((CFWI_cat3s(i,j),i=1,AX),j=1,AY)
      write(110,rec=rec8)((CFWI_cat4a(i,j),i=1,AX),j=1,AY)
      write(111,rec=rec8)((CFWI_cat4s(i,j),i=1,AX),j=1,AY)
      write(110,rec=rec9)((CFWI_cat5a(i,j),i=1,AX),j=1,AY)
      write(111,rec=rec9)((CFWI_cat5s(i,j),i=1,AX),j=1,AY)
    else
```

```
      write(110,rec=rec5)((CDSR_cat1a(i,j),i=1,AX),j=1,AY)
      write(111,rec=rec5)((CDSR_cat1s(i,j),i=1,AX),j=1,AY)
      write(110,rec=rec6)((CDSR_cat2a(i,j),i=1,AX),j=1,AY)
      write(111,rec=rec6)((CDSR_cat2s(i,j),i=1,AX),j=1,AY)
      write(110,rec=rec7)((CDSR_cat3a(i,j),i=1,AX),j=1,AY)
      write(111,rec=rec7)((CDSR_cat3s(i,j),i=1,AX),j=1,AY)
      write(110,rec=rec8)((CDSR_cat4a(i,j),i=1,AX),j=1,AY)
      write(111,rec=rec8)((CDSR_cat4s(i,j),i=1,AX),j=1,AY)
      write(110,rec=rec9)((CDSR_cat5a(i,j),i=1,AX),j=1,AY)
      write(111,rec=rec9)((CDSR_cat5s(i,j),i=1,AX),j=1,AY)
      write(110,rec=rec10)((CLSR(i,j),i=1,AX),j=1,AY)
    endif
   case(2)    ! LFDI
    write(110,rec=rec5)((LFDI_cat1a(i,j),i=1,AX),j=1,AY)
    write(111,rec=rec5)((LFDI_cat1s(i,j),i=1,AX),j=1,AY)
    write(110,rec=rec6)((LFDI_cat2a(i,j),i=1,AX),j=1,AY)
    write(111,rec=rec6)((LFDI_cat2s(i,j),i=1,AX),j=1,AY)
    write(110,rec=rec7)((LFDI_cat3a(i,j),i=1,AX),j=1,AY)
    write(111,rec=rec7)((LFDI_cat3s(i,j),i=1,AX),j=1,AY)
    write(110,rec=rec8)((LFDI_cat4a(i,j),i=1,AX),j=1,AY)
    write(111,rec=rec8)((LFDI_cat4s(i,j),i=1,AX),j=1,AY)
    write(110,rec=rec9)((LFDI_cat5a(i,j),i=1,AX),j=1,AY)
    write(111,rec=rec9)((LFDI_cat5s(i,j),i=1,AX),j=1,AY)
   case(3)    ! FFDI
    write(110,rec=rec5)((FFDI_cat1a(i,j),i=1,AX),j=1,AY)
    write(111,rec=rec5)((FFDI_cat1s(i,j),i=1,AX),j=1,AY)
    write(110,rec=rec6)((FFDI_cat2a(i,j),i=1,AX),j=1,AY)
    write(111,rec=rec6)((FFDI_cat2s(i,j),i=1,AX),j=1,AY)
    write(110,rec=rec7)((FFDI_cat3a(i,j),i=1,AX),j=1,AY)
    write(111,rec=rec7)((FFDI_cat3s(i,j),i=1,AX),j=1,AY)
    write(110,rec=rec8)((FFDI_cat4a(i,j),i=1,AX),j=1,AY)
    write(111,rec=rec8)((FFDI_cat4s(i,j),i=1,AX),j=1,AY)
    write(110,rec=rec9)((FFDI_cat5a(i,j),i=1,AX),j=1,AY)
    write(111,rec=rec9)((FFDI_cat5s(i,j),i=1,AX),j=1,AY)
  end select
  close(110)
  close(111)
  print*,"Number of FDI-values in study area (all months) =",tel
  print*,'Output written to: ',opath//'all_'//finx//GCM//pperiod//
 &       ext2,'or all_fs_***   (daily FDIs)'
  print*,'            and: ',opath//'max_'//finx//GCM//pperiod//
 &       ext2,'or max_fs_***   (spatial maximum FDIs)'
  print*,'            and: ',opath//'mean_'//finx//GCM//pperiod//
 &       ext2,'or mean_fs_***   (spatial mean FDIs)'
  print*,'            and: ',opath//'klima_'//finx//GCM//pperiod//
 &       ext1,'or klims_***   (annual or fire season means/totals)'
  print*,'<>=<>=<>=<>=<>=<>=<>=<>=<>=<>=<>=<>=<>=<>=<>=<>=<>=<>=<>=<>=<>=<>'

  end program fire4era
```

Below the required parameter file “par_fire4era.h”:

```
      integer AX,AY,gnum,maxn,startyr,endyr,AT,fstart,fend,fs,ind,cbp,
     &       CAN
      character pperiod*10,GCM*4
      parameter(AX=1440,AY=721)   ! dim of ERA5 global array
      parameter(gnum=410)     ! number of grid points in study area
      parameter(startyr=1981,endyr=2010,AT=endyr-startyr+1,
     &         pperiod="_1981_2010")
      parameter(fstart=05,fend=11,fs=fend-fstart+1)
      parameter(maxn=gnum*366*AT) ! max possible number of FDI-values
      parameter(GCM="ERA5")
      parameter(cbp=2)     ! see index options below:
       !1 use original breakpoints for FDI categories from literature
       !2 use climatological percentile breakpoints for FDI categories
      parameter(ind=2)     ! see index options below:
       !1 Canadian Fire Weather Index (CFWI) - choose CAN below...
       !2 Lowveld Fire Danger Index (LFDI)
       !3 McArthur Forest Fire Danger Rating (FFDR)
      parameter(CAN=0)     ! index to write out either:
       !0 CDSR
       !1 CFWI
```

“fire4gcm.f” is very similar to “fire4era.f” and was hence not included.
Below the required parameter file “par_fire4gcm.h”:

```
integer AAX,AX,AAY,AY,gnum,maxn,startyr,endyr,AT,fstart,fend,fs,
     &       ind,cbp,CAN
      character pperiod*10,GCM*5
      parameter(AAX=1440,AAY=721) ! dim of ERA5 climatology array
      parameter(AX=162,AY=162)    ! dim of GCM array
      parameter(gnum=119)     ! number of grid points in study area
      parameter(startyr=2071,endyr=2099,AT=endyr-startyr+1,
     &         pperiod="_2071_2099")
      parameter(fstart=05,fend=11,fs=fend-fstart+1)
      parameter(maxn=gnum*366*AT) ! max possible number of FDI-values
      parameter(GCM="miroc")
      parameter(cbp=2)     ! see index options below:
       !1 use original breakpoints for FDI categories from literature
       !2 use climatological percentile breakpoints for FDI categories
      parameter(ind=1)     ! see index options below:
       !1 Canadian Fire Weather Index (CFWI) - choose CAN below...
       !2 Lowveld Fire Danger Index (LFDI)
       !3 McArthur Forest Fire Danger Rating (FFDR)
      parameter(CAN=0)     ! index to write out either:
       !0 CDSR
       !1 CFWI
```

APPENDIX F

```
 program fcdf_gcm

!#####################################################################
!# This FORTRAN program reads the fire danger index values           #
!# calculated for each grid within the study area and:               #
!# a) sort them in ascending order;                                  #
!# b) allocate a probability of non-exceedance to each value;        #
!# c) calculates certain threshold percentiles.                      #
!# It is typically run after 'fire4gcm.f'                            #
!# Before running this program make sure that the parameters         #
!# defined in 'par_fire4gcm.h' is correct.                           #
!# To compile: gfortran fcdf_gcm.f                                   #
!#   an error message might be received when the data array is       #
!#   too big (depending on period) - in such cases the module        #
!#   and main program should be compiled as:                         #
!#      gfortran -c -mcmodel=large fcdf_gcm.f                        #
!#      gfortran fcdf_gcm.o                                          #
!# To run: ./a.out                                                   #
!# Output written to:                                                #
!# 'sorted_all_CFWI.ukmo_2071_2100.txt' (sorted FDIs & F for CDF)    #
!# 'percentiles_CFWI.ukmo_2071_2100.txt' (min,percentiles,max)       #
!#####################################################################
!#    Stephan Steyn   (steynas@ufs.ac.za)          2019              #
!#####################################################################
!
! Brief description of variables used:
! i,j,l,ir,indx,iindx = index used during sorting process
! m = actual number of values (population size)
! k,n = counter for number of values; population + 1
! maxn = maximum possible number of daily FDI-values
! io_status = integer used to test for end-of-file
! CFWI_d = daily value of the Canadian Fire Weather Index (CFWI)
! CDSR_d = daily value of the Canadian Daily Severity Rating (CDSR)
! LFDI_d = daily value of the Lowveld Fire Danger Index (LFDI)
! FFDI_d = daily value of the Forest Fire Danger Index (FFDI)
! CAN = index used for writing out either CFWI or CDSR values
! FDI = sorted fire danger indices
! indx = index of FDI value
! nFDI = placeholder used during sorting process
! iindx = index placeholder used during sorting process
! p99_p ... p75_p = position on percentile in sorted dataset
! p99_l ... p75_l = integer part of position in sorted dataset
! p99_f ... p75_f = fractal part of position in sorted dataset
! p99 ... p75 = respective percentile
!#####################################################################

 ! Declarations ***************************************************
 implicit none
 include 'par_fire4gcm.h'    ! parameter file
 integer :: i,j,k,l,m,n,io_status,ir,iindx,p_l
 integer, dimension(maxn) :: indx
 real :: nFDI,fk,fm,fn,p_p,p_f,p90_half,p90_quarter,pk
 real, dimension(100) :: p
 real, dimension(maxn) :: CFWI_d,CDSR_d,LFDI_d,FFDI_d,FDI,F
 character :: path*27,finx*5,ext1*4

 ! Defining characters and initialising values ********************
 path="/home/steynas/Results4GCMs/" ! Path to input/output data
     ! directory on cluster - use path*27
c    path="/run/media/stephan/SS_Transcend/Results4GCMs/" ! Path to
```

```
      ! input/output data directory on external - use path*45
    ext1=".txt"
    select case (ind)
     case (1)
      if (CAN.eq.1) then
       finx="CFWI."          ! Fire danger index indicator
      else
       finx="CDSR."          ! Fire danger index indicator
      endif
     case (2)
      finx="LFDI."           ! Fire danger index indicator
     case (3)
      finx="FFDI."           ! Fire danger index indicator
    end select
    print*,"Period selected:",startyr,"-",endyr,"=",AT,"years total"
    print*,"Index selected: ",finx

    ! Initialising values
    m=0
    n=0
    io_status=0
    nFDI=0.
    FDI=0.

    ! Reading daily FDI values for entire grid within study area *****
    print*,"Reading data for ",finx
    if (finx.eq."CDSR.") then
     finx="CFWI."   ! CDSR is in same input file as CFWI
    endif
    open(101,file=path//'all_'//finx//GCM//pperiod//ext1) ! file from
                              ! which all daily FDIs are read
    do while (io_status.eq.0)    ! Start looping through data -----
     n=n+1
     select case(ind)
      case(1)    ! CFWI
       read(101,100,iostat=io_status) CFWI_d(n),CDSR_d(n)
      case(2)    ! LFDI
       read(101,200,iostat=io_status) LFDI_d(n)
      case(3)    ! FFDI
       read(101,200,iostat=io_status) FFDI_d(n)
     end select
    enddo    ! while-loop ends
    close(101)
    m=n-1
    print*,"Population size =",m
100   FORMAT (f5.1,3X,f5.1)
200   FORMAT (f5.1)
300   FORMAT (f5.1,3X,f11.10)

    ! Sorting FDI-values in ascending order according to the
    ! "heapsort" method explained in: Press, W.H., Flannery, B.P.,
    ! Teukolsky, S.A. and Vetterling, W.T., 1986. Numerical Recipes.
    ! Cambridge: Cambridge University Press.
    ! The index l will be decremented from its initial value during
    ! the "hiring" (heap creation) phase. Once it reaches 1, the index
    ! ir will be decremented from its initial value down to 1 during
    ! the "retirement-and-promotion" (heap selection) phase.
    select case(ind)
     case(1)    ! CFWI
      if (CAN.eq.1) then
       FDI=CFWI_d
      else
       FDI=CDSR_d
      endif
     case(2)    ! LFDI
       FDI=LFDI_d
```

```
      case(3)    ! FFDI
         FDI=FFDI_d
    end select
    if (m.lt.2) then
      GOTO 500    ! nothing to order
    endif
    ! initialize indices for hiring and retirement-promotion phase
    l=m/2+1
    ir=m
    do i=1,m
      indx(i)=i
    enddo
    sorting: do
      if (l.gt.1) then    ! still in hiring phase
        l=l-1
        nFDI=FDI(l)
        iindx=indx(l)
      else    ! in retirement-promotion phase
        nFDI=FDI(ir)    ! clear a space at the end of the array
        iindx=indx(ir)
        FDI(ir)=FDI(1)    ! retire the top of the heap into it
        indx(ir)=indx(1)
        ir=ir-1
        if (ir.eq.1) then    ! done with the last promotion
          FDI(1)=nFDI
          indx(1)=iindx
          exit sorting
        endif
      endif
      i=l
      j=l+l    ! set up to place nFDI in its proper level
      do while (j.le.ir)
        if (j.lt.ir) then
          if (FDI(j).lt.FDI(j+1)) then
            j=j+1
          endif
        endif
        if (nFDI.lt.FDI(j)) then    ! demote nFDI
          FDI(i)=FDI(j)
          indx(i)=indx(j)
          i=j
          j=j+j
        else
          j=ir+1    ! set j to terminate do-while loop
        endif
      enddo
      FDI(i)=nFDI
      indx(i)=iindx
    enddo sorting
500   CONTINUE

    ! Calculating probabilities of non-exceedance ********************
    fn=real(n)
    do k=1,m
      fk=real(k)
      F(k)=(fk/fn)
    enddo
    print*,'min FDI =',FDI(1),'F(1) =',F(1)
    print*,'max FDI =',FDI(m),'F(max) =',F(m)

    ! Calculating select percentiles *********************************
    fm=real(m)
    do k=1,99
      fk=real(k)
      p_p=(fk*fn/100.)            ! th observation in sorted dataset
      p_l=int(p_p)                ! lower integer
```

```
  p_f=p_p-p_l                ! fractal part
  if (p_p.le.fm) then
    p(k)=FDI(p_l)+p_f*(FDI(p_l+1)-FDI(p_l))
  else
    p(k)=FDI(m)
  endif
 enddo
 ! half of 90th percentile
 p90_half=.5*p(90)
 ! quarter of 90th percentile
 p90_quarter=.25*p(90)
 print*,'============================================================'
 print*,'Recommended cut-off levels for FDRS (own proposal)'
 print*,'p99 =       ',p(99)
 print*,'p93 =       ',p(93)
 print*,'p73 =       ',p(73)
 print*,'p30 =       ',p(30)
 print*,'============================================================'

 ! Writing sorted values and probabilities for CDF to file ********
 if (ind.eq.1.and.CAN.eq.0) then
   finx="CDSR."     ! change finx back to CDSR for output file
 endif
 open(102,file=path//'sorted_all_'//finx//GCM//pperiod//ext1)
 do k=1,m
   write(102,300) FDI(k),F(k)
 enddo
 close(102)
 open(103,file=path//'percentiles_'//finx//GCM//pperiod//ext1)
 write(103,300) FDI(1),F(1)
 do k=1,99
   fk=real(k)
   pk=fk/100.
   write(103,300) p(k),pk
 enddo
 write(103,300) FDI(m),F(m)
 close(103)
 print*,'Output written to: ',path//'sorted_all_'//finx//GCM//
&pperiod//ext1,'     (sorted FDIs and probs for CDF)'
 print*,'                ',path//'percentiles_'//finx//GCM//
&pperiod//ext1,'     (min,percentiles,max)'
 print*,'<>=<>=<>=<>=<>=<>=<>=<>=<>=<>=<>=<>=<>=<>=<>=<>=<>=<>=<>=<>'

 end program fcdf_gcm
```

APPENDIX G

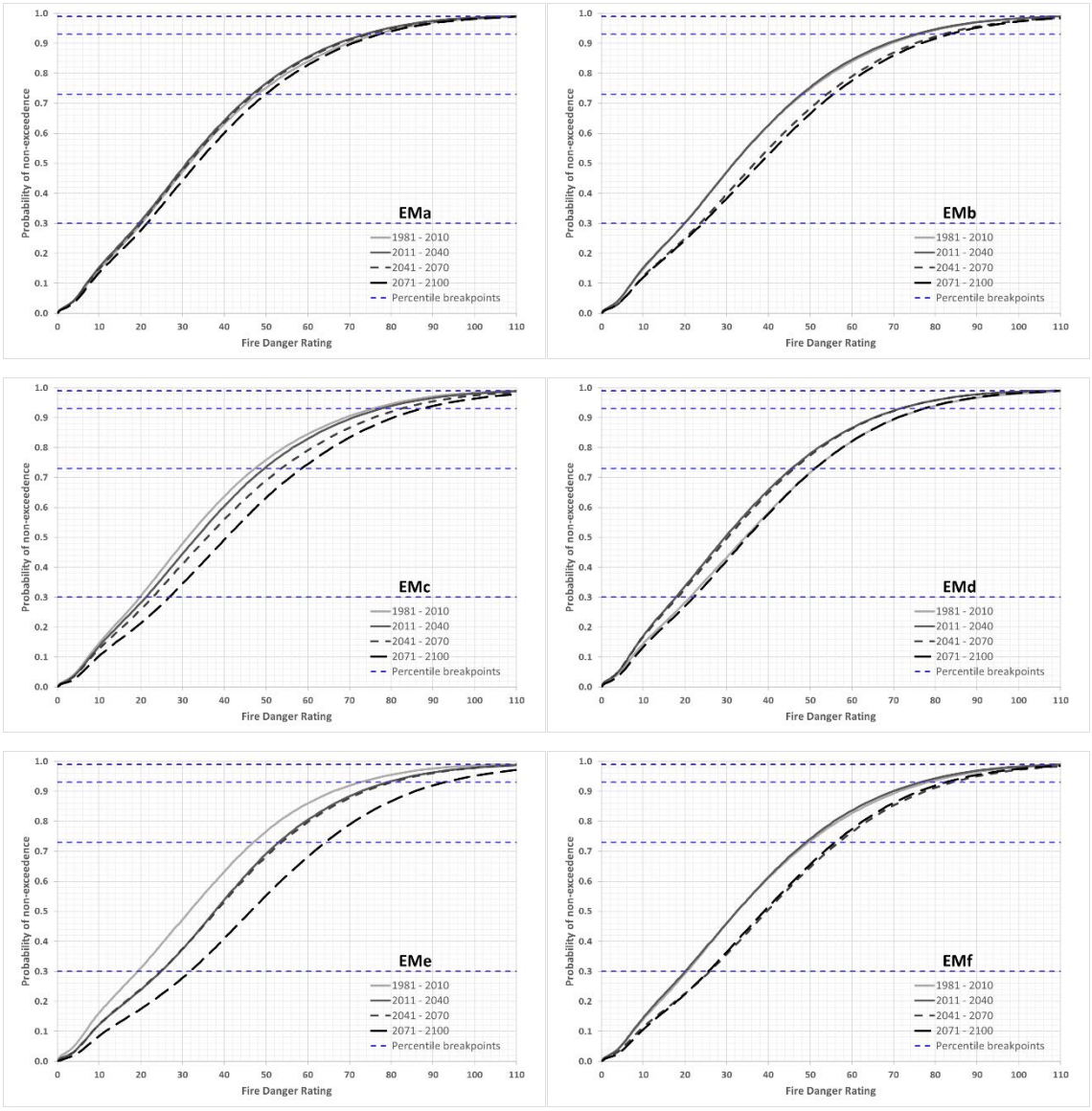

Cumulative distribution functions of the fire season CFWI for four consecutive 30-year periods over the central grassland biome of South Africa. EMa – Emf represent the six ensemble members listed in Figure 9.4.

APPENDIX H

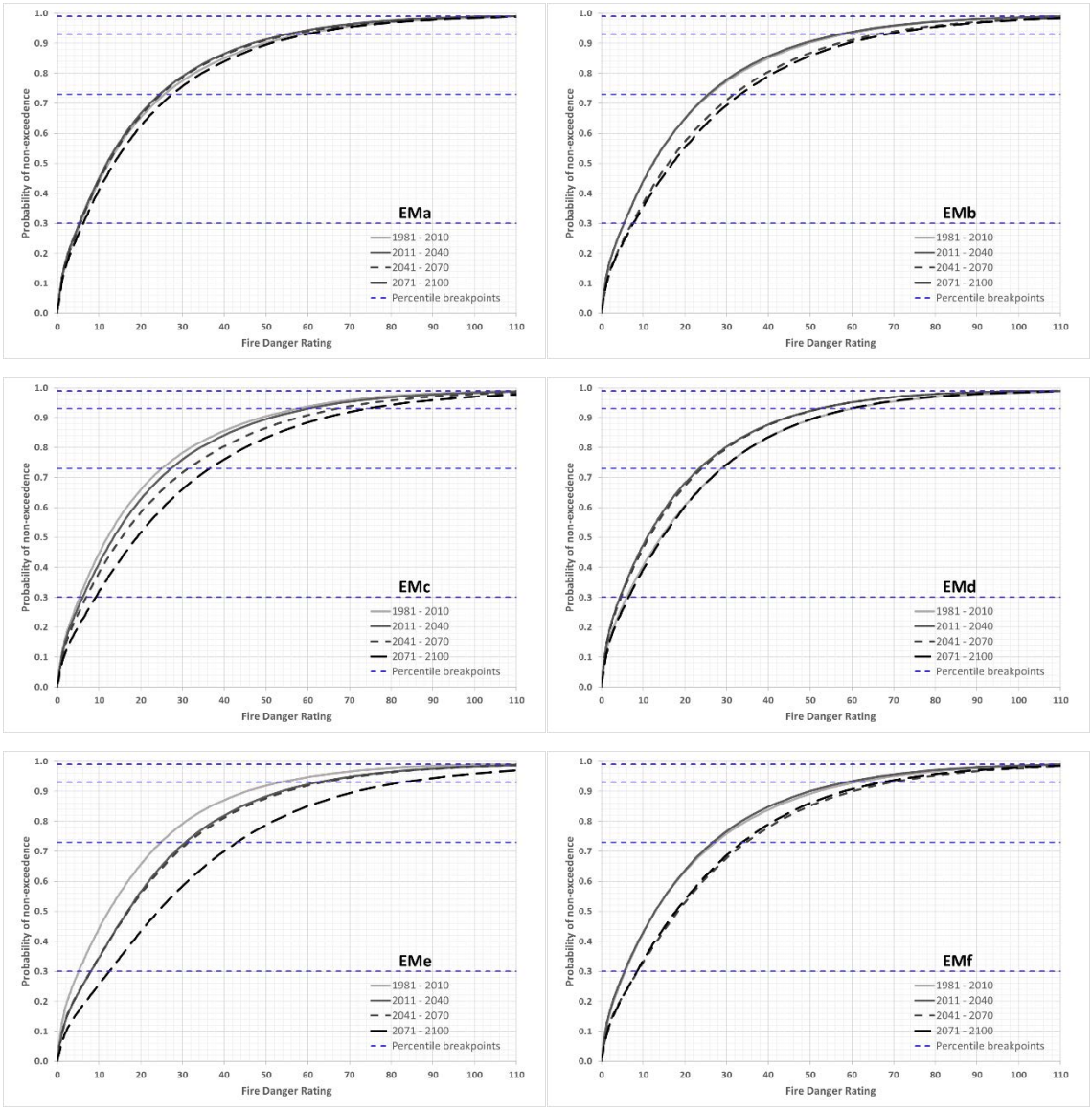

Cumulative distribution functions of the fire season CDSR for four consecutive 30-year periods over the central grassland biome of South Africa. EMa – Emf represent the six ensemble members listed in Figure 9.4.

APPENDIX I

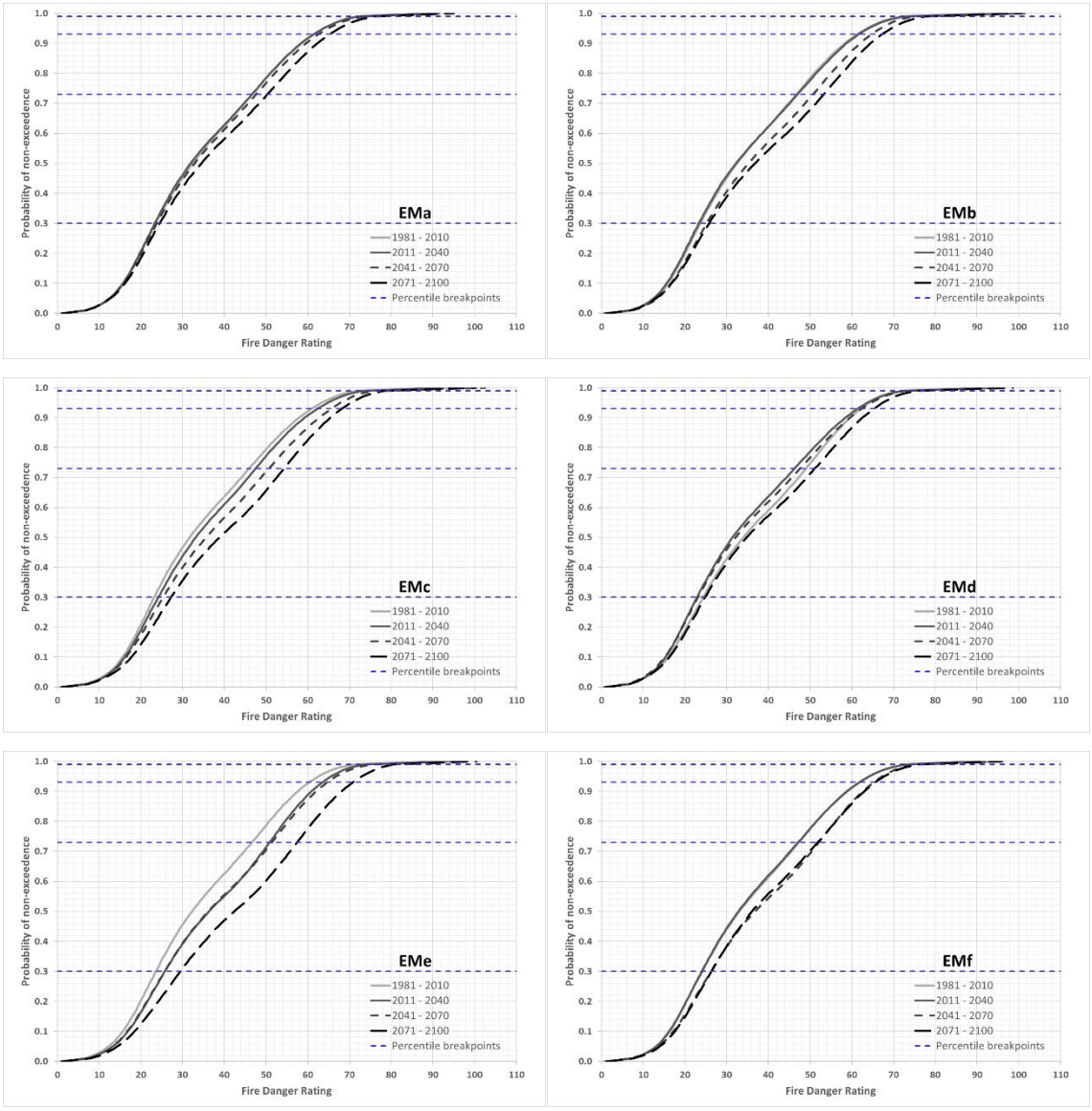

Cumulative distribution functions of the fire season LFDI for four consecutive 30-year periods over the central grassland biome of South Africa. EMa – Emf represent the six ensemble members listed in Figure 9.4.

APPENDIX J

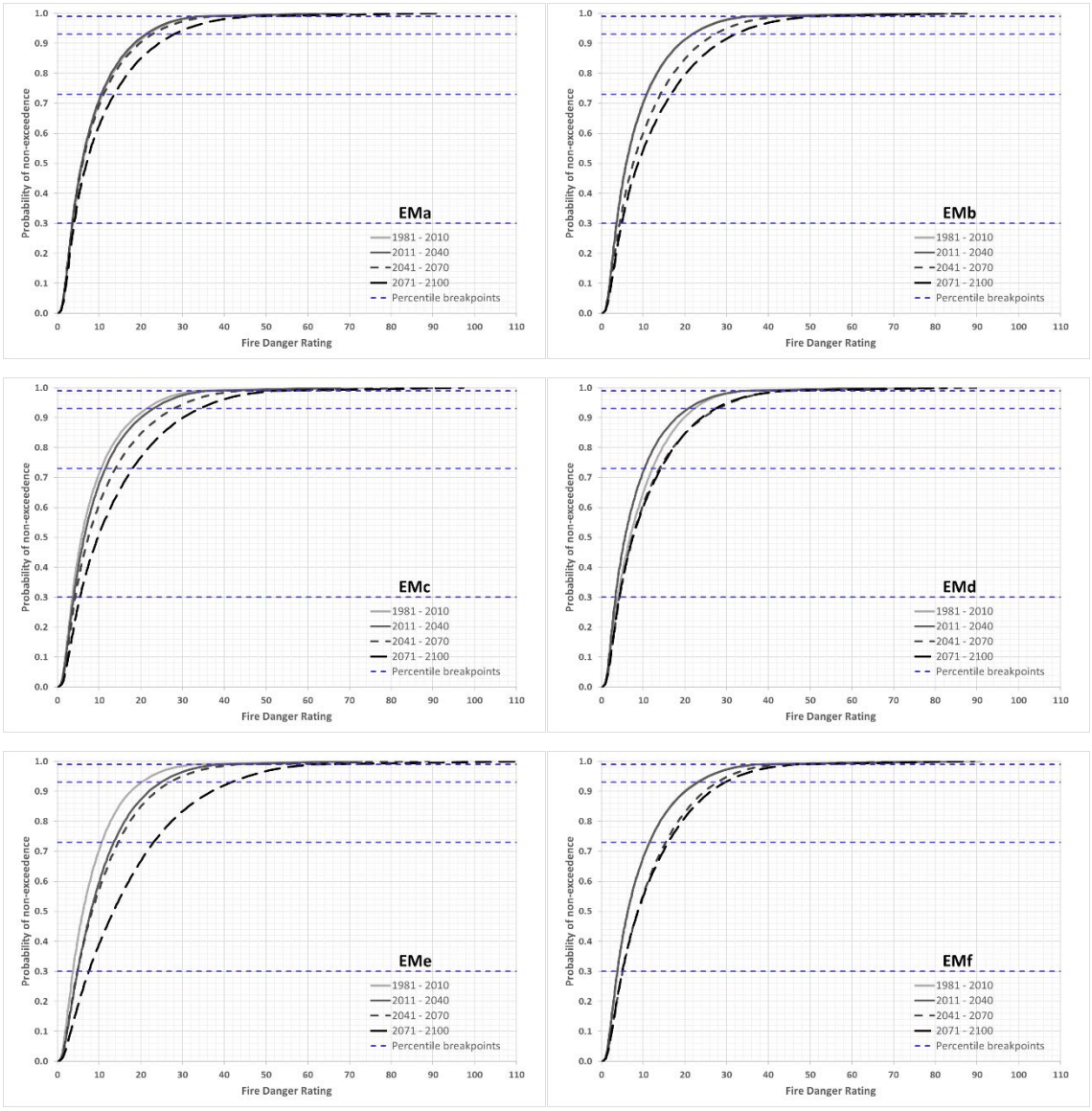

Cumulative distribution functions of the fire season FFDI for four consecutive 30-year periods over the central grassland biome of South Africa. EMa – Emf represent the six ensemble members listed in Figure 9.4.

APPENDIX K

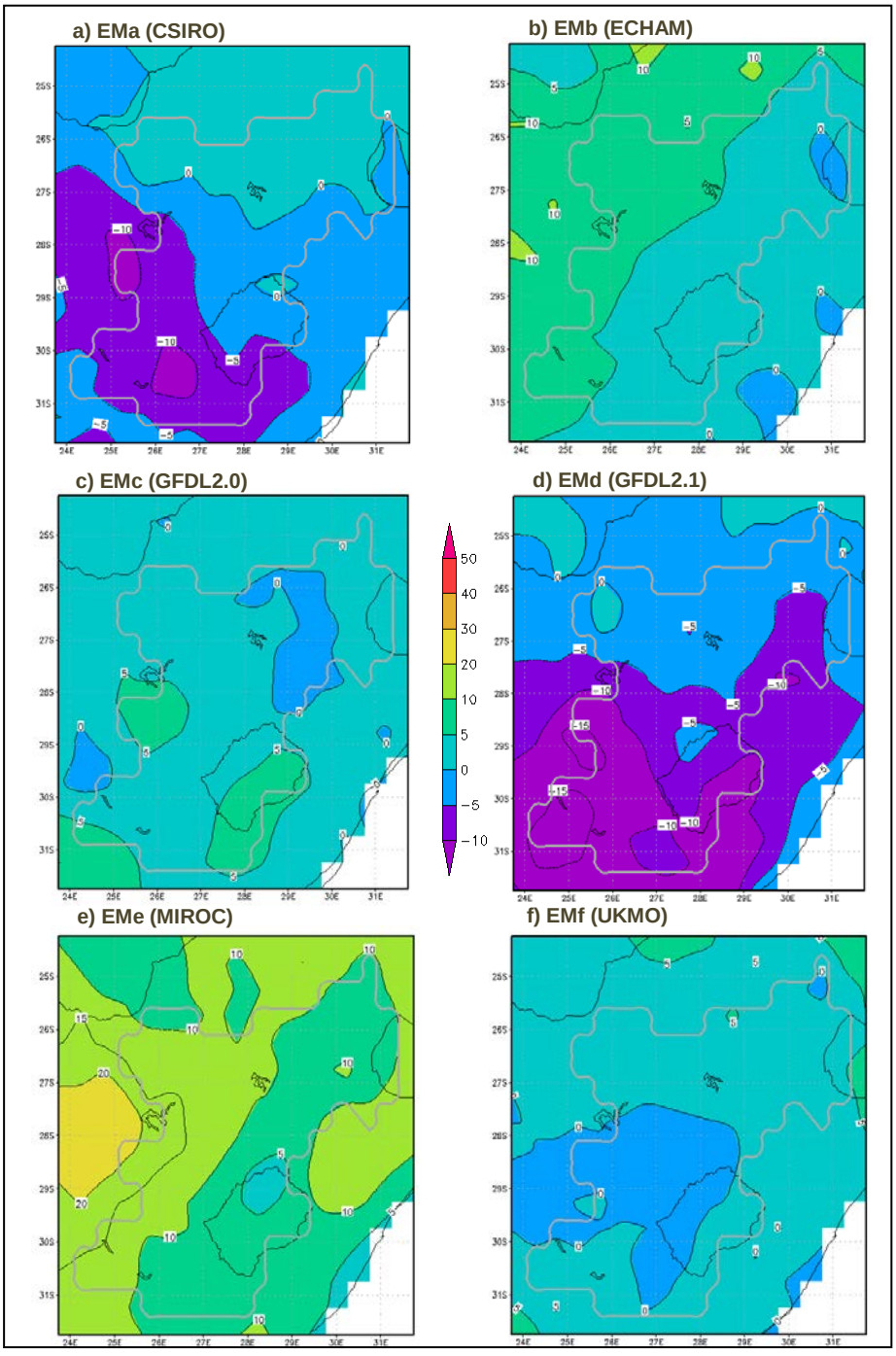

Spatial distribution of changes in mean annual occurrences of very high and extreme danger days combined according to the CFWI for the period 2011 – 2040 relative to the climatological base period (1981 – 2010). The grey polygon delineates the central grassland biome.

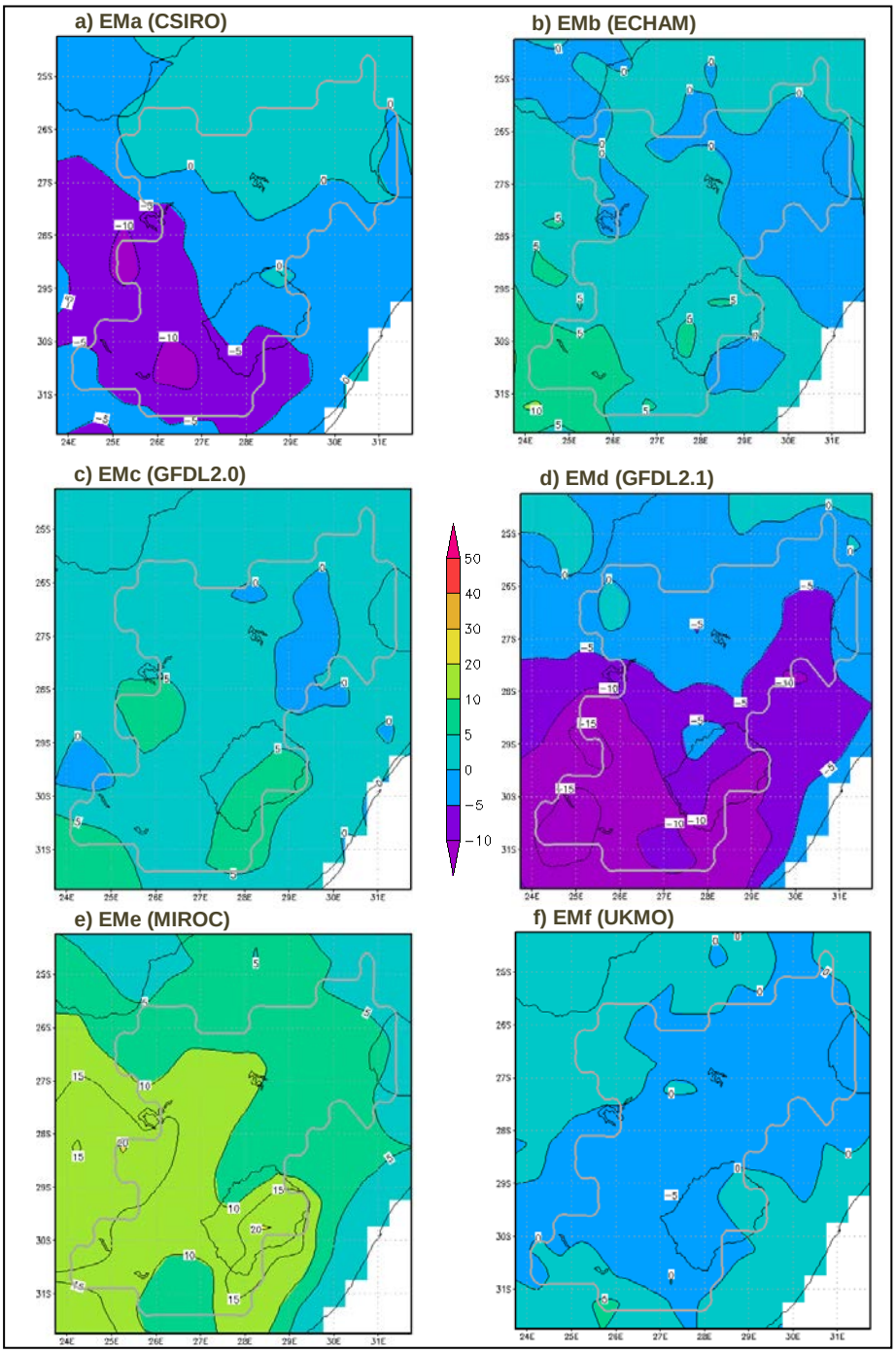

Spatial distribution of changes in mean annual occurrences of very high and extreme danger days combined according to the CDSR for the period 2011 – 2040 relative to the climatological base period (1981 – 2010). The grey polygon delineates the central grassland biome.

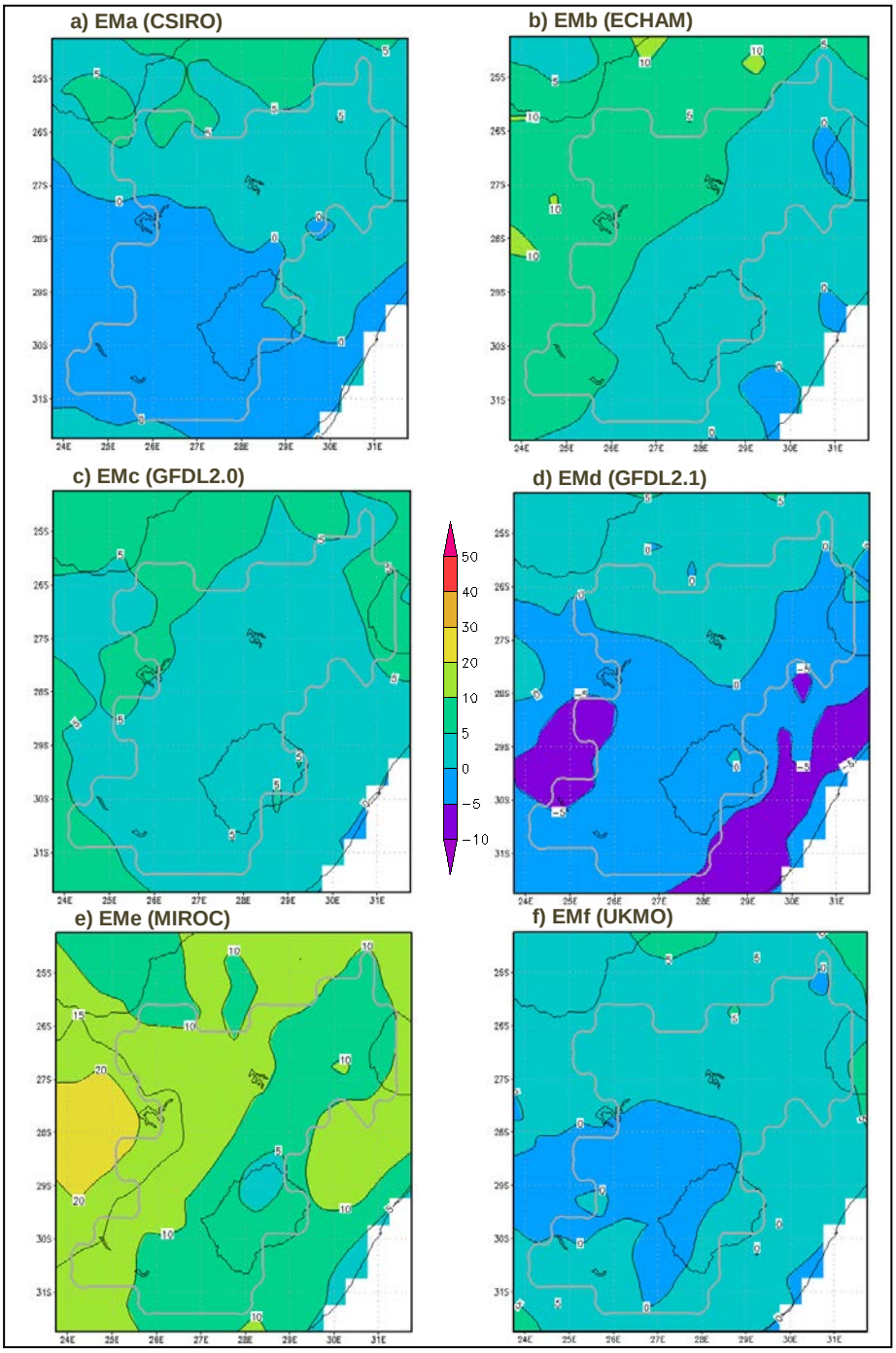

Spatial distribution of changes in mean annual occurrences of very high and extreme danger days combined according to the LFDI for the period 2011 – 2040 relative to the climatological base period (1981 – 2010). The grey polygon delineates the central grassland biome.

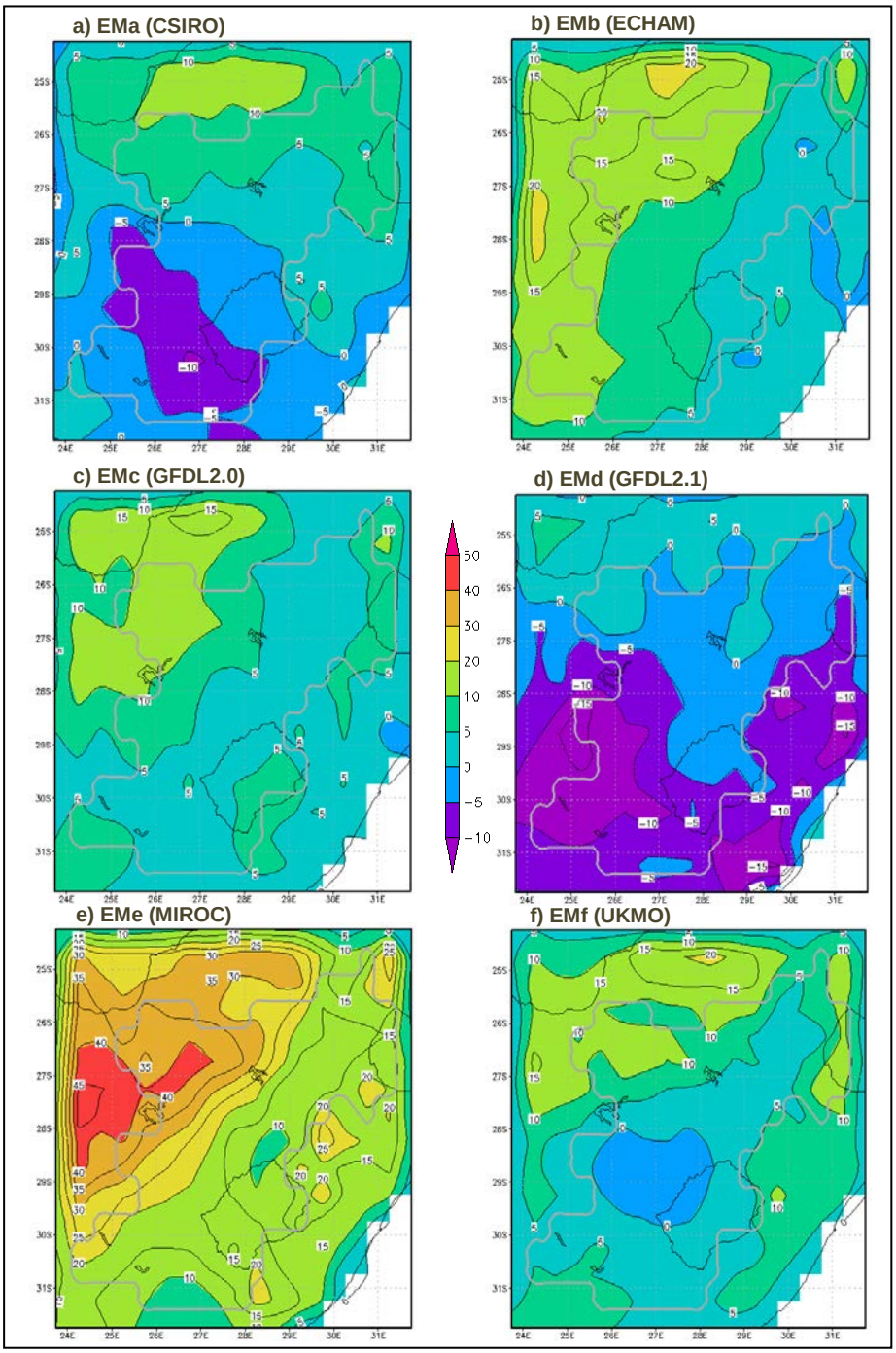

Spatial distribution of changes in mean annual occurrences of very high and extreme danger days combined according to the FFDI for the period 2011 – 2040 relative to the climatological base period (1981 – 2010). The grey polygon delineates the central grassland biome.

APPENDIX L

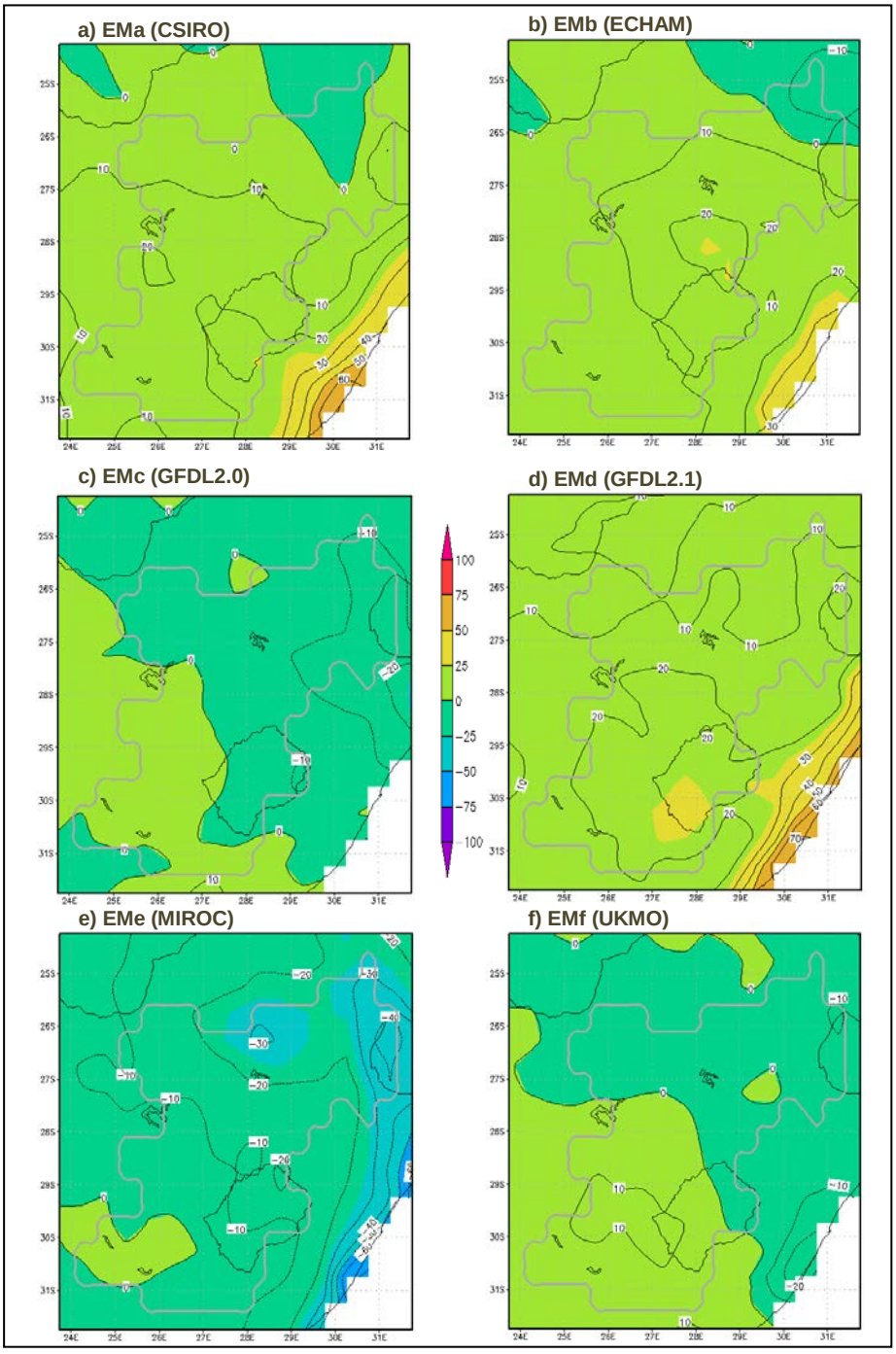

Spatial distribution of changes in mean fire season total precipitation for the period 2011 – 2040 relative to the climatological base period (1981 – 2010). The grey polygon delineates the central grassland biome.

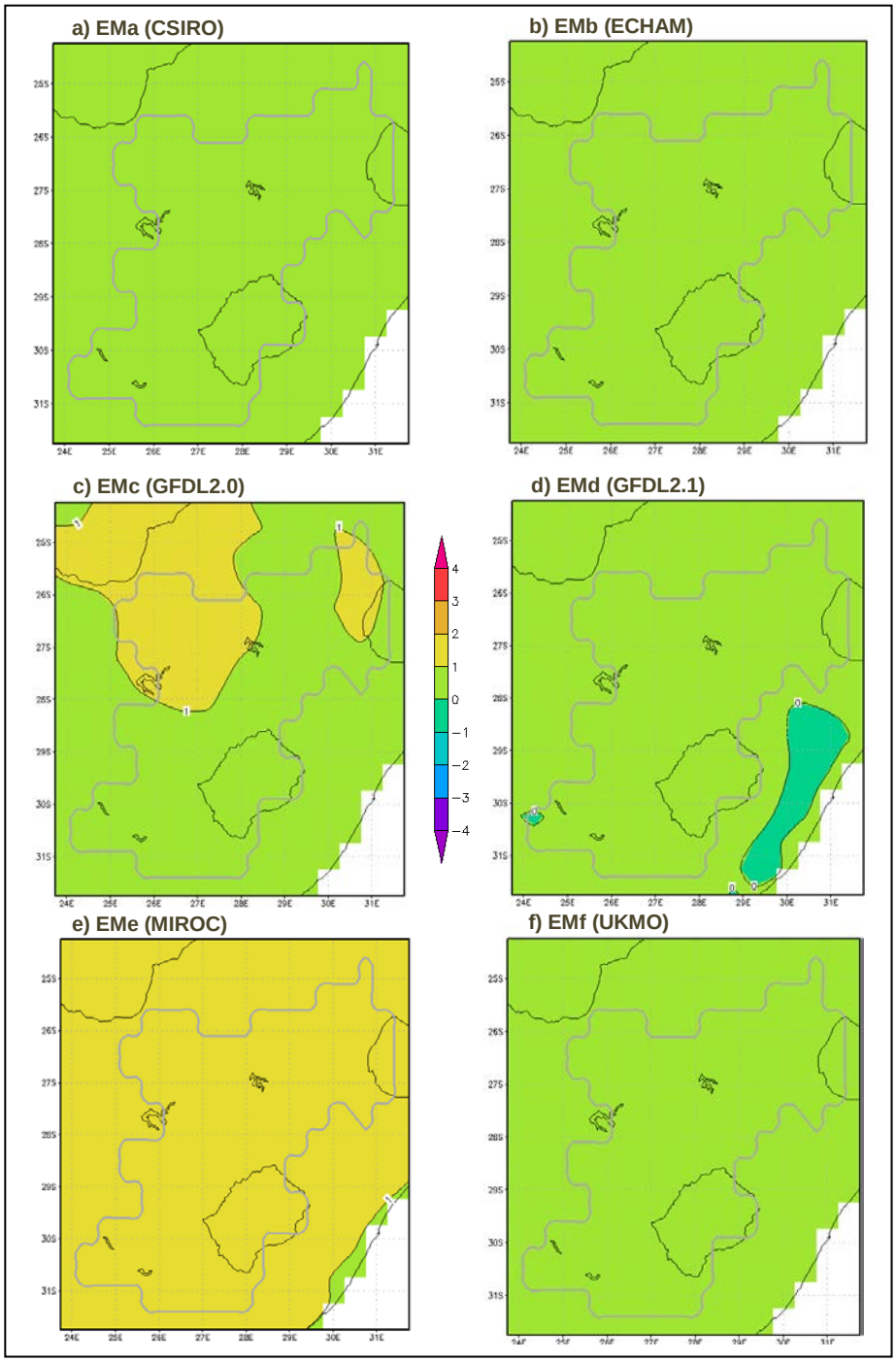

Spatial distribution of changes in mean fire season maximum temperature for the period 2011 – 2040 relative to the climatological base period (1981 – 2010). The grey polygon delineates the central grassland biome.

APPENDIX M

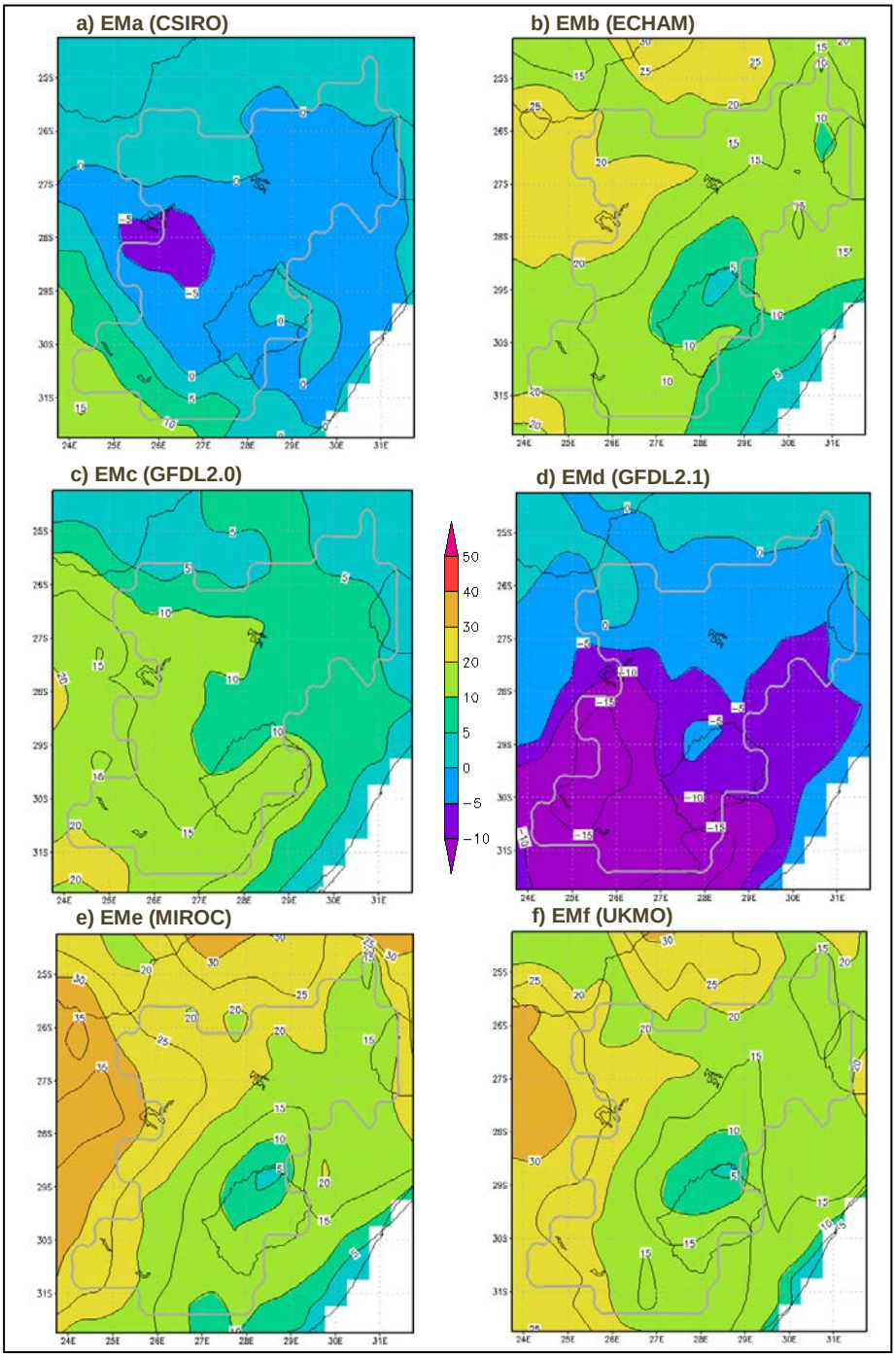

Spatial distribution of changes in mean annual occurrences of very high and extreme danger days combined according to the CFWI for the period 2041 – 2070 relative to the climatological base period (1981 – 2010). The grey polygon delineates the central grassland biome.

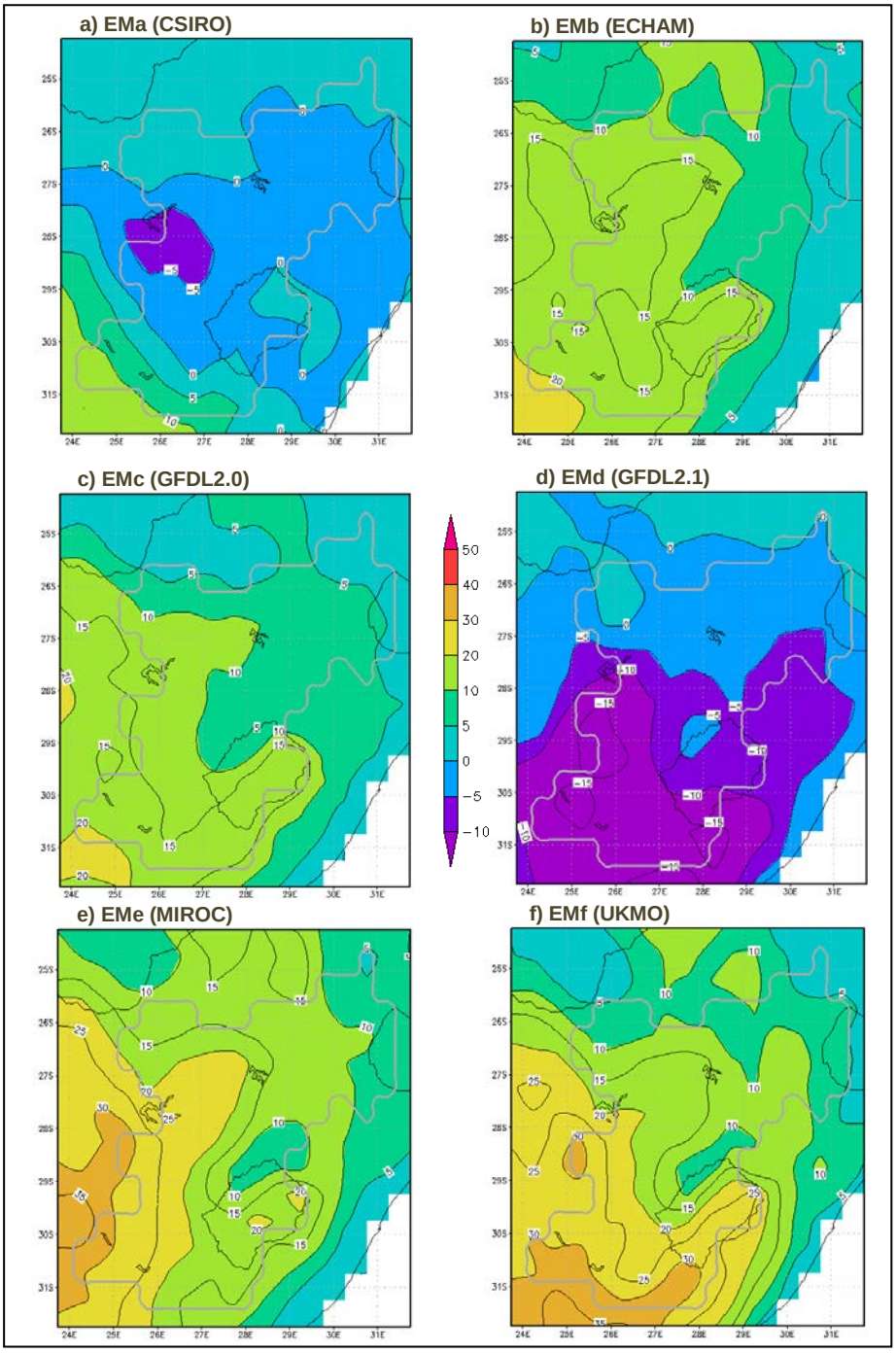

Spatial distribution of changes in mean annual occurrences of very high and extreme danger days combined according to the CDSR for the period 2041 – 2070 relative to the climatological base period (1981 – 2010). The grey polygon delineates the central grassland biome.

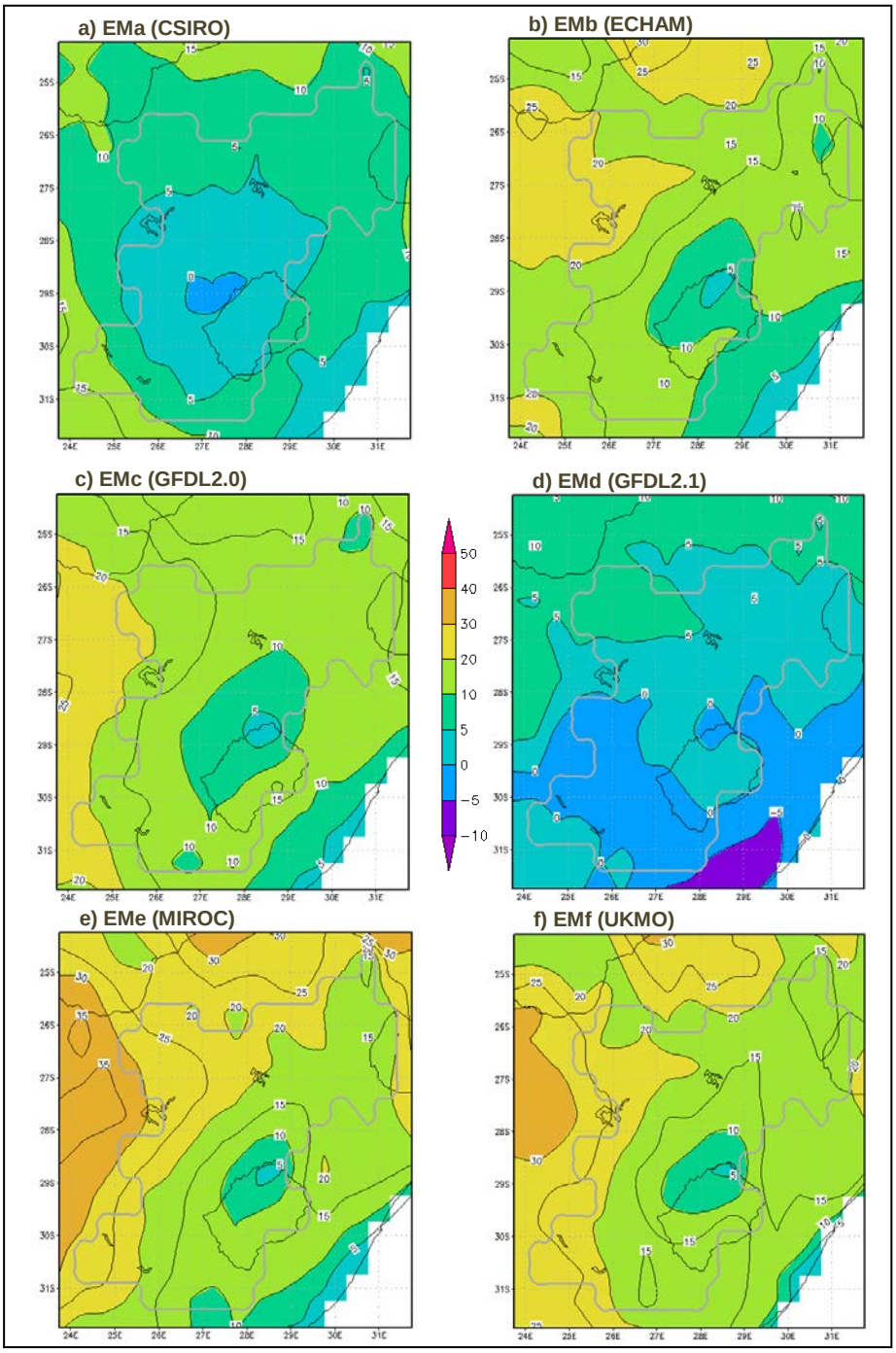

Spatial distribution of changes in mean annual occurrences of very high and extreme danger days combined according to the LFDI for the period 2041 – 2070 relative to the climatological base period (1981 – 2010). The grey polygon delineates the central grassland biome.

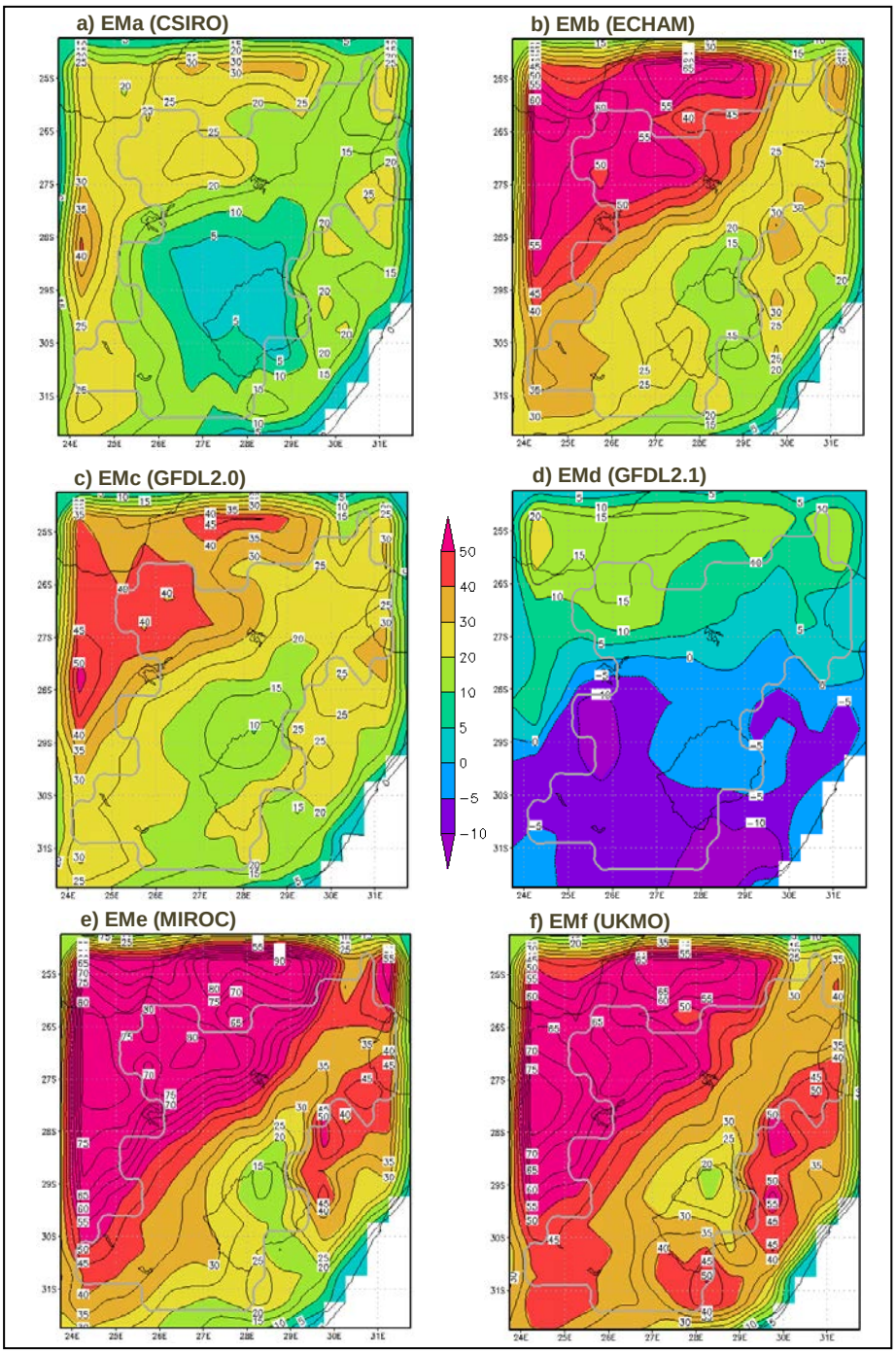

Spatial distribution of changes in mean annual occurrences of very high and extreme danger days combined according to the FFDI for the period 2041 – 2070 relative to the climatological base period (1981 – 2010). The grey polygon delineates the central grassland biome.

APPENDIX N

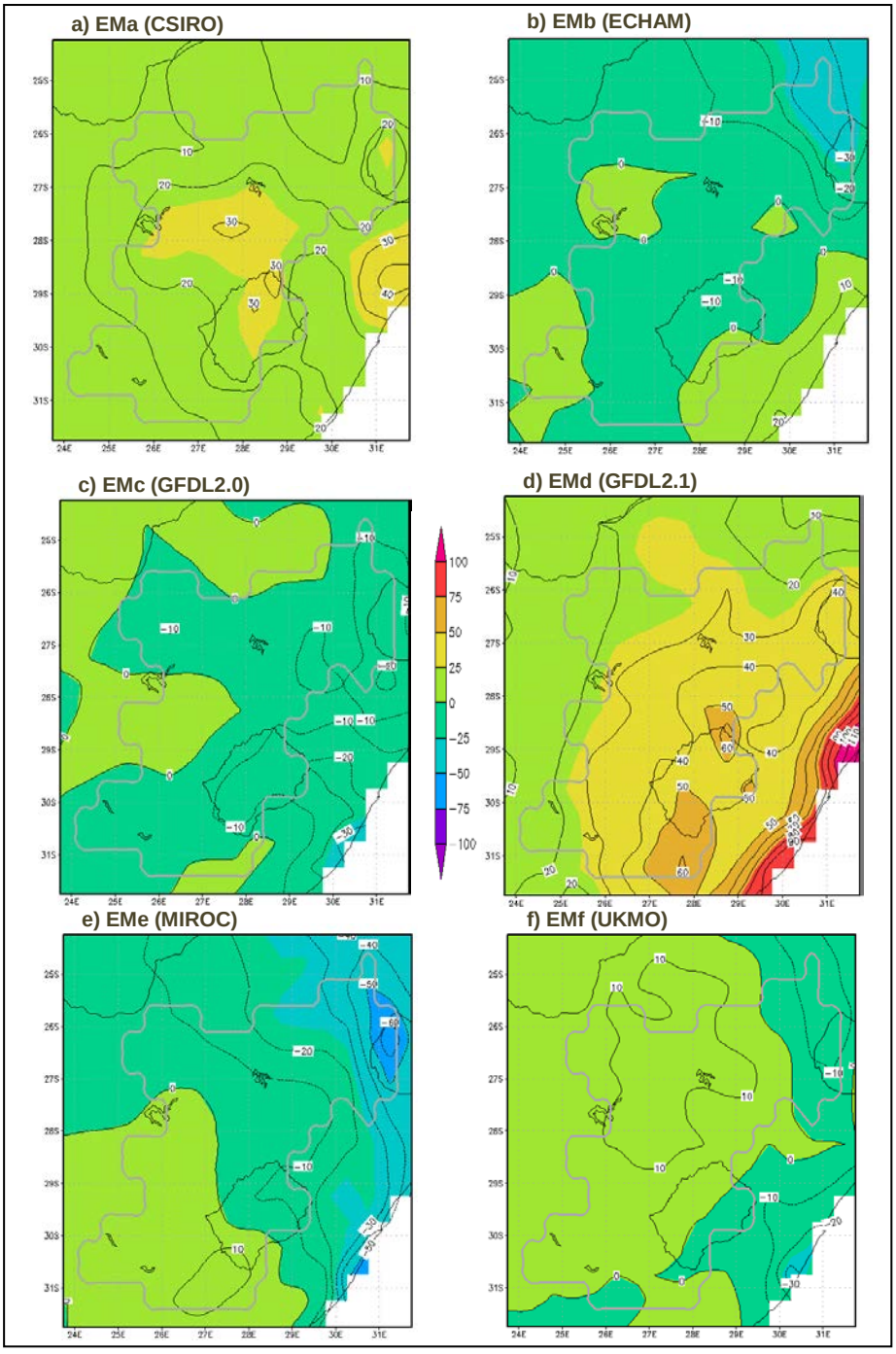

Spatial distribution of changes in mean fire season total precipitation for the period 2041 – 2070 relative to the climatological base period (1981 – 2010). The grey polygon delineates the central grassland biome.

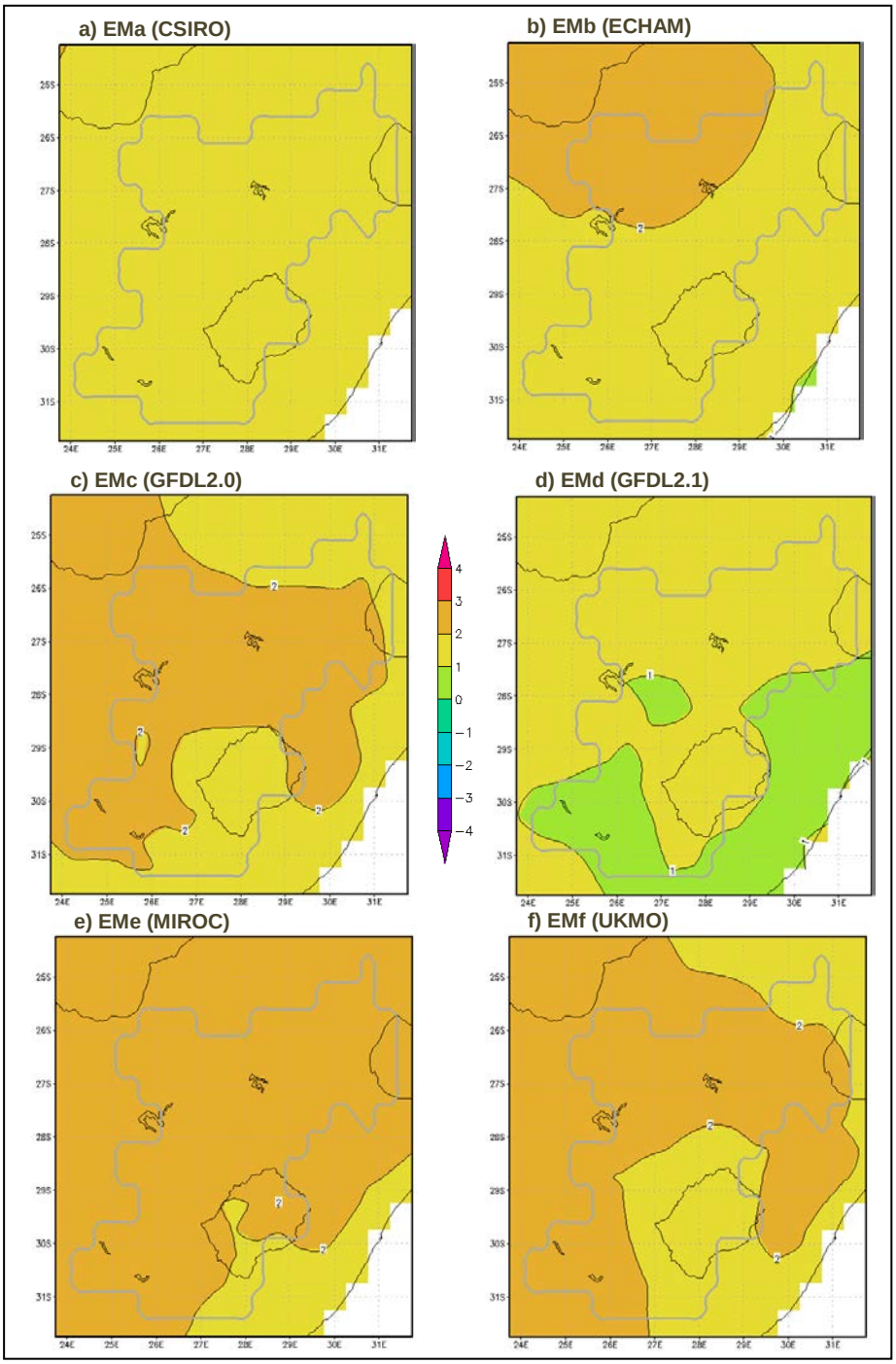

Spatial distribution of changes in mean fire season maximum temperature for the period 2041 – 2070 relative to the climatological base period (1981 – 2010). The grey polygon delineates the central grassland biome.

APPENDIX O

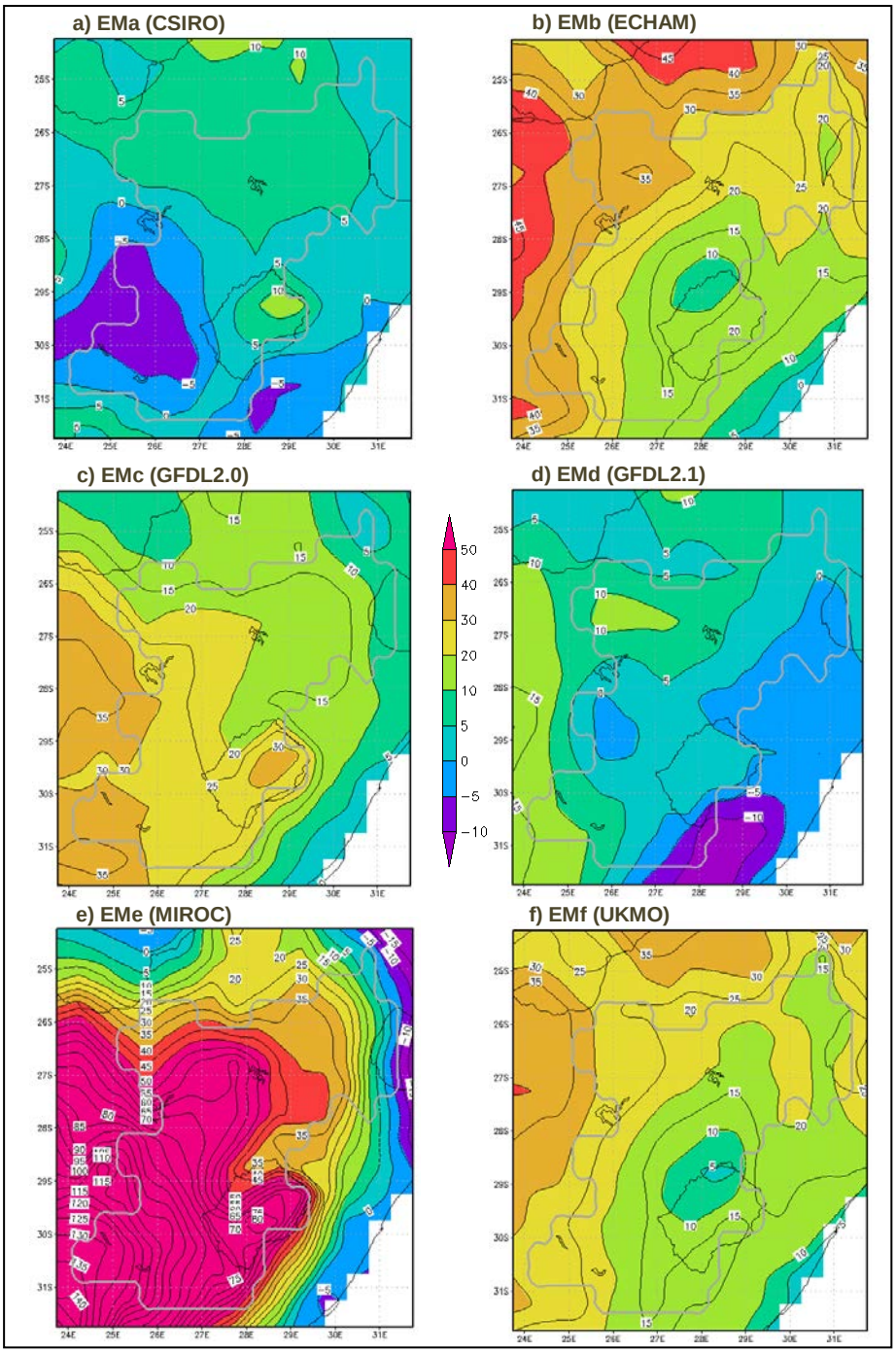

Spatial distribution of changes in mean annual occurrences of very high and extreme danger days combined according to the CFWI for the period 2071 – 2100 relative to the climatological base period (1981 – 2010). The grey polygon delineates the central grassland biome.

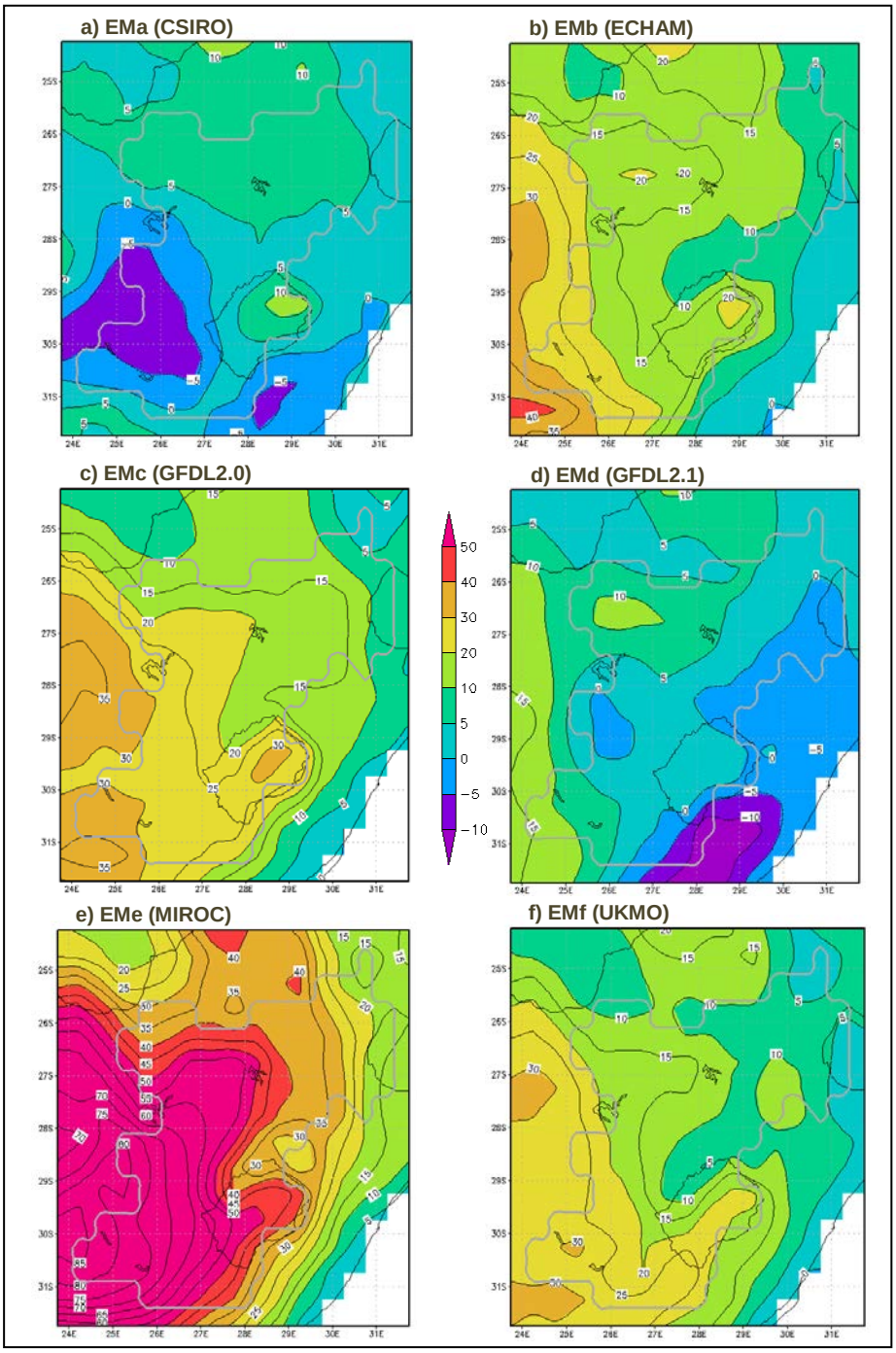

Spatial distribution of changes in mean annual occurrences of very high and extreme danger days combined according to the CDSR for the period 2071 – 2100 relative to the climatological base period (1981 – 2010). The grey polygon delineates the central grassland biome.

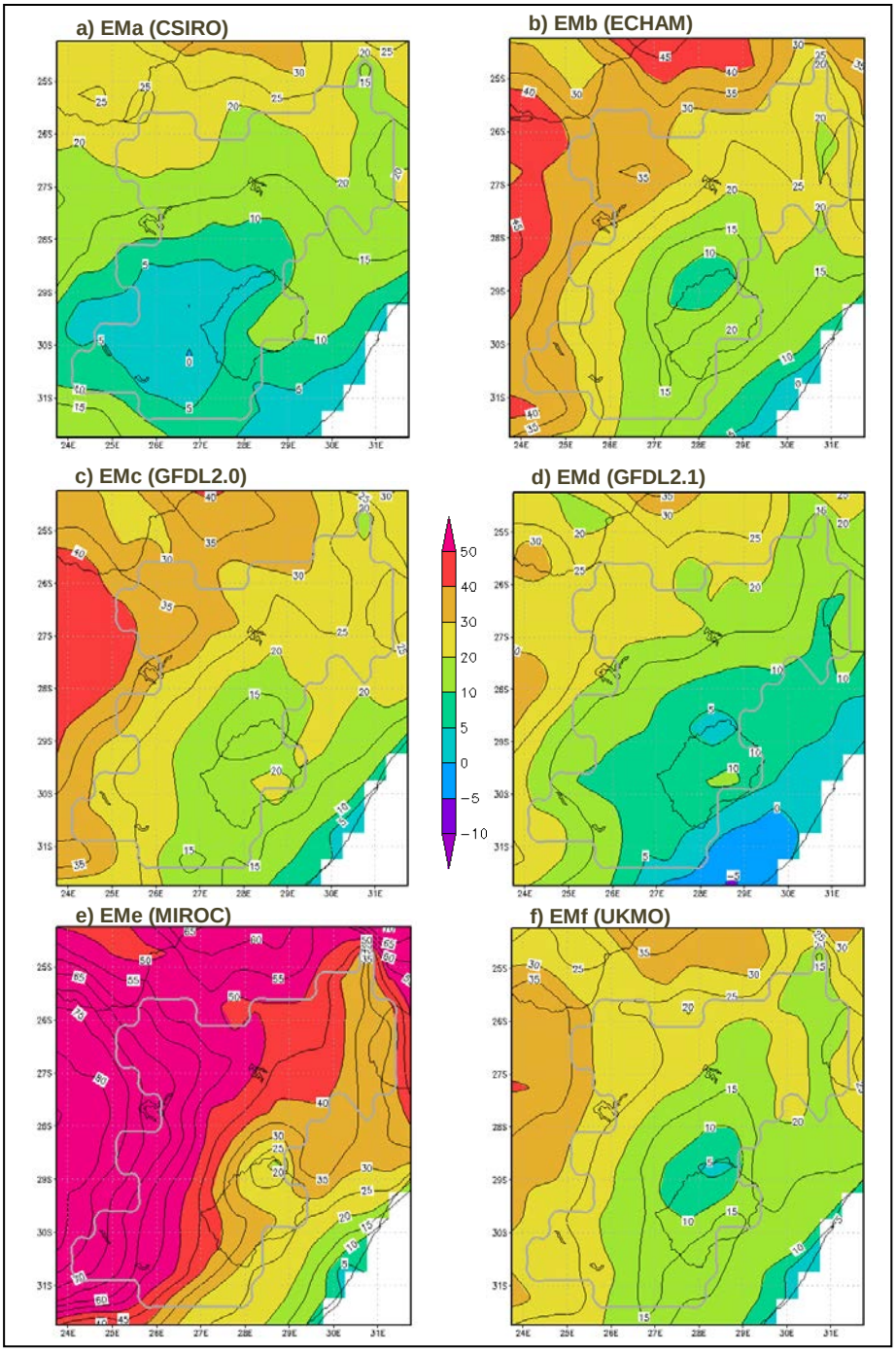

Spatial distribution of changes in mean annual occurrences of very high and extreme danger days combined according to the LFDI for the period 2071 – 2100 relative to the climatological base period (1981 – 2010). The grey polygon delineates the central grassland biome.

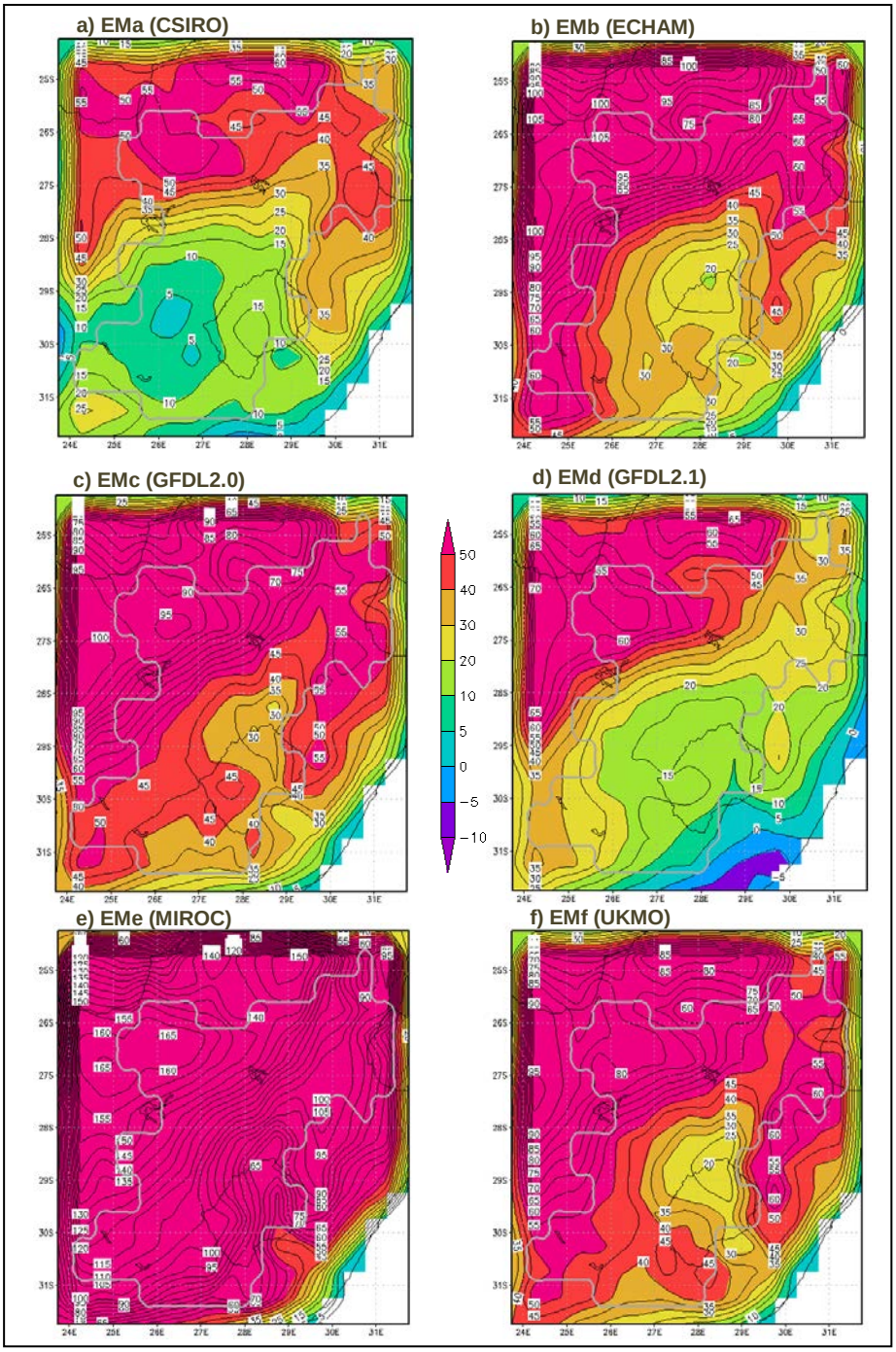

Spatial distribution of changes in mean annual occurrences of very high and extreme danger days combined according to the FFDI for the period 2071 – 2100 relative to the climatological base period (1981 – 2010). The grey polygon delineates the central grassland biome.

APPENDIX P

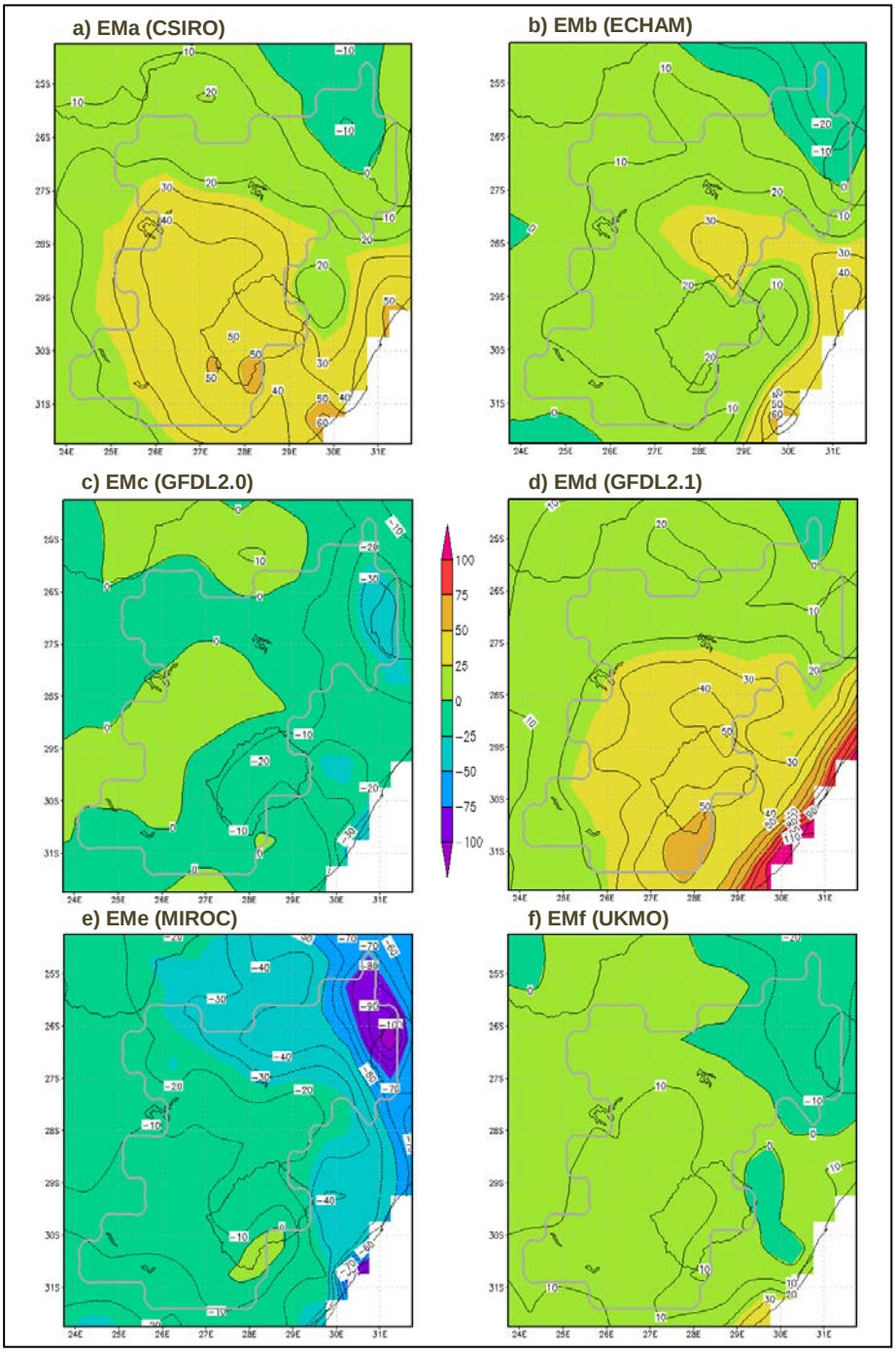

Spatial distribution of changes in mean fire season total precipitation for the period 2071 – 2100 relative to the climatological base period (1981 – 2010). The grey polygon delineates the central grassland biome.

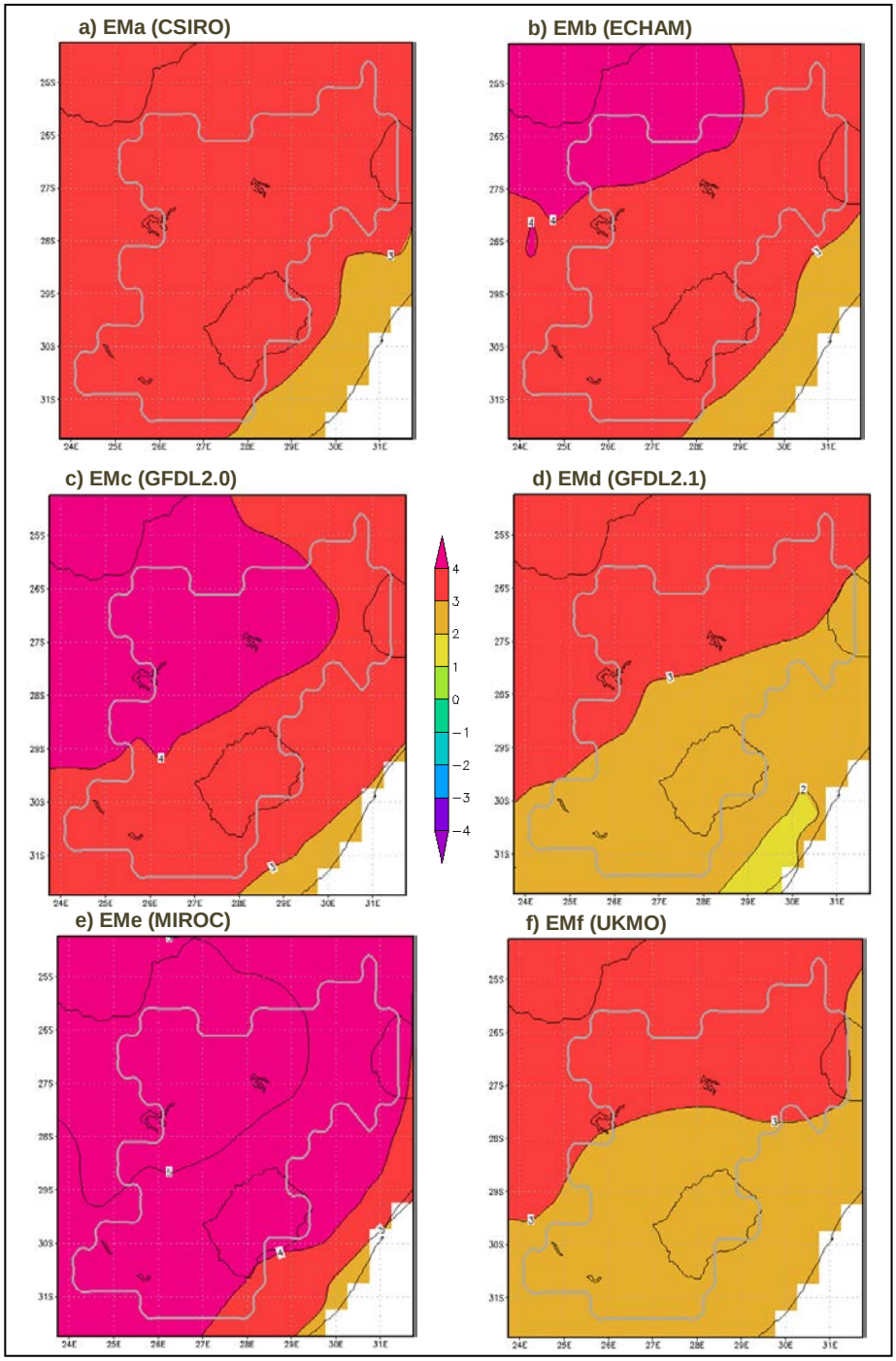

Spatial distribution of changes in mean fire season maximum temperature for the period 2071 – 2100 relative to the climatological base period (1981 – 2010). The grey polygon delineates the central grassland biome.